CORA Cork Open Research Archive
Cartlann Taighde Oscailte Chorcaí

Title	Impurity profiling and synthesis of precursors to the hallucinogenic amphetamine DOB
Authors	Quille, Jonathan
Publication date	2015
Original Citation	Quille, J. 2015. Impurity profiling and synthesis of precursors to the hallucinogenic amphetamine DOB. PhD Thesis, University College Cork.
Type of publication	Doctoral thesis
Rights	© 2015, Jonathan Quille. - http://creativecommons.org/licenses/by-nc-nd/3.0/
Download date	2026-10-30 10:41:44
Item downloaded from	https://hdl.handle.net/10468/2963

UCC
University College Cork, Ireland
Coláiste na hOllscoile Corcaigh

Impurity Profiling and Synthesis of Precursors to the Hallucinogenic Amphetamine DOB

by Jonathan Quille BSc



A thesis presented for the degree of

DOCTOR OF PHILOSOPHY

to

National University of Ireland, Cork

Department of Chemistry,
University College Cork

September, 2015

Supervisors: Dr J.J. Keating and Dr Dara Fitzpatrick

Head of Department: Professor Martyn Pemble

Abstract

DOB (4-bromo-2,5-dimethoxyamphetamine) is a newly emerging hallucinogenic amphetamine that sparked serious health warnings in Ireland, following its first seizure back in 2003. Known more commonly as "snowball", this drug is highly potent and may be used as a substitute to ecstasy (MDMA) and lysergic acid diethylamide (LSD). To date, the work carried out on the impurity profiling of DOB is limited in comparison to amphetamine, methamphetamine and MDMA.

In this work, the impurity profile of 4-bromo-2,5-dimethoxyphenyl-2-propanone (4-Br-2,5-P2P) is explored. This ketone is a direct precursor to DOB. Its more versatile non-bromo analogue, 2,5-dimethoxyphenyl-2-propanone (2,5-P2P) is also examined, as in addition to DOB, it may be used in the synthesis of a range of several other hallucinogenic amphetamines.

A number of different routes to both 2,5-P2P and 4-Br-2,5-P2P were investigated. For each of these routes, the impurities produced were carefully isolated. Following isolation, the impurities were fully characterised (by ^{1}H-NMR/^{13}C-NMR spectroscopy, IR, MS), in order to aid structure elucidation. Compounds not easily resolved by flash column chromatography were analysed by LC-MS and/or independently synthesised for the purpose of attaining reference standards.

Adaptation of the well-known 'phenylacetic acid route' to synthesis of both 2,5-P2P and 4-Br-2,5-P2P, was found to provide low yields of the expected ketone products. Four impurities were isolated during the preparation of both ketones. The yield of one of these impurities (possessing a dibenzylketone core), was greatly influenced by the amount of acetic anhydride reagent used during the reaction. Having carried out the reaction with several different equivalents of acetic anhydride, it was found that formation of the 'dibenzylketone' could not be eliminated. This may increase its likelihood of being detected in the final drug product.

The 'Darzens route', having very recently emerged as a synthetic route to amphetamine and MDMA precursors, was discovered to be a viable route for manufacture of 2,5-P2P and 4-Br-2,5-P2P. Despite execution of the reaction being more tedious, the route provides superior yields (≈50–60%) to those achieved using the 'phenylacetic acid route' (≈35–38%).

Incorporation of a bromine atom (at the aromatic 4-position) is required at some stage during synthesis of DOB. The bromination of many intermediates/starting materials was therefore also examined in detail. Bromination of the acid starting material 2,5-dimethoxyphenylacetic acid (2,5-PAA) was found to be clean and high yielding. This was in stark contrast to the bromination of the benzaldehyde starting material, the ketone precursor 2,5-P2P and the dibenzylketone-based impurity. Numerous brominated products were isolated from each of these reactions, many of which were novel compounds, and previously unreported as impurities in the literature. The unpredictable/nondescript nature of these brominations is likely to have a significant impact on the impurity profile of illicitly produced DOB.

Declaration

I hereby declare that the submitted work for the thesis entitled “Impurity Profiling and Synthesis of Precursors to the Hallucinogenic Amphetamine DOB” is entirely my own. Any reference made to the works of others is clearly cited, the details of which can be found in the bibliography at the end of this thesis. The work contained within this thesis has not been presented at this, or any other university, as part of another degree.

Signature:_____

Jonathan Quille

Date:_____

Acknowledgements

I would like to sincerely thank my supervisors Dr J.J. Keating and Dr Dara Fitzpatrick for their support and guidance throughout my PhD. Their open door policy and willingness to help made it much easier to iron out any issues I had in relation to my research.

I would like to thank my fellow research group member Richard O'Connor for his support also. Richard acted as a mentor to me in the first few months of my PhD (and beyond!) and was always willing to offer advice and support in whatever way he could. Richard is a fantastic source of organic chemistry knowledge and really helped me to find my feet in the lab.

I would like to acknowledge the moral support of my other lab mates also – Roisín, Mike, Kate and Fiona. Thank you for all of your help and for providing great banter in the lab.

I would like to thank Dr Amy Nagle and Dr Elaine Stack in the analytical division for their support and for keeping me entertained during lunch/tea breaks.

I would like to acknowledge the support of the various students and academic/technical staff in the Chemistry department, in particular Dr Lorraine Bateman and Dr Dan McCarthy in providing NMR support, and Dr Simon Lawrence and Dr Kevin Eccles involved in providing crystallography support.

I would like to acknowledge the financial support for my research provided by the Irish Research Council (IRC) and the Irish Separation Science Cluster (ISSC).

Finally, I would like to thank my close friends and family for their emotional support throughout the last few years. To my parents Ellen and Donncha, who to this day, still do not fully understand what I have been doing for the last few years, I would like to say a huge thanks. To my sisters Mary-Ellen and Laura and my brother Jason I would also like to say thanks. To my friend Darren, a fellow eternal student, I would like to say thanks for offering your support, and understanding exactly what I'm going through. Lastly, I would like to thank my girlfriend Lisa. You have been my rock. Thank you for putting up with me and for understanding that when I say I will be done in the lab in 20 minutes, this may in reality be anything between 20 and 200!

Table of Contents

ABSTRACT ..... **I**

DECLARATION ..... **III**

ACKNOWLEDGEMENTS ..... **V**

TABLE OF CONTENTS ..... **VII**

TABLE OF FIGURES ..... **XIII**

TABLE OF TABLES ..... **XXI**

ABBREVIATIONS ..... **XXIV**

CHAPTER 1 – INTRODUCTION **1**

1.1 Drugs of abuse and their classification **1**

1.2 ATS **4**

1.2.1 History of Amphetamine and ATS 4

1.2.2 The amphetamine family 7

1.2.2.1 Phenethylamines *9*

1.2.2.2 Amphetamines *10*

1.2.2.3 N-substituted phenethylamines/amphetamines *11*

1.2.3 Structure-activity relationships 12

1.2.4 Pharmacology 18

1.2.5 The use and domestic/worldwide seizures of ATS 23

1.2.6 Control and Legislation of ATS 29

1.2.6.1 US Legislation *33*

1.2.6.2 UK Legislation *33*

1.2.6.3 Irish Legislation *34*

1.2.7 DOB and the '2,5-dimethoxy' class of amphetamines 37

1.3 Impurity profiling **42**

1.3.1 Impurity profiling *via* the direct analysis of a street sample of an illicit drug 44

1.3.2. Impurity profiling *via* the controlled synthesis and identification of impurities produced 45

1.3.3 Impurity profiling – Case studies 48

1.3.3.1 Impurity profiling of 4-MTA (30) *48*

1.3.3.2 Impurity profiling of MDMA (17) *50*

1.4 Clandestine laboratories and ATS manufacture **51**

1.5 Synthesis of ATS 54

1.5.1 Amphetamine synthesis 54

1.5.1.1 Synthesis via phenyl-2-propanone (P2P) 55

1.5.1.2 Syntheses not involving P2P 64

1.5.2 Synthesis of methamphetamine (14) and MDMA (17) 66

1.5.3 Synthesis of DOB and other 'D series' amphetamines 68

1.6 Clandestine manufacture of ATS – 'A cat and mouse game' 70

1.6.1 2-Methyl glycidic esters 71

1.6.2 APAAN 73

1.6.3 Esters of phenylacetic acid 75

1.6.4 P2P bisulfite adduct 77

1.7 Emerging drugs 78

1.7.1 Synthetic cannabinoids 81

1.7.2 Synthetic cathinones 82

1.7.3 Phenethylamines 83

1.7.4 Piperazines 85

1.7.5 Ketamine 86

1.7.6 Plant based substances 87

1.7.6.1 Khat 87

1.7.6.2 Kratom 87

1.7.6.3 Salvia divinorum 88

1.7.7 Miscellaneous substances 89

1.7.7.1 Aminoindanes 89

1.7.7.2 Phenylcyclidine-type substances 89

1.7.7.3 Tryptamines 90

1.8 Research outline 93

CHAPTER 2 – IMPURITY PROFILING OF THE BROMINATION OF 2,5-DIMETHOXYBENZALDEHYDE 97

2.1 Introduction 97

2.1.1 Bromination of 2,5-dimethoxybenzaldehyde (72) in the literature 98

2.2 In-house bromination of 2,5-dimethoxybenzaldehyde (72) 101

2.2.1 Detection of minor impurities of the bromination of 2,5-dimethoxybenzaldehyde (72) 104
2.2.2 Attempted isolation and identification of detected impurities using ^{1}H-NMR and LC-MS 106

2.3 Definitive structure assignment of detected impurities and the need for reference standards 111
2.3.1 Selective synthesis of 6-bromo-2,5-dimethoxybenzaldehyde (165) 113
2.3.2 Selective synthesis of 3-bromo-2,5-dimethoxybenzaldehyde (169) 122
2.3.3 Differentiation of regioisomeric products of the bromination of 2,5-dimethoxybenzaldehyde (72) by LC-MS/MS 124
2.3.4 Selective synthesis of 3,6-dibromo-2,5-dimethoxybenzene (168) 126
2.3.5 Selective synthesis of 4,6-dibromo-2,5-dimethoxybenzaldehyde (170) 128
2.3.6 Selective synthesis of 4,6-dibromo-5-hydroxy-2-methoxybenzaldehyde (167) 134

2.4 Summary 138

CHAPTER 3 – SYNTHESIS AND IMPURITY PROFILING OF 2,5-DIMETHOXYPHENYL-2-PROPANONE AND ITS 4-BROMO COUNTERPART 143

3.1 The phenylacetic acid (PAA) reaction 143
3.1.1 The PAA route to ketone precursors of ATS 147
3.1.2 Impurity profiling of the PAA reaction 148

3.2 The PAA route to 2,5-P2P (92) 154
3.2.1 Impurities of the PAA route to 2,5-P2P (92) 155
3.2.1.1 Aldehyde impurity (72) 155
3.2.1.2 Monomeric enol acetates (E/Z)-(219) 156
3.2.1.3 Dimeric enol acetate (220) 160
3.2.1.4 Dibenzylketone (221) 162
3.2.2 Investigation into the effects of varying the number of equivalents of Ac_2O, on the yields of 2,5-P2P (92) and dibenzylketone (221) 163

3.3 The PAA route to 4-Br-2,5-P2P (159) 166
3.3.1 Preparation of 4-bromo-2,5-dimethoxyphenylacetic acid (164) 167
3.3.2 PAA route to 4-Br-2,5-P2P (159) using 4-Br-2,5-PAA (164) 168
3.3.3 Impurities of the PAA route to 4-Br-2,5-P2P (159) 168
3.3.3.1 4-Bromo aldehyde impurity (160) 169

3.3.3.2 4-Bromo-monomeric enol acetates (223) *170*
3.3.3.3 Dibromo-dimeric enol acetate (222) *171*
3.3.3.4 Dibromo-dibenzylketone (224) *172*
3.3.4 Investigation into the effects of varying the number of equivalents of Ac_2O, on the yields of 4-Br-2,5-P2P (159) and dibenzylketone (224) 173

3.4 The Darzens reaction 175
3.4.1 Stereochemical outcome and assignment of *cis*/*trans* 176
3.4.2 Subsequent reactions of glycidic esters 178
3.4.3 Synthesis of ATS precursors *via* Darzens condensation 179

3.5 Darzens route to 2,5-P2P (92) and 4-Br-2,5-P2P (159) 180
3.5.1 Barium's synthetic methodology and optimisation of reaction conditions 181
3.5.2 Comparison of optimised 'Barium' method *vs.* 'Et_2O' method and characterisation of recovered glycidic esters 185
3.5.2.1 Methyl 2-methyl-3-(2,5-dimethoxyphenyl)glycidate (161) *185*
3.5.2.2 Ethyl 2-methyl-3-(2,5-dimethoxyphenyl)glycidate (239) *189*
3.5.5.3 Methyl 2-methyl-3-(4-bromo-2,5-dimethoxyphenyl)glycidate (162) *191*
3.5.5.4 Ethyl 2-methyl-3-(4-bromo-2,5-dimethoxyphenyl)glycidate (240) *193*
3.5.3 Saponification, acidification and decarboxylation of glycidic esters to produce 2,5-P2P (92) and 4-Br-2,5-P2P (159) 194

3.6 Nitrostyrene route to 2,5-P2P (92) 198

3.7 Degradation of 2,5-P2P (92) 199

3.8 Summary 207

CHAPTER 4 – IMPURITY PROFILING OF THE BROMINATION OF 2,5-DIMETHOXYPHENYL-2-PROPANONE AND ITS DIMERIC ANALOGUE 1,3-BIS(2,5-DIMETHOXYPHENYL)-2-PROPANONE 209

4.1 Illicit synthesis of DOB 209
4.1.1 Synthesis of 4-Br-2,5-P2P (159) 210

4.2 Impurity profiling of the bromination of 2,5-P2P (92) 212
4.2.1 Terminal α-keto-bromo compounds (252) and (253) 212
4.2.2 Benzyl-bromo compounds (250) and (251) 214
4.2.3 Bromination of 2,5-P2P (92) using excess Br_2 218

4.3 Impurity profiling of the bromination of 1,3-bis(2,5-dimethoxyphenyl)-2-propanone (221) 219

4.3.1 Independent synthesis of a series of aromatic ring–brominated dibenzylketones 220

4.3.1.1 Aldehyde bromination 224

4.3.1.2 Formation of monomeric nitrostyrenes 224

4.3.1.3 Formation of monomeric nitroalkanes 226

4.3.1.4 Preparation of dimeric nitrostyrenes 233

4.3.1.5 Anticancer activity of nitrostyrenes 242

4.3.1.6 Preparation of dibenzylketones 244

4.3.2 Confirmation of the presence of several aromatic ring–brominated dibenzylketones, as impurities of the bromination of 1,3-bis(2,5-dimethoxyphenyl)-2-propanone (221) 252

4.3.3 Attempted synthesis and identification of suspected benzyl-bromo products 254

4.4 Impurity profiling of the Leuckart reaction of dibenzylketones (221) and (224) with formamide 257

4.4.1 Step 1: The 'Leuckart-Wallach reaction' 259

4.4.2 Step 2: Hydrolysis of *N*-formyl intermediates to produce dimeric amines 269

4.5 Summary 271

CHAPTER 5 – EXPERIMENTAL 275

5.1 General procedures 275

5.2 Experimental details pertaining to work outlined in Chapter 2 279

5.2.1 Impurity profiling of the bromination of 2,5-dimethoxybenzaldehyde (72) 279

5.2.2 Selective synthesis of 6-bromo-2,5-dimethoxybenzaldehyde (165) 281

5.2.3 Preparation of 3-bromo-2,5-dimethoxybenzaldehyde (169) 283

5.2.4 Preparation of 3,6-dibromo-2,5-dimethoxybenzene (168) 285

5.2.5 Attempted synthesis of 4,6-dibromo-2,5-dimethoxybenzaldehyde (170) *via* 6-bromo aldehyde (165) 285

5.2.6 Attempted synthesis of 4,6-dibromo-2,5-dimethoxybenzaldehyde (170) *via* 4-bromo aldoxime (182) 286

5.2.7 Selective synthesis of 4,6-dibromo-2,5-dimethoxybenzaldehyde (170) *via* 6-bromo aldoxime (181) 287

5.2.8 Selective synthesis of 4,6-dibromo-5-hydroxy-2-methoxybenzaldehyde (167) 288

5.3 Experimental details pertaining to work outlined in Chapter 3 289

5.3.1 Preparation and impurity profiling of 2,5-dimethoxyphenyl-2-propanone (92) *via* the 'PAA route' 289

5.3.2 Preparation of 4-bromo-2,5-dimethoxyphenylacetic acid (164) 291

5.3.3 Preparation and impurity profiling of 4-bromo-2,5-dimethoxyphenyl-2-propanone (159) *via* the 'PAA route' 292

5.3.4 Preparation and impurity profiling of 2,5-dimethoxyphenyl-2-propanone (92) *via* the 'Darzens reaction' 294

5.3.5 Preparation and impurity profiling of 4-bromo-2,5-dimethoxyphenyl-2-propanone (159) *via* the 'Darzens reaction' 297

5.3.6 Preparation of 2,5-P2P (92) *via* the 'nitrostyrene route' 300

5.4 Experimental details pertaining to work outlined in Chapter 4 301

5.4.1 Impurity profiling of the bromination of 2,5-dimethoxyphenyl-2-propanone (92)..... 301

5.4.2 Preparation of 1-bromo-1-(2,5-dimethoxyphenyl)-2-propanone (250) 303

5.4.3 Preparation of 1-bromo-1-(4-bromo-2,5-dimethoxyphenyl)-2-propanone (251)..... 304

5.4.4 Preparation of monomeric nitrostyrenes (280), (281) and (282) 304

5.4.5 Preparation of monomeric nitroalkanes (283), (284) and (285)..... 306

5.4.6 Preparation of dimeric nitrostyrenes (290)–(298) 308

5.4.7 Preparation of dibenzylketones (221), (224) and (257)–(260) *via* dimeric nitrostyrenes (290)–(298) 314

5.4.8 Impurity profiling of the bromination of 1,3-bis-(2,5-dimethoxyphenyl)-2-propanone (221) 317

5.4.9 Attempted selective synthesis of benzyl-bromo dibenzylketones 317

5.4.10 Impurity profiling of the Leuckart reaction of 1,3-bis(2,5-dimethoxyphenyl)-2-propanone (221) and formamide..... 318

5.4.11 Impurity profiling of the Leuckart reaction of 1,3-bis(4-bromo-2,5-dimethoxyphenyl)-2-propanone (224) and formamide..... 320

5.5 Appendix 323

OVERALL SUMMARY AND FUTURE WORK 327

DISSEMINATION OF RESEARCH FINDINGS 330

REFERENCES 333

Table of Figures

Figure 1.1: Classification of “designer drugs” based on general chemical structure....3
Figure 1.2: Amphetamine (10) and Benzedrine® inhaler....5
Figure 1.3: Comparison of hallucinogenic activity between methoxy substituted ATS ((35) and (20)) and their ring-locked counterparts ((52) and (53)) 14
Figure 1.4: Hallucinogenic amphetamine interacting with the ligand binding domain of human 5-HT_{2A} receptor 15
Figure 1.5: Various sites whereby the phenethylamine/amphetamine backbone can be modified/substituted.... 15
Figure 1.6: Structural features of stimulants, hallucinogens and entactogens 17
Figure 1.7: Mechanism of action of stimulant ATS on synaptic terminal of dopamine neurons.... 20
Figure 1.8: General structure of 5-HT receptor 21
Figure 1.9: Global seizures of ATS, 2002-2011.... 23
Figure 1.10: Countries reporting the highest amphetamine (10) seizures, 2010-2011.... 24
Figure 1.11: ETS seizures in selected countries, 2007-2011 25
Figure 1.12: Use of ATS (excluding ETS) in 2011 25
Figure 1.13: Lifetime use of 'legal substances' in EU among persons aged 15–24, 2011.... 28
Figure 1.14: National drug policy documents adopted in Europe from 2009 31
Figure 1.15: Irish National drug policy developments *vs*. international and EU developments.... 36
Figure 1.16: Proposed scheme for the metabolism of DOB in rats.... 39
Figures 1.17: Powdered DOB (left) and DOB impregnated onto blotter paper (right).... 39
Figure 1.18: Headline from Cork newspaper ‘Evening Echo’ amid public warnings about DOB 40
Figure 1.19: Synthetic methodology used to manufacture DOB in a clandestine laboratory detected in Australia, 1980.... 41
Figure 1.20: Hyphenated analytical technologies.... 44
Figure 1.21: Chemical structures of impurities found in 4-MTA (30) synthesised by the Leuckart route 48
Figure 1.22: TIC chromatogram (‘impurity profile’) of crude 4-MTA (30).... 49
Figure 1.23: Impurity profiling of MDMA.... 50
Figure 1.24: Small scale ‘kitchen’ clandestine laboratory.... 51
Figure 1.25: Custom-made reaction vessel (900 litres) 52
Figure 1.26: Large scale MDMA laboratory detected in the Netherlands in October 2013 52
Figure 1.27: Dectections of illicit ATS laboratories in Europe, 2001-2009.... 53
Figure 1.28: Synthesis of amphetamine *via* P2P *vs*. all other routes.... 55
Figure 1.29: Individual seizures of P2P (in litres) in Europe, 2009.... 56
Figure 1.30: General outline of amphetamine synthesis *via* P2P intermediate 57

Figure 1.31: Common routes to the amphetamine precursor P2P (65) 58
Figure 1.32: P2P from benzyl cyanide starting material (79) 59
Figure 1.33: Naphthalene impurities arising from the hydrolysis of 4-Me-APAAN (83) 60
Figure 1.34: Nitrostyrene route to P2P (65) 61
Figure 1.35: Benzaldoxime (90) and nitrile (91) impurities arising from the Henry-Knoevengel condensation of benzaldehyde (72) and nitroethane 61
Figure 1.36: Oxime impurity from the iron reduction of nitrostyrene (73) 62
Figure 1.37: Common routes to amphetamine (10) from P2P (65) 62
Figure 1.38: Leuckart route to amphetamine 63
Figure 1.39: Reductive amination of P2P (65) 63
Figure 1.40: Oxime route to amphetamine 63
Figure 1.41: Nitrostyrene route to amphetamine 64
Figure 1.42: Amphetamine from allylbenzene (96) 64
Figure 1.43: Routes commonly used in methamphetamine synthesis from ephedrine/pseudoephedrine, adapted to amphetamine synthesis from phenylpropanolamine (95) 65
Figure 1.44: Synthetic routes to methamphetamine 66
Figure 1.45: Synthetic routes to MDMA used in illicit manufacture 68
Figure 1.46: Seized material containing PMK glycidate (MMDMG) (113) 72
Figure 1.47: P2P from a benzyl cyanide starting material *via* APAAN 73
Figure 1.48: Amount (kg) of material encountered as well as the number of incidents involving APAAN, communicated *via* PICS by quarter, 2012–2013 74
Figure 1.49: Proposed origin of the *N*-methyl-2-phenylacetamide impurity (120) in illicitly manufactured methamphetamine 76
Figure 1.50: Masking and unmasking of P2P as its bisulfite adduct (121) 77
Figure 1.51: P2P bisulfite adduct (121) discovered in a drug production facility in the Netherlands in 2008 77
Figure 1.52: Flexibility in ATS manufacture *via* use of alternative/masked precursors 78
Figure 1.53: Number of NPS (cumulative) reported at the global level, 2009 to 2013 79
Figure 1.54: Global emergence of NPS by group, prior to 2008 and from 2008–2012 80
Figure 1.55: Classification of phenethylamines 83
Figure 1.56: Synthesis of *N*-benzyl substituted phenethylamines 85
Figure 1.57: Classification of tryptamines 91
Figure 1.58: Worldwide examples of legal responses to NPS 92
Figure 1.59: Synthetic routes to 2,5-P2P (92) and 4-Br-2,5-P2P (159) 94

Figure 1.60: Starting materials/intermediates that may be subjected to bromination during synthesis of DOB 95
Figure 2.1: Formation of 4-bromo (160) and 6-bromo (165) aldehydes 100
Figure 2.2: Different pathways of electron flow from the 2-methoxy group into the aromatic ring ... 101
Figure 2.3: Aromatic regions of ^{1}H-NMR spectra of 4-bromo (160) (left) and 6-bromo (165) (right) aldehydes 104
Figure 2.4: Region of δ 10.27–10.46 ppm of ^{1}H-NMR spectrum of the crude product and that of the first recovered fraction following flash column chromatography 105
Figure 2.5: HPLC chromatogram of crude reaction from the bromination of 2,5-dimethoxybenzaldehyde (72) 105
Figure 2.6: Tentative structures assigned to impurities recovered in fractions 1 and 2 106
Figure 2.7: Individual HPLC runs (DAD signal @ 210 nm) of the SM (72), and the 4-bromo (160) and 6-bromo (165) regioisomers 107
Figure 2.8: Individual HPLC runs (DAD signal @ 210 nm) of the proposed impurities, two isolated (167) and (168), and two present as a mixture (169) and (170) 108
Figure 2.9: Overlays of TIC signals (ESI+) for SM (72), expected products (160) and (165), and selected impurities (167), (169) and (170) 109
Figure 2.10: Extracted MS spectra from TIC signals obtained in Figure 2.9 109
Figure 2.11: Extracted mass spectra for compound (167) in both positive and negative mode 111
Figure 2.12: 'Takao' synthesis of 6-bromo-2,5-dimethoxybenzaldehyde 113
Figure 2.13: 'Sato' synthesis of 6-bromo-2,5-dimethoxybenzaldehyde 113
Figure 2.14: Dubost's approach to the *ortho*-bromination of benzaldehydes 114
Figure 2.15: Mechanistic proposal for *ortho*-bromination 115
Figure 2.16: Aromatic region (δ 6.76–7.38) of ^{1}H-NMR spectrum of benzaldoxime (180) 116
Figure 2.17: ^{1}H-NMR spectrum of (*Z*)-(181) (@ 400 MHz) 119
Figure 2.18: ^{1}H-NMR spectrum of (*E*)-(181) (@ 400 MHz) 120
Figure 2.19: Comparison of the yields of 6-bromo-2,5-diethoxybenzaldehyde (183) obtained using 'standard' bromination and Dubost's methodology 122
Figure 2.20: Literature procedure for the preparation of 3-bromo-2,5-dimethoxybenzaldehyde (169) 123
Figure 2.21: Three regioisomeric compounds produced during the bromination (Br_2/AcOH) of (72) . 124
Figure 2.22: Targeted MS/MS spectra (ESI+) (@ *m/z* 246.98) of 4-bromo (160), 6-bromo (165) and 3-bromo (169) compounds 125
Figure 2.23: Ions produced from the fragmentation of compounds of general structure (189) 126
Figure 2.24: Literature procedure for the preparation of 3,6-dibromo-2,5-dimethoxybenzene (168) 127

Figure 2.25: Proposed synthesis of 4,6-dibromo aldehyde (170) *via* the attempted bromination of 6-bromo aldehyde (165) 129
Figure 2.26: Proposed synthesis of 4,6-dibromo aldehyde (170) *via* 4-bromo aldoxime (182)..... 129
Figure 2.27: Proposed synthesis of 4,6-dibromo aldehyde (170) *via* 6-bromo aldoxime (181)..... 131
Figure 2.28: ^{1}H-NMR spectra of (*E*)-(191) (top) and (*Z*)-(191) (bottom) (@ 400 MHz) 132
Figure 2.29: Attempts to synthesise 4,6-dibromo-2,5-dimethxoybenzaldehyde (170) 134
Figure 2.30: Literature bromination of phenol (192) 134
Figure 2.31: Preparation of phenol (167) 136
Figure 2.32: Distinguishable analytical/spectroscopic features of detected impurities (169), (170), (168) and (167) 138
Figure 2.33: Individual HPLC runs (DAD signal @ 210 nm) of the four selectively synthesised standards (169), (170), (167) and (168) 139
Figure 2.34: Overlays of impurity and standard chromatograms from Figures 2.8 and 2.33 139
Figure 2.35: Chromatogram overlays of all compounds – SM (72), expected products (160) and (165) and impurities (169), (170), (167) and (168) encountered during the bromination of 2,5-dimethoxybenzaldehyde (72) 140
Figure 3.1: Dakin-West reaction of PAA and Ac_2O 145
Figure 3.2: Cyclic mechanistic proposal for the formation of ketone (P2P)..... 145
Figure 3.3: Scheme outlining formation of ketone (65) *via* 'nucleophilic catalysis'..... 146
Figure 3.4: Recent examples of the use of the PAA route to P2P (65)..... 147
Figure 3.5: Compounds recovered from impure amphetamine associated with the PAA route..... 149
Figure 3.6: Different reaction pathways for formation of P2P (65) and dibenzylketone (80) 151
Figure 3.7: Cyclic mechanistic proposal for formation of P2P (65) and dibenzylketone (80) 152
Figure 3.8: Proposed scheme for formation of enol acetate by-products..... 152
Figure 3.9: Synthesis of 2,5-P2P (92) from 2,5-PAA (108) *via* the PAA route 154
Figure 3.10: Structures and isolated yields of impurities recovered from the synthesis of 2,5-P2P (92) *via* the PAA reaction..... 155
Figure 3.11: ^{1}H-NMR spectrum of mixture of (*E*)-(219) and (*Z*)-(219) enol acetates (@ 400 MHz)..... 157
Figure 3.12: Magnified section of NOESY spectrum obtained for mixture of (*E*)- and (*Z*)-enol acetates of 2,5-P2P 158
Figure 3.13: Differences in chemical shift values that may be used to tentatively assign (*E*)- or (*Z*)-conformation to enol acetate (219)..... 160
Figure 3.14: Chart comparing isolated yields of monomeric (92) and dimeric (221) ketones, obtained when the number of eqv. of Ac_2O is varied during the PAA reaction 165
Figure 3.15: Synthesis of DOB precursor (159), whereby bromination takes place prior to PAA reaction 166

Figure 3.16: Structures and isolated yields of impurities recovered from the synthesis of 4-Br-2,5-P2P (159) *via* the PAA reaction 169
Figure 3.17: ^{1}H-NMR spectrum of (*Z*)-4-bromo enol acetate (223) (@ 400 MHz) 170
Figure 3.18: Chart comparing isolated yields of monomeric (159) and dimeric (224) ketones, obtained when the number of eqv. of Ac_2O is varied during the PAA reaction 174
Figure 3.19: Mechanism of formation of glycidic esters 175
Figure 3.20: Assignment of *cis* and *trans* isomers of the MDMA pre-precursor 'MMDMG' (113) 178
Figure 3.21: Proposed heat induced decarboxylation of a glycidic acid 179
Figure 3.22: One-pot alkyl elimination/decarboxylation of ethyl 3-phenyl glycidate (236) 179
Figure 3.23: Synthesis of 2,5-P2P (92) as outlined by Barium 180
Figure 3.24: Barium's methodology applied to the synthesis of 2,5-P2P (92) *via* ethyl glycidate (239) 182
Figure 3.25: Synthesis of 4-Br-2,5-P2P (159) *via* a methyl/ethyl glycidate intermediate 183
Figure 3.26: Modified procedure for the preparation of 2,5-dimethoxy glycidic esters 185
Figure 3.27: Assigning geometry of *cis*/*trans* isomers of methyl glycidate (161), based on differences in δ values of particular signals 187
Figure 3.28: ^{1}H-NMR spectra of both *cis*-(161) (top spectrum) and *trans*-(161) (bottom spectrum) methyl glycidates 188
Figure 3.29: A 'quartet of doublets' observed in the ^{1}H-NMR spectrum of *trans* ethyl glycidate (239), corresponding to the CH_2 protons of the ester group 190
Figure 3.30: The AB part of an ABX_3 type spectrum of 2-ethoxycylohexenone 191
Figure 3.31: Comparison of selected ^{1}H-NMR signals between 4-bromo-*trans*-methyl (162) and 4-bromo-*trans*-ethyl (240), for assigning geometry of (240) 194
Figure 3.32: Yields of glycidic acids (241) and (242) from glycidic esters (161), (239), (162) and (240) 195
Figure 3.33: Characteristic ^{1}H-NMR/^{13}C-NMR signals of glycidic acids (241) and (242) 195
Figure 3.34: Optimised method for the preparation of ketone precursors (92) and (159) *via* 2-methyl glycidate intermediates 197
Figure 3.35: Nitrostyrene route to 2,5-P2P (92) 198
Figure 3.36: Benzaldoxime (90) and benzonitrile (91) impurities isolated by Griffin, during the nitrostyrene route to 2,5-P2P (92) 199
Figure 3.37: Highest yields obtained for the 'Darzens', 'Nitrostyrene' and 'PAA' routes to 2,5-P2P (92) 199
Figure 3.38: HPLC chromatograms (@ 254 nm) of (A) pure aldehyde (72) and (B) "pure" ketone sample isolated previously by Griffin 200

Figure 3.39: Overlays of HPLC runs (@210 nm) of pure aldehyde (72), pure ('fresh') ketone (92) and an aged sample (≈2.5 years) of ketone (92) synthesised *via* the 'Nitrostyrene route' 201
Figure 3.40: ^{1}H-NMR spectra of 'fresh' ketone (92) (top) and 'aged' ketone (92) (bottom) 202
Figure 3.41: Plot of ratio of aldehyde (72) : ketone (92) over time 203
Figure 3.42: Plot of ratio of aldehyde (72) : ketone (92) over time, for ketone synthesised *via* the 'PAA', 'Darzens' and 'Nitrostyrene' routes 204
Figure 3.43: Photolysis of dibenzylketone (80) 205
Figure 3.44: Plausible route for formation of benzaldehyde (72) following photolysis of 2,5-P2P (92) 206
Figure 4.1: Shulgin's DOB synthesis 210
Figure 4.2: Synthetic strategies, based on PAA route, to DOB precursor (159) 211
Figure 4.3: Compounds identified following bromination of 2,5-P2P (92) 212
Figure 4.4: Proposed scheme for selective benzylic bromination of ketones (92) and (159) 215
Figure 4.5: Selective benzylic bromination of 2,5-P2P (92) and 4-Br-2,5-P2P (159) 216
Figure 4.6: Protons that may resonate in the region of δ 6–6.5 ppm, owing to compounds formed during the bromination (@ 2.2 eqv. Br_2) of 2,5-P2P (92) 218
Figure 4.7: Aromatic ring-brominated dibenzylketones chosen for independent synthesis 220
Figure 4.8: Synthesis of a symmetric dibenzylketone *via* phase-transfer catalysis 221
Figure 4.9: Synthesis of an asymmetric dibenzylketone *via* a dibenzyl cadmium reagent 221
Figure 4.10: General synthesis of substituted dibenzylketones *via* the Henry-Knoevenagel condensation methodology 222
Figure 4.11: Proposed synthetic route to selected dibenzylketones ((221), (224) and (257)–(260)) ... 223
Figure 4.12: 'Henry-Knoevenagel condensation' 224
Figure 4.13: Synthesis of monomeric nitrostyrenes 225
Figure 4.14: Distinguishing *cis* and *trans* isomers using *J* values in ^{1}H-NMR spectroscopy 226
Figure 4.15: Procedures attempted for the preparation of monomeric nitroalkanes 226
Figure 4.16: ^{1}H-NMR spectrum of dinitro-dimeric impurity (286), containing expanded regions of interest (@ 400 MHz) 227
Figure 4.17: Assignment of individual ^{1}H-NMR/^{13}C-NMR signals of the bridging chain positions of (286) 229
Figure 4.18: Mechanism of formation of desired nitroalkane (268) and dinitro dimer (288) 230
Figure 4.19: Comparison of 'triplet' signals corresponding to CH_2 protons α- to nitro group, for non-bromo (283), 4-bromo (284) and 6-bromo (285) nitroalkanes 232
Figure 4.20: Coupling of aldehydes and nitroalkanes *via* Henry-Knoevenagel condensation 233
Figure 4.21: Reduction of two different dimeric nitrostyrenes, yielding dibenzylketone (257) 236
Figure 4.22: Effect of chain length on the geometric conformation of methylenedioxy-nitrostyrene product formed 237

Figure 4.23: Effect of chain length on the geometric conformation of 4-methylthio-nitrostyrene product formed 238
Figure 4.24: Difference in the ^{1}H-NMR δ values of the vinyl proton, between the (*E*)- and (*Z*)-isomers of methylthio-substituted nitrostyrene (301) 239
Figure 4.25: Through-space interactions observed in the NOESY spectra of (*E*)-(301) and (*Z*)-(301) nitrostyrenes..... 239
Figure 4.26: Proposed orientations of (*E*)- and (*Z*)-isomers, giving rise to the allylic splitting (only observed in (*Z*)-isomer) 240
Figure 4.27: Interaction between vinyl and allylic protons on (*Z*)-nitrostyrene (298)..... 241
Figure 4.28: Single crystal analysis of (*E*)- and (*Z*)-isomers of dimeric nitrostyrene (294)..... 242
Figure 4.29: Examples of α-aryl analogues of MDMA that reduce viability of a Burkitt's lymphoma cell line (L3055) 243
Figure 4.30: Preparation of dibenzylketones *via* the iron reduction of dimeric nitrostyrenes 245
Figure 4.31: HRMS evidence for the presence of oxime intermediate (306) during the preparation of dibenzylketone (260) 245
Figure 4.32: Proposed formation of oxime intermediate (306)..... 246
Figure 4.33: Methodology used previously within the research group, to selectively prepare oxime-type impurities..... 246
Figure 4.34: Individual HPLC runs (@ 210 nm) of all six prepared dibenzylketones 247
Figure 4.35: Collision-induced dissociation (CID) of regioisomeric dibenzylketone pairs, (257) and (258) (monobromo), and (224) and (260) (dibromo) 248
Figure 4.36: Proposed fragmentation pattern of dibenzylketone (258), giving rise to the most abundant fragment/daughter ions observed in Figure 4.35..... 249
Figure 4.37: HPLC chromatograms (@ 210 nm) of attempted separation of six dibenzylketones using Agilent Zorbax SB-C18, 3.5 µm, 2.1×30 mm column 250
Figure 4.38: HPLC chromatograms (@ 210 nm) of attempted separation of six dibenzylketones using Agilent Zorbax Eclipse XDB-C18, 1.8 µm, 4.6×50 mm column 251
Figure 4.39: Optimised HPLC separation of six novel dibenzylketones 251
Figure 4.40: Aromatic regions of ^{1}H-NMR spectra of crude bromination experiments, showing tentative evidence for the presence of dibenzylketones (221), (257) and (224) 252
Figure 4.41: Stacked HPLC chromatograms (@ 210 nm) of crude samples from bromination experiments of (221) (in 0.5–2.0 eqv. of Br_2). Previously prepared dibenzylketones (221), (257) and (224) are outlined in boxed regions 253
Figure 4.42: 'Selective' benzylic bromination of dibenzylketones (221), (257) and (224)..... 254
Figure 4.43: The δ 5.93–6.29 ppm region of the ^{1}H-NMR spectrum of the crude product of the bromination (2 eqv. of Br_2) of dibenzylketone (221)..... 256

Figure 4.44: Impurities arising from the Leuckart reaction of 2,5-P2P (92) with formamide 257
Figure 4.45: Leuckart route to dimeric amines (327) and (328) from dibenzylketones (221) and (224) 259
Figure 4.46: Basis for the observation of two sets on signals ('rotamers') in the ^{1}H-NMR/^{13}C-NMR spectra of some *N*-formyl compounds 260
Figure 4.47: ^{1}H-NMR spectra of non-bromo (329) (top) and dibromo (330) (bottom) *N*-formyl intermediates (@ 600 MHz) 263
Figure 4.48: Mechanism for the formation of pyrimidines (331) and (332) 265
Figure 4.49: ^{1}H-NMR spectrum of pyrimidine (331) highlighting four different groups of signals 266
Figure 4.50: Conditions whereby the intensity of a 'quaternary' carbon signal may become diminished in a ^{13}C-NMR spectrum 268
Figure 4.51: Comparison of the regioselectivity of bromine substitution, following bromination (Br_2/AcOH) of compounds (108) and (92) 271
Figure 4.52: Pyrimidine (331), a secondary impurity of DMA (31), synthesised *via* the PAA and Leuckart routes 273
Figure 5.1: 'Agilent LC-MS system', Chemistry Department, University College Cork 276
Figure 5.2: Comparison of IUPAC and customised compound naming systems 278

Table of Tables

Table 1.1: Psychoactive phenethylamine analogues 9

Table 1.2: Psychoactive amphetamine analogues 10

Table 1.3: Psychoactive *N*-substituted phenethylamine/amphetamine analogues 11

Table 1.4: Number of cases and seizures of ATS in Ireland, 2003-2012 26

Table 1.5: ATS named in Schedule I and II of UN Convention on Psychotropic Substances, 1971 32

Table 1.6: Examples of 'D series' amphetamines 37

Table 1.7: 'Characteristic' impurities from various synthetic routes to several ATS 46

Table 1.8: Table of impurities identified in 4-MTA (30) 49

Table 1.9: Number of P2P laboratories seized in the US prior to and following its control 56

Table 2.1: Bromination of 2,5-dimethoxybenzaldehyde as reported in the literature 99

Table 2.2: Reaction of aldehyde (72) with varying reaction times and equivalents of Br_2 102

Table 2.3: Yield, R_f, m.p., IR and HRMS data for 4-bromo (160) and 6-bromo (165) products 103

Table 2.4: Yield, R_f, IR and HRMS data for benzaldoxime (180) 116

Table 2.5: Yield, R_f, m.p., IR and HRMS data for 4-bromo benzaldoxime (182) 118

Table 2.6: R_f, m.p., IR and HRMS data for isomeric benzaldoximes (*E*)-(181) and (*Z*)-(181) 121

Table 2.7: Yield, R_f, m.p., IR and HRMS data for 3-bromo phenol (188) 123

Table 2.8: Yield, R_f, m.p., IR and HRMS data for 3-bromo aldehyde (169) 124

Table 2.9: R_f, m.p., IR and elemental analysis data for 3,6-dibromo compound (168), isolated previously as a product of the bromination of 2,5-dimethoxybenzaldehyde (72) 127

Table 2.10: R_f, m.p., IR and HRMS data for isomeric dibromo benzaldoximes (*E*)-(191) and (*Z*)-(191) 131

Table 2.11: Yield, R_f, m.p., IR and HRMS data for 4,6-dibromo aldehyde (170) 133

Table 2.12: Selective demethylation of a number of 2,5-dimethoxybenzaldehydes 135

Table 2.13: R_f, m.p., IR and HRMS data for dibromo phenol (167) 136

Table 2.14: Identity of each signal in Figure 2.34 140

Table 3.1: Reaction by-products from PAA reaction identified by Allen, Krawczyk and Forbes 149

Table 3.2: Yield, R_f, IR and HRMS data for ketone (92) 154

Table 3.3: Yield, R_f, IR and HRMS data for the mixture of enol acetates (*E*/*Z*)-(219) 156

Table 3.4: Yield, R_f, IR and HRMS data for dimeric enol acetate (220) 160

Table 3.5: Yield, R_f, m.p., IR and HRMS data for dibenzylketone (221) 162

Table 3.6: Early literature examples of the PAA route, showing the outcome of varying the number of eqv. of Ac_2O used 163

Table 3.7: Isolated yields for each of the products of the PAA reaction to 2,5-P2P (92), using different eqv. of Ac_2O 164

Table 3.8: Yield, R_f, m.p., IR and HRMS data for 4-Br-2,5-PAA (164) 167

Table 3.9: Yield, R_f, m.p., IR and HRMS data for 4-Br-2,5-P2P (159) 168

Table 3.10: R_f, m.p., IR and HRMS data for (*Z*)-4-bromo enol acetate (223)..... 170
Table 3.11: Yield, R_f, m.p., IR and HRMS data for dimeric enol acetate (222) 171
Table 3.12: Yield, R_f, m.p., IR and HRMS data for dibenzylketone (224)..... 172
Table 3.13: Isolated yields obtained for each of the products of the PAA reaction to 4-Br-2,5-P2P (159), using different eqv. of Ac_2O 173
Table 3.14: Comparison of optimised Barium method (A) *vs.* Et_2O method (B) during the synthesis of glycidate (161)..... 185
Table 3.15: Yield, R_f, m.p., IR and HRMS data for *trans* methyl glycidate (161)..... 186
Table 3.16: R_f, m.p., IR and HRMS data for *cis* methyl glycidate (161) 187
Table 3.17: Comparison of optimised Barium method (A) *vs.* Et_2O method (B) during the synthesis of glycidate (239)..... 189
Table 3.18: Yield, R_f, m.p., IR and HRMS data for *trans* ethyl glycidate (239)..... 189
Table 3.19: Comparison of optimised Barium method (A) *vs.* Et_2O method (B) during the synthesis of glycidate (162)..... 192
Table 3.20: Yield, R_f, m.p., IR and HRMS data for 4-bromo *trans* methyl glycidate (162) 192
Table 3.21: Comparison of optimised Barium method (A) *vs.* Et_2O method (B) during the synthesis of glycidate (240)..... 193
Table 3.22: Yield, R_f, m.p., IR and HRMS data for 4-bromo *trans* ethyl glycidate (240)..... 193
Table 3.23: Yield, R_f, m.p., IR and HRMS data for non-bromo (241) and 4-bromo (242) glycidic acids 195
Table 4.1: Yields and number of impurities isolated, from reaction steps in Figure 4.2..... 211
Table 4.2: Yield, R_f, m.p., IR and HRMS data for terminal-bromo compounds (252) and (253) 213
Table 4.3: Yield, R_f, IR and HRMS data for benzyl-bromo compound (250)..... 216
Table 4.4: Yield, R_f, IR and HRMS data for aromatic-4-bromo benzyl-bromo compound (251) 217
Table 4.5: Yield, R_f, m.p., IR and HRMS data for monomeric nitrostyrenes (280), (281) and (282) 225
Table 4.6: Yield, R_f, m.p., IR and HRMS data for dimeric-dinitro impurity (286)..... 229
Table 4.7: Yield, R_f, m.p., IR and HRMS data for monomeric nitroalkanes (283), (284) and (285)..... 231
Table 4.8: Yield, R_f, m.p., IR and HRMS data, as well as some key structural features, of novel dimeric nitrostyrenes (290)–(298) 234
Table 4.9: *In vitro*, antiproliferative effects (EC_{50}) of previously published nitrostyrene (305) against in-house prepared nitrostyrenes (290) and (297)..... 244
Table 4.10: Yield, R_f, m.p., IR and HRMS data for novel dibenzylketones (221), (224) and (257)–(260) 247
Table 4.11: Attempted benzylic bromination of dibenzylketones (221), (257) and (224), using different eqv. of NBS 255
Table 4.12: ^{1}H-NMR δ values of shifts observed in the region of 6.0–6.30 ppm, following bromination of dibenzylketone (221) by Br_2..... 255

Table 4.13: Yield, R_f, m.p., IR and HRMS data for dimeric *N*-formyl compounds (329) and (330) 259
Table 4.14: Yield, R_f, m.p., IR and HRMS data for pyrimidine impurities (331) and (332) 265
Table 4.15: Yield, R_f, m.p., IR and HRMS data for dimeric amines (327) and (328) 269

Abbreviations

^{13}C-NMR	carbon-13 nuclear magnetic resonance
^{1}H-NMR	proton nuclear magnetic resonance
25C-NBOMe	2-(4-chloro-2,5-dimethoxyphenyl)-*N*-[(2-methoxyphenyl)methyl]ethanamine
2C	2,5-dimethoxyphenethylamine
2C-B	4-bromo-2,5-dimethoxyphenethylamine
2C-C	4-chloro-2,5-dimethoxyphenethylamine
2C-D	2,5-dimethoxy-4-methylphenethylamine
2C-E	2,5-dimethoxy-4-ethylphenethylamine
2C-I	2,5-dimethoxy-4-iodophenethylamine
2C-P	2,5-dimethoxy-4-*n*-propylphenethylamine
2CT-2	2,5-dimethoxy-4-ethylthiophenethylamine
2CT-7	2,5-dimethoxy-4-propylthiophenethylamine
2D	two-dimensional
4-MA/PMA	4(*para*)-methoxyamphetamine
4-MTA	4-methylthioamphetamine
5-HT	5-hydroxytryptamine
AAS	Atomic Absorption Spectroscopy
ABq	AB quartet
Ac_2O	acetic anhydride
ADHD	Attention Deficit Hyperactivity Disorder
AI	aminoindane
ANN	Artificial Neural Networks
APCI	Atmospheric Pressure Chemical Ionisation
aq.	aqueous
ATS	Amphetamine-Type Stimulants
br s	broad singlet
BZP	1-benzylpiperazine
calc.	calculated
CASE	Comprehensive Actions against Synthetic drugs in Europe
CE	Capillary Electrophoresis
CHAIN	Collaborative Harmonised Amphetamine INitiative
CHAMP	Collaborative Harmonisation of Methods for Profiling of amphetamine-type stimulants
CID	collision-induced dissociation
CND	Commission on Narcotic Drugs

CNS	Central Nervous System
conc.	concentrated
CZE	Capillary Zone Electrophoresis
d	doublet
DA	dopamine
DAD	diode-array detector
DAT	dopamine transporter
DCE	1,2-dichloroethane
DCM	dichloromethane
DEA	Drug Enforcement Administration
DEE	diethyl ether
DIY	do-it-yourself
DMA	2,5-dimethoxyamphetamine
DMMA	2,5-dimethoxy-*N*-methylamphetamine
DMSO	dimethyl sulfoxide
DOB	4-bromo-2,5-dimethoxyamphetamine
DOC	4-chloro-2,5-dimethoxyamphetamine
DOET	2,5-dimethoxy-4-ethylamphetamine
DOI	2,5-dimethoxy-4-iodoamphetamine
DOM/STP	2,5-dimethoxy-4-methylamphetamine
EAS	electrophilic aromatic substitution
EDG	electron donating group
EDPS	European Drug Profiling System
EELS	Europol Ecstasy Logo System
EILS	Europol Illicit Laboratory comparison System
EJUP	European Joint Unit on Precursors
EMCDDA	European Monitoring Centre for Drugs and Drug Addiction
eqv.	equivalent
ESDS	Europol Synthetic Drug System
ESI	electrospray ionisation
Et_2O	diethyl ether
EtOAc	ethyl acetate
ETS	Ecstasy-Type Substances
EU	European Union
EWG	electron withdrawing group
EWS	Early Warning System

FCC	flash column chromatography
fd	fine doublet (*J*≈3 Hz)
FDA	Food and Drug Administration
Frag	fragmentation voltage
FTIR	Fourier transform infrared
GABA	gamma amino butyric acid
GC	Gas Chromatography
GDNU	Garda National Drugs Unit
GPCR	G-protein coupled receptors
GTP	guanosine-5'-triphosphate
HCA	Hierarchical Cluster Analysis
HHS	Department of Health and Human Services
HPLC	High Performance Liquid Chromatography
HPTLC	High Performance Thin Layer Chromatography
HRMS	High Resolution Mass Spectrometry
HSE	Health Service Executive
IC	Ion Chromatography
ICP	Inductively Coupled Plasma
INCB	International Narcotics Control Board
*i*PrOH	isopropyl alcohol/2-propanol
IR	infrared
LC-MS	Liquid Chromatography-Mass Spectrometry
LDA	Linear Discriminant Analysis
LSD	lysergic acid diethylamide
m	multiplet
m.p.	melting point
m/z	mass to charge ratio
MA	methamphetamine
MAO	monoamine oxidase
mCPP	1-(3-chlorophenyl) piperazine
MDA	3,4-methylenedioxyamphetamine
MDAI	5,6-methylenedioxy-2-aminoindane
MDEA	3,4-methylenedioxy-*N*-ethylamphetamine
MDMA	3,4-methylenedioxy-*N*-methamphetamine
MDMMA	3,4-methylenedioxy-*N*,*N*-dimethylamphetamine
MI	molecular ion

MRM	Multiple Reaction Monitoring
MS	Mass Spectrometry
MS/MS	tandem mass spectrometry
MW	microwave
NFI	Netherlands Forensic Institute
NMDA	*N*-methyl-D-aspartate
NMR	Nuclear Magnetic Resonance
NOE	Nuclear Overhauser Effect
NOESY	Nuclear Overhauser Effect SpectroscopY
NSAID	Non-Steroidal Anti-Inflammatory Drug
OCG's	Organised Crime Gangs
org.	organic
OTC	over-the-counter
P2P	phenyl-2-propanone
PAA	phenylacetic acid
PAAD	Phenylacetic Acid and its Derivatives
PCA	Principle Component Analysis
PICS	Precursor Incident Communication System
PiHKAL	Phenethylamines I Have Known And Loved
PMMA	*para*-methoxy-*N*-methylamphetamine
q	quartet
QQQ	triple quadrupole (mass analyser)
QTOF	quadrupole time-of-flight
R_f	retardation factor
rt	room temperature
s	singlet
SAR	Structure-Activity Relationship
sat.	saturated
SERS	Surface-Enhanced Ramen Spectroscopy
SI	Statutory Instruments
SM	starting material
SMART	Synthetics Monitoring: Analysis, Reporting and Trends
t	triplet
TEA	triethylamine
TFMPP	1-(3-trifluoromethylphenyl) piperazine
THF	tetrahydrofuran

TIC	Total Ion Count
TLC	Thin Layer Chromatography
TMA	3,4,5-trimethoxyamphetamine
TMA-2	2,4,5-trimethoxyamphetamine
TOF	time-of-flight
t_R	retention time
UK	United Kingdom
UN	United Nations
UNCND	United Nations Commission on Narcotic Drugs
UNODC	United Nations Office on Drugs and Crime
US	United States
VMAT	vesicular monoamine transporter
δ	chemical shift value

Chapter 1 – Introduction

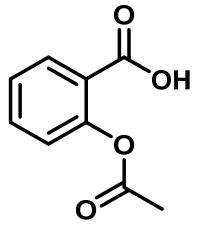
1.1 Drugs of abuse and their classification

The number of compounds that have been abused, (used for non-medical reasons) and have the potential to be abused, is vast. Classification of these drugs is difficult and is the subject of much debate; no one system is without flaw of some form or another. A number of approaches have been taken to classify these drugs and these include:[1]

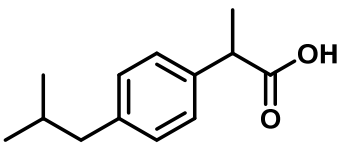
1. By origin – based on whether the drug is a natural product, semi synthetic or totally synthetic.
2. By general effect – based on the physiological response following ingestion of the drug. On this basis drugs can fall into more than one category and this may depend on the dose.
3. By use – based on how the drug is used or abused. These classes include predator drugs/date rape drugs, club drugs, human-performance drugs and inhalants.
4. By schedule – based on the State's legal categorisation of a drug. The State will regulate and control certain classes of drugs based on their potential to be abused and cause harm.

Classification based on general physiological response (point 2 above) is one of the more widely accepted and easily understood of these classifications. The major flaw of this form of classification is that some drugs may have a combination of effects and the predominant effect experienced may depend on the dose administered.[2] According to this system, drugs can be categorised as follows:

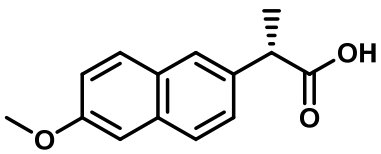
Analgesics: These drugs are commonly used to relieve pain. Drugs that can be found in this group include aspirin **(1)**, ibuprofen **(2)**, naproxen **(3)** and morphine. Aspirin and related compounds belong to a group called Non-Steroidal Anti-Inflammatory Drugs (NSAIDS) and stop pain by reducing fever and inflammation. Morphine reduces pain *via* opioid receptor agonism and blocking the transmission of nerve impulses.



(1)



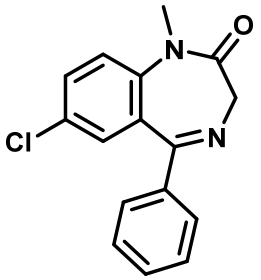
(2)



(3)

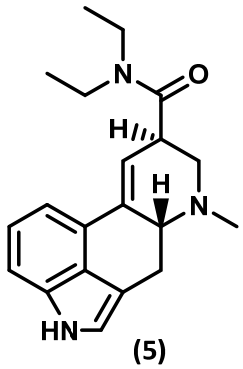
Depressants: This category of drugs depresses functions of the central nervous system (CNS), resulting in a slowed heartbeat, a reduction in anxiety and sometimes the promotion of sleep. Depressant drugs include barbiturates, tranquilisers, sleep aids and ethanol. Benzodiazepines (e.g. diazepam **(4)**

(Valium®)), a common class of depressant, work by interacting with gamma amino butyric acid (GABA) receptors, generating an inhibitory response.

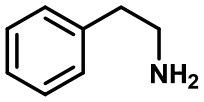


(4)

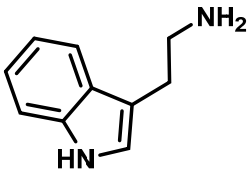
Hallucinogens: Hallucinogens are compounds that alter the perception of time and reality with movements, thoughts, perceptions, vision and hearing all being affected. Lysergic acid diethylamide (LSD) **(5)**, mescaline and marijuana are hallucinogenic. Also, stimulants like amphetamine and methamphetamine often become hallucinogens at higher doses. Generally most hallucinogens are based on, and related to, two key molecules – phenethylamine **(6)** and tryptamine **(7)**.



(5)

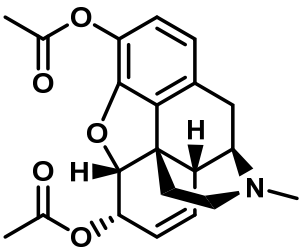


(6)

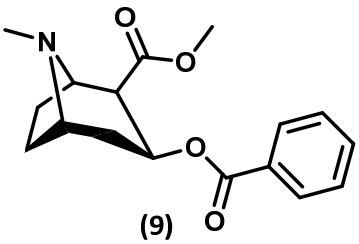


(7)

Narcotics: This drug class has analgesic effects and tends to depress the CNS and promote sleep. The opiate alkaloids, including morphine, codeine, heroin **(8)**, oxycodone and hydrocodone are common examples of narcotics.



(8)



(9)

Stimulants: Unlike the narcotics and depressants, this drug class stimulates functions of the CNS, induces alertness and interferes with sleep. Cocaine **(9)**, amphetamine and methamphetamine are common

stimulants and these may become hallucinogenic at higher doses. The mechanism of action of stimulants, in particular the amphetamines, will be discussed in detail later in Section 1.2.4.

Within the immense group of drugs of abuse known to man, lies a particular subset known as 'designer drugs'. These drugs are primarily synthetic in origin and have been described as "chemicals created for recreational use to evade drug legislation, usually by modification of the molecular structures of existing drugs".[2] Given the fact that they are mostly synthetic in origin, it is drugs belonging to this subset that are of most interest to scientists working in the area of organic impurity profiling.

From a scientists'/chemists' point of view, classification of these "designer drugs" is often based on general chemical structure as it does not suffer the same degree of ambiguity as the 'classification by general effect' grouping does. Based on general chemical structure, the designer drugs fall under a number of families of molecules (phenalkylamines, piperazines etc.) and these are summarised in Figure 1.1. Some of the compounds in this figure have only arisen very recently and will be discussed in greater detail in Section 1.7 ('Emerging Drugs').

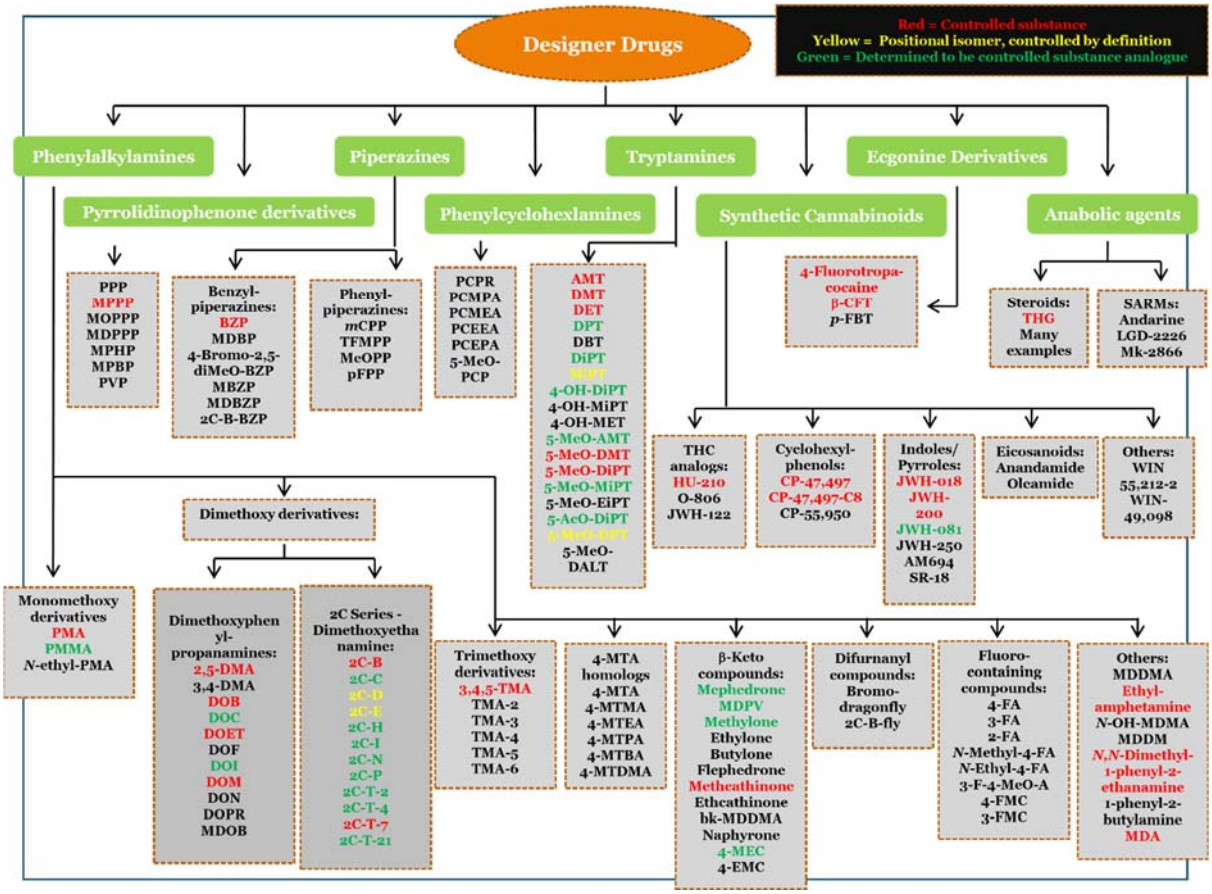
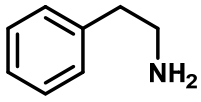


Figure 1.1: Classification of "designer drugs" based on general chemical structure[3]

Of interest to our research group are the family of designer drugs known as phenalkylamines. This class is also referred to as Amphetamine-Type Stimulants (ATS), defined by the UNODC as "synthetic

stimulants, including amphetamine, methamphetamine, methcathinone and ecstasy-type substances (e.g. MDMA and its analogues)".[4] The key structural features of these compounds will be discussed in Section 1.2.2.

Compounds belonging to this group are based on the phenethylamine **(6)** backbone and modification of this basic structure, by substitution of the phenyl ring or ethylamine side-chain, leads to a diverse range of compounds with varying pharmacological effects.



(6)

This potential for structural diversity means that ATS may fall under a number of categories including stimulants, hallucinogens and entactogens. The common structural features associated with compounds belonging to each of the stimulant, hallucinogenic and entactogenic categories, are summarised later in Figure 1.6.

The versatility of this group makes it impossible to classify the ATS into just one category based on the 'classification by general effect' system. This is made even more complicated by the fact that the predominant effect experienced may depend on the dose taken; as mentioned earlier, many compounds typically regarded as 'stimulants', are known to become hallucinogenic at higher doses.

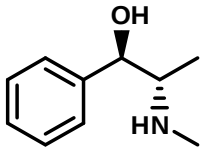
The structures of ATS and their pharmacology, will be discussed in greater detail in Sections 1.2.2 and 1.2.4.

One of the most basic modifications of the phenethylamine backbone is the addition of a methyl group α to the primary amine on the side chain. This modification lead to the first major designer drug/modified phenalkylamine to become a worldwide, problematic drug of abuse – amphetamine.

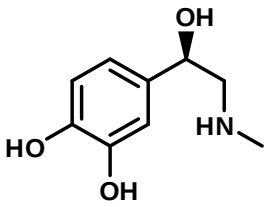
1.2 ATS

1.2.1 History of Amphetamine and ATS

Amphetamine (or alpha-methylphenethylamine) **(10)** is a potent CNS stimulant. It was first synthesised in 1887 by Romanian pharmacologist L. Edeleano.[5] It was not until the late 1920's, whilst American chemist Gordan Alles was looking for an alternative to ephedrine **(11)**, that its array of pharmacological effects was uncovered. Alles reported that amphetamine dramatically reduced fatigue, increased alertness and gave a sense of confident euphoria. Alles went on to carry out further research on the animal and human testing of amphetamine, and developed "modified" amphetamines that resembled naturally occurring adrenaline **(12)**.[6]



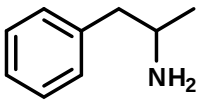
(11)



(12)

It was at this time that the enormous medicinal potential of amphetamine was being explored and it promised to bring about great improvement in the treatment of a vast number of illnesses such as epilepsy and schizophrenia.[5]

Alles submitted a patent for amphetamine in September 1930 and this patent was granted in 1932.[6] Working with the pharmaceutical giant Smith, Kline and French, Alles sold the company the rights to market his amphetamine in exchange for 5% royalties on all sales as well as generous funding for research, thus giving rise to Benzedrine® (Figure 1.2).



(10)



Figure 1.2: Amphetamine (10) and Benzedrine® inhaler[7]

The active constituent of Benzedrine® was amphetamine in its volatile base form and came to market in 1933 in the US, as an inhaler for use in the treatment of nasal congestion.[8] The over-the-counter (OTC) inhaler was used widely by asthmatics and sufferers of hay fever and colds.

The use of Benzedrine® and its variants, including the benzedrine sulphate tablet form, increased greatly worldwide in the 1930's, with the drug being used to treat a growing list of illnesses:

- In 1935, doctors in the US began prescribing Benzedrine® to treat narcolepsy, a condition in which people suffer sudden attacks of deep sleep.
- In 1936, Smith, Kline and French began to sell Benzedrine® as 10 mg tablets without prescription in the US, and over 50 million Benzedrine® tablets were sold within the first 3 years of their availability.[9]
- In 1937, Smith, Kline and French began a huge advertising campaign that saw sales of benzedrine sulphate tablets soar, the drug now offering to effectively treat depression and psychiatric conditions.

It was also in 1937 that amphetamine, now available in tablet form, was said to have a "positive effect" on children suffering from attention deficit hyperactivity disorder (ADHD), improving their

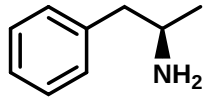
concentration and performance in school. In the years that followed, other ailments for which amphetamine was put to use as a treatment included obesity, Parkinson's disease, alcoholism, morphine and codeine addiction, seasickness, migraines, head injuries and irradiation sickness.[5,8] Although it was made available by prescription only in the US in 1939, its production, and approval by those in the medical profession, was not curtailed.[9] Its fame as a 'cure-all' drug meant that by 1940, it may have been considered one of the greatest medical breakthroughs, alongside such drugs as insulin and penicillin.[6] It was reported at the time, by experts and those in advertising, that amphetamine was not only the very first antidepressant but the very first specific medicine for a mood disorder. In addition, it was among one of the first drugs to be developed through research managed by drug companies.

Given its stimulant action and availability OTC, amphetamine abuse was almost inevitable. Its non-medical use was said to have begun as soon as the Benzedrine® inhalers became available; students recruited for psychological testing of amphetamine in the 1930's, were said to have started using amphetamine to combat fatigue and allow for last-minute "cramming" for exams.[6] Its abuse greatly increased during World War 2 with German, Japanese and British soldiers using amphetamine to counteract fatigue during long missions. Its demand became so high that, by the end of the war, large surpluses of amphetamine were dumped by American troops in Japan, leading to the first epidemic of widespread amphetamine abuse.[10] Truck drivers were also among the first to start abusing amphetamine, using it to stay awake during long journeys; the nature of their work greatly aiding the distribution of amphetamine.

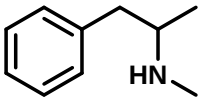
In the post-war years high achievers such as athletes and those in entertainment and business, were using amphetamine to combat fatigue.[8] By the late 1960's, at the peak of its popularity, ten million Americans were regular users of amphetamine; annual production of amphetamine reached 10 billion tablets by 1970 with perhaps 50–70% diverted to the black market.[9]

Reports on the ill effects of amphetamine began in the 1930's with *Time* magazine condemning the promiscuous use of the "powerful but poisonous brain stimulant" in 1937.[6] By the late 1950's, researchers recognised that amphetamines were addictive and may cause severe psychotic conditions. In 1965, all amphetamines became illegal without prescription in the United States (US) and in 1970 the Food and Drug Administration (FDA) greatly restricted the legal use of amphetamines.[8]

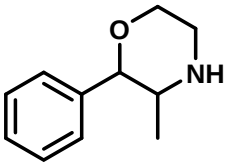
Having said this, amphetamine-type substances continued to be prescribed and are still available today, mainly for use in treating narcolepsy and ADHD, as well as acting as an aid to weight loss. Some of these amphetamine-type substances still used today include dextroamphetamine **(13)** (Dexedrine®), methamphetamine **(14)** (Desoxyn®), phenmetrazine **(15)** (Preludan®), methylphenidate **(16)** (Ritalin®) and amphetamine itself.[8]



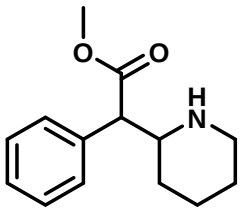
(13)



(14)



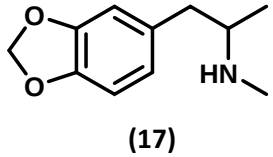
(15)



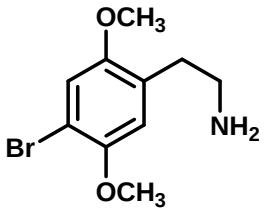
(16)

The licit use of amphetamine and related substances is perhaps becoming more restricted. However, the prescribing of amphetamines has greatly increased in recent years especially in the treatment of ADHD. Aderall®, originally released by Richwood pharmaceuticals, contains a mixture of *R*- and *S*-amphetamine salts and is available in several countries worldwide, including Ireland and the US. Aderall® is currently the most commonly prescribed treatment for juvenile ADHD in the US. America's consumption of medicinal amphetamine has risen almost tenfold since 1995 and exceeded 2.5 billion doses in 2005.[6]

Amphetamine is among the oldest synthetic drugs but following its widespread abuse in the middle of the 20th century, use of substituted phenethylamines (or ATS) quickly followed.[11] Recreational use of ring-substituted phenethylamines (such as 3,4-methylenedioxy-*N*-methylamphetamine **(17)** (MDMA)) arose in the 1960's. In 1971, several of these ring-substituted phenethylamines were included in Schedules I or II of the United Nations Convention on Psychotropic Substances. Although a few were added later (for example MDMA **(17)** in the mid 1980's and 4-bromo-2,5-dimethoxyphenethylamine (2C-B) **(18)** in 2001) most of these are now considered 'old phenethylamines'.[11]



(17)

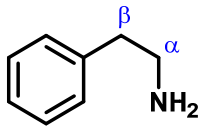


(18)

The new age for phenethylamines/ATS began with the publication of the book 'PiHKAL' in 1991 (discussed later in Section 1.7.3).[12] By 2013, nearly 100 illicit phenethylamines had been documented in the European Union.[11]

1.2.2 The amphetamine family

Amphetamine and amphetamine-type stimulants (ATS) are a primarily synthetic family of compounds, based on the phenethylamine backbone.[13] The phenethylamine core, which is responsible for its hallucinogenic properties, consists of a primary amine separated from a phenyl ring by two carbon atoms.[14]

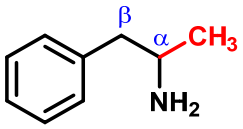


(6)

Chemical modification of the phenethylamine skeleton gives rise to a vast number of potential pharmacologically active compounds. These modifications involve either alteration of the substitution pattern of the phenyl ring and/or alteration of the substituents on the ethylamine side chain.[15] Varying the substitution patterns will in turn, alter the pharmacological effects of the drug; this will be discussed later under 'structure-activity relationships' (Section 1.2.3).

The variability and versatility of the phenethylamine backbone has become of particular interest to clandestine chemists as it allows for the variation and optimisation of the desired pharmacological effect. As well as this, introduction of new substituents allow clandestine chemists to create "legal" amphetamines which are not yet scheduled, thus keeping one step ahead of the law.[16]

As mentioned, alterations to the phenethylamine structure can take place at the phenyl ring or at the ethylamine side chain, at various positions. For example, the amphetamine family core structure is composed of a phenethylamine skeleton with a methyl (CH_3) group at the α-carbon:



(10)

In order to summarise the numerous pharmacologically active compounds based on the phenethylamine backbone, one can place these compounds into 3 distinct groups. These groups cover the common traditional ATS, i.e. those that arose prior to *ca*. 2000. The new age ATS will be discussed later under 'emerging drugs' (Section 1.7.3). The traditional ATS are summarised as follows:

1. The phenethylamines – Basic core structure is phenethylamine **(6)**.
2. The amphetamines – Basic core structure is phenethylamine with a methyl group (CH_3) at the α-carbon **(10)**.
3. The *N*-substituted phenethylamines/amphetamines – Basic core structure is phenethylamine/amphetamine with at least 1 alkyl/hydroxyl group attached to the nitrogen atom of the ethylamine side chain, e.g. methamphetamine **(14)**.

1.2.2.1 Phenethylamines

The countless phenethylamine analogues arise as a result of varying the substitution on the phenyl ring. Listed below (Table 1.1)[15] are some of the common phenethylamine analogues:

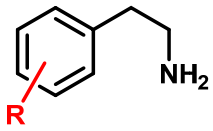


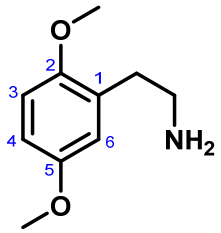
Table 1.1: Psychoactive phenethylamine analogues

Entry	R	Name	Common name
(6)	H	Phenethylamine	
(19)	2,5-$(MeO)_2$	2,5-Dimethoxyphenethylamine	**2C-H**
(20)	3,4,5-$(MeO)_3$	3,4,5-Trimethoxyphenethylamine	**Mescaline**
(21)	2,5-$(MeO)_2$-4-EtS	2,5-Dimethoxy-4-ethylthiophenethylamine	**2CT-2**
(22)	2,5-$(MeO)_2$-4-PrS	2,5-Dimethoxy-4-propylthiophenethylamine	**2CT-7**
(23)	3,5-$(MeO)_2$-4-Al	4-Allyloxy-3,5-dimethoxyphenethylamine	**Allylescaline**
(24)	2,5-$(MeO)_2$-4-Me	2,5-Dimethoxy-4-methylphenethylamine	**2C-D**
(25)	2,5-$(MeO)_2$-4-Et	2,5-Dimethoxy-4-ethylphenethylamine	**2C-E**
(26)	2,5-$(MeO)_2$-4-*n*Pr	2,5-Dimethoxy-4-*n*-propylphenethylamine	**2C-P**
(18)	2,5-$(MeO)_2$-4-Br	4-Bromo-2,5-dimethoxyphenethylamine	**2C-B**
(27)	2,5-$(MeO)_2$-4-Cl	4-Chloro-2,5-dimethoxyphenethylamine	**2C-C**
(28)	2,5-$(MeO)_2$-4-I	2,5-Dimethoxy-4-iodophenethylamine	**2C-I**

Many of these compounds were unheard of until the 1990's. In 1991, the American chemist Dr Alexander Shulgin, together with his wife Ann, published the controversial book 'PiHKAL' (Phenethylamines I Have Known and Loved) – A Chemical Love Story".[12] In this book, Shulgin describes the structure and chemistry of scores of novel psychoactive phenethylamines and amphetamines. In addition to the procedures used to synthesise these compounds, Shulgin describes the effective human dose of the drug and its physiological response. The effects of many of these compounds were personally assessed by Shulgin and his colleagues in their detailed "trip reports". By publishing PiHKAL in book format, freely available to the public, Shulgin's discoveries were allowed to "escape the limits of professional research labs". Shulgin regarded the many psychedelic phenethylamines he produced to be valuable tools for self-exploration.

Common to many of the phenethylamine analogues described by Shulgin is the 2,5-dimethoxy pattern on the phenyl ring.[15] Compounds with this core structure became known as the '2C' drugs; 2C arising from the primary amine being separated from the phenyl ring by 2 carbon atoms.

The two methoxy groups at the 2- and 5-positions are said to be responsible for the hallucinogenic properties of 2C-H **(19)**.



(19)

Basic structure of the '2C' class

Another common feature of the '2C' class is the presence of a hydrophobic 4-substituent (alkyl, halogen, alkylthio etc.), shown in Table 1.1 (entries **(21)–(28)**) which is said to increase the hallucinogenic potency of the drug.[14]

1.2.2.2 Amphetamines

As mentioned previously, the basic structure of amphetamine **(10)** is a phenethylamine backbone with a methyl group attached to the α-carbon. This methyl group greatly lowers the effective dose required to induce a psychotropic response and it does this by increasing the lipophilicity and resisting its deactivation by the enzyme monoamine oxidase (MAO).[15] Also, amphetamines possess a stereocenter and in many cases, the pharmacological response differs between one enantiomer and the next.

As with the phenethylamines, structural variability of the psychoactive amphetamines can be brought about by changing the substituents on the phenyl ring. Listed below (Table 1.2) are some of the common psychoactive amphetamines. Many of these were also first synthesised by Shulgin.

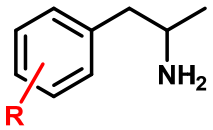


Table 1.2: Psychoactive amphetamine analogues

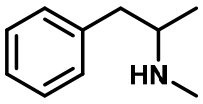
Entry	R	Name	Common name
(10)	H	Amphetamine	
(29)	4-MeO	4(*para*)-Methoxyamphetamine	**4-MA, PMA**
(30)	4-MeS	4-Methylthioamphetamine	**4-MTA**
(31)	2,5-$(MeO)_2$	2,5-Dimethoxyamphetamine	**DMA, 2,5-DMA**
(32)	2,5-$(MeO)_2$-4-Me	2,5-Dimethoxy-4-methylamphetamine	**DOM, STP**
(33)	2,5-$(MeO)_2$-4-Et	2,5-Dimethoxy-4-ethylamphetamine	**DOET**
(34)	2,4,5-$(MeO)_3$	2,4,5-Trimethoxyamphetamine	**TMA-2**
(35)	2,5-$(MeO)_2$-4-Br	4-Bromo-2,5-dimethoxyamphetamine	**DOB**
(36)	2,5-$(MeO)_2$-4-Cl	4-Chloro-2,5-dimethoxyamphetamine	**DOC**
(37)	2,5-$(MeO)_2$-4-I	2,5-Dimethoxy-4-iodoamphetamine	**DOI**
(38)	3,4,5-$(MeO)_3$	3,4,5-Trimethoxyamphetamine	**TMA**
(39)	3,4-$CH_2(O)_2$	3,4-Methylenedioxyamphetamine	**MDA**

As with the '2C' series of phenethylamines, the 2,5-dimethoxy pattern also produces potent hallucinogenic amphetamines, (entries **(31)–(37)**, Table 1.2) with 4-substitution increasing the potency of these compounds. The amphetamine equivalent of the '2C' series of phenethylamines is sometimes referred to as the 'D' series[2], the simplest of which is DMA **(31)**.

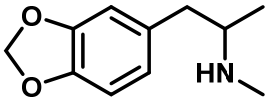
1.2.2.3 N-substituted phenethylamines/amphetamines

As the name suggests, this set of compounds is characterised by the presence of one or more alkyl/hydroxyl groups on the nitrogen atom of the ethylamine side chain.

N-Methylamphetamine **(14)** and MDMA ('ecstasy') **(17)** are two well-known examples of these *N*-substituted compounds and are two of the most problematic drugs of abuse worldwide today.



(14)



(17)

Listed below (Table 1.3) are several more examples of the commonly encountered psychoactive *N*-substituted phenethylamines/amphetamines:

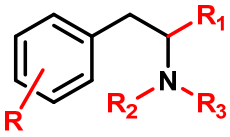


Table 1.3: Psychoactive *N*-substituted phenethylamine/amphetamine analogues

Entry	R	R_1	R_2	R_3	Name	Common name
(14)	H	Me	Me	H	*N*-Methylamphetamine	**MA**
(40)	H	Me	Et	H	*N*-Ethylamphetamine	
(41)	H	Me	Me	Me	*N,N*-Dimethylamphetamine	
(42)	H	H	Me	Me	*N,N*-Dimethylphenethylamine	
(17)	3,4-$CH_2(O)_2$	Me	Me	H	3,4-Methylenedioxy-*N*-methylamphetamine	**MDMA**
(43)	3,4-$CH_2(O)_2$	Me	Me	Me	3,4-Methylenedioxy-*N,N*-dimethylamphetamine	**MDMMA**
(44)	3,4-$CH_2(O)_2$	Me	Et	H	3,4-Methylenedioxy-*N*-ethylamphetamine	**MDEA**
(45)	4-MeO	Me	Me	H	*para*-Methoxy-*N*-methylamphetamine	**PMMA**
(46)	2,5-$(MeO)_2$	Me	Me	H	2,5-Dimethoxy-*N*-methylamphetamine	**DMMA**
(47)	2,5-$(MeO)_2$-4-Br	Me	Me	H	4-Bromo-2,5-dimethoxy-*N*-methylamphetamine	

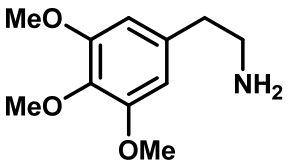
This section demonstrates the versatility of the phenethylamine backbone and how substitution of both the phenyl ring and the ethylamine backbone has given rise to numerous compounds with varying physiological effects. In the next section, the relationship between the specific structure of these compounds and their pharmacological response will be discussed.

1.2.3 Structure-activity relationships

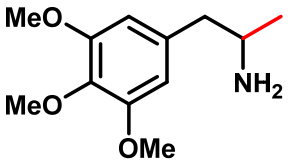
It has long been understood that a relationship exists between the structure of amphetamine (i.e. the substitution pattern) and its pharmacological effect. This phenomenon is referred to as the 'structure-activity relationship' (SAR). The principle has even been exploited by clandestine chemists in creating designer drugs; manipulating the substitution pattern of the amphetamine molecule has allowed them to amplify the many desired pharmacological effects. Knowledge in this area has been greatly enhanced by a number of scientists, namely Alexander T. Shulgin, David E. Nichols, Richard A. Glennon and Aaron P. Monte.

The amphetamine compounds of most interest to our research group are those exhibiting hallucinogenic properties and it is the SAR of this hallucinogenic class of amphetamines which will be the focus of this section.

Shulgin carried out extensive work in the synthesis of numerous substituted amphetamines.[12] As well as the synthesis, he was also interested in the pharmacological effects of these compounds. Mescaline **(20)**, is a naturally occurring phenethylamine, isolated from the peyote cactus (*Lophophora williamsii*). Shulgin used this compound as a standard against which many other phenethylamine/amphetamine based analogues were compared. The degree of potency of many of his novel drugs was evaluated against it.[17] One major find was that when an α-methyl group was added on the ethylamine side chain of mescaline **(20)**, creating the amphetamine TMA **(38)**, the hallucinogenic potency increased almost two-fold. As explained in the book '*Drugs and the Brain*'[18] addition of the α-methyl group blocks enzymatic removal of the nitrogen (by the enzyme MAO), slowing metabolism and therefore increasing the potency.



(20)

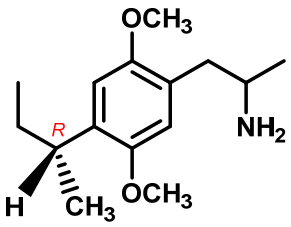


(38)

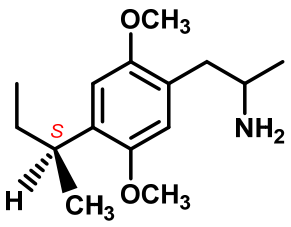
Once knowledge of the affinity of amphetamines for the specific 5-hydroxytrytamine receptor (5-HT_2) was established (see 'pharmacology', Section 1.2.4), Glennon and Nichols carried out further studies on how substitution affects activity. They found that methoxy groups in the 2- and 5-positions of the phenyl ring produced optimal affinity for the receptor, and that methylation, ethylation and

bromination at the 4-position also increased affinity.[19] Shulgin outlined in his paper on DOB in 1971, that hallucinogenic activity increases, with increasing number of alkoxy substituents, with an apparent maximum at tri-substitution.[20] Glennon also found that *N*-methylation decreased activity in most of these compounds except for the '2C' series of compounds.[21]

The hallucinogenic activity of 'D' series (2,5-dimethoxy) amphetamines bearing a range of alkyl groups (methyl, ethyl etc.) at the aromatic 4-position was examined by Oberlender.[22] It was found that the hallucinogenic activity of these D series compounds is reduced when the alkyl chain exceeds *n*-propyl in length, or is branched. Also, for one of the analogues tested, the presence of a stereogenic centre on the alkyl group did not give rise to stereoisomers with different activities, with the *R*- and *S*-enantiomers of the 4-(*R*/*S*)-2-butyl compound, **(48)** and **(49)**, having no significant difference in activity.

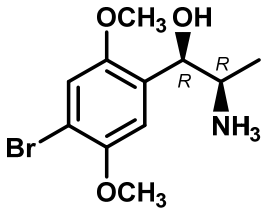


(48)



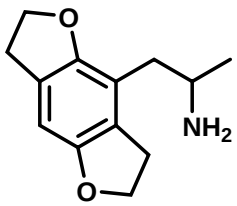
(49)

In a study by Glennon *et al*. in 2004,[23] attempts were made to reduce the lipophilicity of DOB **(35)** and other 4-substituted analogues, in order to hinder their passage across the blood-brain barrier. This was carried out as it was feared that the compound would evoke undesirable effects if sufficient levels accumulated in the brain. The compound used in this study **(50)**, incorporated a hydroxyl group at the β-carbon of the ethylamine side chain of DOB **(35)**. The compound, when tested, was >15 less potent than the analogous *R*-(DOB).

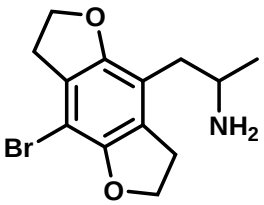


(50)

In more recent studies, Monte *et al.*[24] have demonstrated that the more rigid analogues of D series amphetamines, whereby the methoxy groups are locked/fused into dihydrofuran rings, have a much higher affinity for 5-HT_2 receptor subtypes (e.g. the rigid analogue of DMA **(31)** is dihydrofuran **(51)**). Bromination of the rigid analogue **(51)** at the aromatic 4-position results in a compound with a 100-fold greater affinity for the 5-HT_{2A} receptor, thus making 1-(8-bromo-2,3,6,7-tetrahydrobenzo[1,2-b:4,5-b']difuran-4-y)-2-aminopropane **(52)** one of the most potent hallucinogens known to man.



(51)



(52)

As with many of the rules/trends observed in SAR studies, there are exceptions. The aforementioned 'locking' of the alkoxy groups into rings does not always evoke an increase in hallucinogenic activity. Nichols[25] also observed the same increase in affinity as Monte when the methoxy groups of DOB **(35)** were locked into dihydrofuran rings (as in compound **(52)**). However, locking of the distal methoxy groups (at the aromatic 3- and 5-positions of mescaline **(20)**) into dihydrofuran rings, results in a complete loss of activity at the 5-HT_{2A} receptor (for compound **(53)**) (Figure 1.3).

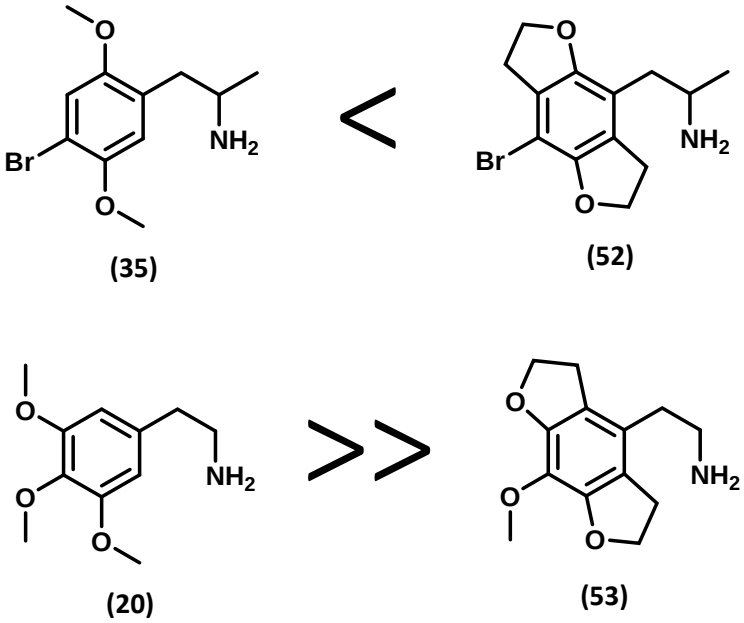


Figure 1.3: Comparison of hallucinogenic activity between methoxy substituted ATS ((35) and (20)) and their ring-locked counterparts ((52) and (53))[25]

The results of this work show that many of the trends that have been outlined in SAR studies cannot be taken for granted; much more research is required to gain a better understanding of what specific receptors are targeted (e.g. 5-HT_{2A}, 5-HT_{2B}, 5-HT_{2C} etc.) by each group of psychoactive compounds and what orientation the molecules adopt once they bind to a given receptor.

Monte and co-workers[24] have summarised (as shown in Figure 1.4) some of the structural features that may be important within the phenethylamine type hallucinogens, for receptor recognition and activation.

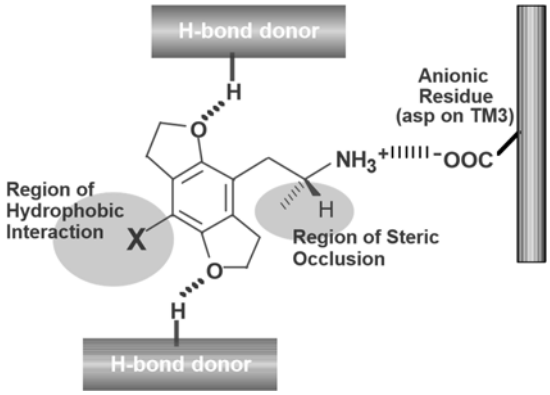


Figure 1.4: Hallucinogenic amphetamine interacting with the ligand binding domain of human 5-HT$_{2A}$ receptor[25]

These structural features include:

- The amino group – The protonated amino group has a strong attraction (*via* ionic bonding) for the deprotonated aspartic acid residue found on the serotonin receptor (5-HT$_{2A}$).
- 'Region of hydrophobic interaction' – This area of the receptor has a particular affinity for atoms or groups of an oily, non-water soluble nature and this hydrophobic interaction with the receptor is said to stabilise the complex. This is evident by the fact that many of the most potent phenethylamine hallucinogens have atoms such as bromine, iodine or sulphur at this position.
- The 2,5-alkoxy groups – The two oxygen atoms at these positions undergo hydrogen bonding with hydrogen bond donating sites on the receptor and therefore are essential for efficient binding and thus activation of the receptor.
- 'Region of steric occlusion' – For efficient binding and activation of the receptor, the ethylamine side chain cannot have bulky groups at the α-position. In fact, nothing larger than a methyl group will be tolerated here in order to elicit a hallucinogenic response.

A summary of the SAR of hallucinogenic phenethylamines/amphetamines at the 5-HT$_2$ receptors was adapted from the work by Griffin *et al.*[26] and is shown below:

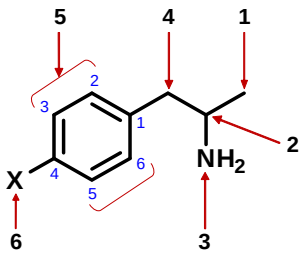


Figure 1.5: Various sites whereby the phenethylamine/amphetamine backbone can be modified/substituted

Position 1: α-methyl group

- Removing the methyl group decreases hallucinogenic potency → Amphetamines more potent than phenethylamines
- However, homologation of group > methyl diminishes potency[27]

Position 2: Stereogenic centre

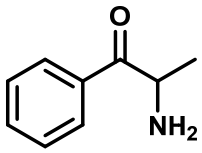
- *R*-enantiomer more potent than *S*-enantiomer in general (some exceptions, e.g. MDMA **(17)**)
- Most substances produced as racemates however[11]

Position 3: Terminal amine

- *N*-methylation decreases hallucinogenic potency (*N*-methyl DOB **(47)** ≈ 10 times less potent than DOB **(35)**)[27]
- However, *N*-methylation may increase stimulant potency (methamphetamine **(14)** twice as potent as amphetamine **(10)**)
- *N*-benzyl, *N*-(bromobenzyl) and *N*-(iodobenzyl) derivatives of 2C-H **(19)** increase potency[11]

Position 4: Benzylic substituent

- Hydroxyl group decreases hallucinogenic potency
- Keto group also often decreases hallucinogenic potency (amphetamine **(10)** about 2 times more potent than cathinone **(54)**)[28]



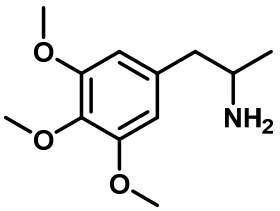
(54)

Position 5: Aromatic ring substituents (at positions 2-, 3-, 5- and 6-)

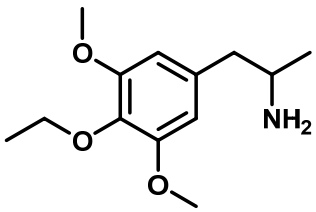
- 2,5-dialkoxy analogues = very potent hallucinogens[15]
- ↑ number of alkoxy groups = ↑ potency, however cut-off is 3 alkoxy groups[20]

Position 6: *Para* ring substituent

- Methyl more hallucinogenic than H (e.g. DOM **(32)** >> DMA **(31)**) and methyl > methoxy[20]
- Et, *i*-Pr more potent than Me (e.g. DOEt **(33)** >> DOM **(32)** and escaline **(55)** 6 times more active than mescaline **(20)**)[19]



(20)

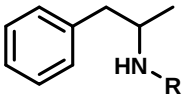


(55)

- Br and I more potent than Et, *i*-Pr (e.g. DOB **(35)**, DOI **(37)** >> DOEt **(33)**)
- NH_2, OH, COOH inactive due to hydrophilic nature
- Chirality: 4-(*R*)-2-butyl **(48)** and 4-(*S*)-2-butyl **(49)** equipotent
- Branching: 4-*iso*-butyl more potent than 4-*sec*-butyl
- Some mono-substituted compounds (e.g. 4-MTA **(30)**) particularly toxic *in vivo*[2,11]
- Alkylthio group "enhances intellectual function"[19]

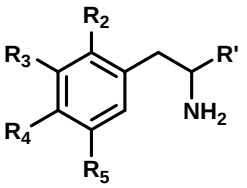
The phenethylamines/amphetamines are best known for their stimulant, hallucinogenic and to a lesser extent, entactogenic activity. It appears that for psychostimulant action, the optimal structure is a simple amphetamine backbone with an unmodified ring and possibly *N*-methylation of the amino group. Hallucinogenic activity is most associated with compounds with an amphetamine backbone, alkoxy groups at the 2- and 5- ring positions and a hydrophobic group (e.g. Br, I) at the 4-position.[2] ATS that are considered entactogenic/empathogenic often bear a methylenedioxy substituent on the phenyl ring, as well as methyl/ethyl groups on both the *N* atom of the amino group, and at the α-carbon. These features are summarised in Figure 1.6.

Stimulants



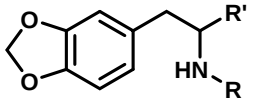
R = H; Amphetamine **(10)**
R = CH_3; Methamphetamine **(14)**

Hallucinogins



R' = H, R_3,R_4,R_5 = OCH_3; Mescaline **(20)**
R' = CH_3, R_2,R_5 = OCH_3, R_4 = Br; DOB **(35)**

Entactogens



R' = CH_3, R = CH_3; MDMA **(17)**
R' = CH_3, R = C_2H_5; MDEA **(44)**

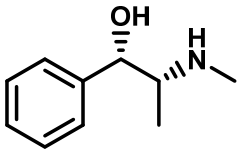
Figure 1.6: Structural features of stimulants, hallucinogens and entactogens[29]

The mode of action of ATS as stimulants, hallucinogens and entactogens is discussed in more detail in Section 1.2.4 ('Pharmacology').

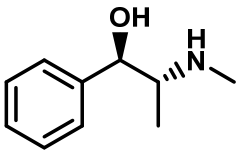
1.2.4 Pharmacology

Amphetamine and amphetamine-type stimulants (ATS) often evoke a psychotropic response. These agents can alter perception, mood and behaviour and lead to extended periods of attention and wakefulness.[15]

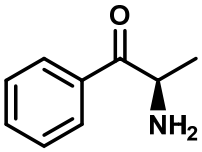
Ever before the synthesis and study of amphetamine itself, many other natural hallucinogenic and mood-enhancing amphetamine-related substances had been used. For centuries, compounds derived from plants have been used for this purpose. The plants commonly used include those of the genus *Ephedra* and the tree *Catha edulis*, known as "khat" in Arabic and Swahili and "myrrha" in East Africa.[9] *Ephedra sinica*, known commonly in China as *Ma huang*, has been used in Asia since Neolithic times and was used in the treatment of asthma and upper respiratory tract infections. It was not until 1887 that its active component ephedrine **(11)** was identified. Ephedrine has been used as a popular appetite suppressant and widely used by athletes to boost performance. Today, ephedrine and its epimer pseudoephedrine **(56)**, are among the most widely used precursors to methamphetamine in clandestine laboratories.[30]



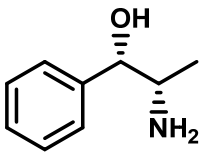
(56)



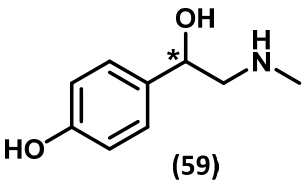
(11)



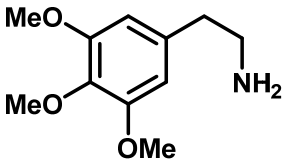
(57)



(58)



(59)



(20)

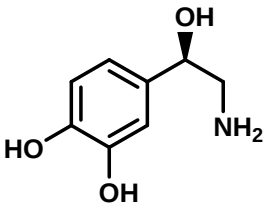
The tree *Catha edulis* (khat), is native to Kenya and Somalia and is widely cultivated in Yemen. Its leaves contain the amphetamine-type compounds (*S*)-cathinone **(57)** and norpseudoephedrine **(58)**. Khat, used by up to 85% of adult males in north Yemen, is associated with feelings of contentment, suppression of fatigue and appetite loss. Khat is often referred to as 'natural amphetamine' as it has similar effects and mode of action.[28] It is also habit forming, and induces paranoia and other behavioural disturbances.

Synephrine **(59)**, a drug similar in structure to amphetamine, is found in citrus plants including *Citrus aurantium* (bitter orange).[9]

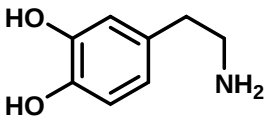
Mescaline **(20)**, an alkaloid and phenethylamine analogue, is derived from the peyote cactus *Lophophora williamsii* and related species, and has been used by Native Americans and even the Aztecs for thousands of years. Its psychedelic properties led to the Aztecs using it to predict the future and other such practices.[9] Mescaline was first isolated from the peyote cactus in 1896 by Heffter, and its structure confirmed by total synthesis in 1919 by Ernst Spath.[31] The 'religious' use of peyote in the US, has been protected by Federal law since 1965.

Other plants known to contain natural amphetamines, including amphetamine and methamphetamine, are the *Acacia* species (e.g. *Acacia rigidula*) and Egyptian jasmine (*Jasminium grandflourum*).[9]

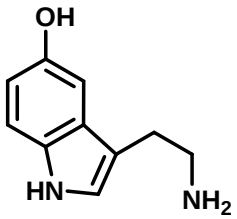
These naturally occurring ATS, as well as the many synthetic amphetamines, produce their pharmacological effects by modulating structurally similar, endogenous neurotransmitters. These neurotransmitters include noradrenaline **(60)**, dopamine (DA) **(61)** and serotonin **(62)**.



(60)



(61)



(62)

By mimicking endogenous neurotransmitters, ATS have the ability to:

- Release and inhibit the release of catecholamines.
- Release and inhibit the reuptake of serotonin.
- Act as direct agonists at serotonin receptors producing hallucinogenic effects.

Modification of the phenethylamine backbone has produced an array of ATS, some of which are classed as stimulants, some as hallucinogens and others as entactogens (see Figure 1.6 for typical structures). The mode of action of each class is different and thus each evokes a very different physiological response.

One way in which amphetamines are known to elicit a physiological response is *via* release of catecholamines (noradrenaline, DA etc.). This mechanism is said to be responsible for the stimulant effect common to many of the amphetamine-type compounds. The ATS can reverse the action of catecholamine transporters (e.g. Dopamine transporter (DAT)) at the synaptic terminal of neurons (Figure 1.7).[32]

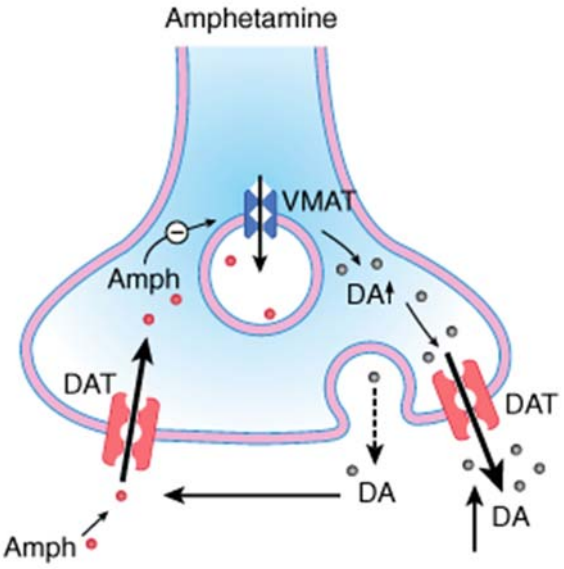


Figure 1.7: Mechanism of action of stimulant ATS on synaptic terminal of dopamine neurons[32]

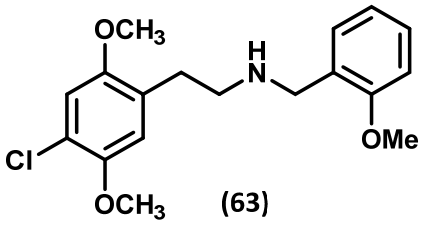
Certain ATS, being structurally similar to catecholamines, affect dopamine (DA) transport. The effects on DA transport includes depletion of vesicular DA, reversal of DAT (efflux of dopamine into synaptic cleft) and DA uptake inhibition. Stimulant ATS compete with DA for Na^+/Cl^--dependant-DAT, competitively inhibiting DA reuptake, hence increasing DA concentration in the synaptic cleft. The ATS, using the DAT, then enters the presynaptic nerve terminal and is transported into dopamine-containing vesicles *via* the vesicular monoamine transporter (VMAT), which release DA into the cytosol in exchange. After the vesicular DA stores have been depleted, the increased cytosolic concentration of DA in the presynaptic nerve terminal (relative to the synaptic cleft) facilitates reverse transport of DA *via* DAT, resulting in DA efflux into the synaptic cleft.[33]

The effect on the individual is typically increased arousal and a decrease in the ability to sleep. Overdose of such stimulants is associated with a sympathomimetric toxidrome.[2] A toxidrome is a syndrome/condition caused by dangerous levels of toxins in the body and symptoms of a sympathomimetric toxidrome include anxiety, delusions, diaphoresis, hyperreflexia, paranoia and seizures.

Another well studied mechanism by which ATS elicit a strong pharmacological response is *via* the interaction with the 5-HT_2 receptor subclass. This mechanism is said to be responsible for the hallucinogenic effect that some ATS induce. In humans, serotogenic hallucinogens produce intense effects on visual, auditory, tactile and olfactory perception. Much of the research carried out in this area has been conducted by D. E. Nichols and R. A. Glennon. The work by Nichols in particular, not only enhanced our knowledge of the SAR of a library of phenethylamines, but also inferred knowledge of the 5-HT receptor's three-dimensional structure.[31]

The 5-HT_2 family belongs to a group of receptors known as G-protein-coupled receptors (GPCR). Within the 5-HT_2 family, there are subfamilies of receptors including the 5-HT_{2A} and 5-HT_{2C} receptors which are most associated with the action of hallucinogenic amphetamines. Both of these receptor types are localised in the periphery and CNS, and there is 80% genetic homology between both.[34] Although phenethylamine based hallucinogens have been shown to bind to both 5-HT_{2A} and 5-HT_{2C} receptors,[35] studies by Fiorella *et al.*[36] suggest that the 5-HT_{2A} receptor plays a more prominent role in the action of hallucinogens.

The 5-HT_{2A} receptor is coded by the HTR2A gene on chromosome 13 in humans.[34] It plays a role in appetite control, thermoregulation and sleep. It also effects cardiovascular function, muscle contraction and plays an important role in neuropsychiatric disorders.[37] *N*-benzyl substituted phenethylamines (e.g. 25C-NBOMe **(63)**, see Section 1.7.3) have been described as super potent and selective 5-HT_{2A} receptor agonists.[38]



(63)

The 5-HT_{2C} receptor is closely homologous to the 2A-subtype. It regulates dopamine and serotonin release and is a target for the treatment of anxiety, obesity and stimulant addiction.[39]

In general, 5-HT receptors are composed of a seven transmembrane α-helix domain protein, with continuing loops of protein connecting the inside (cytoplasm) to the outside (synaptic cleft) of the cell. Connected to the cytoplasmic side of the 5-HT receptor is the GTP (Guanosine triphosphate) binding protein (known as the G protein). This G protein is made up of three subunits, α, β, and γ (Figure 1.8).[25]

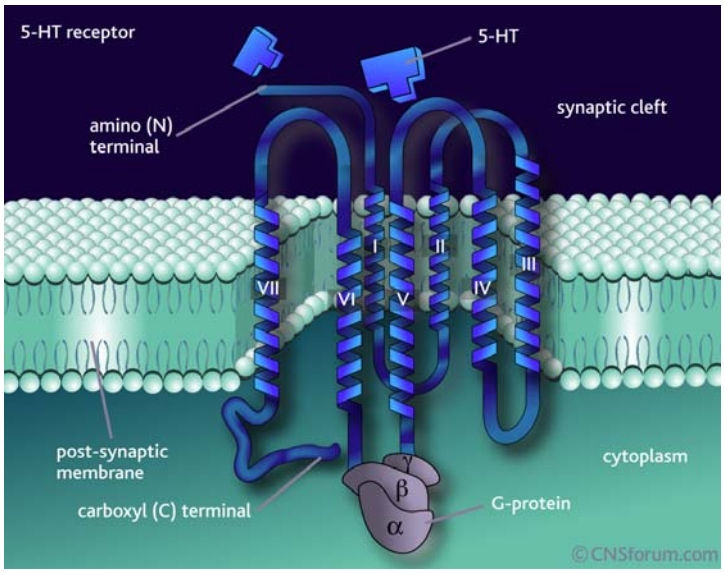


Figure 1.8: General structure of 5-HT receptor[40]

The mechanism which affords a hallucinogenic response begins with a neurotransmitter (e.g. 5-HT) or ATS molecule in the synapse, binding (*via* electrostatic forces) to the receptor (extracellular). The neurotransmitter fits the binding pocket of the receptor and with this binding comes a change in the arrangement and orientation of the alpha helices. The change in conformation of the transmembrane helices, forces the G protein to dissociate from the receptor. The now free G protein binds to molecules of GTP in the cytoplasm, initiating a series of biochemical changes in the neuron, including changes in calcium levels. This complex sequence of events is known as a signalling cascade, and in a process which is not yet fully understood, leads to an alteration in consciousness.[25]

ATS that exerted unique psychological effects in humans that were different to (or even a mixture of) the stimulant and hallucinogenic classes, were coined 'entactogens' in the 1980's.[41] Although for years they were considered as another type of hallucinogen, it was decided that these compounds should be categorised into a class of their own; these compounds not only produced a unique response in humans, but they also did not follow the same 'rules' as other hallucinogens, in terms of their SAR. This suggested that they had a different mode of action.

This group contained mainly ring-substituted amphetamine derivatives like MDMA **(17)** and MDEA **(44)**. Entactogens like MDMA are said to evoke a subtle, easily controllable altered state of consciousness with an emphasis on emotional aspects, relaxation, feelings of happiness, heightened self-acceptance and empathy, openness for communication and decrease of fear.[29] Entactogens are said to evoke their unique response by causing the release of serotonin from central axon boutons (presynaptic terminal).[2] Nichols showed that the mode of action of entactogens differed to stimulants, in that entactogens do not appear to have the ability to block re-update of dopamine. His work (using mainly rat brain models) also showed that the mechanism of action also differs to that of a well-known hallucinogen DOM **(32)**, in that the entactogens are able to release serotonin and inhibit the reuptake of serotonin and noradrenaline **(60)** into nerve terminals. In human models, entactogens were also shown to evoke a different response to stimulant and hallucinogenic amphetamines.[29] Stimulant and hallucinogenic amphetamines are known to enhance the secretion of cortisol, prolactin and growth hormone. However, it was found that the entactogen tested (MDEA **(44)**) did not cause the secretion of growth hormone.

The short and long term effects of ATS have been well studied. Even in small doses these drugs may cause numerous cardiovascular problems including an elevated heart rate, high blood pressure and hypothermia. Long term use of these drugs may trigger aggressive or violent behaviour, cause severe structural and functional changes to the brain and lead to the development of psychosis.[42]

1.2.5 The use and domestic/worldwide seizures of ATS

Globally, the most reliable source of information relating to the use, supply and trafficking of drugs is the United Nations Office on Drugs and Crime (UNODC). The UNODC, established in 1997, is the global leader in the fight against drugs and international crime. It works closely with all UN Member States to gather information on drug use, and produces extensive reports each year; the most significant of which is the World Drug Report.

According to the UNODC World Drug Report 2013 (covering data collected to the end of 2011), the market for ATS is expanding: seizures and consumption levels are increasing, manufacture seems to be spreading and new markets are developing.[43] The number of ATS seized worldwide has risen significantly in the last decade. Included in this group of ATS are amphetamine, methamphetamine, methcathinone, MDMA and its analogues. A new high was reached in 2011 with 123 tons of ATS seized worldwide, compared with 74 tons in 2010 (66% rise) and a doubling since 2005 (60 tons) (Figure 1.9). Seizures increased across all regions, with Asia, North America and Europe registering dramatic increases.

(Note: The quantities stated (in tons) reflect the bulk weight of seizures, with no adjustment for purity.)

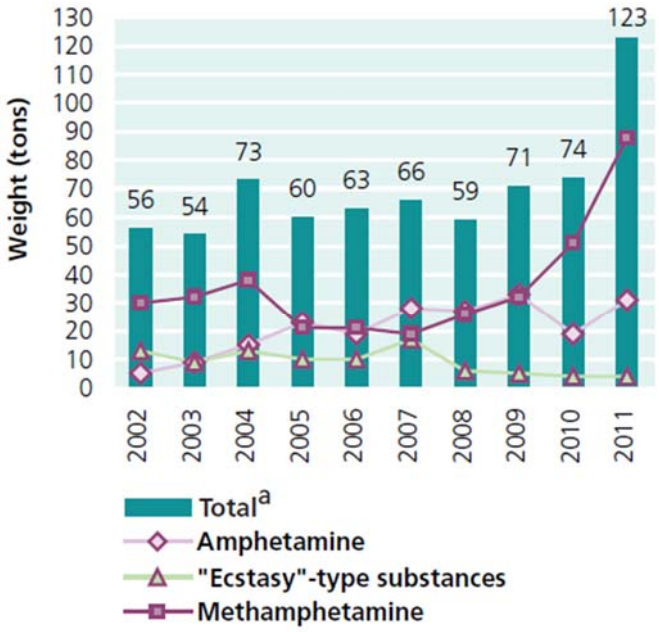


Figure 1.9: Global seizures of ATS, 2002-2011[43]

The overall increase in ATS seizures is largely due to surging methamphetamine seizures, which grew by 73%, from 51 tons in 2010 to 88 tons in 2011. Methamphetamine accounts for 71% of global ATS seizures. Mexico seized the largest amount of methamphetamine, more than doubling, from 13 tons to 31 tons, from 2010 to 2011. Methamphetamine manufacture seems to be spreading also, with new

facilities being detected in Poland and Russia. There is also an indication of increased manufacturing activity in Central America.

Amphetamine seizures have also increased in 2011 (compared to 2010), the most significant of which taking place in the Near and Middle East and South-West Asia, from 14 tons in 2010 to 20 tons in 2011. The highest amphetamine seizures were registered by Saudi Arabia (11 tons), the Syrian Arab Republic (4 tons) and Jordan (4 tons) (Figure 1.10). In Europe, particularly Russia, seizures of amphetamine increased from 142 kg in 2010 to more than 2 tons in 2011.

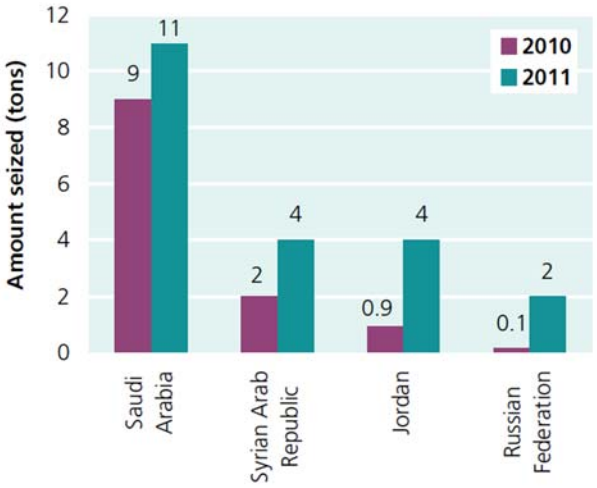
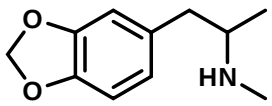


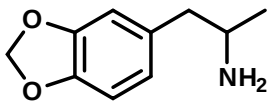
Figure 1.10: Countries reporting the highest amphetamine (10) seizures, 2010-2011[43]

Amphetamine seizures have increased in the Middle East in particular, where the drug is available largely in pill form, sold as "captagon" pills.

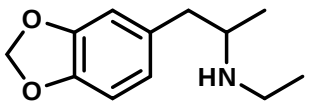
Seizures of 'ecstasy-type substances' (ETS) have been stable or declining globally since 2008.
(Note: According to the UNODC, ecstasy-type substances include those believed to be ecstasy (e.g. MDMA **(17)**, MDA **(39)**, MDEA **(44)**) which may not have been confirmed by forensic testing.)



(17)



(39)



(44)

At 3.6 tons (compared with 3.8 tons in 2010), seizures of ETS deceased by 5% in 2011, reflecting fewer reported seizures in Canada and China. However in Europe, seizures of ETS increased from 1.3 tons in 2010 to 1.7 tons in 2011. By country, the US reported the highest seizures of ETS (926 kg) in 2011, followed by Netherlands (583 kg) and France (409 kg) (Figure 1.11).

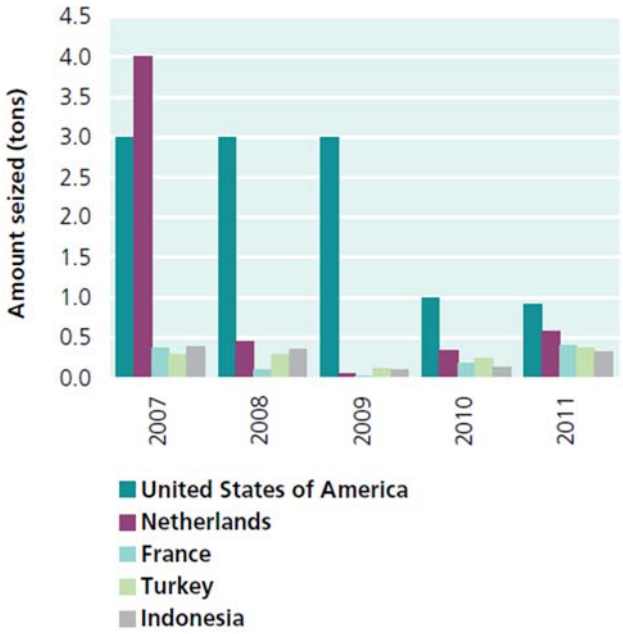


Figure 1.11: ETS seizures in selected countries, 2007-2011[43]

The use of ATS (excluding ETS) is increasing in most regions. In 2011, an estimated 0.7% of the global population aged 15–64, or 33.8 million people, had used ATS (excluding ETS) in the preceding year (Figure 1.12). The European average is slightly lower at 0.5%. The prevalence of ETS use in 2011 (19.4 million, or 0.4% of the population) was lower than in 2009.

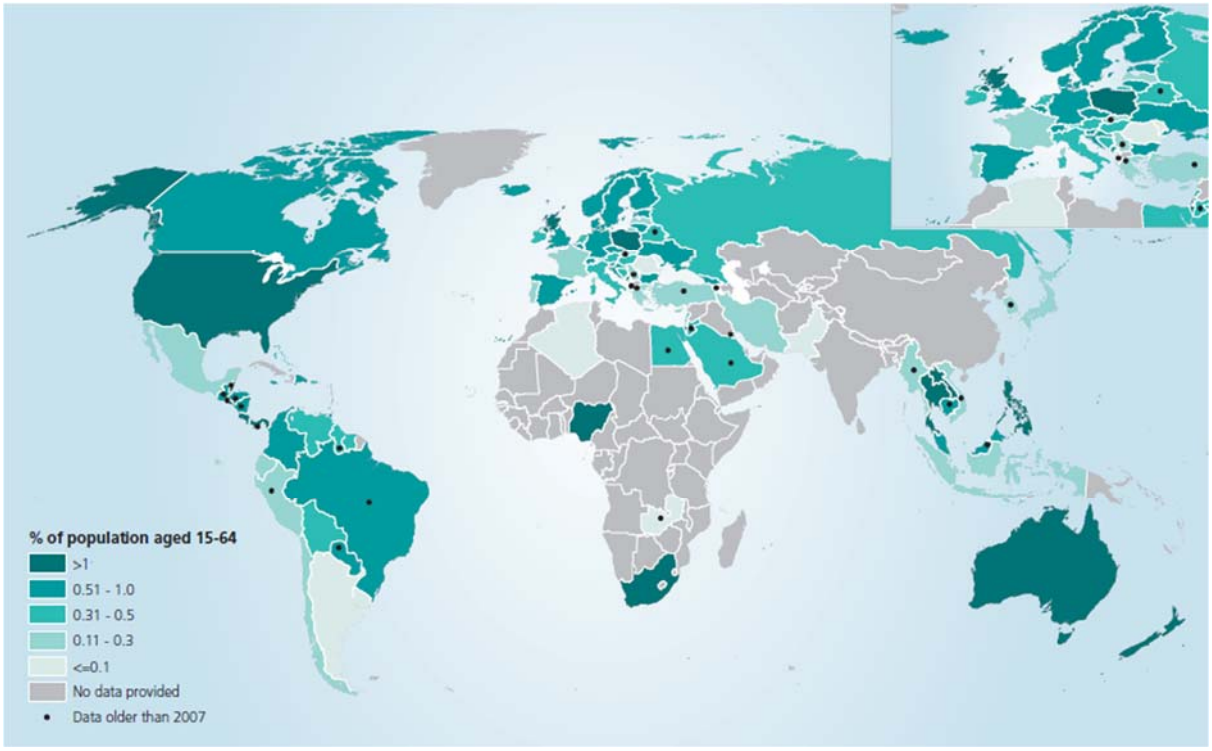


Figure 1.12: Use of ATS (excluding ETS) in 2011[43]

The manufacture of ATS will be discussed in greater detail later in Section 1.4 – 'clandestine laboratories and ATS manufacture'.

Within the European Union, two major organisations deal with the prevention of drug related crime and collection of data. These are Europol and the EMCDDA (European Monitoring Centre for Drugs and Drug Addiction). According to the most recent report by the EMCDDA (published in May 2014), the total number of seizures of ATS (comprising of amphetamine **(10)**, methamphetamine **(14)** and MDMA **(17)**) was 47,200 in the EU. This figure accounted for 29,000 seizures/5.5 tons of amphetamine (slight downward trend, return to 2003 levels), 7,000 seizures/0.3 tons of methamphetamine (increase on previous years) and 11,200 seizures/4 million MDMA tablets (downward trend).

It is estimated that around 3.4% of the EU population have tried amphetamines/methamphetamine in their lifetime (age 15–64), with 1.2 million (0.9%) young adults (15–34) having used it in the last year.[44] For MDMA, the lifetime prevalence is 3.1%, with 1.3 million (1%) young adults (15–64) using it in the last year.

In Ireland, the primary sources of information on drug related crimes can be found in the Annual Reports of An Garda Siochana and the Health Research Boards *Drugnet Ireland* newsletter. Table 1.4, adapted from An Garda Siochana reports 2003-2012, outlines the number of cases and details of the ATS seized in Ireland in recent years.[45-54] (Note: Number of cases in bold text. Zero cases denotes no mention of particular drug in report. "–" symbol denotes no data for number of cases provided: in years 2011 and 2012 data is represented as estimated street value as opposed to number of cases)

Table 1.4: Number of cases and seizures of ATS in Ireland, 2003-2012[45-54]

	2003	2004	2005	2006	2007	2008	2009	2010	2011	2012
Amphetamine	211	145	119	236	194	152	81	89	-	-
	(67,787g, 1,019 tabs)	(92,417 g)	(10,515 g, 19,452 tabs)	(37,922 g, 6,399 tabs)	(54,933 g, 10,395 tabs)	(8,217 g, 946 tabs)	(56,540 g, 432 tabs)	(26,463 g)	(35,876 g, 24 tabs)	(22, 809 g, 1,562 tabs)
Methamphetamine	1	1	14	20	5	26	27	20	-	-
	(0.5 g)	(0.6 g)	(55 g)	(136 g)	(10.2 g)	(4,633 g)	(1,124 g)	(404 g)	(3,272 g)	(1,411 g)
MDMA	1001	793	653	769	948	763	94	30	-	-
	(604 g, 1,205,055 tabs)	(1,098,169 tabs)	(3,444 g, 327,142 tabs)	(106 g, 146,013 tabs, 1.5 L)	(12,516 g, 119,127 tabs)	(1,144 g, 100,635 tabs)	(3,352 g, 18,736 tabs)	(1,429 g, 398 tabs)	(827 g, 101, 850 tabs)	(5,824 g, 164,943 tabs)
MDEA	66	5	1	2	2	0	0	0	-	-
	(12.3g, 5,401 tabs)	(153 tabs)	(7 tabs)	(9 tabs)	(7 tabs)				(2.7 g, 15,812 tabs)	(6 g, 2,984 tabs)
DOB	16	8	1	0	0	0	0	0	0	0
	(81,353 tabs)	(816 tabs)	(30 tabs)							
Mescaline	0	0	0	0	0	0	3	0	-	0
							(9 plants)		(5.4 g)	
2C-B	0	0	0	0	0	0	0	0	-	-
									(20,225 tabs)	(1 g, 22 tabs)
Fluoroamphetamine	0	0	0	0	0	0	0	0	-	-
									(0.5 g)	(294 g)
PMMA	0	0	0	0	0	0	0	0	-	-
									(391 g)	(316 g)
2C-E	0	0	0	0	0	0	0	0	0	-
										(0.05 g)

The use (per head of population) of 'traditional' ATS (amphetamine, methamphetamine and MDMA) in Ireland is above average European figures. In a drug prevalence survey carried out by the Irish National Advisory Committee on Drugs (NACD) in 2008, the percentage of those surveyed claiming to have tried amphetamine/methamphetamine in their lifetime was 4%.[55] A more recent figure quoted in an EMCDDA report for 2014, stated this to be 4.5% for Ireland. The European average for those having tried amphetamine/methamphetamine in their lifetime is 3.7%.

For MDMA, lifetime prevalence in Ireland is reported to be 5% (according to 2007 NACD report)[55] or 6.9% (according to EMCDDA, 2014)[44] substantially higher than the 3.1% European average.

According to the figures in Table 1.4, the number of 'cases' (brought to court) involving amphetamine in Ireland has been decreasing steadily in recent years, peaking in 2006 with 236 cases. Care must be taken however when interpreting these figures. Although the results suggest a positive reduction in the number of seizures, the greater detail provided by the Garda Annual Reports tell a different story. As can be seen in Table 1.4 for 2009, the figure for the number of cases, standing at 81, is the lowest in recent years (since before 2003). When the greater detail of these seizures is looked at, a total haul of 56,540 g of amphetamine was seized in 2009, the highest figure since 2004, so the perception that the popularity of amphetamine is decreasing is not justified. These figures suggest that either drug operations are generally getting larger or the Gardaí/customs officers are targeting the big operators. This discrepancy highlights one of the many flaws in the reporting of seizures of illicit drugs by both An Garda Siochana and international agencies. In relation to the reporting of seizures by An Garda Siochana, a major issue is consistency; the way in which seizures are reported differs from year to year. For example, up until 2010, emphasis was put on the number of cases involving each drug. However, from 2011 onwards, emphasis was put on the street value with no mention of the number of cases. This makes it more difficult to compare seizures over the years. Another issue encountered during the reporting of drug seizures, is the fact that drugs may be seized in a number of different forms, including powders, tablets, capsules, on blotter paper or in plant form (if the drug is of natural origin). The purity level of seized drugs also varies considerably, depending on the extent to which the drug is cut. More recently too, tablets are being produced as mixtures of a number of illicit substances.

The most common methodology used by international agencies is reporting of the mass of bulk material seized. The issue with this methodology is that seized drugs range from high purity (e.g. pure powders) to low purity (e.g. heavily cut tablets) so what may appear to be a substantial haul of tablets may only equate to a low mass of active ingredient. The method of using estimated street value is becoming more popular and the public find this method easier to relate to. However, as with any underground market, it is difficult for enforcement agencies to know for sure how much drug users are paying, and the value of the drug on the street may fluctuate over time, making long term comparison of figures difficult.

What may be useful for comparison purposes is reporting of the mass of pure active ingredient and from this, the number of doses that could be attained from this mass. This information, alongside the total mass of substances acquired and estimated street value would allow for simpler comparison of seizures. For this to work internationally, all countries that contribute to the UNODC World Drug Report and EMCDDA Annual Reports would have to adopt the same reporting procedures.

An interesting observation from the Garda Annual reports, is the increase in new classes of drugs in recent years. Some of those belonging to the phenethylamine/ATS class (e.g. PMMA **(45)**, 2C-E **(25)**) are shown in Table 1.4. This follows the surge in numbers of 'head shops' selling 'legal highs' in 2009/2010 and subsequent legislation (see Section 1.7) in 2010/2011 controlling their sale. A 'head shop' is a retail outlet specialising in tobacco paraphernalia used in the consumption of tobacco, 'legal highs' and 'party powders'. These new phenethylamines/ATS are classified under 'New Psychoactive Substances (NPS)' and within Europe in 2011, Ireland had the highest lifetime prevalence rate (16.3%) among young people (aged 15-24) for these substances (Figure 1.13). These NPS/emerging drugs are discussed in greater detail in Section 1.7.

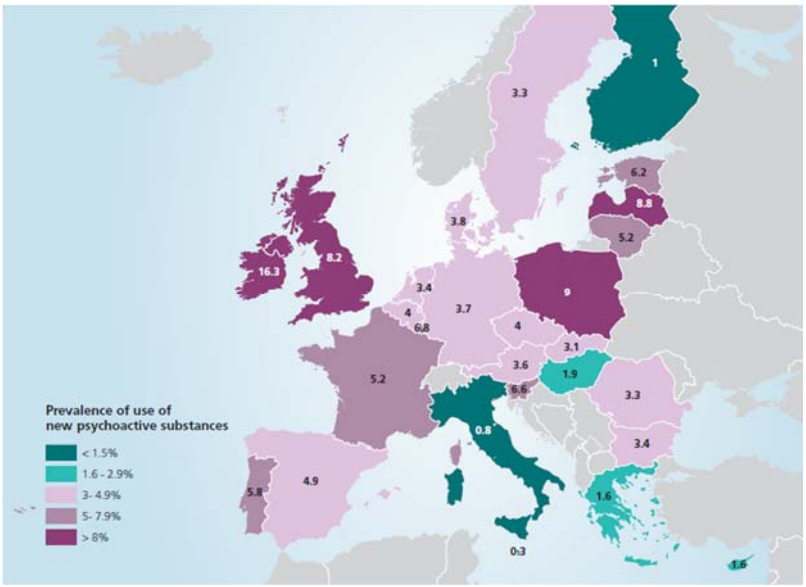


Figure 1.13: Lifetime use of 'legal substances' in EU among persons aged 15–24, 2011[43]

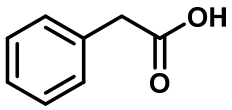
Interestingly, large seizures of these NPS continue to be made despite their prohibition. One may have thought that there would be a much greater drop off in seizures of these drugs, given that they were originally sought after as a 'legal' alternative to existing banned substances. It appears that there is still a demand for these substances and supply is greatly facilitated by online head shops. Evidence suggests that these drugs may continue to be a problem for at least the next few years.[4]

1.2.6 Control and Legislation of ATS

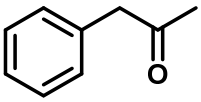
Control of the supply, trafficking and management of data relating to illicit drugs is not only managed by national police forces, but also carried out by international agencies like the UNODC. The UN's Commission on Narcotic Drugs (CND) published a new political declaration and plan of action to tackle the world drug problem in 2009.[56] They also passed a Resolution (52/12) to improve data collection, reporting and analysis in order to monitor the implementation of these new drug policy documents. An example of one of the programs run under the UNODC is the 'SMART' program:[57]

- The *Synthetics Monitoring: Analysis, Reporting and Trends (SMART)* program was launched by the UNODC in 2008 and aims to provide information on the patterns of trafficking and use of synthetic drugs, by supporting countries to better monitor trends, while improving methods for exchanging comparable information.

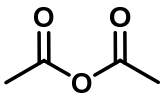
In terms of the control of precursors, the *UN Convention Against Illicit Traffic in Narcotic Drugs and Psychoactive Substances of 1988*, provides for measures to prevent the diversion of precursor chemicals frequently used in the illicit manufacture of drugs, such as ephedrine **(11)**, phenylacetic acid (PAA) **(64)**, phenyl-2-propanone (P2P) **(65)**, and acetic anhydride (Ac_2O) **(66)**.



(64)



(65)



(66)

As well as the UNODC, the International Narcotics Control Board (INCB) is the other main international body involved in precursor control.[30] It monitors UN Member States control over precursor chemicals and assists governments in preventing the diversion of such chemicals into the illicit market. Examples of some of the programs being run by the INCB to control precursor chemicals are:

- The *Pre-Export Notification Online (PEN Online) system* – the cornerstone of international precursor control in terms of monitoring licit trade in, and preventing the diversion of, precursors. The system is used by 146 UN Member States and Territories.
- The *Precursor Incident Communication System (PICS)* – allows relevant law enforcement and regulatory authorities to report and share information on individual seizures of precursors, including incidents involving chemicals previously not known to have been used in illicit drug manufacture.
- '*Operation Pila*' – Launched by the INCB between July 2009 and March 2010 in the framework of Project Prism. It monitors global trade of key amphetamine precursors P2P **(65)** and PAA **(64)**, and methamphetamine precursors ephedrine **(11)** and pseudoephedrine **(56)**. Operation

Pila was intended to generate intelligence on precursor trafficking and identify weaknesses in mechanisms for precursor control at national and regional levels.

Within the EU, it is increasingly common for Member States to set up joint task forces for complex and large-scale investigations, by combining the manpower, knowledge and technical capacity of different law enforcement agencies such as the police, customs, coast guard and revenue services.[58] A number of collaborative projects/initiatives have been set up in the EU to combat drug crime. These include:

- *Joint Action Concerning the Information Exchange, Risk Assessment and Control of New Synthetic Drugs* (1997) – An EU wide initiative aimed at sharing information, establishing a risk assessment procedure and laying out of a mechanism for the eventual control of 'new synthetic drugs'. New synthetic drugs were defined as those that had a limited therapeutic value and were not listed in the 1971 UN Convention on Psychotropic Substances, yet posed a serious threat to public health.[11] An important aspect of this Joint Action was the setting up of the *Early Warning System (EWS)* which highlights compounds that are deemed high risk to health. The number of new compounds submitted to the EMCDDA EWS has been increasing in recent years, with reports of about one new substance per week in 2013.[59]
- *EU Council Decision on Information Exchange, Risk Assessment and Control of New Psychoactive Substances* (2005/357/JHA) – This superseded the 'Joint Action' of 1997, leading to a more comprehensive and robust system for monitoring what then became known as 'new psychoactive substances'.
- *Project SYNERGY* – Developed by Europol and Member States in 2005, this project "gathers and exploits relevant information in the area of synthetic drugs and precursors, available within and outside of the Member States, in order to identify new criminal targets and target groups, support and co-ordinate law enforcement investigations and identify links between different investigations, whilst enhancing information exchange, knowledge and experience."[58] Project SYNERGY also includes the *Europol Illicit Laboratory Comparison System* (EILS), the *Europol Ecstasy Logo System* (EELS) and *Europol Synthetic Drug System* (ESDS).
- *European Union Training Course on Combatting Illicit Synthetic Drugs Laboratories* – Regularly provided by Europol since 1999.
- *European Joint Unit on Precursors* (EJUP) (2003) – A multi-national, multidisciplinary operational unit to investigate serious criminal activity in the field of precursor chemicals.
- *Collaborative Harmonised Amphetamine INitiative (CHAIN) Project* (2005) – Initiative by EU on the profiling of amphetamine for law enforcement purposes whereby significant seizures may be forensically matched. This superseded the Swedish *Comprehensive Actions against Synthetic*

drugs in Europe (CASE) project, a pilot project on the profiling of amphetamine, in which seizure data and intelligence was provided to Europol.

- *Collaborative Harmonisation of Methods for Profiling of Amphetamine Type Stimulants (CHAMP)* - A project, funded by the sixth framework program of the European Commission, aimed at the harmonisation of profiling methods (e.g. GC-MS) and the creation of a common database in a drug profiling perspective.[60]
- *European Drug Profiling System* (EDPS) (2010) – A law-enforcement driven 3-year project involved in profiling of amphetamine, implementation of forensic profiling of MDMA and a feasibility study on forensic profiling of heroin and cocaine.[61]

At a national level, drug policy documents are continuously being published and examples of some of these documents (in Europe) can be seen in Figure 1.14.

Country	Name of policy document	Time span	Scope	Notes
Bulgaria	National strategy for the fight against drugs	2009–13	Illicit drugs	Complemented by an action plan (2009–13)
Ireland	National drugs strategy – interim	2009–16	Illicit drugs	Will be replaced by a substance misuse strategy also covering alcohol
Spain	National drug strategy	2009–16	Illicit drugs, alcohol and tobacco	Complemented by an action plan (2009–12)
Cyprus	National strategy on drugs	2009–12	Illicit drugs	
Hungary	National strategy for tackling the drugs problem	2010–18	Illicit drugs	Will be complemented by action plans
Slovakia	National anti-drug strategy	2009–18	Illicit drugs	Will be complemented by action plans
Croatia	Action plan on combating narcotic drugs abuse	2009–12	Illicit drugs	Second action plan under the national strategy 2006–12

Sources: Reitox national focal points.

Figure 1.14: National drug policy documents adopted in Europe from 2009[56]

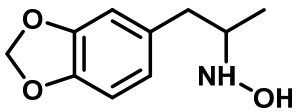
Within Ireland, domestic control of illicit drugs is carried out by the Garda National Drugs Unit (GNDU). In the control of drugs and implementation of drug laws, it liaises with internal agencies such as Revenue's Custom Service, the Irish Navy and the Police Service of Northern Ireland, as well as EU and international law enforcement agencies.[54] The GDNU carries out long term strategic and short term tactical investigations into activities of Organised Crime Gangs (OCG's) based both in Ireland and on the European continent. It works with other European Police forces and has strategic partners in the United Kingdom (UK), Spain, Holland and Belgium; countries where OCG's affecting the Irish jurisdiction tend to be most proactive.

Worldwide drug legislation pertaining to the control of ATS was introduced almost universally in the late 60's and early 70's. Abuse of amphetamine, as described in Section 1.2.1, had reached a phenomenal level, particularly in the US, by the late 1960's. This brought about the need for new legislation to control its supply and availability. The UN International Convention on Psychotropic

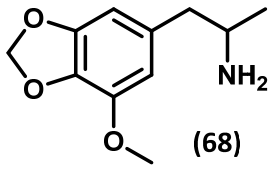
Substances (1971) is the basis for worldwide control of psychotropic drug use. Interpretation of this treaty varies from country to country with some able to control any chemical with a chemical structure (generic) or pharmacology (analogue) that is similar to a known scheduled drug. Other countries have chosen to control each new drug (specific) as it becomes available. The latter allows new chemicals to be created to evade legislation.[2] The Convention on Psychotropic Substances, groups compounds into four Schedules (I, II, III, IV) based on their risk to human health and thus level of restriction, with compounds in Schedule I having the highest risk to public health. Currently, there are 16 compounds belonging to the phenethylamine/ATS class included in Schedule I and II of the 1971 Convention on Psychotropic Substances (Table 1.5).

Table 1.5: ATS named in Schedule I and II of UN Convention on Psychotropic Substances, 1971[11]

Substance	Common name	Entry #
UN 1971 Convention (Schedule I)		
4-Bromo-2,5-dimethoxyamphetamine	DOB	**(35)**
2,5-Dimethoxyamphetamine	DMA	**(31)**
2,5-Dimethoxy-4-ethylamphetamine	DOEt	**(33)**
N-(3,4-Methlenedioxyamphetamine)hydroxylamine	*N*-Hydroxy-MDA	**(67)**
N-Ethyl-3,4-methylenedioxyamphetamine	MDEA	**(44)**
3,4-Methylenedioxymethamphetamine	MDMA	**(17)**
3,4,5-Trimethoxyphenethylamine	Mescaline	**(20)**
5-Methoxy-3,4-methylenedioxyamphatamine	MMDA	**(68)**
4-Methylthioamphetamine	4-MTA	**(30)**
4-Methoxyamphetamine	4-MA, PMA	**(29)**
2,5-Dimethoxy-4-methylamphetamine	DOM, STP	**(32)**
3,4-Methylenedioxyamphetamine	MDA	**(39)**
3,4,5-Trimethoxyamphetamine	TMA	**(38)**
UN 1971 Convention (Schedule II)		
4-Bromo-2,5-dimethoxyphenethylamine	2C-B	**(18)**
α-Methylphenethylamine	Amphetamine	**(10)**
N,α-Dimethylphenethylamine	Methamphetamine	**(14)**



(67)



(68)

Other treaties set out by the UN in relation to drugs are the *Single Convention on Narcotic Drugs, 1961* (amended by the 1972 protocol) and the *Convention against Illicit Traffic in Narcotic Drugs and Psychotropic Substances, 1988*.[62]

The UN treaties may be the basis for worldwide drug legislation but given the difference in interpretation and the difference in what drug types are most problematic, legislation differs from country to country. Here, a brief outline of the legislation in the US, UK and Ireland will be discussed.

This legislation is primarily based on '*Misuse of Drugs Act, 1977 and 1984*' (Ireland), '*Misuse of Drugs Act, 1971*' (UK) and '*Controlled substances Act, 1970*' (US).

1.2.6.1 US Legislation

The *Controlled Substances Act, 1970*[63] is the main piece of drug legislation used in the US today. It groups psychoactive drugs into five Schedules. Schedule I contains substances having the highest potential for abuse whilst possessing little medicinal use. A number of agencies can determine if the Schedule needs to be changed, including the Drug Enforcement Administration (DEA), the Department of Health and Human Services (HHS) and the Food and Drug Administration (FDA). Schedule I covers many hallucinogens and stimulants and names a large number of compounds including MDMA **(17)** and DOB **(35)**, whilst amphetamine **(10)** and methamphetamine **(14)** are named in Schedule II. The legislation is set up so that amendments can be made quickly and is updated very regularly. Amendments in 2014 include the placement of 10 synthetic cathinones into Schedule I (07/03/2014 - 79 FR 12938) and placement of 4 synthetic cannabinoids into Schedule I (10/02/2014 – 79 FR 7577).[63]

1.2.6.2 UK Legislation

The UK legislation today is based mainly on the *Misuse of Drugs Act, 1971*.[64] This Act replaced the *Dangerous Drugs Act, 1965* and the *Drugs (Prevention of Misuse) Act, 1964*. The *Misuse of Drugs Act, 1971* was introduced to "make new provision with respect to dangerous or otherwise harmful drugs and related matters and for purposes connected therewith".[64] Important amendments to this legislation, pertaining to compounds in the ATS class, include:[11]

- 1977 – Generic definition of phenethylamines introduced to the Misuse of Drugs Act. This captured a range of ring-substituted phenethylamines.
- 2001 – Further 35 phenethylamine-type compounds not captured by generic definition, were added by name.
- 2013 – Temporary generic legislation introduced that included a number of benzofurans, indanylalkylamines, and certain NBOMe compounds.

In the 1977 amendment to the *Misuse of Drugs Act*, Part I of Schedule 2, paragraph 1(c) defines Class A phenethylamines as: "any compound structurally derived from phenethylamine, an *N*-alkylphenethylamine, α-methylphenethylamine, an *N*-alkyl-α-methylphenethylamine, α-ethylphenethylamine, or an *N*-alkyl-α-ethylphenethylamine by substitution in the ring to any extent with alkyl, alkoxy, alkylenedioxy or halide substituents, whether or not further substitution in the ring by one or more other univalent substituents."

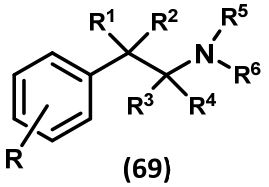
Under this definition, the following criteria must be satisfied in the structure **(69)** below:

R^5 = H or alkyl

$R^6 = R^3 = R^1 = R^2$ = H

R^4 = H, methyl or ethyl

R = alkyl, alkoxy, alkylenedioxy or halogen (either singly or in any combination) with or without any other univalent substituents in the ring



(69)

In Schedule 2 of this Act, controlled substances are grouped into 3 classes (A, B and C) with Class A being most harmful and carrying the harshest punishments. The legislation is very detailed in its specific naming of compounds; In Class A for example, more than 40 ATS are named including 4-bromo-2,5-dimethoxyamphetamine (DOB) **(35)**. Amphetamine **(10)** itself is included in Class B, whilst substances like cathinone **(54)** are found in Class C. The subsequent modification orders (1977 and 2001) have amended the legislation to keep up with emerging drugs of abuse.

1.2.6.3 Irish Legislation

Prior to the *Misuse of Drugs Act, 1977 and 1984*, a number of other acts were in existence to control the supply of drugs.[65,66] These include:

The Poisons Act, 1870

The Pharmacy Act, 1875

The Dangerous Drugs Act, 1934

The Medical Preparations (Control of sale) Regulations, 1966

The Medical Preparations (Control of Amphetamines) Regulations, 1969

Both of the *Medical Preparations Regulations* ('66 and '69) specifically named amphetamines and were introduced to prohibit the manufacture, sale and distribution of amphetamines and their derivatives. The *Misuse of Drugs Act, 1977 (No. 12/1977)* and *1984 (No. 18/1984)* were much more detailed pieces of legislation and describe controls relating to manufacture, cultivation, licensing, importation, administration, supply, possession with/without intent to supply, record keeping, documentation, prescription writing, destruction and safe custody of scheduled substances. New substances are not 'added' to a list, but are 'declared' by Government Declaration Orders to be equivalent to existing drugs under the *Misuse of Drugs Act*. Ireland uses a 'generic' system where possible, in which substances within a defined chemical 'family' are automatically considered controlled drugs.[67]

Back when they were first introduced, a major flaw within the *Misuse of Drugs Acts* was that all substances were placed into one category or schedule. This led to the re-classification of 'controlled drugs' in *The Misuse of Drugs Regulations, 1988 (S.I. No. 328/1988)*. This *Misuse of Drugs Regulations, 1988,* categorised controlled drugs into five Schedules. These Schedules classified drugs based on how 'dangerous' they were from a physical, social and mental health perspective as well as their potential for abuse. For example, drugs falling into Schedule 1 are deemed most 'dangerous' and are subject to more stringent controls.

Phenethylamines and their derivatives (ATS) fall under Schedules 1, 2, 3 and 4 of the *Misuse of Drugs Regulations, 1988* and are listed both by name and generically. For example, cathinone **(54)**, mescaline **(20)** and 4-methyl-2,5-dimethoxyamphetamine (DOM) **(32)** are named in Schedule 1, while amphetamine **(10)** is named in Schedule 2. The generic legislation covering ATS is found under paragraph 1 (c) of Schedule 1 and uses similar wording to that used in the UK legislation (*Misuse of Drugs Act, 1971* (1977 amendment)): "any substance structurally derived from phenethylamine, an *N*-alkylphenethylamine, α-methylphenethylamine, an *N*-alkyl-α-methylphenethylamine, α-ethylphenethylamine, or an *N*-alkyl-α-ethylphenethylamine by substitution in the ring to any extent with alkyl, alkoxy, alkylenedioxy or halide substituents, whether or not further substitution in the ring by one or more other univalent substituents."

A number of new amendments ("Statutory Instruments" (SI)) have been introduced since 1988 including the *Misuse of Drugs (Amendment) Regulations, 1993 (S.I. No. 342/1993)*, which cover substances like khat, 4-methylaminorex and *N*-hydroxy-3,4-methylenedioxyamphetamine, and also the *Misuse of Drugs (Amendment) Regulations Act, 2006 (S.I. No. 53/2006)* which, in response to a death due to 'magic mushrooms', psilocin or its esters and any substances, products, preparations or other fungi containing them, were designated controlled drugs.

In recent years, a series of drug-related legislative changes took place in response to the appearance of 'head shops' selling 'legal highs' *ca.* 2009.[59] Over 200 substances (both generic and specific) were controlled under the *Misuse of Drugs Act 1977 (Controlled Drugs) (Declaration) Order 2010 (S.I. No. 199/2010)*. Subsequently, the *Criminal Justice (Psychoactive Substances) Act (S.I. No. 401/2010)* was adopted in late 2010. This led to the number of 'head shops' falling from more than 113 to 19 during 2010, with the remaining outlets no longer selling such substances. The *Misuse of Drugs Act 1977 (Controlled Drugs) (Declaration) Order 2011 (S.I. No. 551/2011),* controlled 60 additional substances, including many cathinones and synthetic cannabinoids, in November 2011.

In a unexpected ruling by the Court of Appeal on March 10th 2015, the possession of many of the substances controlled under the *Misuse of Drugs Act 1977* (and subsequent amendments) was made 'legal'.[68] The possession of drugs such as MDMA, magic mushrooms and other psychoactive substances was deemed legal following the ruling that Section 2(2) of the Act (the provision empowering the

Government to declare substances as controlled) was unconstitutional. The Government quickly responded to this by producing the *Misuse of Drugs (Amendment) Bill 2015*,[69] signed into law by the President on the following evening of March 11th 2015. This bill allowed for two new paragraphs (1A and 1B) to be added to Schedule 1 of the *Misuse of Drugs Act 1977*, and for several of the Statutory Instruments specified in Schedule 2 to have "statutory effect as if it were an Act of the Oireachtas". As before, the possession of many psychoactive substances, including those previously available in 'head shops', is illegal in Ireland.

A historical look at legislation and control measures pertaining to drugs in Ireland, and a comparison to international and EU developments can be found in Figure 1.15.

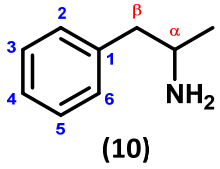
International and EU developments		National developments
	1934	Dangerous Drugs Act 1934
UN Single Convention on Narcotic Drugs	1961	
	1966	Report of the Commission of Inquiry on Mental Illness
UN Convention on Psychotropic Substances	1971	Report of the Working Party on Drug Abuse
	1973	Ireland joins the European Economic Community
	1977	Misuse of Drugs Act 1977
	1983	Report of Special Government Task Force on Drug Abuse
	1984	Misuse of Drugs Act 1984
UN Convention Against Illicit Trafficking in Narcotic Drugs and Psychotropic Substances	1988	
European Plan to Combat Drugs	1990	
	1991	Government Strategy to Prevent Drug Misuse
Report on the European Plan to Combat Drugs	1992	
EU Plan to Combat Drugs 1995–1999	1995	
	1996	First report of the Ministerial Task Force on Measures to Reduce the Demand for Drugs
	1997	Local drugs task forces become operational
UN General Assembly Special Session on the World Drug Problem	1998	
EU Drugs Strategy 2000–04 EU Action Plan on Drugs 2000–04	2000	National Advisory Committee on Drugs established
	2001	'Building on experience: national drugs strategy 2001–2008' launched
	2004	Mid-term review of the national drugs strategy
EU Drugs Strategy 2005–12 EU Drugs Action Plan 2005–08	2005	Regional drugs task forces become operational
	2007	Report of the Working Group on Drugs Rehabilitation
EU Drugs Action Plan 2009–12	2009	National Drugs Strategy (interim), 2009–16 launched
	2010	Criminal Justice (Psychoactive Substances) Act 2010 becomes law
	2012	Steering group report on a national substance misuse strategy

Figure 1.15: Irish National drug policy developments *vs*. international and EU developments[67]

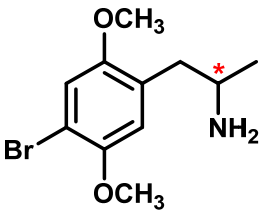
1.2.7 DOB and the '2,5-dimethoxy' class of amphetamines

The amphetamine DOB (4-bromo-2,5-dimethoxyamphetamine) **(35)** became of interest to our research group following large seizures of the drug in Ireland between 2003 and 2005. It is deemed a 'designer drug', a compound based on illicit amphetamine **(10)** but structurally modified to yield a compound with a very different pharmacological response. These modifications often yield compounds that do not fall under existing legislation and thus are deemed 'legal'. DOB was first synthesised in 1967 by Alexander Shulgin and first reported in the literature in 1971.[20] Together with many other novel phenethylamines/amphetamines, it was later published in Shulgin's controversial book PiHKAL.[12]

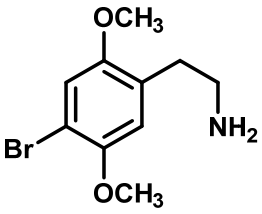
DOB **(35)** differs in structure from amphetamine **(10)** in the substitution pattern of the phenyl ring. DOB **(35)** has methoxy groups at the 2- and 5-positions and a Br atom at the 4-position of the aromatic ring.



(10)



(35)



(18)

DOB belongs to a subclass of amphetamines known as the '2,5-dimethoxy' class, sometimes referred to as the 'D series'.[2] Replacement of the Br atom, at the aromatic 4-position of DOB, with other atoms or groups, gives rise to several other 'D series' compounds. Examples of a few of these are shown in Table 1.6:

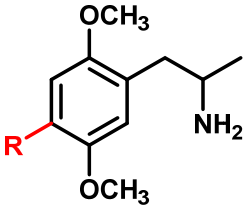


Table 1.6: Examples of 'D series' amphetamines

Entry	R	Common name
(35)	Br	**DOB**
(34)	OCH_3	**TMA-2**
(37)	I	**DOI**
(36)	Cl	**DOC**
(32)	CH_3	**DOM**
(70)	NO_2	**DON**

As mentioned previously, methoxy groups at the 2- and 5-positions increase the hallucinogenic potency (relative to ring-unsubstituted analogues) and a hydrophobic group in the aromatic 4-position (e.g. bromine) resists the drug to oxidative metabolism, thus extending its bioavailability.[15] DOB, having an

α-methyl group on the side chain, is an amphetamine and lasts much longer in the body than its phenethylamine counterpart 2C-B **(18)**.[70] The α-methyl group affords increased potency *in vivo* and results in a longer duration of action.[71] DOB has one stereogenic centre giving rise to two enantiomers. As with most of the hallucinogenic amphetamines, the *R*-enantiomer of DOB is more active than the *S*-enantiomer, although most illicit samples are made up of racemic mixtures. No specific study has fully evaluated the potency of the *S*-enantiomer, however the *R*-enantiomer is thought to be roughly twice as potent as the racemic mixture (Effective hallucinogenic dose for *R*-enantiomer = 1–1.5 mg *vs.* 1–3 mg for the racemate).[27]

With a typical human dose of 1–3 mg, DOB is one of the most potent hallucinogenic members of the amphetamine family. It has a relatively slow onset of action of up to 3 h which greatly increases the danger of accidental overdose.[72] The drug also has a relatively long half-life, with its duration of action between 18 and 30 h.[12] At low doses (0.4 mg), one experiences a distinct enhancement of visual perception, a strengthening of colours and a general feeling of well-being. At higher doses (2.8 mg) there is a feeling of near loss of consciousness and optical hallucinations. Typical symptoms of acute intoxication include convulsions, articular vascular spasms, vomiting, diarrhoea, tingling in the limbs and psychosis with restlessness. Deaths due to DOB intoxication have been reported in the literature.[73-75] In one case, a 21 year old female was found to have ingested at least 9.3 mg of DOB.

DOB is both a stimulant and a hallucinogen. The hallucinogenic effects of DOB have been attributed to 5-HT_{2A} and 5-HT_{2C} receptor agonism, binding in a similar fashion to the benzodifuran-based hallucinogenic amphetamine depicted previously in Figure 1.4. Following intravenous administration, DOB accumulates quickly in the lungs, reaches maximum concentration in the liver in 0.5–1.5 h, in the plasma after 2–3 h and finally in the brain after 3–6 h.[76] Similar results are observed when DOB is orally ingested, however the initial accumulation in the lungs is not observed. Metabolism of DOB has not been fully investigated in humans but many animal studies have been carried out. In a study of the metabolism of DOB in rats,[77] metabolic pathways identified include *O*-demethylation followed by oxidative deamination to the corresponding ketone, as well as deamination followed by reduction to the corresponding alcohol. This pathway appears to be followed in humans too as studies have shown that the 5-*O*-desmethyl metabolite of DOB (2-methoxy-5-hydroxy-4-bromoamphetamine) is the most common metabolite in human urine following ingestion of the drug. The results from the rat pharmacokinetic study appear to reflect the long lasting effects experienced by humans, with slow elimination (up to 32 h) in rats models. Other metabolic pathways identified were *O*,*O*-bisdemethylation, or hydroxylation of the side chain followed by *O*-demethylation and deamination to the corresponding alcohol.[70,71] The metabolism of DOB in rats was proposed in a paper by Ewald *et al*.[71] and is outlined in Figure 1.16.

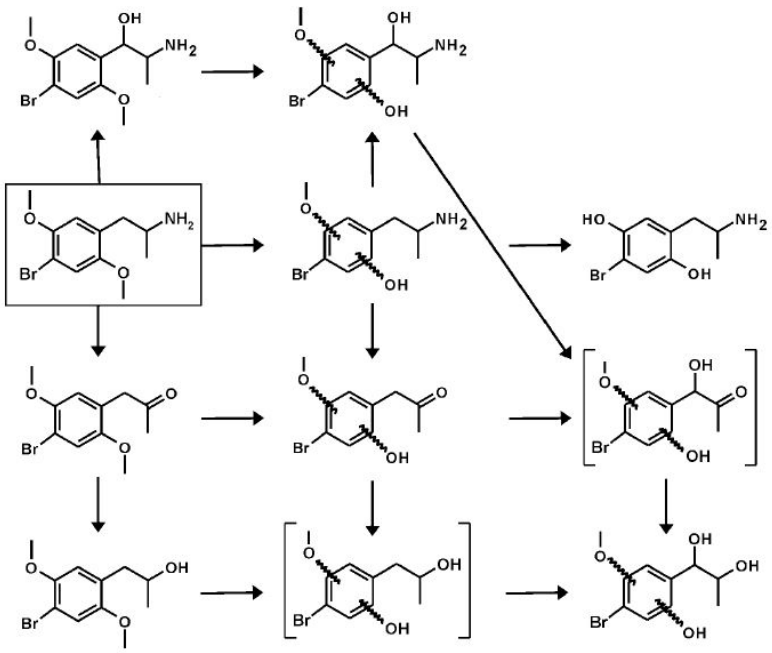


Figure 1.16: Proposed scheme for the metabolism of DOB in rats[71]

On the street DOB is also referred to as “brolamphetamine”, “bromo-DMA”, “bromo”, “golden eagle”, “LSD-25”, “snowballs” and “super ecstasy”. It can be found in tablet form, powdered or on blotting paper (Figure 1.17).

The earliest reported seizure of DOB took place in 1976 in Australia. In 1982, a number of patients were admitted to hospital in Sydney with suspected DOB toxicity.[75] DOB was also reported on the street in Germany in 1981.[78] Once again in the 1990’s, following release of PiHKAL in 1991, DOB became problematic, with use most notable in Australia, US and Italy.[16,71] The DEA in the US keeps track of seizures of emerging drugs of abuse and between 2005 and 2009, six seizures of DOB were reported in their monthly bulletins.[79] In all of these cases DOB was found on blotting paper that mimicked the type of blotting paper in which LSD **(5)** is usually impregnated (Figure 1.17).



Figures 1.17: Powdered DOB (left) and DOB impregnated onto blotter paper (right)[80,81]

Sporadic seizures of DOB have been occurring worldwide in recent years. A number of seizures of DOB were reported by An Garda Siochana in Ireland between 2003 and 2005 according to their Annual Reports.[45-47] The largest seizure of DOB was reported in 2003, with 82,000 tablets seized in Dublin. There were also reports of the drug being used in Cork, Limerick, Tipperary, Mayo and Galway.[82,83] The seizures sparked numerous health warnings (Figure 1.18), as the drug was being sold as MDMA on the street.

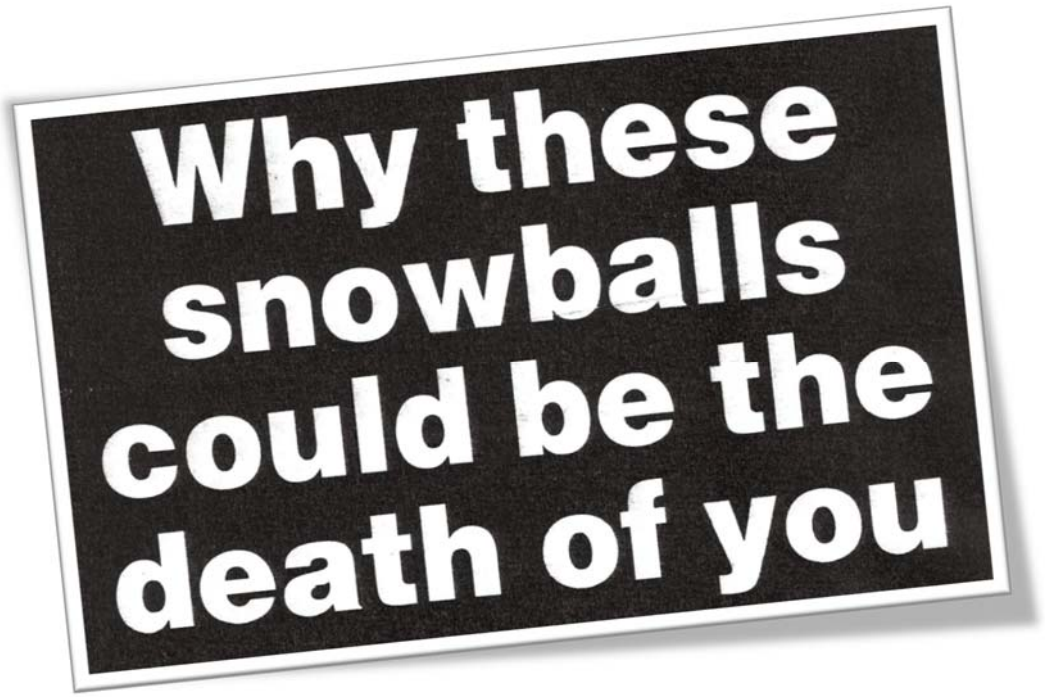
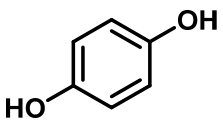


Figure 1.18: Headline from Cork newspaper 'Evening Echo' amid public warnings about DOB[84]

Given that the effective and lethal doses of DOB are much lower than those of MDMA, the risk of accidental overdose is quite high. The hallucinogenic effect of DOB also caused public anxiety with many cases of psychotic episodes reported. One case in Galway reported a man driving into a wall while under its influence, whilst another case involved a man removing his eye during a period of drug-induced psychosis.[83] The popularity of the drug in Ireland then quickly dropped off after this with 816 tablets seized in 2004 and 30 tablets seized in 2005.[46,47] Apparently there have been very small seizures since, but these have not been included in any of the Garda Annual Reports, as DOB may be listed with the figures for 'ecstasy'.[85] One such seizure was reported by the EMCDDA (5 tablets seized in Ireland in 2007).[86] However, this figure was not reported in the 2007 Annual Report by the Gardaí (Table 1.4).[49]

There have been very few reports pertaining to the clandestine manufacture of DOB and the synthetic routes employed. In a paper by Delliou *et al.*, reference is made to 2 clandestine laboratories involved in DOB manufacture.[87] One of the laboratories, detected in the UK in 1981, manufactured DOB *via* an 8-step synthesis starting with hydroquinone **(71)**.



(71)

Another laboratory, discovered in Victoria, Australia in 1980, synthesised DOB using the starting material (SM) 2,5-dimethoxybenzaldehyde **(72)**. The SM **(72)** was converted to the β-nitrostyrene **(73)** *via* the Henry reaction, followed by $LiAlH_4$ reduction to DMA **(31)**. Bromination of DMA **(31)**, using bromine liquid in acetic acid, yielded DOB **(35)**. This route would be expected to be one of the most common routes of manufacture of DOB, as this is the route outlined in PiHKAL (Figure 1.19).[12]

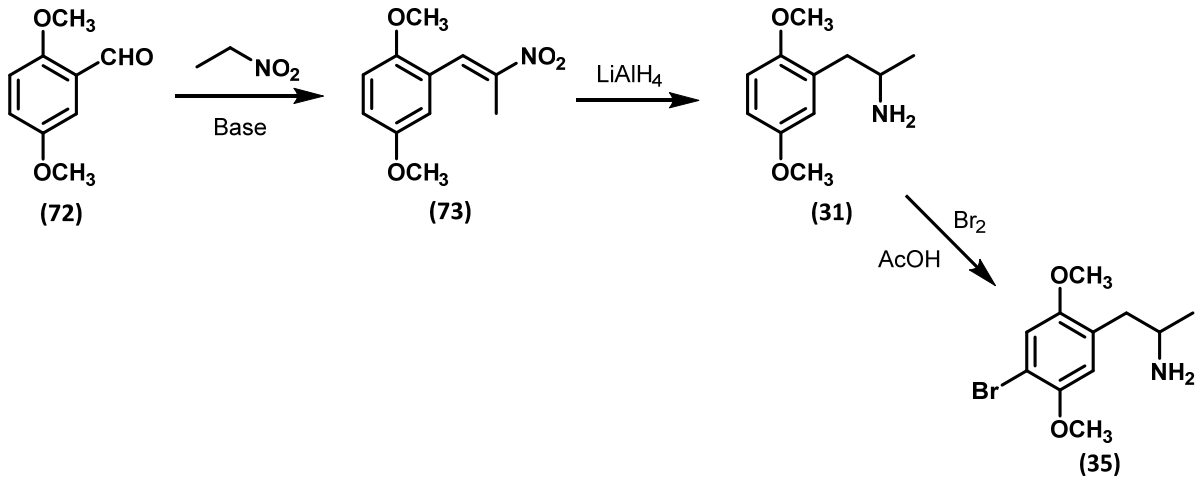


Figure 1.19: Synthetic methodology used to manufacture DOB in a clandestine laboratory detected in Australia, 1980[87]

DOB is probably synthesised by a number of other routes also, as there are many methods of general amphetamine manufacture reported in the literature. These routes will be discussed in Section 1.5.

DOB is a controlled substance in many countries. It was controlled in Ireland under the *Misuse of Drugs Regulations, 1988* (S.I. No. 328/1988), under Schedule 1, paragraph (c) and generically fell under "any substance…structurally derived from phenethylamine... α-methylphenethylamine… by substitution in the ring to any extent with alkyl, alkoxy, alkylenedioxy or halide substituents." It is now controlled under the *Misuse of Drugs (Amendment) Act, 2015*.

In the UK, DOB is specifically named under the *Misuse of Drugs Act, 1971*, Schedule 2, Part 1, Class A (a) but would also fall under part (c), generic legislation similar to that used in Ireland.

In the US, DOB is also named in the *Controlled Substances Act, 1970*, Schedule 1, (d) under "Hallucinogenic substances".

DOB has been analysed by a number of different methods since its first seizure in the 1970's. Overleaf is a summary of some of the literature pertaining to the analytical and spectroscopic analyses of DOB:

- Presumptive test (Marquis reagent) – colour obtained for positive result is first yellow, then turns green.[13,70,88]
- DOB analysed by High Performance TLC (HPTLC), Capillary Zone Electrophoresis (CZE), FTIR, MS and MS/MS by da Costa *et al*.[70]
- Recommended methods for ATS analysis by the UNODC[13] provides Retardation Factor (R_f) values for TLC using a variety of different solvent systems.
- Bell *et al.* has analysed DOB using a rapid method of Surface-Enhanced Raman Spectroscopy (SERS) as an alternative to presumptive colour testing.[72] It is suggested that the low required dose for DOB may not be enough to induce a visible colour change. The 'SERS' method has a detection limit much lower than the active pharmacological dose.
- Kanai *et al.* analysed DOB against a number of related ATS.[89] TLC, IR and ^{1}H-NMR data is given as well as optimised conditions for analysis by GC-MS and LC-MS.

1.3 Impurity profiling

Clandestine manufactured drugs rarely incorporate any form of quality control, with poor purification of products and poor chemical handing. As a result of this, the chemical composition can be highly variable and the final drug product is often a complex mixture of substances.[90] The impurities that arise in the illicit drug can be in the form of inorganic impurities (such as trace metals), natural components, cutting agents (used to dilute active ingredient), residual solvents and organic impurities. It is the organic impurities that are of interest to our research group. The organic impurities encountered are often in the form of residual starting materials from incomplete reaction steps and by-products formed *in situ* from side reactions. The impurities that arise (and their quantities) are dependent on a number of different factors and these include:

- The starting materials used (and their purity)
- The skill level of the manufacturer
- The degree of purification carried out in each step of the process of drug manufacture
- The synthetic route(s) employed to manufacture the drug
- The processing, formulation and storage of the drug post synthesis

Given the number of variables, in terms of how the drug is made, no two batches of illicit drugs will be exactly the same, so each batch is likely to have a unique range (and quantity) of impurities. It is this range of impurities that makes up the 'impurity profile' of a particular batch and acts as a chemical fingerprint. By establishing the impurity profile, the analyst may get a 'history' of the sample, and use this information as a powerful intelligence tool. Drug profiling has been defined as "the extraction of

chosen physical and/or chemical characteristics from the samples and their use as intelligence in the fight against illegal drug trafficking".[91]

The intelligence that can be gained from drug characterisation has been outlined in a report by the UNODC on impurity profiling.[90] The ways in which this information can be used to aid law enforcement include:[92,93]

1. ***Establishing specific links between two or more samples***
   By linking samples based on their impurity profiles the analyst can help link different batches and establish links between suppliers.
2. ***Establishing drug distribution patterns***
   By placing related samples into distinct groups, these groups can then be used to represent different laboratories or different drug related organisations. This would provide useful information in relation to trafficking patterns and distribution networks.
3. ***Identifying the source of drug samples***
   Samples that have been deemed to be related, based on their impurity profiles, may be sourced back to a particular geographical location. This is made much easier when unique starting materials, methods or cutting agents are used that are characteristic of a specific laboratory or region.
4. ***Monitoring methods used for clandestine drug manufacture***
   Examining the impurity profiles can provide information on the synthetic methodology, reaction conditions and chemicals used. This information can be used by law enforcement agencies to identify new target compounds used in clandestine manufacture. Given this intelligence, the agencies can then introduce new controls for precursor chemicals. Route specific impurities (those arising only when a specific route is employed) are particularly useful in determining the mode of synthesis and therefore the precursors used.

The intelligence gathered from impurity profiles may be used by international agencies such as Interpol, Europol, UNODC and EMCDDA. In recent years EU agencies in particular, have been trying to harmonise methods and approaches to impurity profiling and have been encouraging collaborations between laboratories through initiatives like 'CHAIN' and 'CHAMP'. These were discussed in more detail in Section 1.2.6.

There are two main approaches to organic impurity profiling:

Approach 1: The direct analysis of a street sample of an illicit drug.
Approach 2: The controlled synthesis and identification of impurities.

1.3.1 Impurity profiling *via* the direct analysis of a street sample of an illicit drug

A range of chromatographic and spectroscopic techniques are used in this approach.[13] Presumptive tests are often carried out first to determine the main illicit constituent of the sample. These include colour tests, anion tests and microcrystal tests:

- Colour tests: Treatment of a small amount of the drug sample with specified reagents results in a colour change, indicating presence of drug. E.g. Marquis test – used to distinguish between amphetamine and ring-substituted analogues.
- Anion test: Used to indicate which salt of a drug (e.g. sulphate, phosphate) is present based on the reaction with a reagent (e.g. silver nitrate) and the subsequent presence or absence, and solubility, of a precipitate.
- Microcrystal test: Involves the formation of crystals from the reaction of the target compound with a chemical reagent, followed by the analysis of the resulting crystals by means of a polarising microscope and comparison with a reference material, usually photographs of known crystals.

This is then followed by Thin Layer Chromatography (TLC) and more advanced chromatographic methods such as Gas Chromatography (GC), High Performance Liquid Chromatography (HPLC) and Capillary Electrophoresis (CE). In many recent publications hyphenated analytical technologies have been employed.[94] This technology couples modern chromatographic separation techniques to a spectroscopic technique, allowing for the simultaneous separation of analytes and determination of their structural features. Modern hyphenated methods combine LC, GC and CE with structure elucidation methods like Mass Spectrometry (MS), Nuclear Magnetic Resonance (NMR) spectroscopy, Fourier Transform InfraRed (FTIR) spectroscopy and Atomic Absorption Spectroscopy (AAS). Figure 1.20 outlines the many ways in which these methods can be combined.

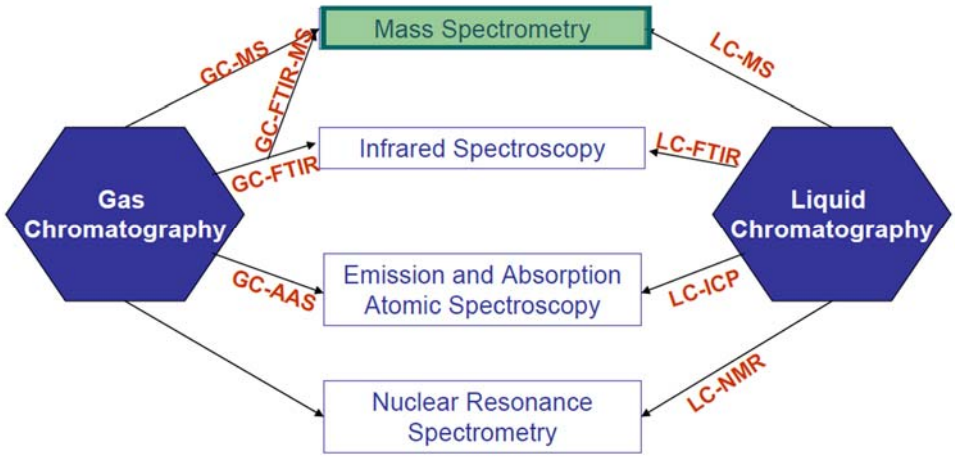


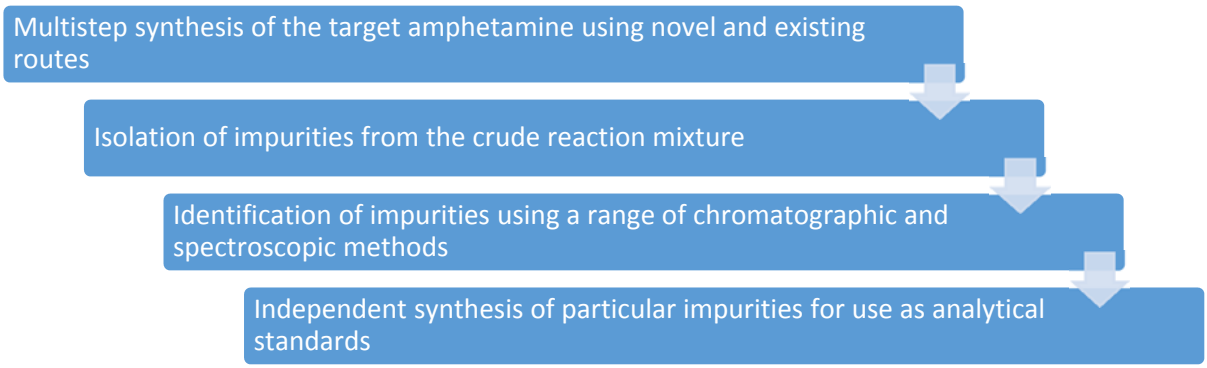
Figure 1.20: Hyphenated analytical technologies[95]

Other methods employed in impurity profiling include:[96]

- Isotope analysis – The abundance of isotopes of elements, such as carbon and nitrogen, can vary due to environmental effects. By comparing $^{13}C/^{12}C$ and $^{15}N/^{14}N$ isotopic ratios, illicit drugs have been linked based on their geographical origin. This method is mainly used for plant based/natural drugs.
- Raman spectroscopy – Using Raman spectroscopy, it has been possible to differentiate the spectra of illicit substances based on differences in the position of the vibrational bands. Also, the spectra can distinguish different hydrated forms of the drug, which could be used to link seizures to a common batch.
- Elemental analysis – Techniques used in impurity profiling, which can detect the levels of individual elements include ElectroThermal AAS (ET-AAS), flame AAS, Inductively coupled plasma (ICP) AAS and Ion Chromatography (IC).
- Statistical and chemometric analysis – When dealing with large volumes of data following chemical analysis, computer based methods can be used to interpret the data and link related batches. These programs include Principle Component analysis (PCA), Hierarchical Cluster Analysis (HCA), Linear Discriminant Analysis (LDA) and Artificial Neural Networks (ANN). These statistical approaches are gaining popularity now that sufficient amounts of data are being generated on impurity profiles of illicit drugs.[60,97,98]

1.3.2. Impurity profiling *via* the controlled synthesis and identification of impurities produced

The second approach to impurity profiling, involving the controlled synthesis and subsequent identification of impurities, is the main focus of our research group. The methodology of this approach involves:



The two approaches to impurity profiling are complementary. Identifying the impurities in an illicit sample is just one aspect. Knowing how they arise is equally important especially in relation to 'route specific' impurities.

In attempting to assess the route of manufacture of a seized drug, emphasis is often put on what are known as 'route specific' impurities. These are impurities that are thought to arise as by-products from a particular method/route of manufacture. The advantage of this, in theory, is that the presence of the particular impurity could indicate the route employed. Publications in recent years however have proven that assigning the 'route specific' label to a particular impurity should be tentative. It appears that a given impurity is only route specific until proven otherwise; in many cases subsequent studies have shown that the impurity labelled 'route specific' arises also in other methods of manufacture.[93] Examples of a number of 'characteristic' impurities arising from various methods of manufacture, for several ATS, were summarised by Stojanovska *et al.* and are shown in Table 1.7.

Table 1.7: 'Characteristic' impurities from various synthetic routes to several ATS[99]

Compound	Synthetic route	Characteristic contaminants
Methamphetamine	Reductive amination	1-Phenyl-2-propanol, amphetamine , 1,3-diphenyl-2-methylaminopropane , *N*-cyanomethyl-N-methyl-1-phenyl-2-propylamine
	Nagai	(2*E*)-*N*-Methyl-3-phenyl-*N*-(1-phenylpropan-2-yl)prop-2-enamide (cis-cinnamoyl derivative of Methamphetamine) , iodoephedrine , *N*-methyl-*N*-(α-methylphenyl)amino-1-phenyl-2-propanone , (*Z*)-*N*-methyl-*N*-(α-methylphenylethyl)-3-phenylpropanamide
	Emde	Chloroephedrine/chloropseudoephedrine , methylephedrine , *N*-formylephedrine , *N*-acetylephedrine, *N*,*O*-diacetylephedrine , *N*-acetylamphetamine
	Birch	1-(1,4-Cyclohexadienyl)-2-methylaminopropane
	Leuckart	α-Benzyl-*N*-methylphenethylamine , α,α^0-dimethyldiphenethylamine , *N*-α,α^0-trimethyldiphenylamine
MDMA	Reductive amination	3,4-Methylenedioxy-*N*-methylbenzylamine , 4-methyl-5-(3,4-methylenedioxyphenyl)-[1,3]-dioxolan-2-one , *N*-methyl-2-methoxy-1-methyl-2-(3,4-methylenedioxyphenyl)-ethanamine , *N*-cyclohexylacetamine , 1,2-methylenedioxy-4-(2-*N*-methyliminopropyl)benzene , *N*-cyanomethyl-*N*-methyl-1-(3,4-methylenedioxyphenyl)-2-propylamine , *N*,*N*-di-[1-(3,4-methylenedioxy)phenyl-2-propyl]methylamine (MDMA dimer)
	Leuckart	*p*-Bromotoluene , *N*-ethylamphetamine , *N*-ethylmethamphetamine , *N*-formylamphetamine , *N*-formyl-MDMA , 5-(1,3-benzodioxol-5-ylmethyl)pyrimidine , 3,4-bis-(1,3-benzodioxol-5-ylmethyl)pyridine
	Wacker oxidation	1-(3,4-Methylenedioxyphenyl)-1-methoxy-2-propanone , methyl-3-(3,4-ethylenedioxyphenyl)-propanoate , 1-(3,4-methylenedioxyphenyl)-1,3-dimethoxypropane , 3-(3,4-ethylenedioxyphenyl)-1,1-dimethoxypropane , 1-(3,4-methylenedioxyphenyl)-1-methoxypropane
	Peracid oxidation	2,4-Dimethyl-3,4-bis(3,4-methylenedioxyphenyl)tetrahydrofuran , 1-(3,4-dimethoxyphenyl)-2-propanone , 1-(3,4-methylenedioxyphenyl)-1-propanone , 2,2,4-trimethyl-5-(3,4-methylenedioxyphenyl)-[1,3]-dioxolane , 1-(3,4-methylenedioxyphenyl)- 1,2-propanedione , 1-methoxy-1-(3,4-methylenedioxyphenyl)-2-propanol
Amphetamine	Emde	Chloronorpseudoephedrine/chloronorephedrine

	Birch	1-(1,4-Cyclohexadienyl)-aminopropane
	Leuckart	α-Benzylphenylethylamineformamide , 4-benzylpyrimidine , 4-methyl-5-phenyl-pyrimidine , 2,4-dimethyl-3,5-diphenylpyridine , 2,6-dimethyl-3,5-diphenylpyridine
DMA	Nitrostyrene	(2-Nitroprop-1-enyl)benzene , benzyl methyl ketoxime , *N*-(β-phenylisopropyl)benzaldime
	Nagai	1-Propenylbenzene , 2-propenylbenzene
	Emde	Chloromethylephedrine/chloromethylpseudoephedrine , 1-dimethylamino-1-phenyl-2-chloropropane
	Birch	1-(1,4-Cyclohexadienyl)-2,2-dimethylaminopropane
PMA	Leuckart	4-(4-Methoxybenzyl)pyrimidine , 4-methyl-5-(4-methoxyphenyl)pyrimidine , 2,4-dimethyl-3,5-di-(4-methoxyphenyl)pyridine , 2,6-dimethyl-3,4-di-(4-methoxyphenyl)pyridine
	Peracid oxidation	4-Methoxyphenol

Unlike the first approach, the second approach to impurity profiling (controlled synthesis and isolation of impurities) allows for pure samples of the impurity to be obtained (or in some cases, selectively synthesised if full isolation is not achieved). These pure samples may then be fully characterised, and their analytical and spectroscopic data (^{1}H-NMR, ^{13}C-NMR etc.) made available to the research community. Availability of these standards, especially for previously unknown compounds, is very important. Standards are needed for chromatographic method development.[100,101] Also, with the arrival of new designer drugs, identification of unknowns is made more difficult when a standard is not available. Traditional forensic chemistry analysis relies on the comparison of an 'unknown' with reference materials.[31] Aside from newly emerging designer drugs, positional isomers of known compounds are also difficult to distinguish (based on MS alone) without the availability of standards and their analytical and spectroscopic data.[102] This highlights the need for reference materials and their full spectroscopic data in order to fully determine the molecular structure of the 'unknown'.

Aside from use as reference materials for comparison purposes, isolation of impurities may also be useful in terms of toxicity or biological testing. Not much work has been carried out to date on the potential toxicity of impurities of ATS. It may be that a particular impurity is much more toxic than the intended active compound. A preliminary study by Finnon *et al.*[103] showed that 'home made' amphetamine becomes toxic to cells at half the concentration of pure amphetamine (purchased from Sigma), possibly suggesting that one or more impurities present at low levels, may be much more toxic than the active ingredient amphetamine.

To date, impurity profiling been put into practice for many of the best known drugs of abuse including MDMA **(17)**,[91,104-109] heroin **(8)**,[110] amphetamine **(10)**,[98,111] methamphetamine **(14)**[60,92,93,112] and cocaine **(9)**.[97,113]

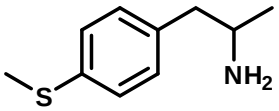
1.3.3 Impurity profiling – Case studies

The following Sections (1.3.3.1 and 1.3.3.2) outline two case studies on the impurity profiling of:

1. A ring-substituted amphetamine – 4-MTA **(30)**
2. MDMA **(17)**

1.3.3.1 Impurity profiling of 4-MTA (30)

Blachut *et al.*[114] carried out the synthesis of 4-MTA **(30)** *via* a number of different variations of the Leuckart method, identified the impurities present based on their MS profiles, and for some novel impurities, carried out their independent synthesis for use as reference standards.



(30)

Figure 1.21 shows the chemical structures of some of the impurities identified in 4-MTA **(30)**, produced using several variations of the Leuckart route. These variations include the "formamide" method, the "formamide/formic acid" method, the "ammonium formate" method and the "ammonium formate/formic acid" method.

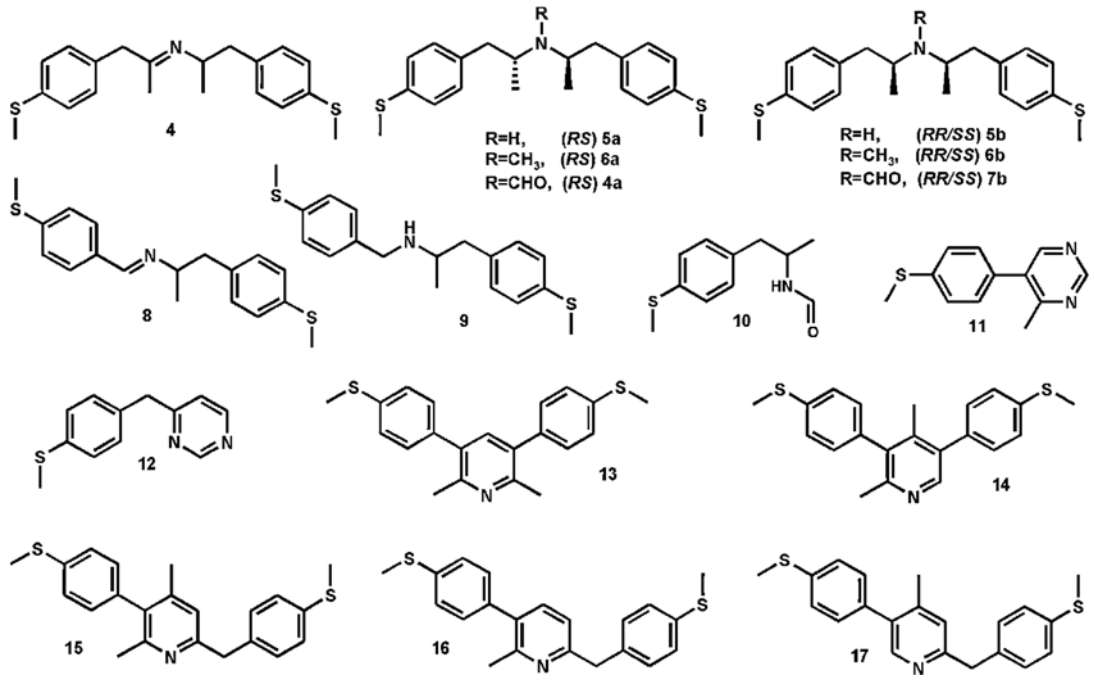


Figure 1.21: Chemical structures of impurities found in 4-MTA (30) synthesised by the Leuckart route[114]

In Figure 1.22 is shown one of the Total Ion Count (TIC) chromatograms (acquired using GC-MS) reported in this study. This specific TIC chromatogram illustrates the impurity profile of a sample of crude 4-MTA **(30)** produced using the "formamide" Leuckart method.

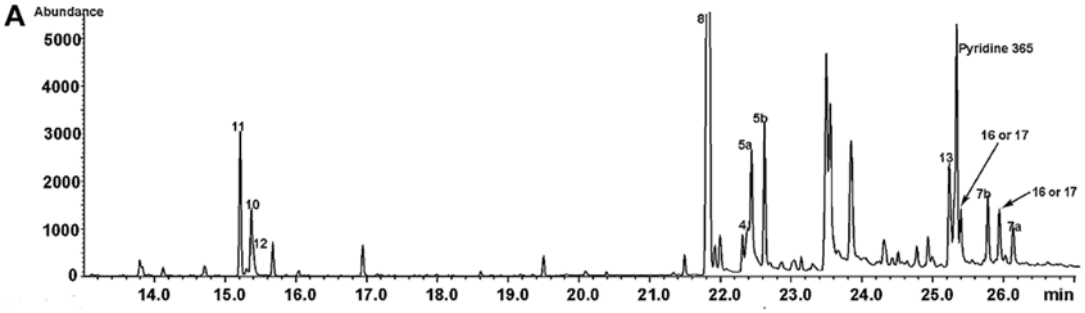


Figure 1.22: TIC chromatogram ('impurity profile') of crude 4-MTA (30)[114]

Table 1.8 outlines the most significant impurities identified in this study, their potential origin and whether or not the impurity was deemed 'route specific'. As well as the 'route specific' markers, Blachut and co-workers were able to identify relationships between the reagent/reagent combinations used and the dominant impurities encountered, with these relationships having some potential in identifying the method of manufacture. For example, when the "formamide" method was used, the presence of pyridine and pyrimidine derivatives was significant. In contrast, when the "ammonium formate" method was used, the quantity of these heterocycles significantly decreased, with the *N*,*N*-di-[β-(4-methylthiophenyl)isopropyl]formamide diastereoisomers **7a**/**7b** (see Table 1.8) being identified as the main by-products.

Table 1.8: Table of impurities identified in 4-MTA (30)[114]

Compound name	Retention time [min]	Molecular formula	Molecular mass	Remarks
4-Methyl-5-(4′-methylthiophenyl)pyrimidine **11**	15.20	$C_{12}H_{12}N_2S$	216	Synthetic route marker
N-formyl-4-methylthioamphetamine **10**	15.37	$C_{11}H_{15}NSO$	209	Intermediate product
4-(4′-Methylthiobenzyl)pyrimidine **12**	~15.40	$C_{12}H_{12}N_2S$	216	Synthetic route marker (coelution with **10**)
N-(1-methyl-2-[4-(methylthio)phenyl]ethyl)-*N*-([4-(methylthio) phenyl]methylene)amine (benzaldimine **8**)	21.80	$C_{18}H_{21}NS_2$	315	Origin: condensation between 4-MTA and 4-methylthiobenzaldehyde
N-(1-methyl-2-[4-(methylthio)phenyl]ethyl)-*N*-[4-(methylthio) benzyl]amine **9**	22.05	$C_{18}H_{23}NS_2$	317	Origin: reduction of **8**
N-[2-(4-methylthiophenyl)-1-methylethyl]-*N*-[2-(4-methylthiophenyl) -1-methylethylidene]amine (ketoimine **4**)	22.33	$C_{20}H_{25}NS_2$	343	Origin: condensation between 4-MTA and 4-methylthiophenylacetone
(*RS*) *N*,*N*-di-[β-(4-methylthiophenyl)isopropyl]amine **5a**	22.40	$C_{20}H_{27}NS_2$	345	Origin: reduction of **4**
(*RR*/*SS*) *N*,*N*-di-[β-(4-methylthiophenyl)isopropyl]amine **5b**	22.59	$C_{20}H_{27}NS_2$	345	Origin: reduction of **4**
(*RR*/*SS*) *N*,*N*-di-[β-(4-methylthiophenyl)isopropyl]methylamine **6b**	23.66	$C_{21}H_{29}NS_2$	359	Origin: reduction of **7b**
(*R*/*S*) *N*,*N*-di-[β-(4-methylthiophenyl)isopropyl]methylamine **6a**	27.73	$C_{21}H_{29}NS_2$	359	Origin: reduction of **7a**
2,6-Dimethyl-3,5-di-(4′-methylthiophenyl)pyridine **13**	25.18	$C_{21}H_{21}NS_2$	351	Synthetic route marker
Pyridine with molecular mass 365	~25.21	$C_{22}H_{23}NS_2$	365	Coelution with **13**, possible structure **15**
2,4-Dimethyl-3,5-di-(4′-methylthiophenyl)pyridine **14**	25.26	$C_{21}H_{21}NS_2$	351	Coelution with unknown pyridine 365, synthetic route marker
Pyridine with molecular mass 365	25.29	$C_{22}H_{23}NS_2$	365	Coelution with **14**, possible structure **15**
4 or 6-Methyl derivative of 2-(4-methylthiobenzyl) -5-(4-methylthiophenyl)pyridine (**16** or **17**)[a]	25.35	$C_{21}H_{21}NS_2$	351	Synthetic route marker
(*RR*/*SS*) *N*,*N*-di-[β-(4-methylthiophenyl)isopropyl]formamide **7b**	25.74	$C_{21}H_{27}NOS_2$	373	Origin: formylation of **5b** synthetic route marker
4 or 6-Methyl derivative of 2-(4-methylthiobenzyl) -5-(4-methylthiophenyl)pyridine (**16** or **17**)[a]	25.90	$C_{21}H_{21}NS_2$	351	Synthetic route marker
(*RS*) *N*,*N*-di-[β-(4-methylthiophenyl)isopropyl]formamide **7a**	26.09	$C_{21}H_{27}NOS_2$	373	Origin: formylation of **5a** synthetic route marker

1.3.3.2 Impurity profiling of MDMA (17)

In a study by Swist *et al.* in 2005,[108] MDMA was synthesised by 5 different synthetic routes: by dissolving metal reduction (Al/Hg), cyanoborohydride reduction ($NaCNBH_3$), borohydride ($NaBH_4$) reduction at low temperature, Leuckart reaction and safrole bromination. The crude reaction mixtures were analysed by GC-MS and the impurities were identified. Some of the impurities (both commonly encountered and route specific) from the Leuckart reaction, reductive amination (by Al/Hg, $NaCNBH_3$ and $NaBH_4$ methods) and safrole bromination routes from this study, are shown in Figure 1.23.

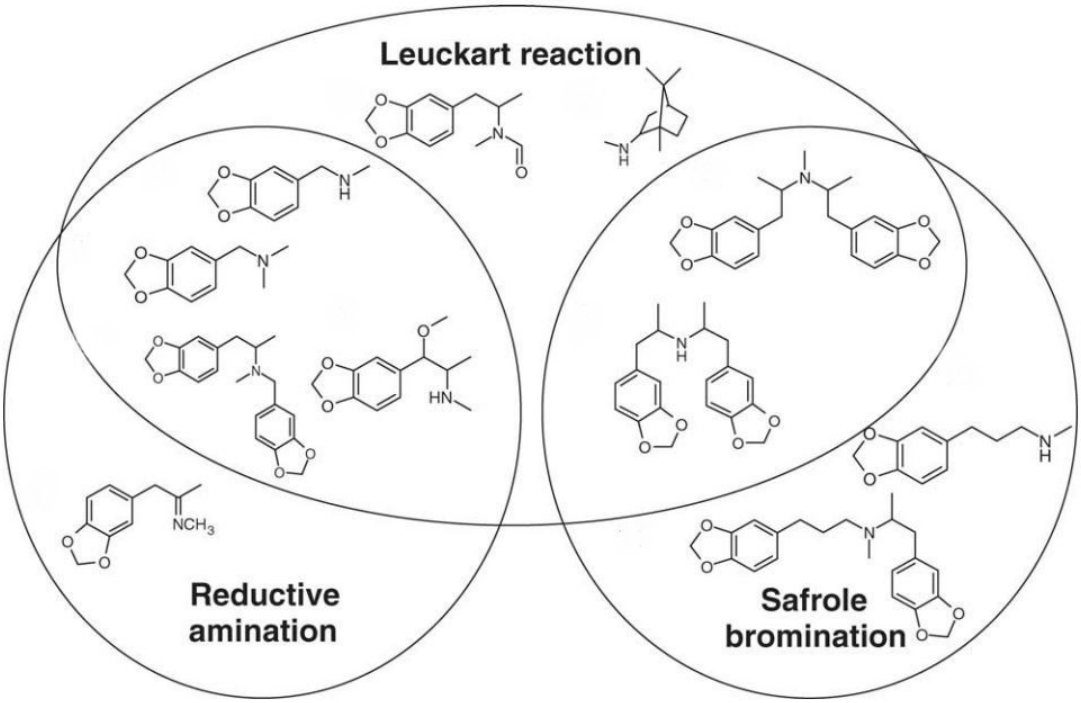
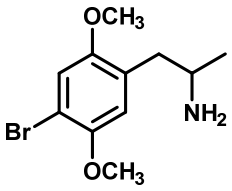
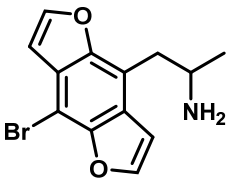


Figure 1.23: Impurity profiling of MDMA[108]

Little work has been carried out to date on the impurity profiling of the relatively new hallucinogenic range of amphetamines. These compounds are of great concern given their behavioural effects and high potency. Within our research group, work is being carried out on the impurity profiling of two hallucinogenic amphetamines: 4-bromo-2,5-dimethoxyamphetamine (DOB) **(35)** and Bromo-DragonFLY **(74)**.



(35)



(74)

The impurity profiling carried out in this body of work will focus mainly on the hallucinogenic amphetamine DOB, its ketone precursor and related non-bromo ketone precursor.

1.4 Clandestine laboratories and ATS manufacture

Clandestine drug manufacture can be defined as "the illegal manufacture, compounding or processing of narcotic, stimulant, hallucinogenic or depressant drugs".[115] Clandestine laboratories can vary greatly in size, complexity and skill level of the chemist/operator involved. In general, clandestine laboratories can be classified as either small scale, medium scale or large scale.

Small scale or 'kitchen laboratories' are those often found in small garages, kitchens, cupboards and even in disused cars (Figure 1.24). The skill level of the operator is usually limited; the operator often following 'cookbook' directions. Improvised equipment and containers are used and the small scale of product recovered, means that production is usually intended for personal use only. In Europe, small scale laboratories for production of ATS are most common in Czech Republic, Estonia, Germany, Lithuania, Poland and the UK.[58]

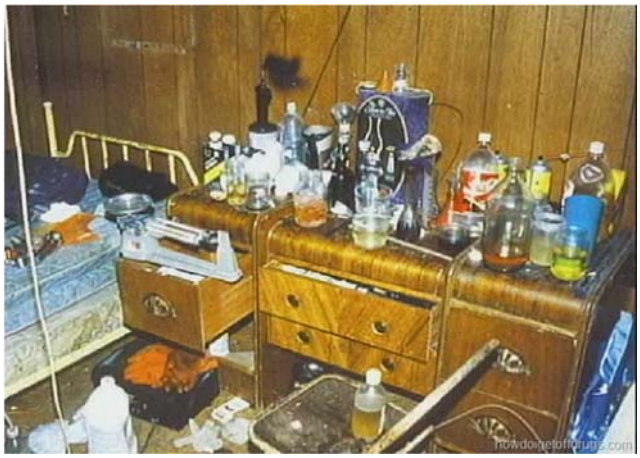


Figure 1.24: Small scale 'kitchen' clandestine laboratory[116]

The medium scale laboratories are those that often occupy an entire room or garage, with more specialised glassware and equipment being used. The operator(s) will often have basic chemical knowledge. With the capacity to produce up to a few kg of material per batch, these laboratories are often involved in small-scale supply of illicit drugs.

Large scale or 'industrial' laboratories are complex in nature. Operators are often chemists, skilled in drug design and synthesis. The laboratory resembles a factory or production line, where batches of up to a few hundred kg/ton are intended to supply both domestic and overseas markets. The equipment/laboratory-ware is large and sophisticated.

High capacity (typically 80–200 L) reaction vessels, industrial heating mantles and tableting machines are common.[58] This equipment is either custom made, diverted from the pharmaceutical industry or sourced from the second-hand market (Figure 1.25).



Figure 1.25: Custom-made reaction vessel (900 litres)[58]

Unlike the small scale laboratories which are almost ubiquitous, the industrial laboratories are usually confined to East and South-East Asia, North America and Central Europe (Particularly Netherlands and Belgium).[57,58,117]

One such 'industrial' scale laboratory was discovered in Belgium in October 2013; it was the largest synthetic drugs production site ever found in the EU.[118] The raid by Belgian Police and Europol experts uncovered an MDMA production facility covering 1000 m^2 and containing high volume equipment. Police seized and removed 35 tons of chemicals and the laboratory contained products and materials estimated to be worth around €3 million. It was estimated that the laboratory had the capacity to produce several hundred kg of MDMA per week, with street value of MDMA being between €2250–6000 per kg (see Figure 1.26).



Figure 1.26: Large scale MDMA laboratory detected in the Netherlands in October 2013[118]

According to the UNODC, the majority (99%) of clandestine laboratories detected worldwide involve the manufacture of ATS.[119] These compounds are attractive to clandestine chemists as, in comparison to other drugs, there is great market potential, relatively low risk and little initial investment. Also, the versatility of starting materials and synthetic methods, together with the fact that the manufacture is not limited to certain geographical locations, means that these ATS laboratories have the potential to be established almost anywhere.

The latest global figures for detections of ATS laboratories can be found in the UNODC World Drug Report 2013[43] and are summarised as follows:

- Methamphetamine laboratories – Most methamphetamine laboratories continue to be reported in the US, where the numbers quadrupled from 2,754 in 2010 to 11,116 in 2011. An increase was also observed in Mexico and Canada with figures of 159 and 35 respectively for 2011. In Europe, 350 laboratories were reported in 2011 with the majority being identified in the Czech Republic (338). Other methamphetamine laboratories were seized in Belgium (1), Russia (4), Poland (2) and New Zealand (109).
- Amphetamine laboratories – Global numbers remain largely stable with 131 laboratories uncovered in 2011 compared to 103 in 2010. The figures for Europe however show that detections of amphetamine laboratories are on the rise again. Of the total worldwide figure for 2011 (131), Europe accounted for most laboratories (69) seized, up slightly on 2010 (62) and much greater again than 2009 (44). Prior to this, detections of amphetamine laboratories had been steadily declining (Figure 1.27).

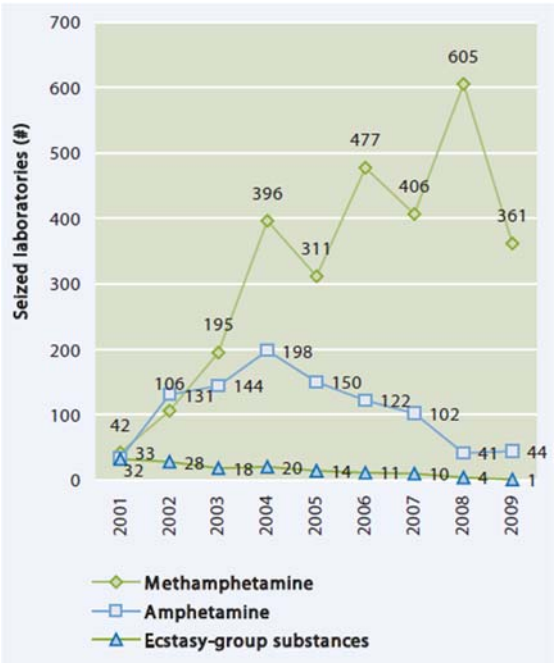


Figure 1.27: Dectections of illicit ATS laboratories in Europe, 2001-2009[57]

Belarus reported an increase in laboratories with nine uncovered in 2011 compared to none in 2010 and two in 2009. Production capacity of amphetamine is also increasing in Europe.[120] In the Netherlands and Belgium for example, use of industrial-scale equipment in amphetamine production facilities is now reported to have resulted in average yields of 40 kg per batch, compared to only 5–8 kg a few years ago.

Outside Europe, Lebanon reported the detection of 3 laboratories manufacturing amphetamine base (powder form) and 2 tablet ('Captagon') laboratories.

- MDMA – Global numbers remain stable with 39 laboratories discovered in 2011, compared to 44 laboratories in 2010. The existence of MDMA laboratories is mainly reported in Oceania, East and South-East Asia and North America. Although no laboratories were detected, Mexico is suspected of becoming a new hub for MDMA manufacture following the seizure of large amounts of precursors/reagents (safrole and methylamine) in 2011. Production is thought to be increasing in Europe also, with seizures of precursor chemicals doubling in the first 10 months of 2013 compared to 2012.[61]

In Ireland, clandestine laboratory detections are very rare. According to the EMCDDA,[56] one methamphetamine laboratory was detected in Ireland in 2008. However, no further information could be found on this from other sources. The largest seizure of methamphetamine in Irish history was seized that same year, with 6 kg of the drug being seized in Birr, Co. Offaly[121] so there may be a link between the two reports. Stronger evidence for clandestine manufacture of methamphetamine in Ireland came in 2012 amid warnings from the Health Service Executive (HSE) to pharmacists to be vigilant for bulk or repeated purchases of OTC products containing pseudoephedrine **(56)**.[122] Pseudoephedrine is a common active ingredient in cold and flu medicines (e.g. Sudafed®) and can be used as a starting material in the synthesis of methamphetamine (see Section 1.5.2). Evidence for this route of methamphetamine manufacture, being used in Ireland, was reported in 2011. One man was questioned by Gardaí after the discovery of a 'backstreet' laboratory in Tralee, Co. Kerry. A quantity of Sudafed® tablets, as well as about €8,000 worth of methamphetamine was found at the site of the makeshift laboratory.[122]

1.5 Synthesis of ATS

1.5.1 Amphetamine synthesis

The number of seizures of clandestine laboratories producing DOB and other 2,5-dimethoxy amphetamines (D series) is quite low, so information in the literature pertaining to the methods used in the synthesis of these compounds is limited. However, given that DOB and other D series compounds

have an amphetamine core structure, it is highly likely that the chemistry involved in amphetamine manufacture may be directly applied to synthesise DOB and related compounds. For this reason, the chemistry of amphetamine synthesis will be discussed in this section.

The synthesis of amphetamine is very versatile, with countless possible synthetic routes and starting materials. Having said this, in a clandestine setting, the choice of synthetic route is often based on the availability of precursors.[15] One such precursor which has been available for many years (either by diversion from legitimate sources or by facile clandestine synthesis) is phenyl-2-propane (P2P) **(65)**. As this intermediate is so commonly used, this synthesis section will be divided into two main parts:

1. Syntheses involving a P2P intermediate
2. Syntheses not involving a P2P intermediate

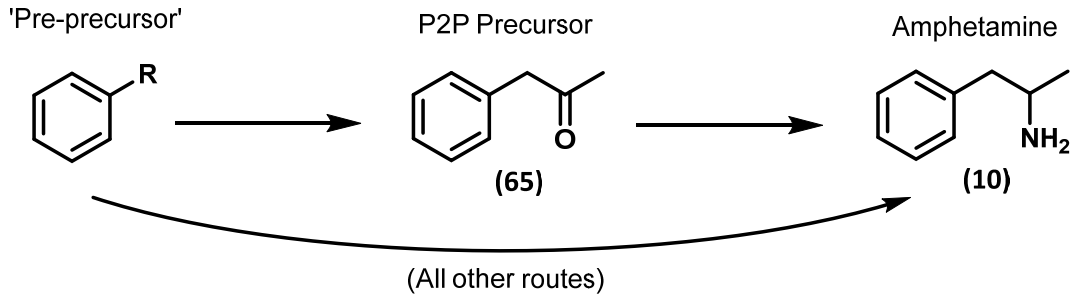


Figure 1.28: Synthesis of amphetamine *via* P2P *vs*. all other routes

1.5.1.1 Synthesis via phenyl-2-propanone (P2P)

In the vast majority of cases, amphetamine synthesis is carried out *via* the P2P **(65)** intermediate (Figure 1.28). In fact, a report published in 2005 by the Central Forensic Laboratory in Poland, states that nearly 100% of all amphetamine from illicit sources used P2P in its manufacture.[123] It is also used in methamphetamine **(14)** synthesis but to a lesser extent.[124] A report in 2005[123] suggests that only about 10% of methamphetamine is synthesised *via* P2P. However, more recent reports suggest a move towards a much higher dependence on P2P in methamphetamine synthesis (see Section 1.5.2 on methamphetamine synthesis).

Prior to 1980, P2P was commercially available on a large scale and was not controlled. As a result, it was widely used by clandestine chemists due to its facile conversion to amphetamine. Given its legitimate use in chemical synthesis, P2P from licit manufacture was often intercepted by criminal gangs for use in amphetamine synthesis. In 1980, P2P became a Schedule ll Controlled Substance in the US.[125] Once the availability of P2P became restricted, its clandestine manufacture increased (Table 1.9).

Table 1.9: Number of P2P laboratories seized in the US prior to and following its control[125]

Year	No. of P2P laboratories seized
1978	2
1979	9
1980	26
1981	38

P2P is also listed in Table I of the UN Convention against Illicit Trafficking in Narcotic Drugs and Psychotropic Substances of 1988, and today its legitimate use is limited. Some of its existing uses today include production of propylhexedrine,[124] cleaning products,[123] and in the pharmaceutical and cosmetic industries.[58] According to a report by Europol in 2007, P2P intercepted from legitimate sources typically originates in China and Russia and this is then smuggled to Europe, where it is used in large-scale amphetamine production in the Netherlands, Belgium and Poland.[58,126] According to a 2005 report, the official price of legitimate P2P is about €100/kg while the mean European black market price is €900/kg.[123]

Russia is the main source of P2P in Europe and this is reflected in figures for the largest individual seizures (in litres) of P2P reported in Europe in 2009 (Figure 1.29).

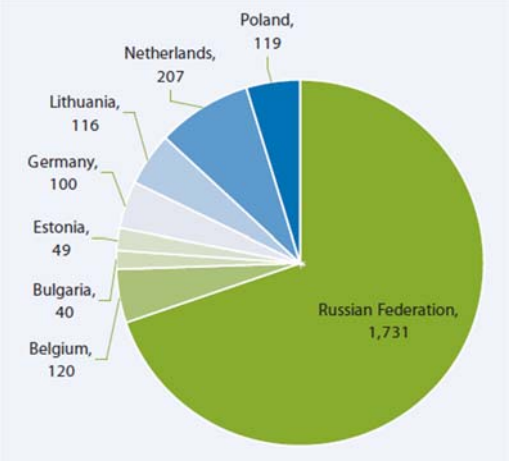


Figure 1.29: Individual seizures of P2P (in litres) in Europe, 2009[117]

Some examples of substantial P2P seizures (individual) reported in recent years are:[117,120]

- Mexico (2012) – 4,669 litres
- China (2012) – 5.8 tons
- Germany (2012) – 70 litres (seized in clandestine laboratory)
- Poland (2012) – 1,400 litres (seized in clandestine laboratory)
- Belgium (2010) – 5,000 litres
- Russia (2009) – 1,731 litres

Given the stricter control on legitimately manufactured P2P in recent years, more and more clandestine chemists are having to synthesise the precursor themselves.[126] This is especially true in Europe with recent reports suggesting that sourcing of P2P is becoming more difficult, with manufacturers now having to import 'pre-precursor' chemicals (such as phenylacetic acid **(64)**) to make P2P.[120]

Finding a method to manufacture P2P is not a problem for the clandestine chemist given the vast number of books, websites and fora dedicated to the 'Do-It-Yourself' (DIY) manufacture of amphetamines and their precursors. These sources provide very detailed information on everything from sourcing starting materials to reaction methods using improvised equipment. Some of the best known of these media include the books *PiHKAL*,[12] *Amphetamine Synthesis* by Otto Snow,[127] and *Secrets of Methamphetamine Manufacture* by Uncle Fester[128] as well as websites like www.designerdrugs.com, www.erowid.org and www.drugs-forum.com.

As P2P is a common intermediate, the synthesis of amphetamine by this methodology can be divided into 2 parts (Figure 1.30):

a) Synthesis of P2P from 'pre-precursors'
b) Synthesis of amphetamine from P2P

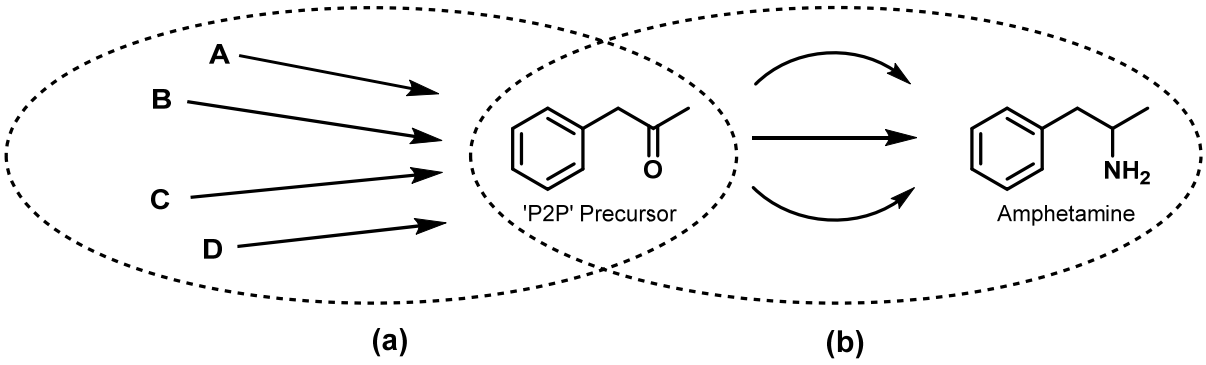


Figure 1.30: General outline of amphetamine synthesis *via* P2P intermediate

a) Synthesis of ketone precursor P2P:

There are many routes to P2P described in the literature, using any number of different starting materials or 'pre-precursors' (represented as A, B, C, D in Figure 1.30). On the website www.erowid.org, one piece by 'Rhodium'[129] outlines ≈20 different routes to P2P. These include several of the more 'traditional' methods, many of which have been abandoned due to restrictions on pre-precursor chemicals, as well as some more elaborate, multi-step procedures. The availability of so many procedures allows for great versatility in the way in which P2P can be manufactured in clandestine laboratories. Some of the routes described by Rhodium are outlined in Figure 1.31.

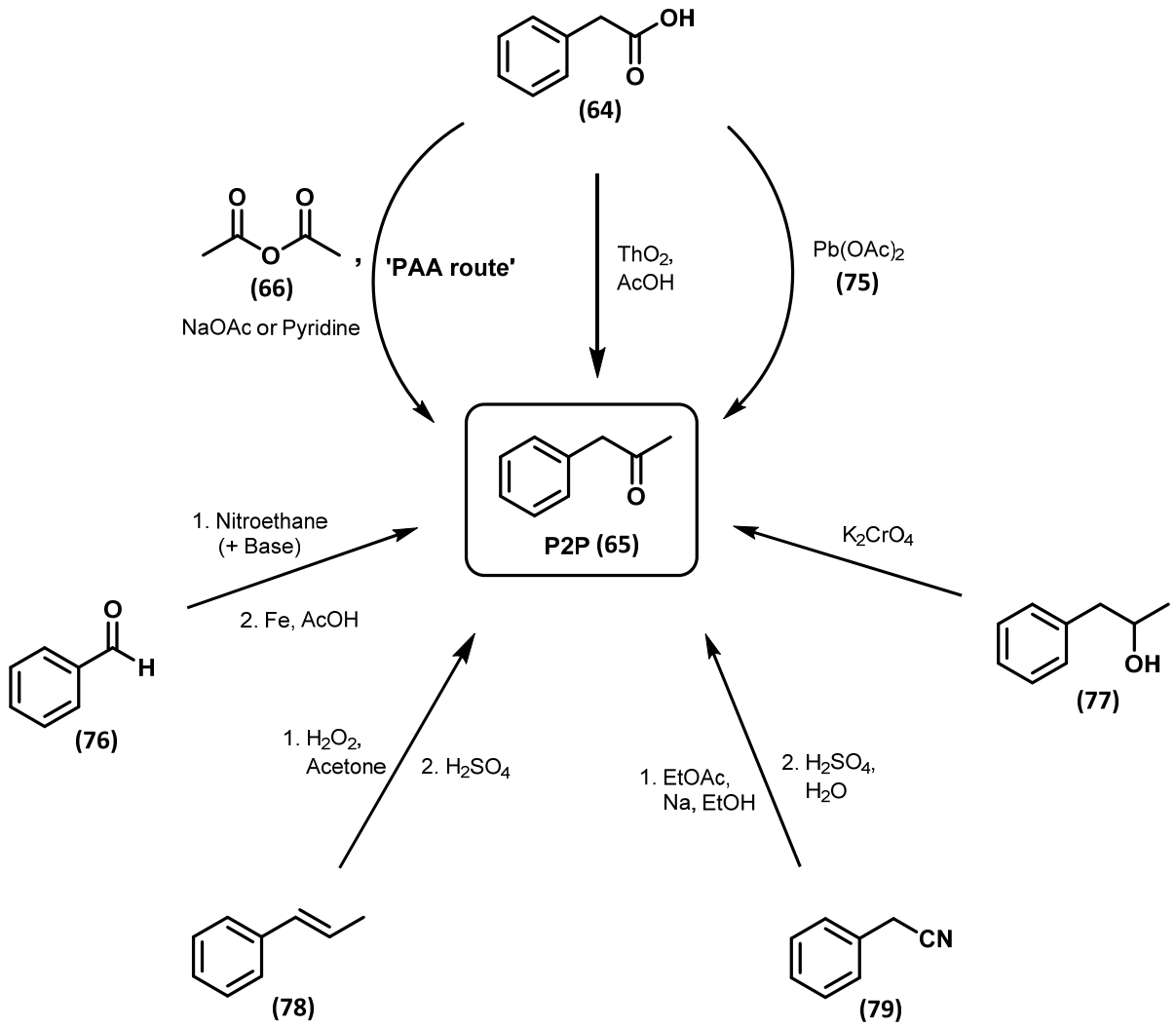


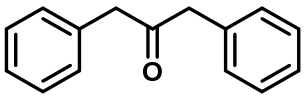
Figure 1.31: Common routes to the amphetamine precursor P2P (65)[1,123,129-131]

A paper published by Frank *et al.* in 1983[125] outlines the most common routes used in the clandestine manufacture of P2P, based on evidence collected from seized laboratories. Some of these routes employed are as follows:

- ***Phenylacetic Acid (PAA) route***:

The most common method of synthesis of P2P used by clandestine chemists, involves refluxing PAA **(64)** and Ac_2O **(66)** with sodium acetate or pyridine (Figure 1.31). This method was found to be utilised in over 75% of cases of P2P manufacture.[125] PAA is a controlled substance but is readily available due to its widespread industrial use. As well as this, Ac_2O is cheap and easy to produce so the use of PAA **(64)** and Ac_2O **(66)** as starting materials has proven to be cost effective, despite only moderate product yields (≈50%) being reported. The typical procedure involves refluxing PAA, Ac_2O and pyridine for about 6 h at 150 °C and quenching of the reaction mixture with 10% aq. HCl.[129] The product can then be isolated *via* fractional distillation or column chromatography. It is important in this method that Ac_2O is used in

a large molar excess (at least 6 equivalents) as the reactive enolate anion intermediate can condense with the ketone product (instead of acetic anhydride) to form a dibenzylketone impurity **(80)**.



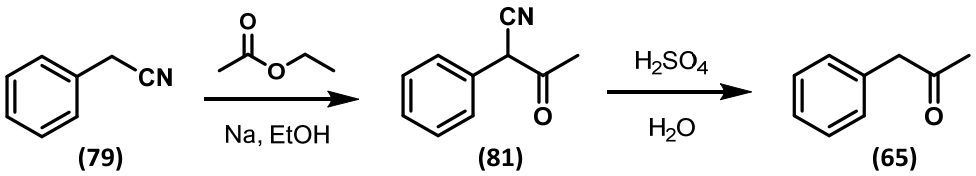
(80)

The dibenzylketone impurity and its origin will be discussed in greater detail in Section 3.1.2.

- ***Via benzyl cyanide***

This route is reported to be used in about 10% of cases.[125] Benzyl cyanide **(79)** is commonly used in the pharmaceutical industry and unlike PAA **(64)**, it is not a controlled substance at national level, in most countries. However, it is on the US DEA's watch list of precursor chemicals (DEA List I of chemicals). Seizures of benzyl cyanide have taken place recently (2012) in the Philippines (2,400 litres) and Lebanon (520 litres).[30]

The route involves 2 steps (Figure 1.32). In the first step benzyl cyanide **(79)** and ethyl acetate (EtOAc) are added to a hot solution of sodium ethoxide (generated *via* addition of sodium to absolute alcohol).[129,130] This results in the formation of 59–64% of α-phenylacetoacetonitrile (APAAN) **(81)**. Detections of APAAN **(81)** are being reported much more frequently in Europe in recent years.[120] It has few legitimate uses but there have been a number of large shipments of the substance reported since 2009. It is known to be used as a precursor to P2P and has only recently been placed under international control (see Section 1.6.2). These controls are yet to be fully implemented at national level in many regions, making for simpler movement/trafficking compared to P2P.



(79) **(81)** **(65)**

Figure 1.32: P2P from benzyl cyanide starting material (79)

In the second step of this synthesis, APAAN **(81)** is exposed to aqueous acid. This hydrolyses the nitrile group and subsequent decarboxylation of the resulting acid gives a yield of 77–86% of P2P **(65)**,[129] although more recent work suggests the yields of this step to be lower.[132,133]

There are a number of naphthalene impurities associated with the hydrolysis step to P2P. Recent work by Power *et al.*[132] on the impurity profiling of 4-methylamphetamine **(82)**, found two such naphthalene impurities (**(85)** and **(86)**) to be produced. Naphthalene **(86)** was independently synthesised and

naphthalene **(85)** was isolated from the impure street sample and characterised (Figure 1.33). These lipophilic impurities were previously thought to be route specific to a method involving the use of ephedrine **(11)** as starting material.

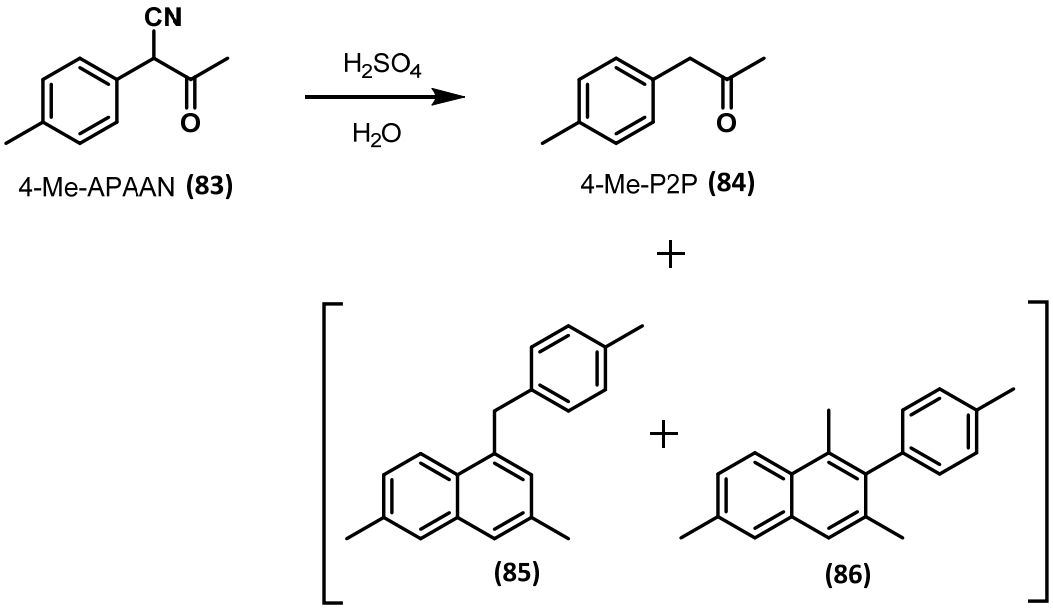


Figure 1.33: Naphthalene impurities arising from the hydrolysis of 4-Me-APAAN (83)[132]

- ***Nitrostyrene route***

Similar to the route involving benzyl cyanide, the nitrostyrene route to P2P occurs in two steps. This method accounts for about 4% of cases of clandestine P2P synthesis.[125] The starting material in this method is benzaldehyde **(76)** and like PAA **(64)**, it is a versatile reagent that can be used as the starting material for a number of different synthetic routes to P2P. Benzaldehyde **(76)**, like benzyl cyanide **(79)**, is not a scheduled substance. Illegitimate trafficking of benzaldehyde was found to have taken place in Europe in 2012, particularly in Estonia (11 kg), Germany (94 kg), Hungary (5 kg), Poland (15 litres) and Russia (6 kg).[30]

The first step in this synthetic route to P2P involves the conversion of benzaldehyde **(76)** to nitrostyrene **(87)**. This is carried out *via* condensation of **(76)** with nitroethane under basic conditions (Henry-Knoevenagel condensation). Nitrostyrene **(87)** can then be converted to P2P **(65)** either by:

(a) One pot reduction with sodium borohydride (60–70% yield)[129] and subsequent hydrolysis of the nitroalkane intermediate **(88)**, or

(b) One pot treatment with iron powder under acidic conditions (75% yield) *via* an oxime intermediate **(89)** (see Figure 1.34).[129]

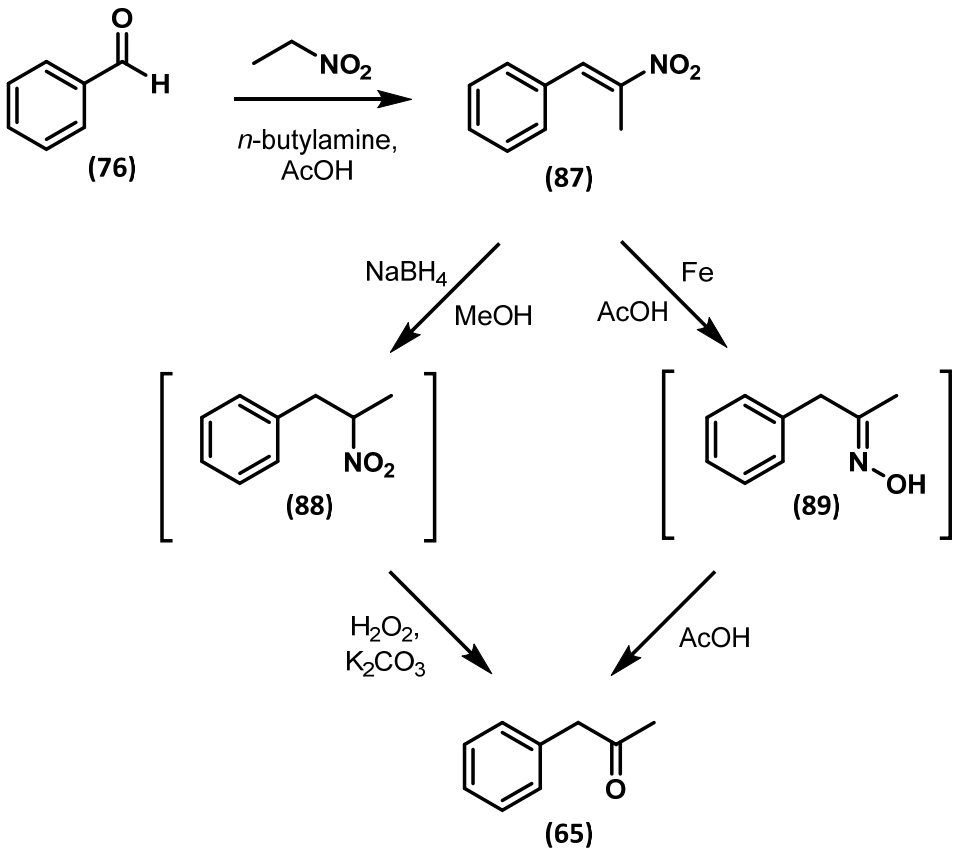


Figure 1.34: Nitrostyrene route to P2P (65)

A small number of impurities are known to arise in each of these two steps to P2P (aldehyde → nitrostyrene and nitrostyrene → ketone). Unpublished work by Griffin and Keating[26] has shown that during the synthesis of ring-substituted nitrostyrene **(73)**, two impurities are produced – benzaldoxime **(90)** and nitrile **(91)** (Figure 1.35). These impurities were recovered in yields of 0.4% and 0.9% respectively.

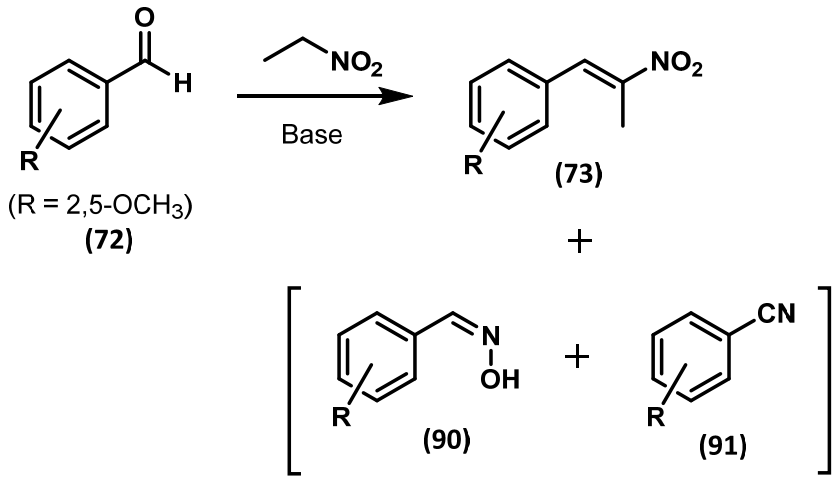


Figure 1.35: Benzaldoxime (90) and nitrile (91) impurities arising from the Henry-Knoevengel condensation of benzaldehyde (72) and nitroethane[26]

Also, during the iron-assisted reduction of nitrostyrene **(73)** to ketone **(92)**, oxime intermediate **(93)** is known to be carried forward as an impurity of ketone **(92)** (Figure 1.36).

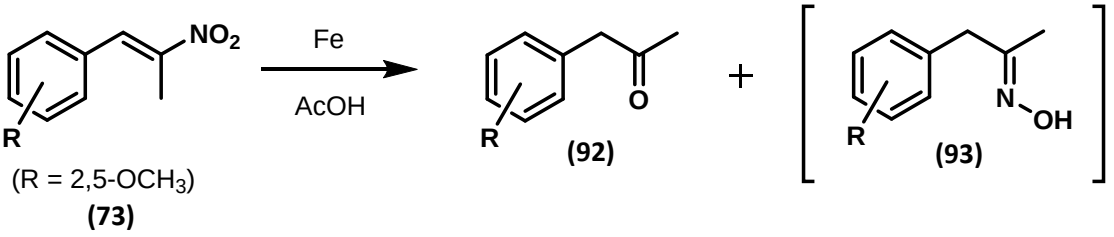


Figure 1.36: Oxime impurity from the iron reduction of nitrostyrene (73)[26]

These are just some of the routes used by clandestine chemists to synthesise P2P, with many more available in the literature. Once successfully synthesised, P2P **(65)** can be converted to amphetamine **(10)**.

b) Synthesis of amphetamine (10) from P2P (65):

Using P2P as a direct precursor, there are three well-known and well-studied routes to amphetamine (Figure 1.37):

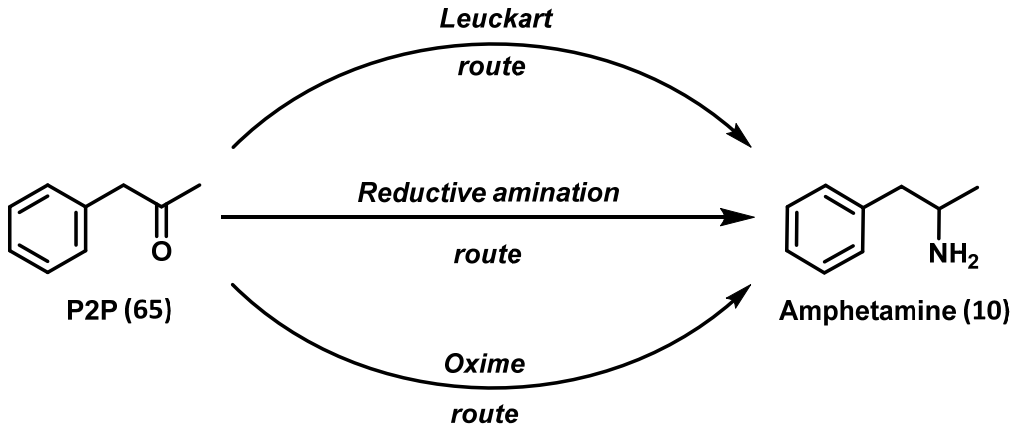


Figure 1.37: Common routes to amphetamine (10) from P2P (65)

- **The Leuckart route:**

The Leuckart route is the most popular method for preparing amphetamine from P2P in the US, UK and the Netherlands.[115] According to a report by Soine *et al.*[115] this route was found to be used in 70–90% of amphetamine clandestine laboratories. The yields from this route are quite low but it is arguably the easiest method to carry out in practice.[57] The Leuckart route occurs in 2 steps. Firstly, P2P **(65)** is condensed with formamide under reflux conditions. This is followed by acid-catalysed hydrolysis of the *N*-formyl intermediate **(94)** affording amphetamine (Figure 1.38).

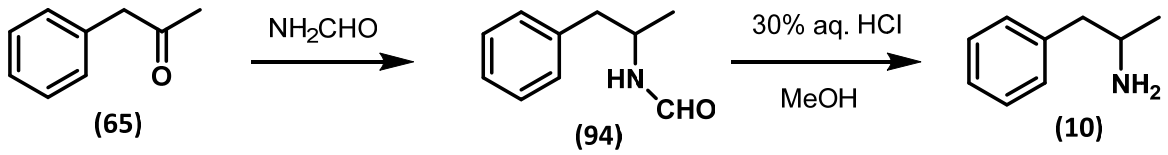


Figure 1.38: Leuckart route to amphetamine

Given the popularity of the Leuckart route, it has been extensively studied. Also, the impurities that arise during this route have been comprehensively documented in the literature.[98,111] These impurities include unreacted starting materials as well as a range of pyridine and pyrimidine impurities characteristic of this route (see Section 4.4). These impurities are of great importance to the impurity profiler in trying to determine the synthetic methodology used.

- **Reductive amination:**

In the reductive amination route, P2P undergoes reduction in the presence of a nucleophilic amine (usually ammonia). Reducing agents used may vary from laboratory to laboratory with those most commonly used including $NaCNBH_3$, $NaBH_4$, Pt/H_2, CuO/H_2, Na/EtOH, Raney Ni/H_2 and Ni plated Zn. These agents reduce the intermediate imine to the amine. A typical reductive amination is shown in Figure 1.39.

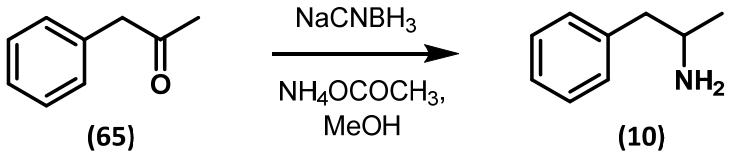


Figure 1.39: Reductive amination of P2P (65)

- **Oxime route:**

This route is not quite as common as the Leuckart and reductive amination routes. The oxime route involves firstly the condensation of P2P **(65)** with hydroxylamine under basic conditions, to form the oxime intermediate **(89)**, after which the route is named. Oxime **(89)** then undergoes reduction with $LiAlH_4$ or Raney Ni/H_2 (Figure 1.40).

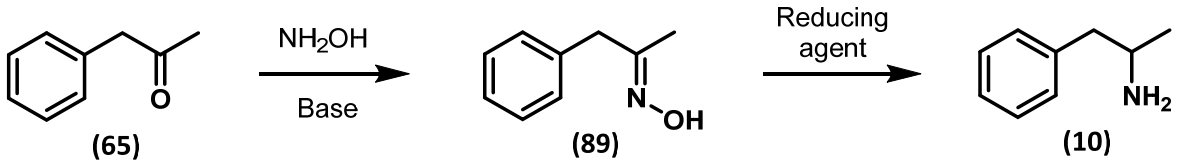


Figure 1.40: Oxime route to amphetamine

1.5.1.2 Syntheses not involving P2P

Synthesis of amphetamine by methods that do not proceed *via* the P2P intermediate are not commonly used. Examples of other precursors from which amphetamine can be synthesised include nitrostyrene **(87)** and phenylpropanolamine **(95)**.

- **Nitrostyrene route to amphetamine:**

As mentioned earlier in Section 1.5.1.1, from benzaldehyde **(76)**, a nitrostyrene intermediate **(87)** can be generated *via* the Henry-Knoevenagel condensation (Figure 1.34). To generate the desired ketone **(65)**, this nitrostyrene underwent catalytic iron reduction. However, in an alternative synthesis, the nitrostyrene **(87)** may be converted to the target amphetamine in a single, high-yielding step. This can be achieved by exposing the nitrostyrene to a strong reducing agent such as $LiAlH_4$. This method, although simple, may not be as common as other routes employed in clandestine laboratories, due to the difficult handling of the water sensitive (and potentially explosive) $LiAlH_4$. Figure 1.41 illustrates the synthesis of amphetamine from nitrostyrene **(87)** *via* this method.

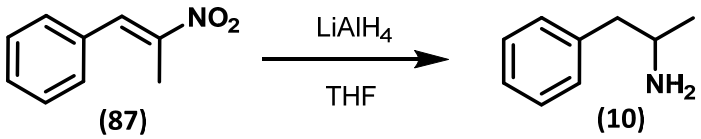


Figure 1.41: Nitrostyrene route to amphetamine

- **From allylbenzene (96):**

Although allylbenzenes may be used to form P2P-type intermediates, they may also be used (*via* an alkyl bromide/iodide reagent) to form the target amine. This is the route described in the original Merck patent for amphetamine synthesis and is still used in illicit manufacture.[15]

In the initial step of the two step synthesis, hydrobromic (HBr) or hydroiodic acid (HI) adds to the double bond of allylbenzene **(96)** to give the 1-phenyl-2-halopropane derivative **(97)**. Subsequent nucleophilic substitution of halide group 'X' by ammonia (NH_3) affords amphetamine **(10)** (Figure 1.42).

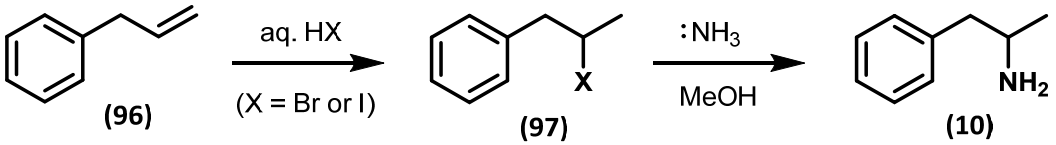
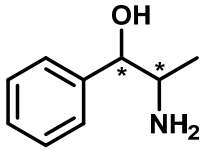


Figure 1.42: Amphetamine from allylbenzene (96)

- **From phenylpropanolamine (95):**

Phenylpropanolamine **(95)** consists of a mixture of *l*-norephedrine and *d*-norephedrine, the *N*-demethylated analogues of ephedrine **(11)** and pseudoephedrine **(56)**.



'phenylpropanolamine' **(95)**

Ephedrine **(11)**/pseudoephedrine **(56)** are commonly used as precursors to methamphetamine **(14)** due to their widespread use in pharmaceutical preparations (e.g. Sudafed®) and thus their availability to clandestine chemists.

Phenylpropanolamine **(95)** on the other hand, has only very limited use in pharmaceutical preparations and thus is not as accessible to clandestine chemists. As a result, the use of phenylpropanolamine in clandestine synthesis, as a precursor to amphetamine, is very rare. Due to the structural similarity of phenylpropanolamine and ephedrine/pseudoephedrine, the well-established routes to methamphetamine from ephedrine/pseudoephedrine, may also be applied to the manufacture of amphetamine from phenylpropanolamine. These routes are summarised below (Figure 1.43).

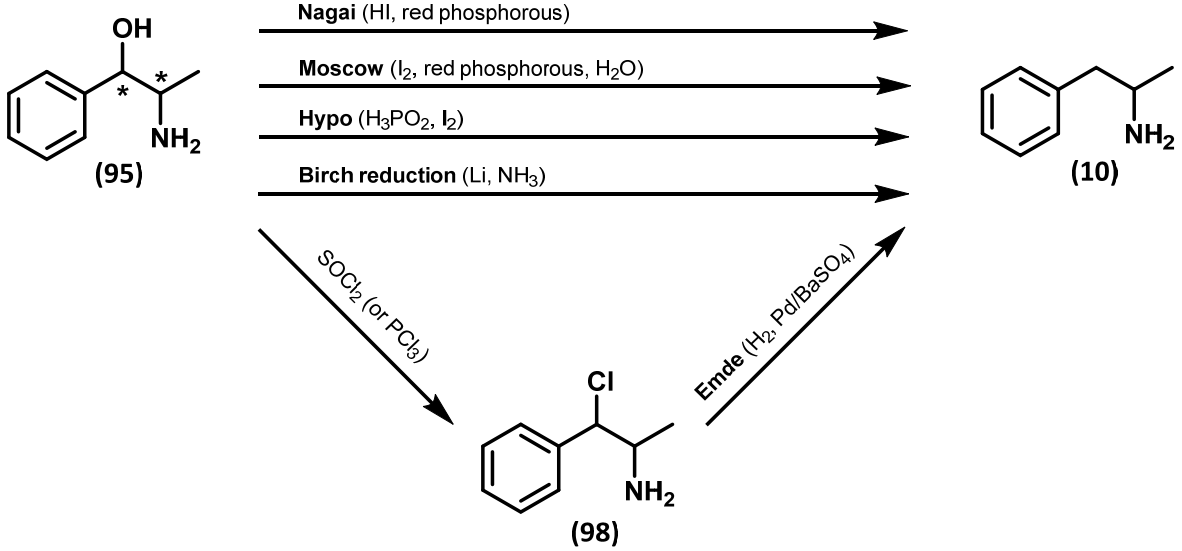


Figure 1.43: Routes commonly used in methamphetamine synthesis from ephedrine/pseudoephedrine, adapted to amphetamine synthesis from phenylpropanolamine (95)[99]

1.5.2 Synthesis of methamphetamine (14) and MDMA (17)

Common routes used in the synthesis of methamphetamine **(14)** were summarised in a paper by Inoue *et al.*[134] and this is depicted in Figure 1.44:

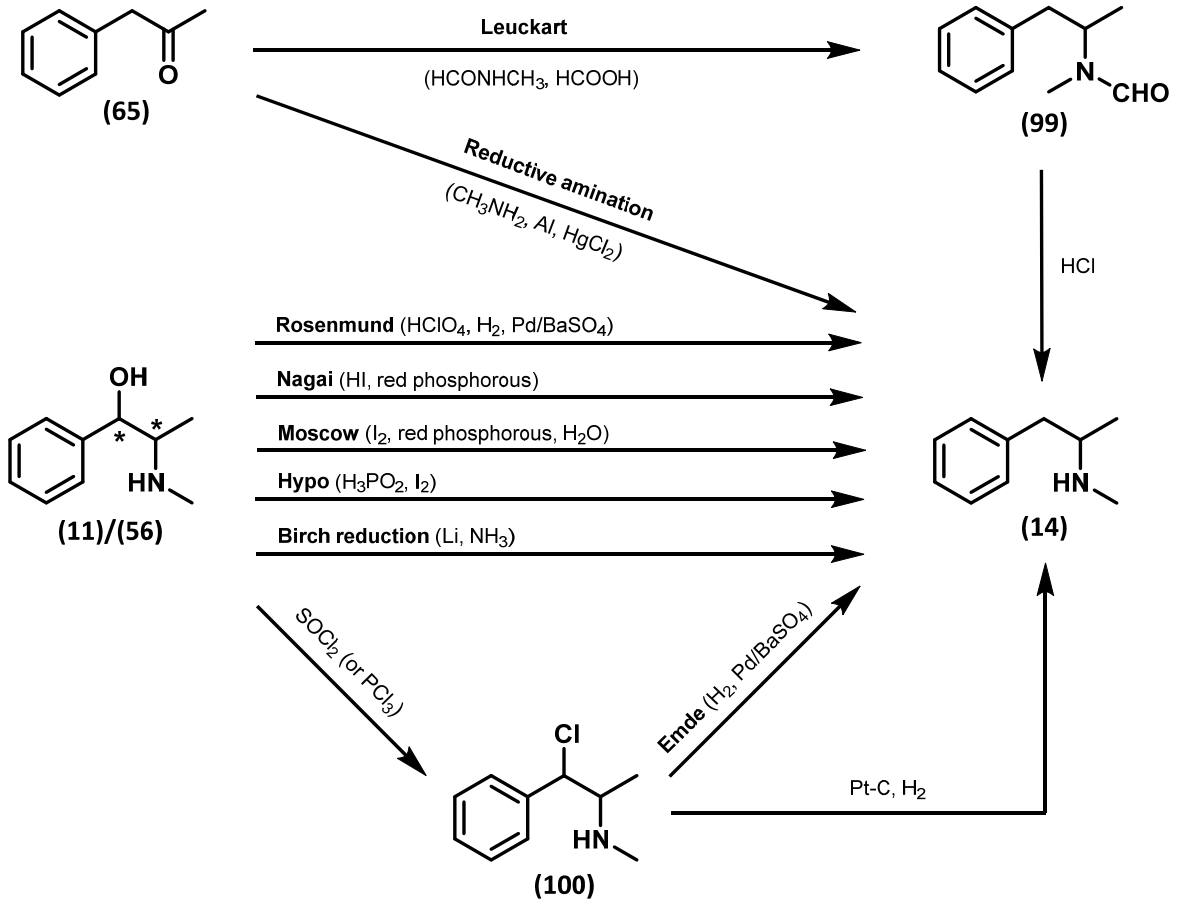


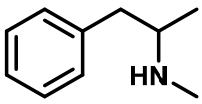
Figure 1.44: Synthetic routes to methamphetamine[134]

As mentioned, there are a number of well-established routes to methamphetamine **(14)** from ephedrine **(11)**/pseudoephedrine **(56)** (e.g. Nagai, Moscow, Birch reduction). The 'ephedrines' are popular starting materials in methamphetamine synthesis, given their widespread use in pharmaceutical preparations and thus their accessibility to clandestine chemists. In recent years, a shift has been observed however, from traditional precursors (ephedrines) to P2P **(65)**. Given stricter controls on the ephedrines, manufacturers of methamphetamine are adapting their methods; use of P2P as a precursor is increasing, especially in Europe, the US and Central America.[93,135] In particular, Mexico's reliance on P2P for methamphetamine manufacture is thought to have greatly increased in recent years.[30] Mexico's seizures of P2P have been gradually increasing and in 2012, for a third consecutive year, Mexico reported the world's largest seizure of P2P (4,699 litres). Seizures of ephedrine/pseudoephedrine have greatly declined in recent years yet production of methamphetamine

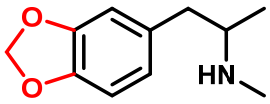
remains high. Based on the profiling of methamphetamine from Mexico, it is estimated that more than 90% of methamphetamine seized by mid-2013 was manufactured using P2P.

P2P can be used as a precursor to synthesise methamphetamine using similar methodology to that used in amphetamine synthesis from P2P (e.g. Leuckart, Reductive amination) (see Section 1.5.1.1). The difference between amphetamine and methamphetamine manufacture from P2P, is the nitrogen source used. Methamphetamines, by definition, possess an *N*-methyl group, so the nitrogen source used must incorporate this *N*-methyl moiety. For example, in the Leuckart reaction to amphetamine, the nitrogen source is formamide (NH_2CHO) whilst for methamphetamine, the nitrogen source is *N*-methyl formamide ($NHCH_3CHO$).

Methamphetamine **(14)** and MDMA **(17)** have been grouped together in this section as essentially, MDMA is a ring-substituted analogue of methamphetamine (3,4-methylenedioxy substituent).



(14)



(17)

In theory, all of the synthetic methods outlined in Figure 1.44 for the synthesis of methamphetamine, could be used to manufacture MDMA. However, in reality, many of the methods used to manufacture methamphetamine **(14)** have never been reported for MDMA **(17)** synthesis. As previously mentioned, availability of starting materials/precursors is a major factor in the choice of synthetic route employed.

In the case of methamphetamine, the phenyl ring is unsubstituted and this simple, common structure means that there are many reagents available as potential precursors, even OTC pharmaceutical preparations (e.g. 'Ephedrines').

In the case of MDMA, the substitution pattern of the phenyl ring (3,4-methylenedioxy) is not commonly encountered in compounds present in pharmaceutical preparations or those used in research. 'Retrofitting' of the 3,4-methylenedioxy feature to methamphetamine or its common precursors would be difficult, especially for inexperienced clandestine chemists. This brings about a need for illicit manufacturers to source precursors that already have this 3,4-methylenedioxy moiety incorporated in their structure, and precursors with this feature are not common. For example, 3,4-methylenedioxy ephedrines are not used in pharmaceutical preparations, therefore they are not available to clandestine chemists.

Routes such as 'Nagai' and 'Moscow' (commonly encountered in methamphetamine synthesis) are not encountered in clandestine laboratories involved in the preparation of MDMA. This greatly limits the number of possible precursors (and thus synthetic routes) that may be used to synthesise MDMA.

Some of the precursors commonly used in MDMA manufacture include piperonal **(101)**, safrole **(102)** and isosafrole **(103)** (Figure 1.45).[99] These materials can all be converted into the P2P analogue of MDMA (3,4-MDP2P or piperonyl methyl ketone (PMK) **(104)**) and using methods described in Section 1.5.1.1 (Leuckart, Reductive amination etc.), the ketone **(104)** can be converted to the target MDMA **(17)**.

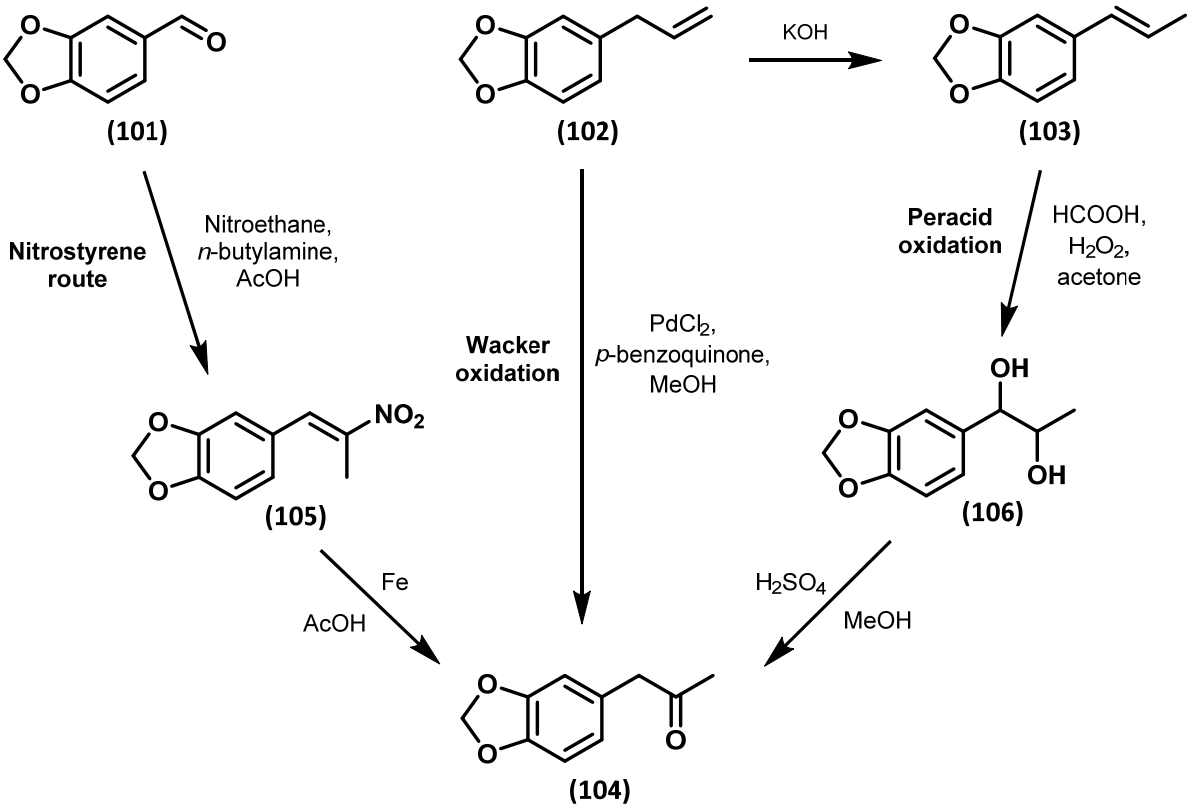
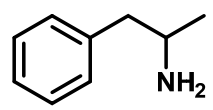


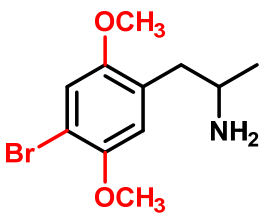
Figure 1.45: Synthetic routes to MDMA used in illicit manufacture[99]

1.5.3 Synthesis of DOB and other 'D series' amphetamines

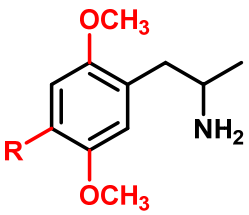
As mentioned previously, the methodology for amphetamine synthesis can be directly applied to synthesise DOB **(35)** and other 2,5-dimethoxyamphetamines ('D series') **(107)**. DOB differs to amphetamine in the substitution pattern of the phenyl ring.



Amphetamine **(10)**



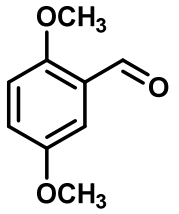
DOB **(35)**



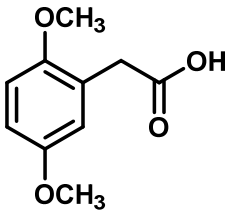
D series **(107)**

The number of synthetic routes used in amphetamine manufacture are vast, but as with MDMA, the substitution pattern of the phenyl ring of DOB and other D series compounds, limits the number of

precursors available to clandestine chemists. Therefore, it is likely that clandestine chemists will intercept/divert 2,5-dimethoxy-substituted starting materials, like 2,5-dimthoxybenzaldehyde **(72)** or 2,5-dimethoxyphenylacetic acid **(108)**, which are used legitimately in the pharmaceutical industry, and are not controlled.

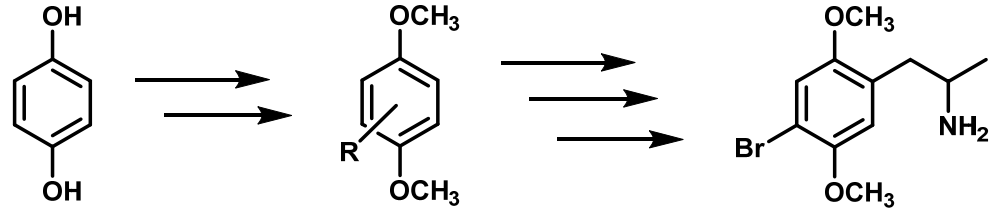


(72)



(108)

Alternatively, the methoxy groups could be introduced by the clandestine chemist. In a clandestine DOB laboratory discovered in the UK in 1981, the 'chemist' was found to be using hydroquinone **(71)** as a starting molecule and converting the hydroxyl groups to methoxy groups as part of their 8-step synthesis:[87]



(71) **(35)**

In the case of DOB, aromatic bromination is also required. This bromination can be carried out in a number of different ways. The most straightforward, and probably most popular method, involves dissolving the starting material in acetic acid, adding excess bromine liquid and stirring at room temperature for several hours. This bromination step can make a big contribution to the impurity profile of illicit DOB. Firstly, the bromination step might not necessarily take place as the first step in the synthesis of DOB. In fact, it may be carried out at any stage of the synthesis. This means that if bromination occurs late in the synthesis, any impurities carried forward from previous steps are susceptible to bromination, giving rise to a new series of brominated impurities. In addition, bromination does not always occur exclusively at the aromatic 4-position. Thus, structural isomers of the expected intermediates (for example, 6-bromo analogues) may give rise to even more potential impurities. The bromination of various intermediates/precursors to DOB is explored throughout this thesis.

1.6 Clandestine manufacture of ATS – 'A cat and mouse game'

A number of developments have been made in controlling the manufacture and trafficking of ATS (and their precursors) in recent years, at both national and international level. A lot of progress has been made in the collaboration and sharing of information/data between national (e.g. research groups/law enforcement) and international (e.g. UNODC/Interpol) bodies. Agencies like the UNODC, Interpol, Europol and EMCDDA have been at the forefront of driving these collaborations. Initiatives like 'CHAMP', set up in the EU, have encouraged partnerships to be established between various European laboratories and help 'harmonise' the way in which different laboratories carry out analyses of drug samples.

Given the developments in the control of existing ATS and their precursors, drug manufacturers have had to adapt in order to avoid detection and continue supplying the illicit drug market. This poses a problem for law enforcement agencies and demonstrates the 'cat and mouse game' that is played between illicit producers attempting to gain access to precursors, and authorities trying to prevent them.[120] To quote the UNODC – "In order to avoid detection, drug trafficking organisations have continued to adapt their manufacturing strategies, and continuing change in the illicit manufacturing process of synthetic substances presents a myriad of new challenges to drug control authorities worldwide".[135]

ATS manufacturers have shown an extraordinary degree of flexibility in how they synthesise drugs in recent years. Some of the strategies used to avoid detection include the use of substitute chemicals, the extraction of precursors from pharmaceutical preparations and most recently, the masking of precursors and the development of alternative methods of synthesis.

One of the major adaptations in the clandestine manufacture of ATS has already been referred to in Section 1.5.2. In some regions (e.g. Mexico) there has been a shift in the precursors predominantly used to manufacture methamphetamine. Traditionally, ephedrines (ephedrine/pseudoephedrine), sourced from pharmaceutical preparations were used, but following stricter control on these substances, manufacturers have switched to using P2P **(65)** (normally associated with amphetamine synthesis) as the preferred precursor.[30]

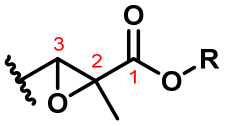
The use of P2P as a precursor to both amphetamine and methamphetamine has been increasing in recent years. This is probably due to the fact that it is a very versatile intermediate compound, with a multitude of ways in which it can be synthesised (from numerous 'pre-precursors') and ways in which it can be converted to the active ATS (see Section 1.5.1.1). This is very much suited to clandestine manufacture as once a particular reagent or pre-precursor becomes flagged for control, another one can be used and a new synthetic approach adopted. Access to P2P however, is becoming more difficult due to enhanced international cooperation by intelligence/law enforcement agencies.[132]

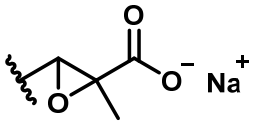
Strategies used in P2P manufacture to avoid detection include the use of alternative 'pre-precursors' and use of 'masked' precursors.[135] Alternative pre-precursors are new (or newly adopted) chemicals not traditionally used as pre-precursors to illicit drugs. Clandestine chemists may also modify the structure or physical form of the precursor into something that is not controlled or more difficult to detect, but is easily converted back to a known precursor. This is referred to as 'masking'. Alternative pre-precursors and masked precursors allow essential molecular building blocks for illicit drugs to be easily trafficked across continents (as non-controlled substances), and upon reaching their destination, converted to known controlled precursors (e.g. P2P **(65)**). Once converted to a known precursor, they may be sent to another location or converted on-site, to the target ATS.

Recent examples of these alternative pre-precursor/masked precursor strategies include the use of 2-methyl glycidic esters, APAAN, esters of phenylacetic acid and the bisulfite adduct of P2P. These are discussed in greater detail in the following sections:

1.6.1 2-Methyl glycidic esters

These compounds, usually found either as their methyl **(109)**/ethyl **(110)** esters, or sodium salts of the acid **(111)**, may be classified as 'alternative pre-precursors'. They have few legitimate uses.[43]

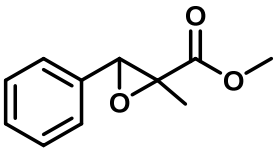




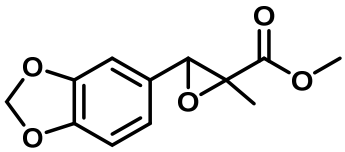
(111)

R = CH_3 = Methyl 2-methyl glycidate **(109)**
R = CH_2CH_3 = Ethyl 2-methyl glycidate **(110)**

The methyl 2-methyl glycidate pre-precursors to P2P **(65)** and 3,4-MDP2P **(104)** (direct precursors to amphetamine **(10)** and MDMA **(17)**) are shown below. The P2P glycidate (methyl 2-methyl-3-phenylglycidate) **(112)** and PMK glycidate ('MMDMG') (methyl 2-methyl-3-(3,4-methylenedioxyphenyl)glycidate) **(113)** are not controlled substances and as a result, their trafficking is much easier than that of the controlled ketone.

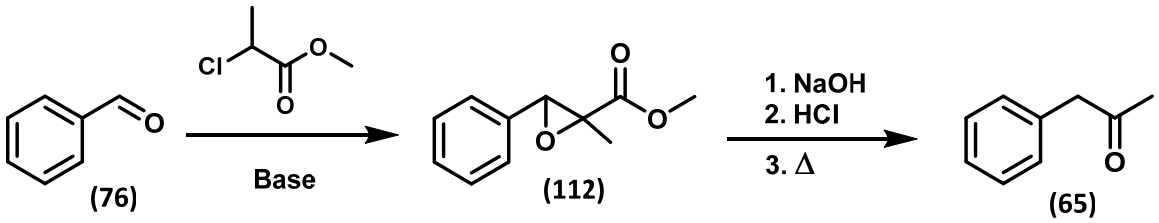


(112)



(113)

Glycidates can be easily converted to ketones (e.g. P2P **(65)**) by the thermal decarboxylation of the glycidic acid (formed after saponification of the glycidic ester). The glycidates can be generated from the reaction of a benzaldehyde **(76)** starting material with a chloro/bromo-propionate reagent in the presence of base (known as 'Darzens condensation'):[136]



As with many of the pre-precursors and masked precursors, the glycidate esters used in clandestine manufacture are thought to be sourced in China and then trafficked to Europe (most likely to the Netherlands) to be converted to the ketone (P2P).[30] According to the literature, the methyl 2-methyl glycidate **(113)** of 3,4-MDP2P **(104)** (precursor to MDMA) (Figure 1.46) is much more commonly encountered than its amphetamine precursor counterpart **(112)**. The synthesis of 3,4-MDP2P **(104)** (*via* glycidate **(113)**) has been described in the literature.[137-139]

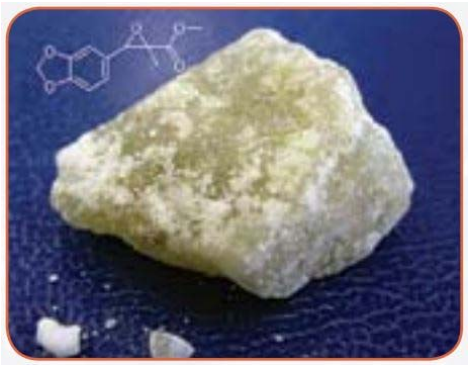
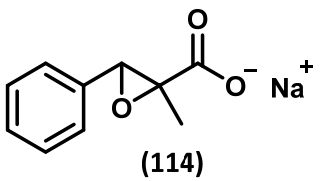


Figure 1.46: Seized material containing PMK glycidate (MMDMG) (113)[140]

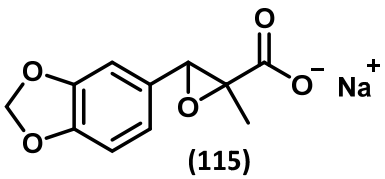
Prior to 2004, there were no reports of glycidic esters (or their salts) used as pre-precursors to ATS. Since 2004, there have been several detections of these materials intended for use in ATS manufacture. Some examples of these detections include:

- **2004** – MMDMG **(113)** seized (5 × 44 gallon drums) in Australia.[139,140]
- **May 2010** – "Small quantity" of MMDMG **(113)** seized in MDMA/methamphetamine laboratory in the Netherlands, along with instructions on how to convert it into 3,4-MDP2P **(104)**.
- **Oct 2010** – 200 kg of "chemicals", consisting of a mixture of 3,4-MDP2P **(104)**, piperonal **(101)** and MMDMG **(113)**, seized in Slovakia.
- **Mar 2011** – 800 kg of MMDMG **(113)** detected in Denmark from air cargo ship destined for the Netherlands (from China).[43]
- **2011** – One conversion laboratory discovered in the Netherlands where MMDMG was being converted to 3,4-MDP2P **(104)**. Other seizures of MMDMG were reported in Belgium, Poland and Estonia.

- **2012** – 420 kg of the sodium salt of 3,4-MDP2P glycidic acid **(115)** seized in Luxembourg (after travelling by air from Hong Kong and destined for the Netherlands). Other reports of the substance were recorded in Estonia and Romania.[30]



(114)

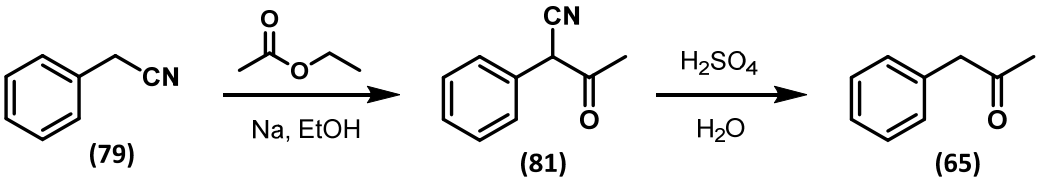


(115)

- **2012** – 100 kg of the sodium salt of P2P glycidic acid **(114)** was seized in a conversion laboratory in the UK, as well as an amount of successfully converted P2P.[141] The sodium salt of the acid can be converted to P2P (*via* heat-induced decarboxylation of the acid) at a practical ratio of about 2 to 1 (i.e. 2 kg of the salt will produce 1 kg of P2P).[30] It was reported that the gang involved had advance orders for a "large amount" of P2P that, if successfully manufactured, could be used to make £5 million worth of amphetamine. The leader of the group had apparently travelled to China to recruit two chemists to demonstrate the conversion procedure and subsequently sponsored their visa applications so that they could travel to the UK and work in the laboratory. In 2013, five members of the gang (including the 2 Chinese 'chemists') received jail terms in the UK totalling over 23 years.
- **2014** – An international operation involving Europol and seven EU Member States was reported by Europol on 3 April 2014.[142] The operation led to the arrest of 8 major players in an international organised crime network that had been active in the EU for several years. It was revealed that the group's key players had organised deliveries of pre-precursors from China, *via* Romania and other EU countries, to the Netherlands from where the business was run. The group had trafficked 650 kg of MMDMG **(113)** and piperonal **(101)** into the EU in 2012-2013.

1.6.2 APAAN

As mentioned in Section 1.5.1.1, P2P **(65)** can be produced from a benzyl cyanide **(79)** pre-precursor *via* an α-phenylacetoacetonitrile (APAAN) intermediate **(81)** (Figure 1.47).



(79) **(81)** **(65)**

Figure 1.47: P2P from a benzyl cyanide starting material *via* APAAN

APAAN **(81)** has, in recent years, become a major concern to law enforcement agencies due to its ever increasing use as a pre-precursor to amphetamine. Compound **(81)** is reported to be easily converted to P2P at a practical ratio of about 1.4 to 1.[30] It is also reported that for clandestine manufacture of P2P **(65)**, it is cheaper to purchase **(81)** and convert it to P2P, than it is to purchase an equivalent amount of commercially prepared P2P **(65)**.[143]

Like the glycidate compounds **(112)** and **(113)**, APAAN **(81)** has very limited legitimate uses, so any large imports are likely to be intended for conversion to P2P.[120] Shipments of APAAN **(81)** typically originate in China and transit numerous European countries, the intended destination being the Netherlands. China is thought to be the main source of manufacture of APAAN but seizures of benzyl cyanide **(79)** in 2012 in the Philippines (2,400 litres) and Lebanon (520 litres) may suggest that manufacture is spreading. Prior to its recent international control, movement and trafficking of APAAN was much easier and there were cases where intercepted APAAN had to be released to traffickers again due to lack of legislation enabling its seizure.[30] The mislabelling and misdeclaration of shipments have been identified as the main *modi operandi* used by traffickers of APAAN. In an attempt to avoid detection, traffickers have also been known to transport APAAN in liquid form or as a two phase mixture consisting of undissolved crystals of APAAN in ethanol or an ethanol-water mixture. APAAN is normally encountered in the form of a white, off-white or pale yellow crystalline powder.[30]

APAAN **(81)** was first discovered in a methamphetamine laboratory in Malaysia in 2006 and reports of large APAAN shipments began in Europe in 2009. More recently, there has been a large number of incidents relayed to the INCB through their PICS system (Figure 1.48).

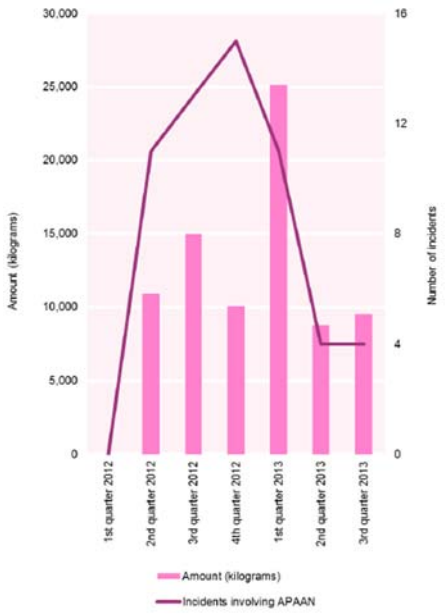


Figure 1.48: Amount (kg) of material encountered as well as the number of incidents involving APAAN, communicated *via* PICS by quarter, 2012–2013[30]

Some of the significant seizures/reports of APAAN **(81)** in recent years include:

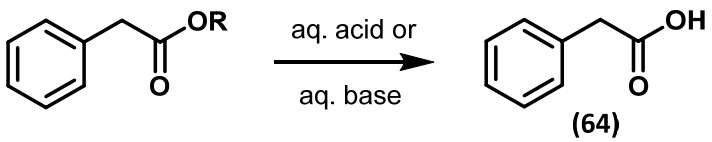
- **2011** – 700 kg seized in Poland.[43]
- **2011** – More than 4 tons intercepted in the Netherlands.[120]
- **2011/2012** – Conversion laboratories dismantled in the Netherlands (8+), Belgium, Germany and Poland.[120]
- **2012** – Seizures in Belgium (7 tons, 23 individual cases), the Netherlands (6.8 tons) and Hungary (3 tons).[30]
- **2012** – Several seizures in Bulgaria in April (330 kg), July (500 kg), August (104 kg) and September (600 kg) of 2012.[143]
- **2012/2013** – In the same investigation outlined in Section 1.4 (Figure 1.26), an organised crime gang involved in trafficking of precursors, was found to have trafficked at least 10.4 tons of APAAN **(81)** into the EU in 2012–2013. The investigation was concluded in early 2014 and the details revealed in a press release on 3 April 2014.[142]

In response to the significant detections and seizures of APAAN **(81)**, a request was submitted in November 2013 by the INCB to the UNCND, to include APAAN in Table I of the UN Convention Against Illicit Traffic in Narcotic Drugs and Psychotropic Substances, 1988. This recommendation was approved at the 57th session of the UNCND held in March 2014.

1.6.3 Esters of phenylacetic acid

Traditionally the most common method of manufacture of the precursor P2P **(65)** was *via* the phenylacetic acid route (see Section 1.5.1.1). Given the prevalence of PAA **(64)** in P2P synthesis, it became an internationally controlled precursor and can be found in Table I of the UN Convention Against Illicit Traffic in Narcotic Drugs and Psychotropic Substances, 1988.[62]

In order to avoid detection, traffickers have, in recent years, begun to 'mask' the PAA pre-precursor as an ester. These esters may be easily converted to PAA upon reaching the clandestine laboratory involved in the production of P2P. This conversion can be carried out *via* base hydrolysis (e.g. aq. NaOH, 'saponification') or by the acid-catalysed hydrolysis (e.g. aq. H_2SO_4) of the ester:



(64)

R = CH_3 **(116)**
R = CH_2CH_3 **(117)**
R = $CH_2CH(CH_3)_2$ **(118)**
R = C_5H_{11} **(119)**

Esters of PAA known to be used as masking agents in the illicit manufacture of ATS include the methyl **(116)**, ethyl **(117)**, isobutyl **(118)** and amyl **(119)** esters[117] with the ethyl ester (ethyl phenyl acetate **(117)**), reported to be the most commonly encountered. Much of the world's supply of **(117)** reportedly originates from China where it is a common ingredient in some pharmaceuticals, agrochemicals, food and cosmetic products.[140]

Significant quantities of these esters have been encountered in Central America in particular, where production of methamphetamine from P2P has now superseded production *via* traditional ephedrines. Seizures of these esters became much more frequent following strengthened controls by Mexican authorities, on PAA and its salts and derivatives in 2010.[117] The extent to which these non-controlled esters were being encountered, led to the establishment of *Operation Phenylacetic Acid and its Derivatives* (PAAD) by the INCB in 2011.[4]

The use of esters as masked pre-precursors essentially adds another step to the synthesis of methamphetamine and this is noteworthy in terms of impurity profiling. A recent study has shown that if some of the ester is not successfully converted (to PAA) and is carried through to the reductive amination step, the *N*-methyl-2-phenylacetamide impurity **(120)** may be produced (Figure 1.49). This impurity may be used as a route specific marker for methamphetamine synthesised *via* the ester → acid → P2P → (*via* reductive amination) methamphetamine route.[144]

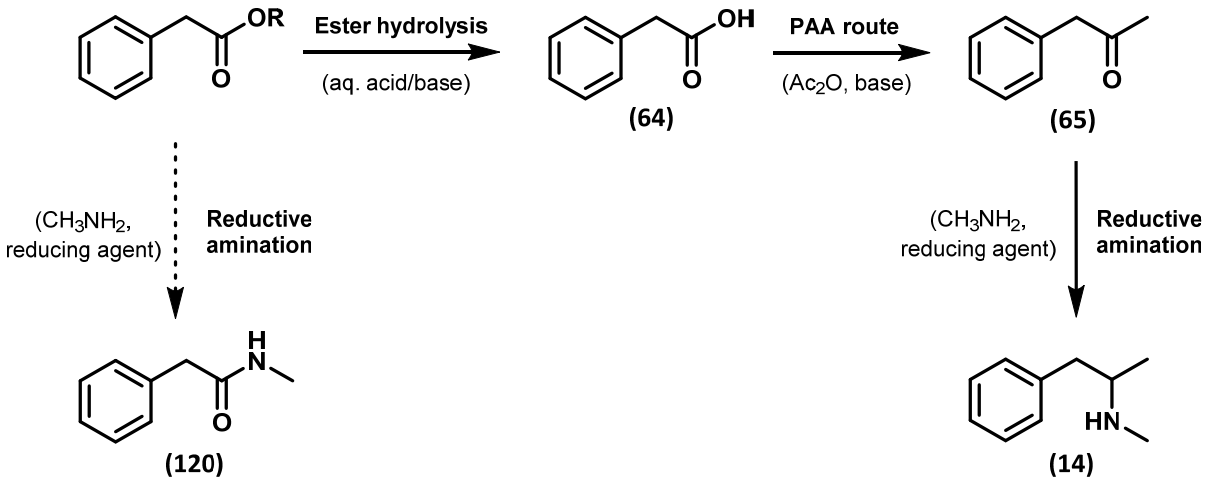


Figure 1.49: Proposed origin of the *N*-methyl-2-phenylacetamide impurity (120) in illicitly manufactured methamphetamine[144]

Examples of recent seizures of esters of PAA, intended for illicit manufacture of ATS include:

- **2008** – "Significant" seizures of methyl **(116)**, ethyl **(117)**, isobutyl **(118)** and amyl **(119)** esters of PAA in Mexico.[117]
- **2010** – 45 tons of ethyl phenyl acetate **(117)** seized in Belize.
- **2011** – 1 ton of ethyl phenyl acetate **(117)** seized by Dutch customs at Schiphol Airport.[140]

- **2012** – 16 tons of ethyl phenyl acetate **(117)** (originating in China) seized in a warehouse in Guatemala.[30]
- **2012** – 72.8 tons and 46,000 litres of ethyl phenyl acetate **(117)** seized in total in Mexico in 2012.

1.6.4 P2P bisulfite adduct

As a way of 'masking' P2P **(65)**, criminal groups have begun to form its bisulfite adduct **(121)**.[57] Conversion of the bisulfite adduct back to its ketone form (i.e. P2P), can be performed without difficulty and without specific chemical knowledge, upon reaching its destination (Figure 1.50).

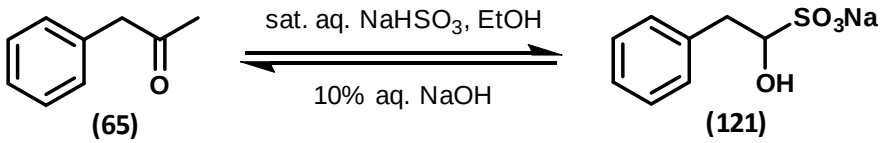


Figure 1.50: Masking and unmasking of P2P as its bisulfite adduct (121)[145]

The bisulfite adduct **(121)** is not easily recognised by law enforcement. P2P **(65)** is generally found in the form of a pale yellow liquid whilst the bisulfite adduct is found as a white, moist, crystalline solid resembling damp sea salt.[43,117] Bisulfite **(121)** was found in a large-scale illicit drugs production site in the Netherlands in 2008. Following investigation by Dutch police and the Netherlands Forensic Institute (NFI), the laboratory was found to be converting **(121)** to P2P **(65)** on site (Figure 1.51). Also, 2,600 kg of **(121)** was seized during a customs clearance at the Russian/Latvian border in 2009.[57]



Figure 1.51: P2P bisulfite adduct (121) discovered in a drug production facility in the Netherlands in 2008[57]

The formation of **(121)** may serve additional purposes other than the masking of P2P. According to the literature,[145] formation of the bisulfite adduct of an aldehyde or ketone may be used as a purification process: to a crude/impure sample of ketone/aldehyde, aq. sodium bisulfite is added, resulting in the subsequent formation of the bisulfate adduct (as a precipitate). The precipitate is then collected and converted back to the desired 'pure' aldehyde/ketone (using aq. NaOH or $NaHCO_3$).

Also, the adduct **(121)** may act as a stable form of P2P, thus extending its shelf life. P2P and its ring substituted ketone analogues have been found in the literature[146] and within our research group (Section 3.7), to undergo degradation (most likely light induced) over time. The solid bisulfite adducts of P2P and its analogues are much easier to 'handle' as they are more resistant to degradation.[145]

The use of these non-controlled pre-precursors and masked precursors highlights the flexible nature of ATS manufacture and reflects the response of drug traffickers to the tighter controls placed on traditional ATS precursors. Some of these alternative/masked precursors, as well as their relationship to more traditional precursors are summarised in Figure 1.52.

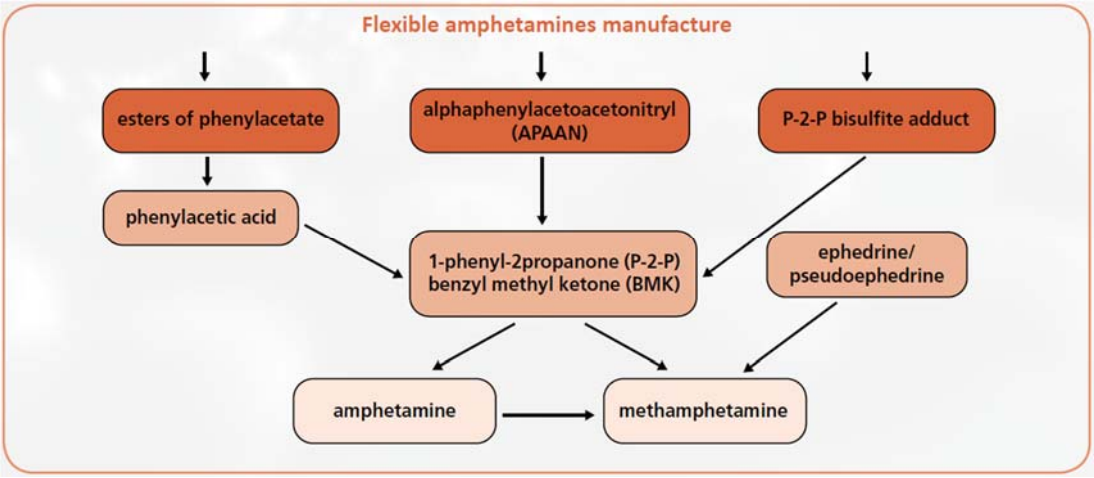


Figure 1.52: Flexibility in ATS manufacture *via* use of alternative/masked precursors[140]

1.7 Emerging drugs

In recent years, terms such as 'Novel (or New) Psychoactive substances' (NPS), 'legal highs', 'designer drugs' and 'emerging drugs' have been increasingly used in both research and in the media. The terms may be used interchangeably as many substances that have recently appeared (or reappeared) on the drug market may technically fit into all of these categories. To avoid confusion, definitions of each of these terms is given below:[43]

- *New psychoactive substance (NPS)* – defined by the UNODC as "substances of abuse, either in a pure form or a preparation, that are not controlled by the 1961 Single Convention on Narcotic Drugs or the 1971 Convention on Psychotropic Substances, but which may pose a public health threat. In this context, the term 'new' does not necessarily refer to new inventions but to substances that have recently become available".
- *Legal highs* – "an umbrella term for the unregulated (new) psychoactive substances or products intended to mimic the effects of controlled drugs. The term encompasses a wide range of synthetic and/or plant-derived substances and products, which are offered as 'legal highs'

(emphasising the idea of legality), 'research chemicals' (implying legitimate research use), 'party pills' (an alternative to 'party drugs') and 'herbal highs' (stressing the plant origin) etc.. They are frequently sold *via* the internet or in 'smart shops' or 'head shops' and in some cases are intentionally mislabelled, with purported ingredients differing from the actual composition".

- *Designer drugs* – defined by the EMCDDA and Europol as "substances designed to mimic the effects of known drugs by slightly altering their chemical structure in order to circumvent existing controls".
- *Emerging drugs* – not defined by UNODC or EMCDDA but often referred to in same context as NPS.

According to the UNODC, the multitude of NPS and the speed with which they have emerged in all regions of the world, is one of the most notable trends in drug markets over the past 5 years.[43] Substances falling under the definition of 'legal highs' posed the greatest challenge, with those involved in the illicit trade showing considerable innovation in the development of new production processes, products and marketing opportunities. The suppliers are able to adapt rapidly to control measures and use the internet to effectively market, sell and distribute recreational drugs.[2] Figure 1.53 demonstrates the increase in numbers of NPS reported globally in recent years.

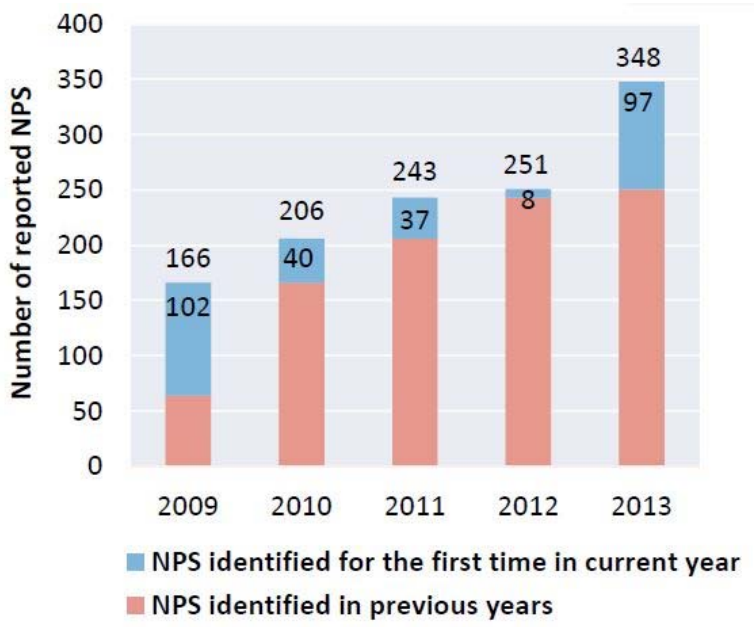


Figure 1.53: Number of NPS (cumulative) reported at the global level, 2009 to 2013[4]

By the end of 2013, 348 NPS were identified, most of which were reported since 2008. This well exceeds the total number of psychoactive substances currently controlled by international drug conventions (234 substances).[43]

Using the UNODC classification system, NPS are classified as follows:[147]

- Synthetic cannabinoids
- Synthetic cathinones
- Phenethylamines
- Piperazines
- Ketamine
- Plant-based substances
    - Khat (*Catha edulis*)
    - Kratom (*Mitragyna speciosa*)
    - *Salvia divinorum*
- Miscellaneous substances
    - Aminoindanes
    - Phenylcyclidine-type substances
    - Tryptamines

Many of these compounds are represented schematically under 'drugs of abuse' (Section 1.1, Figure 1.1).

The number of NPS identified globally has greatly increased in recent years and some of these substances (especially the synthetic cannabinoids and synthetic cathinones) were almost unheard of prior to 2008 (Figure 1.54).

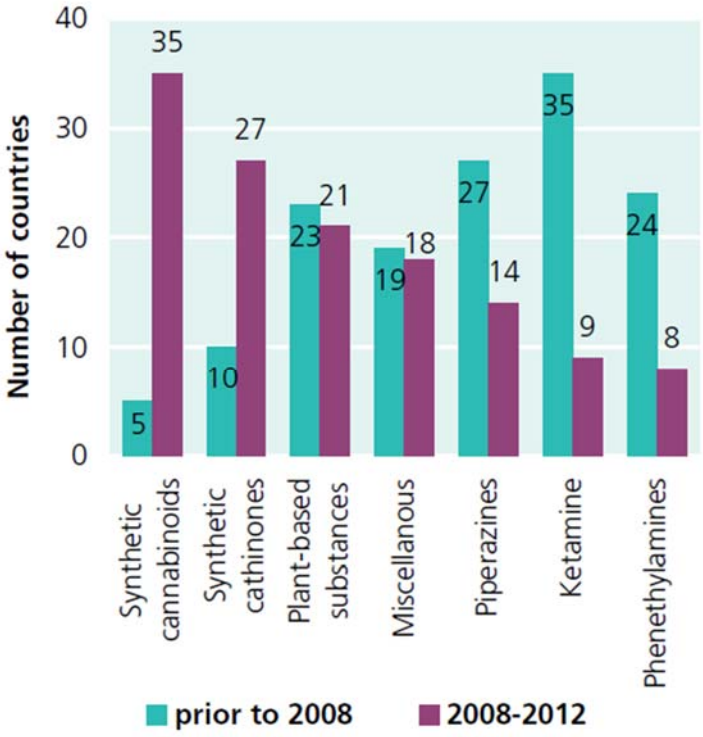
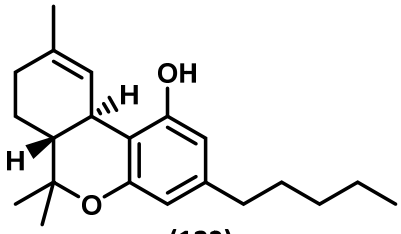


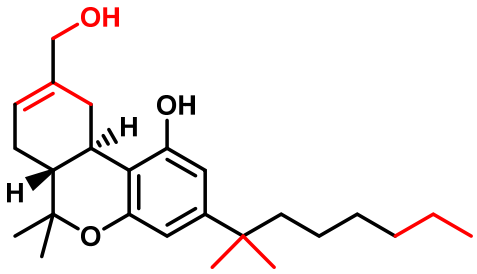
Figure 1.54: Global emergence of NPS by group, prior to 2008 and from 2008–2012[43]

1.7.1 Synthetic cannabinoids

Currently the most widely used NPS are the synthetic cannabinoids.[43,147] They are often mixed with various herbal mixtures and sold under the name 'Spice'. Other names include K2, Moon Rocks, Yucatan Fire and Skunk. The emergence of these synthetic cannabinoids in 'herbal highs' took place *ca.* 2004 and they share some structural similarities with Δ^9-tetrahydrocannabinol (THC) **(122)**, an active component of *Cannabis sativa*. Cannabinoids structurally similar to THC, are referred to as 'classical cannabinoids'. An example of a classical cannabinoid is 'HU-210' **(123)**, first synthesised in Israel in 1988.[147,148]

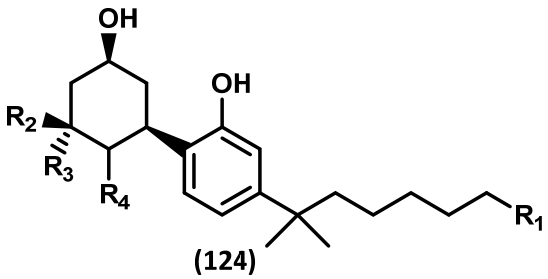


(122)



(123)

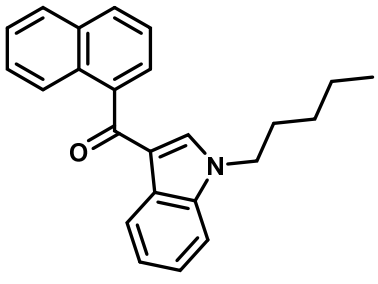
'Non-classical cannabinoids' include cyclohexylphenols ('CP compounds') of general structure **(124)**. These compounds were developed as potential analgesics in the 1980's and have been found in Spice products in numerous countries since 2009. Examples include CP-47,497 **(125)** and CP-47,497-C8 **(126)**.



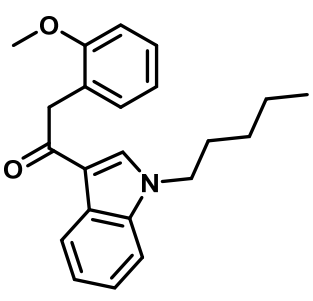
(124)

R_1=CH_3, R_2,R_3,R_4=H **(125)**
R_1=CH_2CH_3, R_2,R_3,R_4=H **(126)**

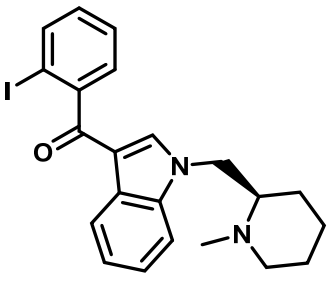
Other structurally dissimilar varieties of synthetic cannabinoids, unrelated to THC, have also emerged on the market. These include aminoalkylindoles, such as naphthoylindoles (e.g. JWH-018 **(127)**), phenylacetylindoles (e.g. JWH-250 **(128)**) and benzoylindoles (e.g. AM-2233 **(129)**).



(127)



(128)



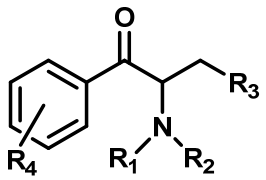
(129)

Similar to cannabis, these substances tend to elevate the mood, aid relaxation and alter perceptions. Negative side effects include increased heart rate, vomiting, agitation, confusion, and hallucinations.[43,149]

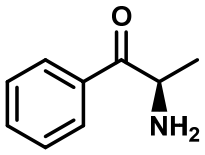
1.7.2 Synthetic cathinones

Cathinone and its derivatives are closely related to the phenethylamine family (which includes amphetamine and methamphetamine), but generally the cathinones are less potent than the phenethylamines.[147] Sometimes they are even classified under phenethylamines or ATS. They are characterised by the presence of a β-keto group on the side chain of the phenethylamine. (*S*)-Cathinone **(57)**, the principle active ingredient in the leaves of the Khat plant, can be considered the prototype for the range of synthetic cathinones that have emerged in recent years.

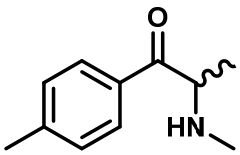
Synthetic cathinones appeared on the drug market in mid 2000's, with methylone **(130)** (a structural derivative of MDMA **(17)**) being the first to be reported to the EMCDDA in 2005.[147] Mephedrone (4-methyl-methcathinone) **(131)** use was first reported in 2007 in Israel and became a major concern in terms of public health, especially in the UK. A recent report suggested that 1.1% of adults (aged 16–59) in England and Wales had used mephedrone in 2011.[59] Subsequently, a generic ban was introduced in the UK, covering many of the mephedrone family.[150] Other synthetic cathinone derivatives, of general structure **(132)**, soon became available by substitution at various positions on the phenyl ring and side chain. Many of the derivatives (e.g. methylone **(130)**) were based on the structures of existing and well known ATS such as amphetamine **(10)**, methamphetamine **(14)** and MDMA **(17)**.



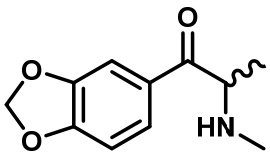
(132)



(57)



(131)

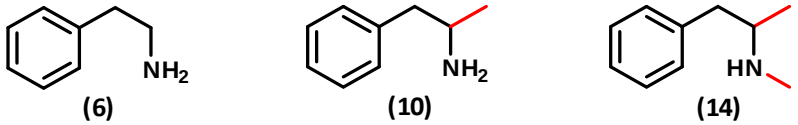


(130)

The synthetic cathinones are currently the most problematic group of NPS in terms of public safety and health.[43] Apart from the 'positive' psychological effects experienced by users, including euphoria, increased alertness, mental stimulation and increased sociability, synthetic cathinones share many of the negative side effects of ATS, including increased heart rate, hypertension, breathing difficulties, anxiety and hallucinations.

1.7.3 Phenethylamines

The structures of many of the commonly known phenethylamines were discussed in Section 1.2.2. 'Phenethylamines' is a broad term covering a large number of compounds, including derivatives of phenethylamine **(6)**, amphetamine **(10)** and methamphetamine **(14)**. 'Phenethylamines' is often used interchangeably with ATS.



(6) **(10)** **(14)**

There is no clear consensus in the literature on what compounds fall under the term phenethylamines. For example, Hill and Thomas[2] group many different phenethylamine related compounds (including the cathinones and aminoindanes) under 'phenethylamines' (Figure 1.55) whilst the cathinones and aminoindanes are classed as entirely separate groups under the UNODC system.[147]

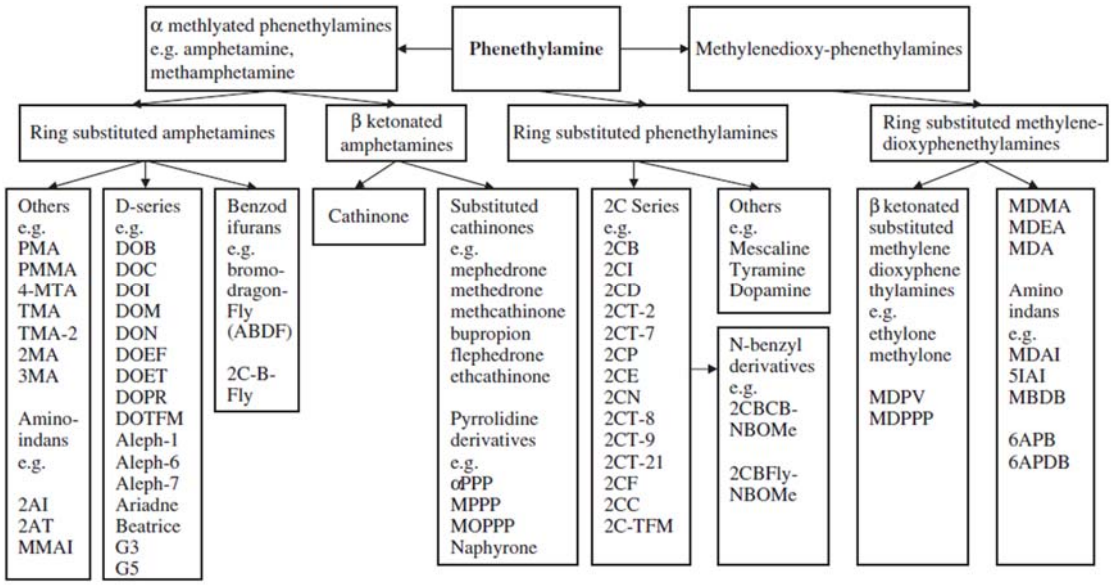


Figure 1.55: Classification of phenethylamines[2]

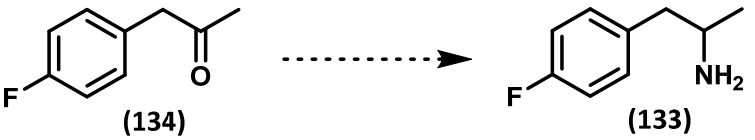
The high degree of structure variability and thus high number of available analogues, means the phenethylamines may induce a number of physiological responses, acting as stimulants, hallucinogens and entactogens. The optimal structural features that evoke each of these responses is outlined in Section 1.2.3 (Figure 1.6).

As mentioned previously, many of the phenethylamines/ATS were first synthesised by Shulgin and co-workers and published in PiHKAL in 1991.[12] Sixteen of these are included in Schedule I and II of the UN Convention of 1971. These are referred to as 'old phenethylamines' according to King *et al.*.[11] In 1997, the EU set up the Early Warning System on NPS and since then, a large number of novel

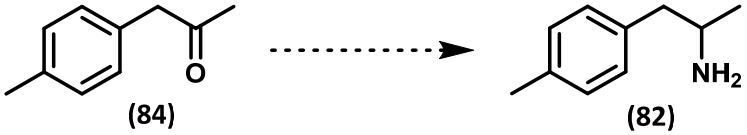
phenethylamines have been reported. In the past 20 years about 100 new phenethylamines have been found in Europe.

Since 2005 in particular, a number of novel 'phenethylamines' have appeared. These fall into 3 groups:

- Substances manufactured to evade controlled precursors or due to shortages in supply of controlled precursors like P2P. Examples include 4-fluoroamphetamine **(133)** and 4-methylamphetamine **(82)**, synthesised from 4-fluoro-P2P **(134)** and 4-methyl-P2P **(84)** respectively (both non-controlled precursors):

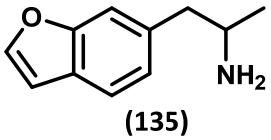


(134) (133)

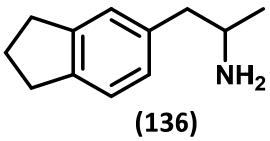


(84) (82)

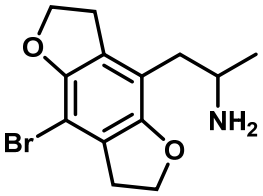
- Substances with fused rings. These include various benzofurans (e.g. 6-APB **(135)**), indanylalkylamines (e.g. 5-IAP **(136)**), dibenzofurans (e.g. DOB-FLY **(52)**) and 2-aminopropylindoles (e.g. 5-IT **(137)**):



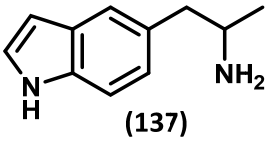
(135)



(136)



(52)



(137)

- The NBOMe-type substances or '*N*-benzyl-phenethylamines' – ATS that are *N*-substituted with a benzyl group (which may itself be ring substituted). These compounds have no history of human use prior to 2010, when they first became available online.[151] They have been described as super potent and selective 5-HT_{2A} receptor agonists.[38,39] They are usually synthesised from the parent phenethylamine, by reductive amination with the appropriate aldehyde, producing the *N*-benzyl product (Figure 1.56). One such compound of this type is

25C-NBOMe **(63)**. Compound **(63)** has been detected in a number of countries, including New Zealand where, in 2012, it was discovered to be on sale as 'legal LSD'.[151]

The way in which these compounds are named infers information about their structure. In the case of 25C-NBOMe **(63)** for example:

- '25-C' refers to the phenethylamine from which it is derived, in this case a 2,5-dimethoxy ('25'), 4-Chloro ('C') phenyl-substituted, phenethylamine.
- 'NB' refers to *N*-benzyl substitution (of the parent phenethylamine).
- 'OMe' refers to the substitution (in this case a methoxy group) on the aromatic ring of the *N*-benzyl moiety.

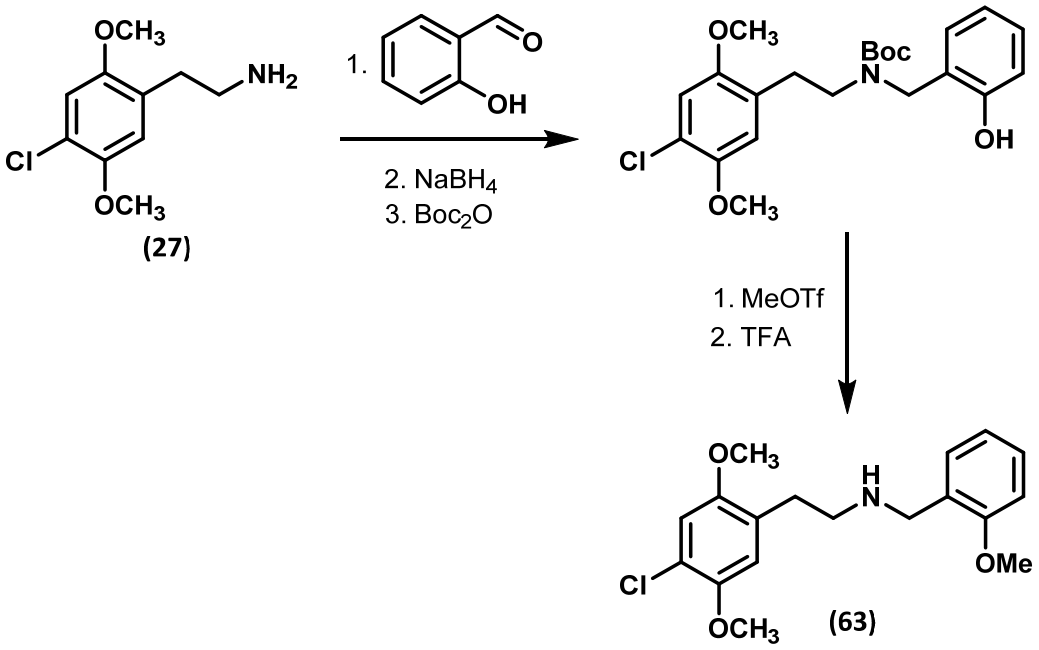


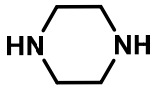
Figure 1.56: Synthesis of *N*-benzyl substituted phenethylamines[38]

1.7.4 Piperazines

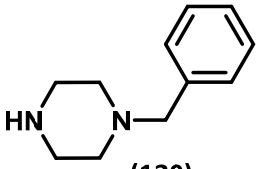
As the name suggests, this compound class is derived from piperazine **(138)**, a pharmaceutical introduced in 1953 for its anthelmintic properties, but later replaced upon development of better alternatives.[43] Derivatisation of the basic piperazine structure **(138)**, often with substituted phenyl/benzyl groups, has given rise to a number of drugs of abuse, including BZP **(139)**, 1-(3-chlorophenyl) piperazine (*m*CPP) **(140)** and 1-(3-trifluoromethylphenyl) piperazine (TFMPP) **(141)**.

The best known piperazine is BZP **(139)**, originally developed as a potential antidepressant drug. However, it was found to have similar properties to amphetamine and therefore was liable to abuse.[147] BZP has euphoric and stimulant properties, and when mixed with TFMPP **(141)** in the club and rave scene, possesses entactogenic properties similar to MDMA. In the late 1990's, BZP emerged as a 'legal

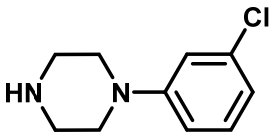
alternative' for MDMA and methamphetamine. In Europe, its use was first reported in Sweden in 1999, but it only became widespread as a NPS from 2004 onwards, until control measures were introduced in 2008 in the EU.



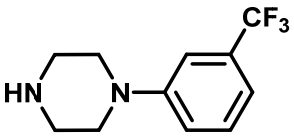
(138)



(139)



(140)

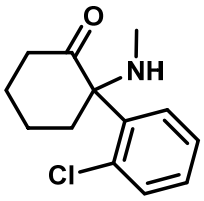


(141)

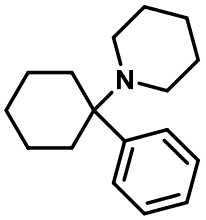
In Ireland, BZP **(139)** became a controlled drug firstly in March 2009 (*Misuse of Drugs Act 1977 (Controlled Drugs) (Declaration) Order 2009 (S.I. No. 121/2009)*).[65] It is now controlled under the *Misuse of Drugs (Amendment) Act, 2015*. Street names for BZP include "Jax", "A2", "Benny Bear", "Legal E" and "Pep X". Adverse effects of BZP include increased heart rate, hypertension, dilation of pupils, nausea, chest pains and hallucinations.

1.7.5 Ketamine

Ketamine **(142)** was synthesised as an anaesthetic in 1962, following the withdrawal of phenylcyclidine (PCP) **(143)**, a structurally similar compound with hallucinogenic effects. Both ketamine **(142)** and PCP **(143)** act as antagonists at *N*-methyl-D-aspartate (NMDA) receptors (glutamate receptor found in brain) and have psychotomimetic as well as anaesthetic properties.[14] Phenylcyclidine **(143)** and its derivatives will be discussed in Section 1.7.7.2.



(142)



(143)

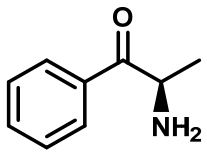
Ketamine is used in veterinary medicine for general anaesthesia and in human medicine to treat depression in patients with bipolar disorder.[43] The misuse of ketamine dates back to the 1980's and 1990's. It is used as a club drug and at raves, notably in South-East Asia, where it is often sold as MDMA. Street names for ketamine include "K", "Special K", "kit kat", "tac", "tic", "cat valium", "cat tranquillizer", "vitamin K", "ket" and "super K". Ketamine use is said to provide feelings of euphoria, increased energy and a sense of calm and serenity. Misuse can lead to an increase in heart rate, slurred speech, severe confusion, disorientation and shifts in perception of reality.

1.7.6 Plant based substances

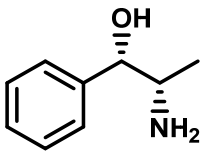
1.7.6.1 Khat

The khat shrub (*Catha edullis*) is a plant native to the horn of Africa and the Arabian Peninsula. Khat chewing is a social custom of communities living in these areas.[43] The psychoactive effects of khat are attributed to the release of (*S*)-cathinone **(57)** and cathine alkaloids (e.g. norpseudoephedrine **(58)**) after chewing. It is thought that cathinone is present at a concentration of about 78–343 mg per 100 g of fresh khat leaves.[28] Compounds **(57)** and **(58)** are controlled under the 1971 UN Convention on Psychotropic Substances but *Catha edullis* is not controlled internationally. Khat is under national control in several countries.

In Ireland, cathinone **(54)** is named in Schedule 1 (paragraph 1) of *The Misuse of Drugs Regulations, 1988 (S.I. No. 328/1988)*. Khat is covered by this legislation under paragraph 5 of the same schedule as "any preparation or other product containing any proportion of a substance or product specified in paragraphs 1, 2, 3 or 4…". Its control is now covered under the recent *Misuse of Drugs (Amendment) Act, 2015*.



(57)



(58)

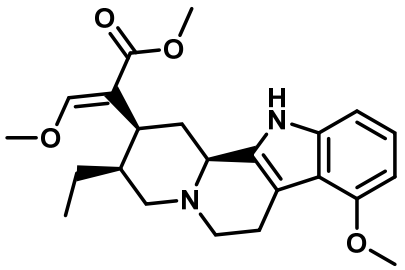
Norpseudoephedrine **(58)** was isolated from khat and identified in 1930, followed by the identification of cathinone **(54)** in 1975. Due to the degradation of cathinone, khat leaves need to be consumed soon after harvesting and therefore fresh leaves of khat are the preferred form of use.[147] The pharmacological effects of khat resemble those of amphetamine use, and includes increased alertness, euphoria, hypertension, anorexia and an increased respiration rate, heart rate and blood pressure. Prolonged use of khat has been linked to adverse effects that range from psychiatric disturbances, to damage of major organs of the body.

1.7.6.2 Kratom

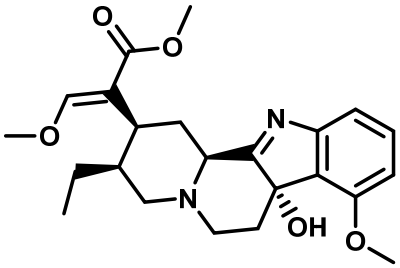
Kratom is a large tree found in South-East Asia, particularly Thailand. Kratom (*Mitragyna speciosa*) has been used in traditional Thai medicine as an anti-diarrhoeal and as a treatment for opioid dependence. However, it is also widely used recreationally, leading to its prohibition in Thailand.[43] It has also been illegal in Australia since 2005. Kratom is widely available *via* the internet, reflecting extensive demand for the product.[14] Kratom is a stimulant at low doses and a sedative at high doses. At low doses, it

tends to increase physical energy and alertness. At higher doses, it helps to reduce physical and emotional pain and generates feelings of well-being before eventually developing its sedative properties.

Over 40 alkaloids have been isolated from Kratom, two of which are shown below – mitragynine **(144)** (first isolated in 1921) and 7-hydroxymitragynine **(145)** (more potent than mitragynine or morphine). Both of these compounds became controlled in Ireland (by name) under the *Misuse of Drugs 1977 (Controlled Drugs) (Declaration) Order 2011 (S.I. No. 551/2011)*. They are now controlled under the *Misuse of Drugs (Amendment) Act, 2015*.



(144)

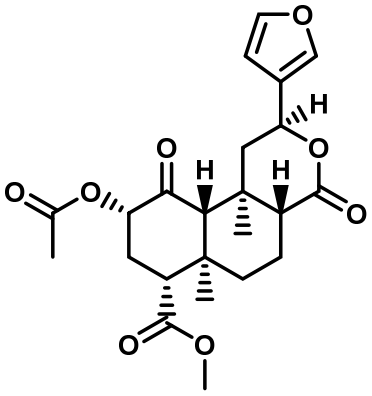


(145)

1.7.6.3 Salvia divinorum

Salvia divinorum is a psychoactive plant indigenous to forest areas in Oaxaca, Mexico. It was traditionally used by Mazatec Indians for religious practices and medicinal purposes, and its use as an NPS dates back to the 1990's.[43,147] Neoclerodane diterpene 'salvinorin A' **(146)** is the active component responsible for the psychoactive effects of the plant.

Salvia divinorum is typically consumed by sucking and chewing the fresh leaves or crushing of the leaves to make a drinkable infusion. Smoking of the dry leaves is also reported and this is said to produce short but intense hallucinations. The effects include various psychedelic experiences and in contrast to other drugs, its use prompts dysphoria (sadness and depression). In addition, it may prompt a decreased heart rate, slurred speech, lack of coordination and possibly loss of consciousness.



(146)

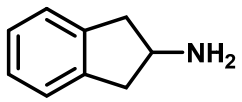
'salvinorin A'

The active component, 'salvinorin A' **(146)** was originally controlled in Ireland (by name) under the *Misuse of Drugs 1977 (Controlled Drugs) (Declaration) Order 2011 (S.I. No. 551/2011)*. It is now covered under the *Misuse of Drugs (Amendment) Act, 2015*.

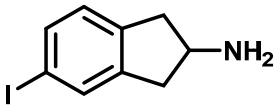
1.7.7 Miscellaneous substances

1.7.7.1 Aminoindanes

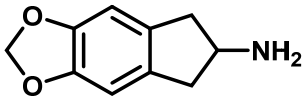
Aminoindanes have arose as NPS in recent years due to their ability to mimic the empathogenic and entactogenic effects of serotonin releasing drugs, such as MDMA.[147] Following legislation controlling the cathinones in the UK in 2010, it was thought that the aminoindanes may be the next wave of 'legal highs' to act as substitutes to controlled drugs.[152] Their use however, has not (yet) come close to the level at which the cathinones were used. The aminoindanes are conformationally rigid analogues of ATS; the 5-membered ring of aminoindane may be envisaged as the cyclic analogue of the ethylamine side chain present in ATS. As a result, the aminoindanes are sometimes placed under the 'phenethylamines' class (see Section 1.7.3, Figure 1.55). 2-Aminoindane (2-AI) **(147)** is a rigid analogue of amphetamine **(10)**. The basic bicyclic structure **(147)** can be modified to produce diverse chemical substances such as 5-iodo-2-aminoindane (5-IAI) **(148)** and 5,6-methylenedioxy-2-aminoindane (MDAI) **(149)**.



(147)



(148)



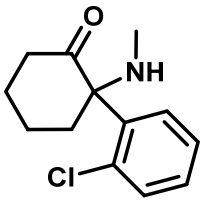
(149)

Aminoindanes may be prepared from indanone, indene or from the intramolecular cyclisation of the acyl chloride derivative of 3-phenyl-2-propionic acid. Aminoindanes are reported to have potent effects on serotonin release and re-uptake, and possess stimulant and entactogenic properties.[152] Street names for MDAI **(149)** include "MDAI gold", while 2-AI **(147)** has been found in party pills known as "pink champagnes". Aminoindanes are commonly found in powder form and crystals, and are usually ingested, but snorting is also possible. MDAI **(149)** and 5-IAI **(148)** are reported to be highly potent selective serotonin releasing agents.

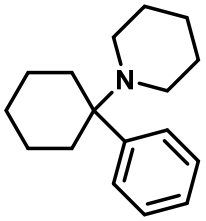
1.7.7.2 Phenylcyclidine-type substances

As reported earlier (Section 1.7.5), phenylcyclidine (PCP) **(143)** is structurally similar to ketamine **(142)** and both are classified as arylcycloalkylamines.[147] PCP was first synthesised in the 1950's and sold until 1967 as an injectable anaesthetic in the US, under the trade names Sernyl® and Sernylan®. It was

withdrawn from the market due to intense negative psychological effects, such as dysphoria, confusion, delirium and psychosis.

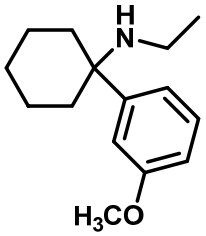


(142)

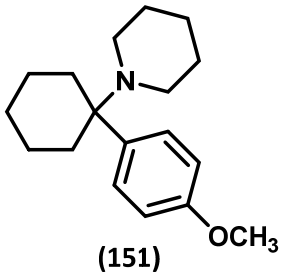


(143)

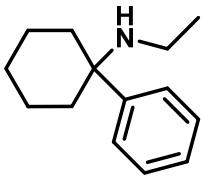
Its recreational use began in the mid 1960's and PCP-type substances first appeared as 'research chemicals' in Europe in 2010. 3-Methoxyeticyclidine (3-MeO-PCE) **(150)** was the first to be reported in the UK in 2010, followed by 4-methoxyphencyclidine (4-MeO-PCP) **(151)** in Norway, Russia and the UK in 2011.



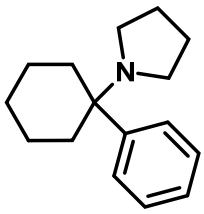
(150)



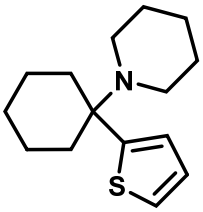
(151)



(152)



(153)

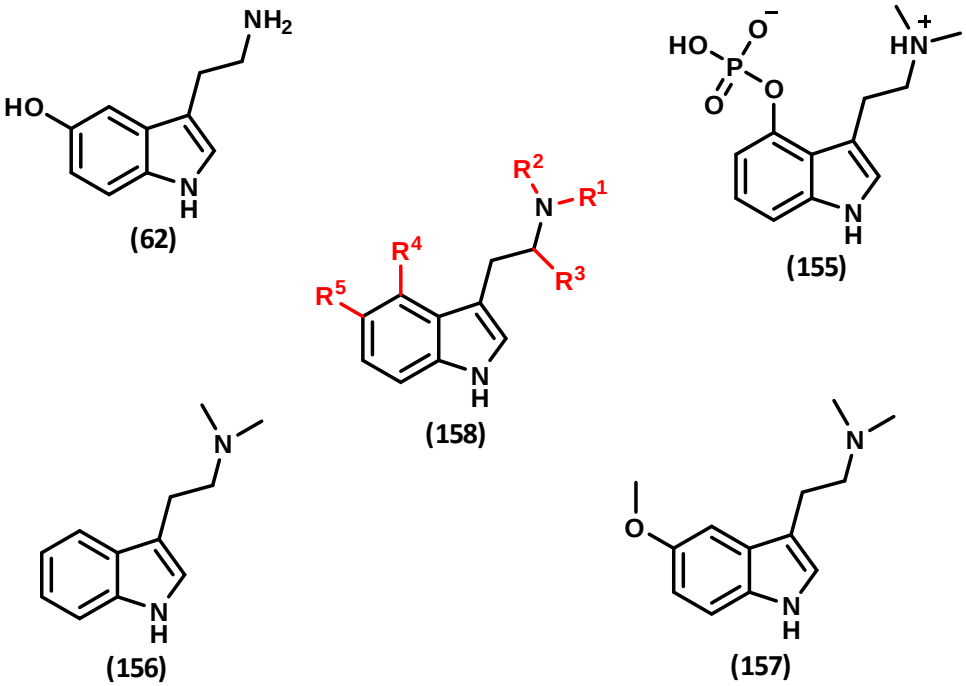


(154)

PCP and phenylcyclohexyl analogues, including eticyclidine (PCE) **(152)**, rolicyclidine (PHP, PCPY) **(153)** and tenocyclidine (TCP) **(154)** are controlled under Schedule I of the 1971 UN Convention but derivatives such as 3-MeO-PCE **(150)** and 4-MeO-PCP **(151)** are not under international control.

1.7.7.3 Tryptamines

Unlike other classes of NPS (e.g. the phenethylamines), many of the tryptamines are naturally occurring compounds: some are natural neurotransmitters (like serotonin **(62)**) while most are psychoactive hallucinogens found in plants, fungi and animals (like psilocybin **(155)** – found in 'magic mushrooms').[147] Other natural tryptamines include dimethyltryptamine (DMT) **(156)** and 5-methoxy-*N*,*N*-dimethyltryptamine (5-MeO-DMT) **(157)**.



A number of synthetic tryptamine derivatives have been produced. Substitution at various positions (R^1–R^5) of generic trytamine **(158)** results in a multitude of synthetic derivatives. Many of these derivatives were produced by Shulgin and co-workers and published in TiHKAL ('Tryptamines I Have Known And Loved')[153] in 1997, a sequel to PiHKAL. A number of tryptamine analogues are summarised in the scheme below (Figure 1.57).

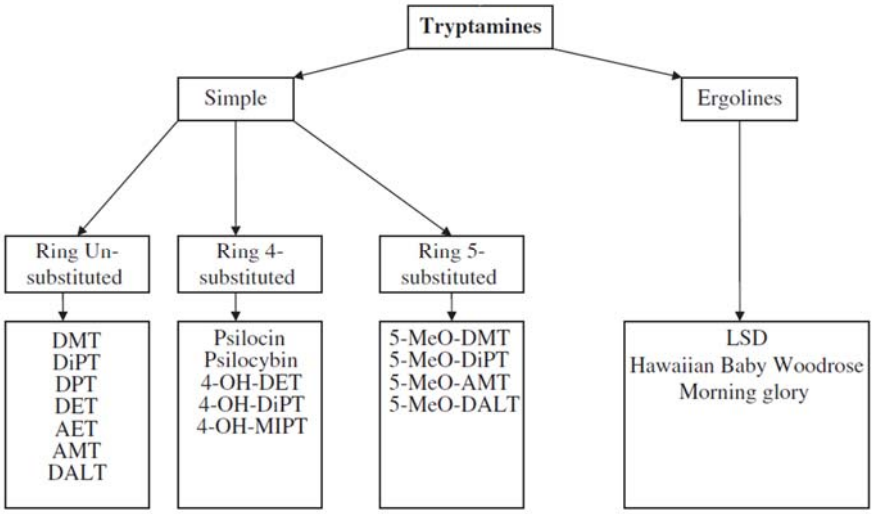


Figure 1.57: Classification of tryptamines[2]

The use of tryptamines leads to a hallucinatory state, linked to auditory, visual and temporal distortions of reality. Natural tryptamines are commonly available in preparations of dried or brewed mushrooms, while tryptamine derivatives are sold in capsule, tablet, powder or liquid form.

The use of NPS in recent years and the rate at which they are emerging (about 1 NPS/week in the EU), has led to international law enforcement agencies playing catch-up with illicit producers. Introducing new legislation to control these new substances was traditionally very slow but more recently (April 2014), the European Parliament endorsed the EU Commission's proposals for a much more rapid system to control these substances.[154] Up to now, it took a minimum of two years to ban a substance in the EU. Under the new rules, the EU will be able to act within just 10 months. In particularly serious cases, the procedure will be shorter still (4 months); substances that are deemed a particularly high risk can be quickly removed from the market for one year while a full risk assessment is being carried out.

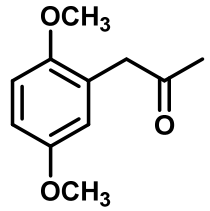
At a national level, a large number of countries have, in recent years, introduced new legislation to control NPS. Example of some of these pieces of legislation are given in Figure 1.58.

Country	System in place	Legislation/Bills
Canada	Analogue control	The Controlled Drugs and Substances Act (CDSA)
United States	Analogue control	Controlled Substances Analogue Enforcement Act (CSA) of 1986: Section 802 (32) (A)
United Kingdom	Generic control	Home Office circular 010/2010. A change to the Misuse of Drugs Act 1971 : Control of mephedrone and other cathinone derivatives
Other countries	Generic control	From 2009-2013 this approach has been used to ban in several european countries to ban NPS.[9]
Denmark	Temporary bans	Consolidated Act no. 748 of 1 July 2008 on Euphoriant Substances (para. 1, 2)
Hungary	Temporary bans	Government Decree 66/2012
New Zealand	Temporary bans	Misuse of Drugs Act (Section 4 (C))
United Kingdom	Temporary bans	Misuse of Drugs Act 1971 (amended by the Police Reform and Social Responsibility Act 2011, Section 151, Schedule 17)
United States	Temporary bans	US Controlled Substances Act, 1986, Part B § 811 (h)
Singapore	Temporary bans	Bill No. 27/2012 (Section 58A, in force since 01.05.2013)
Luxembourg	Rapid procedure	Act of 12 July 1996 on the Reform of the Council of State (lasts between 1-2 months); Grand-Ducal Regulation of 7 October 2004
Norway	Rapid procedure	Regulation of 30 June 1978 No. 8 on narcotics section 3.
Poland	Rapid procedure	Act 29 July 2005
Slovakia	Rapid procedure	Act 139/1998 Collection of 2 April on narcotic drugs and psychotropic substances
Sweden	Rapid procedure	The Narcotic Drugs (Punishments) Act (SFS 1968:64) or the Act on the Prohibition of Certain Goods Dangerous to Health (SFS 1999:42); the Narcotic Drugs Control Ordinance (SFS 1994:1554); Ordinance regarding the Prohibition of Certain Goods Dangerous to Health (SFS 1999:58)
Austria	Specific NPS legislation	Federal Act on the Protection against health hazards in connection with *new psychoactive substances* (2011)
Ireland	Specific NPS legislation	The Criminal Justice (Psychoactive Substances) Act 2010
New Zealand	Specific NPSlegislation	The Psychoactive Substances Bill
Romania	Specific NPS legislation	Law 194/2011 of 10 November 2011

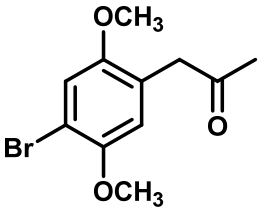
Figure 1.58: Worldwide examples of legal responses to NPS[155]

1.8 Research outline

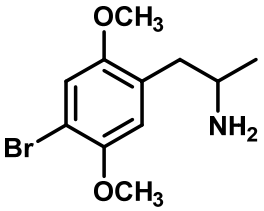
Much of the research work carried out in this thesis centres on the synthesis and impurity profiling of the ketone precursor 2,5-dimethoxyphenyl-2-propanone (2,5-P2P) **(92)** and its 4-bromo derivative (4-Br-2,5-P2P) **(159)**, a direct precursor to the hallucinogenic amphetamine DOB **(35)**.



(92)



(159)



(35)

The research was focussed on the ketone precursors for the following reasons:

- Research into the synthesis and impurity profiling of routes from the ketone precursor to the target amphetamine (e.g. Leuckart route) for these compounds had been well explored previously within our research group.
- The ketone intermediate is a very versatile reagent. Not only can it be used as a precursor to both amphetamine and methamphetamine, but it can itself be synthesised from several 'pre-precursor' chemicals.[120] This means, if a particular pre-precursor becomes more controlled, illicit drug producers may simply switch to another pre-precursor, many of which are well documented in the literature.
- The use of substituted P2P-type precursors (non-controlled) is increasing due to stricter controls on P2P **(65)** (listed on Table I of the UN Convention against Illicit Traffic in Narcotic Drugs and Psychotropic Substances, 1988). For example, recently there have been seizures of 4-fluoroamphetamine **(133)** and 4-methylamphetamine **(82)** synthesised from 4-fluoro-P2P **(134)** and 4-methyl-P2P **(84)** respectively (see Section 1.7.3), avoiding the need to source/manufacture controlled P2P.[11] This may suggest that there may be even more of a shift in the future, from traditional ATS (amphetamine/methamphetamine/MDMA) to substituted analogues, in order to circumvent legislation.

The routes to the P2P-type intermediate investigated include the 'phenylacetic acid (PAA) route', the 'nitrostyrene route' (using aldehyde starting materials **(72)** or **(160)**) and the 'Darzens route' (from aldehyde starting materials **(72)** or **(160)**, *via* glycidate intermediates **(161)** or **(162)**) (Figure 1.59). As described in Sections 1.5.1.1 and 1.6.1, the PAA and nitrostyrene routes are commonly encountered in the clandestine synthesis of amphetamine **(10)** and MDMA **(17)**, whilst the Darzens methodology has only been adopted in very recent years.

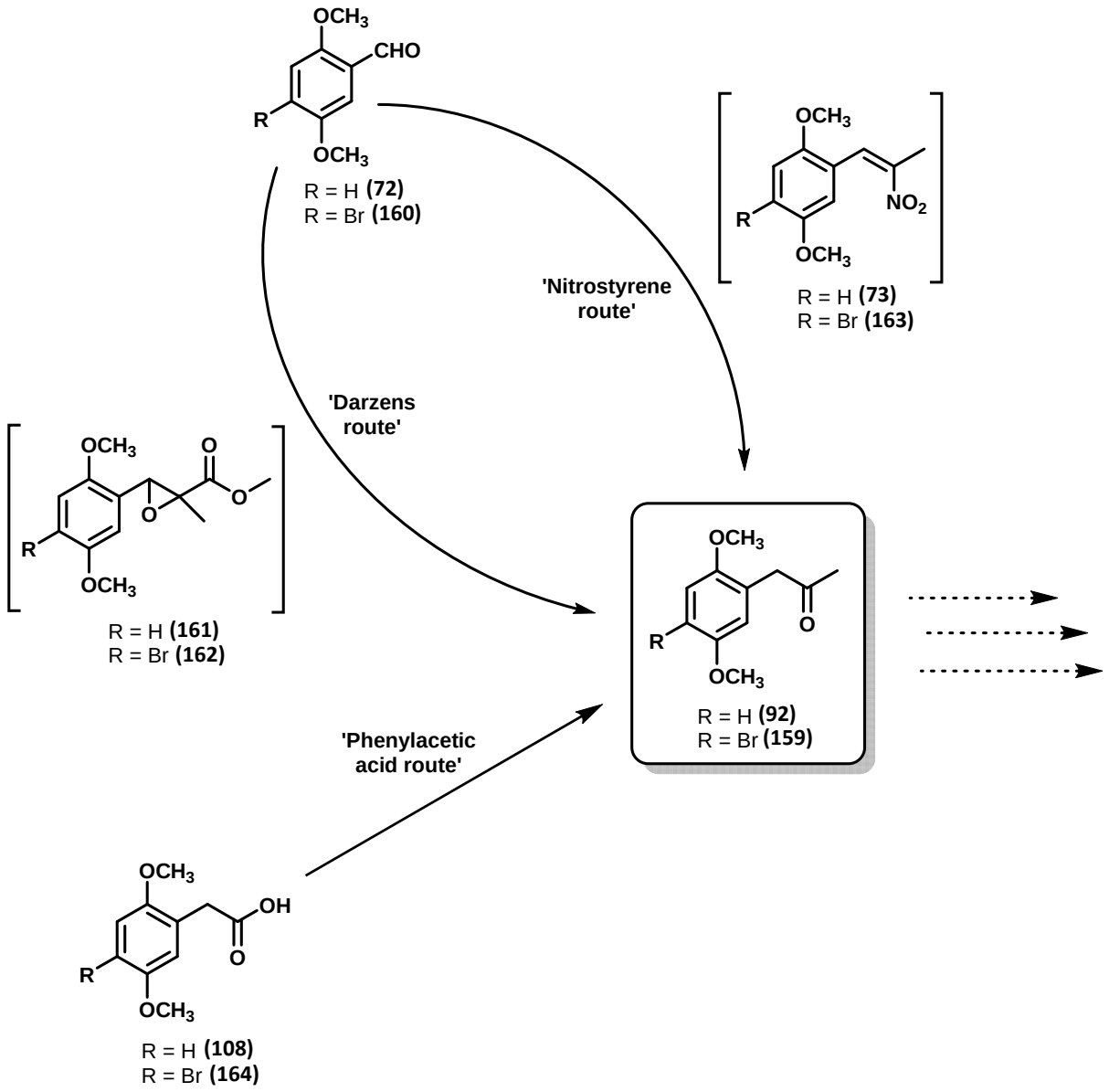


Figure 1.59: Synthetic routes to 2,5-P2P (92) and 4-Br-2,5-P2P (159)

DOB **(35)** is a drug of major interest to our research group, so the bromination of some of the starting materials and intermediates that may be used in the preparation of **(35)**, was also investigated. Aromatic bromine substitution of simple monomeric compounds may be carried out in a single reaction step and several procedures are available in the literature for this. Many of these procedures involve use of elemental bromine (Br_2).

The bromination step may take place at any stage during the multistep synthesis of the target DOB, so this may give rise to a number of potential brominated impurities. For example, in the synthesis of DOB from phenylacetic acid starting material **(108)**, bromination may take place at the start of the synthesis (bromination of the phenylacetic acid starting material), after formation of 2,5-P2P **(92)** or even after the formation of the amphetamine **(31)** (Figure 1.60).

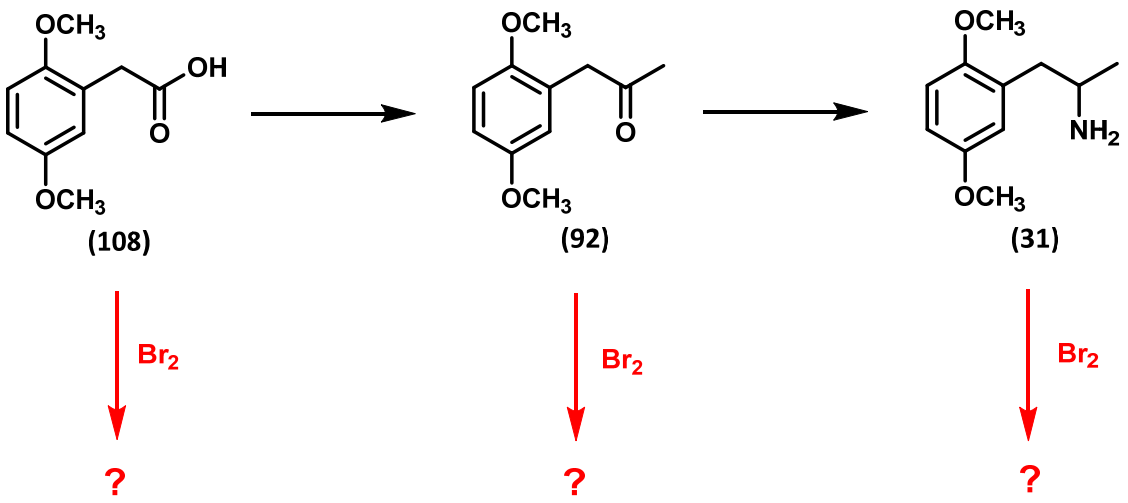


Figure 1.60: Starting materials/intermediates that may be subjected to bromination during synthesis of DOB

Different impurity profiles will result from bromination at various stages of the synthesis. Presumably, the further along the synthetic sequence that bromination takes place, the more likely it is for multiple brominated impurities to arise, given that some impurities/unreacted intermediates get carried forward from one step to the next.

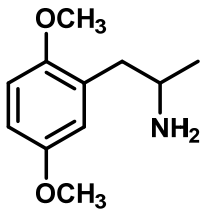
Note: Where possible, the basic synthetic methods used throughout this work are taken from published materials which are accessible to and used by clandestine chemists (websites/books dedicated to clandestine manufacture). Every effort is made to mimic the reaction conditions used by clandestine chemists, in order acquire comparable impurity profiles. However, safety conditions (and scale) also influenced the synthetic protocols used, and these may not be as carefully considered in clandestine laboratories.

Chapter 2 – Impurity profiling of the bromination of 2,5-dimethoxybenzaldehyde

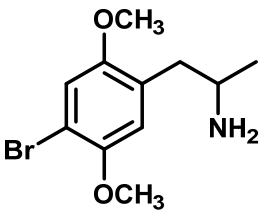
Amphetamines with 2,5-dimethoxy substitution on the phenyl ring, are among the most potent hallucinogens known to man. Introduction of a halogen atom, such as bromine, to the aromatic 4-position enhances the potency even further. Bromination of 2,5-dimethoxybenzaldehyde, a key 'pre-precursor' to DOB and related 2,5-dimethoxyamphetamines, is well reported in the literature. However, impurities other than the 6-bromo regioisomer have not been reported to date. From an impurity profiling viewpoint, this reaction step is important, given that it is an early stage reaction in the sequence to the target amphetamine. Impurities formed at this stage are likely to be carried forward through subsequent reaction steps and may be found in the final drug product. Knowledge of these impurities and how they arise may also be important in assessing potential toxicity of compounds present in the illicit drug product. The work in this chapter relates to the identification of a number of previously unreported impurities of the aforementioned bromination step. Full characterisation of these impurities using techniques such as ^{1}H-NMR, ^{13}C-NMR, IR and HRMS was carried out, as well as matching of the LC-MS profiles of the recovered impurities with in-house synthesised reference standards, for confirmation of molecular structure. This data may be useful to researchers investigating the origin of impurities in illicit amphetamines such as DOB.

2.1 Introduction

The bromination of the hallucinogen DMA **(31)** at the aromatic 4-position, gives rise to an amphetamine of even greater hallucinogenic potency, DOB **(35)**.



(31)



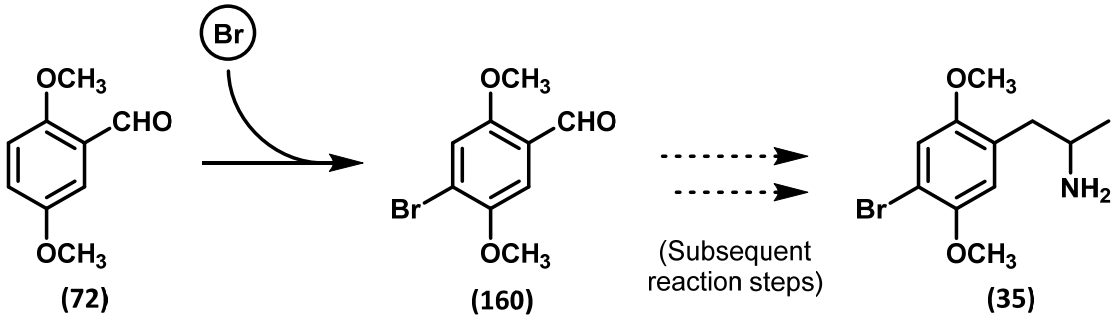
(35)

Derivatives of DMA ('D series' compounds) with hydrophobic groups at the aromatic 4-position, exhibit high 5-HT_{2A} affinity because these groups interact with a specific lipophilic pocket within the receptor binding site. Precursors/pre-precursors to ATS are rarely found to have this hydrophobic group already incorporated into their structure, so clandestine chemists involved in the manufacture of compounds of this type are forced to introduce this group as part of their synthetic protocol.

In the case of DOB, introduction of a Br atom at the aromatic 4-position is required. This bromination step may, in theory, occur at any stage in the synthetic sequence to DOB. In Shulgin's DOB synthesis published in PiHKAL in 1991,[12] the Br atom is introduced after the amine side chain is formed, i.e. it is the final step in the reaction sequence. In many other published routes, bromination is carried out as the first step in the sequence, i.e. bromination of a pre-precursor. From an impurity profiling viewpoint, early stage bromination is important as nondescript (or non regiospecific) bromination of the pre-precursor may occur, giving rise to a number of brominated analogues. These may be carried forward through the reaction sequence and greatly increase the complexity of the impurity profile of the final drug product.

2.1.1 Bromination of 2,5-dimethoxybenzaldehyde (72) in the literature

As discussed in Section 1.5.1.1 of Chapter 1, a common pre-precursor to amphetamine is benzaldehyde **(76)**. In the case of the 'D series' amphetamines, the equivalent would be 2,5-dimethoxybenzaldehyde **(72)**. Bromination at the aromatic 4-position of this compound would result in a direct pre-precursor of DOB **(35)** – i.e. aldehyde **(160)**:



Br = Source of bromine atom (e.g. Br_2)

The synthesis of 4-bromo-2,5-dimethoxybenzaldehyde **(160)**, involving the bromination of 2,5-dimethoxybenzaldehyde **(72)**, is reported a number of times in the literature. In most cases the source of bromine is elemental bromine (Br_2) due to its widespread availability and low cost. Reaction conditions and yields vary slightly and some of the reports concerned with this reaction are summarised in Table 2.1.

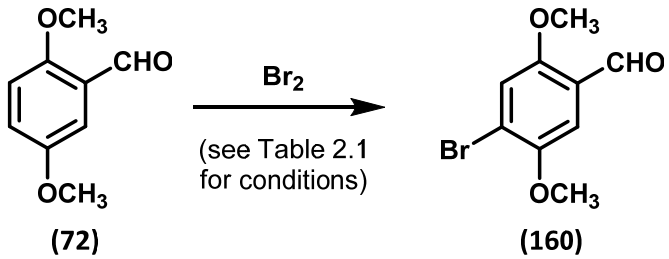
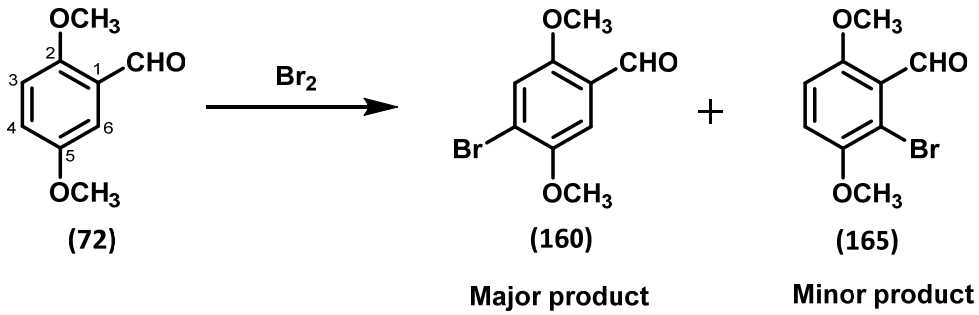


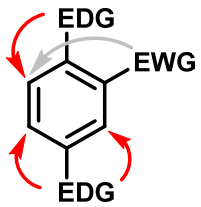
Table 2.1: Bromination of 2,5-dimethoxybenzaldehyde as reported in the literature

Reaction conditions	Purification method	Yield	Source
Br_2 (1.02 eqv.), AcOH, rt, 48 h	Recrystallisation (EtOAc)	**55%**	Simmons *et al.*[156]
Br_2 (1.1 eqv.), AcOH, rt, 12 h	Recrystallisation (EtOH)	**62%**	Koo *et al.*[157]
Br_2 (1.1 eqv.), AcOH, 0 °C–rt, 1 h	Flash column (EtOAc/Hexane)	**56%**	Radomkit *et al.*[158]
Br_2 (1.1 eqv.), AcOH, rt, 4 h	(Not provided)	**45%**	Tisdale *et al.*[159]
Br_2 (1.2 eqv.), AcOH, rt, 24 h	Flash column (EtOAc/Hexane)	**56%**	Griffin[26]
Br_2 (1.0 eqv.), DCM, $SnCl_4$, rt–reflux, 2 h + rt overnight	Recrystallisation (MeOH/H_2O)	**44%**	Bedford *et al.*[160]
Br_2 (1.0 eqv.), DCM, $SnCl_4$, rt–reflux, 2 h + rt overnight	Recrystallisation (MeOH/H_2O)	**66%**	Barfknecht and Nichols[161]
Br_2 (1.0 eqv.), DCM, $SnCl_4$, rt–reflux, 2 h + rt overnight	Flash column (EtOAc/Hexane)	**42%**	Griffin[26]

In most of these reports the 4-bromo product is used as an intermediate in the synthesis of various organic compounds with no concern for impurity profiling, so additional impurities/by-products are rarely mentioned. The first mention of an impurity of this reaction was in a paper by Sardessai *et al.*[162] whereby the 6-bromo regioisomer **(165)** was isolated in a yield of 5% (Br_2 (1.0 eqv.), AcOH, rt, 2–3 days). 6-Bromo **(165)** was also encountered by Griffin *et al.*[26] whereby it was isolated in yields of 24% (Br_2 (1.0 eqv.), dichloromethane (DCM), $SnCl_4$, rt–reflux, 2 h + rt overnight) and 31% (Br_2 (1.2 eqv.), AcOH, rt, 24 h).



Bromination at these particular sites on the aromatic ring and the dominance of the 4-bromo over the 6-bromo isomer can be explained by the principle of electrophilic aromatic substitution, in addition to steric effects. The 2,5-dimethoxybenzaldehyde starting material **(72)** has 2 methoxy groups and one aldehyde group on the aromatic ring. The methoxy groups are electron donating (EDG) and so direct substitution towards the *ortho* and *para* positions (see structure **(166)**). The lone pair of electrons on the oxygen atom of the methoxy groups can feed into the aromatic system making particular sites on the ring more nucleophilic. The aldehyde group is electron withdrawing (EWG) and this directs substitution towards the *meta* position. However, the electron donating effect of the methoxy groups is much greater than the electron withdrawing effect of the aldehyde. Thus the *meta* directing character is very weak.



(166)

Drawing out the resonance structures that result from the lone pair donation into the ring system demonstrates that of the three free ring positions (3, 4 and 6), the 4-position is most nucleophilic (Figure 2.1).

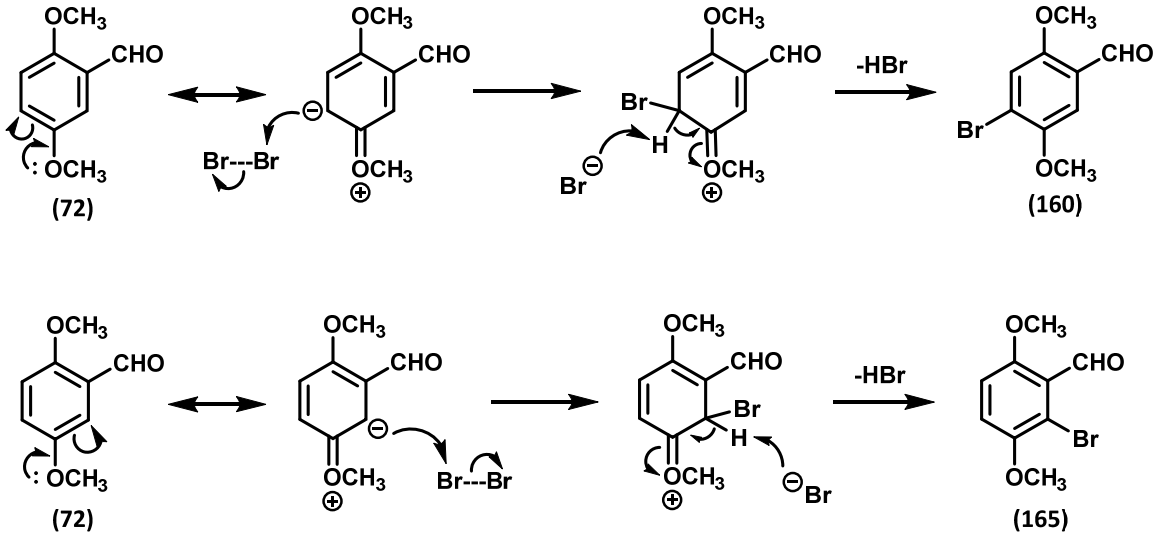


Figure 2.1: Formation of 4-bromo (160) and 6-bromo (165) aldehydes

It may appear from Figure 2.1, that the 4- and 6-positions are equally nucleophilic. However, steric hindrance also plays an important role, with the result that the 4-position is favoured, due to its less hindered nature.

Bromination at the 3-position may also seem in theory to be very favourable. Like the 4-position, it is sterically unhindered and *ortho* to an electron donating methoxy group. Similar to Figure 2.1, where the 5-methoxy group feeds electron density onto the 4- and 6-positions making them nucleophilic, it is just as plausible for the 2-methoxy group to feed electron density onto the 3-position. Also, the aldehyde (EWG) is *meta* directing (weakly in comparison to the electron donating effects of the methoxy groups) and the 3-position is in fact, *meta* to the aldehyde group. These arguments would make the 3-bromo compound **(169)** just as likely (if not more likely) to be a product of the bromination of 2,5-dimethoxybenzaldehyde, as the 4-bromo product **(160)**. In reality, the 3-bromo compound **(169)** has not been documented as a product of this reaction in the literature, to our knowledge. One plausible explanation for this is that the 2-methoxy (EDG) is *ortho* to the aldehyde (EWG) and the flow of electrons from this 2-methoxy group is more likely to move in the direction of the aldehyde ('Pathway B', Figure

2.2) rather than onto the 3-position ('Pathway A', Figure 2.2), making it less likely to exist as a stable resonance form, and thus the 3-position would be less nucleophilic.

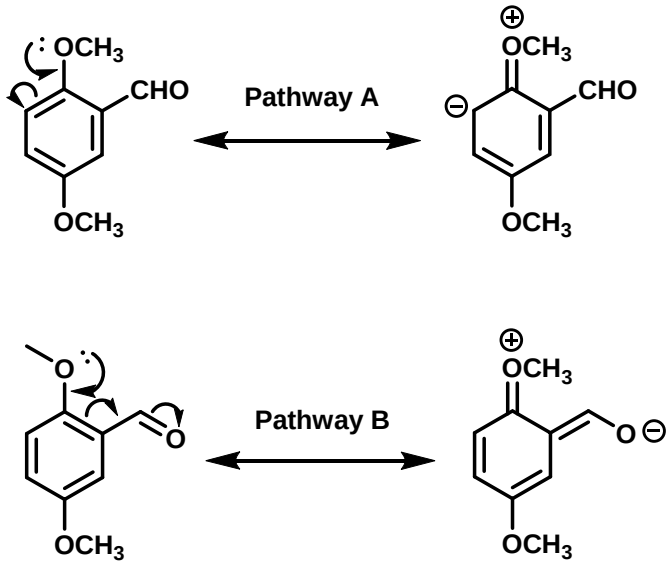


Figure 2.2: Different pathways of electron flow from the 2-methoxy group into the aromatic ring

2.2 In-house bromination of 2,5-dimethoxybenzaldehyde (72)

As mentioned, the bromination of 2,5-dimethoxybenzaldehyde **(72)** may be carried out using a number of reagents/conditions. In this work, the bromination procedure adhered to involved using Br_2 liquid (≈1.2 equivalents) in AcOH at rt for 24 h. This procedure is very common in the literature for brominating a range of compounds (see Table 2.1). It is also a very simple method with accessible reagents, and is reported on websites pertaining to clandestine drug manufacture.[162]

When this reaction was carried out in-house, both the 4-bromo **(160)** and 6-bromo **(165)** products were obtained, with the 4-bromo regioisomer present in a much higher yield than the 6-bromo. Having carried out the reaction a number of times, it was observed that even under the same conditions, the yields of products, amount of unreacted starting material (SM) recovered and the ratio of 4-bromo to 6-bromo products was quite variable. On average however, the yields of 4-bromo-2,5-dimethoxybenzaldehyde **(160)** and 6-bromo-2,5-dimethoxybenzaldehyde **(165)** were found to be 74% and 15% respectively; the ratio of 4-bromo to 6-bromo averaging at 5:1. Results were found to be even more variable when reaction conditions were altered slightly. These slight alterations were carried out in an attempt to emulate the variability of clandestine laboratory manufacture, as it unlikely that the illicit synthesis of ATS is carried out in an environment as controlled as our laboratory. The reaction of 2,5-dimethoxybenzaldehyde **(72)** and Br_2 was carried out at different temperatures and with differing equivalents (eqv.) of Br_2. The results are summarised in Table 2.2.

Table 2.2: Reaction of aldehyde (72) with varying reaction times and equivalents of Br_2

Entry	Temp.	Br_2 (eqv.)	Time (h)	Ratio of 4-bromo:6-bromo:SM*
1	rt	1.2	24	3.1 : 1 : 1.4
2	rt	1.8	40	4.8 : 1 : 0.1
3	40 °C	1.1	24	7.4 : 1 : 2.2
4	50 °C	1.6	24	21.5 : 1 : 0

*Based on ratios of C*H*O shift in ^{1}H-NMR spectra of crude reaction mixtures prior to purification
(Note: For reaction entries 2, 3 and 4, purification of products/SM was not pursued)

Table 2.2 demonstrates some of the trends that may be observed when reaction conditions for the bromination of 2,5-dimethoxtbenzaldehyde are varied.

Firstly, increasing reaction temperature, increasingly favours the formation of the 4-bromo compound **(160)** over the 6-bromo **(165)** (Entry 4, Table 2.2 – ratio of 4-bromo:6-bromo = 21.5 : 1 @ 50 °C). However, one must also consider the boiling point of Br_2 is low (58.8 °C)[163] so when approaching this temperature, it is more likely that a larger amount of Br_2 will remain in the headspace of the reaction vessel or be lost if the reaction vessel is not sealed. One would probably have to use more equivalents of Br_2 to compensate for this loss at higher temperature. This may explain why the reaction did not go to completion (residual starting material present) in Entry 3, Table 2.2. In this reaction, only 1.1 equivalents of Br_2 was used so it seems likely that some of this (>0.1 eqv.) was lost, or remained in the headspace during the reaction.

Secondly, it appears that increasing both the eqv. of Br_2 and to a lesser extent reaction time, pushes the reaction towards completion (full consumption of SM). Increasing Br_2 eqv. does not appear to have a huge effect on the ratio of 4-bromo:6-bromo regioisomers formed (Entry 1 *vs.* Entry 2, Table 2.2).

It may seem that using a large excess of Br_2 would achieve reaction completion and a maximum product yield. However, from a practical point of view, Br_2 can be difficult to remove from the products and if carried forward to subsequent reaction steps may brominate other reactants/products, forming undesired impurities.

In summary, it was found that the suitable conditions for satisfactory reaction completion whilst limiting the effort required to remove residual bromine from the crude reaction mixture, involved using ≈1.2 eqv. of Br_2 for 24 h. If the 4-bromo product **(160)** in particular was desired, slightly elevated temperature (≈30 °C) and a slightly larger excess (+ 0.1–0.2 eqv.) of Br_2 (to compensate for loss of volatile Br_2) were employed.

Yields and ratios of the 4-bromo **(160)** and 6-bromo **(165)** products were slightly different to that obtained by Griffin.[26] In the work by Griffin, isolated yields of **(160)** and **(165)** were 56% and 31% respectively (ratio = 1.8:1), compared to 74% and 15% (ratio = 5:1) achieved using similar conditions (≈1.4 eqv. of Br_2, @ rt for 24 h – see Section 5.2.1). This discrepancy is not surprising because, as

mentioned previously, the reaction outcome (yields and ratio of products) was found to be quite variable for this particular reaction. Isolation of products was achieved by flash column chromatography (EtOAc/hexane) on silica gel and resolution of regioisomers was relatively facile given the difference in R_f values (see procedure – Section 5.2.1). These R_f values, as well as the IR and HRMS data collected for the 4-bromo **(160)** and 6-bromo **(165)** products, are summarised in Table 2.3.

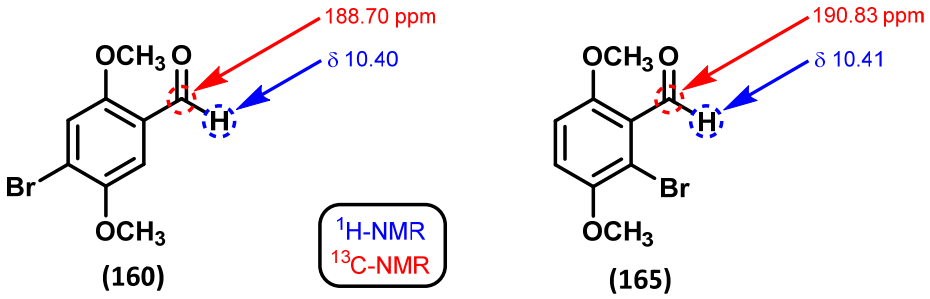


Table 2.3: Yield, R_f, m.p., IR and HRMS data for 4-bromo (160) and 6-bromo (165) products

Compound No.	Yield	m.p. (°C)	R_f*	IRν_{max} (KBr) (cm^{-1})	HRMS ($M+H^+$)⋆ (*m/z*)	
					Calc.	Found
(160)	74%	129–131 (EtOH/H_2O)	0.60	1678 (C=O), 1604, 1575, 1484 (C=C)	244.9813	244.9821
(165)	15%	100–101 (DCM/hexane)	0.26	1690 (C=O), 1599, 1567, 1479 (C=C)	244.9813	244.9808

*mobile phase = 30:70 EtOAc:hexane

⋆molecular ion (M) calculated for ^{79}Br isotope peak

Due to similarities in R_f values, residual SM **(72)** and 4-bromo product **(160)** would quite often co-elute during column chromatography, thus reducing the isolated yield of the 4-bromo product **(160)**. Having said this, recrystallisation of the 4-bromo/SM mixture (from EtOH/H_2O) results in very satisfactory purification of the 4-bromo product **(160)**, given that the SM remains dissolved in the mother liquor.

Differences of R_f values, m.p. and IR spectra can be used to distinguish between the two main products (Table 2.3). Definitive structural assignment (especially for regioisomers) is provided by ^{1}H-NMR. For these compounds, it is the aromatic region of the spectra (δ 6.5–8) which is characteristic. For 4-bromo **(160)**, 2 × 1H singlets are observed in the aromatic region (@ δ 7.25 and 7.34) (Figure 2.3). This is as expected given that the 3- and 6-positions are the only unoccupied positions (only H atom attached) on the ring and these positions are *para* to one another. As *para* splitting is rarely observed in aromatic ring systems (generally <1 Hz if observed), these protons are observed as singlets. For 6-bromo **(165)**, the two unoccupied ring positions are the 3- and 4-positions. As these positions are *ortho* to each other, the expected *ortho* coupling is observed. This results in 2 × 1H doublets being observed in the aromatic region of the ^{1}H-NMR spectrum, each with a coupling constant of 9 Hz (Figure 2.3). These observations are in-line with previously documented data for this particular reaction.[26,162]

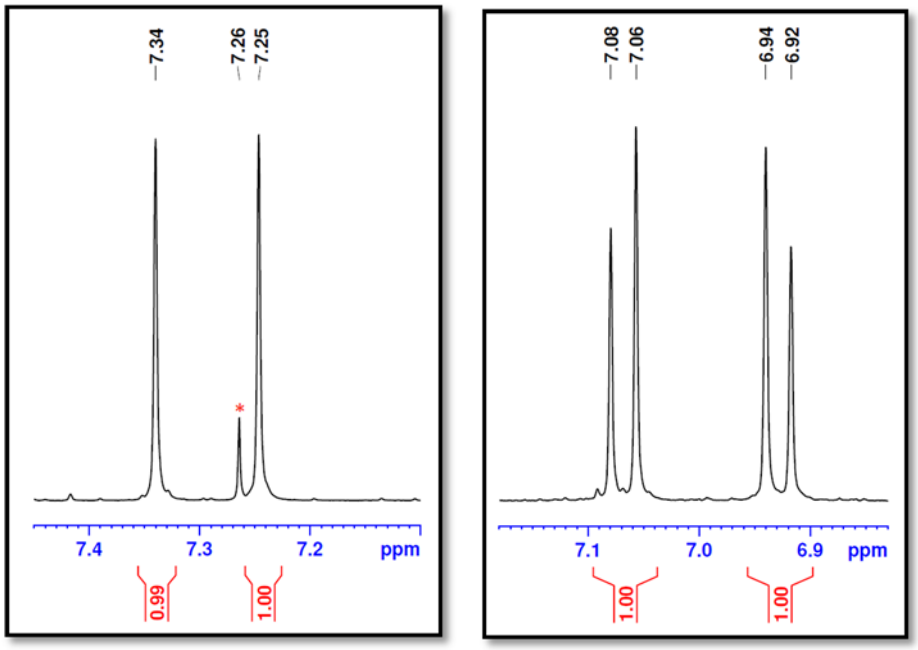


Figure 2.3: Aromatic regions of ^{1}H-NMR spectra of 4-bromo (160) (left) and 6-bromo (165) (right) aldehydes

(= residual solvent – $CHCl_3$)*

2.2.1 Detection of minor impurities of the bromination of 2,5-dimethoxybenzaldehyde (72)

Of the several times that the bromination of 2,5-dimethoxybenzaldehyde **(72)** was carried out, it was observed that a number of minor unidentified baseline shifts were present in the ^{1}H-NMR spectrum of the crude sample, prior to purification by flash column chromatography. The presence of several additional spots was also observed on TLC, none of which corresponded to the known R_f values of the products and SM. Of the minor unidentified shifts in the ^{1}H-NMR spectrum of the crude sample, three were in a similar region to the aldehyde (CHO) proton shifts of the known products (≈ δ 10–10.5) (see structures accompanying Table 2.3). This tentatively suggested that there may be at least 3 unknown impurities that, like the known products, possessed an aldehyde functional group in their structure.

Whilst carrying out flash column chromatography in order to purify the known 4-bromo **(160)** and 6-bromo **(165)** products, the first major fraction collected (at 8/92 EtOAc/hexane) consisted of an enriched sample of these unknown impurities. As depicted in Figure 2.4, this first fraction contained, in addition to trace amounts of the known 4-bromo **(160)** and 6-bromo **(165)** products, a substantial amount of unknown compounds with ^{1}H-NMR signals resonating at δ 10.30, δ 10.32 and δ 10.39. These 'unknown' signals are encircled in orange in Figure 2.4 overleaf.

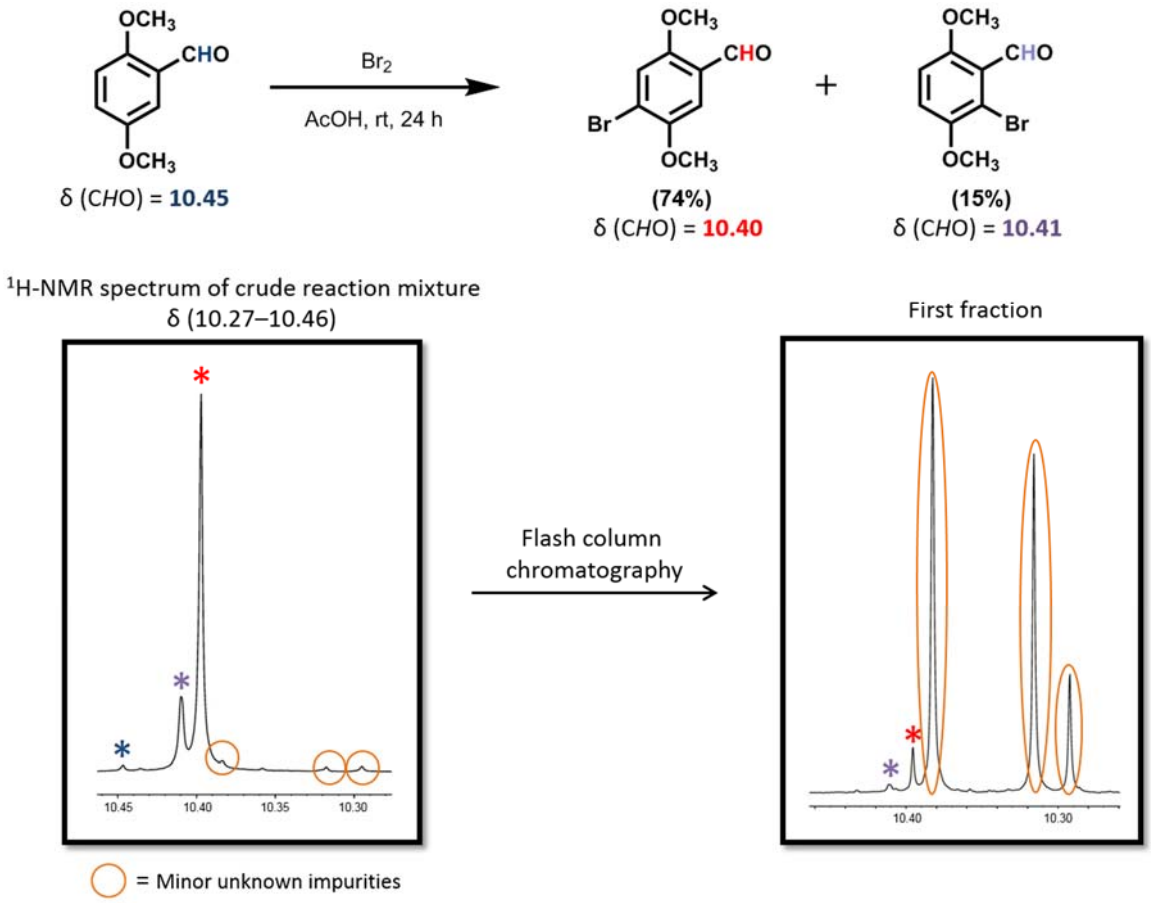


Figure 2.4: Region of δ 10.27–10.46 ppm of ^{1}H-NMR spectrum of the crude product and that of the first recovered fraction following flash column chromatography

Evidence for the presence of a number of unknown impurities in the crude reaction, was also provided by HPLC (Figure 2.5). As well as the two major peaks at 1.4 and 2.3 min (known products **(160)** and **(165)**), there were also a number of smaller peaks at 2.7, 3.5, 4.1 and 4.9 min.

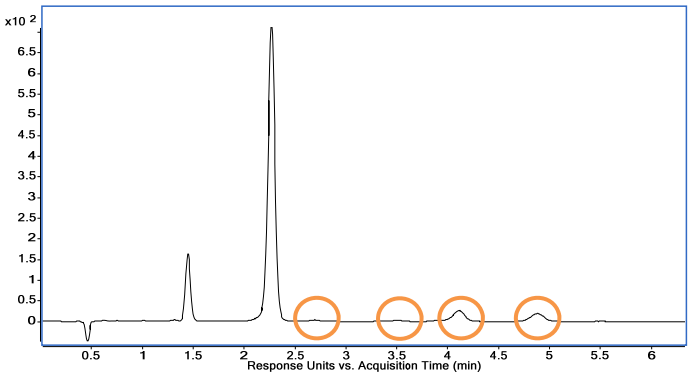


Figure 2.5: HPLC chromatogram of crude reaction from the bromination of 2,5-dimethoxybenzaldehyde (72)

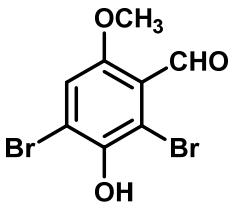
(Mobile phase = 50/50 'CH$_3$CN'/'H$_2$O' (ESI+ mode, isocratic elution – see Section 5.1), flow rate = 1.5 mL/min, column = Agilent Zorbax Eclipse XDB-C18, 3.5 µm, 4.6×75 mm @ 20 °C, injection vol. = 5 µL, signal recorded @ 210 nm)

2.2.2 Attempted isolation and identification of detected impurities using ^{1}H-NMR and LC-MS

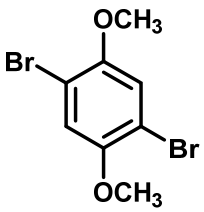
In an attempt to isolate and identify the detected impurities, additional flash column chromatography was carried out on the first recovered fraction. This time however, a lower proportion of EtOAc (1/99 EtOAc/hexane) was used to start with, in an attempt to achieve better resolution of the unknowns. After carrying out slow, thorough column chromatography on this fraction, none of the unknown compounds could be fully isolated. Two main (impure) fractions were recovered from this secondary column, the first recovered at 1/99 EtOAc/hexane and the second at 2/98 EtOAc/hexane. Based on integrations of the shifts present in the ^{1}H-NMR spectra of both of these fractions, it appeared that there were two different compounds present in each fraction, i.e. four unidentified impurities in total, none of which had been previously reported for this reaction.

Based on the ^{1}H-NMR data for these fractions (using integrations of chemical shifts, their location on the δ 0–14 ppm scale and splitting patterns of signals in the aromatic region of the spectrum), tentative structures were assigned to the four impurities (Figure 2.6).

Second column, fraction 1

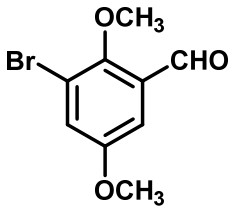


(167)

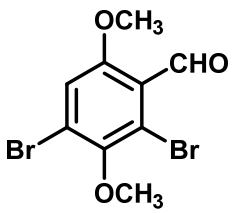


(168)

Second column, fraction 2



(169)



(170)

Figure 2.6: Tentative structures assigned to impurities recovered in fractions 1 and 2

Based on the structures assigned, it was envisaged that for fraction 1, the two impurities may be separated by acid/base extraction, by exploiting the fact that phenol **(167)** may become ionised in a basic (high pH) aqueous solution. This extraction was carried out (Chapter 5, general procedure 5.2.1.1) and was successful in separating the two compounds (**(167)** and **(168)**), allowing for their full characterisation (discussed later in Sections 2.3.4 and 2.3.6).

At this stage, two novel impurities had been isolated from the bromination of 2,5-dimethoxybenzaldehyde **(72)** and another two structures were proposed based on the ^{1}H-NMR spectrum of a mixture.

In order to support the structural evidence provided by ^{1}H-NMR, it was decided to run samples of the recovered impurities (two isolated **(167)** and **(168)**, and two as a mixture **(169)** and **(170)**) on LC-MS. This would provide accurate masses of the impurities, providing further evidence for the (tentatively) assigned structures, as well as establishing if the mixture of impurities (inseparable by flash column chromatography) could be resolved by HPLC.

To start, pure samples of the SM **(72)** and two known products 4-bromo **(160)** and 6-bromo **(165)**, were run so that retention times (t_R) of these could be recorded and compared against a sample of the crude reaction mixture (Figure 2.7).

(Note: All compounds were UV active @ 210 nm and were detected using a Diode Array Detector (DAD)).

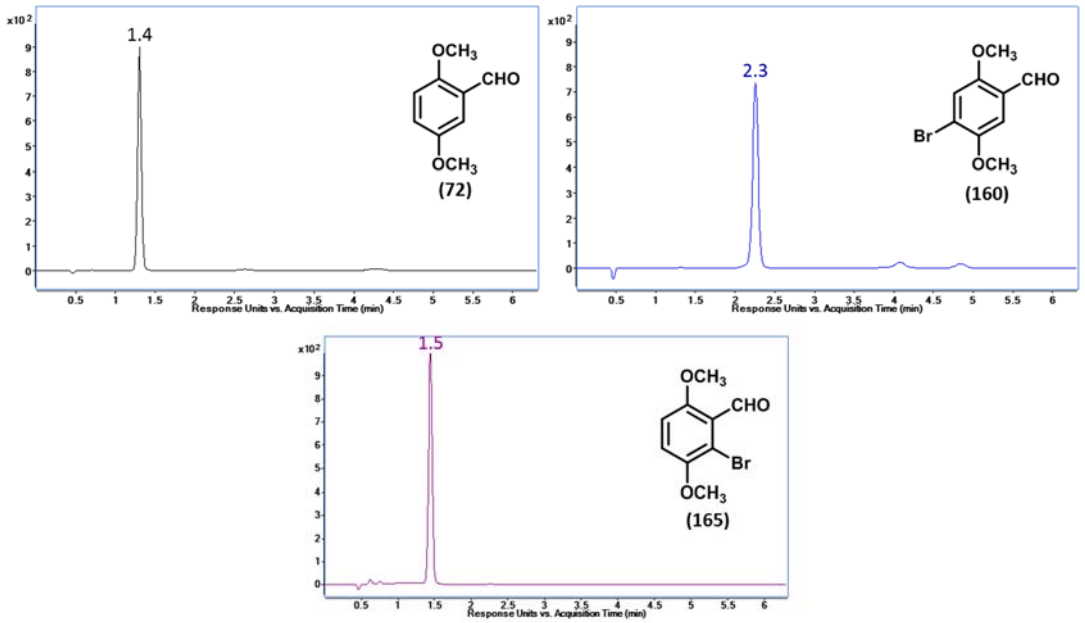


Figure 2.7: Individual HPLC runs (DAD signal @ 210 nm) of the SM (72), and the 4-bromo (160) and 6-bromo (165) regioisomers

*(HPLC acquisition conditions similar to those outlined in Figure 2.5, with the exception of the injection vol. used – 1 µL for **(72)**, 4 µL for **(160)** and 2 µL for **(165)**)*

The HPLC chromatograms show that the SM **(72)** (t_R = 1.4 min), and two known products of the reaction **(160)** (t_R = 2.3 min) and **(165)** (t_R = 1.5 min), all elute within 2.5 min. Also, by comparing retention times, the two major signals in the crude sample run (Figure 2.5) were a match with, as expected, the 4-bromo **(160)** and 6-bromo **(165)** products, run individually in Figure 2.7 above.

Following this, the two isolated impurities **(167)** and **(168)**, and the mixture of impurities **(169)** and **(170)**, were run under the same HPLC conditions used for the SM and known products in Figure 2.7. The chromatograms obtained for the impurity runs are shown in Figure 2.8.

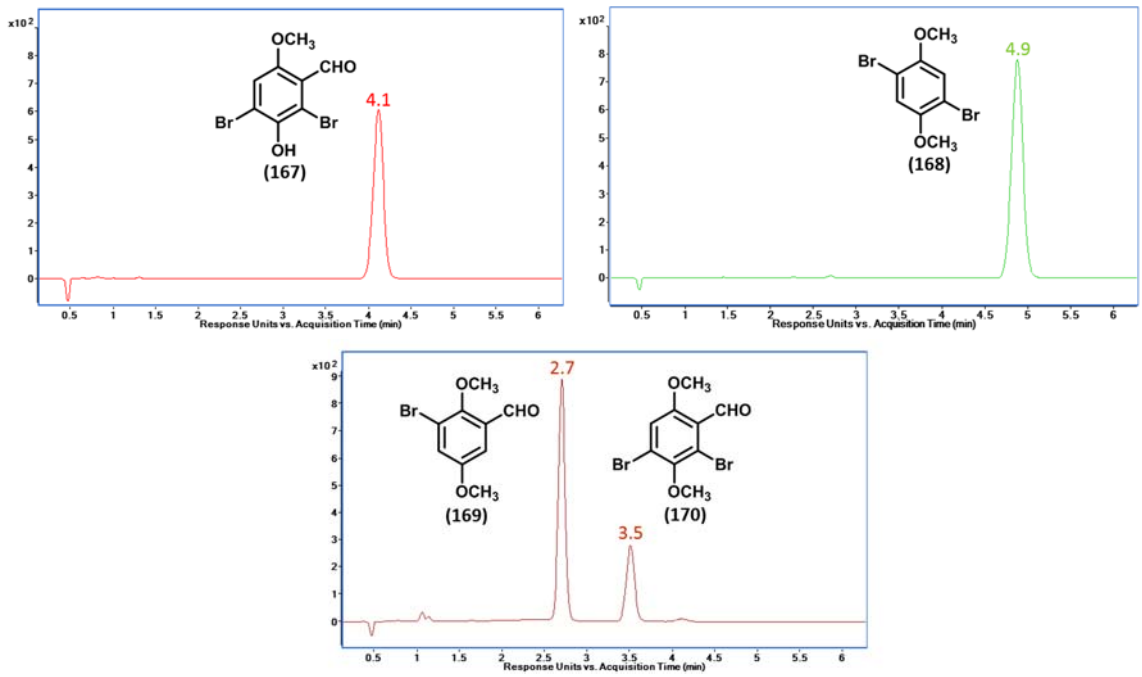


Figure 2.8: Individual HPLC runs (DAD signal @ 210 nm) of the proposed impurities, two isolated (167) and (168), and two present as a mixture (169) and (170)

*(HPLC acquisition conditions similar to those outlined in Figure 2.5, with the exception of the injection vol. used – 8 µL for **(167)**, 5 µL for **(168)** and 5 µL for mixture of **(169)** and **(170)**)*

The retention times of the four impurities were found to be 2.7, 3.5, 4.1 and 4.9 min. These are a good match with the four minor impurity peaks, highlighted earlier (encircled in orange) in the chromatogram of the crude mixture (prior to column chromatography) in Figure 2.5.

The chromatogram of the mixture in Figure 2.8 shows that there is good resolution of the two impurities (**(169)** and **(170)**), that were previously found to be inseparable by flash column chromatography. This is a very positive result as it shows that these compounds would be identified much easier if they were encountered during impurity profiling, as clean mass spectra could be obtained.

Given that it was shown that the starting material, expected products and impurities could be resolved by HPLC, the next step was to attempt to obtain mass spectra of the impurities as evidence that the proposed structures were in agreement. Using slightly altered conditions, more suitable for LC-MS (e.g. reduced flow rate and injection volume) the LC stream was diverted to the MS in order to obtain TIC (Total Ion Count) chromatograms (using ElectroSpray Ionisation in positive mode (ESI+)) for each of the products and impurities. TIC signals for the SM **(72)**, 4-bromo **(160)** and 6-bromo **(165)** products, as well as the impurities **(167)**, **(169)** and **(170)**, were obtained. These individual runs were then overlaid as shown in Figure 2.9. This overlaying of the signals demonstrates that good resolution of the signals is maintained using MS detection (in addition to UV detection).

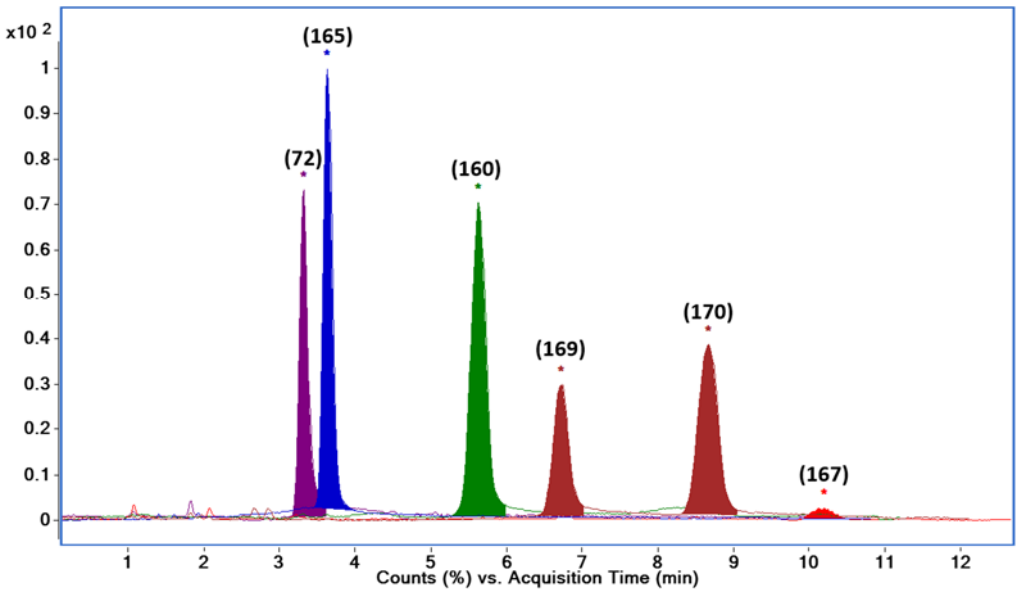


Figure 2.9: Overlays of TIC signals (ESI+) for SM (72), expected products (160) and (165), and selected impurities (167), (169) and (170)

*(Mobile phase = 50/50 'CH$_3$CN'/'H$_2$O' (isocratic), flow rate = 0.6 mL/min, column = Agilent Zorbax Eclipse XDB-C18, 3.5 µm, 4.6×75 mm @ 20 °C, injection volumes = 0.4 µL for **(72)**, 0.5 µL for **(165)**, 2 µL for **(160)**, 3 µL for mixture of **(169)** and **(170)** and 3 µL for **(167)**)*

Good TIC signals (all ESI+) were obtained for the SM **(72)**, 4-bromo **(160)** and 6-bromo **(165)** products and the 3-bromo **(169)** and 4,6-dibromo **(170)** impurities (Figure 2.9). The mass spectra extracted from each of these TIC signals are shown in Figure 2.10.

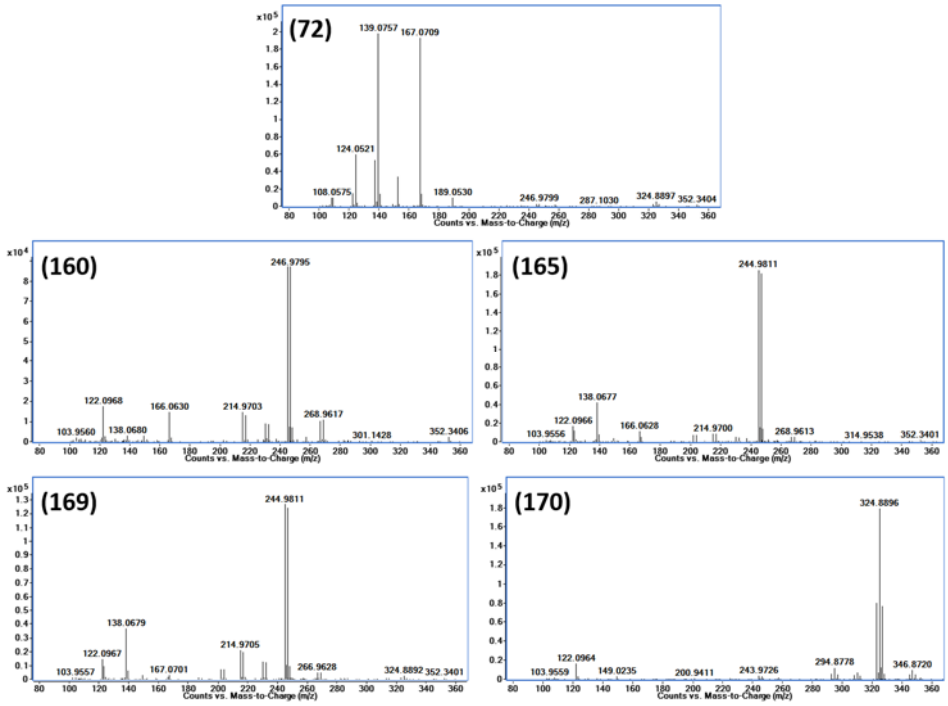


Figure 2.10: Extracted MS spectra from TIC signals obtained in Figure 2.9

(See Chapter 5 for general MS conditions, e.g. source parameters)

The final two mass spectra in Figure 2.10, allow for the assignment of the two peaks in the mixture of what was previously postulated to be 3-bromo **(169)** and 4,6-dibromo **(170)** impurities (see mixture in Figure 2.8). The mass spectrum for **(169)** is very similar to spectra for the 4-bromo **(160)** and 6-bromo **(165)** expected products, having the same abundant 'doublet' molecular ion ($M+H^+$) peak at 245/247 *m/z*. The 'doublet' peak (ratio ≈ 1:1) is indicative of a compound containing one bromine atom as bromine has two naturally occurring common isotopes (^{79}Br and ^{81}Br) that exist in a ratio of ≈ 1:1. As this impurity has the same *m/z* as the 4- and 6-bromo products but has a different t_R, the only other ring position that may be brominated is the 3-position. Thus, this impurity is most likely 3-bromo-2,5-dimethoxybenzaldehyde **(169)**, as was postulated earlier based on the ^1H-NMR signals present in the mixture.

The spectrum for the compound proposed to be structure **(170)**, has a high abundance 'triplet' molecular ion ($M + H^+$) peak at 325 *m/z*, the 'triplet' indicative of a compound containing two bromine atoms. This *m/z* and isotope pattern is in agreement with a dibromo-substituted 2,5-dimethoxybenzaldehyde material. The compound structure proposed earlier, 4,6-dibromo-2,5-dimethoxybenzaldehyde **(170)**, is one of only three possible structures to fit this profile (*vs*. the 3,6-dibromo and 3,4-dibromo theoretical structures).

The remaining two impurities isolated from the bromination of 2,5-dimethoxybenzaldehyde **(72)** were 4,6-dibromo-5-hydroxy-2-methoxybenzaldehyde **(167)** and 3,6-dibromo-2,5-dimethoxybenzene **(168)**. Obtaining MS profiles of these two impurities was not as straightforward as for the other products/impurities. For compound **(167)**, the TIC signal was of very low intensity (see Figure 2.9). This was despite the fact that the compound had a strong UV signal (@ 210 nm). Also, the signal intensity only marginally increased when the injection volume was increased. This suggests that the compound is not sufficiently ionised under these conditions and as a result, its identification by MS may be difficult if an impurity profile was being established. As the compound has a phenol group at the aromatic 5-position, it was envisaged that a much stronger TIC signal may be obtained if the analysis was performed in negative mode, as deprotonation of this phenol group would, in theory, result in ionisation of the compound. However, when the analysis was performed in negative mode (ESI–) (using 5 mmol ammonium formate in mobile phase) the TIC signal was of even lower intensity than that obtained in positive mode. This suggests that the phenol group is not easily deprotonated under these conditions and very little of the total number of analyte molecules are ionised at the source of the instrument. Despite the low TIC signal intensity, mass spectra for compound **(167)** in both positive mode (molecular ion @ 311 *m/z* ($M+H^+$)) and negative mode (molecular ion @ 309 *m/z* ($M-H^+$)) were obtained (Figure 2.11). Again, as observed for dibromo compound **(170)**, highly abundant 'triplet' molecular ions are observed in the extracted mass spectra of compound **(167)** (in both ESI+ and ESI– mode), indicative of dibromination having taken place.

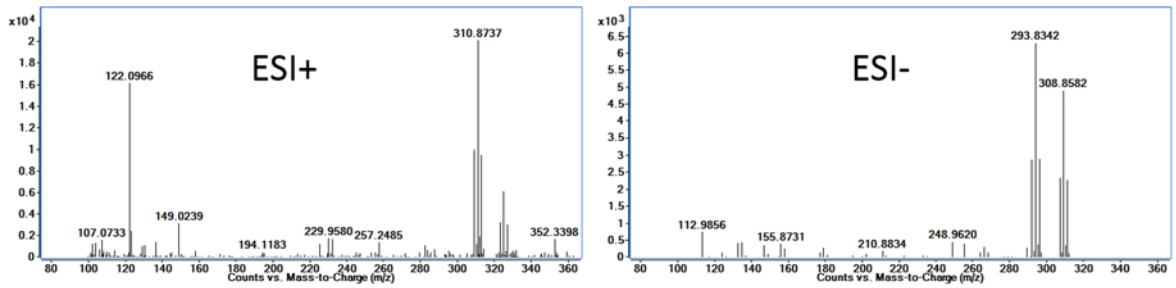


Figure 2.11: Extracted mass spectra for compound (167) in both positive and negative mode

In Figure 2.9, a TIC signal is not shown for the 3,6-dibromo compound **(168)**. This is because despite a strong UV signal (@ 210 nm) at t_R=12.0 min, no corresponding TIC signal was observed, even when the injection volume was increased and the analysis carried out in both positive and negative mode. As a result, no MS profile could be obtained as proof of compound identity. This suggests that the compound is very poorly ionised (to an even greater extent than phenol **(167)**) under these conditions. A probable explanation for this may be that the compound is not suitable for analysis whereby ESI technology is used at the source. ESI technology, used at the source of the MS instrument, is generally suitable for a wide range of small to large organic molecules. However, it is most associated for use in conjunction with charged, polar or basic molecules. The nature of the ionisation process requires that compounds possess ionisable groups (e.g. amines, carboxylic acids, aldehydes, ketones etc.) that may be protonated/deprotonated by mobile phase additive (e.g. formic acid, ammonium formate etc.) before they enter the electrospray chamber. 3,6-Dibromo **(168)**, unlike the other products/impurities of the bromination reaction, does not possess an ionisable group (i.e. aldehyde group) so may not be protonated by mobile phase additives. Thus, as it remains in a neutral form, it is not detected by the mass spectrometer. A possible solution to this issue would be use of alternative source technology, such as Atmospheric Pressure Chemical Ionisation (APCI), which is suitable for compounds that do not possess ionisable groups. However, access to this ionisation source was not available at the time.

2.3 Definitive structure assignment of detected impurities and the need for reference standards

The four compounds identified above have not previously been reported in the literature as impurities of the bromination of 2,5-dimethoxybenzaldehyde **(72)**. In fact, the two dibromo aldehydes (**(167)** and **(170)**) are novel.

At this stage, assignment of the structures of the impurities was largely tentative and it may be argued that there was not enough evidence available to fully support the structures assigned. For example:

- There was no analytical/spectroscopic data available in the literature for the two novel compounds to support the structures assigned.

- One of these novel dibromo impurities **(170)**, had not been isolated from the 3-bromo impurity **(169)**, so full characterisation (including melting point (m.p.), IR spectroscopy etc.) could not be performed. Only MS and crude ^{1}H-NMR data were available to support structure assignment.
- The 3,6-dibromo **(168)**, although isolated, could not be ionised under the MS conditions used, so no MS profile (to indicate molecular weight) was obtained to support the structure assigned to this impurity.

For more comprehensive confirmation of the structures of these impurities, it was decided that standards would need to be obtained to support the evidence already acquired. By obtaining standards, novel impurities that had not been isolated, could be fully characterised and their analytical/spectroscopic data made available to those working in the area of impurity profiling. Also, by running the standards against the recovered impurities on HPLC and matching retention times, much stronger evidence supporting the proposed structures would be provided. Obtaining standards for these compounds was not straightforward:

- 3-Bromo **(169)** was commercially available, but only from a very small number of vendors and only very small amounts (<3 mg) were offered. These small amounts and the high price of the standard would make full characterisation difficult. However, facile preparation of this compound has been reported in the literature (see Section 2.3.2).
- 4,6-Dibromo-2,5-dimethoxybenzaldehyde **(170)** and 4,6-dibromo-5-hydroxy-2-methoxybenzaldehyde **(167)** are both novel compounds. No standards are commercially available and no preparation is reported in the literature.

Given these challenges, it was decided to attempt the independent synthesis of these compounds as reference standards.

As well as the four previously unreported impurities of the bromination reaction, it was also decided to attempt the selective synthesis of the previously reported 6-bromo product **(165)**. Although this compound was fully isolated from the reaction and characterised by ^{1}H-NMR, ^{13}C-NMR, IR etc., it was only recovered in a yield of approximately 15%. As this compound would later be required for use as a starting material in a four step synthesis of a series of dibenzylketones (Chapter 4, Section 4.3.1), the bromination procedure used was not a very efficient method of acquiring a stock of the 6-bromo product **(165)**. Thus a selective, more efficient synthesis of the compound was sought and the results of this are outlined overleaf.

2.3.1 Selective synthesis of 6-bromo-2,5-dimethoxybenzaldehyde (165)

The preparation of 6-bromo-2,5-dimethoxybenzaldehyde **(165)** has been previously reported in the literature. In a paper by Takao *et al.*[164] 6-bromo **(165)** was synthesised *via* dihydroxy aldehyde **(171)**, as outlined in Figure 2.12. According to Takao, bromination of phenol **(171)** results in regiospecific 6-bromination. This is followed by methylation at the 2,5-hydroxy positions (of **(172)**) to give the desired 6-bromo aldehyde **(165)** in an overall yield (over 2 steps) of 55%.

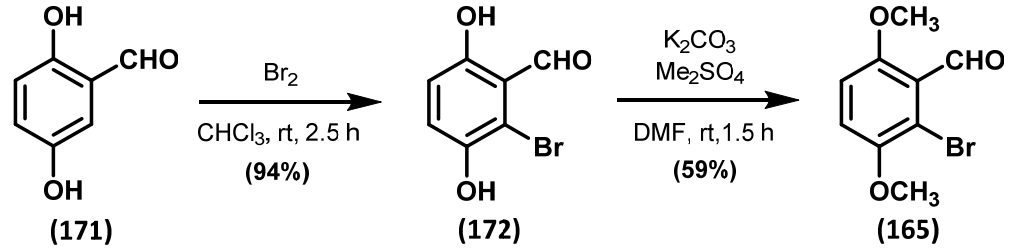


Figure 2.12: 'Takao' synthesis of 6-bromo-2,5-dimethoxybenzaldehyde[164]

Synthesis from 2,5-dimethoxybenzaldehyde **(72)** was performed by Sato *et al.*.[165] Sato's methodology involves using an acetal (Lewis base) to direct lithiation and subsequent bromination to the *ortho* position ('directed *ortho* metalation') (Figure 2.13).

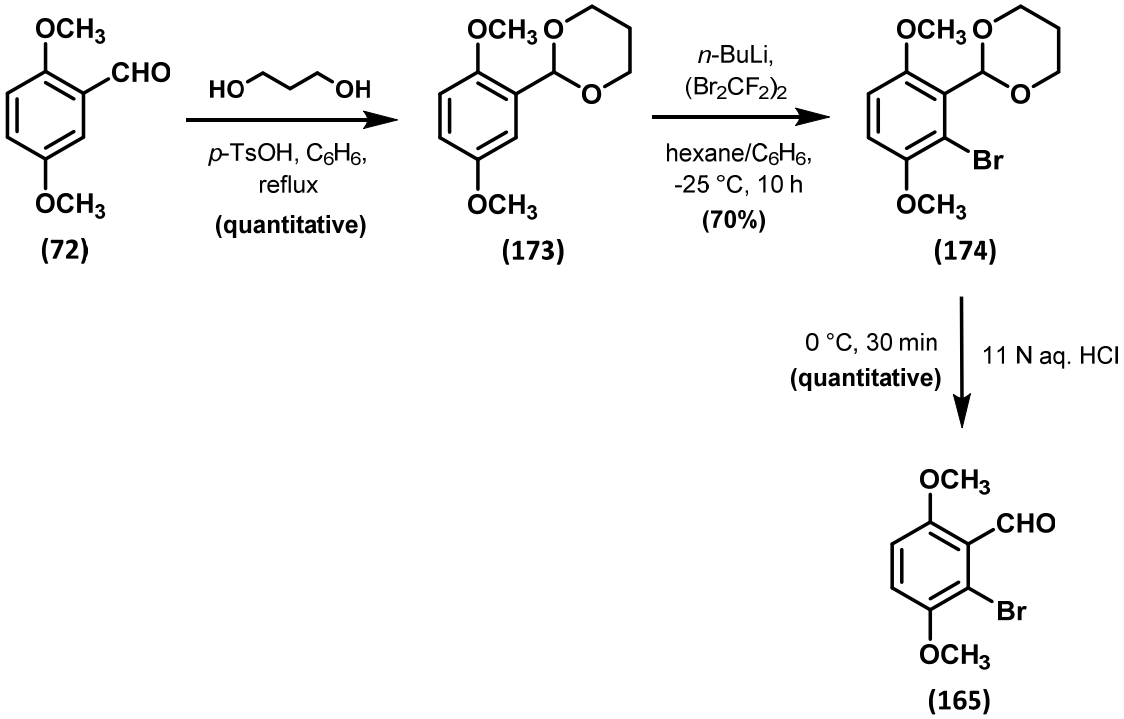
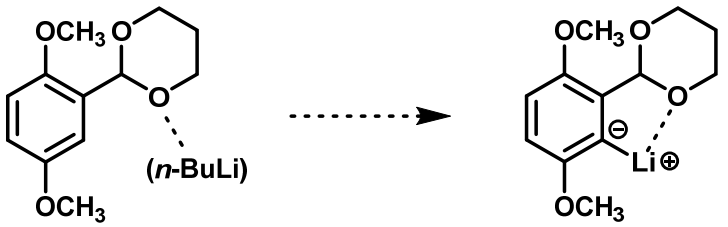


Figure 2.13: 'Sato' synthesis of 6-bromo-2,5-dimethoxybenzaldehyde[165]

Firstly, aldehyde **(72)** undergoes acetylation to form **(173)**, with the acetal acting as a directing group. The acetal is a stronger electron withdrawing group than the aldehyde, with the O atoms of the acetal

acting as a Lewis base. When an alkyl lithium reagent is introduced (e.g. *n*-BuLi), the lithium can act as a Lewis acid and undergoes an acid-base interaction with the O atoms (Lewis base) of the acetal, forming a new alkyllithium intermediate **(175)**:



(175) **(176)**

This very basic alkyllithium **(175)** deprotonates the ring at the nearest available (*ortho*) position (in this case the 6-position) forming aryllithium **(176)**, whilst maintaining the acid-base interaction. This greatly increases the nucleophilicity of the *ortho* position, making it more susceptible to undergo electrophilic aromatic substitution when an electrophile is introduced (e.g. $BrCF_2CF_2Br$). The acetal may then be hydrolysed to the aldehyde upon treatment with aqueous acid. This methodology was also used by Li *et al.*.[166] This method is reported to produce the desired 6-bromo aldehyde **(165)** in an overall yield (over 3 steps) of 70%.

A third synthetic approach to the preparation of *ortho*-brominated aldehydes was explored by Dubost *et al.*.[167] The methodology behind this approach is similar to that used by Sato *et al*.[165] in that the aldehyde is initially converted to a directing group, for the purpose of directing bromination to the *ortho*-position. Although Dubost does not synthesise 6-bromo-2,5-dimethoxybenzaldehyde **(165)**, the method is very successful for a range of other ring-substituted aromatic aldehydes.

Given that (a) the dihydroxy SM **(171)** used in Takao's synthesis was not to hand in the laboratory at the time, (b) Sato's synthesis involved use of hazardous materials (*n*-BuLi/benzene) and (c) Dubost's approach had not been documented for 2,5-dimethoxybenzaldehyde **(72)**, it was decided that in this work, Dubost's method would be explored for the selective synthesis of 6-bromo-2,5-dimethoxybenzaldehyde **(165)**.

Figure 2.14 below outlines the basic methodology used by Dubost in the *ortho*-bromination of a number of ring-substituted benzaldehydes.

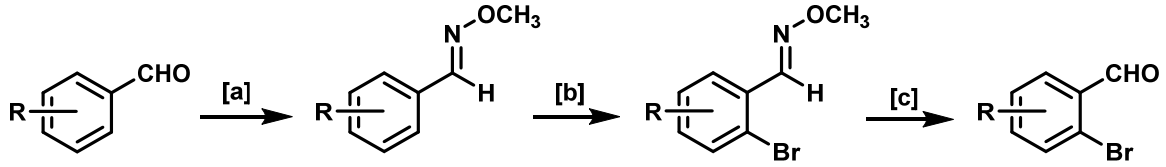


Figure 2.14: Dubost's approach to the *ortho*-bromination of benzaldehydes[167]

([a] = CH_3ONH_2.HCl, pyridine, DCM, rt, 1 h; [b] = NBS, AcOH, $Pd(OAc)_2$, $AgOCOCF_3$, DCE, 120 °C, 24 h; [c] = p-TsOH, $(CH_2O)_n$, THF/H_2O (10:1), 100 °C (MW), 15 min)

The directing group used by Dubost is *O*-methylbenzaldoxime. It directs bromination to the *ortho*-position (Step 2, Figure 2.14) by first forming a cyclometalated complex (Pd^{II} species) **(177)**, and following oxidative addition of NBS, a Pd^{IV} intermediate (benzaldoxime-$Pd(OAc)_2$-NBS complex) **(178)** is formed. Reductive elimination of this species results in the *ortho*-bromination of the benzaldoxime **(179)** and regeneration of the Pd^{II} catalyst (Figure 2.15).

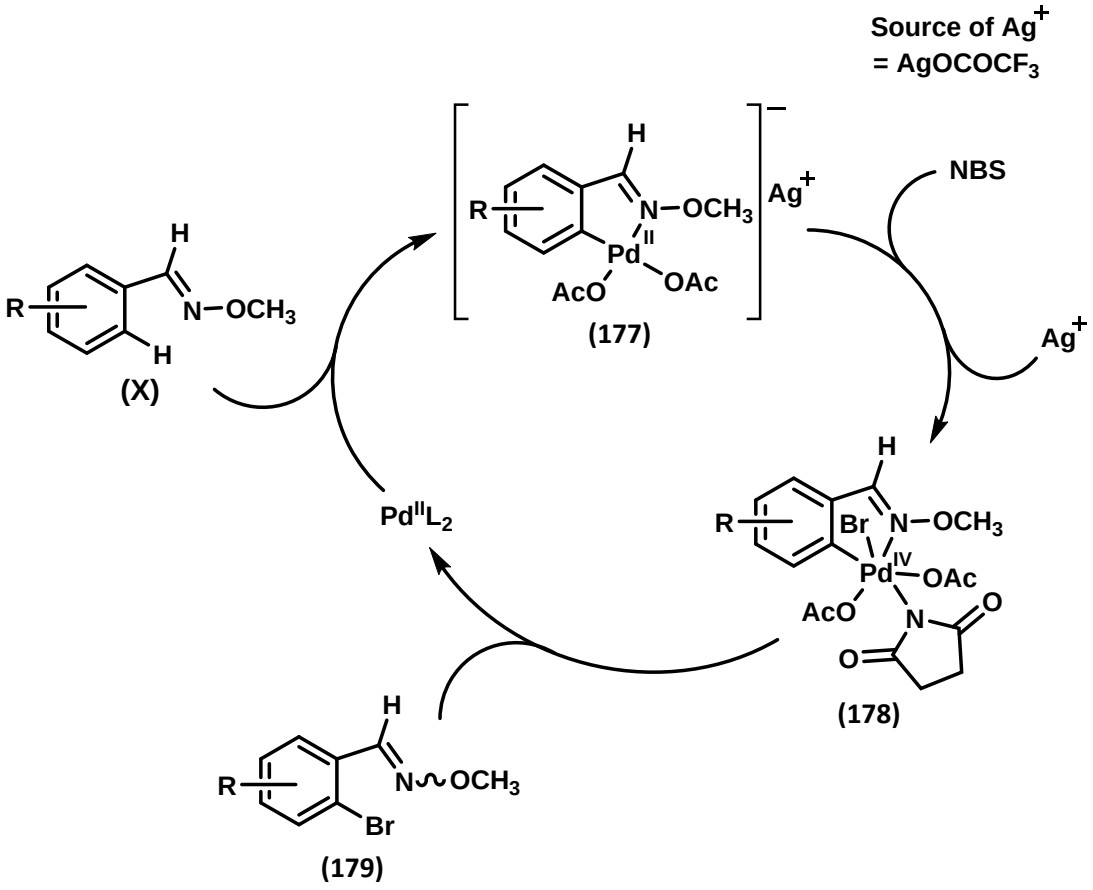
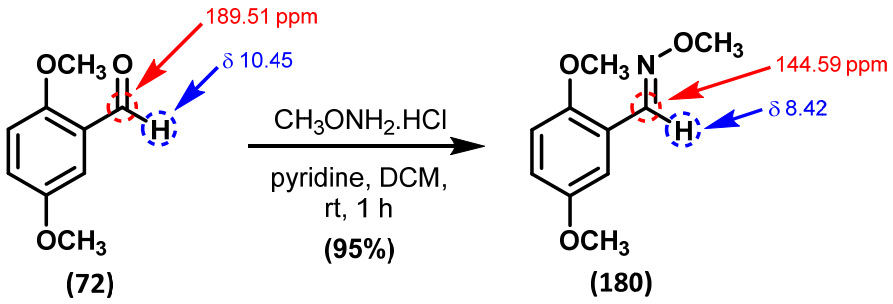


Figure 2.15: Mechanistic proposal for *ortho*-bromination[167]

Using Dubost's selective *ortho*-bromination strategy, we attempted the synthesis of 6-bromo-2,5-dimethoxybenzaldehyde **(165)**. Step one of this synthesis is as follows:



This first step involved conversion of the 2,5-dimethoxy aldehyde **(72)** to the novel benzaldoxime (2,5-dimethoxybenzaldehyde *O*-methyloxime **(180)**). When this step was performed in-house, an almost quantitative yield (95%) of benzaldoxime **(180)** was achieved. This high yield was maintained when the

reaction was scaled up (1 g/5.1 mmol to 4 g/20.5 mmol scale). The R_f, IR and MS data collected for benzaldoxime **(180)** are summarised in Table 2.4.

Table 2.4: Yield, R_f, IR and HRMS data for benzaldoxime (180)

Compound No.	Yield	R_f*	IRν_{max} (NaCl) (cm^{-1})	HRMS (M+H$^+$) (*m/z*)	
				Calc.	Found
(180)	95%	0.77	1577 (C=N), 1600, 1495 (C=C)	196.0974	196.0969

*mobile phase = 50:50 EtOAc:hexane

The product **(180)**, on each occasion, formed as a single isomer. Evidence of reaction completion was obtained from ^{1}H-NMR data. It was signified mainly by the disappearance of the aldehyde proton (@ δ 10.45) and the appearance of an aldoxime proton (@ δ 8.42). The ring substitution pattern was similar for both SM **(72)** and product **(180)** (ABX pattern) with a doublet @ δ 6.82 (*ortho* coupling, ≈9 Hz), a doublet of doublets @ δ 6.90 (*ortho* and *meta* coupling, ≈9 and 3 Hz) and a fine doublet @ δ 7.33 (*meta* coupling, ≈ 3 Hz) being observed in the aromatic region (δ ≈6.0–8.0) of the ^{1}H-NMR spectrum of the product (Figure 2.16).

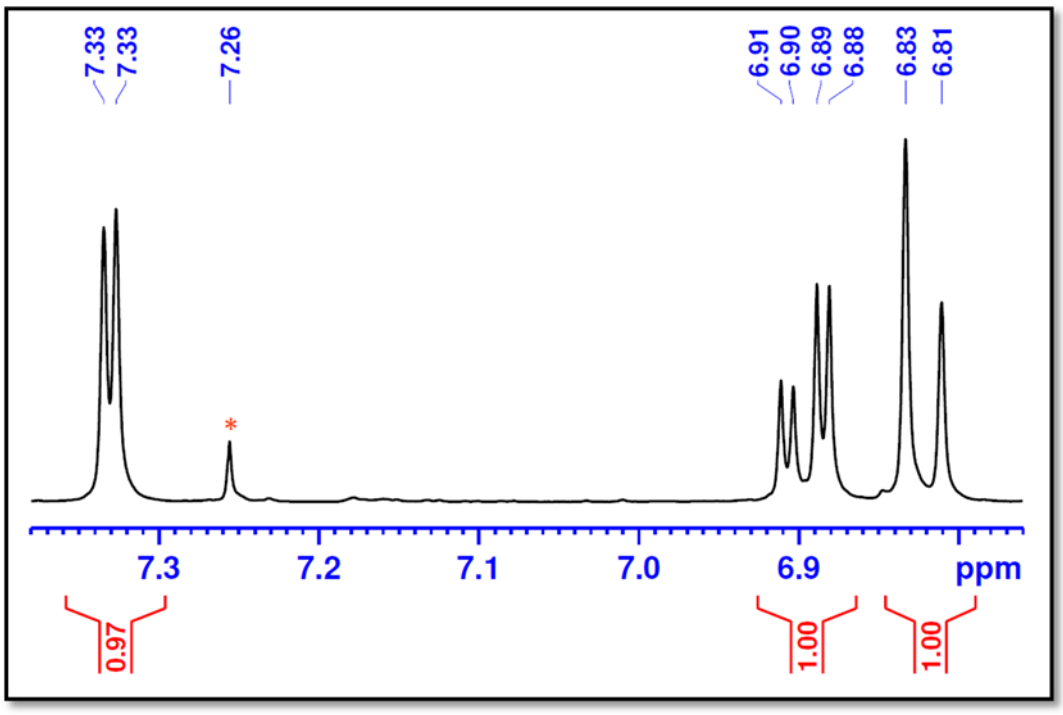


Figure 2.16: Aromatic region (δ 6.76–7.38) of ^{1}H-NMR spectrum of benzaldoxime (180)

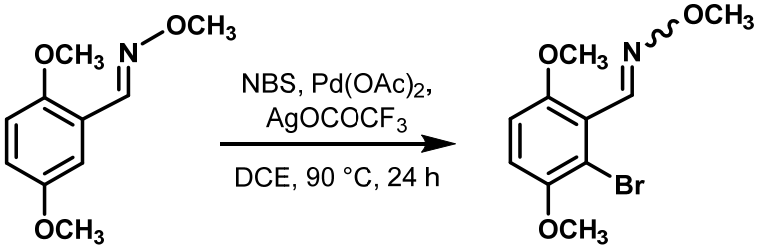
(= residual solvent – $CHCl_3$)*

The product obtained from this reaction was assigned (*E*)-conformation, based solely on the results from Dubost's work. For the vast majority of the initial benzaldoxime compounds (pre-bromination) synthesised by Dubost, the (*E*)-isomers formed exclusively. Nuclear Overhauser Effect (NOE)

spectroscopy ('NOESY') experiments, for one of these compounds, was used as the basis of structure assignment for all compounds. Also, for all compounds whereby the (*E*)-isomer formed exclusively, the aldoxime proton shift (δ) was generally > 8.0. In the single case in which the (*Z*)-isomer formed (to a very small extent), the aldoxime δ was < 8.0 (@ δ 7.73).[167]

During our work, NOE experiment data (both NOESY and NOE difference spectra) were obtained for the 2,5-dimethoxybenzaldehyde *O*-methyloxime product **(180)**. The spectra did not provide any evidence of an interaction between protons about the aldoxime group. At best, this could be used as negative evidence for the ruling out of the (*Z*)-isomer (one may expect interaction between the ring 2-OC*H*$_3$ and the *N*-OC*H*$_3$ in close proximity) but this could not be considered strong enough evidence for assignment of conformation. Due to the fact that the aldoxime proton shift (δ) was > 8.0 (@ δ 8.42), the (*E*)-conformation was assigned to the aldoxime product **(180)** recovered.
The product was obtained in high purity, and so was carried through to the next step (selective *ortho*-bromination) without need for further purification.

The key bromination step was attempted next. The standard conditions used by Dubost *et al*.[167] for this particular reaction step were outlined previously in Figure 2.14. However, it was observed that for the successful manufacture of benzaldoxime compounds with strongly activating aromatic substituents (e.g. methoxy groups), a lower temperature (90 °C *vs*. 120 °C) was required to avoid formation of the electrophilic aromatic substitution (EAS) product. With this in mind, the in-house synthesis of 2,5-dimethoxy compound **(181)**, was carried out at 90 °C. Also observed by Dubost was the fact that the use of a small amount of AcOH in many cases, led to higher yields. However, this was often accompanied by formation of unwanted dibrominated compounds. It was therefore decided that AcOH would be omitted in this work. The reaction conditions thus employed in our synthesis are summarised below:



(180) **(181)**

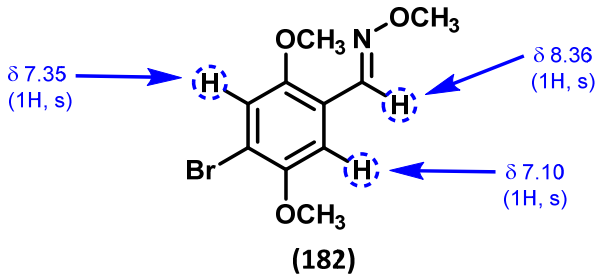
Using the procedure outlined above, the initial ^{1}H-NMR spectrum of the crude reaction mixture revealed the following:

- The reaction did not go to completion. A small amount (<10%) of unreacted SM **(180)** (aldoxime shift @ δ 8.42) remained in the crude product.

- The desired 6-bromo benzaldoxime product **(181)** formed as a mixture of (*Z*)- and (*E*)-isomers ('(*Z*)-**(181)**' and '(*E*)-**(181)**'), in a ratio (*Z*:*E*) of 1:2.
- A small amount of unknown benzaldoxime formed (≈7%) (aldoxime proton shift @ δ 8.36).

Due to reaction incompletion and presence of an unknown benzaldoxime, the concentrated crude reaction mixture was subjected to flash column chromatography on silica gel, in order to purify the reaction products.

The unknown benzaldoxime (aldoxime proton shift @ δ 8.36) was the first compound to elute the column and a pure sample (4.5%) was recovered. This allowed for full characterisation and thus, a compound structure was proposed. Based primarily on the ^{1}H-NMR (aromatic region) and MS data, the compound was assigned as 4-bromo-2,5-dimethoxybenzaldehyde *O*-methyloxime **(182)**. The R_f, m.p., IR and MS data collected for the novel benzaldoxime **(182)** are summarised in Table 2.5.



(182)

Table 2.5: Yield, R_f, m.p., IR and HRMS data for 4-bromo benzaldoxime (182)

Compound No.	Yield	m.p. (°C)	R_f*	IRν_{max} (KBr) (cm^{-1})	HRMS (M+H$^+$)⋆ (*m/z*)	
					Calc.	Found
(182)	4.5%	85–87 (MeOH)	0.77	1591 (C=N), 1611, 1499 (C=C)	274.0079	274.0082

*mobile phase = 50:50 Et_2O:hexane

⋆molecular ion (M) calculated for ^{79}Br isotope peak

MS data revealed that the compound had the same *m/z* as the expected 6-bromo product **(181)** and also possessed a bromine atom (characteristic 'doublet' molecular ion). The aromatic region of the ^{1}H-NMR spectrum (δ ≈6.5–8) contained two singlets (@ δ 7.10 and 7.35). As no splitting of the signals was observed it was assumed that the two ring protons must be *para* to one another. With this information, the most plausible structure that could be assigned is the 4-bromo regioisomer of the expected product. NOE data was also collected for this compound but like the unbrominated aldoxime **(180)**, no strong evidence for either (*E*)- or (*Z*)-conformation was provided. With the aldoxime shift @ δ 8.36 for 4-bromo **(182)**, it was assumed to be the (*E*)-isomer, based on the work by Dubost.[167]

The presence of the 4-bromo impurity may explain why the reaction did not go to completion. Some of the non-bromo SM **(180)** remained in the crude reaction mixture as only one equivalent of NBS was

used and clearly some of this was consumed in the formation of 4-bromo impurity **(182)**. Also, the formation of this 4-bromo (EAS) product was supposed to be avoided by using a lower reaction temperature (90 °C *vs*. 120 °C) according to Dubost.[167] Having said this, a satisfactory yield (67%) of the desired 6-bromo product **(181)** was isolated.

As mentioned, the desired 6-bromo product formed as a mixture of (*Z*)-**(181)** and (*E*)-**(181)** isomers in a ratio (*Z*:*E*) of 1:2. Despite the closeness in R_f values for the (*Z*)-**(181)** and (*E*)-**(181)** isomers (0.49 and 0.47 in 50:50 Et_2O:hexane), pure samples of each were obtained following flash column chromatography. The (*Z*)-isomer eluted first and a pure sample was obtained, allowing for full characterisation (see Table 2.6). The ^{1}H-NMR spectrum obtained for (*Z*)-**(181)** is shown in Figure 2.17.

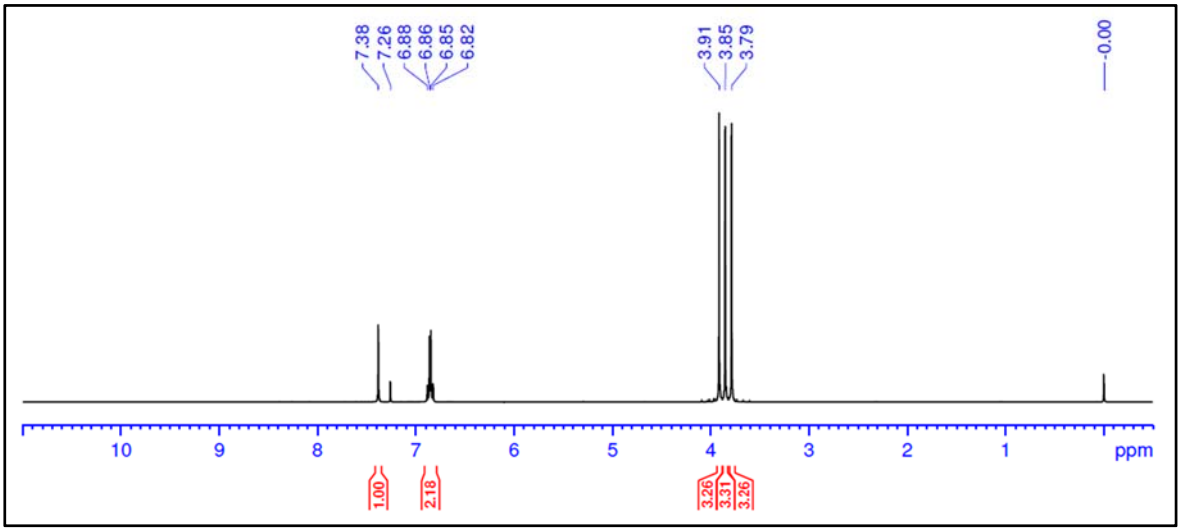


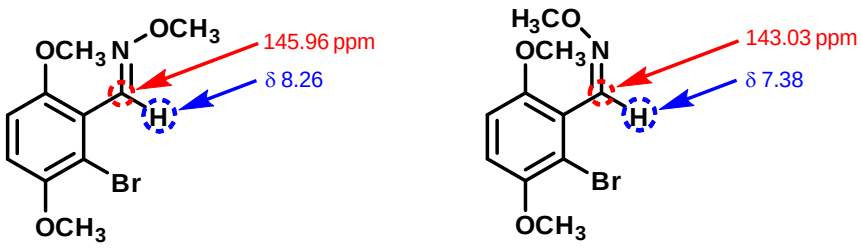
Figure 2.17: ^{1}H-NMR spectrum of (*Z*)-(181) (@ 400 MHz)

Assignment of the compound as the 6-bromo regioisomer was based on the signals present in the aromatic region of the ^{1}H-NMR spectrum (δ ≈6.5–8). Two 'doublets' in close proximity (@ δ 6.84 and 6.87) were present in the aromatic region ('AB pattern'). As the splitting for both doublets was ≈9 Hz (*ortho* coupling), this is in agreement with bromination at the 6-position.

(Note: The distance ($\Delta\nu_{AB}$) between the two *ortho* aromatic proton signals (A and B) is so small, that the 'doublets' referred to above take on an atypical shape, whereby the peaks closest to the centre between the two signals ('inner peaks') are much greater in intensity than those furthest from the centre ('outer peaks'). This atypical shape often resembles, and may be misinterpreted as, a quartet (q) signal. When two closely related doublets take on the appearance of a quartet in this way, the signal observed is often referred to as an AB quartet (ABq).)

A NOESY spectrum was attained for (*Z*)-**(181)**. It was hoped that evidence for the (*Z*)-orientation of the aldoxime group would be represented as a positive interaction between the 2-OC*H*$_3$ group and the *N*-OC*H*$_3$ group. Evidence for this was unfortunately not observed. This may be due to the close proximity

of all three OCH_3 group signals in the ^{1}H-NMR spectrum (all three resonating between δ 3.79 and 3.91). Perhaps if these signals were better resolved, a more obvious interaction may be observed (represented as a positive irradiation↔enhancement relationship in the NOE difference spectrum). Without two-dimensional (2D) NMR evidence, the (*Z*)-assignment was based primarily on the chemical shift value of the aldoxime proton - @ δ 7.38 (*vs*. δ 8.26 for (*E*)-**(181)**). *E*/*Z* geometry may be tentatively assigned also using the ^{13}C-NMR chemical shift of the iminyl carbon. According to Gordon *et al*.,[168] for a range of *para*-substituted benzaldoximes, the iminyl ^{13}C shifts are consistently more downfield for the (*E*)-isomer compared to that of the (*Z*)-isomer. Assignment of (*E*)-**(181)** and (*Z*)-**(181)** based on this methodology was in agreement with the methodology used earlier, based on the aldoxime proton shift:



(*E*)-**(181)** (*Z*)-**(181)**

The (*E*)-isomer eluted closely after the (*Z*)-, with some of (*Z*)-**(181)** in fact, co-eluting with (*E*)-**(181)**. Having said this, a pure sample of (*E*)-**(181)** was obtained following recrystallisation of this fraction (from MeOH), which removed all traces of (*Z*)-**(181)**. The purified sample of (*E*)-6-bromo-2,5-dimethoxybenzaldehyde *O*-methyloxime **(181)** was fully characterised (see Table 2.6). The ^{1}H-NMR spectrum obtained for (*E*)-**(181)** can be found in Figure 2.18.

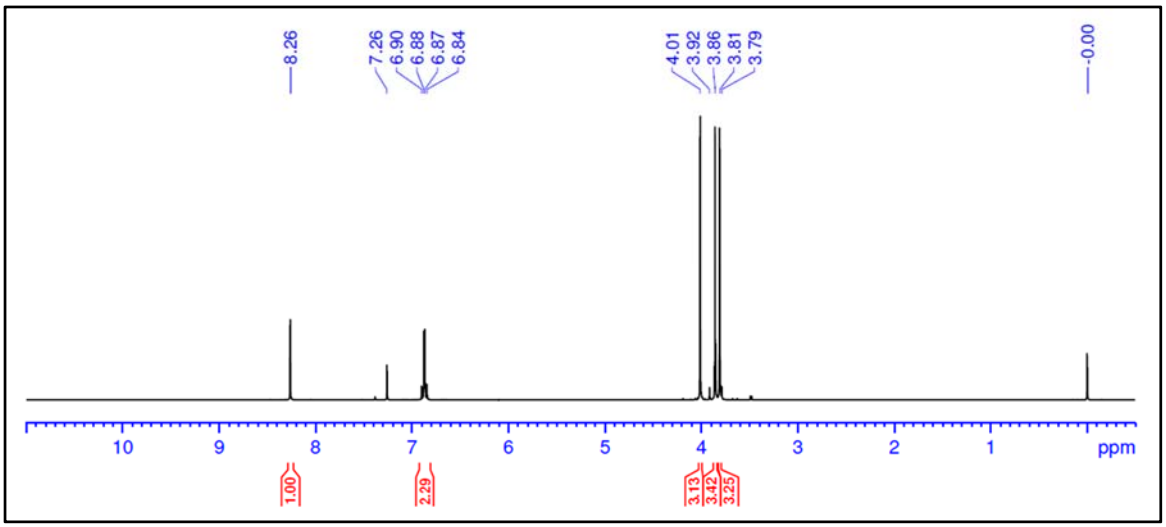


Figure 2.18: ^{1}H-NMR spectrum of (*E*)-(181) (@ 400 MHz)

Similar to (*Z*)-**(181)**, assignment of 6-bromo substitution was based on the aromatic signals in the ^{1}H-NMR spectrum (ABq pattern). Again, NOESY data did not provide strong evidence of conformation so the (*Z*)-assignment was based primarily on the chemical shift value of the aldoxime proton - @ δ 8.26.

The R_f, m.p., IR and MS data collected for novel benzaldoximes (*E*)-**(181)** and (*Z*)-**(181)** are summarised in Table 2.6.

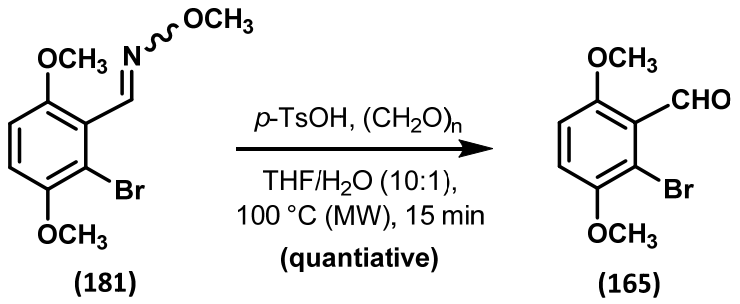
Table 2.6: R_f, m.p., IR and HRMS data for isomeric benzaldoximes (*E*)-(181) and (*Z*)-(181)

Compound No.	m.p. (°C)	R_f*	IRν_{max} (KBr) (cm^{-1})	HRMS ($M+H^+$)⋆ (*m/z*)	
				Calc.	Found
(*E*)-(**181**)	89–91 (MeOH)	0.47	1573 (C=N), 1608, 1483 (C=C)	274.0079	274.0084
(*Z*)-(**181**)	100–103 (MeOH)	0.49	1572 (C=N), 1626, 1596 (C=C)	274.0079	274.0090

*mobile phase = 50:50 Et_2O:hexane

⋆molecular ion (M) calculated for ^{79}Br isotope peak

The final step in the selective synthesis of 6-bromo-2,5-dimethoxybenzaldehyde **(165)** using Dubost's methodology,[167] was removal of the aldoxime directing group. This was carried out under microwave irradiation and afforded the 6-bromo aldehyde **(165)** in a quantitative yield without need for further purification:



The 6-bromo aldehyde **(165)** had been previously isolated and characterised (Table 2.3), and the spectroscopic data acquired for **(165)** produced using Dubost's methodology, were in excellent agreement with this previously collected data.

In summary, the selective synthesis of 6-bromo-2,5-dimethoxybenzaldehyde **(165)** using Dubost's methodology, proved to be very efficient. Compared to the yield from the Br_2/AcOH bromination of 2,5-dimethoxybenzaldehyde **(72)** (15% by General Procedure 5.2.1.1), **(165)** was recovered, using Dubost's method, in an overall yield (over 3 steps) of 63% (General Procedures 5.2.2.1, 5.2.2.2 and 5.2.2.3).

(Note: Collaborative work in the synthesis of dimeric nitrostyrenes (Chapter 4, Section 4.3.1.4) with another member of the research group called for the synthesis of the 6-bromo-2,5-diethoxybenzaldehyde **(183)**. This compound was synthesised also using both the standard (Br_2/AcOH) bromination and Dubost's bromination (see Figure 2.19).

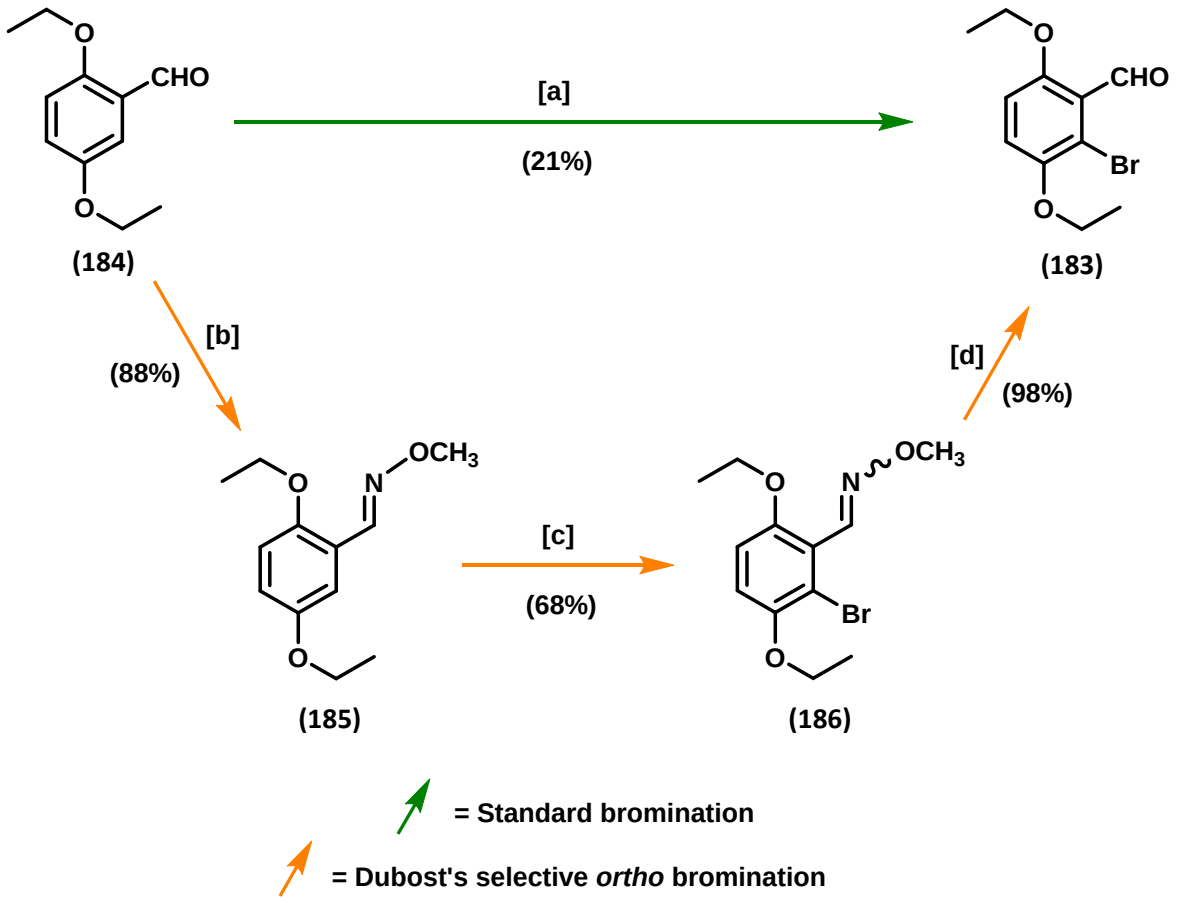


Figure 2.19: Comparison of the yields of 6-bromo-2,5-diethoxybenzaldehyde (183) obtained using 'standard' bromination and Dubost's methodology[167]

([a] = Br_2, AcOH, rt, 24 h; [b] = CH_3ONH_2.HCl, pyridine, DCM, rt, 1 h; [c] = NBS, $Pd(OAc)_2$, $AgOCOCF_3$, DCE, 90 °C, 24 h; [d] = p-TsOH, $(CH_2O)_n$, THF/H_2O (10:1), 100 °C (MW), 15 min)

Similar results to dimethoxy **(165)** were observed, in that **(183)** was obtained in yields of 21% (by standard (Br_2/AcOH) bromination) and 59% (Dubost's method).[167] As the synthesis of this compound is not directly linked to this current work, its experimental procedures and characterisation are reported as an Appendix (Section 5.5) at the end of Chapter 5.

2.3.2 Selective synthesis of 3-bromo-2,5-dimethoxybenzaldehyde (169)

As mentioned previously, the 3-bromo compound **(169)** is commercially available, but is expensive and only available in small amounts. Its preparation however, is reported to be simple and high yielding. A number of reports detailing the synthesis of 3-bromo-2,5-dimethoxybenzaldehyde **(169)**, were found in the literature.[169-172]

The most recent of these,[169] reports a simple two-step synthesis from phenol **(187)**, affording 3-bromo **(169)** in an overall yield (over 2 steps) of 88%. This procedure (carried out by Evano *et al.*) is outlined in Figure 2.20 overleaf.

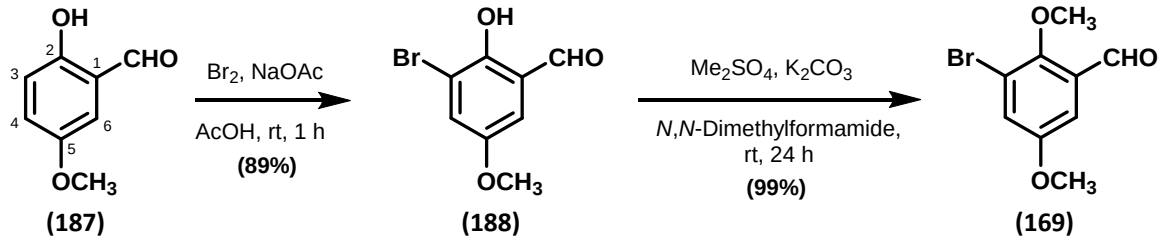


Figure 2.20: Literature procedure for the preparation of 3-bromo-2,5-dimethoxybenzaldehyde (169)[169]

Regioselective substitution of the phenyl ring is achieved by using a phenol group to direct *ortho*-bromination. The phenolic group is a very strong activator (much stronger than methoxy) and will direct substitution *ortho* and *para*. In the case of phenolic aldehyde **(187)** in Figure 2.20, there are two *ortho*-positions (C-1 and C-3) and one *para*-position (C-5). However, the C-1 and C-5 positions are already substituted, meaning the only remaining site for EAS is the 3-position. As a result, the bromination of this phenolic compound **(187)** is highly regiospecific.

Following bromination, the phenolic group may undergo S_N2 substitution, in the presence of a suitable alkylating reagent (e.g. Me_2SO_4), to form the methoxy substituent.

When Evano's synthetic methodology was followed in-house, the 3-bromo phenol **(188)** was recovered from the initial bromination step in a yield of 81%. The product was obtained pure, without need for further purification. The R_f, m.p., IR and MS data collected for **(188)** are summarised in Table 2.7.

Table 2.7: Yield, R_f, m.p., IR and HRMS data for 3-bromo phenol (188)

Compound No.	Yield	m.p. (°C)	R_f*	IRν_{max} (KBr) (cm^{-1})	HRMS ($M+H^+$)⋆ (*m/z*)	
					Calc.	Found
(188)	81%	108–109 (EtOH)	0.74	1655 (C=O), 1611, 1456 (C=C)	230.9657	230.9654

*mobile phase = 50:50 EtOAc:hexane

⋆molecular ion (M) calculated for ^{79}Br isotope peak

The spectroscopic data acquired for 3-bromo phenol **(188)** were in excellent agreement with previously published data.[169] The aromatic region of the ^{1}H-NMR spectrum of **(188)** was most useful in terms of ensuring the regioselectivity of bromine substitution – two finely split doublets ($J \approx 3$ Hz) (@ δ 7.04 and 7.42) indicating the *meta* relationship of the two remaining 'free' (protonated) ring positions.

The second step (methylation of phenol **(188)**) was also high yielding (93%) and the characterisation of this compound is summarised in Table 2.8. Again, these data were in agreement with those published by Evano *et al*..[169]

Table 2.8: Yield, R_f, m.p., IR and HRMS data for 3-bromo aldehyde (169)

Compound No.	Yield	m.p. (°C)	R_f*	IRν_{max} (KBr) (cm^{-1})	HRMS ($M+H^+$)⋆ (*m/z*)	
					Calc.	Found
(169)	93%	64–66 (EtOH)	0.50	1690 (C=O), 1603, 1474 (C=C)	244.9813	244.9807

*mobile phase = 20:80 EtOAc:hexane

⋆molecular ion (M) calculated for ^{79}Br isotope peak

Overall, 3-bromo aldehyde **(169)** was produced in a yield (over 2 steps) of 75%. This was slightly lower than the yield (88%) reported by Evano.[169]

Following characterisation, the ^{1}H-NMR spectrum of **(169)** was compared to the spectrum of the mixture of impurities recovered from the bromination of 2,5-dimethoxybenzaldehyde **(72)** (See Figure 2.6, fraction 2). Although the impurity had not been isolated, there was good agreement between the signals of the un-isolated impurity and the independently synthesised standard. The aromatic region of the ^{1}H-NMR spectrum had initially been most useful for assigning structures to the mixture of impurities, and for the proposed 3-bromo aldehyde **(169)**, this region displayed two finely split doublets ($J \approx 3$ Hz) (@ δ 7.28 and 7.39). This is indicative of aromatic *meta* coupling and the 3-bromo aldehyde **(169)** was the best fit based on this data. With a standard available for comparison, the 3-bromo aldehyde **(169)** could then be confirmed as an impurity of the bromination of 2,5-dimethoxybenzaldehyde **(72)** (Section 2.2).

2.3.3 Differentiation of regioisomeric products of the bromination of 2,5-dimethoxybenzaldehyde (72) by LC-MS/MS

The identification of 3-bromo **(169)** as an impurity of the bromination of 2,5-dimethoxybenzaldehyde **(72)**, meant that together with the previously identified products, 4-bromo **(160)** and 6-bromo **(165)**, there were three products/impurities with the same molecular formula ($C_9H_9BrO_3$) (Figure 2.21).

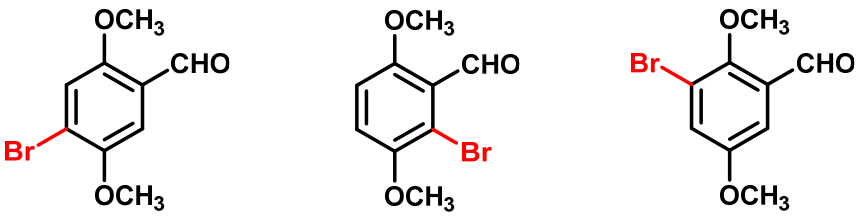


Figure 2.21: Three regioisomeric compounds produced during the bromination (Br_2/AcOH) of (72)

From an impurity profiling perspective, in the absence of ^{1}H-NMR data or standards for use in retention time matching, differentiation of these compounds in a mixture would be difficult as they all have the

same molecular formula/molecular weight. As pure samples of these three compounds had been isolated/selectively synthesised, it was hoped that they could be distinguished by MS. When standard High Resolution Mass Spectra (HRMS) were obtained for each of the three compounds, there was little difference in the mass profiles of each to distinguish between them. All displayed the typical 'doublet' MI peaks ($M+H^+$) at *m/z* 245/247, indicative of a compound containing a single Br atom (see Figure 2.10, mass spectra of **(160)**, **(165)** and **(169)**). As the three regioisomers are structurally different, it was thought that they may have different fragmentation patterns or different ratios of fragment ions. Targeted MS/MS (or 'product ion scan mode') was carried out in an attempt to distinguish between the three regioisomers.

In targeted MS/MS, a specific ion is selected (in this case one of the molecular ions) and fragmented, and only the fragments ('daughter ions') of this ion are detected and observed on the targeted mass spectrum. This gives much more detail regarding which fragments are specifically the product of the targeted precursor ion. In the case of unknowns, these fragments can be pieced together to solve the structure of the parent compound. For each of the three isomers, 4-bromo **(160)**, 6-bromo **(165)** and 3-bromo **(169)**, the molecular ion (@ *m/z* 246.98, $C_9H_9{}^{81}BrO_3$) was targeted and the product MS/MS spectra obtained from each are depicted in Figure 2.22.

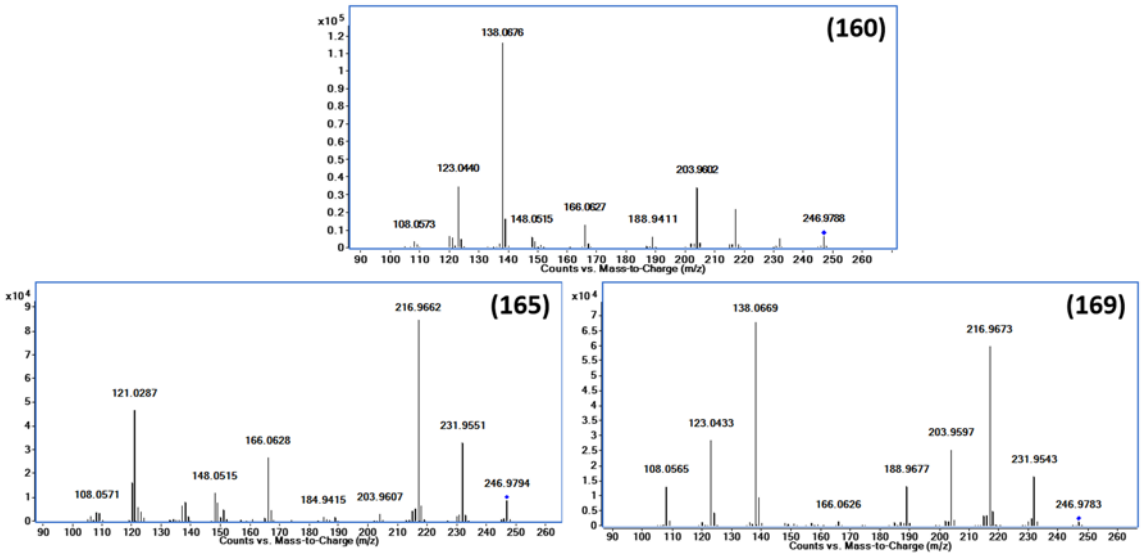


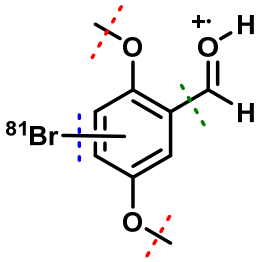
Figure 2.22: Targeted MS/MS spectra (ESI+) (@ *m/z* 246.98) of 4-bromo (160), 6-bromo (165) and 3-bromo (169) compounds

*(m/z 246.98 fragmented in 'ramped collision' mode: slope = 3, offset = 10; HPLC conditions identical to those outlined in Figure 2.9, except for injection volumes used: 1 µL for **(160)**, 0.2 µL for **(165)** and 2 µL for **(169)**)*

The spectra in Figure 2.22 demonstrate that there are differences in the fragmentation patterns, but more so the abundances of daughter ions, between the three compounds. For example:

- The abundance of the daughter ion @ *m/z* 217 is high for 6-bromo **(165)** and 3-bromo **(169)**, but low for 4-bromo **(160)**.
- The abundance of the daughter ion @ *m/z* 138 is high for 4-bromo **(160)** and 3-bromo **(169)**, but low for 6-bromo **(165)**.

Sites of bond cleavage and atom/group losses for compounds of general structure **(189)**, are proposed in Figure 2.23, based on daughter ions produced from the fragmentation of compounds **(160)**, **(165)** and **(169)**.



(189)
m/z 247
(Targetted MI)

Atoms/groups lost from (189)	*m/z* of fragment
$-CH_3$	232
–CHO	217
$-CH_3$ & –CHO	204
$-CH_3$, $-CH_3$ & –CHO	189
$-^{81}Br$	166
$-^{81}Br$ & –CHO	138
$-^{81}Br$, $-CH_3$ & –CHO	123
$-^{81}Br$, $-CH_3$, $-CH_3$ & –CHO	108

Figure 2.23: Ions produced from the fragmentation of compounds of general structure (189)

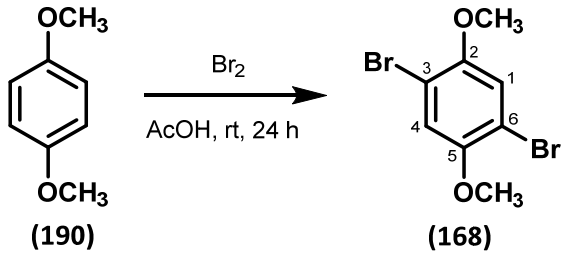
The difference in fragmentation pattern between regioisomers may be exploited in Multiple Reaction Monitoring (MRM) MS, in order to distinguish between the three compounds, when present in a mixture. In MRM-MS, a specific precursor ion is selected (or targeted) for fragmentation (like in the experiment above) but the detector is programmed to only detect specific daughter/product ions (for example, daughter ions @ *m/z* 217 and 138). The instrument also has the ability to calculate the ion ratio (ratio of the abundances/peak areas) between the selected daughter ions (or transitions).

As we had obtained pure samples of each of the regioisomers, MRM-MS was not explored. However, if a method were established whereby only daughter ions @ *m/z* 217 and 138 were detected, the ion ratios between the transitions 247>217 and 247>138 could be used to distinguish between each of the compounds in a mixture. This may eliminate the need to source pure standard compounds.

2.3.4 Selective synthesis of 3,6-dibromo-2,5-dimethoxybenzene (168)

Although the 3,6-dibromo compound **(168)** was commercially available and inexpensive, its facile, one-step synthesis (from a SM available in-house) was reported a number of times in the literature.[173-178]

The method used by Tsutsui *et al.*[173] was pursued in the synthesis of **(168)**, with conditions outlined in Figure 2.24.



(190) **(168)**

Figure 2.24: Literature procedure for the preparation of 3,6-dibromo-2,5-dimethoxybenzene (168)[173]

The *o/p* directing methoxy groups of SM **(190)**, mean that any of the four remaining free sites on the phenyl ring, may be subject to bromination. Initially, monobromination of the aromatic ring is thought to occur at one of the four available chemically equivalent positions (3-, 4-, 1- or 6-). As halogens are deactivating, *o/p* directors, additional EAS would most likely take place at the 4- or 6-positions (if the initial bromination had occurred at the 3-position for example). Given that the product of this reaction is exclusively 3,6-dibromo **(168)**, substitution must favour the less sterically hindered 6-position. No other bromine substitution patterns were observed, for example mono-bromination or tri-bromination. Tri-bromination is unlikely to occur given that dibromo **(168)** is probably too sterically hindered for further EAS.

As expected, the one-step reaction was high yielding, with 88% of **(168)** recovered after recrystallisation from EtOH. The spectroscopic data recovered for **(168)**, prepared according to Figure 2.24, was in excellent agreement with both the literature data[174] and the data collected previously, when it was isolated as a product of the bromination of 2,5-dimethoxybenzaldehyde **(72)**. These previously collected R_f, m.p., IR and elemental analysis data are outlined in Table 2.9.

Table 2.9: R_f, m.p., IR and elemental analysis data for 3,6-dibromo compound (168), isolated previously as a product of the bromination of 2,5-dimethoxybenzaldehyde (72)

Compound No.	m.p. (°C)	R_f*	IRv_{max} (KBr) (cm^{-1})	Elemental analysis	
				Calc. (%)	Found (%)
(168)	143–145 (EtOH)	0.73	1700, 1494 (C=C)	C (32.47) H (2.72)	C (32.43) H (2.63)

*mobile phase = 30:70 EtOAc:hexane

The ^{1}H-NMR spectrum for this molecule was straightforward to assign, where aside from trace solvent, there were only two signals present in the spectrum (@ δ 3.85 and 7.11).

Characterisation of selectively synthesised standards typically involves HRMS but when a sample was submitted for analysis, no molecular ion was found. This was also found to be the case during LC-MS analysis of **(168)**, and as described previously, this is probably due to the unsuitability of the compound for ESI at the source of the MS. As no MS evidence for the compound was acquired, elemental analysis was carried out as proof of molecular formula (see Table 2.9).

As the spectroscopic data of the compound that had been isolated (and characterised) from the bromination of 2,5-dimethoxybenzaldehyde **(72)**, matched that of the selectively synthesised standard, dibromo **(168)** was confirmed as a product of the bromination of **(72)**.

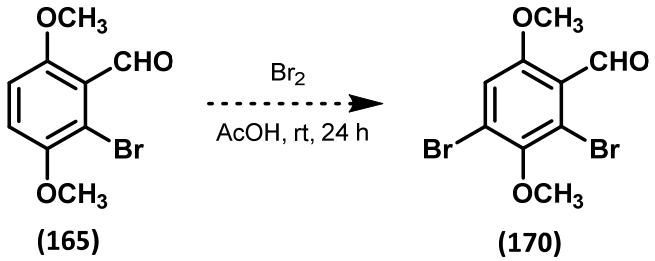
The origin of the dibromo compound **(168)** is still unclear. Given the efficiency and regiospecificity of the bromination of 1,4-dimethoxybenzene **(190)** (as observed during the selective preparation of **(168)**), it may be that this reaction is in fact, part of the pathway by which dibromo **(168)** arises during the bromination of 2,5-dimethoxybenzadehye **(72)**. This pathway can only be proposed on the basis that 1,4-dimethoxybenzene **(190)** is somehow introduced/formed in the reaction vessel, prior to Br_2 exposure. Contamination of the aldehyde SM **(72)** with **(190)** was originally suspected. However no evidence (either by LC-MS or ^{1}H-NMR) for the presence of compound **(190)** (or indeed any other organic compounds), in the commercial sample of **(72)** could be found. This leaves only the possibility that **(190)** is somehow formed as a by-product in the reaction vessel, but how this occurs is not clear. One possible argument for its origin is the deformylation of the aldehyde SM **(72)**. Many of the earliest selective deformylation reactions carried out in the literature[179] involve metal catalysis (e.g. Pd/Rh), so perhaps our reaction is somehow contaminated by a metal-based material. This theory may be investigated by testing a sample of the SM or reagents for metallic substances (by ICP spectroscopy for example). This was not pursued however as part of my work.

2.3.5 Selective synthesis of 4,6-dibromo-2,5-dimethoxybenzaldehyde (170)

Dibromo aldehyde **(170)**, although not isolated by flash column chromatography, was proposed as an impurity of the bromination of 2,5-dimethoxybenzaldehyde **(72)**, based on crude ^{1}H-NMR and MS evidence acquired from the impurity mixture (Figure 2.10, MS spectrum of compound **(170)**). As the compound is not known in the literature, selective synthesis of a standard of **(170)** would be required for full characterisation and for confirmation (by t_R matching) that it is in fact, structurally identical to the impurity recovered (see Section 2.2.2).

A facile synthesis of any compound similar in structure to **(170)**, could not be found in the literature. Subsequently, a number of attempts using various synthetic approaches, were carried out. At first we attempted bromination of 6-bromo aldehyde **(165)** under standard bromination conditions (Br_2/AcOH,

rt, 24 h) in order to investigate if further EAS of the molecule (at C-4) could produce the desired dibrominated product (Figure 2.25).

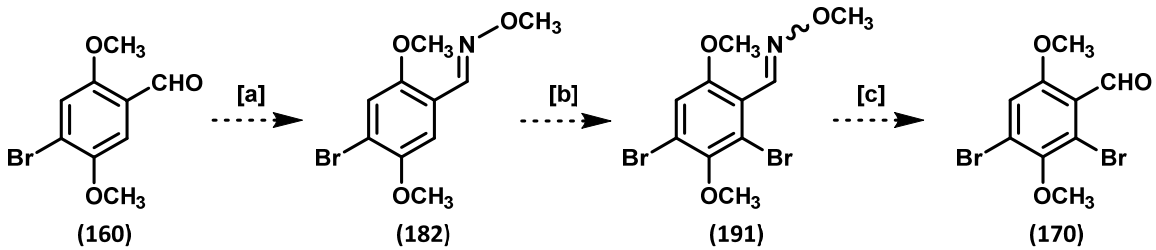


(165) **(170)**

Figure 2.25: Proposed synthesis of 4,6-dibromo aldehyde (170) *via* the attempted bromination of 6-bromo aldehyde (165)

The ^{1}H-NMR spectrum of the crude reaction mixture, following work-up, revealed that only about 6% conversion to the desired product **(170)** was achieved, with the remainder of the sample being unreacted SM **(165)**. As such a low conversion rate was achieved, isolation by flash column chromatography was not pursued and alternative syntheses were explored.

The next attempt was based on methodology used previously, in the selective synthesis of 6-bromo aldehyde **(165)** (Figure 2.14). This procedure[167] allowed for a series of aromatic aldehydes to be selectively *ortho*-brominated. In this attempt, we investigated if the unbrominated aldehyde used previously **(72)**, were replaced by 4-bromo aldehyde **(160)** as a SM, would the *ortho*-bromination procedure result in the formation of 4,6-dibromo **(170)** (Figure 2.26).

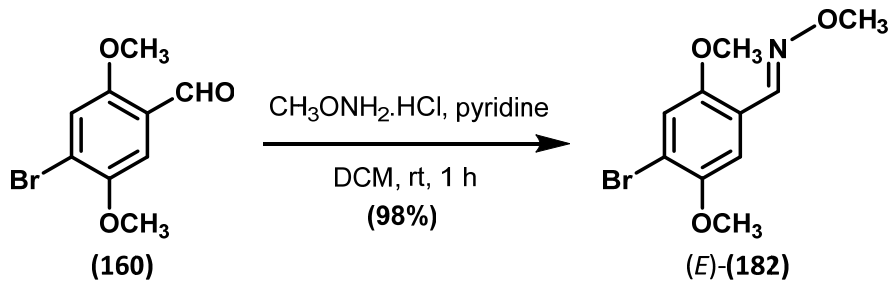


(160) **(182)** **(191)** **(170)**

Figure 2.26: Proposed synthesis of 4,6-dibromo aldehyde (170) *via* 4-bromo aldoxime (182)

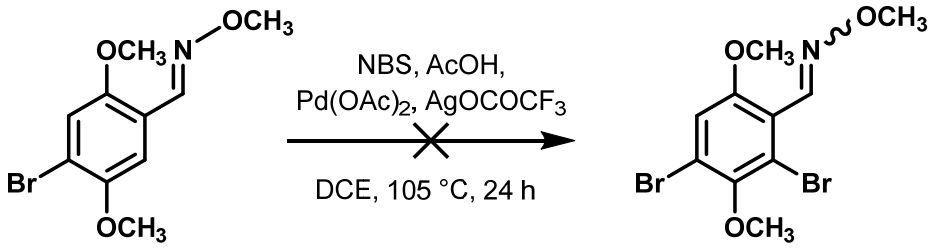
([a] = CH_3ONH_2.HCl, pyridine, DCM, rt, 1 h; [b] = NBS, AcOH, $Pd(OAc)_2$, $AgOCOCF_3$, DCE, 120 °C, 24 h; [c] = p-TsOH, $(CH_2O)_n$, THF/H_2O (10:1), 100 °C (MW), 15 min)

The first step of this reaction produced the desired 4-bromo aldoxime **(182)** in an almost quantitative yield (98%) (see reaction overleaf). As **(182)** had been previously encountered as a by-product in the selective 6-bromination of **(72)** and had been fully characterised (Section 2.3.1), the ^{1}H-NMR and ^{13}C-NMR spectra were compared and found to be in excellent agreement. The 4-bromo benzaldoxime **(182)** recovered, did not require purification and was brought forward to the key bromination step.



(160) (*E*)-**(182)**

During Dubost's selective *ortho*-bromination of methoxy substituted aromatic aldehydes,[167] lower temperature (90 °C *vs*. 120 °C), avoidance of the use of AcOH as an additive and lower equivalents of NBS were all employed, in order to avoid formation of the unwanted dibromo product. These conditions were adhered to during synthesis of 6-bromo aldehyde **(165)** previously in this chapter (see Section 2.3.1). In the current attempted synthesis of 4,6-dibromo **(170)**, it was thought that using the higher temperature, AcOH additive and higher equivalents of NBS may be favourable in forcing bromination of the 4-bromo aldoxime **(182)**. These modified conditions (105 °C, 1 eqv. AcOH, 2 eqv. NBS) were used in the attempted 6-bromination of 4-bromo aldoxime **(182)**:



(182) **(191)**

The resulting ^{1}H-NMR spectrum of the crude reaction mixture indicated that very little conversion took place, with a substantial amount of unreacted 4-bromo aldoxime **(182)** remaining.

This mixture was subjected to flash column chromatography and although several minor unknowns were detected (but not isolated), none of these appeared to correspond to desired dibromo **(191)**. A second attempt at this reaction was made whereby AcOH was omitted and reaction time increased from 24 to 48 h, without any significant change in reaction outcome. It appears that bromine substitution at the 4-position of **(182)** has a significant impact on the reactivity of the remaining ring positions. The aromatic ring must be deactivated to such an extent that, complexation at the 6-position with $Pd(OAc)_2$ and the aldoxime group (as described in Figure 2.15), is very inefficient. Thus, subsequent oxidative addition of NBS to the complex cannot take place.

An additional attempt to synthesise **(170)** was made. In this attempt, bromination of the previously synthesised 6-bromo aldoxime **(181)** was investigated. Standard bromination conditions (Br_2, AcOH) were employed as outlined in Figure 2.27.

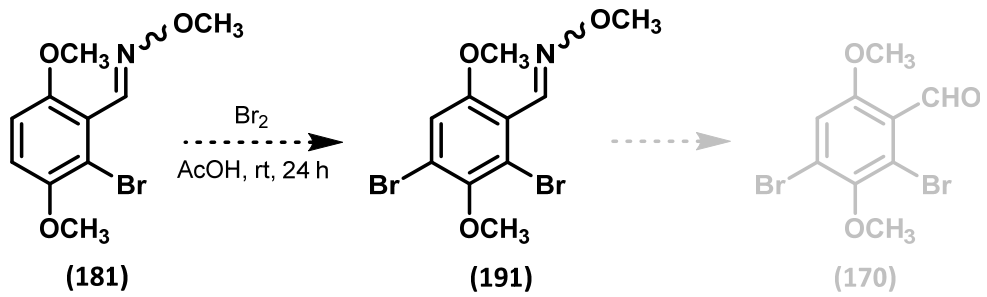


Figure 2.27: Proposed synthesis of 4,6-dibromo aldehyde (170) *via* 6-bromo aldoxime (181)

Following this first bromination step (Figure 2.27), initial evidence from the ^{1}H-NMR spectrum of the crude reaction mixture was promising. Although there was a substantial amount of unreacted 6-bromo aldoxime **(181)** present, there were also a number of new signals that correlated well with what would be expected for the desired 4,6-dibromo aldoxime **(191)**. Following flash column chromatography, both (*E*)-**(191)** and (*Z*)-**(191)** isomers of the desired dibromo aldoxime were recovered in a total combined yield of 29%. As pure samples of both isomers were recovered, full characterisation could be carried out (see Table 2.10).

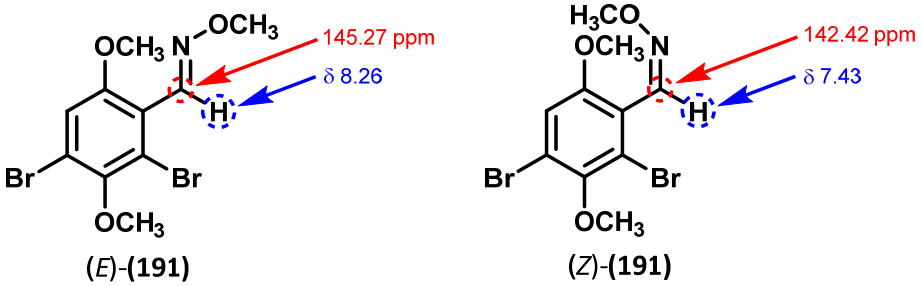
Table 2.10: R_f, m.p., IR and HRMS data for isomeric dibromo benzaldoximes (*E*)-(191) and (*Z*)-(191)

Compound No.	m.p. (°C)	R_f*	IRν_{max} (KBr) (cm^{-1})	HRMS (M+H$^+$)* (*m/z*)	
				Calc.	Found
(*E*)-**(191)**	70–72 (MeOH)	0.58	1582 (C=N), 1545 (C=C)	351.9184	351.9171
(*Z*)-**(191)**	70–72 (MeOH)	0.50	1582 (C=N), 1622, 1552 (C=C)	351.9184	351.9175

*mobile phase = 20:80 Et_2O:hexane

*molecular ion (M) calculated for $^{79}Br_2$ isotope peak

As with the previously encountered aldoximes (Section 2.3.1), assignment of (*E*)- and (*Z*)-configuration was based primarily on the ^{1}H-NMR δ value of the aldoxime proton; generally for (*E*)-, the aldoxime proton shift is > δ 8.0, and for (*Z*)-, this value is < δ 8.0. This assignment is in agreement with the observations made by Gordon *et al.*,[168] whereby for a range of *para*-substituted benzaldoximes, the iminyl ^{13}C shifts are consistently more downfield for the (*E*)-isomer compared to that of the (*Z*)-isomer:



The aromatic region of the ^{1}H-NMR spectra for both of these isomers was straightforward, as there is only one ring proton. Thus, only one singlet is observed for each compound in this region. The ^{1}H-NMR spectra obtained for both (*E*)-**(191)** and (*Z*)-**(191)** can be found in Figure 2.28.

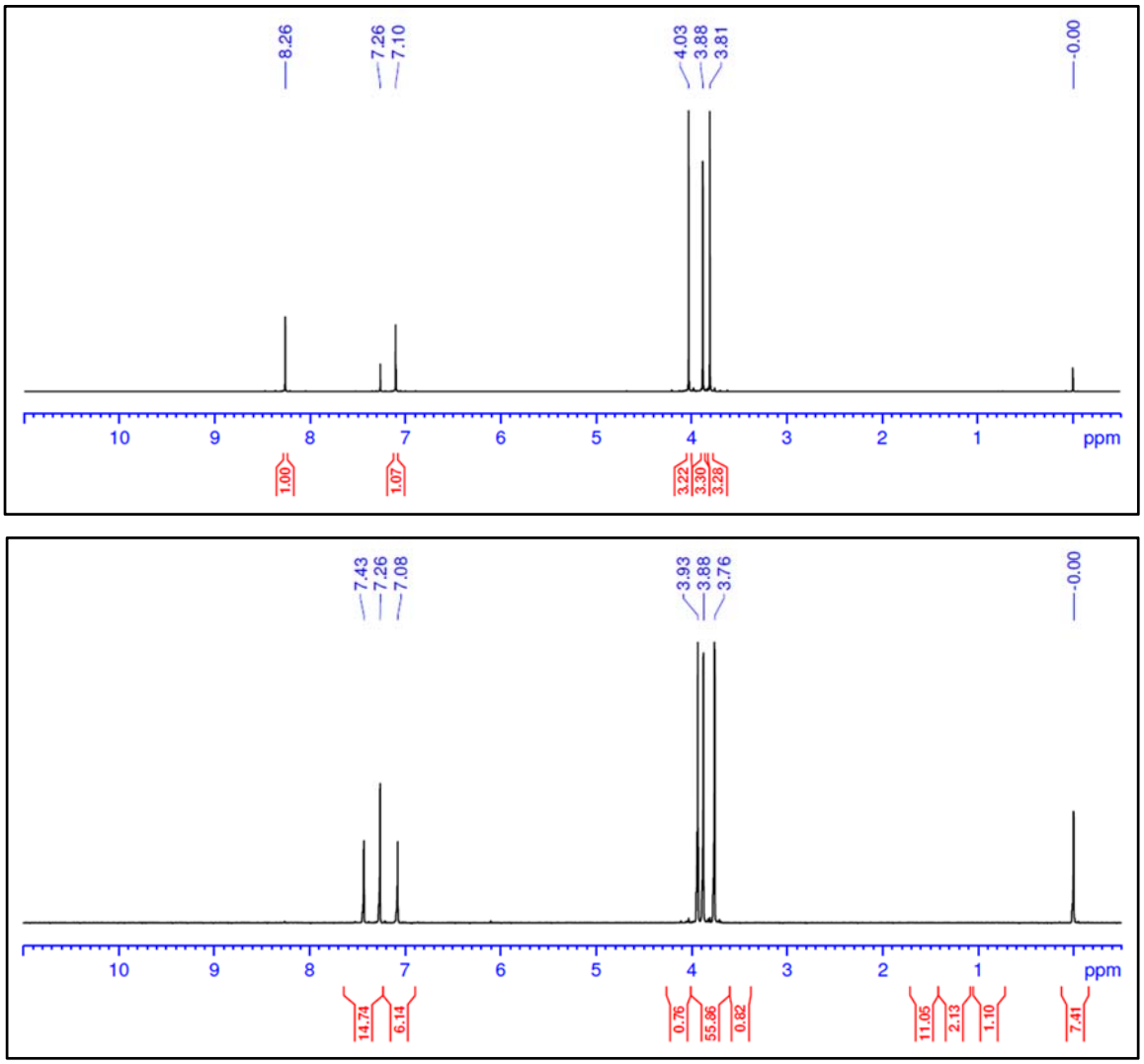
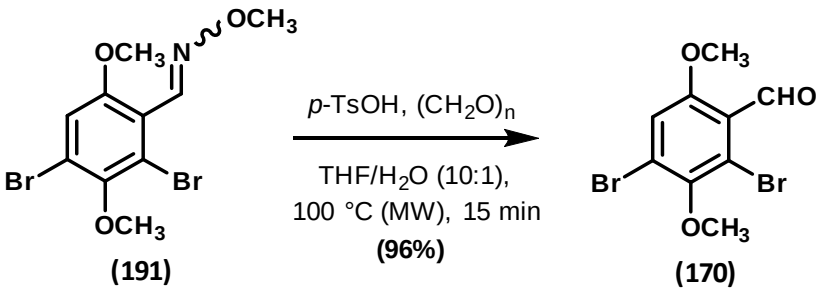


Figure 2.28: ^{1}H-NMR spectra of (*E*)-(191) (top) and (*Z*)-(191) (bottom) (@ 400 MHz)

Following successful synthesis of dibromo aldoxime **(191)**, all that remained in the synthesis of the 4,6-dibromo aldehyde standard **(170)** was removal of the aldoxime directing group. This was carried out using Dubost's microwave method:[167]



The conversion was highly successful, with a 96% yield of the desired 4,6-dibromo aldehyde **(170)** (from the aldoxime *E*/*Z* mixture **(191)**). Considering synthesis from the 6-bromo aldoxime **(181)**, this equates to an overall yield (over 2 steps) of 28%.

The novel dibromo aldehyde **(170)** was recovered pure, allowing for its full characterisation. The R_f, m.p., IR and MS data collected for **(170)** are summarised in Table 2.11.

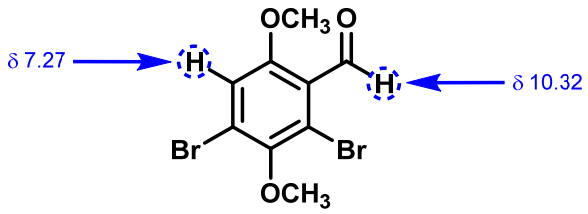
Table 2.11: Yield, R_f, m.p., IR and HRMS data for 4,6-dibromo aldehyde (170)

Compound No.	Yield	m.p. (°C)	R_f*	IRν_{max} (KBr) (cm^{-1})	HRMS ($M+H^+$)⋆ (*m/z*)	
					Calc.	Found
(170)	96%	98–99.5 (DCM/hexane)	0.67	1693 (C=O), 1579, 1546 (C=C)	322.8918	322.8906

*mobile phase = 50:50 Et_2O:hexane

⋆molecular ion (M) calculated for $^{79}Br_2$ isotope peak

The aromatic region of the ^{1}H-NMR spectrum of **(170)** was straightforward, with only one singlet present (@ δ 7.27), corresponding to the single proton present on the aromatic ring. This provides strong evidence that dibromination of the ring has taken place. The shift at δ 10.32 (typical for aldehyde) also suggests that the removal of the aldoxime group ('deprotection') was also successful.



(170)

HRMS data was obtained for a sample of the standard. This exhibited the typical 'triplet' molecular ion (@ *m/z* 325 [middle peak of triplet] for $M+H^+$), characteristic of a compound containing two bromine atoms. The ^{1}H-NMR and MS data were in good agreement with data obtained for the un-isolated impurity of the bromination of 2,5-dimethoxybenzaldehyde **(72)** (Section 2.2.2).

A summary of the various attempts involved in the synthesis of a standard sample of 4,6-dibromo-2,5-dimethoxybenzaldehyde **(170)**, is outlined in Figure 2.29 overleaf.

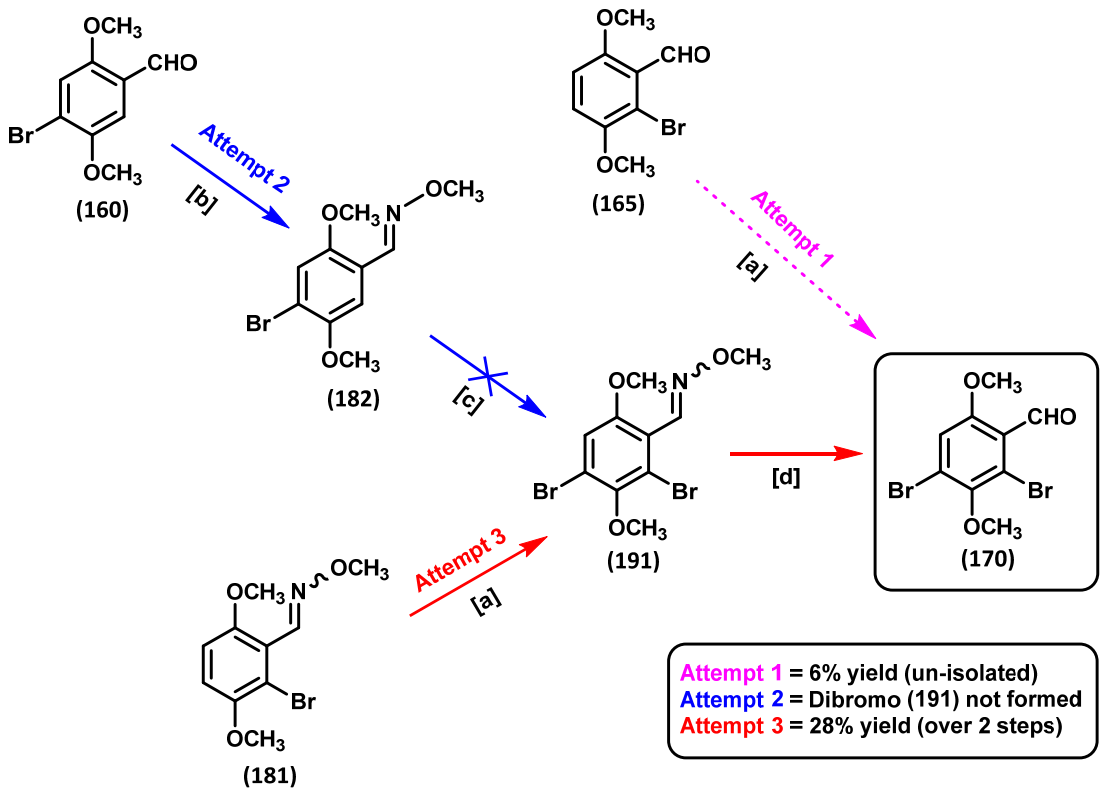


Figure 2.29: Attempts to synthesise 4,6-dibromo-2,5-dimethxoybenzaldehyde (170)

([a] = Br_2, AcOH, rt, 24 h; [b] = $CH_3ONH_2.HCl$, pyridine, DCM, rt, 1 h; [c]= NBS, AcOH, $Pd(OAc)_2$, $AgOCOCF_3$, DCE, 105 °C, 24 h; [d] = p-TsOH, $(CH_2O)_n$, THF/H_2O (10:1), 100 °C (MW), 15 min)

2.3.6 Selective synthesis of 4,6-dibromo-5-hydroxy-2-methoxybenzaldehyde (167)

Novel phenol **(167)** had been fully isolated as an impurity of the bromination of 2,5-dimethoxbenzaldehyde **(72)** (Section 2.2.2). Even though the impurity had already been characterised, comparison with a standard would provide much stronger evidence for the structure assigned. As the compound was novel, no preparation procedure, specific to this structure, was available in the literature. Two approaches were considered for the synthesis of the target phenol **(167)**. The first approach involved starting from commercially available 5-hydroxy-2-methoxybenzaldehyde **(192)**. It was hoped that the phenol group (@ C-5) would be sufficiently activating to direct bromination to both the 4- and 6-positions. However, literature precedence[180] suggested that only monobromination of phenol **(192)** (@ C-4) could be achieved (Figure 2.30).

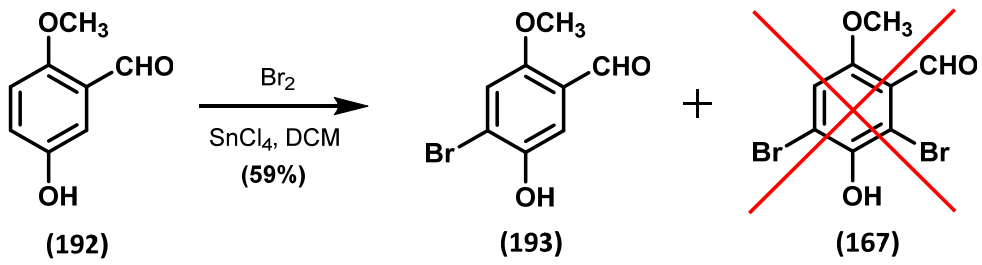


Figure 2.30: Literature bromination of phenol (192)[180]

As encountered previously, introduction of a second bromine atom, to a compound of general structure **(193)**, is difficult and low yielding, so further bromination of **(193)** was not pursued.

The second envisaged approach to dibromo phenol **(167)**, was the selective demethylation (of the 5-methoxy group) of a suitably substituted 2,5-dimethoxy compound. This was made particularly feasible by the fact that 4,6-dibromo-2,5-dimethoxy aldehyde **(170)** had already been synthesised as a standard (Section 2.3.5), making the potential synthesis of phenol **(167)** a one-step process.

In relation to 2,5-dimethoxy aldehydes of general structure **(194)**, selective demethylation, at both the 2- and 5-positions, has been reported in the literature (see Table 2.12). Selective 2-demethylation generally involves treatment of **(194)** with a Lewis acid (e.g. $AlCl_3$ or BCl_3). The Lewis acid forms a cyclic intermediate with the aldehyde/2-methoxy groups. Chloride (Cl^-), displaced from the complexed Lewis acid, attacks the methyl group (of 2-methoxy) forming MeCl (S_N2 reaction). Upon addition of water, the remaining aluminium (or boronic) complex, undergoes hydrolysis to form the desired phenol (at C-2) and boronic acid.[181,182]

In a paper by Ulrich *et al*. published in 1974,[181] selective demethylation at the 5-position of 2,5-dimethoxybenzaldehyde **(72)** was carried out. This was achieved following exposure of the compound to concentrated H_2SO_4. The regioselective demethylation is as a result of the difference in nucleophilicity between the 2- and 5-methoxy groups (5-methoxy > 2-methoxy). A summary of some structurally similar 2,5-dimethoxybenzaldehydes (of general structure **(194)**) that have undergone regioselective demethylation in the literature, can be found in Table 2.12.

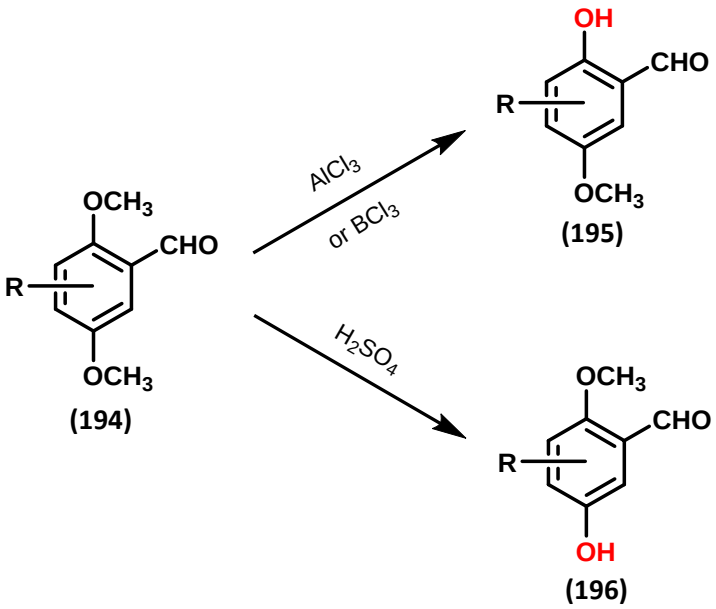


Table 2.12: Selective demethylation of a number of 2,5-dimethoxybenzaldehydes

	R	Reagents/Conditions	Literature source
Selective 2-demethylation →(195)	4-bromo	**BCl_3**, CH_3NO_2, $ZnCl_2$, DCM, rt, 6 h	Maruyama *et al*.[183]
	4-bromo	**$AlCl_3$**, DCM, 0 °C–rt, 4 h	Radomkit *et al*.[158]
	4-methyl	**$AlCl_3$**, NaI, CH_3CN, reflux, 1 h	Lanfranchi *et al*.[184]

	4-iodo	**BCl_3**, DCM, rt, 16 h	Ettrup *et al*.[38]

	R	Reagents/Conditions	Literature source
Selective 5-demethylation →(196)	H	**H_2SO_4** (neat), 0–54 °C, 46 h	Ulrich *et al*.[181]
	4-bromo	**H_2SO_4** (neat), 0–55 °C, 48 h	Rangisetty *et al*.[180]
	6-bromo	**H_2SO_4** (neat), 70 °C, 14 h	Li *et al*.[166]

As selective demethylation of the 5-methoxy group was required for synthesis of phenol **(167)**, conditions outlined by Rangisetty *et al*.[180] (Figure 2.31) were employed in this work.

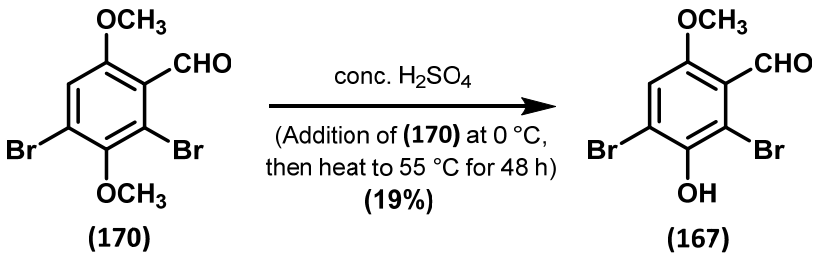


Figure 2.31: Preparation of phenol (167)

Following purification by flash column chromatography, phenol **(167)** was isolated in a yield of 19%. Although the yield was poor, the desired phenol **(167)** was produced in a single synthetic step (from a previously prepared standard **(170)**) and only a small amount of sample was required for comparison of spectroscopic and LC-MS data, with that of the isolated impurity (Section 2.2.2). The R_f, m.p., IR and MS data previously collected for phenol **(167)**, following its isolation as an impurity from the bromination of 2,5-dimethoxybenzaldehyde **(72)**, are summarised in Table 2.13.

Table 2.13: R_f, m.p., IR and HRMS data for dibromo phenol (167)

Compound No.	m.p. (°C)	R_f*	IRν_{max} (KBr) (cm^{-1})	HRMS ($M–H^+$)⋆ (*m/z*)	
				Calc.	Found
(167)	139–140 (EtOH)	0.76	3000 (OH), 1649 (C=O), 1593, 1577, 1561 (C=C)	306.8605	306.8604

*mobile phase = 30:70 EtOAc:hexane

⋆molecular ion (M) calculated for $^{79}Br_2$ isotope peak

The ^{1}H-NMR spectrum of phenol **(167)** was very straightforward to assign, where aside from residual solvent, only four signals (all singlets) were present. These singlets resonated at δ 12.14 (O–H), δ 10.39 (CHO), δ 7.42 (ring proton @ 3-position) and δ 3.90 (methoxy group protons).

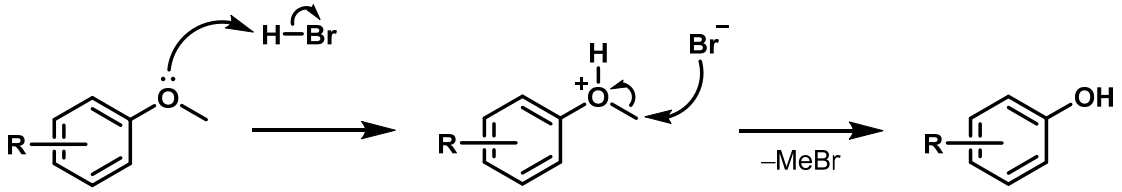
The ^{1}H-NMR and ^{13}C-NMR spectra of the selectively synthesised standard of **(167)** (synthesised according to Figure 2.31), and those of the isolated impurity, were found to be comparable. This confirms compound **(167)** to be an impurity of the bromination of 2,5-dimethoxybenzaldehyde **(72)**.

The origin of **(167)** in this reaction is not clear. To propose a plausible origin, two questions must be answered:

1. Does the 5-*O*-demethylation occur prior to bromination, following monobromination (at position 4 or 6) or following dibromination (at positions 4 and 6)?
2. By what manner does the key *O*-demethylation step take place?

To answer the first question, we have speculated that the 5-*O*-demethylation occurs following dibromination (at positions 4 and 6) of the aromatic ring (i.e. *via* 5-*O*-demethylation of **(170)**). This theory was based on the assumption that if *O*-demethylation of either SM **(72)**, 4-bromo **(160)** or 6-bromo **(165)** were to be part of the pathway to **(167)**, some trace of their phenolic counterparts (precursors to **(167)**, i.e. either **(192)**, **(193)** or 6-bromo-**(196)**) would be found in the crude reaction mixture. No evidence for the presence of these compounds was found. Further support for this may be gained from the fact that the 4,6-dibromo-2,5-dimethoxy compound **(170)** was in fact, detected in the crude reaction mixture following work-up.

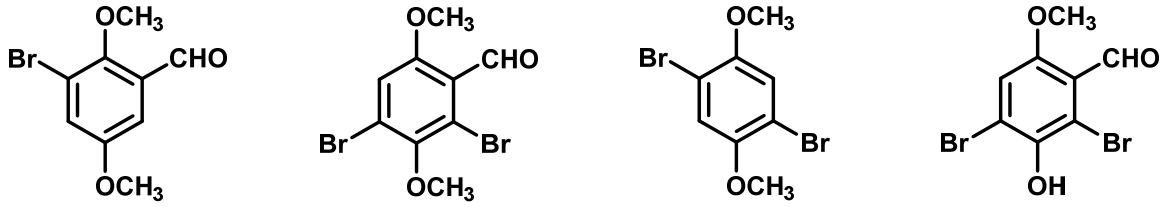
With regard to the second question, one proposal for the *O*-demethylation that could be put forward is one which involves reaction of the methoxy group with HBr. This acid would be expected in the bromination reaction mixture following EAS of SM **(72)** with Br_2 (producing Br^-, existing as HBr in AcOH environment). A simple schematic depicting this HBr mediated *O*-demethylation is shown below:



Several references to this HBr/AcOH demethylation methodology can be found in the literature and it has a particular niche in the regiospecific demethylation of many alkaloids.[185,186]

2.4 Summary

The characterisation of four previously unidentified impurities of the bromination of 2,5-dimethoxybenzaldehyde **(72)** is summarised in Figure 2.32. This figure outlines the key analytical/spectroscopic data that may be used to distinguish between the four impurities.



	(169)	**(170)**	**(168)**	**(167)**
^{1}H-NMR δ (C*H*O)	10.32	10.30	n/a	10.39
^{1}H-NMR δ (aromatic signals)	7.28, 7.39 (d × 2, *J*=3 Hz)	7.27 (s)	7.11 (s)	7.42 (s)
^{13}C-NMR (*C*HO) (ppm)	188.99	190.16	n/a	197.67
IR (C=O) (cm^{-1})	1690	1693	n/a	1649
MS (*m/z*=)	245/247 'doublet' ($M+H^+$)	323/325/327 'triplet' ($M+H^+$)	n/a	307/309/311 'triplet' ($M-H^+$)
m.p. (°C)	64–66 (EtOH)	98–99 (DCM/hexane)	143–145 (EtOH)	139–140 (EtOH)

Figure 2.32: Distinguishable analytical/spectroscopic features of detected impurities (169), (170), (168) and (167)

Following selective synthesis of standards of the four impurities, t_R matching (against the previously recovered impurities) was carried out by HPLC. Firstly, the synthesised standards were run under the HPLC conditions used previously, for the analysis of the SM, known products and recovered impurities (outlined earlier in Figures 2.7 and 2.8). This allowed for the t_R of each of the synthesised standards to be established. The UV signals (DAD @ 210 nm) for the four standard runs are shown in Figure 2.33.

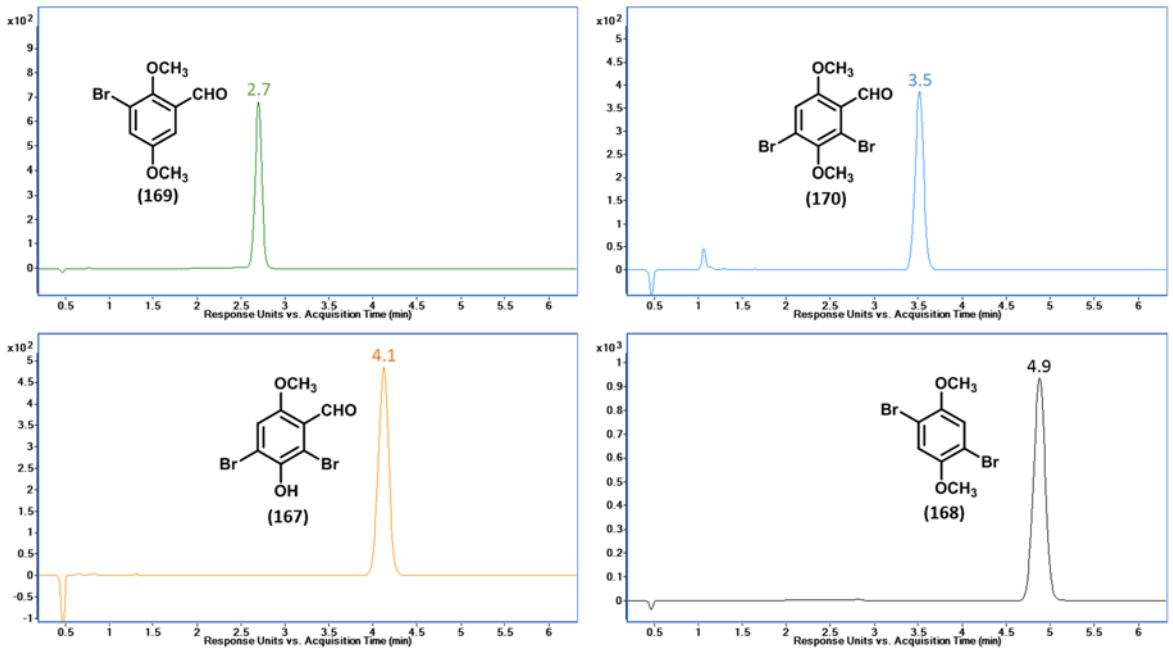


Figure 2.33: Individual HPLC runs (DAD signal @ 210 nm) of the four selectively synthesised standards (169), (170), (167) and (168)

*(HPLC conditions identical to those outlined in Figure 2.5 except for injection volumes used: 2 µL for **(169)**, 5 µL for **(170)**, 12 µL for **(167)** and 3 µL for **(168)**)*

On visual inspection, there appears to be good agreement between the t_R of the recovered impurities (Figure 2.8) and the t_R of the selectively synthesised standards (Figure 2.33). The LC-MS data processing software used, allows for multiple runs to be overlaid. The impurities from Figure 2.8, and standards from Figure 2.33, were overlaid in this manner, making t_R agreement much easier to visualise (Figure 2.34).

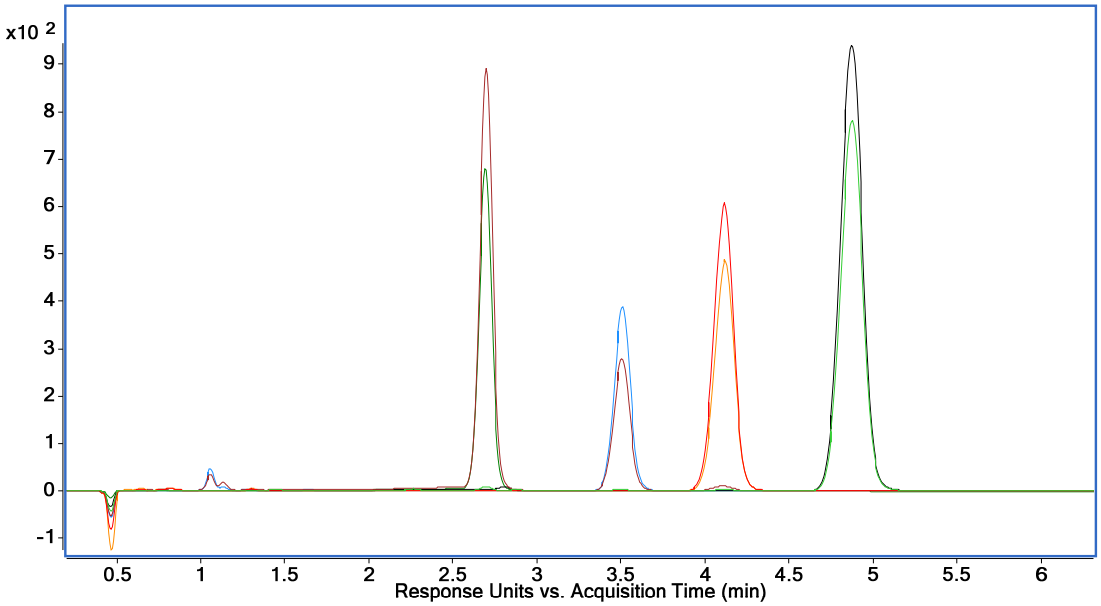


Figure 2.34: Overlays of impurity and standard chromatograms from Figures 2.8 and 2.33

Table 2.14 outlines the identity of each signal in the chromatogram (each set of overlapping signals corresponding to the recovered impurity and synthesised standard).

Table 2.14: Identity of each signal in Figure 2.34

t_R (min)	Peak colour	Impurity or standard?
2.7	Dark Green	Synthesised standard of **(169)**
2.7	Brown	Recovered impurity of **(169)**
3.5	Light Blue	Synthesised standard of **(170)**
3.5	Brown	Recovered impurity of **(170)**
4.1	Orange	Synthesised standard of **(167)**
4.1	Red	Recovered impurity of **(167)**
4.9	Black	Synthesised standard of **(168)**
4.9	Light Green	Recovered impurity of **(168)**

Finally, the SM **(72)**, 4-bromo **(160)** and 6-bromo **(165)** products (from Figure 2.7) were also overlaid with the impurities/standards (see Figure 2.34). Figure 2.35 demonstrates that all compounds identified to date, that may arise during the impurity profiling of the bromination of 2,5-dimethoxybenzaldehyde **(72)**, may be easily separated by HPLC (on a standard C18 column) in a run time of just over 5 minutes.

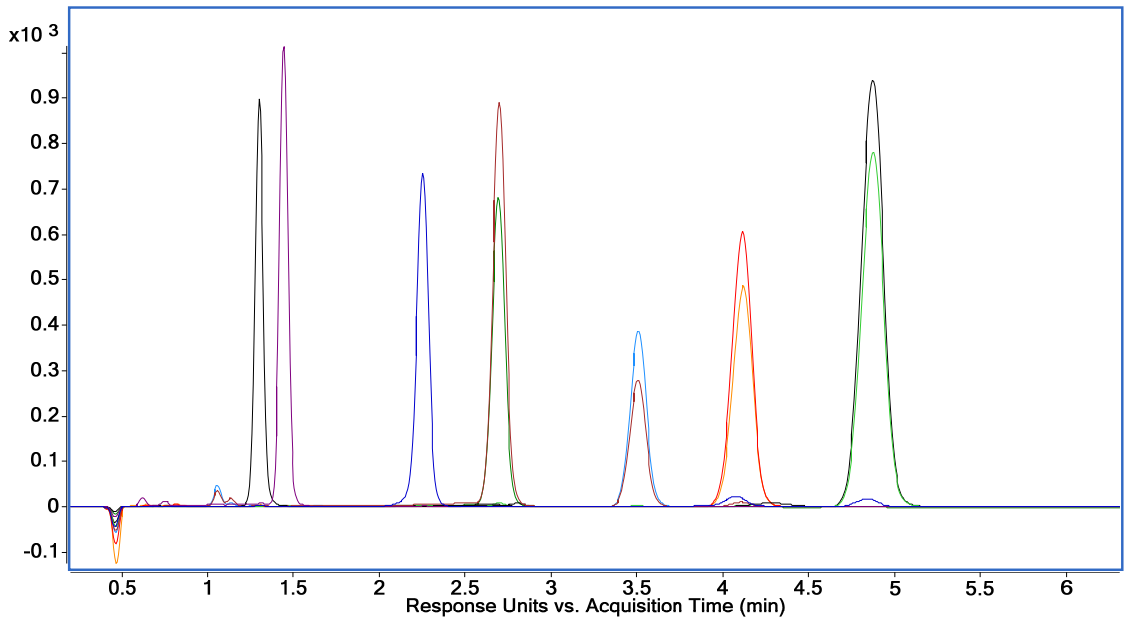
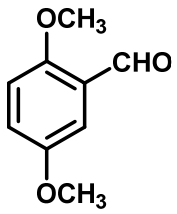
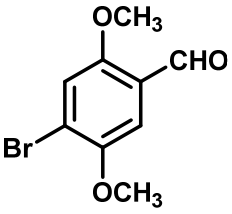


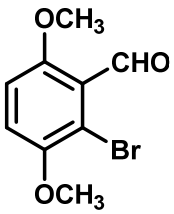
Figure 2.35: Chromatogram overlays of all compounds – SM (72), expected products (160) and (165) and impurities (169), (170), (167) and (168) encountered during the bromination of 2,5-dimethoxybenzaldehyde (72)



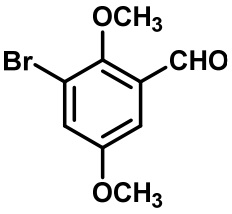
(72)
t_R = 1.4 min



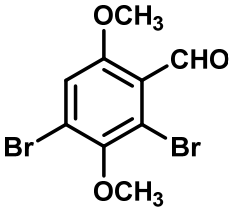
(160)
t_R = 2.2 min



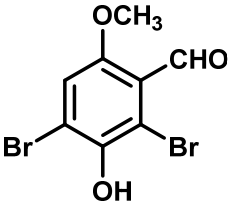
(165)
t_R = 1.5 min



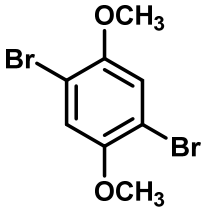
(169)
t_R = 2.7 min



(170)
t_R = 3.5 min



(167)
t_R = 4.1 min



(168)
t_R = 4.9 min

In summary, four impurities of the bromination of 2,5-dimethoxybenzaldehyde **(72)**, not previously reported in the literature, were identified in this chapter. Of these impurities, two were novel compounds. Isolation of two of the impurities (**(167)** and **(168)**) was possible *via* flash column chromatography of the crude reaction mixture, followed by an acid/base extraction. The other two impurities (**(169)** and **(170)**), unresolved by flash chromatography, were separated by HPLC and tentatively identified with the help of a coupled mass spectrometer.

Together with the previously reported 6-bromo impurity **(165)**, selective synthesis of standards of each of the impurities was carried out. This was performed for the purpose of t_R matching (by HPLC) of the selectively synthesised standards and recovered impurities. Excellent agreement between the chromatography of the standards and recovered impurities was achieved. As well as this, good resolution (by HPLC) of all compounds encountered during the bromination of **(72)** (SM, known products and impurities), was accomplished. This resolution would make the identification of impurities present in a mixture (or crude sample), much easier during impurity profiling.

The compounds identified in this work, add to the list of impurities in the literature, that are encountered during the impurity profiling of brominated ATS, in particular DOB **(35)**. These impurities, formed in the early stages of DOB synthesis, may be carried forward through subsequent reaction steps and be found in the final drug product. If detected, they may indicate that bromination of aldehyde **(72)** was part of the synthetic strategy used in the manufacture of the final drug product.

The impurities that are formed and carried through to subsequent reaction steps, may also undergo similar reactions to those of the intended intermediates, thus forming additional 'secondary' by-products. Identification of the source of these additional by-products would be difficult without prior knowledge of the original impurities (from which the by-products arise).

Future work in this area may involve subjecting the isolated impurities (or synthesised standards) to the subsequent reaction steps (e.g. nitrostyrene route to ketone intermediate **(159)**), that the intended products/intermediates would be involved in. This would allow for standard samples of several more potential secondary impurities to be attained.

Chapter 3 – Synthesis and impurity profiling of 2,5-dimethoxyphenyl-2-propanone and its 4-bromo counterpart

The 'phenylacetic acid (PAA) route' is a commonly used method of converting ketone precursors to illicit amphetamine-type stimulants (ATS). Its name is derived from the phenylacetic acid-based starting material used in production of the precursor chemicals. Due to the ease of access to starting materials, its cost-effectiveness and the well reported "recipes" documented in books and online, the route is commonly used in clandestine laboratories. However, the route is by no means an efficient method of synthesising the ketone and thus, many impurities are known to arise.

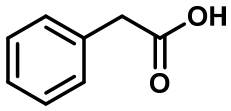
Numerous reports detailing the impurities arising from the manufacture of ketone precursors to amphetamine and MDMA, from PAA starting materials, can be found in the literature. However, the same cannot be said for the hallucinogenic 2,5-dimethoxy class of amphetamines. This chapter outlines a detailed account of the synthesis, isolation, identification and characterisation of such impurities arising from the PAA route to 2,5-dimethoxyphenyl-2-propanane (2,5-P2P) and its 4-bromo analogue (4-Br-2,5-P2P); a key precursor to DOB - the most potent of the 2,5-dimethoxy class of amphetamines.

Also explored in this chapter is the synthesis of 2,5-P2P *via* the 'Darzens route'. In terms of the synthesis of ATS precursors, this route was almost unheard of prior to 2004 but since then, a number of seizures of the uncontrolled glycidate 'pre-precursors' to MDMA and amphetamine, have been reported. With the potential of this methodology to be used in the synthesis of 2,5-P2P, the viability of the route was assessed, and the yields achieved were compared to the other, more common routes to ketone precursors. No significant additional impurities were detected using this route, aside from the 2,5-dimethoxybenzaldehyde starting material, which was present not only due to reaction incompletion, but also as a decomposition product of the glycidate intermediate.

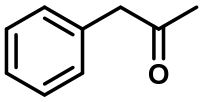
3.1 The phenylacetic acid (PAA) reaction

The 'PAA route', as described previously in Section 1.5.1.1, is reported to be used in over 75% of cases of P2P **(65)** manufacture.[125] The trafficking of PAA **(64)** is controlled (under United Nations Convention against Illicit Traffic in Narcotic Drugs and Psychotropic Substances, 1988).[57] However, it is readily available due to its widespread industrial use and is often diverted from legitimate sources. The European Monitoring Centre for Drugs and Drug Addiction (EMCDDA) reported a sharp rise in seizures

of **(64)** in 2009, with almost 42 tonnes confiscated worldwide.[57] The two countries seizing the most of **(64)** in 2009 worldwide were Mexico and China. In Europe, 2.2 tonnes were seized in 2009, most of which was recovered in Serbia and France.



(64)



(65)

Illicit production of amphetamine precursors was rare in Europe until 2010. Before this, precursors were imported from China/Russia and then converted to amphetamine once they had been trafficked into Europe. In recent years, there have been numerous reports of precursors (e.g. P2P **(65)**) being manufactured from pre-precursors, like PAA **(64)**, within Europe. For example, in Poland, three clandestine facilities manufacturing P2P **(65)** from PAA **(64)**, have been dismantled since the early 2000's. Also, clandestine amphetamine production sites, using **(65)**, were dismantled in Germany and Spain in 2010.[57]

Given the increase in seizures in recent years, PAA **(64)** was rescheduled in 2011, from Table II to Table I of the United Nations Convention against Illicit Traffic in Narcotic Drugs and Psychotropic Substances, 1988. This puts it under the same type of international control as P2P **(65)**.

The origin of the PAA route to ketone precursors is, in most cases, associated with the Dakin-West reaction, although some reports suggest that the first successful conversion of carboxylic acids to ketones should be attributed to work carried out by Perkin and Thorpe in the 19th century.[187] Originally, the Dakin-West methodology (published in 1928)[188] involved the reaction of α-amino acids, in the presence of acetic anhydride (Ac_2O) **(66)** and pyridine, to form β-acetomido ketones. Later, it was used successfully to synthesise ketones from aryl acetic acids, and the mechanism and kinetics of this reaction have been well studied since.[187,189-191]

There has been some dispute around the mechanism of formation of ketone **(65)**.[192] Based on the Dakin-West ideology, the mechanism can be broken down into a number of conceptual steps: (Figure 3.1)

- The first step is an acid-mixed anhydride equilibrium.
- The second step is proton removal from the mixed anhydride **(197)** by a base (sodium acetate or pyridine).
- The third step is attack, by the enolate **(198)** of the mixed anhydride, on one of the carbonyl groups of Ac_2O **(66)**.
- The final step is the decarboxylation of the β-keto acid **(200)** to yield ketone **(65)**.[193]

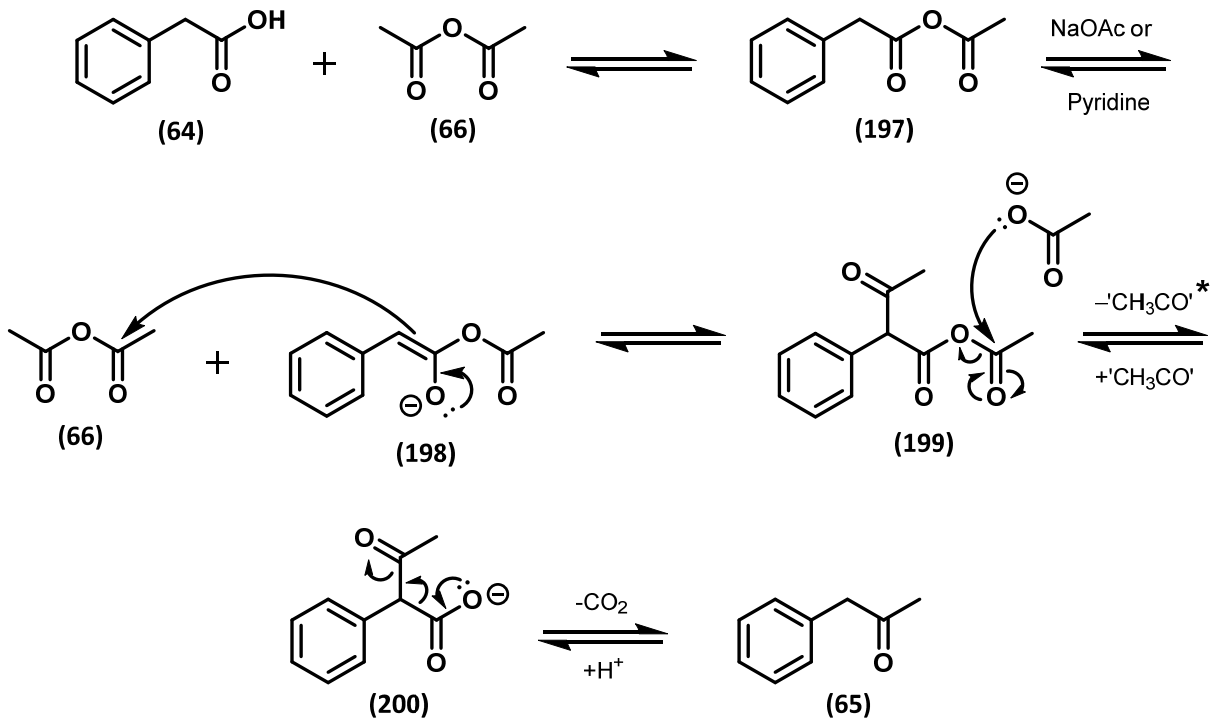


Figure 3.1: Dakin-West reaction of PAA and Ac_2O[193]

('CH_3CO' lost in the form of Ac_2O **(66)**)*

The 'step-wise' Dakin-West mechanism is purely conceptual and others have argued against it. Allinger,[189] suggests that the reaction proceeds *via* a cyclic intermediate (Figure 3.2), whereby the initial mixed anhydride **(197)** reacts with Ac_2O **(66)** in a concerted fashion. The orientation of the anhydride reagent (in this case **(66)**, where R = CH_3 in Figure 3.2) is also important in determining which product is formed. This will be discussed in greater detail later.

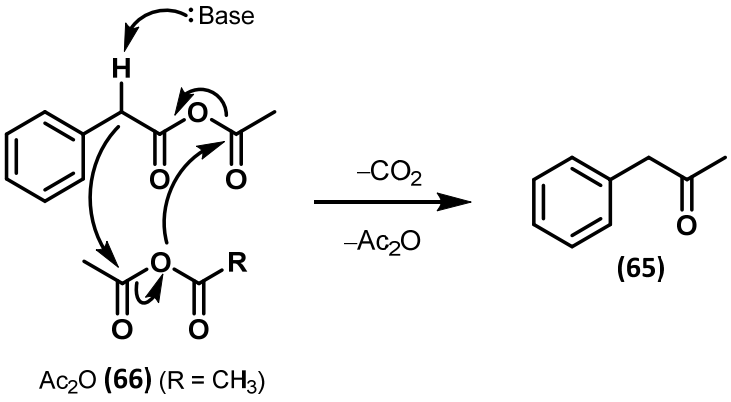
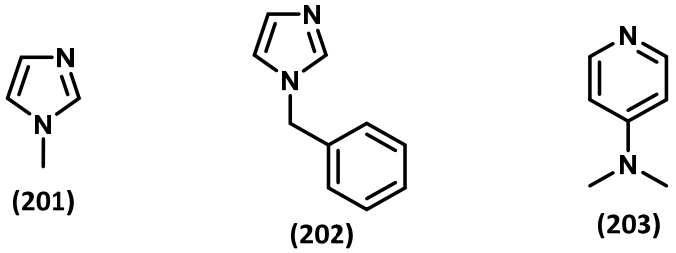


Figure 3.2: Cyclic mechanistic proposal for the formation of ketone (P2P)[189]

A more recent publication,[191] suggests that the choice of catalyst used has a substantial influence on yield of product, in addition to, which product is predominantly formed. In the case of catalysts such as

1-methylimidazole (MIM) **(201)**, 1-benzylimidazole **(202)** and DMAP **(203)**, the predominant product formed is the monomeric ketone P2P and the reaction proposed proceeds *via* 'nucleophilic catalysis'.



This ideology proposes that the catalyst (by first reacting with **(66)**) can generate an effective acylating agent **(205)** and a strong base (acetate **(204)**), as shown in Figure 3.3. The mechanism suggests that the acyl-imidazolium species **(205)** is a much stronger electrophile than the mixed anhydride **(197)**, as the results show very little dimeric ketone **(80)** is formed (compared to when other catalysts such as NaOAc are used, see Section 1.5.1.1).

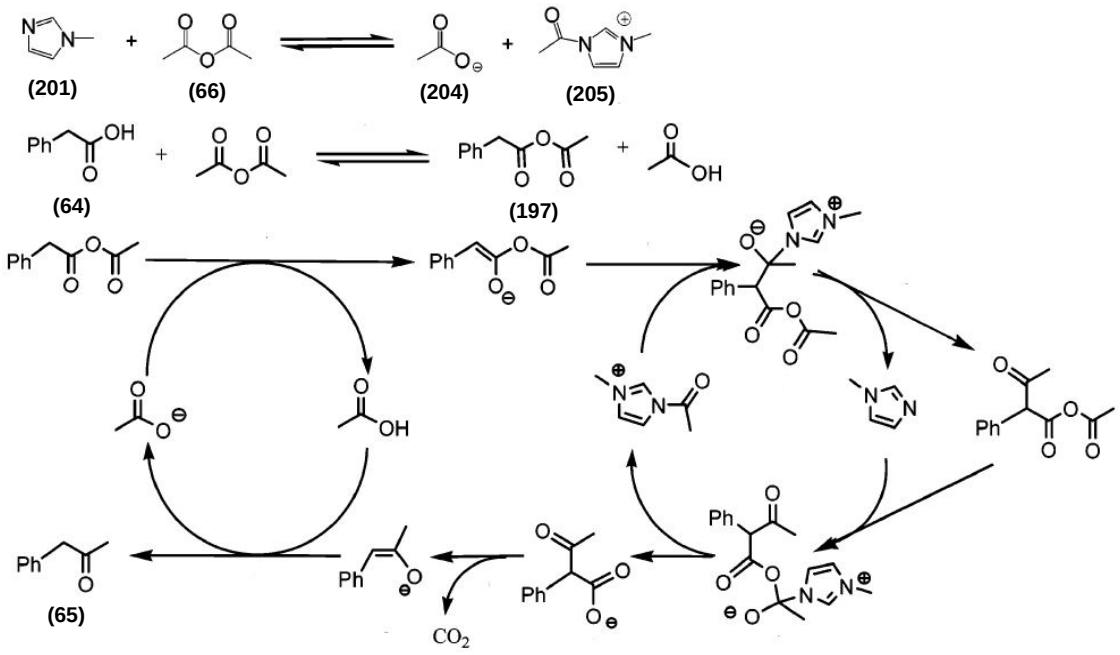
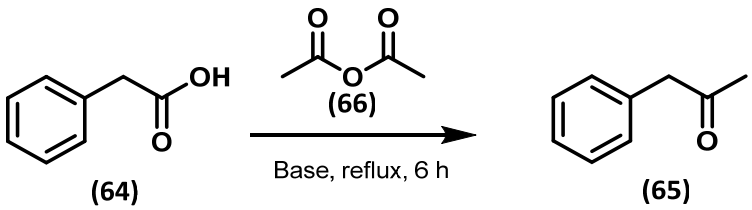


Figure 3.3: Scheme outlining formation of ketone (65) *via* 'nucleophilic catalysis'[191]

The Dakin-West/PAA route methodology used 80 years ago, is still used today. Some literature examples of more recent uses of the PAA reaction to P2P **(65)**, are outlined in Figure 3.4. The structurally simple ketone **(65)** continues to be an important intermediate in the synthesis of an array of bioactive molecules.



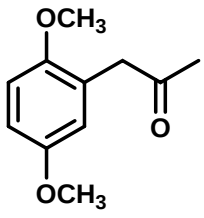
Base used	Ratio of SM (64) : Ac_2O (66)	% yield	Literature source
Pyridine	1 : 6	56	Tran and Bickar, 2006[191]
NaOAc	1 : 10	27	Ammerman *et al.*, 2012[194]
Pyridine	1 : 5	27	Jozwiak *et al*., 2007[195]

Figure 3.4: Recent examples of the use of the PAA route to P2P (65)

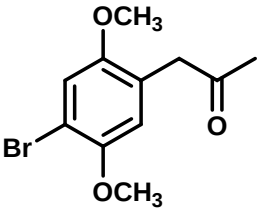
3.1.1 The PAA route to ketone precursors of ATS

It was not until the latter half of the 20th century that the PAA procedure was adopted by clandestine chemists for the manufacture of amphetamine precursors. A number of variations of the PAA route to P2P **(65)** exist in the literature,[129,193] whereby various catalysts/reagents are employed. Based on the reference material/'recipes' used by illicit chemists (books, fora etc.), the typical procedure used involves refluxing PAA **(64)** with Ac_2O **(66)** (at least a 6 fold molar excess of Ac_2O) in the presence of pyridine as a catalyst. These conditions are derived from the early optimisation work carried out to increase the yield of the desired ketone **(65)**. It was found in the early 20th century that for reaction completion (i.e. complete consumption of starting material), at least 3 molar equivalents of **(66)** are required.[192] It was also discovered around this time that using lower equivalents of **(66)**, favoured the formation of dibenzylketone **(80)** over the monomeric ketone (P2P **(65)**).[196] This phenomenon will be discussed in greater detail later (Section 3.2.2).

Note: Little is known about the specific routes employed in the manufacture of the 2,5-dimethoxy class of amphetamines. However, it is reasonable to assume that, as these are structural analogues of amphetamine, similar synthetic protocols and trends would be observed. Thus, it is likely that the PAA route may be used to synthesise 2,5-P2P **(92)** or 4-Br-2,5-P2P **(159)**.



(92)



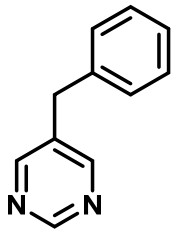
(159)

3.1.2 Impurity profiling of the PAA reaction

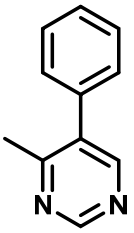
Given the influx of P2P synthesis into Europe in recent years, impurity profiling is important for establishing possible links between samples, providing evidence of the synthetic route employed and establishing if samples of P2P seized are diverted from licit manufacturers or are illicitly produced. In terms of impurity profiling, there have been a number of reports concerning impurities present in seized P2P **(65)**.

A paper by Krawczyk *et al*.[123] reported the analysis of 80 samples of seized P2P (by GC-MS) and identified 36 impurities. Two routes of manufacture of P2P were identified based on the presence of unreacted SM or unreacted intermediate – the PAA route and a route involving benzyl cyanide as SM (see Section 1.5.1.1). For many of the samples, the route of manufacture was not determined. In the case of the PAA route, only the presence of the unreacted SM, PAA **(64)** was used to identify the route used; no other links were made between the impurities identified and manufacture *via* PAA **(64)**.

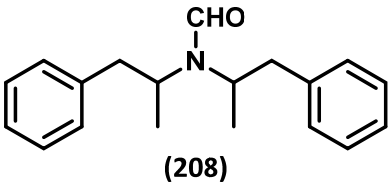
In a report by Forbes *et al*.,[146] analysis was carried out on a sample taken from a clandestine laboratory involved in the manufacture of amphetamine. It was suspected, based on the impurities identified, that the amphetamine was manufactured from P2P **(65)**, which was in turn derived from PAA **(64)**. GC-MS analysis revealed that, aside from the target amphetamine and P2P **(65)** precursor, a number of other compounds were identified. These include impurities associated with the Leuckart route (pyrimidines **(206)**/**(207)**, dimeric *N*-formyl compound **(208)**), and reductive amination route (*N*,*N*-diisopropylamine **(209)**). The Leuckart and reductive amination routes are commonly used to manufacture amphetamine from P2P **(65)** (Section 1.5.1.1).



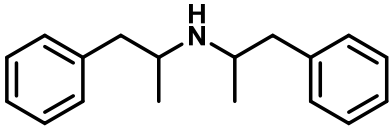
(206)



(207)



(208)



(209)

A number of other compounds present were thought to arise from the synthesis of P2P **(65)** from PAA **(64)**. These impurities are outlined in Figure 3.5.

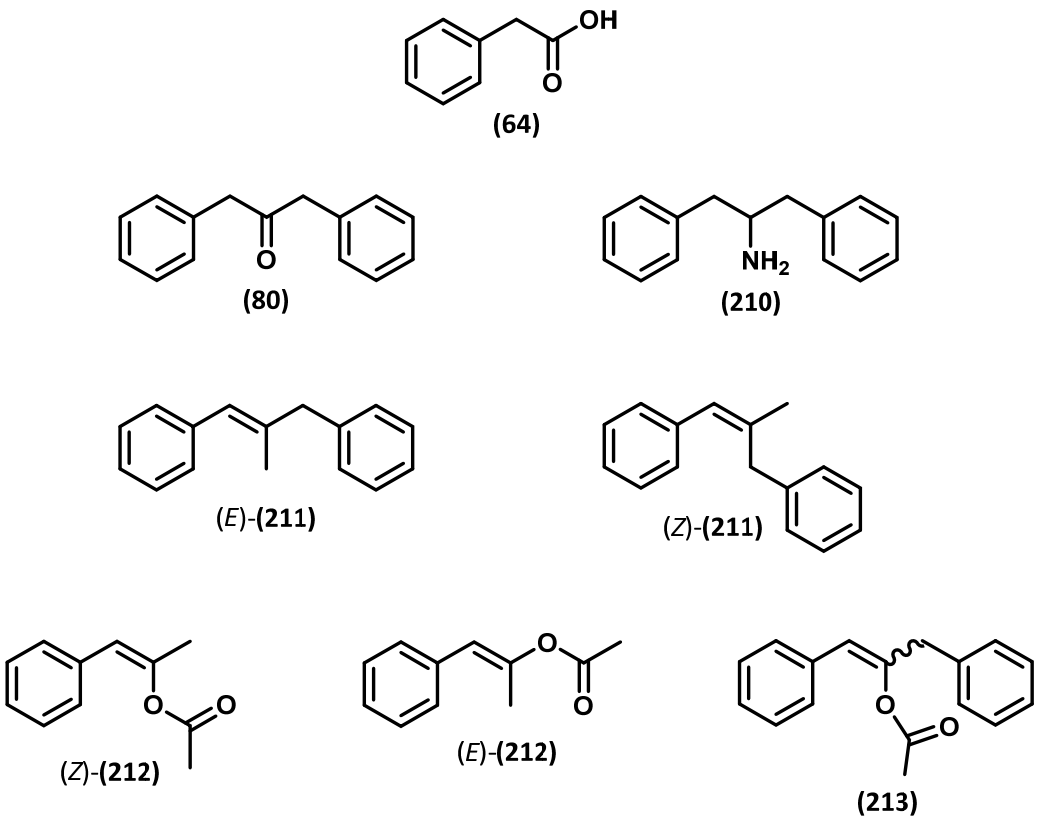


Figure 3.5: Compounds recovered from impure amphetamine associated with the PAA route[146]

All of the compounds shown in Figure 3.5 are thought to arise directly as reaction by-products from the PAA route to P2P **(65)**, except for dimeric amine **(210)**, which is thought to arise as a result of dimeric ketone **(80)** being reduced to the amine under Leuckart reaction conditions.

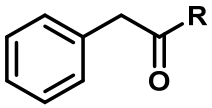
A paper by Allen *et al*.[193] looked specifically at impurities arising during the PAA route to P2P **(65)**. In particular, Allen *et al*. compared two routes, whereby two different catalysts/reagents were used – Ac_2O **(66)** and $Pb(OAc)_2$ **(75)**. Between the two reactions, 21 reaction by-products were identified. These by-products are summarised in Table 3.1. This Table also indicates if the by-product were encountered by Krawczyk[123] or Forbes[146] during their profiling of illicitly produced P2P **(65)**.

Table 3.1: Reaction by-products from PAA reaction identified by Allen, Krawczyk and Forbes[123,146,193]

Entry	Compound name	Allen *et al.*	Krawczyk *et al.*	Forbes *et al.*
	Phenyl-2-propanone **(65)** (intended product)	✓	✓	✓
1	Benzaldehyde **(76)**	✓	✓	✓
2	Methyl benzoate	✓	✓	×
3	Benzyl acetate	✓	✓	×
4	(*Z*)-Phenyl-2-propanone enol acetate (*Z*)-**(212)**	✓	×	✓
5	(*E*)-Phenyl-2-propanone enol acetate (*E*)-**(212)**	✓	×	✓
6	Diphenylmethane	✓	✓	×

7	*cis*-Stilbene	✓	✓	×
8	Bibenzyl **(214)**	✓	×	×
9	(*Z*)-1-Phenyl-2-benzyl-1-propene (*Z*)-**(211)**	✓	×	✓
10	*trans*-Stilbene	✓	×	×
11	1-Phenyl-2-benzyl-2-propene	✓	×	×
12	(*E*)-1-Phenyl-2-benzyl-1-propene (*E*)-**(211)**	✓	×	✓
13	Dibenzylketone **(80)**	✓	✓	✓
14	(*E*)-1,5-Diphenyl-2-methyl-1-pentene-4-one	✓	×	×
15	(*Z*)-1,5-Diphenyl-2-methyl-1-pentene-4-one	✓	×	×
16	(*Z*)-1,3-Diphenyl-2-methyl-1-pentene-4-one	✓	×	×
17	(*E*)-1,3-Diphenyl-2-methyl-2-pentene-4-one	✓	×	×
18	(*Z*)-1,3-Diphenyl-2-methyl-2-pentene-4-one	✓	×	×
19	(*E*)-1,3-Diphenyl-2-methyl-1-pentene-4-one	✓	×	×
20	2,4-Diphenyl-3,5-dimethylphenol	✓	×	×
21	1,3,5-Triphenyl-2,4,6-trimethylbenzene	✓	×	×

The work of Allen *et al.*,[193] provides detailed proposed mechanisms for many of the identified by-products, including entries 4, 5, 9 and 11–21, in Table 3.1. The first of the impurities discussed is dibenzylketone **(80)** (entry 13). To understand how this arises, the mechanism of formation of P2P **(65)** must be looked at, as **(80)** and P2P **(65)** are closely related.



R = CH_3 = **(65)**
R = CH_2Ph = **(80)**

Two of the theories concerning formation of P2P **(65)** were outlined earlier in Figures 3.1 and 3.2. The first of these, the step-wise mechanism (Figure 3.1), begins similarly for both dibenzylketone **(80)** and P2P **(65)**, with formation of the mixed anhydride **(197)** and subsequently, the carbanionic mixed anhydride species **(198)**. It is from here that the mechanism diverges for P2P **(65)** and dibenzylketone **(80)** formation (see Figure 3.6). With regard to P2P **(65)**, the carbanionic mixed anhydride species **(198)** attacks one of the carbonyl groups of the Ac_2O reagent **(66)**, forming the β-keto anhydride **(199)** (red pathway, Figure 3.6). In the case of dibenzylketone **(80)**, the carbanionic species **(198)** attacks the mixed anhydride **(197)**, formed in the previous step (blue pathway, Figure 3.6). The subsequent deacylation and decarboxylation steps are similar to that of P2P **(65)**, as described in Figure 3.1.

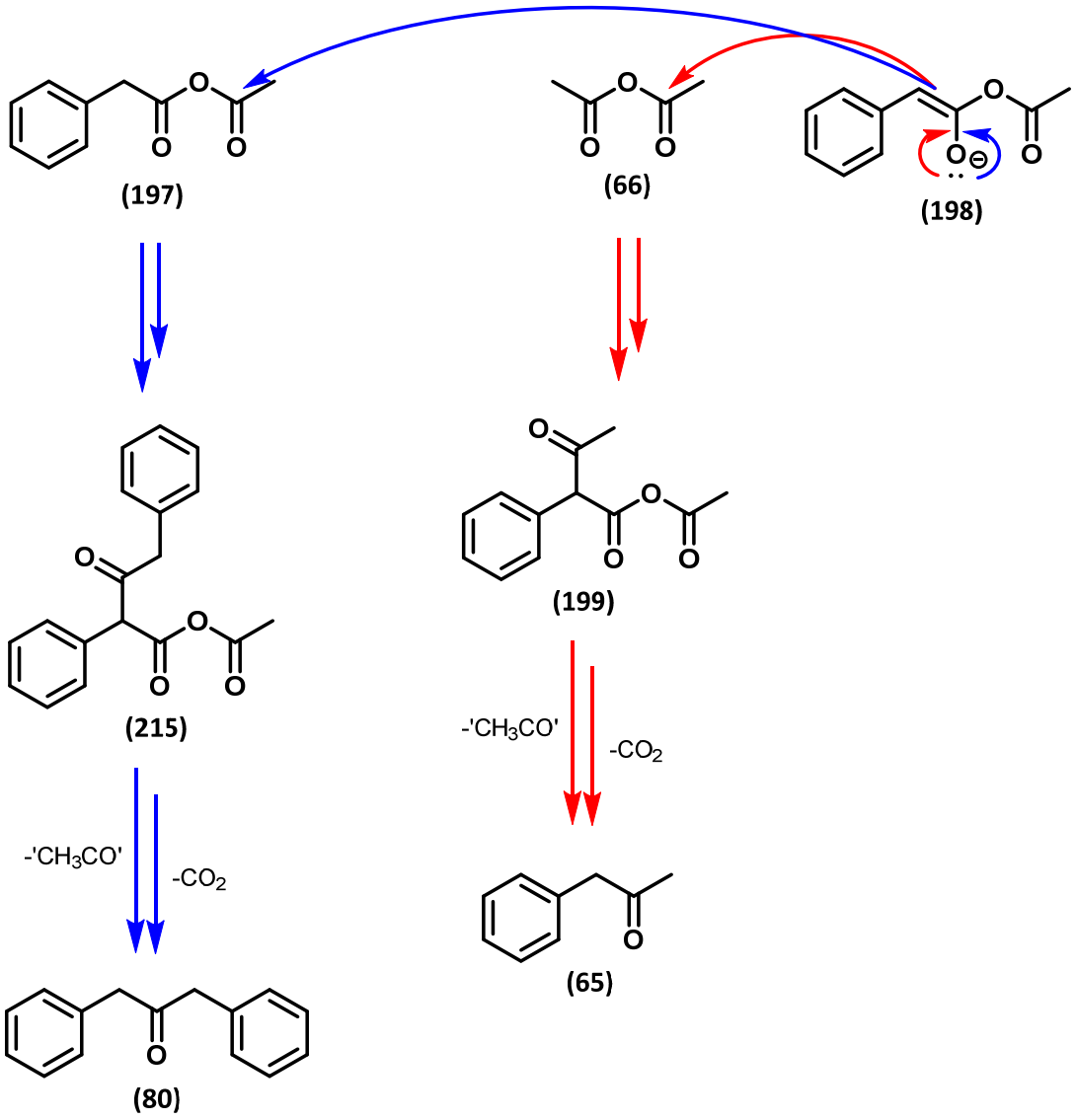


Figure 3.6: Different reaction pathways for formation of P2P (65) and dibenzylketone (80)

A second theory concerning the mechanistic formation of P2P **(65)** (outlined previously in Figure 3.2), proposes that the key step in the reaction involves a cyclic intermediate. As mentioned previously, the orientation of the anhydride species being attacked is important in determining what product is formed. In the case of P2P **(80)** formation, the anhydride being attacked is aligned in such a way that the methyl group is closest to the phenyl ring on the attacking mixed anhydride. This is referred to as 'head to tail' alignment by Allen *et al*..[193] In the case where the phenyl rings of both anhydrides (i.e. two equivalents of the mixed anhydride **(197)**) are aligned so that they are both on the same side ('head to head'), the dibenzylketone **(80)** is formed (Figure 3.7).

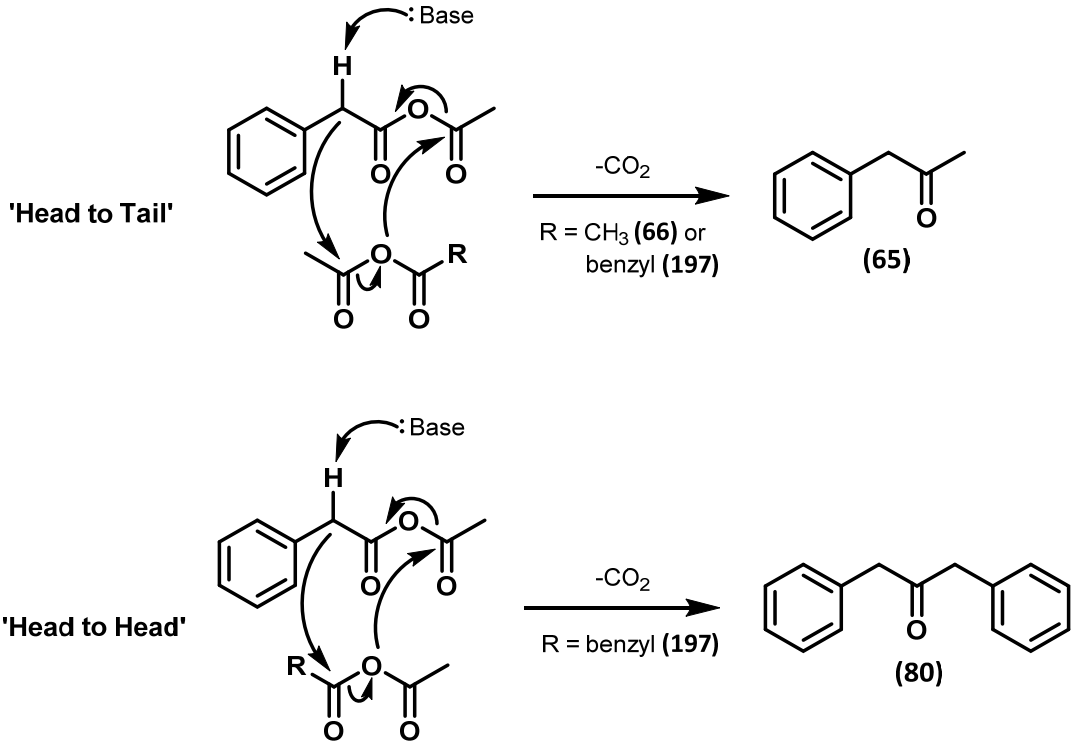
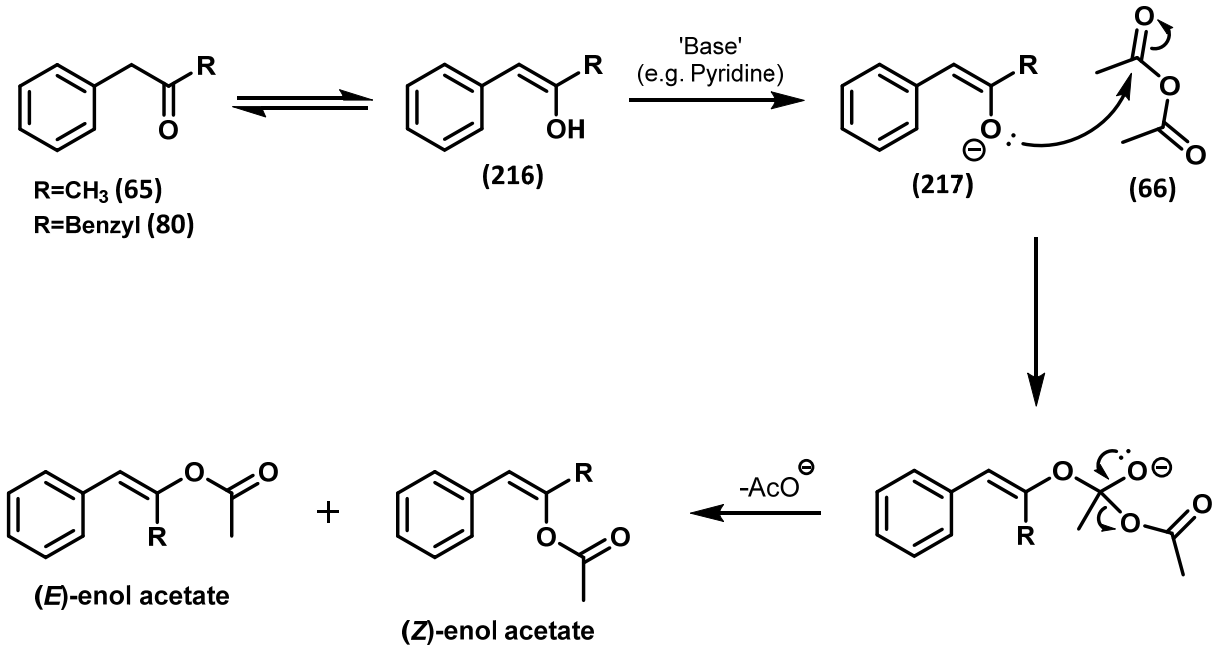


Figure 3.7: Cyclic mechanistic proposal for formation of P2P (65) and dibenzylketone (80)[193]

Another set of by-products deemed significant by Allen *et al.*,[193] were the (*E*)- and (*Z*)-enol acetates of P2P and dibenzylketone (compounds **(212)** and **(213)**). The mechanistic proposal for their formation is outlined in Figure 3.8.



R = CH_3: Mononeric enol acetate(s) **(212)**
R = Benzyl: Dimeric enol acetate(s) **(213)**

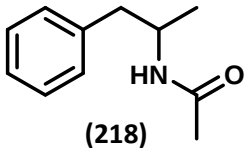
Figure 3.8: Proposed scheme for formation of enol acetate by-products[193]

In Figure 3.8, it is proposed that when the ketone (either **(65)** or **(80)**) undergoes keto-enol tautomerism in the reaction vessel, enol **(216)** is deprotonated (in the presence of base) and the resulting enolate **(217)** nucleophilically attacks acetic anhydride **(66)**, forming the enol acetate. (Alternatively, the enolate **(217)** may be generated following deprotonation of **(65)**/**(80)** at the α-carbon.) Monomeric enol acetates (*E*/*Z*)-**(212)** are the result of P2P **(65)** undergoing this type of reaction. In the case of dibenzylketone **(80)**, dimeric enol acetates (*E*/*Z*)-**(213)** are formed.

Based on the above scheme depicting formation of the enol acetate by-products, selective synthesis of standards of these compounds may be carried out by refluxing the ketone product **(65)** with an excess of Ac_2O **(66)** and pyridine for 48 h. Substantial amounts of these enol acetates may also be recovered if the PAA reaction is carried out at a slightly lower temperature and over a longer period of time (67 h @ ≈120 °C).[197]

Allen *et al*.[193] deemed these enol acetate by-products particularly significant with regard to impurity profiling. He proposed that the enol acetates (*E*/*Z*)-**(212)**, are route specific for the PAA route in which Ac_2O **(66)** is used (as opposed to $Pb(OAc)_2$ **(75)**).

These enol acetates may also undergo additional reactions if carried through to subsequent reaction steps. For example, enol acetate by-products have been associated with the presence of *N*-acetylamphetamine **(218)** in street samples of amphetamine.



(218)

This impurity **(218)** is postulated to be a result of the acetylation of amphetamine (by enol acetate(s)) as it is formed in the final step of the reaction sequence.[146]

3.2 The PAA route to 2,5-P2P (92)

Although many impurities of the PAA route to P2P **(65)** have been reported in works by Allen, Forbes, Krawczyk[123,146,193] and others, their identification is tentative, often solely based on MS data. Also, information on the impurity profiling of the PAA route to the 2,5-dimethoxy class of amphetamines is lacking. In this work, the isolation and identification of a number of such impurities, as well as extensive characterisation by ^{1}H-NMR, ^{13}C-NMR, HRMS and IR, was carried out. This information may be beneficial to the forensic chemist in determining the route employed in the synthesis of a relatively new class of hallucinogenic amphetamines.

Using commercially available 2,5-dimethoxyphenylacetic acid (2,5-PAA) **(108)**, the PAA route to 2,5-dimethoxyphenyl-2-propanone (2,5-P2P) **(92)** was carried out (Figure 3.9) using standard* PAA route conditions.

(*Standard conditions are those which have been commonly used in the synthesis of P2P **(65)** from PAA **(64)** in the literature in recent years[191,195] and involves refluxing the acid SM in 6 equivalents of pyridine and ≈5–6 equivalents of Ac_2O **(66)**.)

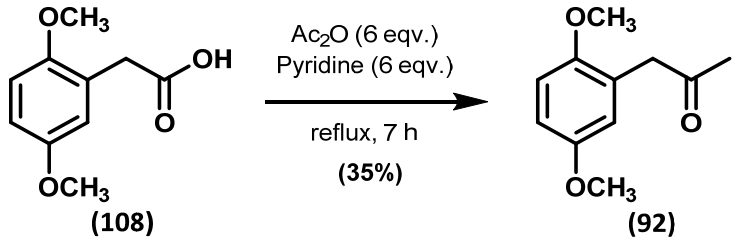


Figure 3.9: Synthesis of 2,5-P2P (92) from 2,5-PAA (108) *via* the PAA route

Following purification by flash column chromatography, the expected ketone **(92)** was isolated in a yield of 35%. This is notably lower than the reported yields (≈50%) for the unsubstituted P2P **(65),** using similar conditions.[129,190] This is likely due to the fact that the 2,5-dimethoxy aromatic ring system is more electron rich and cannot stabilise the carbanionic mixed anhydride intermediate as well as that of the unsubstituted equivalent **(198)**. The R_f, IR and MS data for ketone **(92)** are presented in Table 3.2.

Table 3.2: Yield, R_f, IR and HRMS data for ketone (92)

Compound No.	Yield	R_f*	IRν_{max} (NaCl) (cm^{-1})	HRMS (M+H$^+$) (*m/z*)	
				Calc.	Found
(92)	35%	0.66	1715 (C=O), 1593, 1505 (C=C)	195.1021	195.1015

*mobile phase = 70:30 Et_2O:hexane

Formation of ketone product **(92)** was most evident in the ^{1}H-NMR spectrum of the crude reaction mixture, by the appearance of the 3H, s @ δ 2.13, corresponding to the terminal methyl protons of the ketone side-chain. For all other signals (corresponding to the 2- and 5-methoxy groups, CH_2 protons and aromatic ring protons), there was substantial overlap of signals in the ^{1}H-NMR spectrum of the SM **(108)** and product 2,5-P2P **(92)**. Following isolation of ketone **(92)** by flash column chromatography, a clean ^{1}H-NMR spectrum was obtained. The aforementioned 3H, s @ δ 2.13 (terminal methyl protons) was accompanied by a 2H, s @ δ 3.64 (CH_2 protons α to aromatic ring), 2 × (3H, s) @ δ 3.76 and 3.77 (2 × methoxy group protons) and a multiplet @ δ 6.71–6.82 (aromatic protons). The aromatic ABX pattern, which may be expected for a compound with this particular substitution about the ring, was not observed for ketone **(92)**. The signals overlapped to such an extent that the typical d (*J*≈7 Hz), dd (*J*≈7 and ≈3 Hz) and d (*J*≈3 Hz) signals could not be deciphered.

3.2.1 Impurities of the PAA route to 2,5-P2P (92)

More extensive flash column chromatography revealed that a number of impurities/by products had formed during the above reaction (Figure 3.9). The structures of these (proposed based on spectroscopic data and previously reported impurities of P2P[146,193]), are outlined in Figure 3.10.

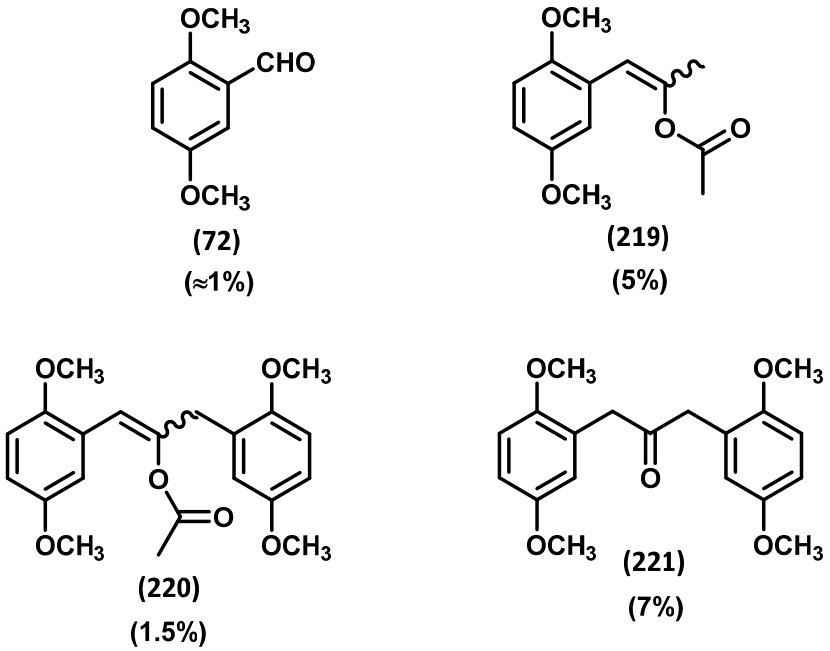
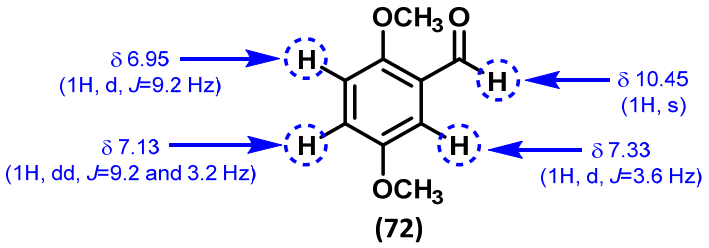


Figure 3.10: Structures and isolated yields of impurities recovered from the synthesis of 2,5-P2P (92) *via* the PAA reaction

3.2.1.1 Aldehyde impurity (72)

The structure of aldehyde impurity **(72)** was easily established as it had been used as a SM in various bromination reactions in Chapter 2; the CHO shift (@ δ 10.45) in the ^{1}H-NMR spectrum, indicated the

presence of an aldehyde functional group and the ABX pattern observed in the aromatic region of the spectrum (see below) indicated the substitution pattern on the phenyl ring. On comparison with the standard material used previously, there was excellent agreement of the spectroscopic data.



(72)

Although no reports of the PAA route to 2,5-P2P **(92)** could be found in the literature, the unsubstituted aldehyde **(76)** had been reported as an impurity of P2P **(65)** synthesised from PAA **(64)** (see Table 3.1, Entry 1). Only one of these reports had postulated a possible origin of the aldehyde **(76)**. In a paper by Forbes *et al*.,[146] it had been observed that P2P **(65)** had a tendency to decompose to aldehyde **(76)**, however no mechanistic explanation was provided. This is likely to be the origin of the 2,5-dimethoxy substituted aldehyde **(72)** encountered during the PAA route to 2,5-P2P **(92)**; similar to the observation made by Forbes *et al*., pure samples of 2,5-P2P **(92)** were found to decompose to aldehyde **(72)** over time. This phenomenon is examined in more detail in Section 3.7.

3.2.1.2 Monomeric enol acetates (E/Z)-(219)

The unsubstituted analogues of (*E*)- and (*Z*)-enol acetates **(219)**, had been previously reported as impurities of P2P (see Table 3.1, Entries 4 and 5 **(212)**) and their origin was proposed in Figure 3.8.
The novel 2,5-dimethoxy enol acetate **(219)** was recovered, after flash column chromatography, as a mixture of geometric isomers (ratio of *Z*:*E* = 4:1) in a total combined yield of 5%. As the isomers could not be resolved, the R_f, IR and MS data collected was that of the mixture. These data are summarised in Table 3.3 below.

Table 3.3: Yield, R_f, IR and HRMS data for the mixture of enol acetates (*E*/*Z*)-(219)

Compound No.	Yield	R_f*	IRν_{max} (NaCl) (cm^{-1})	HRMS (M+H$^+$) (*m/z*)	
				Calc.	Found
(*E*/*Z*)-**(219)**	5%	0.68	1756 (C=O), 1678 (C=C), 1606, 1583 (aromatic C=C)	237.1127	237.1122

*mobile phase = 70:30 Et_2O:hexane

Initially, the signals in the ^{1}H-NMR spectrum for the (*E*)- and (*Z*)-enol acetates could not be distinguished and were simply referred to as 'major' and 'minor' isomers. The ^{1}H-NMR spectrum of this *E*/*Z* mixture can be found in Figure 3.11.

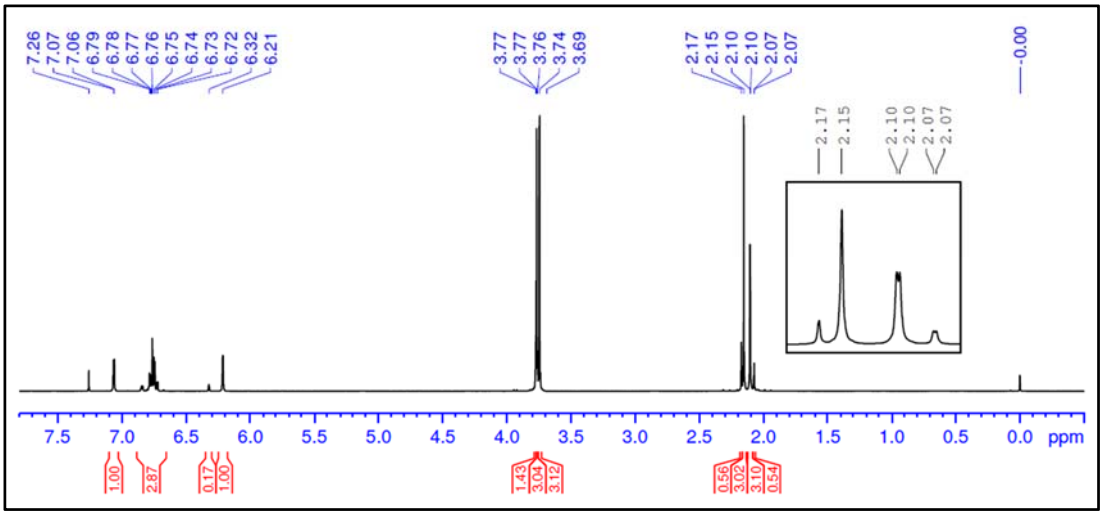
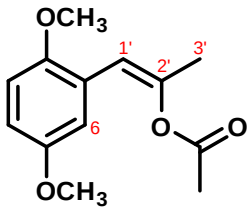
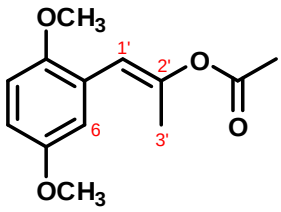


Figure 3.11: ^{1}H-NMR spectrum of mixture of (*E*)-(219) and (*Z*)-(219) enol acetates (@ 400 MHz)

For each isomer, there were two methyl (C*H*$_3$) signals in the region of δ 2–2.2 in the ^{1}H-NMR spectrum, corresponding to the acetyl protons (COC*H*$_3$) and those on C-3'. These could be distinguished from one another due to the fine allylic splitting (*J*≈1 Hz) of the signal corresponding to the protons on C-3'.



(*Z*)-**(219)**



(*E*)-**(219)**

There was substantial overlap of the aromatic signals, as well as the methoxy signals, of both isomers in the ^{1}H-NMR spectrum. Fortunately, the acetyl methyl signal (COC*H*$_3$) and alkene signal (H-1') for both compounds were well resolved and these were used (*via* NOESY experiments) to distinguish between (*E*)-**(219)** and (*Z*)-**(219)**. NOESY spectra identify interactions through space, between protons on the same compound. If two protons (or sets of equivalent protons) are close in space, a signal, at the intersection of where the two ^{1}H-NMR spectra have been plotted against each other, will be observed. The initial NOESY experiment exhibited 3 possible interactions that could be used to assign (*E*)- and (*Z*)-geometry to the major and minor isomers. These are as follows:

- Interaction between proton on C-1' and protons on C-3' (Major isomer: Interaction 'A')
- Interaction between proton on C-6 and COC*H*$_3$ protons (Major isomer: Interaction 'B')
- Interaction between proton on C-6 and protons on terminal C-3' (Minor isomer: Interaction 'C')

A magnified section of the NOESY spectrum obtained is shown in Figure 3.12 overleaf.

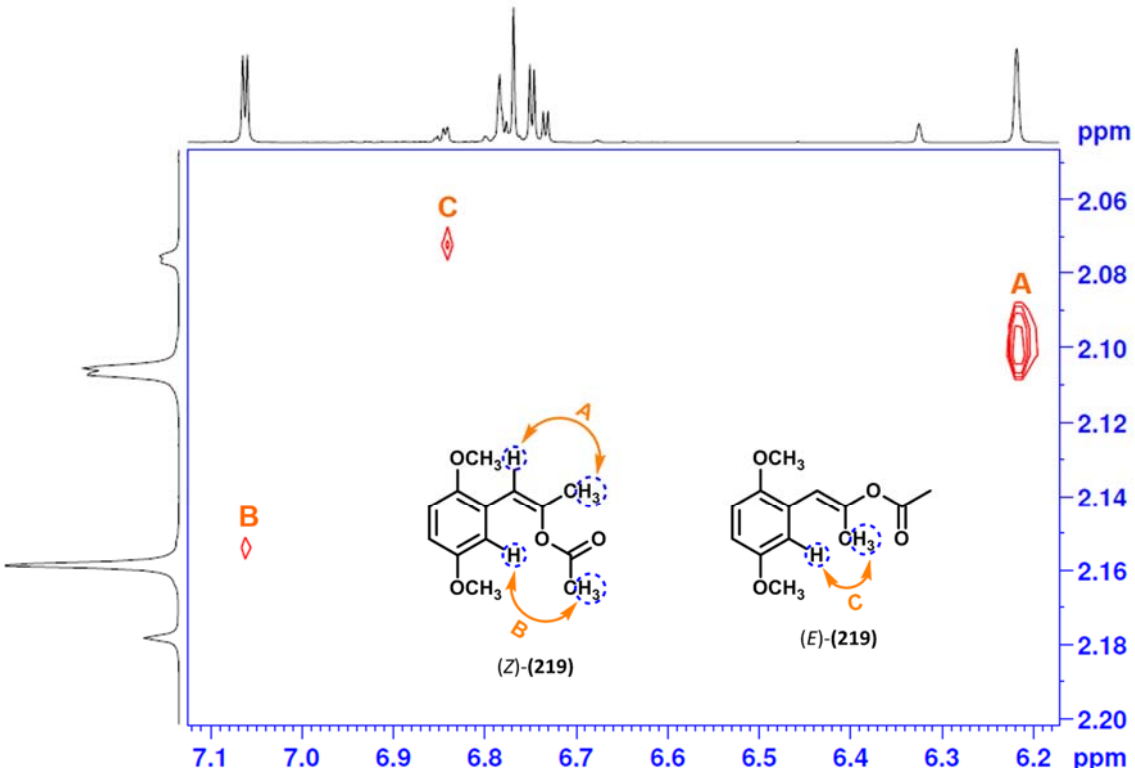


Figure 3.12: Magnified section of NOESY spectrum obtained for mixture of (*E*)- and (*Z*)-enol acetates of 2,5-P2P

In order to support the evidence observed in the NOESY spectrum, NOE difference experiments were carried out. With NOE difference experiments, each of the two interacting protons (or sets of protons) are irradiated individually. If there is a strong NOE interaction between the 2 protons, the particular proton that is being irradiated (negative phase) will cause the interacting proton signal to become enhanced (in the positive phase) and thus become substantially larger than other signals in the spectrum. This substantiates what is observed in the NOESY spectra, as NOESY data can often suffer from background noise/false positives which could be mistaken for a positive interaction.

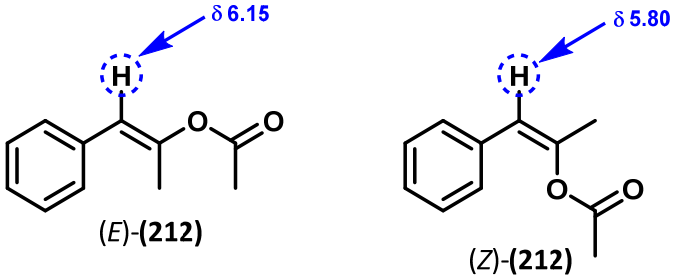
The first interaction observed in the NOESY spectrum (between proton on C-1' and protons on C-3' of the major isomer) was reiterated by the NOE difference results. When the signal at δ 2.10 (protons on C-3) was irradiated, the signal at δ 6.21 (proton on C-1') became enhanced. The *vice versa* experiment was the same, in that when the signal at δ 6.21 was irradiated, the signal at δ 2.10 became enhanced. This interaction suggested that for the major isomer, the proton on C-1' and protons on C-3' are relatively close in space and likely to be on the same plane. This would suggest that the major isomer is in the (*Z*)-conformation. No interaction is observed between the corresponding proton on C-1' and protons on C-3' for the minor isomer.

The other two key interactions observed in the NOESY spectrum, between proton on C-6 and COCH_3 protons of the major isomer, and between proton on C-6 and protons on terminal C-3' of the minor

isomer, could not be corroborated by the NOE difference data, as there was no obvious enhancement of any signals when selected signals were irradiated.

With the first interaction observed on the NOESY spectrum supported by NOE difference, we assigned the major isomer as (*Z*)- and the minor as (*E*)-.

Tentative assignment of (*E*)- and (*Z*)-conformation, based on the ^{1}H-NMR chemical shift (δ) value of the vinyl proton (on C-1') is also possible. A study by House *et al.*[198] has shown that for a range of enol acetates, the ^{1}H-NMR chemical shift (δ) of the vinyl proton of the (*E*)-isomer, is generally more downfield (by about 0.2–0.3 ppm) than the corresponding vinyl proton chemical shift of the (*Z*)-. For example, in the case of the unsubstituted enol acetates encountered earlier (impurities of PAA route to P2P **(65)**), there is a difference (Δδ) of 0.35 ppm:



(*E*)-**(212)** (*Z*)-**(212)**

Others[199] have used this difference in ^{1}H-NMR δ values as the basis of assigning geometric isomerism to a range of enol acetates of similar structure (with different substituents on the aromatic ring). The difference in δ value of the vinyl protons of our (*E*)-**(219)** and (*Z*)-**(219)** enol acetates is 0.11 ppm (vinyl proton of (*E*)-**(219)** = δ 6.32 and (*Z*)-**(219)** = δ 6.21). Although this value is smaller than the range quoted by House *et al.* (0.2–0.3 ppm), the values may still be used for tentative assignment of geometric isomerism, in the absence of other supporting data such as 2D–NMR.

As well as the ^{1}H-NMR δ values of the vinyl protons, there is also a difference (≈0.2 ppm) in the δ value for the proton on C-6, between the (*E*)-**(219)** and (*Z*)-**(219)** isomers. This may be due to the deshielding (through space) of the proton on C-6 of (*Z*)-**(219)**, by the oxygen atom of the acetate group. This observation is significant as the more downfield signal of the (*Z*)-isomer (@ δ 7.06, 1H, d, *J*=3.2 Hz) is now well resolved from all other aromatic proton signals, compared to that of the (*E*)-isomer, whereby all aromatic signals are overlapping (Figure 3.13). This difference in δ value and resulting resolution of the signal from other aromatic protons, may again be used as tentative evidence for the assignment of (*E*)- or (*Z*)-conformation.

The ^{13}C-NMR spectrum of the mixture of (*E*)-**(219)** and (*Z*)-**(219)** isomers was complex, with assignment of signals corresponding to (*E*)- or (*Z*)- only possible due to the large difference in signal intensities between the isomers (ratio of *Z*:*E* = 4:1). Fortunately, most signals were resolved from one another. For overlapping signals ($COCH_3$ signal for (*E*)-**(219)** and (*Z*)-**(219)**), resolution was achieved by running the sample at a higher frequency. At 75 MHz, both signals were unresolved, each resonating at 21.12

ppm. At 150 MHz, the signals became partially resolved, resonating at 21.09 ppm ((*E*)-isomer) and 21.11 ppm ((*Z*)-isomer). Interestingly, there was a substantial difference in the chemical shift value (nearly 4 ppm) of the terminal methyl carbon (C-3'), between the (*E*)-**(219)** and (*Z*)-**(219)** isomers. Similar to the vinyl proton signals in the ^{1}H-NMR spectrum, the C-3' ^{13}C-NMR signal may be used to tentatively assign (*E*)- or (*Z*)-conformations to enol acetates of similar structure (see Figure 3.13).

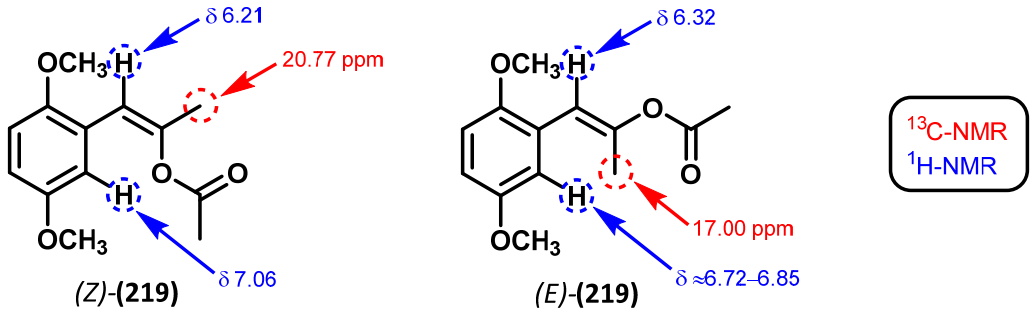
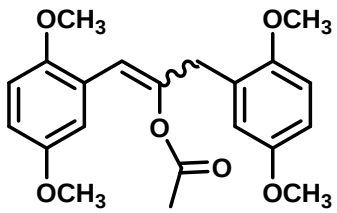


Figure 3.13: Differences in chemical shift values that may be used to tentatively assign (*E*)- or (*Z*)-conformation to enol acetate (219)

3.2.1.3 Dimeric enol acetate (220)

As outlined in Figure 3.10, the dimeric enol acetate **(220)** was also recovered as an impurity of the PAA reaction to 2,5-P2P **(92)**. The proposed formation of the unsubstituted dimeric enol acetate **(213)** was outlined previously in Figure 3.8.

The novel dimeric enol acetate **(220)** was recovered, after column chromatography, as a single isomer in a yield of 1.5%. The R_f, IR and MS data collected for **(220)** are summarised in Table 3.4.



(220)

Table 3.4: Yield, R_f, IR and HRMS data for dimeric enol acetate (220)

Compound No.	Yield	R_f*	IRν_{max} (NaCl) (cm^{-1})	HRMS (M+H$^+$) (*m/z*)	
				Calc.	Found
(220)	1.5%	0.56	1756 (C=O), 1672 (C=C), 1608, 1584 (aromatic C=C)	373.1651	373.1649

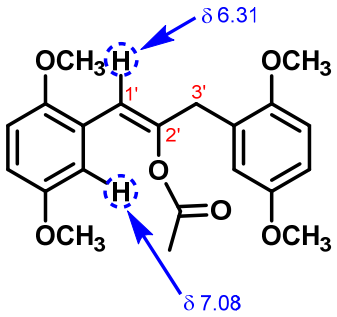
*mobile phase = 70:30 Et_2O:hexane

Assignment of (*E*)- or (*Z*)-isomerism to the recovered dimeric enol acetate **(220)**, was based on evidence collected for monomeric enol acetates (*E*)-**(219)** and (*Z*)-**(219)**, as summarised in Figure 3.13. These very

general 'rules' may be used to tentatively assign conformation, in the absence of other supporting data (such as 2D–NMR).

Previously, the ^{1}H-NMR δ value of the vinyl proton was used to distinguish (*E*)-**(219)** from (*Z*)-**(219)** (value generally more downfield for the (*E*)-isomer). As we had recovered only a single isomer of dimeric enol acetate **(220)** (vinyl proton = δ 6.31), no comparison of chemical shift values could be made and thus, tentative assignment based on this methodology was not possible.

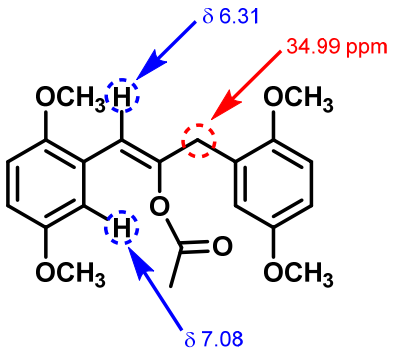
Another theory used for (*E*)/(*Z*) assignment of the monomeric enol acetates was the position, in the ^{13}C-NMR spectrum, of the signal corresponding to C-3' (terminal methyl carbon). Again this was not useful as this methyl signal was not present in the dimer **(220)**. The final piece of data (^{1}H-NMR) used for tentative (*E*)/(*Z*) assignment was the δ value of the ring proton on C-6. This was found previously, to be more downfield (by ≈0.2 ppm) of all other aromatic protons, for the (*Z*)-isomer. Given that the recovered dimer **(220)** reflected this (proton on C-6 = δ 7.08), it was initially assigned (*Z*)-conformation:



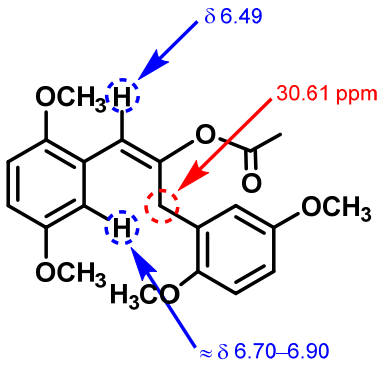
(*Z*)-**(220)**

Similar to the monomeric enol acetates (*E*)-**(219)** and (*Z*)-**(219)**, NOESY and NOE difference spectra were obtained for dimer **(220)** in an attempt to obtain solid evidence of conformation. A possible interaction, between H-1' and H-3' protons, was observed in the NOESY spectrum (which may indicate (*Z*)-isomerism). However, as there was substantial overlap of all methoxy proton signals, and the signal corresponding to H-3' in the ^{1}H-NMR spectrum (all signals resonating between δ 3.70 and 3.80), the interaction observed may not necessarily be between H-1' and H-3' protons.

Interestingly, when a ^{1}H-NMR spectrum of a sample of the dimeric enol acetate was obtained 11 months later, it was found that *E*/*Z* isomerisation had taken place over time. Having a sample of the mixture meant that comparison of particular ^{1}H-NMR/^{13}C-NMR signals could be made, making assignment of (*E*)- or (*Z*)-conformation more straightforward (according to previous 'rules'):



(*Z*)-**(220)**



(*E*)-**(220)**

3.2.1.4 Dibenzylketone (221)

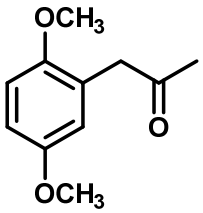
The final impurity (in Figure 3.10) to be isolated by column chromatography, was the novel dibenzylketone **(221)**. Proposals for the mechanistic formation of this compound were outlined in Section 3.1.2. Dibenzylketone **(221)** was recovered in a yield of 7%. The R_f, m.p., IR and HRMS data collected for **(221)** are summarised in Table 3.5 below.

Table 3.5: Yield, R_f, m.p., IR and HRMS data for dibenzylketone (221)

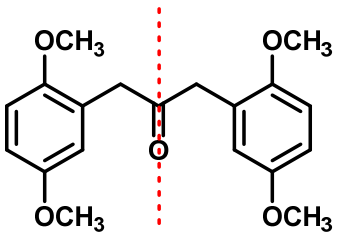
Compound No.	Yield	m.p. (°C)	R_f*	IRν_{max} (KBr) (cm^{-1})	HRMS (M+H$^+$) (*m/z*)	
					Calc.	Found
(221)	7%	59–60	0.54	1718 (C=O), 1616, 1592, 1506 (C=C)	331.1545	331.1531

*mobile phase = 70:30 Et_2O:hexane

The ^{1}H-NMR spectrum obtained for dibenzylketone **(221)** was straightforward; the axis of symmetry about the carbonyl group meant that the spectrum was similar to that of monomeric ketone **(92)**.



(92)



(221)

The clear differences between the ^{1}H-NMR spectra for monomeric ketone **(92)** and dibenzylketone **(221)** were:

- For dibenzylketone **(221)**, all methoxy protons were isochronous (12H, s @ δ 3.74, as opposed to 2 × (3H, s) @ δ 3.76 and 3.77 for **(92)**).
- The upfield signal @ δ 2.13 for **(92)** (corresponding to the terminal methyl protons) was absent in the spectrum of dibenzylketone **(221)**.

The remaining signals, corresponding to CH_2 protons (@ δ 3.64 for **(92)** and δ 3.69 for **(221)**) and aromatic ring protons (@ δ 6.71–6.82 for **(92)** and δ 6.67–6.80 for **(221)**), were very similar.

In the context of P2P **(65)** synthesis, ring-unsubstituted dibenzylketone **(80)** is reported to be a very common and significant impurity. As outlined by Stojanovska *et al.*,[99] dibenzylketone **(80)** is difficult to separate from P2P, so non-commercial P2P is likely to contain the dibenzylketone impurity. As a result, when this impure P2P is used to produce amphetamine, dibenzylketone **(80)** will undergo the same reactions, forming additional secondary by-products such as 1,3-diphenyl-2-aminopropane **(210)** (see Figure 3.5). This concept, with regard to our ring-substituted dibenzylketone **(221)**, is investigated in Section 4.4.

3.2.2 Investigation into the effects of varying the number of equivalents of Ac_2O, on the yields of 2,5-P2P (92) and dibenzylketone (221)

The presence of dibenzylketone **(80)**, as a product of the PAA reaction to P2P **(65)**, was reported in a number of papers in the first half of the 20th century. Its formation was associated with reactions in which the number of eqv. of Ac_2O **(66)** used (compared to PAA **(64)**) is 'low' (≈2 or less eqv.). Research by Hurd *et al.* in 1933,[196] outlined that dibenzylketone **(80)**, was the sole product (48–61% yield) of the PAA reaction whereby the number of eqv. of Ac_2O (or molar ratio of PAA to Ac_2O) used was 2 (see Table 3.6). In a later publication (1936)[200] these results were rescinded, and it was declared that P2P **(65)** was also produced in the reaction (yield of dibenzylketone **(80)** = 41%, yield of P2P **(65)** = 16%). Work carried out on optimisation of the yield of P2P from this particular reaction, found that using a higher number of eqv. of Ac_2O, actually favoured the formation of P2P.[201] However, the presence/yields of dibenzylketone was not alluded to. Later, King and McMillan[202] carried out similar work (using high eqv. of Ac_2O) and found that when 5 eqv. of Ac_2O were used, P2P was obtained in a yield of 56%, in addition to dibenzylketone (24%). Some of the results of these bodies of work are outlined in Table 3.6.

Table 3.6: Early literature examples of the PAA route, showing the outcome of varying the number of eqv. of Ac_2O used

Eqv. of Ac_2O	Reaction conditions	Yield of (65)	Yield of (80)	Literature source
2	KOAc (0.07 eqv.), reflux, 2 h	16%	41%	Hurd and Thomas, 1936[200]
8	NaOAc (8 eqv.), 145–150 °C, 20 h	56%	?	Magidson and Garkusha, 1941[201]
13	NaOAc (0.8 eqv.), 145–150 °C, 20 h	51%	?	Magidson and Garkusha, 1941[201]
5	Pyridine (6 eqv.), reflux, 6 h	56%	24%	King and McMillan, 1951[202]

? = Dibenzylketone **(80)**, not referred to in paper

Based on these literature results, it appears that the dominant product formed (either P2P **(65)** or dibenzylketone **(80)**) is dependent on the number of eqv. of Ac_2O used. If P2P is the desired product, a 'high' number of eqv. (≈5 or more) is required. If dibenzylketone formation is favoured, a 'low' number of eqv. (≈2 or less) is required.

No single, comprehensive study could be found in the literature, whereby the effect of varying the number of eqv. of Ac_2O, influences the yields of monomeric **(65)** and dimeric **(80)** ketones, during the PAA reaction to P2P (or its derivatives). Although the study by Magidson and Garkusha[201] had involved varying eqv. of Ac_2O, the number of molar eqv. used were always high (≥ 8). Also, as the study focussed purely on optimising the yield of P2P **(65)**, the presence/yield of dibenzylketone **(80)** was not referred to.

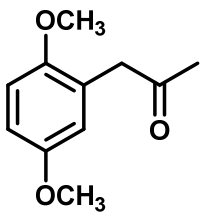
In this work, it was decided that the effect of varying the eqv. of Ac_2O, during the PAA reaction to 2,5-P2P **(92)**, would be evaluated. In addition to the reaction outlined earlier (see Figure 3.9), in which the number of eqv. of Ac_2O used (compared to 2,5-PAA **(108)**) was 6, the reaction was also performed at 1, 3 and 12 eqv.. The yields obtained for each of the products of these reactions are outlined in Table 3.7 (see Figure 3.10 for compound structures).

Table 3.7: Isolated yields for each of the products of the PAA reaction to 2,5-P2P (92), using different eqv. of Ac_2O

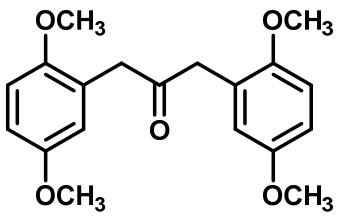
Eqv. of Ac_2O	Yields				
	(92)	(221)	(72)	(219)	(220)
1	11%	20%	Trace*	Trace*	ND⋆
3	22%	14%	Trace*	6%	Trace*
6	35%	7%	≈1%	5%	1.5%
12	39%	6%	Trace*	2%	Trace*

*Trace = Amount detected <1% and not fully isolated
⋆ND = Not detected

The yields of greatest significance in Table 3.7, are those of the monomeric ketone **(92)** and dimeric ketone **(221)**. These are presented in the form of a bar chart in Figure 3.14.



(92)



(221)

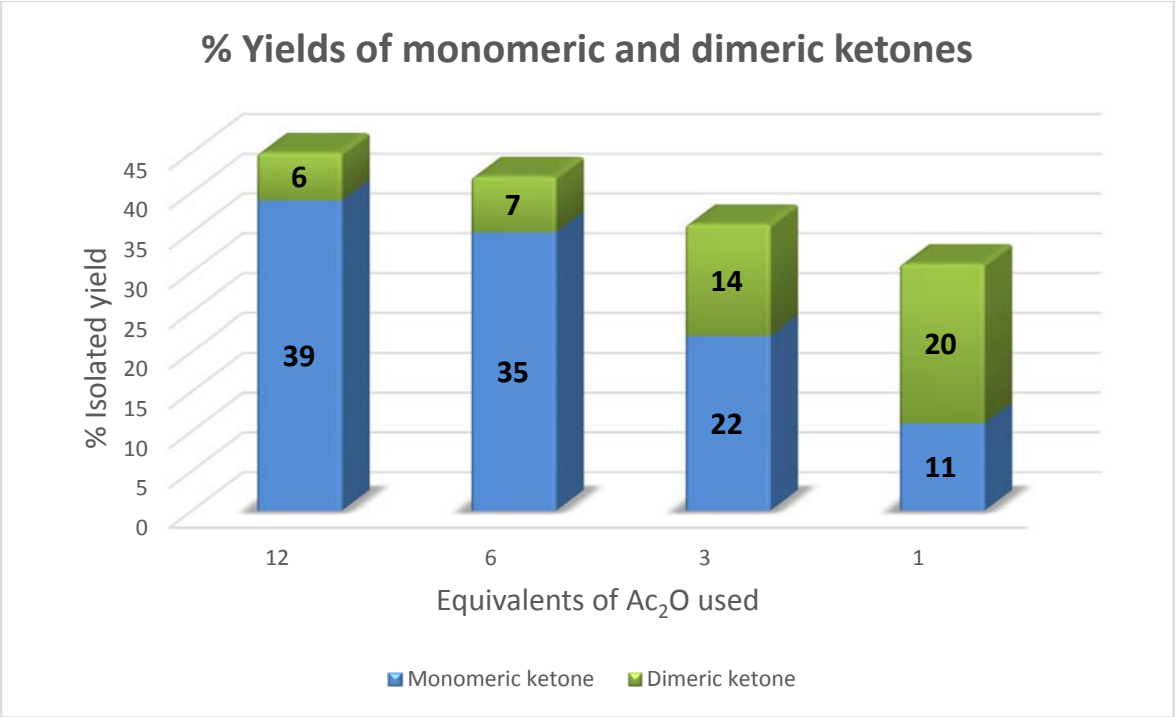


Figure 3.14: Chart comparing isolated yields of monomeric (92) and dimeric (221) ketones, obtained when the number of eqv. of Ac_2O is varied during the PAA reaction

The results of the above experiments are largely in agreement with the findings[201,202] for the unsubstituted monomeric **(65)** and dimeric **(80)** ketones – the dominant product formed (either monomeric or dimeric ketone), is dependent on the number of eqv. of Ac_2O used in the reaction. Based on the apparent trend in Figure 3.14, it would appear that the point at which the monomeric **(92)** and dimeric **(221)** ketones may be produced in equal amounts is at ≈2 eqv. of Ac_2O.

Another inference that could be made from the data presented in Figure 3.14, is that after about 6 eqv., the amount of Ac_2O used does not have a large influence on the yields and ratio of products, i.e. there is neither a substantial increase in monomeric ketone **(92)**, nor decrease in dimeric ketone **(221)**. Therefore, attempts at increasing yields of **(92)**, or eliminating formation of **(221)**, by increasing the eqv. of Ac_2O (beyond ≈6), would probably be ineffective.

As mentioned in Section 3.1, a recent publication[191] suggested that the choice of catalyst used has a substantial effect on the major product formed. In this paper, the PAA reaction (with PAA **(65)** as SM), was performed using a range of different catalysts. Among the catalysts used were pyridine (as used in our method previously) and triethylamine (TEA). When pyridine (6 eqv.) was used as catalyst, P2P **(65)** and dibenzylketone **(80)** were produced in a ratio of 70:30 respectively (in a combined yield of 80%). When TEA (1 eqv.) was used, P2P and dibenzylketone were produced in a ratio of 6:94 respectively (73% total yield). These findings suggest that the major product formed can be reversed, from P2P (in the case of pyridine) to dibenzylketone (in the case of TEA). Using this methodology, it was hoped that by using TEA as catalyst, a selective synthesis of our dimeric ketone **(221)** could be performed. However,

when TEA (1 eqv.) was employed in the PAA reaction using our 2,5-PAA SM **(108)**, both the expected major product **(221)** and minor product **(92)** were only detected in trace amounts in the ^{1}H-NMR spectrum of the crude reaction mixture. Evidence for a number of other compounds, not previously encountered during the PAA route to 2,5-P2P **(92)**, was indicated by ^{1}H-NMR, but purification/identification of these was not pursued.

Another concept put forward in this paper[191] was that, by changing the wash procedure at the end of the reaction, the formation of both monomeric **(219)** and dimeric **(220)** enol acetates could be greatly reduced. According to the authors, the enol acetates are formed during workup, when the ketone products react with residual acetic acid. When this procedure was carried out, by washing the initial organic phase with potassium bicarbonate, the presence of enol acetates in the final crude product was reported to be reduced from ≈30% to <2%. When this new wash procedure (using sodium bicarbonate) was applied in the course of our work, there was found to be no reduction in the quantities of enol acetates **(219)**/**(220)** present.

3.3 The PAA route to 4-Br-2,5-P2P (159)

As mentioned in Chapter 1, of the several known 2,5-dimethoxy ('D series') amphetamines, DOB **(35)** is the most potent hallucinogen. In this thesis, a specific emphasis is put on the bromination of many of the intermediates used in the synthesis of DOB **(35)**, as the introduction of the bromine atom (at the aromatic 4-position) may take place at any stage of the synthesis. For example, bromination may take place prior to the PAA reaction, as outlined in Figure 3.15.

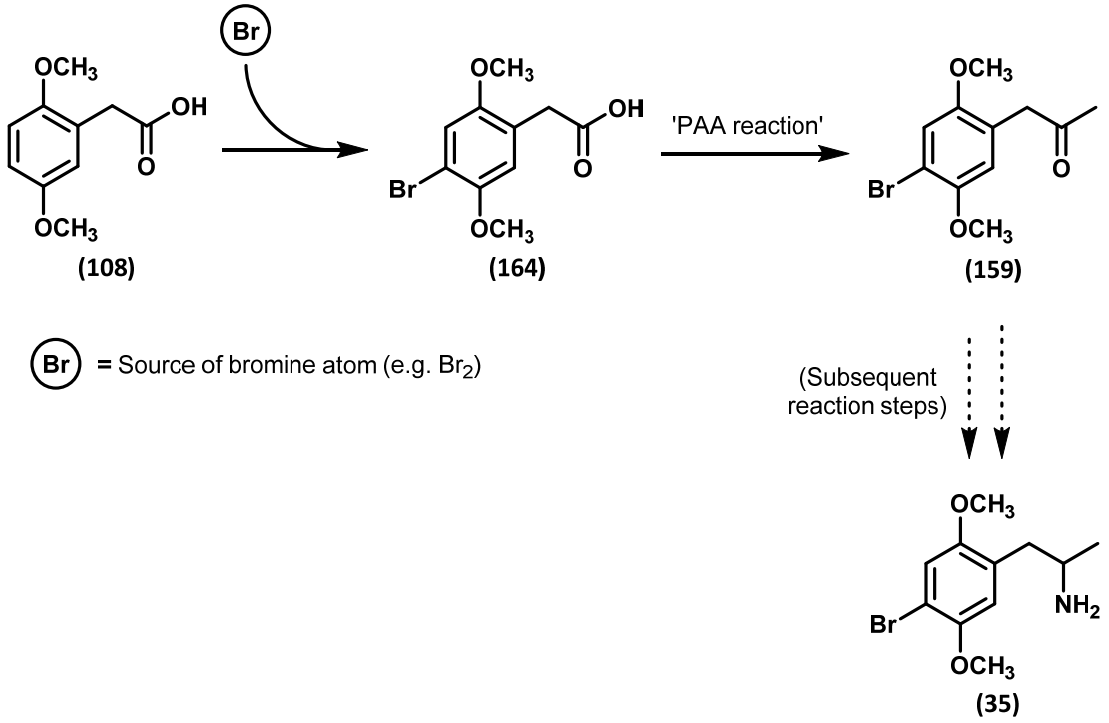
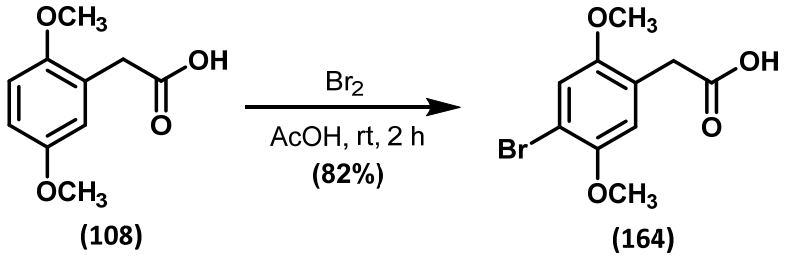


Figure 3.15: Synthesis of DOB precursor (159), whereby bromination takes place prior to PAA reaction

3.3.1 Preparation of 4-bromo-2,5-dimethoxyphenylacetic acid (164)

Following the methodology outlined in Figure 3.15, the first step to be carried out was bromination of 2,5-PAA **(108)**. Literature precedence[39,203] for the bromination of commercially available 2,5-PAA **(108)**, indicated that high yields (68–92%) of 4-Br-2,5-PAA **(164)** could be attained under 'standard' bromination conditions (Br_2, AcOH). Using these standard conditions (General procedure 5.3.2.1) in-house, resulted in an 82% yield of desired product **(164)**.



(108) **(164)**

Occasionally, these standard brominations are carried out at 0 °C in the literature. In order to investigate if there may be a difference in reaction outcome (change in yields or formation of other regioisomers), the above reaction was also carried out at 0 °C (as opposed to rt). The yield obtained for this reaction was very similar (within 5%) to that obtained when the reaction was carried out at rt, and no other regioisomers were detected in the recovered product.

The R_f, m.p., IR and MS data collected for 4-Br-2,5-PAA **(164)** are summarised in Table 3.8 below.

Table 3.8: Yield, R_f, m.p., IR and HRMS data for 4-Br-2,5-PAA (164)

Compound No.	Yield	m.p. (°C)	R_f*	IRν_{max} (KBr) (cm^{-1})	HRMS ($M+H^+$)⋆ (*m/z*)	
					Calc.	Found
(164)	82%	125–127 (EtOH/H_2O)	0.49	1706 (C=O), 1501 (C=C)	274.9919	274.9908

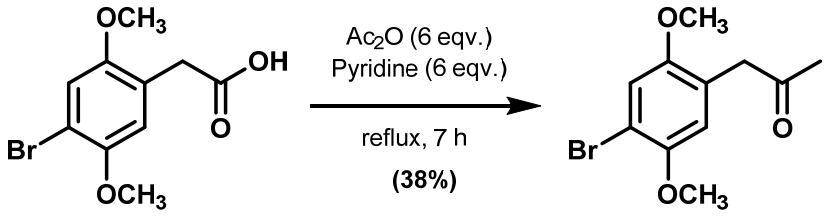
*mobile phase = 50:50 THF:hexane

⋆molecular ion (M) calculated for ^{79}Br isotope peak

Evidence for formation of 4-bromo product **(164)** by ^{1}H-NMR, was most notable in the aromatic region of the spectrum. Unlike the SM **(108)**, in which an overlapping ABX system (multiplet) was observed, two well resolved singlets (δ 6.79 and 7.08) were observed in the aromatic region of the ^{1}H-NMR spectrum of **(164)**. Bromination at the 4-position of **(108)**, resulted in the remaining two free ring positions (C-3 and C-6) being *para* to one another. As *para* splitting is rarely observed in aromatic ring systems, the two remaining ring protons were observed, as expected, as two singlets. The remaining signals in the ^{1}H-NMR spectrum of **(164)**, (methoxy protons @ δ 3.79 and 3.84 and CH_2 protons @ δ 3.63), were similar to those of the SM **(108)**. All spectroscopic data collected for 4-Br-2,5-PAA **(164)** were in good agreement with previously published data.[39]

3.3.2 PAA route to 4-Br-2,5-P2P (159) using 4-Br-2,5-PAA (164)

Successful synthesis of 4-Br-2,5-PAA **(164)**, meant that similar to the non-brominated acid **(108)** (Section 3.2.1), it could be used in the PAA reaction to produce a ketone precursor to DOB **(35)**. The ketone precursor in this instance is 4-bromo-2,5-dimethoxyphenyl-2-propanone (4-Br-2,5-P2P) **(159)** and its synthesis was carried out under 'standard' PAA conditions as outlined below:



(164) **(159)**

Following flash column chromatography and recrystallisation (to remove dimeric enol acetate impurity **(222)**), the 4-bromo ketone **(159)** was isolated in a yield of 38%. This value is similar to that obtained for the non-bromo ketone **(92)** (35%). The R_f, m.p., IR and MS data collected for 4-Br-2,5-P2P **(159)**, are presented in Table 3.9 below.

Table 3.9: Yield, R_f, m.p., IR and HRMS data for 4-Br-2,5-P2P (159)

Compound No.	Yield	m.p. (°C)	R_f*	IRν_{max} (KBr) (cm^{-1})	HRMS ($M+H^+$) (*m/z*)	
					Calc.	Found
(159)	38%	59–60.5 (DCM/hexane)	0.48	1709 (C=O), 1498 (C=C)	273.0126	273.0124

*mobile phase = 70:30 Et_2O:hexane

The presence of a 3H, s @ δ 2.16, in the ^{1}H-NMR spectrum of the crude reaction mixture, was the most obvious indication of successful product formation. This signal corresponds to the terminal methyl group (i.e. CH_3 protons) of the ketone side-chain of **(159)**. Again, two singlets were observed in the aromatic region of the ^{1}H-NMR spectrum (1H, s @ δ 6.72 and 1H, s @ δ 7.07), indicating that the 4-bromo substituent had remained intact throughout the reaction. The other signals present in the ^{1}H-NMR spectrum (2 × (3H, s) @ δ 3.77 and 3.84 (methoxy protons) and 2H, s @ δ 3.64 (CH_2 protons)), were similar to those of SM **(164)**.

3.3.3 Impurities of the PAA route to 4-Br-2,5-P2P (159)

Following extensive flash column chromatography/purification by recrystallisation, several additional compounds were recovered from the PAA reaction to 4-Br-2,5-P2P **(159)**. The structures and isolated yields of these compounds are outlined in Figure 3.16.

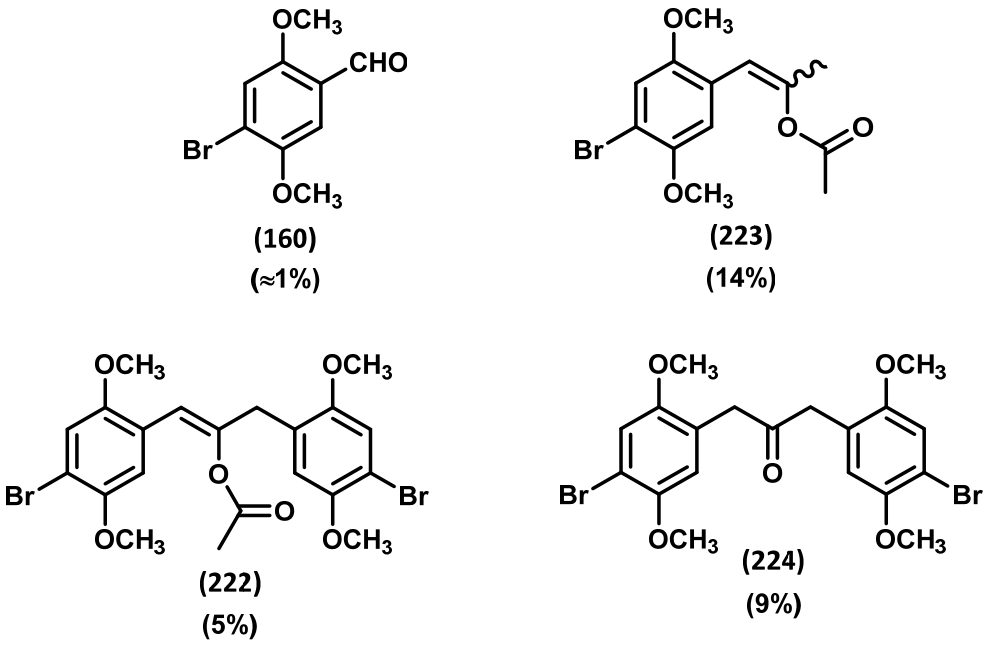
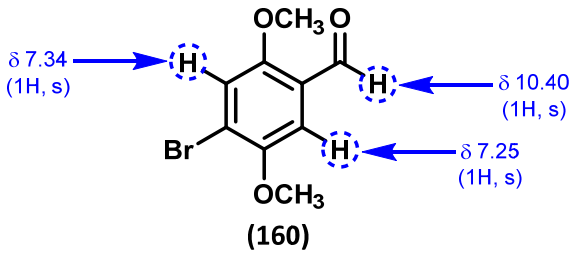


Figure 3.16: Structures and isolated yields of impurities recovered from the synthesis of 4-Br-2,5-P2P (159) *via* the PAA reaction

The impurities recovered were found to be of the same general structure as those recovered during the PAA reaction to 2,5-P2P **(92)** (see Figure 3.10). This made their identification much more straightforward. Also, given the aromatic 4-substitution of all impurities, the aromatic regions of the ^{1}H-NMR spectra were much easier to interpret (all signals = singlets), allowing for the signals of compounds in a mixture, to be distinguished.

3.3.3.1 4-Bromo aldehyde impurity (160)

4-Bromo aldehyde **(160)** was the first impurity to elute the flash column. The downfield shift at δ 10.40 was indicative of aldehyde functionality and the two singlets in the aromatic region of the ^{1}H-NMR spectrum indicated 4-substitution of the phenyl ring.



(160)

Confirmation of compound structure was greatly assisted by the availability of a fully characterised reference sample; 4-bromo aldehyde **(160)** had been isolated as the main product of the bromination of 2,5-dimethoxybenzaldehyde **(72)** in Chapter 2.

3.3.3.2 4-Bromo-monomeric enol acetates (223)

Similar to the non-bromo PAA reaction to 2,5-P2P **(92)**, the novel monomeric (*E*)-**(223)** and (*Z*)-**(223)** enol acetates of 4-bromo ketone **(159)** were recovered from the flash column. In total, the isolated yield of monomeric enol acetates recovered was 14%. This was substantially higher than the 5% recovery of non-bromo (*E*)-**(219)** and (*Z*)-**(219)** enol acetates. Another difference between the non-bromo and 4-bromo PAA reactions was that during flash column chromatography for the 4-bromo PAA reaction, a small sample of one of the enol acetates ((*Z*)-**(223)**) was recovered pure, allowing for its full characterisation. The ^{1}H-NMR spectrum obtained for this compound can be found in Figure 3.17.

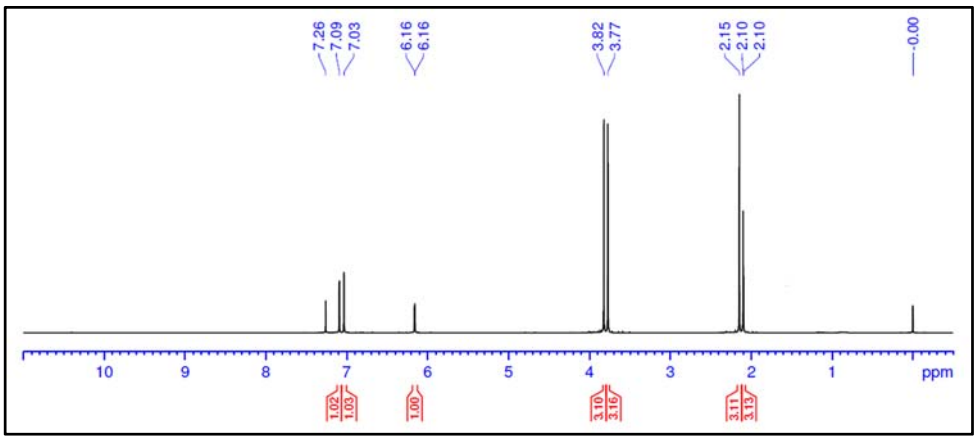
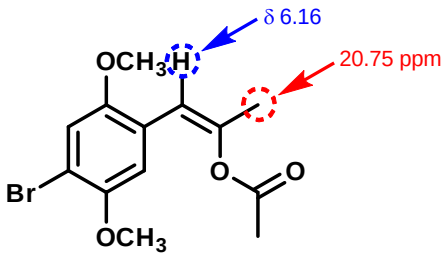


Figure 3.17: ^{1}H-NMR spectrum of (*Z*)-4-bromo enol acetate (223) (@ 400 MHz)

The R_f, m.p., IR and MS data for 4-bromo (*Z*)-**(223)** enol acetate are presented in Table 3.10 below. As before, assignment of (*Z*)/(*E*)-conformation was based the chemical shift values of particular signals in the ^{1}H-NMR/^{13}C-NMR spectra of the compounds, relative to one another (see Section 3.2.1.2).



(*Z*)-**(223)**

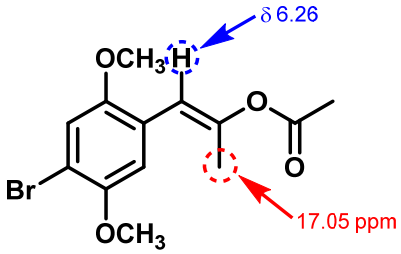
Table 3.10: R_f, m.p., IR and HRMS data for (*Z*)-4-bromo enol acetate (223)

Compound No.	m.p. (°C)	R_f*	IRν_{max} (KBr) (cm^{-1})	HRMS (M+H$^+$)* (*m/z*)	
				Calc.	Found
(223)	63.5–65 (DCM/hexane)	0.79	1748 (C=O), 1682 (C=C), 1491 (aromatic C=C)	315.0232	315.0225

*mobile phase = 70:30 Et_2O:hexane

*molecular ion (M) calculated for ^{79}Br isotope peak

Additional evidence supporting the assignment of (*Z*)-conformation in this instance, was gained by comparing the ^{1}H-NMR signal corresponding to the proton on C-1' of both isomers. In the case of the isolated '(*Z*)-isomer', this signal (resonating at δ 6.16) is observed as a finely split doublet (*J*=0.6 Hz), whereas the corresponding signal in the '(*E*)-isomer' (resonating at δ 6.26, as shown below) appears as a singlet. Of the two isomers, it seems more plausible that this allylic splitting (with the protons on C-3') would occur in the (*Z*)-isomer rather than the (*E*)-isomer. In the (*Z*)-conformation, the proton on C-1' is likely to have an eclipsed relationship (based on Newman projection) with one of the protons on C-3', which may result in splitting. In the (*E*)-conformation, the CH_3 group is pointing downwards (on an entirely different plane) so any interaction of the proton on C-1' with this group, is much more unlikely. The (*E*)-**(223)** enol acetate co-eluted the flash column with the remainder of (*Z*)-**(223)** enol acetate.



(*E*)-**(223)**

Although (*E*)-**(223)** was not isolated in its pure form, the ^{1}H-NMR/^{13}C-NMR signals (from the mixture of (*Z*)-**(223)** and (*E*)-**(223)**) corresponding to (*E*)-**(223)**, could be identified by process of elimination. Having said this, as with the non-bromo enol acetates, the ^{13}C-NMR spectrum was run at 125 MHz to fully resolve all signals in the mixture.

3.3.3.3 Dibromo-dimeric enol acetate (222)

As mentioned, dimeric enol acetate **(222)** had co-eluted from the flash column with 4-bromo ketone **(159)**. Recrystallisation of this mixture (from MeOH), resulted in the enol acetate **(222)** selectively crystallising out of solution, with 4-bromo ketone **(159)** remaining in solution (mother liquor). The novel dimer **(222)** was isolated in a total yield of 5%. The R_f, m.p., IR and MS data for dimeric enol acetate **(222)** are presented in Table 3.11.

Table 3.11: Yield, R_f, m.p., IR and HRMS data for dimeric enol acetate (222)

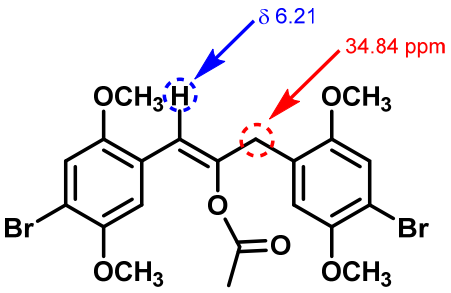
Compound No.	Yield	m.p. (°C)	R_f*	IRv_{max} (KBr) (cm^{-1})	HRMS (M+H$^+$)⋆ (*m/z*)	
					Calc.	Found
(222)	5%	139–141 (MeOH)	0.53	1764 (C=O), 1673 (C=C), 1496 (aromatic C=C)	528.9861	528.9861

*mobile phase = 70:30 Et_2O:hexane

⋆molecular ion (M) calculated for $^{79}Br_2$ isotope peak

Only a single isomer of the dimer **(222)** was recovered. Having only one isomer made assignment of (*E*)/(*Z*) conformation more difficult as the δ values of the various signals (e.g. alkene proton on C-1'), could not be compared between one isomer and another. The compound recovered was assigned the (*Z*)-conformation for the following reasons:

- In the case of structurally similar, non-bromo dimeric enol acetate, only the (*Z*)-**(219)** was recovered from the flash column. The (*E*)-**(219)** isomer only arose after *E*/*Z* isomerisation had occurred, over a period of several months.
- Again, with the non-bromo dimer, there was a substantial difference in the ^{13}C-NMR chemical shift value of C-3', between the (*Z*)-**(220)** (@ 34.99 ppm) and (*E*)-**(220)** (@ 30.61 ppm) isomers. As the chemical shift value of C-3', in the case of dibromo dimer **(222)**, resonated at 34.84 ppm, the compound was assumed to be in the (*Z*)-conformation.



(*Z*)-**(222)**

3.3.3.4 Dibromo-dibenzylketone (224)

The final impurity in Figure 3.16, that was recovered from the PAA reaction to 4-Br-2,5-P2P **(159)**, was the novel dibenzylketone **(224)**. The impurity was isolated from the flash column in a yield of 9%. The R_f, m.p., IR and MS data for dibenzylketone **(224)** are outlined in Table 3.12.

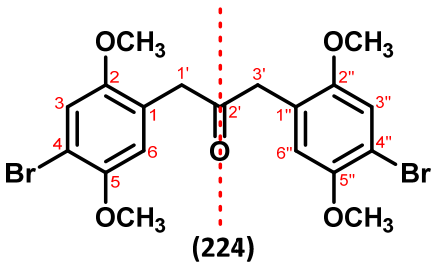
Table 3.12: Yield, R_f, m.p., IR and HRMS data for dibenzylketone (224)

Compound No.	Yield	m.p. (°C)	R_f*	IRν_{max} (KBr) (cm^{-1})	HRMS (M+H$^+$)⋆ (*m/z*)	
					Calc.	Found
(224)	9%	147–149	0.40	1723 (C=O), 1604, 1583, 1500 (C=C)	486.9756	486.9753

*mobile phase = 70:30 Et_2O:hexane

⋆molecular ion (M) calculated for $^{79}Br_2$ isotope peak

The ^{1}H-NMR spectrum obtained for dibenzylketone **(224)** was not complex. This lack of complexity was as a result of the axis of symmetry about the carbonyl group. Only five signals were observed in the ^{1}H-NMR spectrum of **(224)** due to the isochronous nature of the protons on C-1'/C-3', 2-methoxy/2''-methoxy, C-3/C-3'', 5-methoxy/5''-methoxy and C-6/C-6''.



(224)

3.3.4 Investigation into the effects of varying the number of equivalents of Ac_2O, on the yields of 4-Br-2,5-P2P (159) and dibenzylketone (224)

As described in Section 3.2.2, a study of the PAA reaction was conducted whereby the number of equivalents (eqv.) of Ac_2O **(66)** was varied, in order to establish how this may affect the isolated yields of monomeric and dimeric ketones. The results of this study (for the PAA reaction to 2,5-P2P **(92)**) were summarised in Table 3.7 and Figure 3.14.

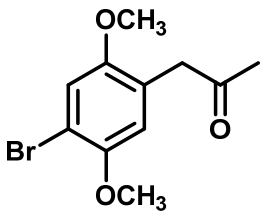
This study was repeated for the PAA reaction to 4-Br-2,5-P2P **(159)** and the isolated yields of 4-bromo monomeric ketone **(159)**, dimeric ketone **(224)**, and other impurities **(160)**, **(223)** and **(222)**, at 1, 3 and 6 eqv. of Ac_2O, were established. The results of these experiments are summarised in Table 3.13.
(Note: The experiment whereby 12 eqv. of Ac_2O were used was not repeated in this case, as it was found previously (for 'non-bromo' PAA reaction) to have little effect (*vs.* the 6 eqv. of Ac_2O experiment) on yields of monomeric and dimeric ketone products).

Table 3.13: Isolated yields obtained for each of the products of the PAA reaction to 4-Br-2,5-P2P (159), using different eqv. of Ac_2O

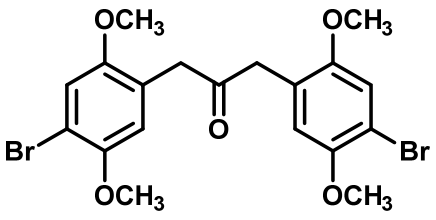
Eqv. of Ac_2O	Yields				
	(159)	(224)	(160)	(223)	(222)
1	16%	26%	Trace*	2%	3%
3	31%	13%	Trace*	10%	5%
6	38%	9%	≈1%	14%	5%

*Trace = Amount detected <1% and not fully isolated

As was performed for non-bromo monomeric and dimeric ketones **(92)** and **(221)** (in Figure 3.14), the yields of their brominated counterparts **(159)** and **(224)** were compared on a bar chart (see Figure 3.18).



(159)



(224)

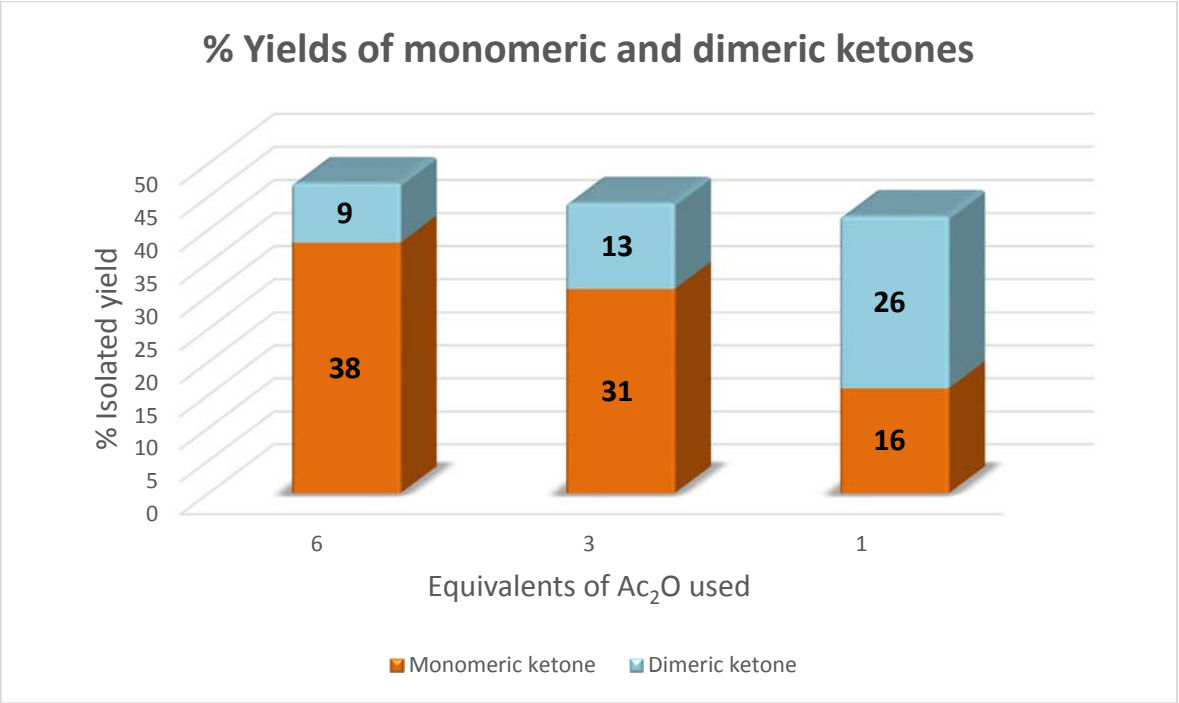


Figure 3.18: Chart comparing isolated yields of monomeric (159) and dimeric (224) ketones, obtained when the number of eqv. of Ac_2O is varied during the PAA reaction

The results of these experiments on the PAA reaction to 4-Br-2,5-P2P **(159)**, are more or less in line with those observed for the 'non-bromo' PAA reaction experiments (i.e. the predominant ketone formed (monomeric/dimeric) is highly dependent on the number of eqv. of Ac_2O used in the reaction).

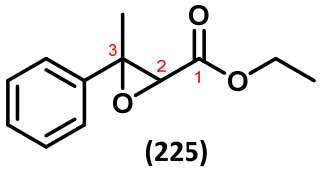
The PAA route is a well-established method of synthesising ketone precursors to ATS. Another method, which has only appeared in recent years, involves a glycidate intermediate and is referred to as the 'Darzens reaction'. This method, in the context of 2,5-dimethoxy ketone precursors, will be explored in the next section.

3.4 The Darzens reaction

The use of glycidic ester compounds (glycidates) as 'alternative pre-precursors' to illicit ATS, is a very recent phenomenon. The synthesis of glycidate pre-precursors to MDMA and amphetamine, as well as some recent examples of seizures, were briefly discussed earlier (Section 1.6.1).

Although the first synthesis of a glycidic ester was described by Erlenmeyer in 1892, it was Darzens (after whom the reaction is named) who developed the reaction.[136] As well as being important intermediates in organic synthesis, many glycidates (e.g. ethyl 3-methyl-3-phenylglycidate **(225)**) are used in the flavours and fragrances industry.[204]

(Note: The generally accepted numbering system for glycidates is shown below for compound **(225)**, with the carbonyl carbon of the ester assigned number 1. In the interest of consistency, the numbering system used in the assignment of ^{1}H-NMR/^{13}C-NMR spectra in the Experimental section does not follow this convention. Instead, a generalised system, as outlined in Section 5.1, is used.)



(225)

"strawberry aldehyde"

The 'Darzens reaction' involves the condensation of a carbonyl compound (most often a phenone or aldehyde) with an α-halo ester **(226)** in the presence of a base, to form an α,β-epoxy ester (glycidic ester) **(227)**. The mechanism of this reaction is outlined in Figure 3.19.

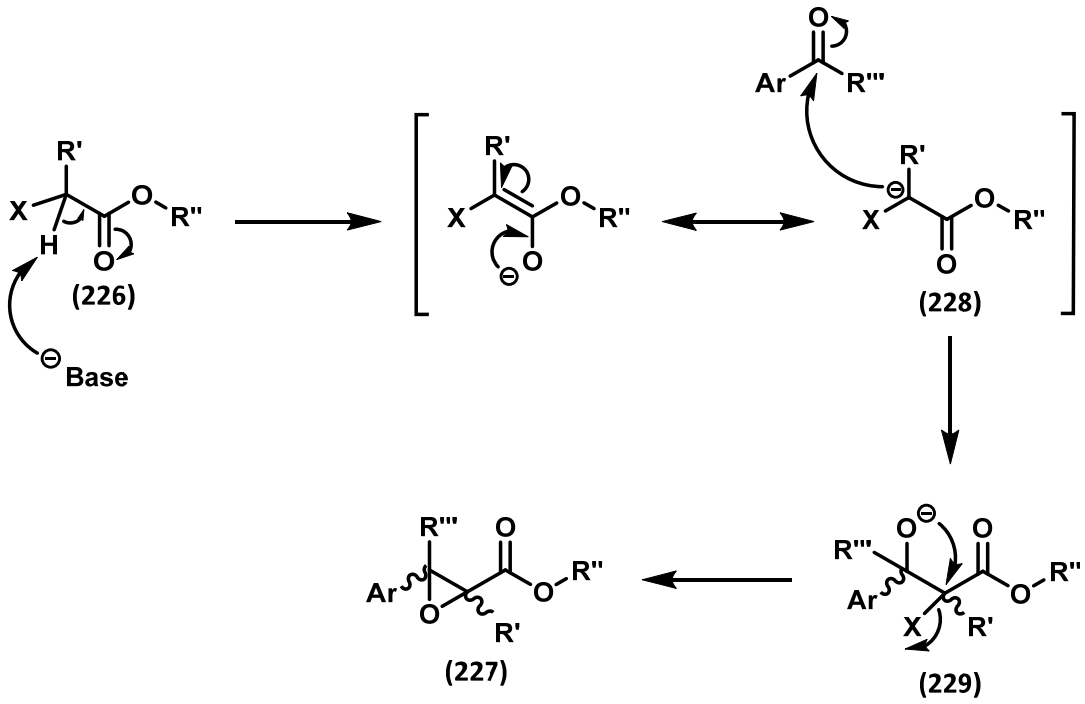


Figure 3.19: Mechanism of formation of glycidic esters

Crouch *et al.*[205] describes the reaction as a two-step process:

- Step 1 = Base-mediated aldol reaction of an α-halocarbonyl compound with an aldehyde or ketone,
- Step 2 = Intramolecular nucleophilic substitution reaction to form an epoxide or oxirane.

The mechanism outlined in Figure 3.19, describes the Darzens reaction in very general terms. There are a number of aspects of the reaction (conditions etc.) which have important practical implications on reaction outcome (products formed/yields, stereochemistry etc.). Some of these considerations include:

- Which R' and R'' groups are used (in α-halo ester **(226)**)
- What halogen ('X') atom is used (in α-halo ester **(226)**)
- What carbonyl compound is used (aldehyde (R'''= H) *vs.* ketone (R'''= Alkyl)
- What base is used
- What solvent is used

In terms of α-halo ester **(226)**, various R', R'' and X groups may be used. The R'/R'' groups tend to be short alkyl chains (e.g. methyl or ethyl) and the halogen atom is usually either Cl or Br. As shown in Figure 3.19, the carbonyl compound used is often an aromatic aldehyde or ketone; the greater inherent electrophilicity of the aldehyde making it much more widely used than the ketone.

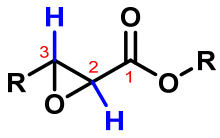
A number of bases have been used for this reaction in the literature, including potassium hydroxide (KOH).[205,206] However, sodium alkoxides (e.g. sodium methoxide (NaOMe) and sodium ethoxide (NaOEt)) are by far the most widely used.[136,207-209] These are often generated *in situ* from the reaction of sodium with the appropriate alcohol (MeOH or EtOH). One important caveat, when using a sodium alkoxide as base, is that the alkoxide used must match the ester (R'') of the α-halo ester **(226)**, as transesterification may occur,[210] resulting in a mixture of glycidic ester products.

A number of solvents have also been used in the formation of glycidic esters. Alcohols (MeOH or EtOH) are used in the case of *in situ* generated sodium alkoxides, the choice of alcohol used being determined by the nature of the ester group on **(226)**. Other solvents used include Et_2O[211,212] and THF.[205,206,213]

3.4.1 Stereochemical outcome and assignment of *cis*/*trans*

Depending on reaction conditions (including choice of solvent) and the specific structures involved, the glycidic ester produced may be only *cis*, *trans* or a mixture of the two. The stereochemical aspect comes into play after the carbanionic species **(228)** attacks the aldehyde/ketone, forming a pair of diastereoisomeric halohydrins **(229)**. The intramolecular S_N2 reaction that follows produces the *cis* and/or *trans* glycidate **(227)**.

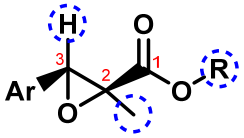
The assignment of *cis*/*trans* isomers of glycidic esters is straightforward for compounds of general structure **(230)**.



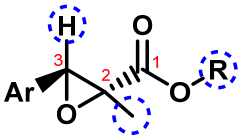
(230)

For these compounds (with hydrogen atoms on both carbons of the epoxide ring), the ^{1}H-NMR coupling constants (*J* values) may be used to assign geometry.[205] For structures whereby the hydrogen atoms on the epoxide ring are *cis* to one another, the *J* values are typically 3.9–4.9 Hz. For *trans*-hydrogens, the *J* values are about 1.5–2.0 Hz.

In terms of 2-methyl glycidates (used in ATS manufacture), this rule cannot be applied due to the fact that there are no hydrogen atoms present on both C-2 and C-3 of the epoxide ring. In the literature, assignment of the geometry of these compounds, is based on relative chemical shift (δ) values. Roux-Schmitt *et al*.[210] set out general 'rules' for the assignment of *cis* and *trans* isomers of the following general structure **(231)**:



***cis*-(231)**

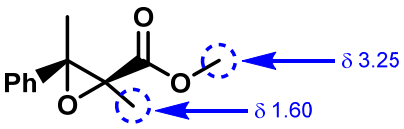


***trans*-(231)**

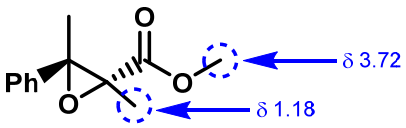
Based on the δ values in the ^{1}H-NMR spectrum, of the proton on C-3, the methyl group protons and the protons of the ester group (R), the following general rules apply:

- For δ values of proton on C-3 and protons on R, ***trans* is more downfield than *cis***
- For δ value of methyl protons, ***cis* is more downfield than *trans***

An explanation as to why these general rules are observed was provided by Johnson and Bade[214] in their attempt to assign the geometry of the isomers of **(232)** shown below:



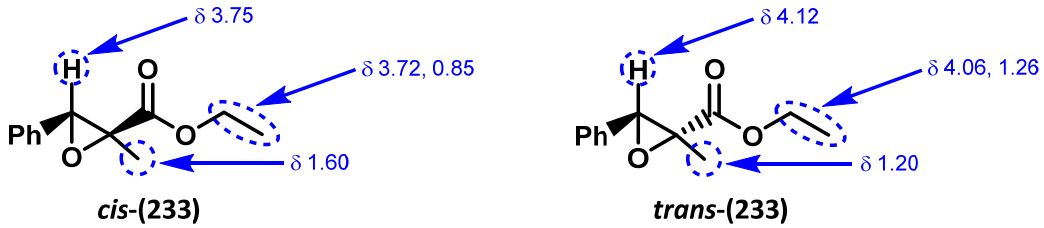
***cis*-(232)**



***trans*-(232)**

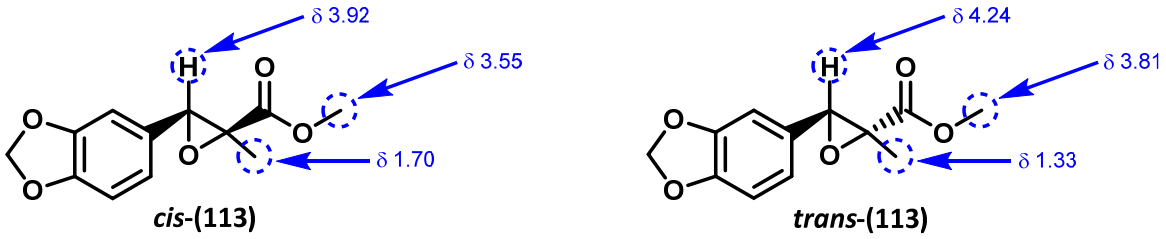
The authors point out that models of the two isomers indicate severe crowding of the phenyl ring, unless it is out of plane with respect to the epoxide C–C bond. This would direct the deshielding cone of the aromatic ring at the *cis* methyl group. As a result, the *cis* methyl group protons resonate at δ 1.60 (deshielded with respect to *trans* methyl protons at δ 1.18) and the *cis* methyl ester protons resonate at δ 3.25 (shielded with respect to the *trans* methyl ester protons at δ 3.72).

Valente and Wolfhagen[215] cite a similar explanation for the observation in ethyl 2-methylglycidate **(233)**. Their model shows that the ethoxy protons are located, part of the time, directly over the phenyl ring in the *cis* isomer, and are subject to increased shielding due to "induced ring currents". They use this theory to assign the geometry of many glycidates, including the isomers of ethyl 2-methyl-3-phenylglycidate **(233)**:



***cis*-(233)** ***trans*-(233)**

Evidence supporting these general rules has been provided by advanced ^{1}H-NMR techniques, such as NOESY. For example, NOSEY was used by Collins *et al.*[139] in the assignment of *cis*-**(113)** and *trans*-**(113)** isomers of a glycidate pre-precursor to MDMA (Figure 3.20). The evidence provided by NOESY experiments was found to be in agreement with the assignment rules laid out previously.



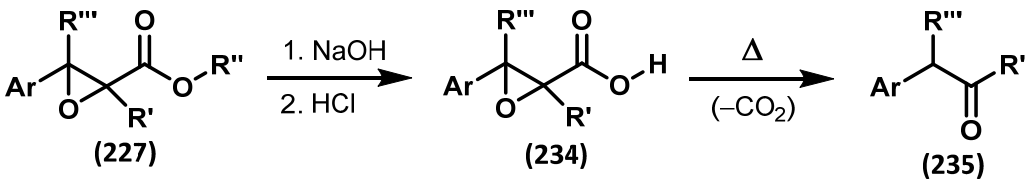
***cis*-(113)** ***trans*-(113)**

Figure 3.20: Assignment of *cis* and *trans* isomers of the MDMA pre-precursor 'MMDMG' (113)

3.4.2 Subsequent reactions of glycidic esters

As mentioned previously, glycidic esters are important intermediates in the synthesis of organic compounds, often being used in subsequent reactions to form other desirable intermediates/products. One of the most common transformations involves conversion of the glycidate to a carbonyl compound. The reaction (*via* a glycidate intermediate) is frequently used in carbonyl homologation.[214] It is this methodology which has recently been exploited in the synthesis of ketone precursors to ATS.

The method whereby glycidates are converted to carbonyl compounds involves saponification of the glycidic ester, followed by decarboxylation:



(227) **(234)** **(235)**

The widely accepted saponification mechanism is said to yield a sodium salt (attack of $^{-}$OH on carbonyl of ester and subsequent loss of the O–R'' moiety), which upon treatment of aq. acid, forms the glycidic acid **(234)**. The heat induced decarboxylation of the glycidic acid **(234)**, is thought to proceed *via* a 5-membered cyclic transition state (Figure 3.21).[216]

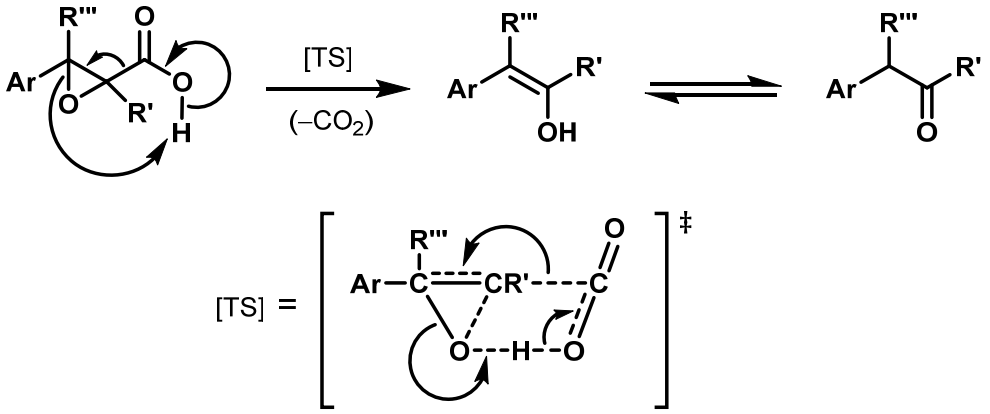


Figure 3.21: Proposed heat induced decarboxylation of a glycidic acid[216]

For some glycidic esters, in which a ≥2 carbon ester moiety (R'') is present (e.g. ethyl, *t*-butyl), decomposition/pyrolysis may be carried out in such a way that the glycidate may be directly converted to the carbonyl in a one pot reaction.[216,217] This involves elimination of the alkyl side chain of the ester through a concerted six-membered transition state, followed by decarboxylation of the resulting acid intermediate, as outlined previously. This eliminates the need to work-up and isolate the acid intermediate. The one-pot alkyl elimination/decarboxylation was carried out by Josa *et al.*[216] on ethyl 3-phenyl glycidate **(236)** (Figure 3.22).

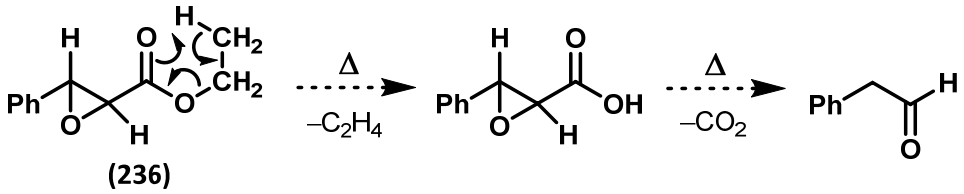
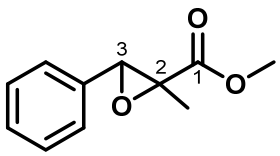


Figure 3.22: One-pot alkyl elimination/decarboxylation of ethyl 3-phenyl glycidate (236)[216]

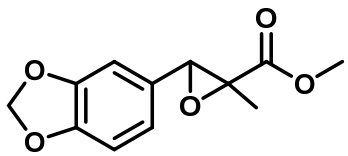
3.4.3 Synthesis of ATS precursors *via* Darzens condensation

In terms of ATS manufacture, the recent use/seizures of glycidate pre-precursors was described earlier (Section 1.6.1). Included in this Section are the 2-methyl glycidate pre-precursors to amphetamine and MDMA (**(112)** and **(113)**). As of yet, these compounds (shown overleaf) are not controlled and the trafficking of these 'alternative pre-precursor' chemicals is much easier than that of the controlled ketone.



(112)

Methyl 2-methyl-3-phenylglycidate



(113)

Methyl 2-methyl-3-(3,4-methylenedioxyphenyl)glycidate
'MMDMG'

Given the increased use of glycidate pre-precursors to amphetamine and MDMA in recent years, it was decided to investigate if this method would be a plausible route to ketone precursors of the 'D series' (2,5-dimethoxy) class of amphetamines. Also, by carrying out the independent synthesis, any by-products, which may potentially arise as impurities in the final drug, could be identified.

3.5 Darzens route to 2,5-P2P (92) and 4-Br-2,5-P2P (159)

Reports of the illicit synthesis of 2,5-P2P **(92)**, *via* a glycidate pre-precursor, could not be found in the literature. However, a procedure by 'Barium' posted on erowid.org (website dedicated to clandestine drug manufacture) gave details of the synthesis of **(92)** from 2,5-dimethoxybenzaldehyde **(72)**.[218] Barium's synthesis is outlined in Figure 3.23 below.

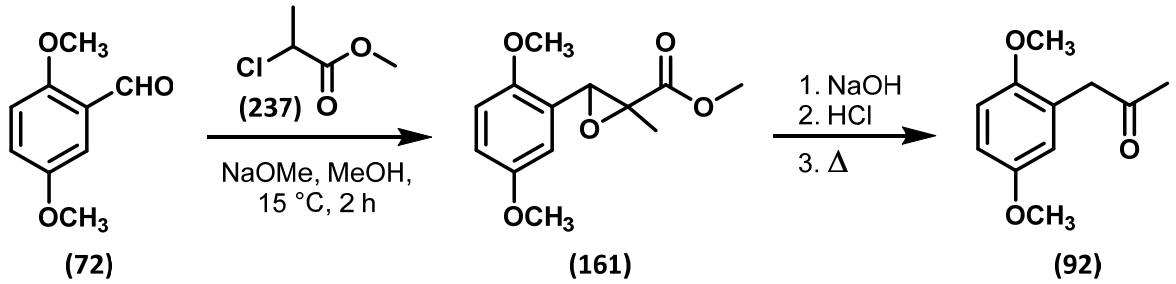


Figure 3.23: Synthesis of 2,5-P2P (92) as outlined by Barium[218]

As this was the only glycidate synthesis (involving the 2,5-dimethoxy moiety) that could be found, it was decided to follow Barium's methodology in this work to see if yields were comparable, if any impurities arose and if the method could be applied to structurally similar compounds.

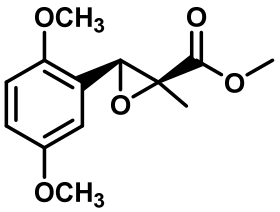
In addition to the methyl 2-chloropropionate reagent **(237)** used above (producing the methyl glycidic ester), reactions were also carried out using ethyl 2-chloropropionate **(238)**. This is due to the fact that the methyl and ethyl glycidic esters are the most commonly encountered, in the synthesis of amphetamine and MDMA precursors.

3.5.1 Barium's synthetic methodology and optimisation of reaction conditions

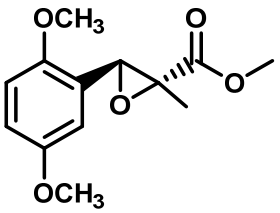
Barium's synthesis is unusual in that, although the process involves a number of steps (formation of glycidic ester, saponification of ester, decarboxylation), none of the intermediates (either glycidic ester or glycidic acid) are worked-up or isolated. Nevertheless, Barium reports an overall yield of 77% for ketone product **(92)**. When Barium's procedure was followed in-house, very different results were obtained. This resulted in extensive optimisation of reaction conditions being carried out, in an attempt to replicate Barium's reaction yield.

The crude product obtained using Barium's full method, contained approx. 50% 2,5-dimethoxybenzaldehyde **(72)**. Initially it was not known if the presence of **(72)** was as a result of unreacted SM being carried through to final product, or whether it was the result of degradation of intermediates/product. The reaction was repeated in the same fashion, with aliquots being taken at different intervals (for ^{1}H-NMR analysis), to track reaction progress. The first of these aliquot samples, taken after 2 h (time in which glycidic ester formation should be complete), revealed that a substantial amount (≈50%) of SM **(72)** remained. The reaction was left stirring overnight and following analysis of an aliquot by ^{1}H-NMR, the reaction did not appear to progress much further. Heating of the reaction to 55 °C for an additional 24 h did not drive the reaction to completion, with ≈15% **(72)** remaining. These results show that using Barium's methodology, reaction completion (for initial glycidic ester **(161)** formation) could not be achieved, despite extended reaction time and additional heating.

As glycidic ester **(161)** is a novel compound, its isolation and characterisation was carried out in order to make the spectroscopic/analytical data available for impurity profiling purposes. Following a simple work-up, the initial ^{1}H-NMR spectrum of the concentrated crude reaction mixture, suggested that the glycidic ester had formed as a mixture of *cis*-**(161)** and *trans*-**(161)** isomers (ratio 1:1).



cis-**(161)**



trans-**(161)**

(Note: Although only one *cis* and one *trans* isomer are depicted for each glycidate in this chapter, it is assumed that the other enantiomers of each are also formed. However, as both *cis* enantiomers and both *trans* enantiomers cannot be distinguished from one another by ^{1}H/^{13}C-NMR, they are grouped together in this work. No additional attempts were made to assign the absolute stereochemistry of any specific enantiomers.)

Following flash column chromatography, the isomers of **(161)** were recovered (as a mixture) in a total combined yield of 46%. Despite co-elution of *cis* and *trans* isomers, for a number of fractions recovered,

a white crystalline substance formed upon evaporation of eluent. This substance, when carefully removed from selected fractions, was found to consist of a pure sample of one of the glycidic ester isomers (according to ^{1}H-NMR). This selective crystallisation of one of the isomers meant that it could be fully characterised. The characterisation of this isomer, as well as stereochemical assignment of both isomers, will be discussed later (Section 3.5.2.1).

Barium's procedure was repeated once again and as heating had helped to improve yield previously, the reaction was set to 55 °C (following addition of NaOMe) and left stirring for 24 h. Similar to the previous attempt, ≈20% SM **(72)** remained after 24 h. Despite reaction incompletion, the mixture was carried forward to the second stage of Barium's synthesis (i.e. saponification with NaOH, acidification with 15% aq. HCl and decarboxylation by heating). Following work-up of the final crude reaction mixture, the ^{1}H-NMR spectrum revealed that, in addition to the expected ketone product **(92)**, ≈50% of the sample consisted of aldehyde **(72)**. The substantial presence of aldehyde **(72)** would suggest that in addition to reaction incompletion, breakdown of one of the intermediates/product to aldehyde **(72)** must also be contributing to the poor yield of ketone **(92)**. In previous attempts to isolate and characterise glycidic ester intermediate **(161)**, evidence of degradation of **(161)** was observed during flash column chromatography. The instability of this intermediate, during Barium's synthesis, may very likely be contributing to low product yield, and recovery of unwanted aldehyde **(72)**.

Synthesis of 2,5-P2P **(92)** *via* the ethyl glycidate **(239)**, was also attempted using Barium's methodology (Figure 3.24). To avoid any risk of transesterification, the solvent and base used were EtOH and NaOEt.

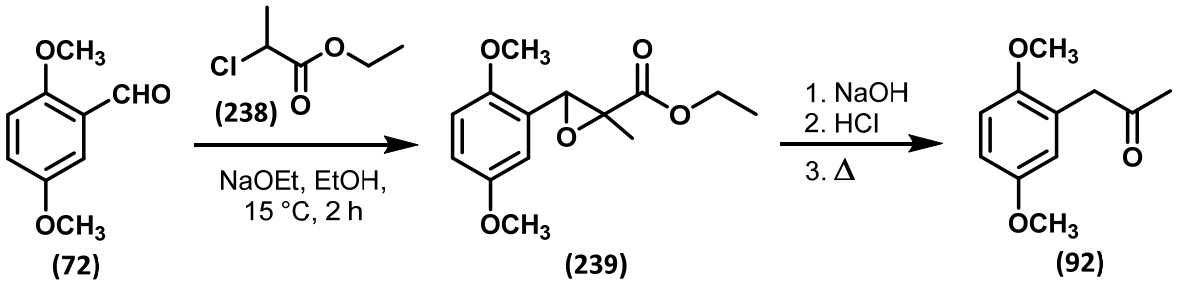


Figure 3.24: Barium's methodology applied to the synthesis of 2,5-P2P (92) *via* ethyl glycidate (239)

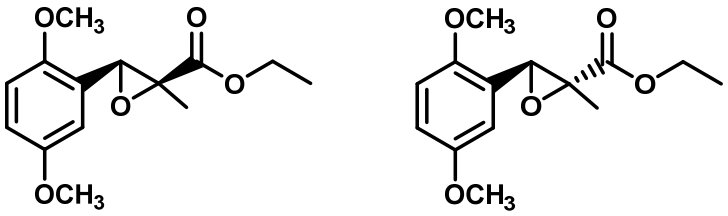
Following Barium's procedure *verbatim* yielded similar results to those obtained for synthesis *via* methyl glycidate **(161)** – the final crude sample of ketone **(92)**, contained a substantial amount (≈50%) of aldehyde **(72)**. Like before, some optimisation of the reaction was carried out. By following reaction progression (by taking aliquots for ^{1}H-NMR analysis) and isolating the glycidate intermediate, it was discovered that working with the ethyl glycidate **(239)** is more favourable than the methyl glycidate **(161)** for the following reasons:

a) Reaction completion (i.e. complete consumption of SM **(72)**), was achieved using the ethyl glycidate intermediate **(239)** (after 16 h stirring @ rt). This represents an improvement on the

≈80% conversion achieved for methyl glycidate intermediate **(161)** (after heating/stirring for 2 days).

b) Following isolation by flash column chromatography, the yield of ethyl glycidate **(239)** was greater than that of methyl glycidate **(161)** (56% *vs.* 46%). Also, the amount of aldehyde **(72)** recovered from the flash column during isolation of ethyl glycidate **(239)** was much lower than that of methyl glycidate **(161)**, suggesting that degradation of ethyl glycidate **(239)** occurs to a much lesser extent.

Upon isolation, ethyl glycidic ester intermediate **(239)** (yield = 56%), was found to exist as a mixture of *cis*-**(239)** and *trans*-**(239)** isomers (ratio = 1:1), which could not be resolved by flash column chromatography. Characterisation of these isomers and their stereochemical assignment will be discussed later (Section 3.5.2.2).



cis-**(239)** *trans*-**(239)**

2,5-P2P **(92)**, synthesised *via* a glycidic ester intermediate, may be used as a precursor to a range of 'D series' amphetamines, such as DOB **(35)**. In relation to the potential use of glycidates in DOB **(35)** synthesis, introduction of the bromine atom may, in theory, take place prior to formation of the glycidate. With this in mind, Barium's methodology was applied to 4-bromo aldehyde **(160)**, in an attempt to produce the DOB precursor 4-Br-2,5-P2P **(159)** (Figure 3.25).

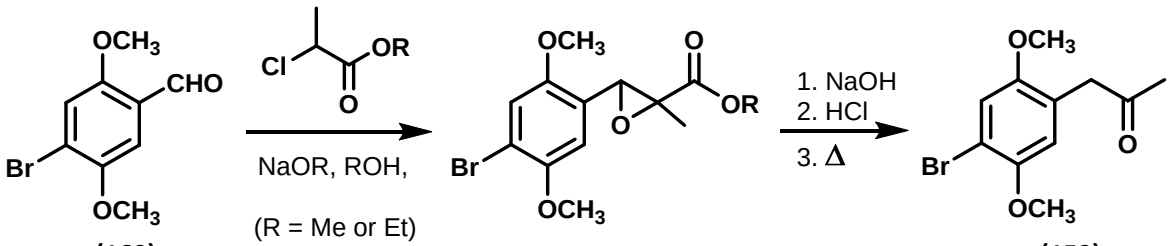
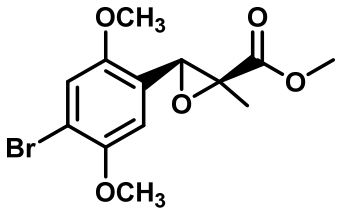


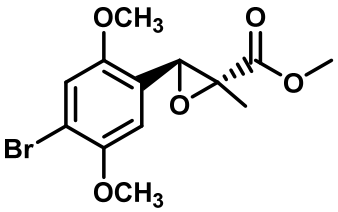
Figure 3.25: Synthesis of 4-Br-2,5-P2P (159) *via* a methyl/ethyl glycidate intermediate

As was observed for the non-bromo glycidates **(161)** and **(239)**, reaction completion had not taken place within 2 h (Barium's method), for both the methyl **(162)** and ethyl **(240)** 4-bromo glycidic esters. Further heating and increased reaction times were again assessed in an attempt to drive the reaction to completion. For the 4-bromo methyl glycidic ester **(162)**, the reaction needed to be heated to 65 °C (to fully dissolve the SM **(160)**) and after 2 days of heating/stirring, only 70% conversion was achieved. This

equated to an isolated yield of **(162)** of 40% following column chromatography. As observed for the non-bromo glycidates, the product formed as a mixture of *cis*-**(162)** and *trans*-**(162)** isomers (ratio = 1:1).



cis-**(162)**



trans-**(162)**

For 4-bromo ethyl glycidic ester **(240)**, despite extended reaction time (up to 3 days) and additional heating (@ 65 °C), only a trace amount of product was detected by ^{1}H-NMR. Given this poor conversion, purification by flash column chromatography was not pursued.

Barium's procedure had proven to be an unpredictable and inconsistent method of producing ketone precursors (both non-brominated and brominated) to 'D series' amphetamines, despite the promising yield quoted on the web (≈77% for ketone **(92)**).[218] Even after reaction optimisation (by heating and extending reaction time), reaction completion for formation of the glycidate intermediate, could only be reached for one of the compounds (**(239)**). This suggests that the method is not versatile and cannot be used across a range of structurally similar analogues. Also, there was found to be poor reproducibility of reaction outcome, with the yield of a given reaction varying from one day to the next.

The principle weakness in Barium's methodology, especially for the 4-bromo compounds, was reaction incompletion during initial glycidic ester formation. This obviously leads to a reduction in overall product yield but also, attempts to separate glycidic ester from SM by flash column chromatography, lead to breakdown of the glycidic ester in some cases.

The formation of glycidic esters has been well explored in the literature and there is great variability in reaction conditions (base/solvent used etc. – Section 3.4). Modification of Barium's method was explored in order to assess how it may affect reaction outcome. One simple modification involved changing the solvent used in the reaction, whereby MeOH/EtOH were replaced by Et_2O. This minor alteration gave rise to greatly improved reaction yields (see Section 3.5.2), as well as a change in the stereochemical outcome of the glycidic esters produced. This new procedure is outlined in Figure 3.26.

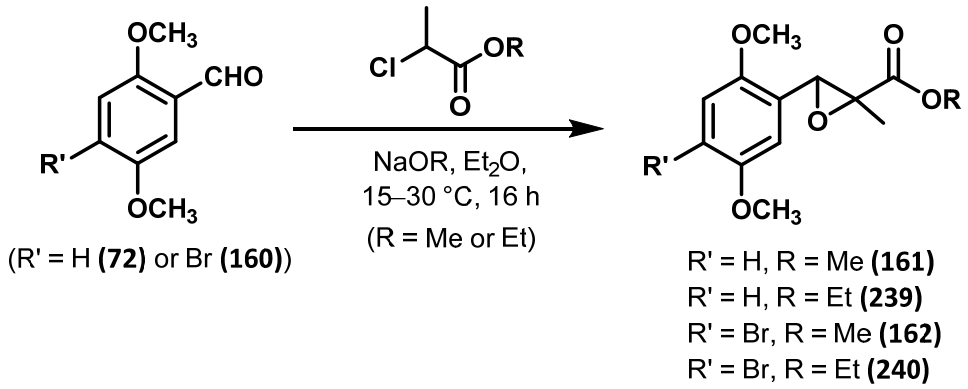
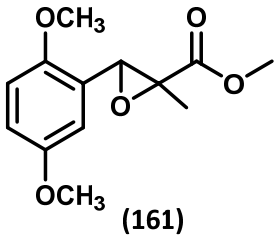


Figure 3.26: Modified procedure for the preparation of 2,5-dimethoxy glycidic esters

3.5.2 Comparison of optimised 'Barium' method *vs.* 'Et$_2$O' method and characterisation of recovered glycidic esters

The Barium method that had given the highest product yield of glycidic ester (after optimisation), and the method in which Et$_2$O was used as solvent, were compared. The yields obtained for both of these methods, as well as the characterisation of each of the glycidic esters produced, is outlined in this section.

3.5.2.1 Methyl 2-methyl-3-(2,5-dimethoxyphenyl)glycidate (161)



(161)

Table 3.14: Comparison of optimised Barium method (A) *vs.* Et$_2$O method (B) during the synthesis of glycidate (161)

Method	Reaction conditions	Reaction completion?*	Additional purification★ required?	Isolated yield	Geometry of product(s)
A	NaOMe, MeOH, 55 °C, 40 h	No	Yes	46%	*cis* + *trans* (Ratio = 1:1)
B	NaOMe, Et$_2$O, 30 °C, 16 h	Yes	No	92%	*trans* only

*As indicated by ^{1}H-NMR spectrum of crude reaction

★By flash column chromatography

The yield of glycidate obtained using method B is vastly greater than that of method A. Also, as reaction completion was achieved using method B, there was no need to purify the product by flash column chromatography. Therefore, once work-up of the crude reaction was complete, the product could be directly used in subsequent reaction steps (saponification/decarboxylation).

Aside from reaction yield, the other major difference between the two methods was the geometry of the resulting glycidic ester product. As mentioned previously, depending on the conditions, a specific reaction may give only *cis*, *trans* or a mixture of the two.[219] How the solvent alone influences this is not fully understood. However, it has been suggested that the solvent has an effect on reaction kinetics, influencing the rate/reversibility of particular steps in the reaction mechanism. According to Tung *et al.,*[219] normally the Darzens condensation leads to a mixture of *cis* and *trans* isomers (as observed using Barium's method). In this case, it is thought that the kinetically (or sterically) favoured *trans* isomer is initially formed but under the basic reaction conditions, epimerisation to the *cis* isomer occurs over time. It is possible that the solvent used may promote/inhibit this epimerisation to the extent that only one isomer is formed.

According to Roux-Schmitt *et al*.,[210] the difference in geometry from one reaction to the next is attributed to how the solvent affects the reversibility of the initial aldolisation step. If a particular solvent can influence this aldolisation step to become irreversible (in favour of *trans* for example) whilst remaining reversible for *cis*, eventually the equilibrium will favour exclusive formation of *trans*. Therefore, the ability of Et_2O as solvent, to produce exclusively the *trans* isomer in our work, may be attributed to either of these explanations (i.e. ability to influence either the rate of epimerisation or reversibility of the aldolisation step).

Using Et_2O as solvent, the glycidate **(161)** was produced in a single isomeric form, in a yield of 92%. For reasons outlined below, this was assigned *trans* conformation. The R_f, m.p., IR and MS data for *trans* methyl glycidate **(161)** are presented in Table 3.15 below.

Table 3.15: Yield, R_f, m.p., IR and HRMS data for *trans* methyl glycidate (161)

Compound No.	Yield	m.p. (°C)	R_f*	IRν_{max} (KBr) (cm^{-1})	HRMS ($M+H^+$) (*m/z*)	
					Calc.	Found
trans-**(161)**	92%	46–48	0.59	1729 (C=O), 1591, 1500 (C=C)	253.1076	253.1072

*mobile phase = 70:30 Et_2O:hexane

As mentioned, the Barium method had produced methyl glycidate **(161)** as a mixture or *cis*/*trans* isomers. By chance, during flash column chromatography, one of these isomers selectively crystallised out of solution. This isomer, which did not match the ^{1}H-NMR spectrum of the isomer isolated from the

Et_2O method, was assigned *cis* geometry. The R_f, m.p., IR and MS data for *cis* methyl glycidate **(161)** are presented in Table 3.16 below.

Table 3.16: R_f, m.p., IR and HRMS data for *cis* methyl glycidate (161)

Compound No.	m.p. (°C)	R_f*	IRν_{max} (KBr) (cm^{-1})	HRMS ($M+H^+$) (*m/z*)	
				Calc.	Found
cis-**(161)**	78–79.5 (Et_2O/hexane)	0.58	1754 (C=O), 1612, 1499 (C=C)	253.1076	253.1076

*mobile phase = 70:30 Et_2O:hexane

Given that the ^{1}H-NMR spectra of both isomers were available, assignment of geometry was made on the basis of the chemical shift value (δ) 'rules' outlined in Section 3.4.1. The ^{1}H-NMR signals that were most useful in assigning the geometry of the two isomers are highlighted in Figure 3.27.

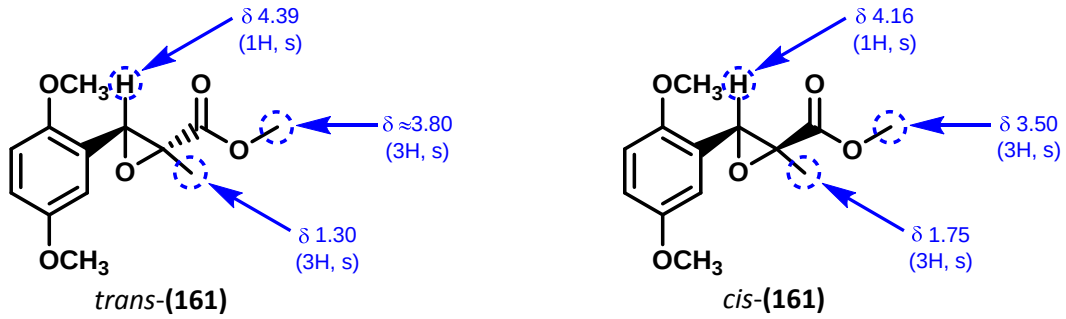


Figure 3.27: Assigning geometry of *cis*/*trans* isomers of methyl glycidate (161), based on differences in δ values of particular signals

Based on the 'rules' set out by Roux-Schmitt *et al*.,[210] the δ values of the proton on C-3 and protons on the ester group (methoxy protons in this case) are more downfield for the *trans* isomer, whilst the δ value of the methyl protons is more downfield for the *cis*. These rules were applied to methyl glycidate **(161)**, the isomers of which were assigned accordingly (Figure 3.27). The ^{1}H-NMR spectra of both isomers can be found in Figure 3.28.

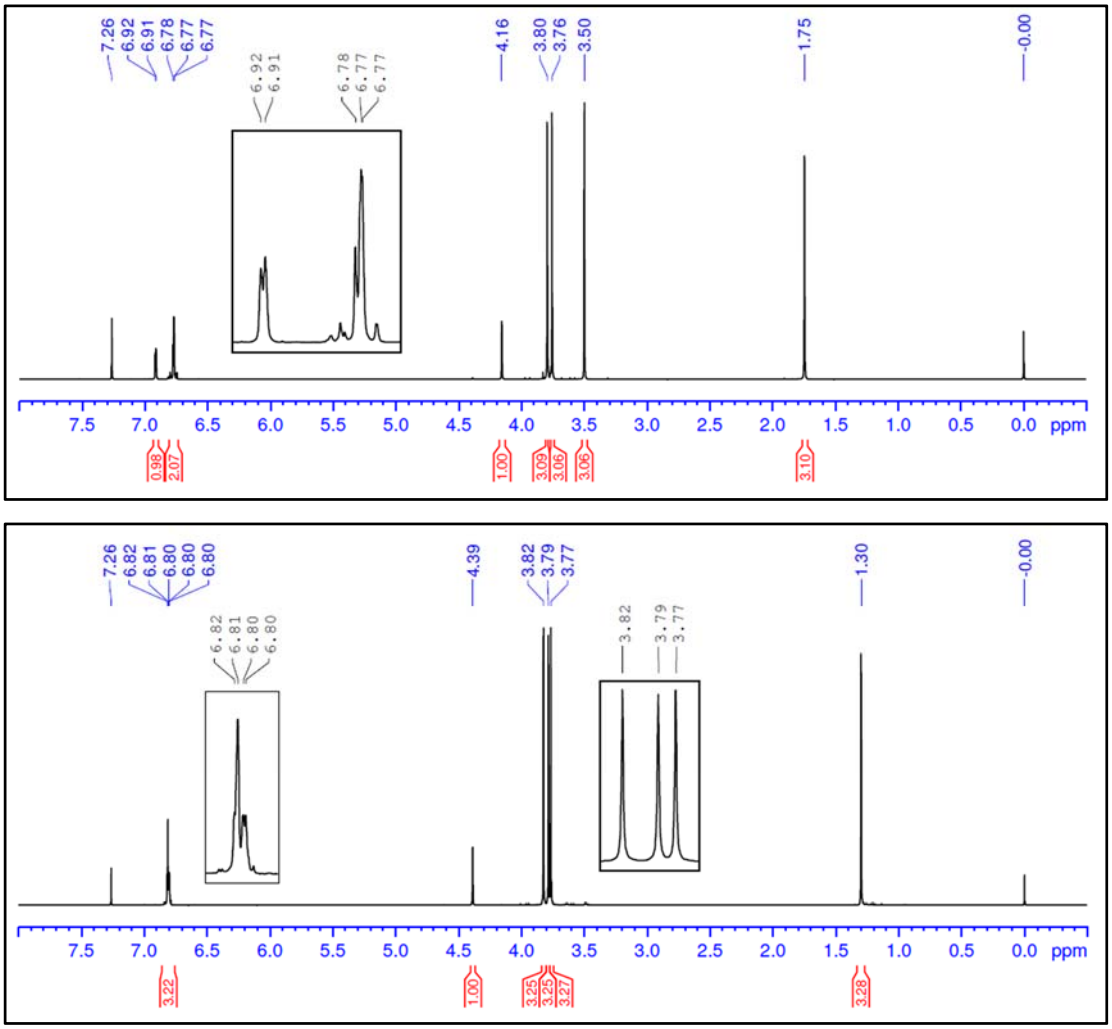
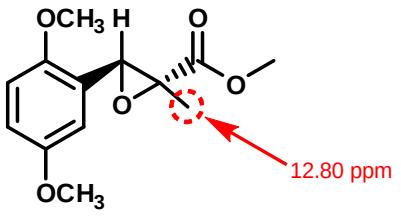


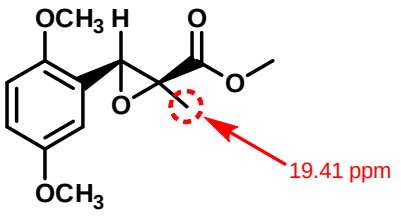
Figure 3.28: ^{1}H-NMR spectra of both *cis*-(161) (top spectrum) and *trans*-(161) (bottom spectrum) methyl glycidates

Another minor difference between the ^{1}H-NMR spectra of the two isomers can be found in the aromatic region. Although one may expect to observe the ABX pattern for the three ring protons, an indiscernible multiplet (@ δ 6.79–6.84) is observed for *trans*-**(161)**. However, for *cis*-**(161)**, slightly better resolution of the aromatic signals is observed: an apparent ABq signal (@ δ 6.78) and a distinct doublet (@ δ 6.91, *J*=3 Hz, corresponding to H-6).

In terms of the ^{13}C-NMR spectra, only one signal may possibly be useful in distinguishing between the two isomers (due to a sufficiently large difference in chemical shift). This signal corresponds to the carbon of the 2-methyl group. The δ value of this signal, for both isomers, is shown below.

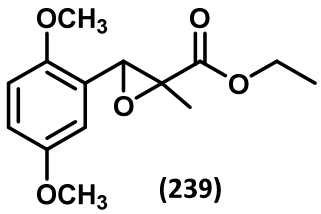


trans-**(161)**



cis-**(161)**

3.5.2.2 Ethyl 2-methyl-3-(2,5-dimethoxyphenyl)glycidate (239)



(239)

Table 3.17: Comparison of optimised Barium method (A) *vs.* Et_2O method (B) during the synthesis of glycidate (239)

Method	Reaction conditions	Reaction completion?*	Additional purification★ required?	Isolated yield	Geometry of product(s)
A	NaOEt, EtOH, rt, 16 h	Yes▲	No	56%	*cis* + *trans* (Ratio = 1:1)
B	NaOEt, Et_2O, 30 °C, 16 h	Yes	No	88%	*trans* only

*As indicated by ^{1}H-NMR spectrum of crude reaction
★By flash column chromatography
▲Replicate reactions, under same conditions, did not go to completion and thus required additional purification

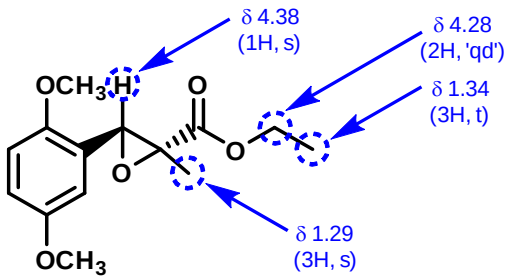
The yield of glycidate produced *via* method B was much greater that of method A. Although reaction completion had been achieved in one case using Barium's methodology (method A), this was not always observed (see Note▲ under Table 3.17). Similar to methyl glycidate **(161)**, method B (solvent = Et_2O) produced the glycidate exclusively in the *trans* form, in an excellent yield (88%). The R_f, m.p., IR and MS data for *trans* ethyl glycidate **(239)** are presented in Table 3.18 below.

Table 3.18: Yield, R_f, m.p., IR and HRMS data for *trans* ethyl glycidate (239)

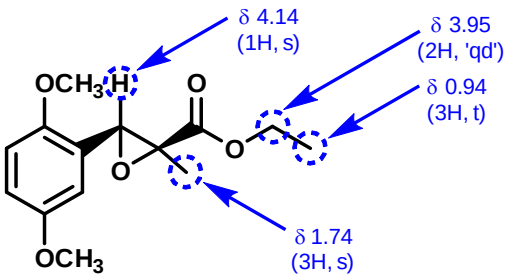
Compound No.	Yield	m.p. (°C)	R_f*	IRν_{max} (NaCl) (cm^{-1})	HRMS (M+H$^+$) (*m/z*)	
					Calc.	Found
trans-**(239)**	88%	≈30	0.63	1732 (C=O), 1592, 1505 (C=C)	267.1232	267.1230

*mobile phase = 70:30 Et_2O:hexane

Method A produced the ethyl glycidate **(239)** as mixture of *cis*/*trans* isomers that were inseparable by flash column chromatography. Despite the lack of resolution, both isomers were assigned geometry based on the general 'rules' outlined in Section 3.4.1 (see overleaf). Also, despite the lack of a pure sample of *cis*-**(239)**, the fact that a pure sample of *trans*-**(239)** was available (from method B) meant that by process of elimination, all ^{1}H-NMR/^{13}C-NMR signals of *cis*-**(239)** could be assigned.



trans-**(239)**



cis-**(239)**

An unusual feature, observed in the ^{1}H-NMR spectra of both isomers, was the splitting pattern of the CH_2 protons of the ester group. One may expect to observe a quartet signal for these protons. Instead, additional splitting is observed, in the form of an apparent quartet of doublets ('qd') (Figure 3.29).

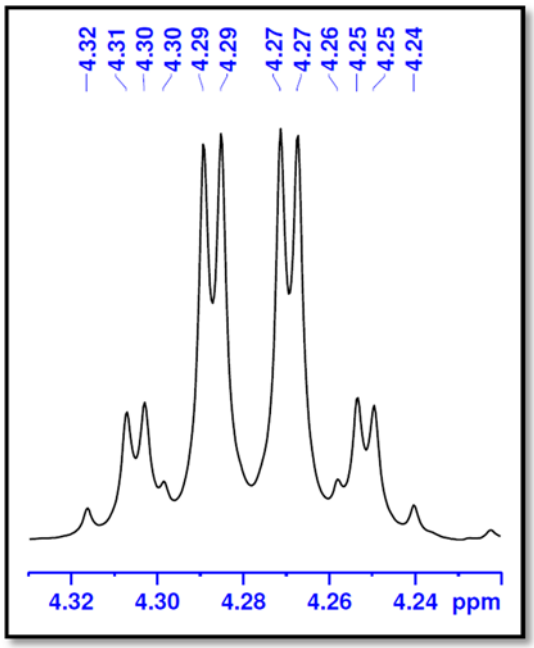


Figure 3.29: A 'quartet of doublets' observed in the ^{1}H-NMR spectrum of *trans* ethyl glycidate (239), corresponding to the CH_2 protons of the ester group

The apparent quartet of doublets observed is in fact, part of an ABX_3 system. This is a feature that is common to ethyl groups in chiral molecules. As outlined by Günther,[220] if a molecule contains an asymmetric carbon, the magnetic equivalence of neighbouring protons or groups of protons can break down. The result of this, for our ethyl glycidates, is that the two protons ("A" and "B") of the CH_2 group are diastereotopic. This adds considerable complexity to the spectrum, as each of the two protons (A and B) will couple to the CH_3 ("X_3") protons (in general, produces a quartet, J≈7 Hz) as well as coupling to each other (J≈14 Hz). In the case where the diastereotopic shift between the 2 protons (A and B) is large enough for full resolution, a quartet, in which each line is split further into two, is observed. A good example of this is observed for 2-ethoxycyclohexenone (Figure 3.30).

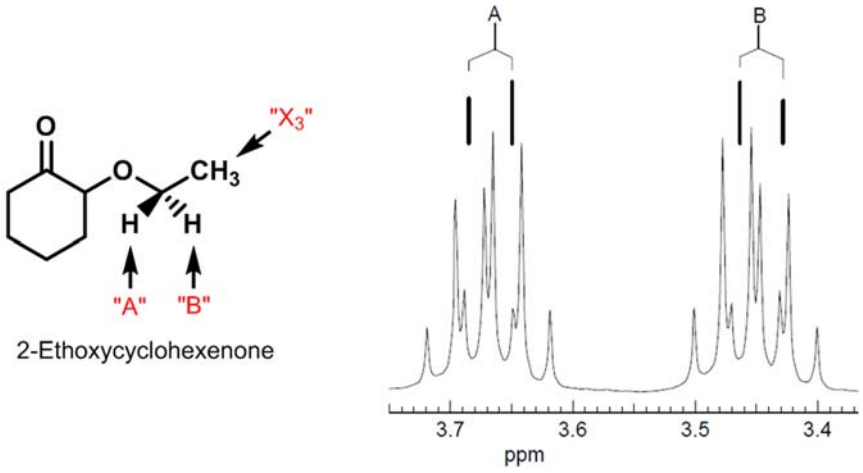


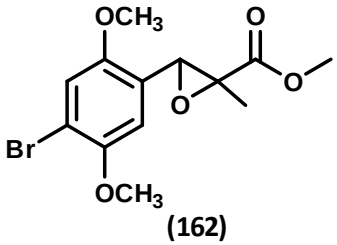
Figure 3.30: The AB part of an ABX$_3$ type spectrum of 2-ethoxycylohexenone[221]

In many molecules with this ethoxy moiety, interpretation is not so clear. Often, the value of J_{AB} is equal to about twice that of J_{AX}, the result being that within the signal for proton A, for example, several of the lines are superimposed. Also, if the diastereotopic shift is small, considerable overlap of A and B signals will take place, to the extent where they can resemble a quartet of doublets. This appears to be the case for both isomers of ethyl glycidate **(239)** (Figure 3.29).

In the ^{1}H-NMR spectra, another feature that may be used to possibly distinguish between the two isomers is the splitting pattern of the aromatic ring protons. Similar to methyl glycidate **(161)**, the signals corresponding to the three aromatic ring protons are better resolved for *cis*-**(239)** compared to *trans*-**(239)**. For *trans*-**(239)**, all three protons resonate in a very narrow range (from δ 6.80–6.81), almost resembling a singlet. For *cis*-**(239)**, an apparent ABq signal (@ δ 6.76) and a distinct doublet (@ δ 6.93, *J*=3 Hz, corresponding to H-6) are observed.

The ^{13}C-NMR spectra of both isomers are very similar. Only the chemical shift value of the carbon of the 2-methyl group may be used to possibly distinguish between the two isomers: similar to methyl glycidate **(161)**, this signal resonates at a more downfield position (≈19 ppm) for *cis*-**(239)**, compared to ≈13 ppm for *trans*-**(239)**.

3.5.5.3 Methyl 2-methyl-3-(4-bromo-2,5-dimethoxyphenyl)glycidate (162)



(162)

Table 3.19: Comparison of optimised Barium method (A) *vs.* Et_2O method (B) during the synthesis of glycidate (162)

Method	Reaction conditions	Reaction completion?*	Additional purification⋆ required?	Isolated yield	Geometry of product(s)
A	NaOMe, MeOH, 65 °C, 48 h	No	Yes	40%	*cis* + *trans* (Ratio = 1:1)
B	NaOMe, Et_2O, 30 °C, 16 h	Yes	No	83%	*trans* only

*As indicated by ^{1}H-NMR spectrum of crude reaction
⋆By flash column chromatography

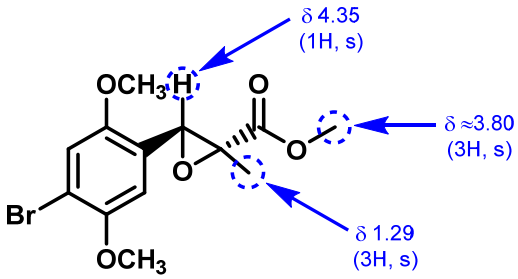
Similar to the non-bromo glycidates **(161)** and **(239)**, the yield of product recovered using Et_2O as solvent (Method B) was far superior to Barium's method, even after optimisation. Method B (Table 3.19) produced the desired glycidic ester exclusively in the *trans* form in a yield of 83%. The R_f, m.p., IR and MS data for 4-bromo *trans* methyl glycidate **(162)** are presented in Table 3.20 below.

Table 3.20: Yield, R_f, m.p., IR and HRMS data for 4-bromo *trans* methyl glycidate (162)

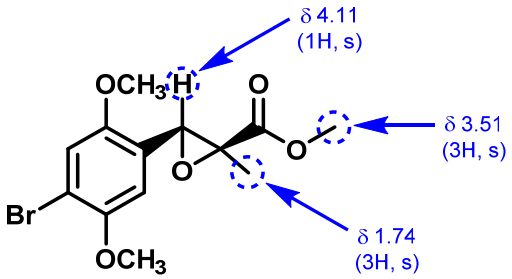
Compound No.	Yield	m.p. (°C)	R_f*	IRν_{max} (KBr) (cm^{-1})	HRMS ($M+H^+$)⋆ (*m/z*)	
					Calc.	Found
trans-**(162)**	83%	105–106 (MeOH)	0.65	1738 (C=O), 1496 (C=C)	331.0181	331.0174

*mobile phase = 70:30 Et_2O:hexane
⋆molecular ion (M) calculated for ^{79}Br isotope peak

Method A produced the 4-bromo methyl glycidate **(162)** as mixture of *cis*/*trans* isomers that were inseparable by flash column chromatography. Despite the lack or resolution, both isomers were assigned geometry based on the general 'rules' outlined in Section 3.4.1:

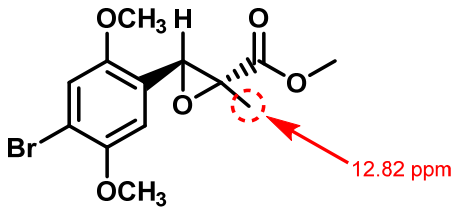


4-Bromo-*trans*-**(162)**

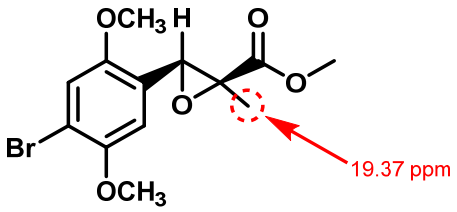


4-Bromo-*cis*-**(162)**

All other signals in the ^{1}H-NMR spectra (of both *cis*-**(162)** and *trans*-**(162)**) were very similar. For the ^{13}C-NMR spectra, only the signals corresponding to the carbon of the 2-methyl group may possibly be used to distinguish between the two isomers. The δ value of this signal, for both isomers, is shown overleaf.

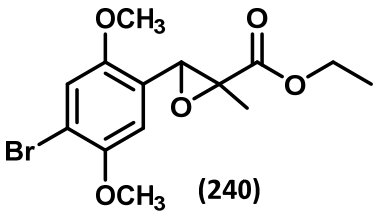


4-Bromo-*trans*-**(162)**



4-Bromo-*cis*-**(162)**

3.5.5.4 Ethyl 2-methyl-3-(4-bromo-2,5-dimethoxyphenyl)glycidate (240)



(240)

Table 3.21: Comparison of optimised Barium method (A) *vs.* Et_2O method (B) during the synthesis of glycidate (240)

Method	Reaction conditions	Reaction completion?*	Additional purification★ required?	Isolated yield	Geometry of product(s)
A	NaOEt, EtOH, 65 °C, 72 h	No▲	–	–	–
B	NaOEt, Et_2O, 30 °C, 16 h	Yes	No	85%	*trans* only

*As indicated by ^{1}H-NMR spectrum of crude reaction
★By flash column chromatography
▲Only trace amount of product detected, purification by column chromatography not pursued

In the case of 4-bromo-ethyl glycidate **(240)**, method A could not realistically be used as a method of producing the glycidic ester, as only a trace amount was detected by ^{1}H-NMR spectroscopy. Method B on the other hand, produced the desired glycidic ester exclusively in a single isomeric form (assumed *trans*) in a yield of 85%. The R_f, m.p., IR and MS data for 4-bromo *trans* ethyl glycidate **(240)** are presented in Table 3.22 below.

Table 3.22: Yield, R_f, m.p., IR and HRMS data for 4-bromo *trans* ethyl glycidate (240)

Compound No.	Yield	m.p. (°C)	R_f*	IRν_{max} (KBr) (cm^{-1})	HRMS (M+H$^+$)★ (*m/z*)	
					Calc.	Found
trans-**(240)**	85%	94–96 (MeOH)	0.68	1736 (C=O), 1496 (C=C)	345.0338	345.0323

*mobile phase = 70:30 Et_2O:hexane
★molecular ion (M) calculated for ^{79}Br isotope peak

Although in this case we did not have pure samples of both isomers to assist in the assignment of geometry, the product obtained above was assumed to be *trans*-**(240)**, based on the similarity of δ values of selected signals (in ^{1}H-NMR spectrum), to 4-bromo *trans* methyl glycidate **(162)**, characterised previously (Figure 3.31).

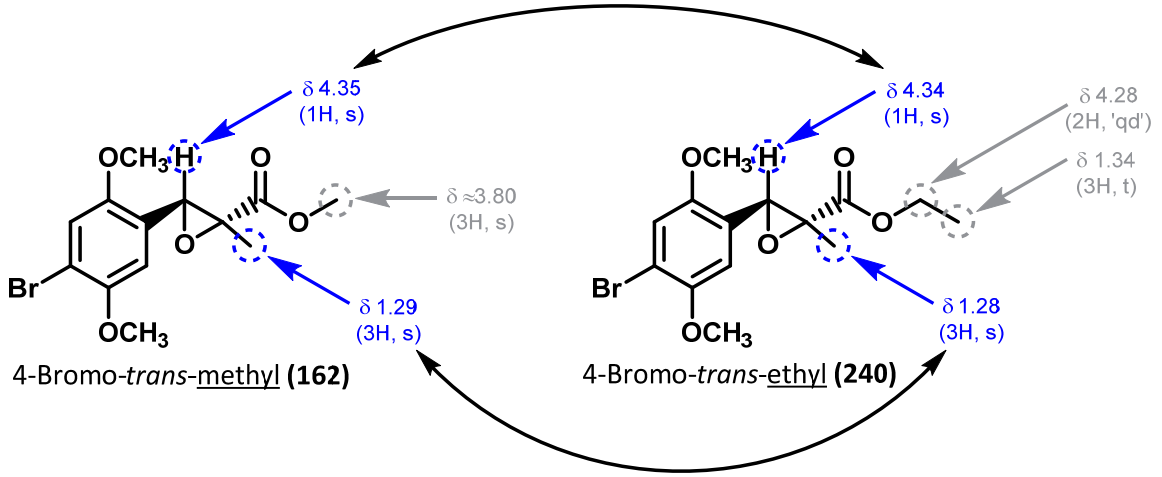


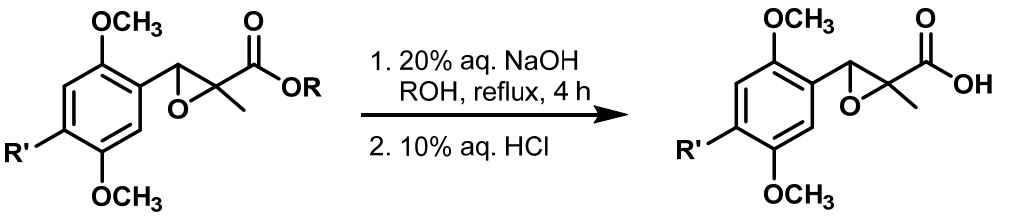
Figure 3.31: Comparison of selected ^{1}H-NMR signals between 4-bromo-*trans*-methyl (162) and 4-bromo-*trans*-ethyl (240), for assigning geometry of (240)

Also, the lack of a CH_3 carbon (corresponding to 2-methyl group) in the ^{13}C-NMR spectrum, in the region of ≈19 ppm, helped to rule out **(240)** as the *cis*-isomer.

3.5.3 Saponification, acidification and decarboxylation of glycidic esters to produce 2,5-P2P (92) and 4-Br-2,5-P2P (159)

Poor reaction yield of the ketone product **(92)**, was previously found to be a result of a combination of factors, using Barium's methodology. Among these are reaction incompletion and breakdown of glycidic ester intermediate. It was also found that when Barium's saponification/decarboxylation step was carried out (without isolation of the acid intermediate), substantial aldehyde **(72)** was present in the crude reaction. This implies that optimisation of the saponification/decarboxylation steps also needs to be carried out to produce the desired ketone in reasonable yields.

In a number of other literature procedures for the production of aldehydes/ketones *via* glycidates, the intermediate acid is worked-up and isolated before undergoing heat-induced decarboxylation.[31,137,209,212,213] This methodology was applied (as outlined in Sections 5.3.4 and 5.3.5, Procedure B) to the glycidic esters synthesised thus far, producing the intermediate glycidic acids in excellent yields (Figure 3.32).



R' = H, R = Me **(161)**
R' = H, R = Et **(239)**
R' = Br, R = Me **(162)**
R' = Br, R = Et **(240)**

R' = H **(241)** (**87%** from **(161)**)
(**88%** from **(239)**)
R' = Br **(242)** (**95%** from **(162)**)
(**97%** from **(240)**)

Figure 3.32: Yields of glycidic acids (241) and (242) from glycidic esters (161), (239), (162) and (240)

Isolation of novel glycidic acids **(241)** and **(242)**, allowed for their full characterisation. The R_f, m.p., IR and MS data for non-bromo glycidic acid **(241)** and 4-bromo glycidic acid **(242)** are outlined in Table 3.23 below.

Table 3.23: Yield, R_f, m.p., IR and HRMS data for non-bromo (241) and 4-bromo (242) glycidic acids

Compound No.	Yield	m.p. (°C)	R_f*	IRν_{max} (KBr) (cm^{-1})	HRMS ($M+H^+$) (*m/z*)	
					Calc.	Found
(241)	87–88%★	95–98	0.15	≈3000 (OH), 1715 (C=O), 1498 (C=C)	239.0919	239.0920
(242)	95–97%★	121–123	0.09	≈3000 (OH), 1705 (C=O), 1495 (C=C)	317.0025▲	317.0023

*mobile phase = 50:50 EtOAc:hexane
★see Figure 3.32
▲molecular ion (M) calculated for ^{79}Br isotope peak

Due to the fact that they share the core 2-methyl-3-phenyl glycidate structure, the ^{1}H-NMR and ^{13}C-NMR spectra of the glycidic esters and glycidic acids are similar. The obvious differences being the lack of methyl/ethyl group signals (from ester) and the appearance of a low intensity, broad singlet in the ^{1}H-NMR spectra of the acids (Figure 3.33). In addition to these, there is also a slight difference in the chemical shift value (^{13}C-NMR) between the ester carbonyl carbon and the acid carbonyl carbon (acid more downfield by ≈7 ppm).

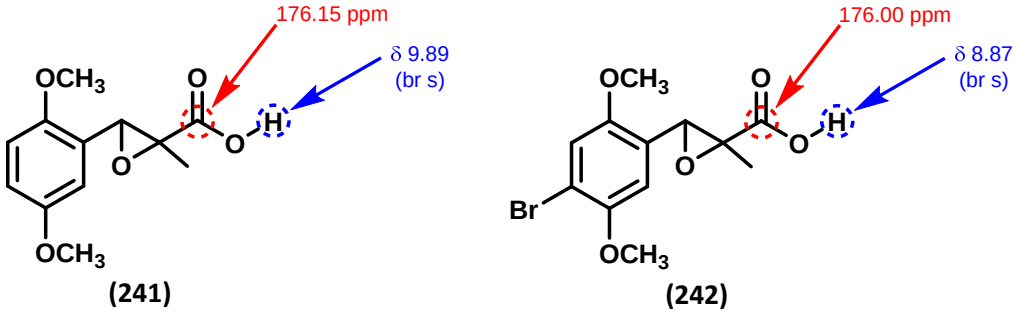
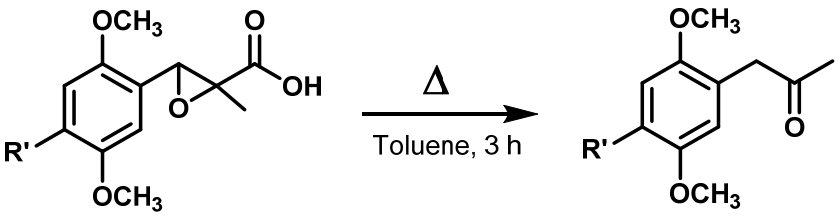


Figure 3.33: Characteristic ^{1}H-NMR/^{13}C-NMR signals of glycidic acids (241) and (242)

Another obvious difference between the glycidic esters and glycidic acids was observed in the IR spectra, in the region of ≈3000 cm^{-1}. For the esters, a number of sharp signals were observed in this region, corresponding to various C–H stretching frequencies. For the acids, these C–H stretching frequencies were enveloped by a very broad O–H stretching frequency, arising from the carboxylic acid functional group.

Decarboxylation of the acids **(241)** and **(242)**, was all that remained in the synthesis of the ketone precursors **(92)** and **(159)**. In the literature, decarboxylation (by heating) of the neat glycidic acid is often carried out. In this case, for ease of handling, the neat acid was dissolved in a small amount of toluene before heating. This was found to have no effect on the yield of ketone produced, when compared to neat heating.

Following work-up of the crude product, the ^{1}H-NMR spectra (for both non-bromo and bromo products) revealed that a trace amount of aldehyde was present. However, this amount was very small in comparison to the level observed using Barium's method (≈50%). The presence of the aldehyde called for the crude product to be purified by flash column chromatography. Following this, the non-bromo **(92)** and 4-bromo **(159)** ketones were recovered in yields of 65% and 71% respectively:



R' = H **(241)**
R' = Br **(242)**

R' = H **(92) (65%)**
R' = Br **(159) (71%)**

A good yield of ketones **(92)** and **(159)** would be expected in this work, based on work carried out by Billman and Tonnis,[207] who found the decarboxylation of a series of glycidic acids to be most efficient for compounds baring electron donating groups on the aromatic ring.
As both ketones **(92)** and **(159)**, had been previously synthesised and characterised (Sections 3.2 and 3.3), comparison of spectroscopic data with that of authentic samples was used as proof of structure.

Our work had shown that Barium's procedure, despite the promising reported yield, could not be used as a viable method of synthesising ketone precursors to 'D series' amphetamines. There were several sources of poor product yield in the method, namely the initial glycidic ester formation and decarboxylation steps. By optimising reaction conditions, a viable method of producing ketone precursors was established, whereby overall yields (from aldehyde to ketone) of 50–59% were achieved (Figure 3.34).

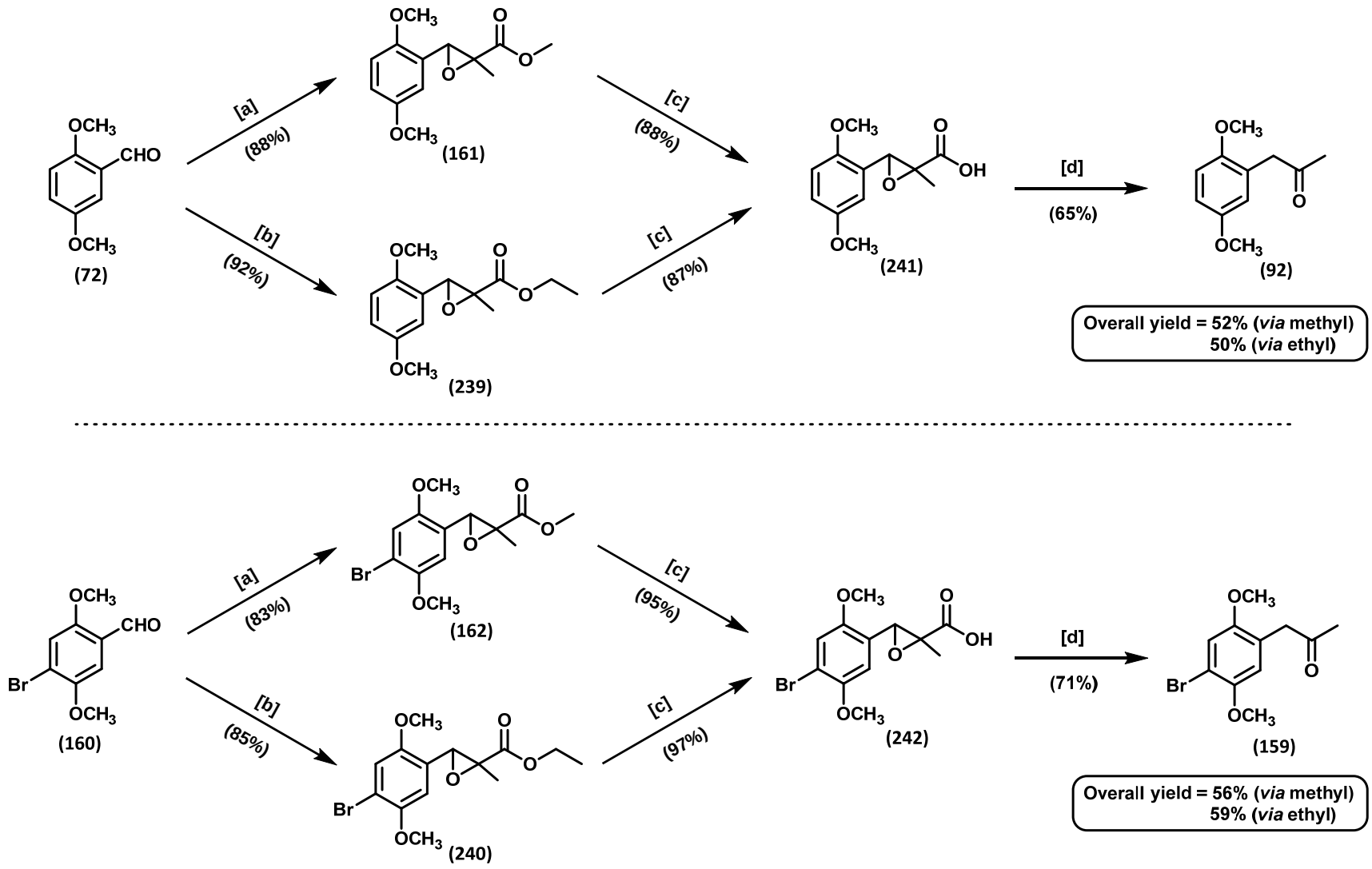


Figure 3.34: Optimised method for the preparation of ketone precursors (92) and (159) *via* 2-methyl glycidate intermediates

*([a] = Chloropropionate reagent **(237)**, NaOMe, Et_2O, 30 °C, 16 h; [b] = Chloropropionate reagent **(238)**, NaOEt, Et_2O, 30 °C, 16 h; [c] = Step 1 – MeOH or EtOH, 20% aq. NaOH, reflux, 4 h; Step 2 – 10% aq. HCl; [d] = 115–120 °C, toluene, 3 h)*

In terms of impurity profiling, only the aldehyde **(72)** may be envisaged as a potential impurity of the 'Darzens route' to 2,5-P2P **(92)**. Its presence in illicitly manufactured 2,5-P2P **(92)** may be attributed to reaction incompletion (for initial glycidic ester formation), breakdown of glycidic ester/acid intermediates or as will be discussed later (Section 3.7), degradation of ketone product **(92)**. No additional reaction by-products were detected for this route of manufacture. This is despite only moderate yields of **(92)** and **(159)** (65% and 71% respectively) in the final decarboxylation step. Aside from a trace amount of aldehyde SM in the crude mixture of these reactions, the remaining loss of yield was attributed to combustion/pyrolysis products that were insoluble in Et_2O.

3.6 Nitrostyrene route to 2,5-P2P (92)

Up to this point, two routes to ketone precursors of 'D series' amphetamines have been explored in this chapter – the PAA route and the Darzens route. Another viable route, common to amphetamine synthesis (Section 1.5.1.1) is one which involves a nitrostyrene intermediate. Although this methodology had been explored by a previous member of our research group,[26] it was decided to repeat the process to see if the yield could be reproduced and also assess how the yield of 2,5-P2P **(92)** obtained, compared to those of the other two routes.

The reaction conditions used by Griffin[26] are outlined in Figure 3.35 below.

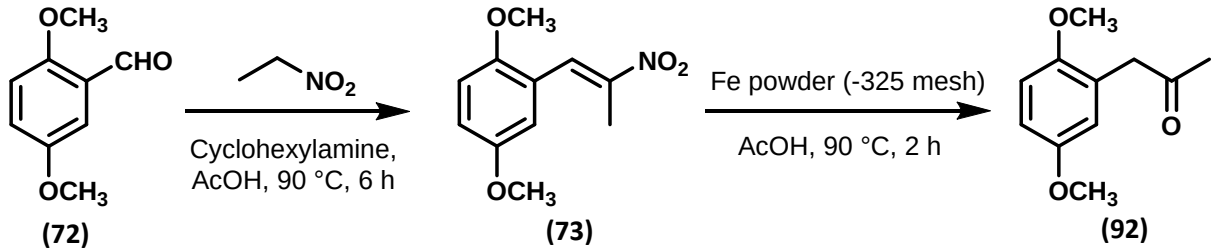


Figure 3.35: Nitrostyrene route to 2,5-P2P (92)[26]

Griffin[26] had achieved a yield of 87% for the formation of nitrostyrene **(73)**, and a 79% yield for the reduction of the nitrostyrene to 2,5-P2P **(92)**. This equates to an overall yield (over two steps) of 69%. When this procedure was followed *verbatim*, yields of 82% and 88% were attained, equating to a 72% overall yield. This suggests that the method is robust and has good reproducibility. Isolation of impurities of this route was not pursued during the course of this work. However, Griffin had previously isolated two impurities (**(90)** and **(91)**), both associated with the initial nitrostyrene formation step (Figure 3.36). Unreacted aldehyde SM **(72)** was also recovered.

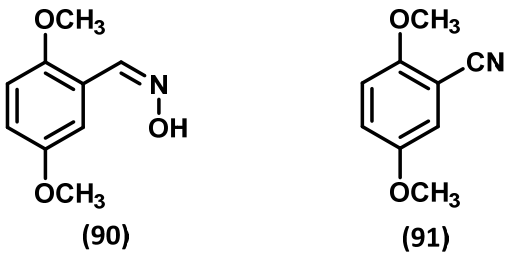


Figure 3.36: Benzaldoxime (90) and benzonitrile (91) impurities isolated by Griffin, during the nitrostyrene route to 2,5-P2P (92)[26]

A comparison of the best yields achieved for each of the three routes to 2,5-P2P **(92)**, explored in this chapter, is outlined in Figure 3.37.

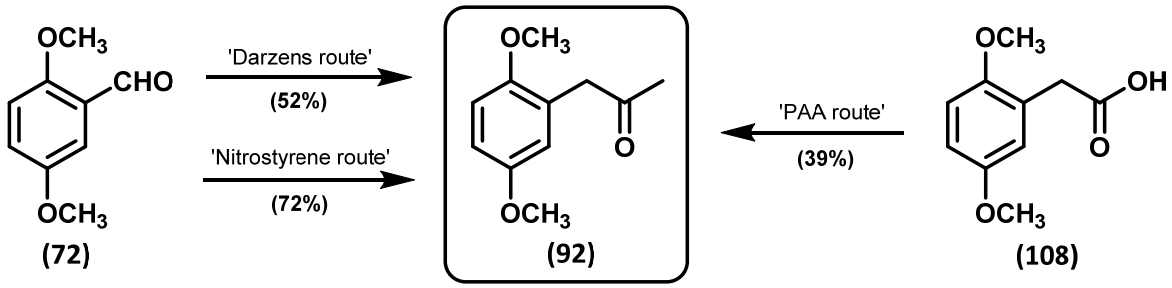
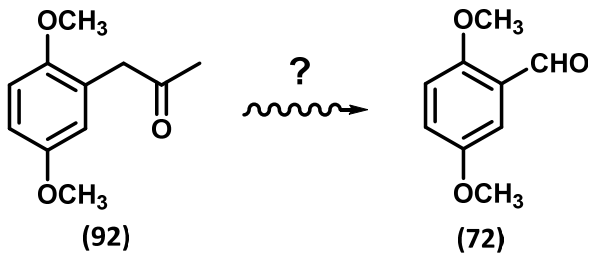


Figure 3.37: Highest yields obtained for the 'Darzens', 'Nitrostyrene' and 'PAA' routes to 2,5-P2P (92)

3.7 Degradation of 2,5-P2P (92)

The impurity profile of 2,5-P2P **(92)** may be highly variable from one sample to the next, depending on the route of manufacture. This is due to individual routes having their own set of associated impurities. One impurity that was found to be present in each of the routes explored was 2,5-dimethoxybenzaldehye **(72)**. This may be expected (due to reaction incompletion) for routes whereby the aldehyde **(72)** is used as a SM (e.g. 'Nitrostyrene' and 'Darzens' routes). However, aldehyde **(72)** was also detected during the 'PAA route', which uses a carboxylic acid SM **(108)**. One possible explanation for this is the degradation of 2,5-P2P **(92)** to aldehyde **(72)**:



In terms of the impurity profiling of illicitly manufactured ATS, there are very few reports which allude to the possible degradation of ketone precursors. Forbes and Kirkbride,[146] in carrying out work on the

impurity profiling of the amphetamine precursor P2P **(65)**, noted that **(65)** had a tendency to decompose to benzaldehyde **(76)**. The authors however, did not offer a mechanistic explanation for this, stating "it is not yet clear whether heat, or oxygen, or both are responsible for this decomposition". Schneiders *et al.*,[126] who also worked on the impurity profiling of illicitly manufactured P2P **(65)**, found traces of benzaldehyde **(76)** in all P2P samples tested. They referred to the fact that benzaldehyde **(76)** may be present due to its use as a SM or as a result of "transformed" P2P **(65)** (citing Forbes and Kirkbrides paper[146]).

A number of other reports however, attribute the presence of benzaldehyde **(76)** (and any other by-products formed from it) to its use as a SM, for example, in the nitrostyrene route, with no mention of possible P2P degradation.[131] This may lead to incorrect assignment of synthetic route during impurity profiling.

Degradation of ketone 2,5-P2P **(92)**, was also found to occur over time. We first became alerted to this when a "pure" sample of 2,5-P2P **(92)**, synthesised ≈3 years previously by Griffin,[26] appeared to contain substantial aldehyde **(72)** (based on δ (CHO) @ δ 10.45 in the ^{1}H-NMR spectrum). In addition to the ^{1}H-NMR evidence, a sample of the aged ketone and a sample of aldehyde **(72)** were run on HPLC. When compared, there was found to be good agreement between the t_R of aldehyde **(72)** (2.59 min) and the t_R of the largest peak in Griffins "pure" ketone sample (2.56 min) (Figure 3.38).
(Note: The sample prepared by Griffin had been stored in a sealed glass sample vial and left on the bench, i.e. at ambient temperature and exposed to light. It was assumed that no effort had been made to exclude air or cap the sample with an inert gas such as N_2.)

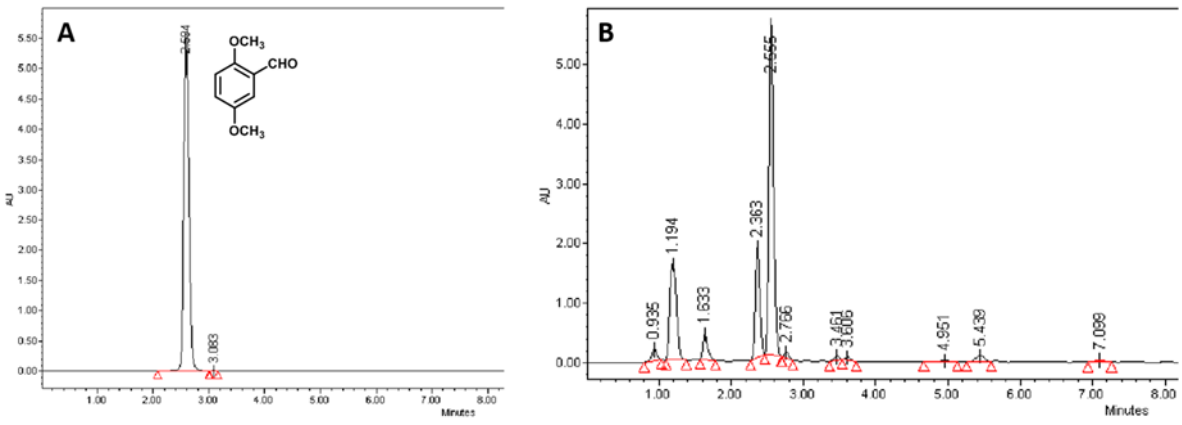


Figure 3.38: HPLC chromatograms (@ 254 nm) of (A) pure aldehyde (72) and (B) "pure" ketone sample isolated previously by Griffin[26]

(Waters 'Alliance' HPLC system (see Section 5.1), mobile phase = 50/50 CH_3CN/H_2O (isocratic), flow rate = 1 mL/min, column = Waters Nova-Pak® C18, 4 µm, 3.9×150 mm @ rt, inj. vol. = 1 µL)

It was clear that this degradation takes place slowly over time; no trace of aldehyde **(72)** was detected within a week of isolating ketone **(92)**. It was decided to track the progression of degradation over time by taking small aliquots (≈10 mg) of ketone **(92)**, for analysis by ^{1}H-NMR spectroscopy.

(Note: All samples of ketone **(92)** prepared in-house and used in this degradation study were stored under similar conditions. The samples, having been concentrated *in vacuo* (in a round bottom flask) following purification or work-up, were sealed under Parafilm® and left in the fume hood. Having said this, the Parafilm® seal, on a number of occasions failed, meaning the sample was uncovered for periods of time.)

Tracking of the degradation of in-house prepared samples was firstly carried out on a batch of 2,5-P2P **(92)**, synthesised *via* the 'Nitrostyrene route'. A HPLC run of an aged sample from this batch (after ≈2.5 years), revealed that like Griffin's sample (Figure 3.38), there was substantial aldehyde **(72)** present, in addition to other unidentified degradation products (Figure 3.39).

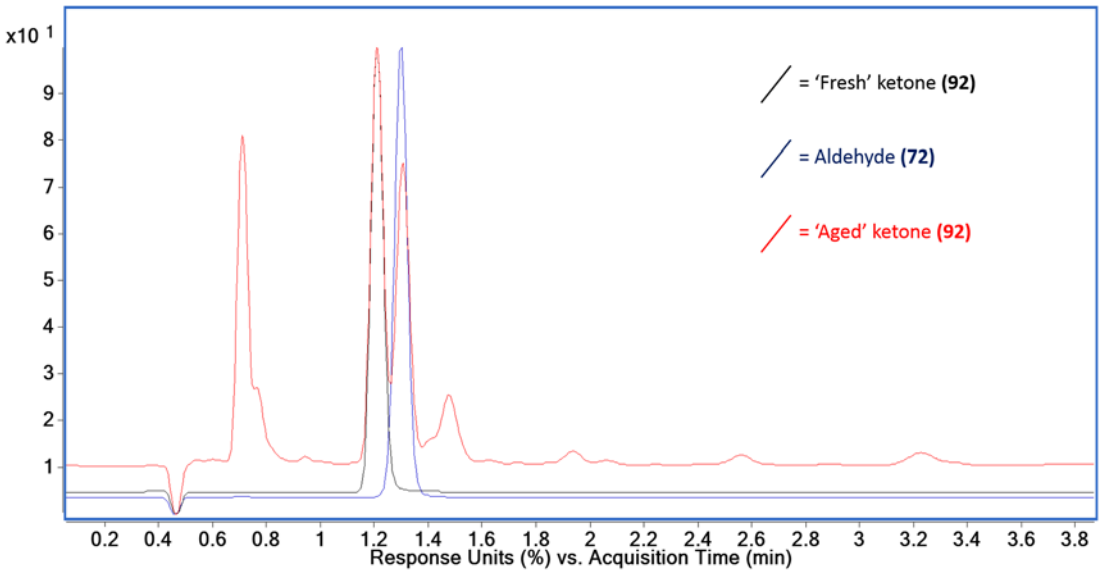


Figure 3.39: Overlays of HPLC runs (@210 nm) of pure aldehyde (72), pure ('fresh') ketone (92) and an aged sample (≈2.5 years) of ketone (92) synthesised *via* the 'Nitrostyrene route'

(Carried out on Agilent LC-MS system (see Section 5.1), mobile phase = 50/50 'CH$_3$CN'/'H$_2$O' (isocratic), flow rate = 1.5 mL/min, column = Agilent Zorbax Eclipse XDB-C18, 3.5 µm, 4.6×75 mm @ 20 °C)

^{1}H-NMR evidence of this degradation of ketone **(92)** to aldehyde **(72)** can be found in Figure 3.40. This is most evident by the presence of the characteristic aldehyde shift (@ δ 10.44) in the 'aged' ketone.

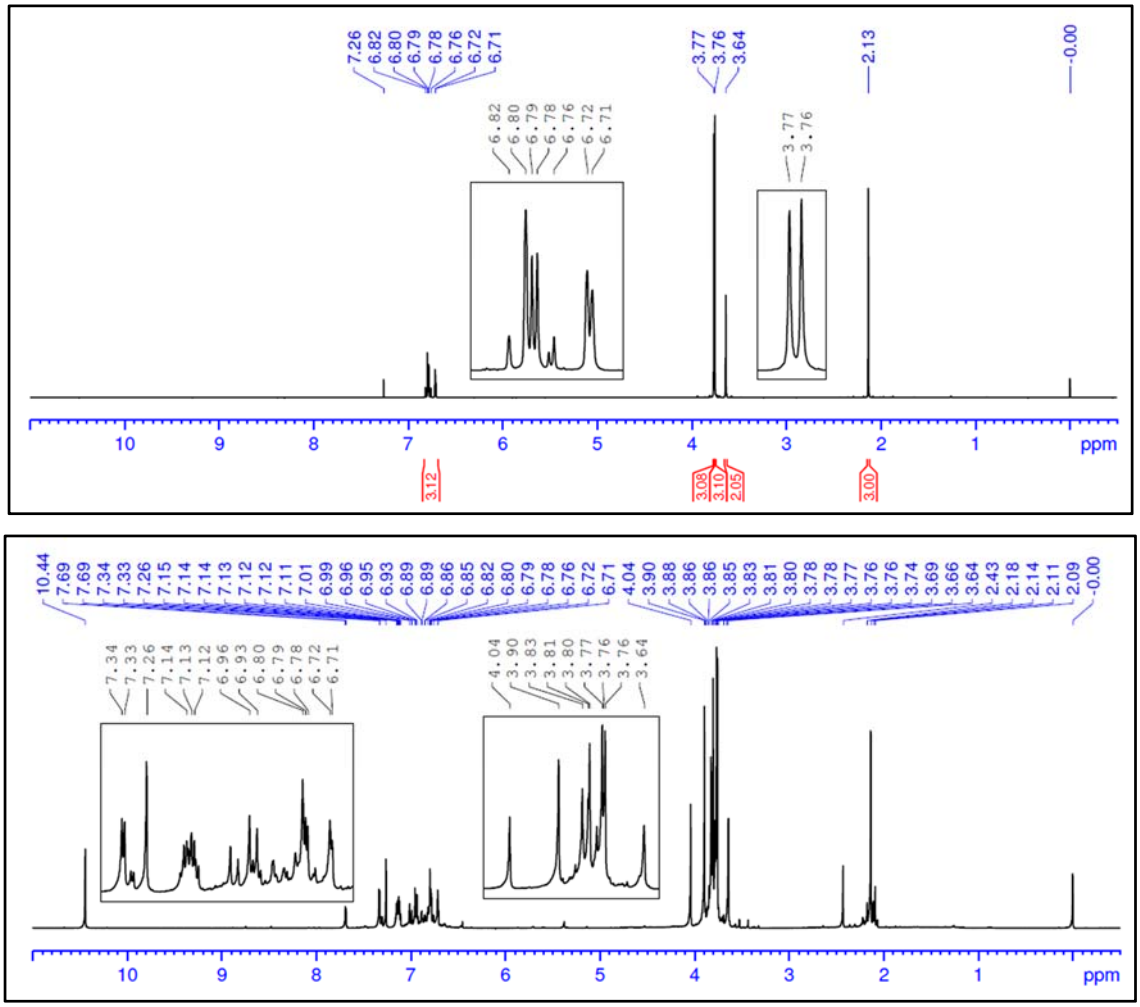
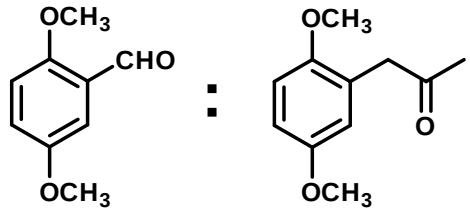


Figure 3.40: ^{1}H-NMR spectra of 'fresh' ketone (92) (top) and 'aged' ketone (92) (bottom)

Figure 3.41 consists of a graph outlining the ratio of aldehyde **(72)** to ketone **(92)** over a period of about 3.5 years (originally synthesised in-house *via* the 'Nitrostyrene route'). The ratio was calculated based on the integration of the aldehyde (CHO) shift and the integration of the ketone CH_3 signal shift (÷ 3):



(72) **(92)**

$$\frac{\int \text{Peak area under } CHO \text{ shift}}{1} : \frac{\int \text{Peak area under } CH_3 \text{ shift}}{3}$$

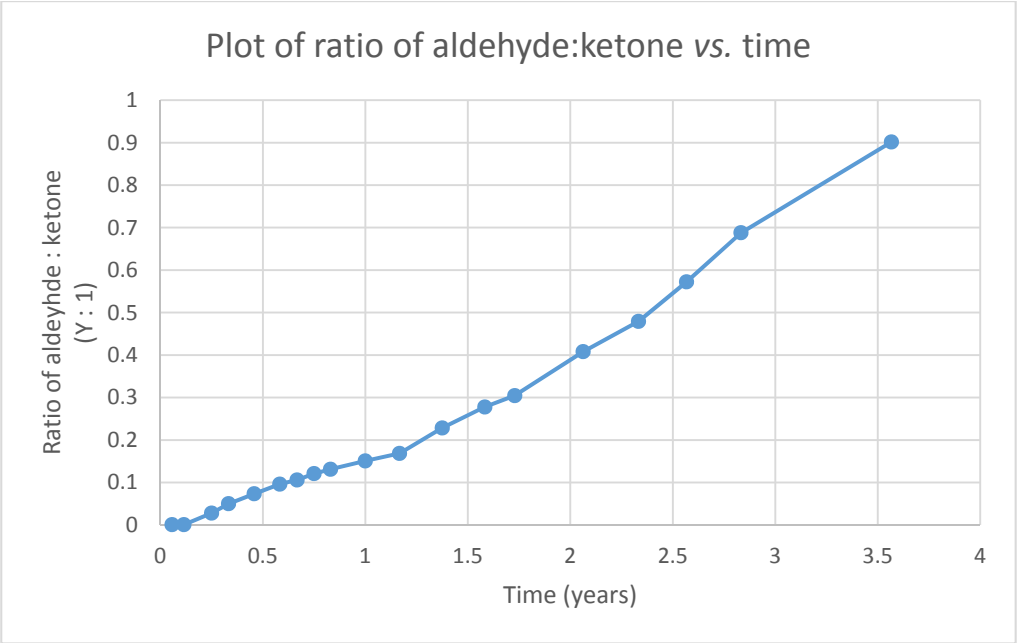


Figure 3.41: Plot of ratio of aldehyde (72) : ketone (92) over time

Initially it was not clear how this degradation was occurring. What was clear was that the degradation was somehow induced by either light, heat, oxygen (or possibly a combination). This was made evident by the fact that a sample of the ketone, stored in a freezer (@ –18 °C), did not show any signs of degradation, even after one year of storage. In an attempt to test if the degradation may be light induced, a fresh sample of the ketone was placed under short wave (≈254 nm) and long wave (≈365 nm) light for ≈3 h. It was thought that if the degradation was largely influenced by light, accelerated degradation at one of these wavelengths may occur. However, no evidence of degradation was observed over the 3 h period.

To rule out if degradation was a consequence of the synthetic route employed (due to a residual compound or species in the sample), tracking of the progress of degradation was also carried out on ketone samples recovered from the two other synthetic routes explored – the 'PAA route' and 'Darzens route'. The samples of 2,5-P2P **(92)** synthesised *via* these routes were stored in a similar manner to the sample prepared *via* the 'Nitrostyrene route' described earlier (i.e. in a round bottom flask in the fume hood with the neck covered in Parafilm®). Plots of the degradation of **(92)** synthesised *via* the 'PAA route' and 'Darzens route', combined with a section of the plot from Figure 3.41 (for the 'Nitrostyrene route'), are depicted in Figure 3.42.

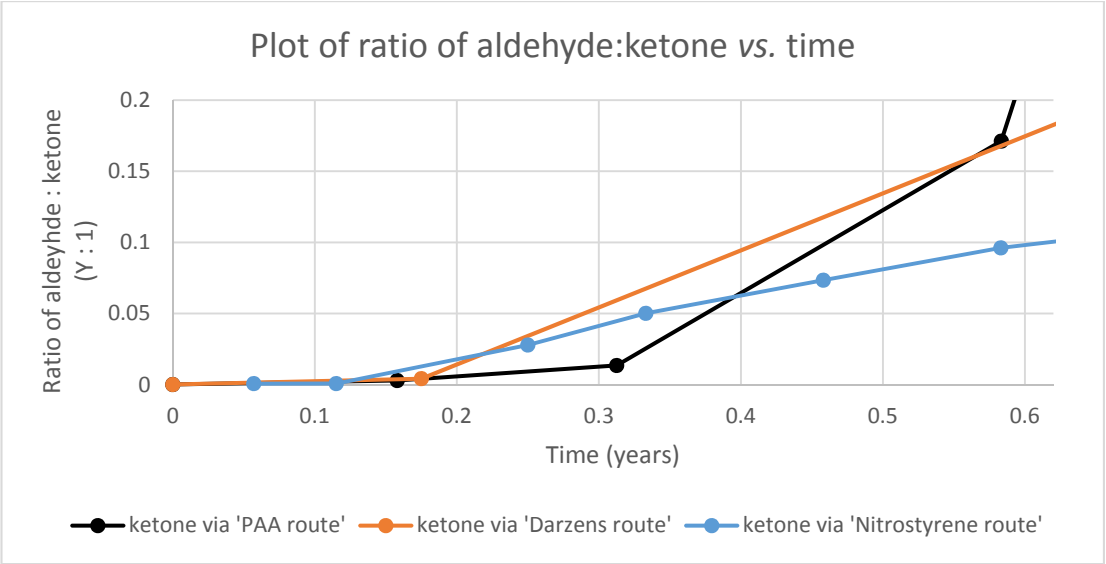
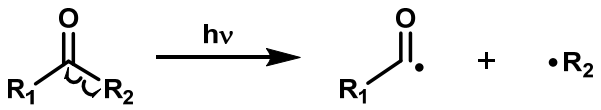


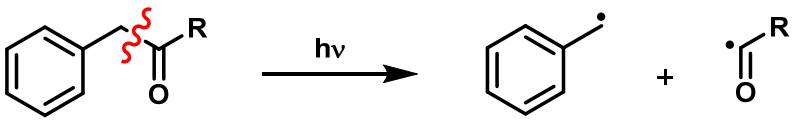
Figure 3.42: Plot of ratio of aldehyde (72) : ketone (92) over time, for ketone synthesised *via* the 'PAA', 'Darzens' and 'Nitrostyrene' routes

The plots in Figure 3.42 suggest that despite the method used to manufacture 2,5-P2P **(92)**, degradation is evident within a few months of manufacture. Having said this, the rate of degradation is different from one route to the next. However, this may be due to the different samples having different levels of exposure to air (due to Parafilm® failure).

A mechanistic basis for this phenomenon may be provided by literature in the field of photochemistry. Carbonyl compounds are commonly known to undergo α-cleavage (or Norrish type I reaction). In this process, a bond adjacent to the carbonyl is homolytically broken and a pair of radicals is formed:[222]



The α-cleavage will almost always favour bond breakage between the carbonyl group and the more substituted adjacent carbon atom. The initial pair of radicals will often seek to produce stable products. This is usually achieved through the abstraction of a hydrogen atom from another fragment, and/or recombination of the radical with other radical species. In particular, α-aryl ketones have been well studied in terms of their photochemistry. Of this group of compounds, P2P **(65)** and dibenzylketone **(80)** have been well explored, mainly due to the ease in which they produce benzyl radicals **(243)** during photolysis:[223,224]



R = CH_3 **(65)**
R = CH_2Ph **(80)**

(243)

The photolysis of dibenzylketone **(80)** is well described by Ruziska *et al.*.[225] In homogenous solutions, the photolysis of dibenzylketone **(80)** promotes it to the singlet excited state (S_1). This undergoes intersystem crossing (ISC) to the triplet state (T_1), which undergoes rapid primary α-cleavage, followed by slower decarbonylation (Figure 3.43). The triplet radical pairs (^{3}D and ^{3}D') formed, must intersystem cross to singlet radical pairs (^{1}D and ^{1}D') before they recombine with other radicals forming either bibenzyl **(214)** or the SM **(80)**.

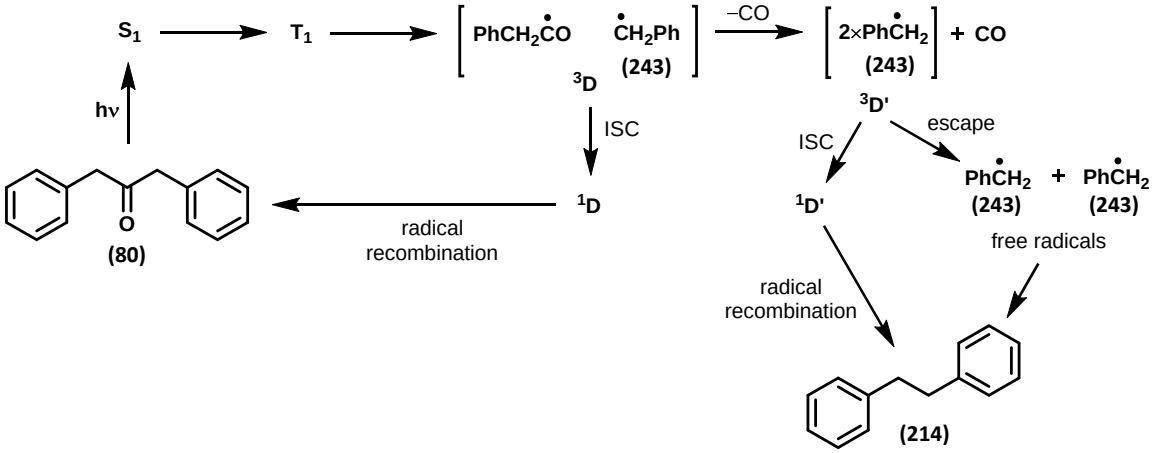
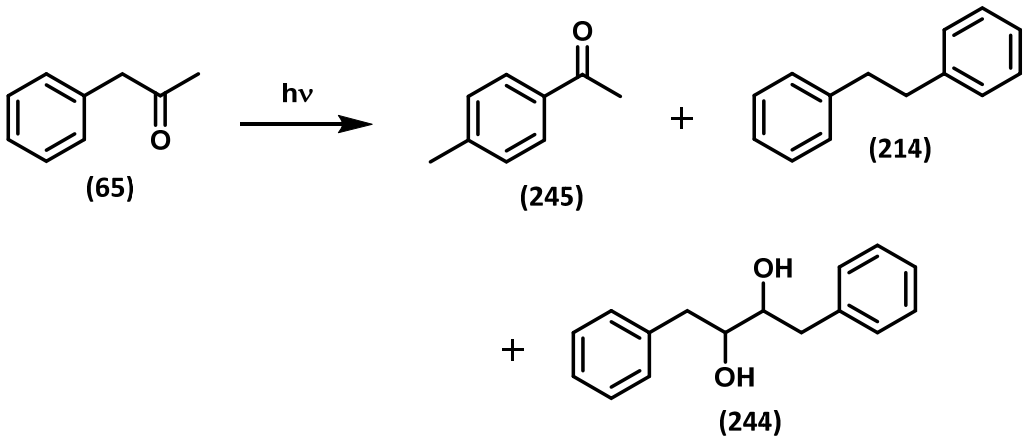


Figure 3.43: Photolysis of dibenzylketone (80)[225]

Alternatively, one of the triplet radical pairs (^{3}D') may escape the solvent cage, to produce free benzyl radicals. These free benzyl radicals **(243)** may recombine to form bibenzyl **(214)**, undergo oxidation (e.g. with copper(II) chloride to form benzyl chloride) or be trapped by oxygen to produce peroxy radicals. In the case of P2P **(65)**, other products such as pinacol **(244)** and ketone **(245)** may result from photolysis. As reported by Houk,[226] irradiation of P2P **(65)** in hexane results in the following:



A number of papers have reported the detection of benzaldehyde **(76)** following photolysis of P2P **(65)**.[227,228] As mentioned, a paper by Ruziska *et al.*[225] refers to the fact that free benzyl radicals **(243)** may become trapped by oxygen to produce peroxy radicals. A paper by Tada *et al.*[229] goes another step further and describes how this peroxy radical may abstract a hydrogen atom from another species,

forming hydroperoxide, which upon loss of water forms benzaldehyde **(76)**. This proposed path is the most plausible explanation for the origin of benzaldehyde **(72)** in aged samples of 2,5-P2P **(92)**. The pathway outlined by Tada *et al.*[229] was adapted to depict the degradation of 2,5-P2P **(92)** in Figure 3.44.

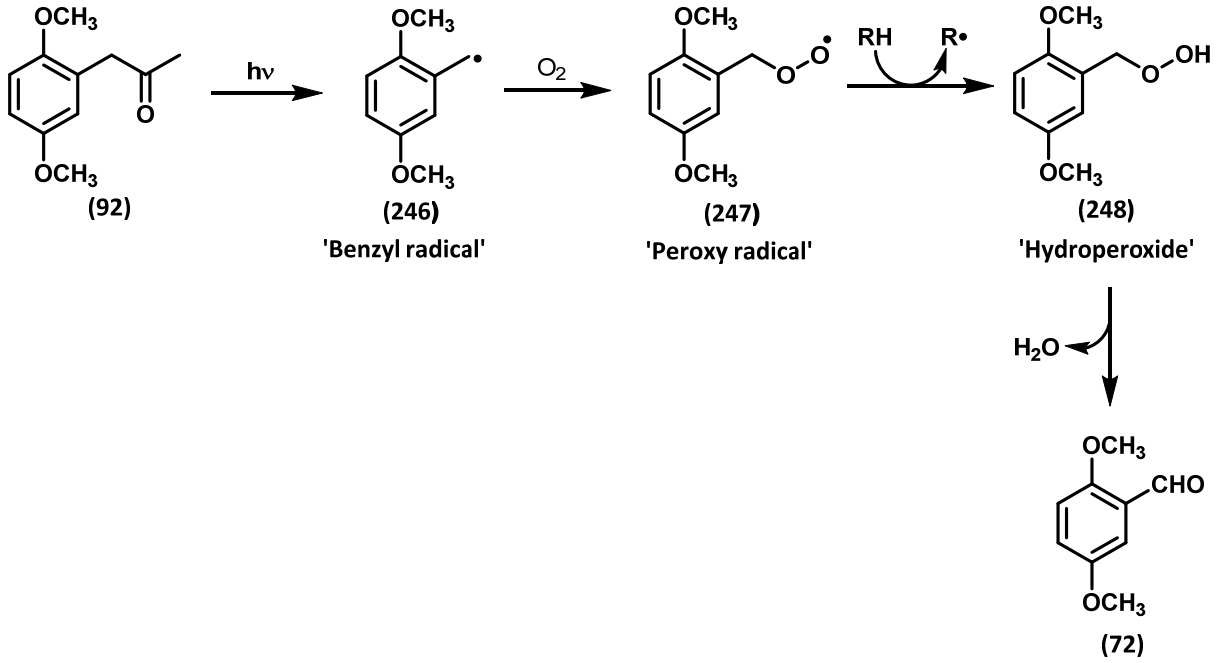
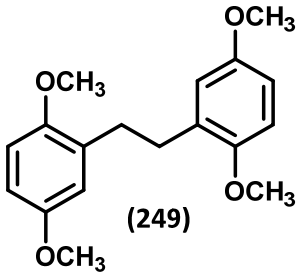


Figure 3.44: Plausible route for formation of benzaldehyde (72) following photolysis of 2,5-P2P (92)

Many papers cite bibenzyl **(214)** to be a major product of the photolysis of α-aryl ketones (Figure 3.43). However, even after prolonged degradation of 2,5-P2P **(92)**, no evidence could be found (in the ^{13}C-NMR DEPT135 spectrum – *C*H_2 signals in negative phase) for the presence of ring-substituted bibenzyl **(249)**.



A possible explanation for this is that the benzyl radicals **(246)** formed are scavenged by O_2 at a faster rate, than the rate of recombination of benzyl radicals (to form bibenzyl **(249)**).[230]

The bibenzyl compound **(214)** has previously been shown to be an impurity of illicitly manufactured P2P **(65)** (Table 3.1). In a paper by Allen *et al.*,[193] bibenzyl **(214)** was determined to be 'route specific' to the PAA route, whereby $Pb(OAc)_2$ **(75)** is used instead of Ac_2O **(66)**. Based on what we have learned from the literature on photolysis of α-aryl ketones, it would be incorrect to assign this impurity as 'route specific' given that under certain photolysis conditions (absence of O_2), bibenzyl **(214)** has been shown to be a light-induced degradation product of P2P **(65)**.

3.8 Summary

As shown in Figure 3.37, three synthetic routes to 2,5-P2P **(92)** were explored in this chapter. Of these, two were looked at in great detail – the 'PAA route' and the 'Darzens route'.

For the PAA route to 2,5-P2P **(92)**, a number of impurities were isolated and characterised including the aldehyde **(72)**, monomeric enol acetate **(219)**, dimeric enol acetate **(220)** and dibenzylketone **(221)**. Dibenzylketone **(221)** is an important impurity due to its difficult isolation (from 2,5-P2P **(92)**) and its ability to undergo similar reactions to **(92)**, if carried through to subsequent reaction steps.

The effect of varying the equivalents of Ac_2O **(66)** used, on the yields of both 2,5-P2P **(92)** and dibenzylketone **(221)**, was explored. It was found that the dominant product formed (either 2,5-P2P **(92)** or dibenzylketone **(221)**) was highly dependent on the number of equivalents of Ac_2O **(66)** used. Interestingly, it was found also that even when a large excess of Ac_2O is used (12 eqv.), the formation of the dimeric impurity **(221)** cannot be avoided. As a result, clandestine manufacturers would find it very difficult to avoid formation of the impurity, making it likely to be carried forward to subsequent reaction steps (for example, the Leuckart reaction – see Section 4.4). In addition to 2,5-P2P **(92)**, the PAA route to its 4-bromo counterpart (4-Br-2,5-P2P **(159)** – precursor to DOB **(35)**), was also explored. The results obtained were similar to those of 2,5-P2P **(92)**.

The 'Darzens route', which uses a glycidic ester intermediate, is a relatively new method of synthesising ketone precursors to illicit ATS. The route was examined as a possible route of manufacture of 2,5-P2P **(92)**. Only one procedure was found[218] (on a website dedicated to clandestine chemistry) for the synthesis of 2,5-P2P **(92)** *via* a glycidate intermediate. The procedure, if followed *verbatim*, results in a very poor yield of **(92)**, with substantial aldehyde **(72)** present. However, optimisation of the reaction (by changing solvent and work-up procedure) resulted in much greater yields, making it a viable route to 2,5-P2P **(92)**, as well as 4-Br-2,5-P2P **(159)**.

The degradation of 2,5-P2P **(92)** was highlighted also in this chapter. It was found that as ketone **(92)** aged (most likely due to photolysis-induced α-cleavage), aldehyde **(72)** became more abundant in the sample. This was monitored by ^{1}H-NMR spectroscopy and HPLC. A plausible scheme for the degradation process was also proposed based on photolysis literature.[229] This was proposed based on the assumption that in the presence of O_2, aldehyde **(72)** is the dominant degradation product formed. Possible future work in this area may involve placing the sample under vacuum (or under a blanket of N_2) to investigate if the bibenzyl compound **(249)** forms predominantly. It is important for this degradation phenomenon to be highlighted, as some of the literature on impurity profiling uses the degradation products (e.g. aldehyde **(76)** and bibenzyl **(214)**) to incorrectly assign route of manufacture.

Chapter 4 – Impurity profiling of the bromination of 2,5-dimethoxyphenyl-2-propanone and its dimeric analogue 1,3-bis(2,5-dimethoxyphenyl)-2-propanone

DOB is the most potent of the 'D series' amphetamines. Its synthesis will inevitably require introduction of a bromine atom at the aromatic 4-position. This bromination, unlike other steps in the sequence, may in theory be carried out at various different stages of the synthesis. The point at which the bromination is carried out is very important from an impurity profiling perspective. Bromination of one particular SM/intermediate may be very 'clean' and high yielding, whist another may result in a low yield with numerous unwanted impurities. Also, the later in the synthetic sequence that the bromination step takes place, the more intermediates/by-products will be present and thus susceptible to bromination.

Two compounds which may be present as intermediates/by-products in the synthesis of DOB are 2,5-P2P and its dimeric analogue 1,3-bis(2,5-dimethoxyphenyl)-2-propanone ('dibenzylketone'). The impurity profiling of the bromination of these two compounds is examined in this chapter. Identification/characterisation of many of the compounds produced is carried out. In the case of some poorly resolved or novel compounds, selective synthesis is performed as a way of attaining reference standards. LC-MS is also utilised in an attempt to identify complex mixtures of compounds that are poorly resolved by flash column chromatography.

The Leuckart route to DOB (from 2,5-P2P) has been investigated previously within our research group. A number of pyridine, pyrimidine and *N*-formyl-based impurities were found to arise during this route of manufacture. The dibenzylketone, a potential major impurity of 2,5-P2P, is thought to possess similar reactivity and if subjected to Leuckart reaction conditions, may result in a series of dimeric impurities (pyrimidines etc.) also being present in the final drug product. The potential of these compounds, to arise as impurities of DOB, is investigated also in this chapter.

4.1 Illicit synthesis of DOB

Very little is known about the specific routes used by clandestine chemists in the manufacture of DOB **(35)**. A paper by Delliou[87] reported the methodology used by two laboratories that were dismantled by authorities. One of these laboratories synthesised DOB *via* the aldehyde→nitrostyrene→amine→4-bromo-amine (DOB) route (Figure 1.19), whilst the other synthesised DOB *via* an eight-step sequence

using a hydroquinone SM **(71)** (see Section 1.2.7). As no more recent reports could be found, it can be assumed that books/fora dedicated to clandestine chemistry, are being used as the primary source of information on DOB manufacture.

Alexander T. Shulgin was the first to report the synthesis of DOB in 1971. This synthesis, together with the synthesis of many other phenethylamines/amphetamines, were compiled in PiHKAL, published in 1991.[12] This book is likely to be used as an information source for clandestine chemists. Shulgin's method was in fact, found to be used in the first clandestine laboratory described previously, and is summarised in Figure 4.1. In this method, bromination is carried out as the final step in the sequence and according to the work by Griffin,[26] DOB is formed exclusively, and in high yield during the bromination step. The only reported potential impurity of this step is DMA **(31)**, arising only when an insufficient amount of Br_2 is used.

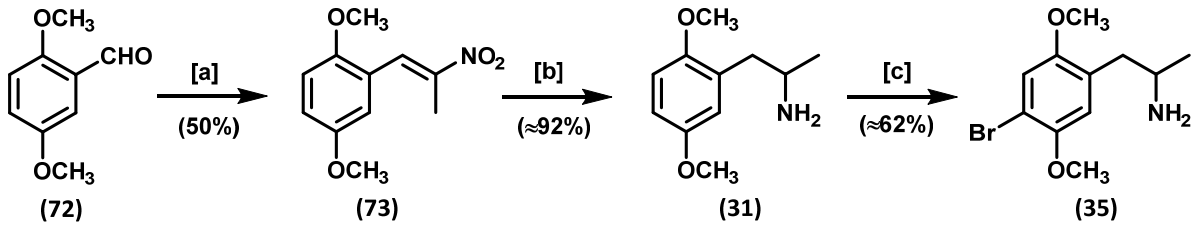


Figure 4.1: Shulgin's DOB synthesis[12]

([a] = $CH_3CH_2NO_2$, AcOH, NH_4OAc, 100 °C, 3 h; [b] = $LiAlH_4$, Et_2O, reflux, 20 h; [c] = Br_2, AcOH, rt, 3 h)

Alternatively, a number of methods exist whereby DOB pre-precursors undergo bromination at the beginning of the sequence. Two of these methods have already been explored in this work – the bromination of 2,5-dimethoxybenzaldehyde **(72)** (see Section 2.2) and the bromination of 2,5-dimethoxyphenylacetic acid (2,5-PAA) **(108)** (see Section 3.3.1). The efficiencies of these two methods are vastly different. The bromination of 2,5-PAA **(108)** was found to produce the desired 4-bromo product **(164)** exclusively, and in a high yield (82%). In the bromination of aldehyde **(72)**, a good yield of 4-bromo aldehyde **(160)** was produced (74%). However, at least 5 other brominated compounds were detected as impurities of this latter reaction. These impurities may be carried forward through subsequent reaction steps and possibly form additional ('secondary') by-products.

These results highlight the fact that, the point in the reaction sequence at which bromination takes place and the intermediate chosen to undergo bromination, may have a substantial influence on the impurity profile of illicitly produced DOB **(35)**.

4.1.1 Synthesis of 4-Br-2,5-P2P (159)

The brominated ketone precursor to DOB (4-Br-2,5-P2P **(159)**) has been previously synthesised in this work *via* the 'PAA' and 'Darzens' routes (Chapter 3). Its synthesis, *via* the 'PAA route', involved

bromination of the acid SM **(108)** (Step 1), followed by the 'PAA reaction' (Step 2) (Figure 4.2, blue route). Step 1 was clean and efficient while Step 2 was low yielding, with four impurities recovered following flash column chromatography (yields and number of impurities outlined in Table 4.1). In a possible alternative synthesis of 4-Br-2,5-P2P **(159)**, the order of these steps may be reversed so that the 'PAA reaction' occurs first, followed by bromination of the ketone **(92)** (Figure 4.2, red route). Step 1 of this method had been previously carried out (Section 3.2) and was found to produce the ketone **(92)** in low yield, with four impurities recovered (Table 4.1). The outcome of the bromination (using Br_2/AcOH) of 2,5-P2P **(92)** is not known.

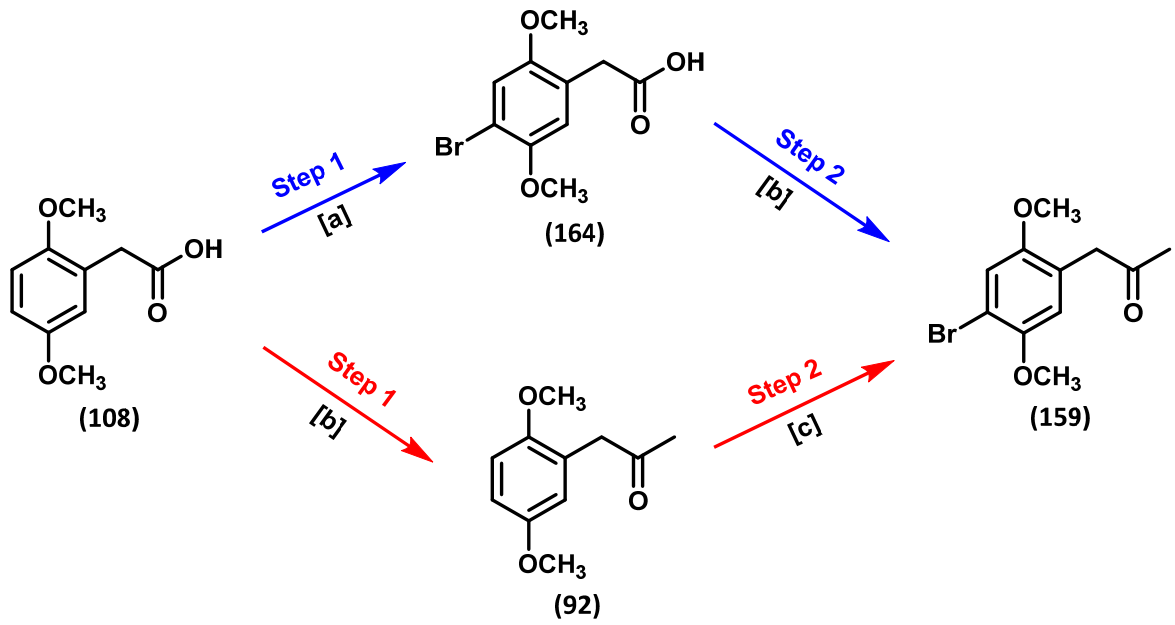


Figure 4.2: Synthetic strategies, based on PAA route, to DOB precursor (159)

([a] = Br_2 (1.2 eqv.), AcOH, rt, 2 h; [b] = pyridine (6 eqv.), Ac_2O, (6 eqv.), Δ, 7 h; [c] = Br_2 (1.2 eqv.), AcOH, rt, 24 h)

Table 4.1: Yields and number of impurities isolated, from reaction steps in Figure 4.2

	% Yield	No. of impurities isolated
Step 1	82	0
Step 2	38	4
Step 1	35	4
Step 2	?	?

The bromination (Br_2/AcOH) of 2,5-P2P **(92)** is not documented in the literature, so it is unlikely to be pursued as a method of synthesising DOB precursors. However the reaction is likely to occur (inadvertently) if the bromination of DMA **(31)** (contaminated with 2,5-P2P **(92)**) were attempted. For this reason, potential impurities arising from this bromination were investigated. The findings from this work are outlined in the following Section.

4.2 Impurity profiling of the bromination of 2,5-P2P (92)

When 2,5-P2P **(92)** was subjected to 'standard' bromination conditions (Br_2 (1.2 eqv.), AcOH, rt, 24 h), several compounds were produced, based on the ^{1}H-NMR spectrum of the crude reaction following work-up. Surprisingly, only a trace amount of 4-Br-2,5-P2P **(159)** was detected, which equated to a mere 1% isolated yield following flash column chromatography. This rules out the red route in Figure 4.2 as a viable method of synthesising 4-Br-2,5-P2P **(159)** from the acid SM **(108)**.

Aside from a small amount of unreacted SM **(92)**, the remaining compounds in the mixture had not previously been encountered. Based on ^{1}H-NMR evidence, it was suspected that bromination had occurred at the benzylic position (due to presence of signals @ δ ≈6) and at the terminal α-keto position (due to presence of signals @ δ ≈4.2). Following flash column chromatography, a number of compounds were identified. Some were fully isolated and characterised, others, which were unresolved, were identified following comparison with selectively synthesised standards. The compounds identified (three of which were fully isolated) are summarised in Figure 4.3. Their characterisation is discussed in the next section.

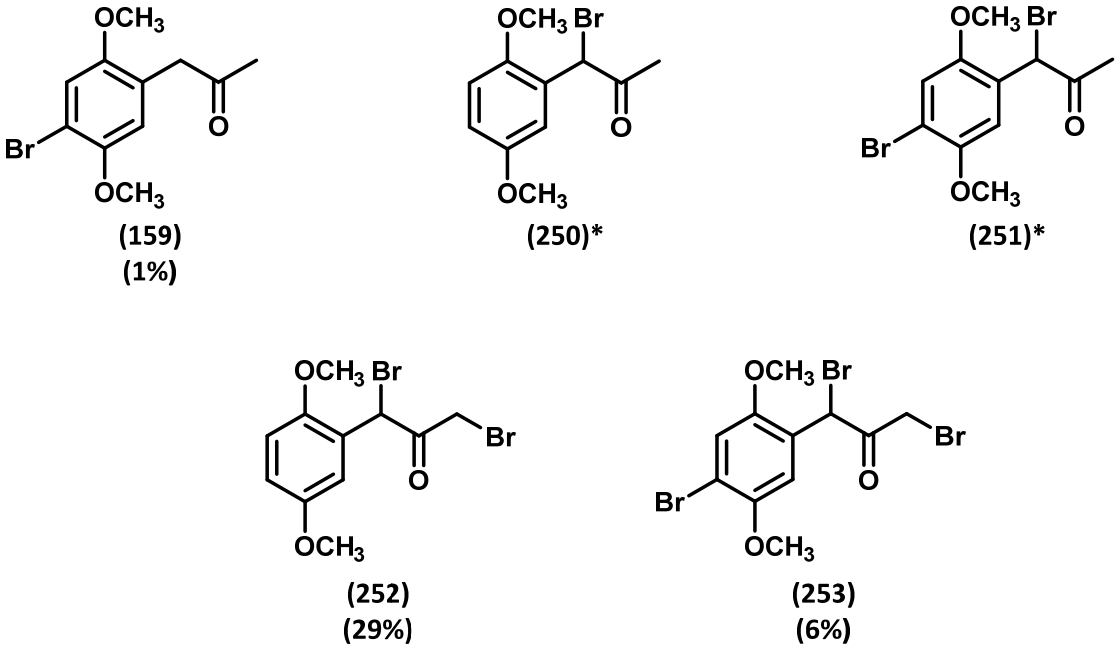


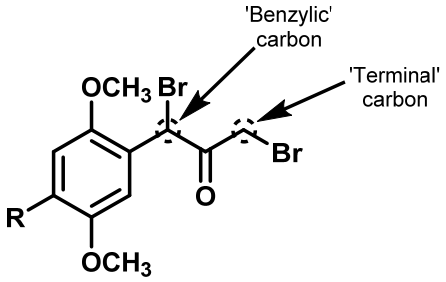
Figure 4.3: Compounds identified following bromination of 2,5-P2P (92)

(= compound not isolated)*

4.2.1 Terminal α-keto-bromo compounds (252) and (253)

As indicated in Figure 4.3, two compounds were isolated from the bromination of 2,5-P2P **(92)**, with a bromine atom at the terminal carbon of the ketone side chain. As both of these compounds were fully

isolated, their characterisation and subsequent identification could be carried out. These data are presented in Table 4.2 below.



R = H **(252)**
R = Br **(253)**

Table 4.2: Yield, R_f, m.p., IR and HRMS data for terminal-bromo compounds (252) and (253)

Compound No.	Yield	m.p. (°C)	R_f*	IRν_{max} (cm^{-1})	HRMS (M+H$^+$) (*m/z*)	
					Calc.	Found
(252)	29%	80–82 (EtOH)	0.68	1742 (C=O), 1588, 1502 (C=C)	350.9231*	350.9225
(253)	6%	(Oil)	0.81	1733 (C=O), 1578, 1506 (C=C)	428.8337$^\blacktriangle$	428.8326

*mobile phase = 70:30 Et_2O:hexane
*molecular ion (M) calculated for $^{79}Br_2$ isotope peak
$^\blacktriangle$molecular ion (M) calculated for $^{79}Br_3$ isotope peak

For the first compound **(252)**, whereby no aromatic ring bromination had taken place, structure elucidation was provided by ^{1}H-NMR spectroscopy. The signals that were most useful in terms of structure determination were as follows:

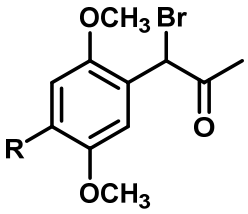
- Aromatic signals (δ 6.8–7.05 region) – Splitting characteristic of an ABX pattern was observed, i.e. 1H, **d** (*J*=9 Hz), 1H, **dd** (*J*=9 and 3 Hz) and 1H **d** (*J*=3 Hz). This indicates that no further substitution of the aromatic ring had taken place, compared to that of SM **(92)**.
- 1H, singlet in region of δ ≈6 – Indicative of benzylic bromination.
- 2 × 1H doublets (*J*=13 Hz) @ δ ≈4.2 – Indicative of bromination at the terminal carbon of the ketone side chain. The geminal coupling (*J*=13 Hz) arises from the two diastereotopic protons adjacent to the terminal bromine atom. This phenomenon has been observed for structurally similar compounds in the literature.[231]

Bromine substitution at two sites was also evident based on the MS data for **(252)**. A triplet molecular ion (M+H$^+$) was observed (ratio ≈ 1:2:1, lowest *m/z* peak of triplet @ ≈351 representing the $^{79}Br_2$ isotope in Table 4.2 above), which would indicate that the molecule possesses two bromine atoms.

The ^{1}H-NMR spectrum of the second compound **(253)** was similar to that of the first **(252)**, in that the same evidence for benzylic and terminal bromination was observed. There was however, a great difference in the aromatic region for compound **(253)**, with two singlets being observed. This is indicative of additional substitution at the aromatic 4-position. Evidence of this is supported by ^{13}C-NMR spectroscopy, with one more 'quaternary' carbon signal and one less C–H signal observed in the spectrum of aromatic 4-bromo **(253)**, compared to that of non-bromo **(252)**. The additional bromine substitution was also evident in the mass spectrum of **(253)**; the quartet molecular ion ($M+H^+$) (ratio ≈ 1:3:3:1) indicating that the molecule possesses three bromine atoms (lowest *m*/*z* peak of quartet @ ≈429 representing the $^{79}Br_3$ isotope in Table 4.2).

4.2.2 Benzyl-bromo compounds (250) and (251)

Compounds that were brominated at the benzylic position (without also being brominated at the terminal position) were detected during the 'standard' bromination of 2,5-P2P **(92)** (see Figure 4.3). However, these compounds (**(250)** and **(251)**) could not be separated by flash column chromatography (due to co-elution).



R = H **(250)**
R = Br **(251)**

By comparing the integration of the benzylic protons of **(250)** and **(251)**, with those of the isolated terminal/benzyl-bromo compounds **(252)** and **(253)**, it was estimated that **(250)** and **(251)** were produced in approximate yields of 17% and 4% respectively. As these compounds were novel, it was decided to carry out their independent synthesis as a way of acquiring reference standards.

Although the selective benzylic bromination of 2,5-P2P **(92)** was not documented in the literature, procedures successful for structurally similar compounds (such as P2P **(65)**), were available. In the case of P2P **(65)**, some authors found selective benzylic bromination to occur under 'standard' bromination conditions.[232,233] However, in the case of 2,5-P2P **(92)**, this selective bromination clearly does not occur (Section 4.2). The most common selective benzylic bromination methods in the literature involve the use of *N*-bromosuccinimide (NBS) in a radical-type mechanism. Radical initiation may be light induced, by chemical means (e.g. azobisisobutyronitrile (AIBN), benzoyl peroxide) or both.[234-236] A scheme explaining selective benzylic bromination was proposed by McMurry.[237] An adaptation of this scheme, showing benzylic bromination of ketones **(92)** and **(159)**, is outlined in Figure 4.4.

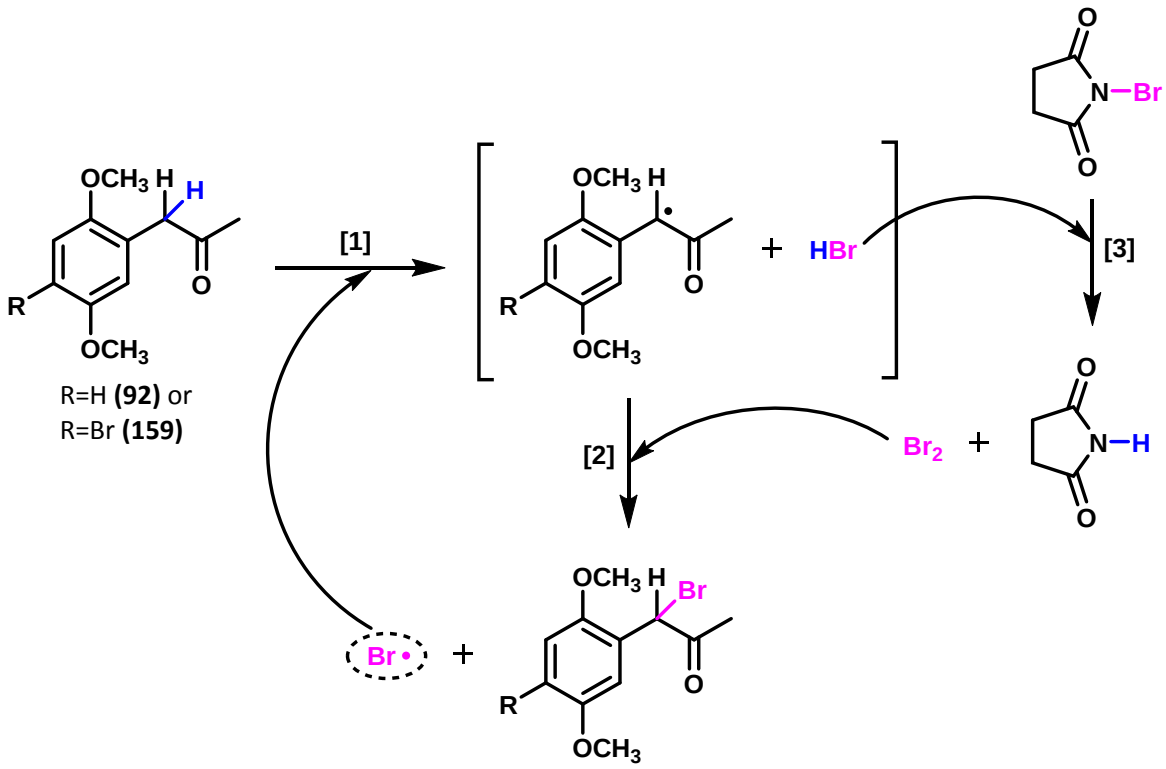
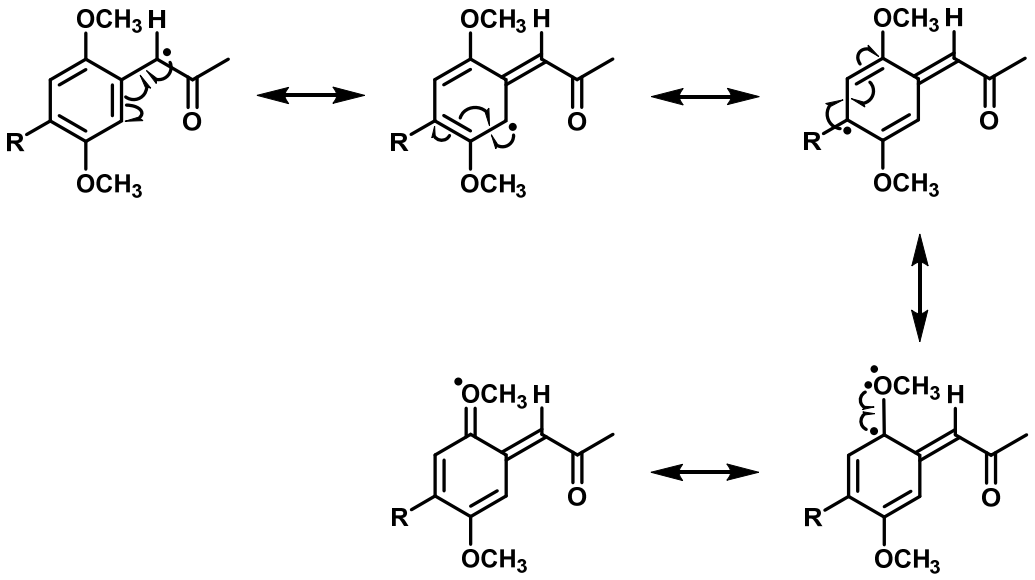
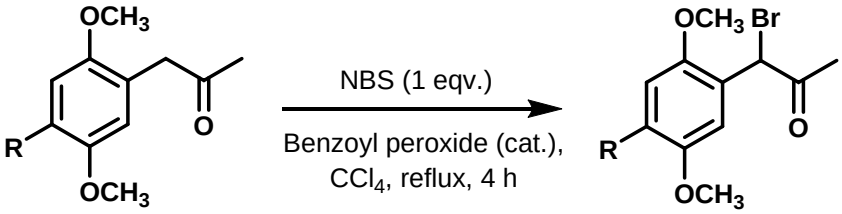


Figure 4.4: Proposed scheme for selective benzylic bromination of ketones (92) and (159)[237]

The first step in this scheme involves abstraction of a benzylic hydrogen atom by a bromine radical (Br•). This initial Br• is probably generated following attack of Br_2 by the homolytic product of the radical initiator. This abstraction of the benzylic hydrogen generates a stabilised intermediate benzyl radical, which reacts with Br_2 in the second step to yield the benzyl-bromo product and a Br• radical. The Br• radical cycles back into the reaction to carry on the chain. The Br_2 necessary for reaction with the benzyl radical is produced in the third step above, by a concurrent reaction of HBr and NBS. The reaction is said to occur exclusively at the benzylic position because the benzyl radical intermediate is stabilised by resonance:



The methodology used in the selective synthesis of benzyl-bromo compounds **(250)** and **(251)**, is outlined in Figure 4.5. It was adapted from a procedure used by Lange *et al.*.[238]



R = H **(92)**
R = Br **(159)**

R = H **(250) (74%)**
R = Br **(251) (53%)**

Figure 4.5: Selective benzylic bromination of 2,5-P2P (92) and 4-Br-2,5-P2P (159)

When the selective bromination, as outlined in Figure 4.5, was performed using 2,5-P2P **(92)**, a yield of 74% of benzyl-bromo **(250)** was isolated following flash column chromatography. The R_f, IR and MS data collected for **(250)** are summarised in Table 4.3.

Table 4.3: Yield, R_f, IR and HRMS data for benzyl-bromo compound (250)

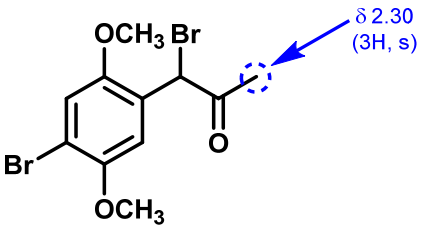
Compound No.	Yield	R_f*	IRν_{max} (NaCl) (cm^{-1})	HRMS ($M+H^+$)⋆ (*m/z*)	
				Calc.	Found
(250)	74%	0.58	1734 (C=O), 1588, 1506 (C=C)	273.0126	273.0120

*mobile phase = 70:30 Et_2O:hexane
⋆molecular ion (M) calculated for ^{79}Br isotope peak

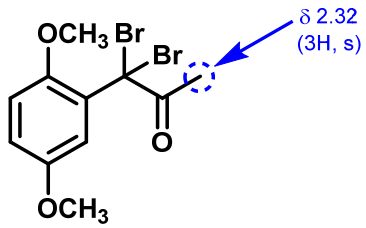
The ^{1}H-NMR spectrum obtained for **(250)** was as expected. The typical ABX splitting was observed for the aromatic ring protons at positions 3, 4 and 6 (i.e. 1H, **d** (*J*=9 Hz), 1H, **dd** (*J*=9 and 3 Hz) and 1H **d** (*J*=3 Hz). The benzylic proton, adjacent to the bromine atom, resonates at δ 5.87, the methoxy group protons at δ 3.77 and 3.82, and the terminal methyl protons at δ 2.27. Successful product formation was indicated in the ^{13}C-NMR spectrum, by the disappearance of a CH_2 carbon @ 45.54 ppm (negative phase in DEPT135) and the appearance of a new C–H carbon signal (@ 51.45 ppm).

Also detected during column chromatography was SM **(92)** (≈15%), as well as trace amounts of aromatic 4-bromo compound **(251)**, and what was speculated to be dibromo benzyl compound **(254)**. Dibromination at the benzylic position had also been observed by Podgoršek *et al.*[235] during selective benzylic bromination of P2P **(65)**.

(Note: As a pure sample of **(254)** was not obtained during this work, it could not be fully characterised. Its identity therefore is speculative.)



(251)



(254)

Keeping the number of eqv. of NBS at 1 was important for minimising formation of the dibromo benzyl compound **(254)**; using an excess of NBS was found to produce a substantial amount of **(254)** which was difficult to resolve, by column chromatography, from desired product **(250)**. The presence of dibromo **(254)** was most evident in the ^{1}H-NMR spectrum by the appearance of a singlet at δ 2.32, presumably arising from the protons of its terminal methyl group.

The selective benzylic bromination procedure, when carried using 4-Br-2,5-P2P **(159)**, produced benzyl-bromo **(251)** in a 53% isolated yield, following flash column chromatography. The R_f, IR and MS data collected for **(251)** are summarised in Table 4.4.

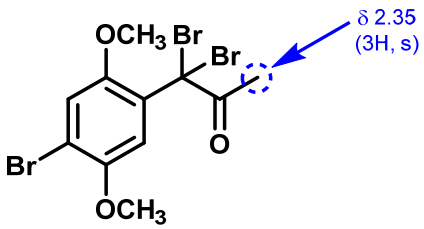
Table 4.4: Yield, R_f, IR and HRMS data for aromatic-4-bromo benzyl-bromo compound (251)

Compound No.	Yield	R_f*	IRν_{max} (NaCl) (cm^{-1})	HRMS (M+H$^+$)* (*m/z*)	
				Calc.	Found
(251)	53%	0.72	1733 (C=O), 1576, 1496 (C=C)	350.9231	350.9240

*mobile phase = 70:30 Et_2O:hexane

*molecular ion (M) calculated for $^{79}Br_2$ isotope peak

The yield was lower than that of its ring unsubstituted counterpart **(250)**, mainly due to a lower degree of reaction completion. Improved consumption of SM could be achieved using excess NBS but again this leads to formation of what was speculated to be dibromo-benzyl product (in this case **(255)**), which is difficult to resolve from the intended product **(251)**. At 1 eqv. of NBS, the suspected dibromo-benzyl **(255)** is only formed in a trace amount, its presence indicated by a singlet at δ 2.35.



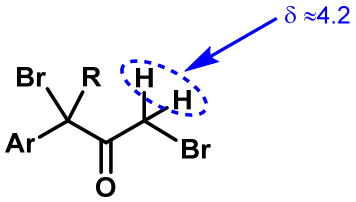
(255)

(Note: As dibromo-benzyl **(255)** was not isolated and characterised, its presence could only be speculated based on the presence of a possible C*H*$_3$ signal (on C-3') and the absence of a benzyl/methylene proton(s) signal (on C-1') in the ^{1}H-NMR spectrum of the mixture.)

The ^{1}H-NMR spectrum of the intended product **(251)** was as expected. The two singlets in the aromatic region indicated that the 4-bromo substituent had remained intact, the singlet (at δ 5.86) was indicative of successful benzylic bromination and the 3H, singlet (at δ 2.30) ruled out any possible 'terminal' bromination.

4.2.3 Bromination of 2,5-P2P (92) using excess Br_2

When the bromination outlined in Section 4.2 was carried out using an excess of Br_2 (2.2 eqv.), the impurity profile of the resulting crude reaction mixture was quite different. Although purification of the crude reaction mixture (by column chromatography) was not pursued, a number of general conclusions could be made by comparing the ^{1}H-NMR data with that of compounds recovered from the 'standard' bromination (1.2 eqv. Br_2) experiment. Firstly, it became clear that using excess Br_2 resulted in highly efficient bromination at the terminal carbon of the ketone side chain. This was evident by the low abundance of signals in the region of δ 2–2.5, typical of terminal methyl ('CH_3') protons. Also, there were a number of new signals in the region of δ ≈4.2. Based on evidence collected for benzyl/terminal-bromo compounds (**(252)** and **(253)**), it may be assumed that a number of compounds of general structure **(256)**, had formed during the bromination reaction.



(256)

R = H or Br

Secondly, a number of signals in the region of δ 6–6.5, that had not previously been observed (during 'standard' bromination), may indicate even more extensive bromination at the terminal position. The protons highlighted in Figure 4.6 below, may all resonate in the region of δ 6–6.5. As no such compounds had been isolated in this work, this is purely speculative. Having said this, compounds of similar structure[231] were found to produce signals resonating in this region.

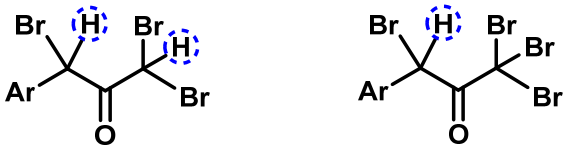
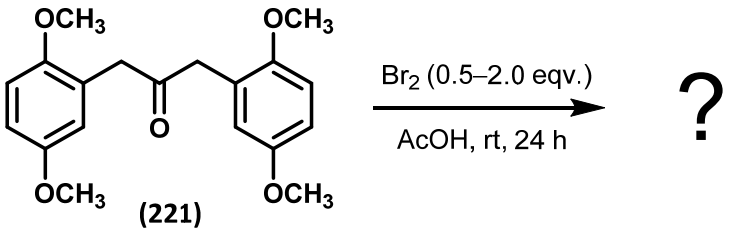


Figure 4.6: Protons that may resonate in the region of δ 6–6.5 ppm, owing to compounds formed during the bromination (@ 2.2 eqv. Br_2) of 2,5-P2P (92)

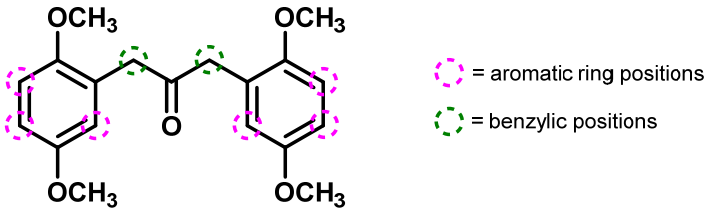
4.3 Impurity profiling of the bromination of 1,3-bis(2,5-dimethoxyphenyl)-2-propanone (221)

1,3-Bis(2,5-dimethoxyphenyl)-2-propanone ('dibenzylketone') **(221)** was previously isolated as an impurity form the PAA route to 2,5-P2P **(92)** (Section 3.2.1.4). Similar to 2,5-P2P **(92)**, it may become exposed to Br_2 if the bromination step is carried out in the latter stages of DOB **(35)** synthesis. As with 2,5-P2P **(92)**, it was decided to investigate what compounds are likely to form if dibenzylketone **(221)** were to become subjected to Br_2, in a clandestine laboratory setting. The number of equivalents (eqv.) of Br_2 used was shown previously to have a substantial effect on product profile, so in the case of dibenzylketone **(221)**, four different eqv. of Br_2 were used – 0.5, 1.0, 1.5 and 2.0 eqv. (see Experimental – Section 5.4.8.1).



According to the ^{1}H-NMR spectra of the crude samples recovered from these bromination experiments, several compounds were produced, with the level of complexity increasing with increasing Br_2 equivalents. Although flash column chromatography was attempted, none of the compounds produced could be isolated and thus identified. Identification of compounds present in the mixture was made even more difficult due to the nature of the dibenzylketone **(221)** structure, with significant overlap of all methoxy/methylene proton signals and all aromatic ring proton signals in the ^{1}H-NMR spectra.

In the case of 2,5-P2P **(92)**, bromination (by Br_2) was found to occur at a number of different sites on the molecule – at the benzylic carbon, at the terminal methyl carbon and at the 4-position (*para*) of the aromatic ring. Due to its dimeric nature, the dibenzylketone **(221)** does not possess a terminal methyl group so it may be envisaged that bromination by Br_2, would most likely occur at the benzylic and aromatic ring positions.



There was strong evidence in the crude ^{1}H-NMR spectra (of the bromination reactions of **(221)**), for benzylic bromination, with a number of signals present in the region of δ ≈6 ppm. As for possible

bromination of the aromatic ring, this was difficult to establish due to extensive signal overlap in the methoxy (δ 3.5–4) and aromatic (δ 6.5–7.5) regions of the ^{1}H-NMR spectra.

As attempts to isolate and thus identify the bromination products (by column chromatography) had failed, it was decided to attempt the controlled independent synthesis of several standards as potential products of the bromination reaction. The availability of these reference materials would greatly aid the identification of unknowns.

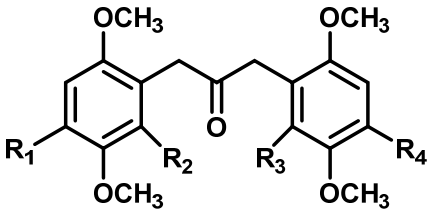
As mentioned, bromination of dibenzylketone **(221)** is most likely to occur at the benzylic and/or aromatic ring positions. With this in mind, the reference standards to be synthesised were divided into two distinct groups:

- Those which vary in the bromination about the **aromatic rings** and
- Those with varying degrees of bromine substitution at the **benzylic positions**

The synthesis of these compounds is discussed in the following sections.

4.3.1 Independent synthesis of a series of aromatic ring–brominated dibenzylketones

In choosing which compounds were to be synthesised as potential bromination products, the findings from previous bromination experiments were taken into consideration. In the 'standard' bromination (by Br_2) of 2,5-P2P **(92)** (Section 4.2), aromatic ring bromination was found only to occur at the 4-position (*para* to ketone side chain). However, in the case of other compounds, such as 2,5-dimethoxybenzaldehyde **(72)** (Section 2.2) significant bromination at the 6-position (*ortho* to aldehyde substituent) was also found to occur. Based on these results, it was decided to independently synthesise five dibenzylketone standards with different bromine substitution patterns at the *ortho*/*para* positions (Figure 4.7). Synthesis of non-bromo dibenzylketone **(221)** was also performed for use in later benzylic bromination experiments (Section 4.3.3).



R_1,R_2,R_3,R_4 = H **(221)**
R_1 = **Br**, R_2,R_3,R_4 = H **(257)**
R_2 = **Br**, R_1,R_3,R_4 = H **(258)**
R_1,R_3 = **Br**, R_2,R_4 = H **(259)**
R_1,R_4 = **Br**, R_2,R_3 = H **(224)**
R_2,R_3 = **Br**, R_1,R_4 = H **(260)**

Figure 4.7: Aromatic ring-brominated dibenzylketones chosen for independent synthesis

A number of methodologies exist in the literature concerning the synthesis of compounds possessing a dibenzylketone core. One such method was attempted previously (Section 3.2.2) and involved a modified version of the PAA route (whereby an alternative base is used), that favours the formation of the dimeric dibenzylketone compound over the monomeric ketone.[191] This was shown previously to be unsuccessful for the selective synthesis of our dibenzylketone **(221)**. Another method used in the synthesis of symmetric dibenzylketones involves using pentacarbonyl iron ($Fe(CO)_5$) to couple two equivalents of benzyl halide **(261)**, in the presence of a phase-transfer catalyst (Figure 4.8).[239]

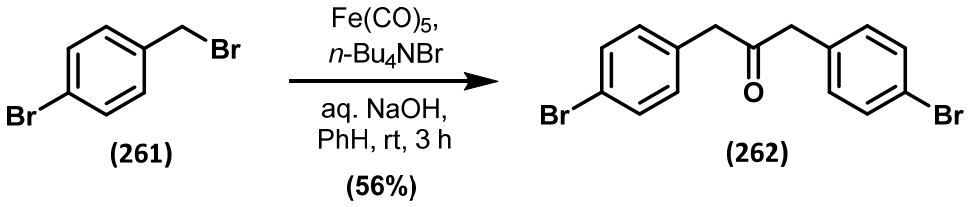


Figure 4.8: Synthesis of a symmetric dibenzylketone *via* phase-transfer catalysis[239]

In terms of asymmetric dibenzylketones, Turro and Weed[223] published a procedure involving the reaction of an acid chloride with an *in-situ* generated dibenzyl cadmium reagent. The dibenzyl cadmium reagent **(263)** had been generated from the reaction of the Grignard reagent ($PhCH_2MgCl$) with cadmium chloride ($CdCl_2$):

$$2\ PhCH_2MgCl + CdCl_2 \rightarrow (PhCH_2)_2Cd + 2\ MgCl_2$$

The acid chloride **(264)** had been generated from the reaction of the carboxylic acid **(265)** with thionyl chloride ($SOCl_2$) (Figure 4.9). The acid chloride **(264)** generated, then reacts with dibenzyl cadmium **(263)**, to form the desired asymmetric dibenzylketone **(266)**:

$$(PhCH_2)_2Cd + 2\ (4\text{-}MePh)CH_2COCl \rightarrow 2\ PhCH_2COCH_2(4\text{-}MePh) + CdO$$

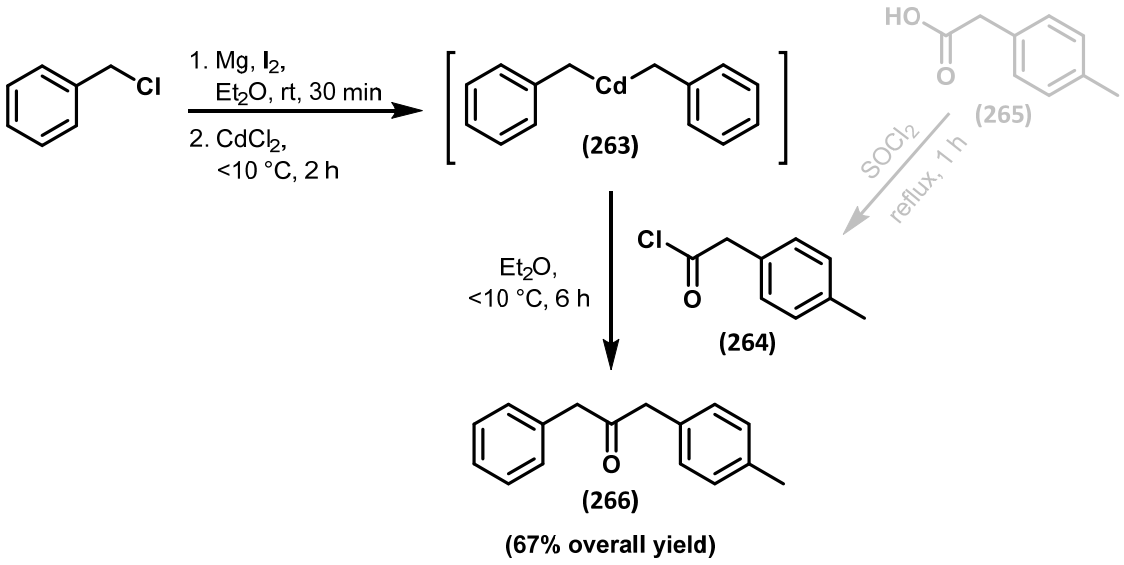


Figure 4.9: Synthesis of an asymmetric dibenzylketone *via* a dibenzyl cadmium reagent[223]

Included in our previous list of target compounds (Figure 4.7) were both symmetric and asymmetric dibenzylketones. It was decided that a single methodology would be chosen, that would be suitable for both types of dibenzylketones. One such procedure, that was found to be successful for a range of ring-substituted dibenzylketones, involved use of the Henry-Knoevenagel condensation for the coupling of substituted benzaldehydes **(267)** to substituted nitroalkanes **(268)**.[240,241] A very generalised overview of this methodology is presented in Figure 4.10.

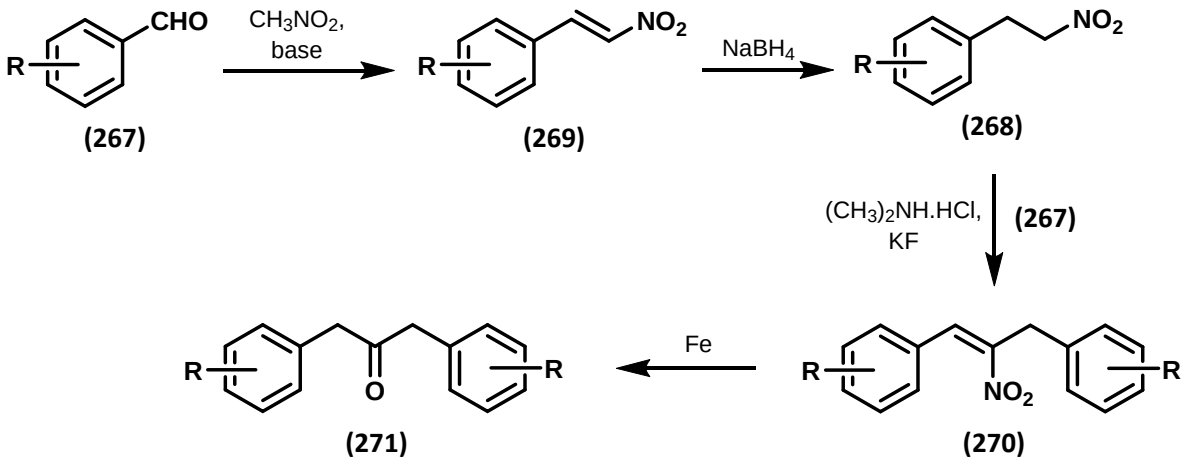


Figure 4.10: General synthesis of substituted dibenzylketones *via* the Henry-Knoevenagel condensation methodology[241]

The method involves firstly the Henry-Knoevenagel condensation of a suitably substituted benzaldehyde **(267)** with nitromethane (CH_3NO_2) to produce (*E*)-1-aryl-2-nitroethene ('nitrostyrene') **(269)**. This monomeric nitrostyrene **(269)** is then reduced with $NaBH_4$ to give a 1-aryl-2-nitroethane ('nitroalkane') **(268)**. A second Henry-Knoevenagel condensation (using *N*,*N*-dimethylamine.HCl ($(CH_3)_2NH.HCl$) and potassium fluoride (KF)), of this nitroalkane **(268)** with the appropriate benzaldehyde **(267)** affords a 1,3-bis(aryl)-2-nitro-1-propene ('dimeric nitrostyrene') **(270)**. Finally, the dimeric nitrostyrene **(270)** can be reduced to the desired dibenzylketone **(271)**, using iron powder in glacial acetic acid.

In order to apply this methodology to our selected dibenzylketones (Figure 4.7), suitable ring-substituted starting materials (2,5-dimethoxy) would be required. Also, given that the bromine substitution is so regiospecific for each of the dibenzylketones, the bromine atom would need to be incorporated at the required ring position on both the aldehyde **(267)** and nitroalkane **(268)**, prior to the key Henry-Knoevenagel coupling step. All five brominated dibenzylketones chosen for selective synthesis, can be manufactured from aldehydes substituted at the aromatic 4- and 6-positions. Fortunately, the suitably substituted 4- and 6-bromo aldehydes (**(160)** and **(165)**) had previously been prepared in Chapter 2. Using these previously synthesised materials as building blocks in the

methodology outlined in Figure 4.10, a scheme for the selective synthesis of our chosen dibenzylketones (of general structure **(275)**) was proposed (Figure 4.11).

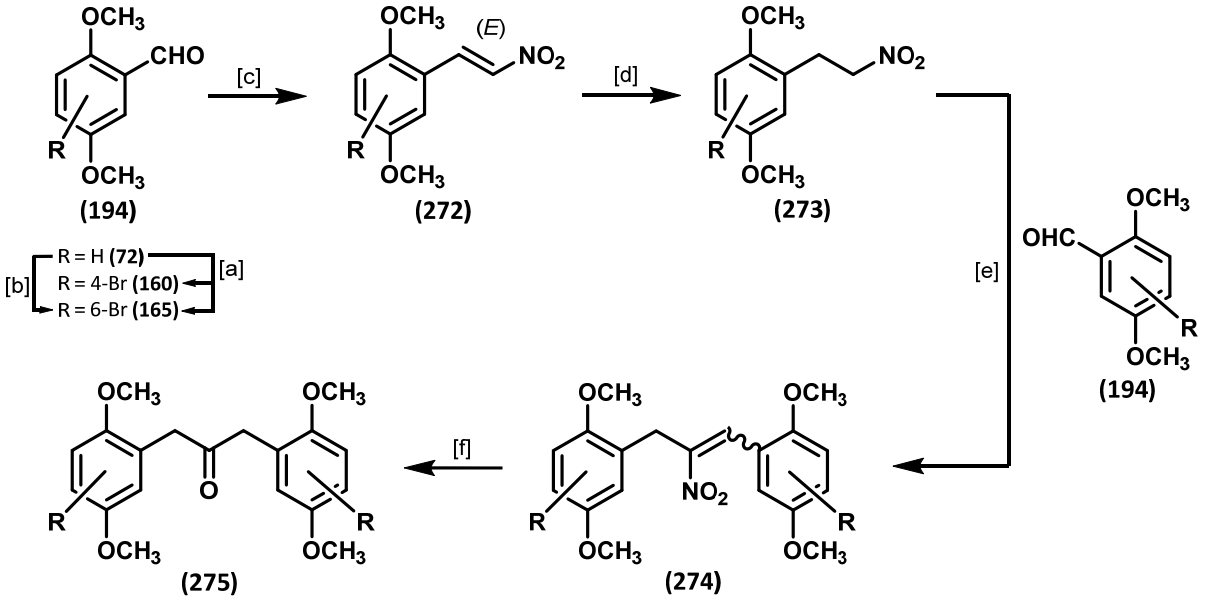


Figure 4.11: Proposed synthetic route to selected dibenzylketones ((221), (224) and (257)–(260))

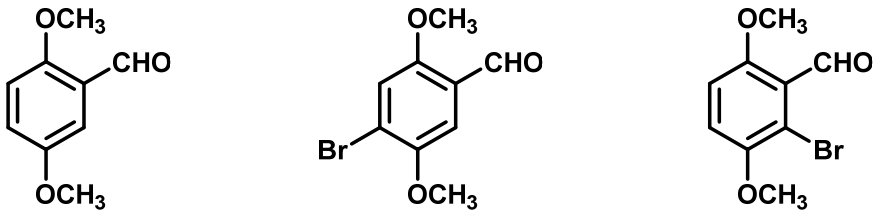
([a] = Br_2, AcOH, rt, 24 h, see Section 2.2; [b] = 3 step synthesis, see Section 2.3.1; [c] = CH_3NO_2, cyclohexylamine, AcOH, 90 °C, 6 h; [d] = $NaBH_4$, silica gel, iPrOH, $CHCl_3$, rt, ≈1.5 h; [e] = $(CH_3)_2NH.HCl$, KF, toluene, reflux (Dean-Stark trap), 24 h; [f] = Fe, AcOH, 90 °C, 2–4 h)

The synthesis of selected dibenzylketones (according to Figure 4.11), as well as a detailed account of the characterisation of isolated intermediates, is described in the following sections. For clarity, the sequence is divided into five subsections, representing each of the five key steps:

- Aldehyde bromination
- Monomeric nitrostyrene **(272)** formation (Henry-Knoevenagel condensation)
- Reduction of monomeric nitrostyrene **(272)** to nitroalkane **(273)**
- Formation of dimeric nitrostyrene **(274)** (2nd Henry-Knoevenagel condensation)
- Iron reduction of dimeric nitrostyrene **(274)** to dibenzylketone **(275)**

4.3.1.1 Aldehyde bromination

Three different aldehydes **(72)**, **(160)** and **(165)**, were required for the synthesis of all six dibenzylketones (including non-bromo **(221)** – see Figure 4.7).



(72) **(160)** **(165)**

Non-bromo aldehyde **(72)** was commercially available and was used in the synthesis of 4- and 6-bromo aldehydes (**(160)** and **(165)**), as described in Chapter 2. In summary, the 'standard' bromination of aldehyde **(72)**, produced 4-bromo **(160)** and 6-bromo **(165)** aldehydes (in a one-pot reaction) in yields of 74% and 15% respectively (following column chromatography). Alternatively, the 6-bromo aldehyde **(165)** could be synthesised *via* a three-step synthesis (using a benzaldoxime directing group), offering a superior yield (over three steps) of 59% (see Section 2.3.1).

Although bromination of aldehyde **(72)** was previously found to occur at different ring positions (e.g. @ the 3-position), the amounts detected were very small. Thus, it was considered unlikely that bromination at positions other that the 4- and 6- would occur for dibenzylketone **(221)**. Therefore, selective synthesis of the chosen aromatic ring-brominated dibenzylketone standards (see Figure 4.7) was limited to substitution about the 4- and 6-positions. This meant that there was only need for three aldehyde building blocks – **(72)**, **(160)** and **(165)**.

4.3.1.2 Formation of monomeric nitrostyrenes

The method by which nitrostyrenes are synthesised, as described in Figure 4.12, may be referred to as the 'Henry-Knoevenagel condensation'. The name is derived from the fact that it is considered a combination of the 'Henry reaction' and the 'Knoevenagel condensation'. The product of the Henry reaction is typically a β-nitro alcohol **(278)**, formed from the reaction of a carbonyl compound (e.g. aldehyde **(276)**) with a nitroalkane **(277)** (Figure 4.12).

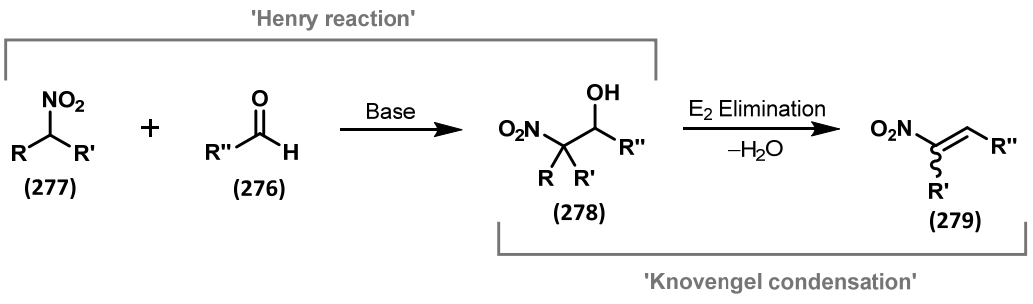
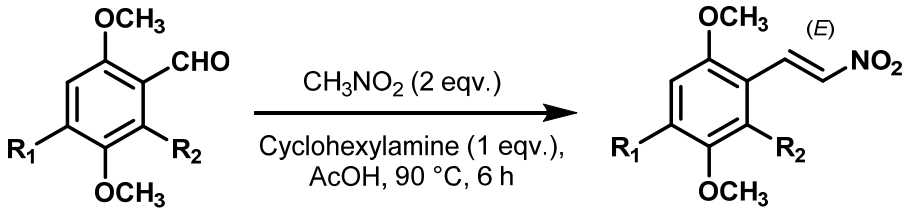


Figure 4.12: 'Henry-Knoevenagel condensation'

In the specific case whereby an acidic proton is available (i.e. when R = H in **(278)**), E_2-type elimination of water tends to take place to form the nitroalkene **(279)**. This elimination step is a feature of the Knoevenagel condensation, hence the name 'Henry-Knoevenagel condensation'.

As outlined in Figure 4.13, three monomeric nitrostyrenes were synthesised *via* the Henry-Knoevenagel condensation. The methodology used was similar to that of McNamara *et al*.[241] and Kodukulla *et al*..[240]



R_1=R_2= H **(72)**
R_1= Br, R_2= H **(160)**
R_1= H, R_2= Br **(165)**

R_1=R_2= H **(280)**
R_1= Br, R_2= H **(281)**
R_1= H, R_2= Br **(282)**

Figure 4.13: Synthesis of monomeric nitrostyrenes

The three monomeric nitrostyrenes were isolated, following recrystallisation, in excellent yields. The R_f, m.p., IR and MS data for non-bromo **(280)**, 4-bromo **(281)** and 6-bromo **(282)** nitrostyrenes are outlined in Table 4.5 below.

(Note: No reference to 6-bromo nitrostyrene **(282)** could be found in the literature so it is assumed to be novel.)

Table 4.5: Yield, R_f, m.p., IR and HRMS data for monomeric nitrostyrenes (280), (281) and (282)

Compound No.	Yield	m.p. (°C)	R_f*	IRν_{max} (KBr) (cm^{-1})	HRMS ($M+H^+$) (*m/z*)	
					Calc.	Found
(280)	85%	116–118 (EtOH/H_2O)	0.47	1621, 1579 (C=C), 1350 (NO_2)	210.0766	210.0757
(281)	76%	156–158 (EtOH/H_2O)	0.63	1628, 1604, 1502 (C=C), 1563, 1346 (NO_2)	287.9871⋆	287.9882
(282)	92%	124–126 (EtOH/H_2O)	0.39	1630, 1595, 1510 (C=C), 1570, 1342 (NO_2)	287.9871⋆	287.9878

*mobile phase = 50:50 Et_2O:hexane
⋆molecular ion (M) calculated for ^{79}Br isotope peak

All three monomeric nitrostyrenes were assigned *trans* conformation. This was based on the values of the vicinal coupling constants (^3J) between the two vinyl protons. It is widely accepted that for hydrogen

atoms that are *cis* to one another, ^3J is usually in the range of 6–12 Hz. For *trans* hydrogens, this is typically 14–18 Hz (Figure 4.14).[242]

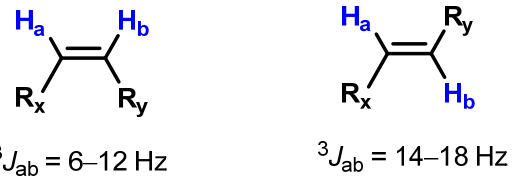


Figure 4.14: Distinguishing *cis* and *trans* isomers using *J* values in ^{1}H-NMR spectroscopy

For all three nitrostyrenes **(280)**, **(281)** and **(282)**, two doublets were observed at δ ≈8 ppm with *J* values ≈14 Hz. As a result, *trans* isomerism was assigned to each.

The expected aromatic ring splitting patterns were observed for the three nitrostyrenes. For non-bromo nitrostyrene **(280)**, the typical ABX pattern (in the form of a 1H, **d** (*J*=9 Hz) (@ δ 6.91), 1H, **dd** (*J*=9 and 3 Hz) (@ δ 7.02) and 1H **d** (*J*=3 Hz) (@ δ 6.97)) was observed. For 4-bromo **(281)**, two singlets were observed (@ δ 6.93 and 7.20) – the lack of signal splitting a result of the *para* relationship between the two hydrogen atoms. For the novel 6-bromo nitrostyrene **(282)**, two doublets (*J*=9 Hz) were observed (@ δ 6.91 and 7.00), the *J* value indicating *ortho* (^3J) splitting.

The monomeric nitrostyrenes were easily purified by recrystallisation. Upon isolation they were carried forward to the next step in the sequence – reduction by $NaBH_4$.

4.3.1.3 Formation of monomeric nitroalkanes

Two procedures were attempted for the preparation of monomeric nitroalkanes **(283)**, **(284)** and **(285)**. The first procedure ([A], Figure 4.15), was taken from the clandestine chemistry website 'erowid.org'.[243] In this instance, the non-bromo nitroalkane **(283)** was featured as an intermediate in the synthesis of 2C-B **(18)**, the phenethylamine equivalent of DOB **(35)**.

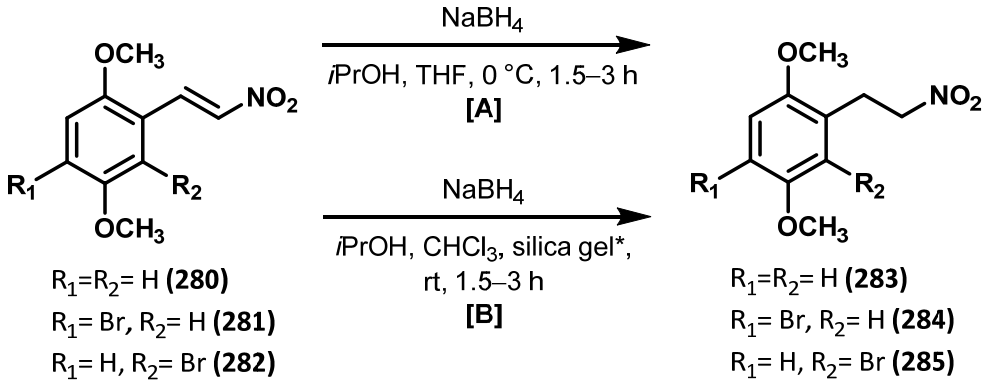
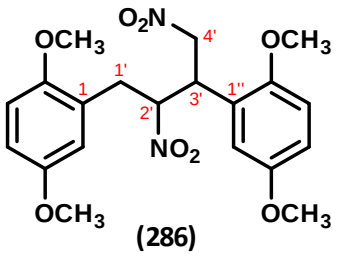


Figure 4.15: Procedures attempted for the preparation of monomeric nitroalkanes

*(*silica gel used = Merck Kieselgel 60, particle size 40–63 µm)*

Procedure [A], when used in the preparation of non-bromo **(283)**, was reported to give a yield of 89.5%.[243] Also reported was the presence of a trace amount (<2%) of a "dimeric impurity". However, attempts to remove or identify this impurity were not conducted in this study. The amount of this impurity formed was reported to be much higher when a lower number of eqv. of $NaBH_4$ (2.5 *vs.* 4 eqv.) were used.

When the procedure was carried out in-house (using non-bromo **(280)**), the ^{1}H-NMR spectrum of the crude reaction indicated that an impurity was indeed present, in addition to the desired product **(283)**. The presence of the impurity called for purification of the desired monomeric nitroalkane **(283)** by flash column chromatography. Following purification, **(283)** was recovered in a yield of 73%, much lower than the 89.5% quoted earlier.[243] The impurity was recovered in a yield of 7%, despite a large excess (4.15 eqv.) of $NaBH_4$ being used. Following characterisation of the impurity and a historical review of the literature on nitrostyrene reductions by $NaBH_4$, a structure of the novel impurity was proposed:



(286)

The ^{1}H-NMR spectrum of **(286)** (see Figure 4.16) revealed that although the compound contains two stereocentres, only one diastereoisomer was predominantly formed, with only trace evidence for the presence of the other (minor) diastereoisomer. No attempt was made to determine the ratio of major and minor diastereoisomers or the specific stereochemistry of the predominant diastereoisomer encountered.

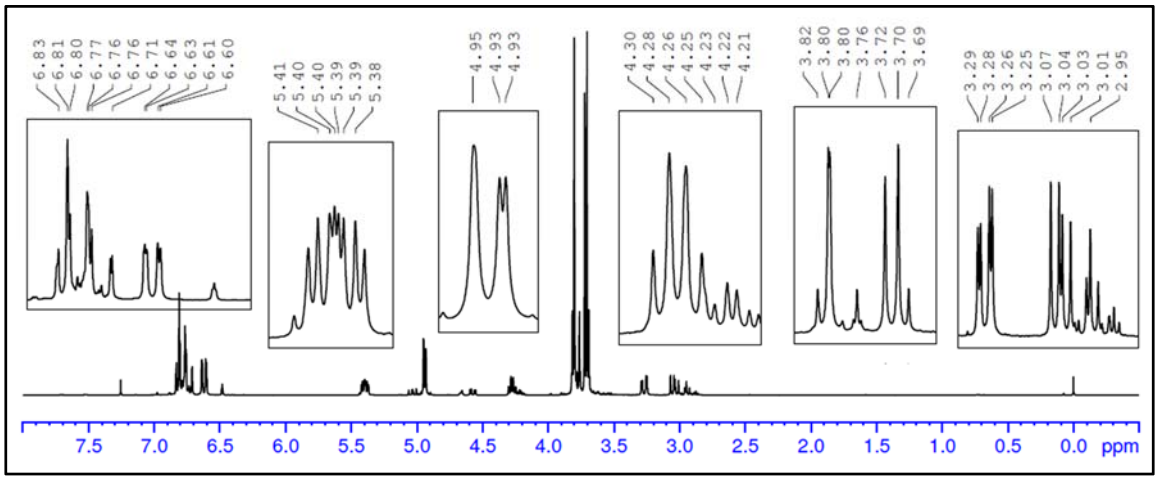
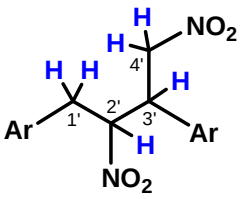


Figure 4.16: ^{1}H-NMR spectrum of dinitro-dimeric impurity (286), containing expanded regions of interest (@ 400 MHz)

Assignment of the molecular structure of the major diastereoisomer of **(286)** was facilitated by 1D-NMR as well as 2D-NMR techniques (e.g. COSY and HSQC).

In terms of the ^{1}H-NMR spectrum, there was extensive overlap of all aromatic ring protons. As a result, no attempt could be made to individually assign any of the six aromatic ring protons resonating in the region of δ 6.60–6.84. There was also some overlap of methoxy group protons, with two of the four groups being isochronous (signal resonating @ δ 3.81 integrating for six protons). The other two methoxy group signals were resolved (@ δ 3.71 and 3.73).

The protons present on the chain bridging the two aromatic rings (on C-1'–C-4'), gave rise to signals with complex splitting; the diastereotopic nature of the protons on C-1' and C-4' greatly contributing to this. In theory, six signals may be observed, arising from the six individual protons of the bridging chain:



(286)

(Ar = 2,5-dimethoxyphenyl)

In reality, only five individual signals could be distinguished, resonating at:

- δ 3.04 (1H, m)
- δ 3.27 (1H, dd, J_{gem}=14.2 Hz, J_{AB}=3.2 Hz)
- δ 4.28 (1H, m)
- δ 4.95 (2H, m)
- δ 5.40 (1H, m)

For many of these signals, the splitting observed did not aid assignment, with most existing as complex multiplets. There is clearly some overlap of signals also, as only five (of the six expected) signals were observed.

Any information regarding the connectivity of protons, that may have been provided by splitting patterns in the ^{1}H-NMR spectrum, could instead be gained from COSY data. By plotting two ^{1}H-NMR spectra against one another, correlations (generally ^{2}J–^{4}J) between neighbouring protons can be established using COSY. Such correlations allowed for the protons on C-1'/C-4' to be distinguished from those on C-2'/C-3'. This knowledge suggested that of the five signals listed above, those resonating at δ 3.04, 3.27 and 4.95 arise from the protons on C-1'/C-4', and those at δ 4.28 and 5.40 arise from protons on C-2'/C-3'. Distinguishing between protons on C-1' and C-4', and protons on C-2' and C-3' was then possible, based on sufficient differences in chemical shift values (δ) between signals. For example, taking the protons on C-2'/C-3' (δ 4.28 and 5.40), the more downfield of the two signals (δ 5.40) most likely arises from the proton on C-2', due to its close proximity to the electron withdrawing nitro group.

The same ideology was used to distinguish between the protons on C-1' (δ 3.04, 3.27) and those on C-4' (δ 4.95).

Using this assignment of ^{1}H-NMR signals, in conjunction with HSQC data, allowed for more straightforward assignment of individual ^{13}C-NMR signals. With regard to ^{1}H-NMR/^{13}C-NMR signals of the bridging chain (C-1'–C-4'), the following HSQC correlations were observed:

- δ 3.04, 3.27 ↔ 33.29 ppm
- δ 4.28 ↔ 43.98 ppm
- δ 4.95 ↔ 75.39 ppm
- δ 5.40 ↔ 87.67 ppm

Assignment of each of these ^{1}H-NMR/^{13}C-NMR signals is summarised in Figure 4.17:

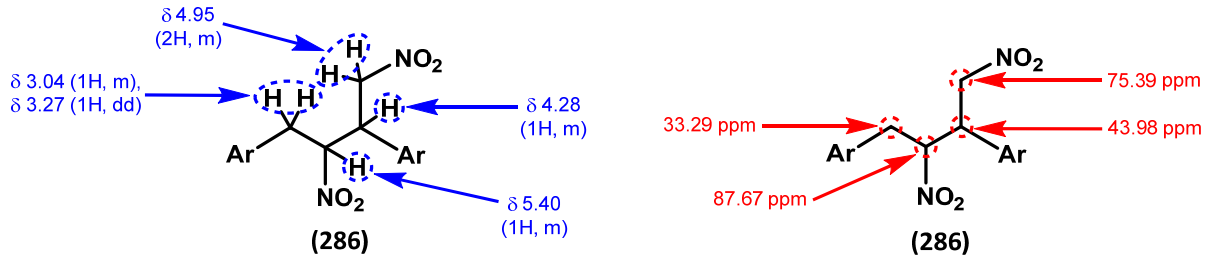


Figure 4.17: Assignment of individual ^{1}H-NMR/^{13}C-NMR signals of the bridging chain positions of (286)

Individual assignment of many of the other ^{1}H-NMR and ^{13}C-NMR signals (methoxy groups, aromatic ring positions) was not possible, so these are of little use in structure elucidation.

Additional evidence supporting structure assignment was provided by HRMS. This is outlined below in the characterisation of dimeric impurity **(286)** (Table 4.6).

Table 4.6: Yield, R_f, m.p., IR and HRMS data for dimeric-dinitro impurity (286)

Compound No.	Yield	m.p. (°C)	R_f*	IRν_{max} (KBr) (cm^{-1})	HRMS (M+H$^+$) (*m/z*)	
					Calc.	Found
(286)	7%	140–143 (EtOH)	0.25	1589, 1505 (C=C), 1554, 1375 (NO_2)	421.1611	421.1624

*mobile phase = 50:50 Et_2O:hexane

One of the first reports on the occurrence of these dimeric impurities was published in 1956 by Shechter *et al.*.[244] In this paper, the authors reveal that during the reduction of several nitroalkenes by a number of complex hydrides (including $NaBH_4$), consecutive Michael-type reactions occur in which "the salt of the nitroalkane, adds to the initial conjugated nitroolefin to yield a salt of the corresponding 1,3-

dintroalkane". The authors also reported that 'normal addition' (addition of nitroalkene to borohydride) helped to minimise dimer formation.

This phenomenon was also encountered by Coutts *et al.*[245] during the synthesis of a *N*-hydroxy homologue of DOM **(32)**. Coutts attributes the formation of the dinitro dimer **(288)** to the same Michael-type, consecutive reaction proposed by Shechter. Coutts also provides a more detailed mechanistic basis for the phenomenon (Figure 4.18).

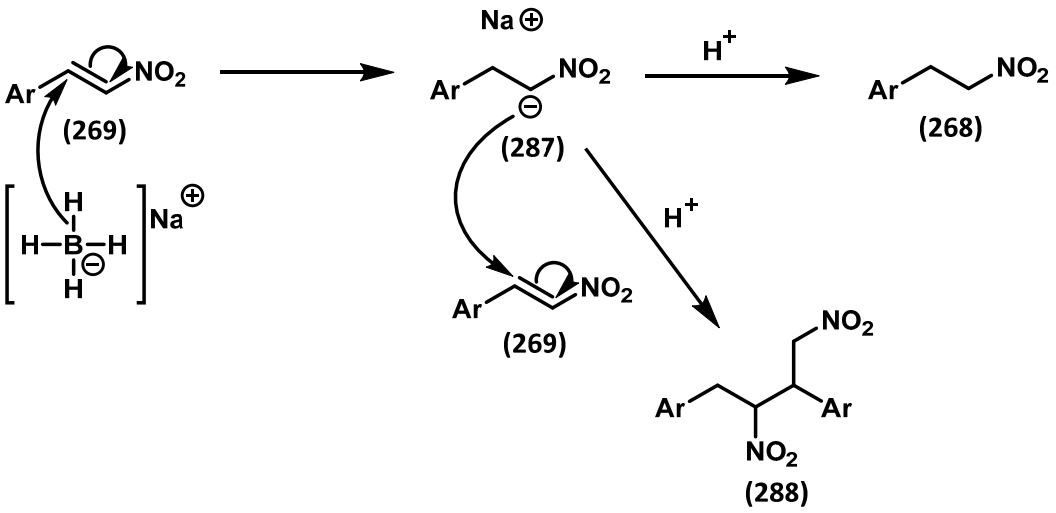
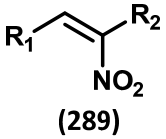


Figure 4.18: Mechanism of formation of desired nitroalkane (268) and dinitro dimer (288)

(Note: In work by Coutts et al.,[245] Ar group = 4-Me-2,5-dimethoxyphenyl)

As described in Figure 4.18, following initial attack by hydride and formation of the resonance stabilised carbanion intermediate **(287)**, the reaction can continue on two different paths. In the first path, the carbanion may become protonated, forming the desired monomeric nitroalkane **(268)**. Alternatively, the carbanion may attack the initial nitrostyrene SM **(269)**, forming a dimeric carbanionic species which, following protonation, yields the dimeric impurity **(288)**.

Attempts to minimise the formation of these dimeric impurities were carried out by Meyers and Sircar.[246] For nitroalkenes of general structure **(289)**, the formation of dimeric impurities was found to be influenced by pH.



(289)

For many nitroalkenes, in which R_1=alkyl, formation of the dimer was found to be completely suppressed when the pH was maintained between 3 and 6. For other nitroalkenes, this methodology was found to be ineffective, none more so than for β-aryl, vinyl-unsubstituted nitroalkenes (R_1=Ar, R_2=H ("nitrostyrenes")). Our nitrostyrene **(280)**, would fall under this group.

Work by Sinhababu and Borchardt,[247] offered a successful procedural change that overcame the issue of dimer formation, in the reduction of these nitrostyrenes. In this new procedure, silica gel (1–3 g/mmol of nitrostyrene) and chloroform ($CHCl_3$) were used to suppress dimer formation. The silica gel used in this reaction (type not specified) would act as an insoluble protic phase. It was proposed that the highly polar and negatively charged intermediate **(287)** would adsorb onto the silica surface and consequently accept a proton, forming nitroalkane **(268)**. This would occur before the intermediate **(287)** had the opportunity to undergo Michael addition to the nitrostyrene SM **(269)**. Using $CHCl_3$ as solvent was advantageous due to the greater inherent density (which facilitated the suspension of silica in the reaction medium) and low dielectric constant (which minimised dissolution of the charged intermediate **(287)**). The procedure was shown to be highly successful for a range of ring-substituted nitrostyrenes, providing high yields of desired nitroalkanes (90–98%) and suppressing formation of dinitro dimers. The procedure has since been adopted by a number of others.[240,241] Owing to the previous formation of dimer **(286)**, in the synthesis of nitroalkane **(283)**, the procedure was also adopted in our work (Procedure [B], Figure 4.15). Having applied this new procedure to the preparation of nitroalkanes **(283), (284)** and **(285)**, excellent yields (≥93%) of the desired monomeric nitroalkanes, were achieved. Also, the formation of dimeric-dinitro impurities was almost eradicated, with no greater than 1% being detected in any of the reactions. This meant that purification by column chromatography was not required and the nitroalkanes could be carried through to the next step in the reaction sequence.

The R_f, m.p., IR and MS data for non-bromo **(283)**, novel 4-bromo **(284)** and novel 6-bromo **(285)** nitroalkanes, are outlined in Table 4.7.

Table 4.7: Yield, R_f, m.p., IR and HRMS data for monomeric nitroalkanes (283), (284) and (285)

Compound No.	Yield	m.p. (°C)	R_f*	IRν_{max} (cm^{-1})	HRMS ($M+H^+$) (*m/z*)	
					Calc.	Found
(283)	73% [A]★ 96% [B]★	(Oil)	0.68	1503 (C=C), 1552, 1379 (NO_2)	212.0923	212.0918
(284)	99% [B]★	74–76 (EtOH)	0.45	1500 (C=C), 1545, 1379 (NO_2)	290.0028▲	290.0034
(285)	93% [B]★	61–63	0.35	1479 (C=C), 1550, 1386 (NO_2)	290.0028▲	290.0027

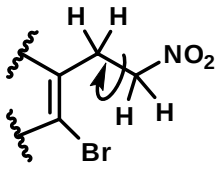
*mobile phase = 50:50 Et_2O:hexane

★[A]/[B] refers to procedures outlined in Figure 4.15

▲molecular ion (M) calculated for ^{79}Br isotope peak

Visually, the progress of the reduction reaction was easy to monitor. The reaction which begun a bright orange colour, faded to almost colourless upon complete consumption of starting material. Reaction completion was also clearly signified by the appearance of triplet signals @ δ ≈3.5 and 4.5 and the

disappearance of doublets (× 2) @ δ ≈8, in the ^{1}H-NMR spectra of **(283)**, **(284)** and **(285)**. The triplet signals correspond to the two methylene group protons of the nitroalkane side-chain. Interestingly, it appears that additional splitting of the 'triplet' signals occurs for the 6-bromo nitroalkane **(285)** (see Figure 4.19).



(285)

This is presumably due to restricted rotation of the nitroalkane side chain due to the steric bulk imposed by the bromine atom. This restricted rotation would result in a breakdown of the equivalence of the two geminal protons at each CH_2 group, meaning they may couple to neighbouring protons independently.

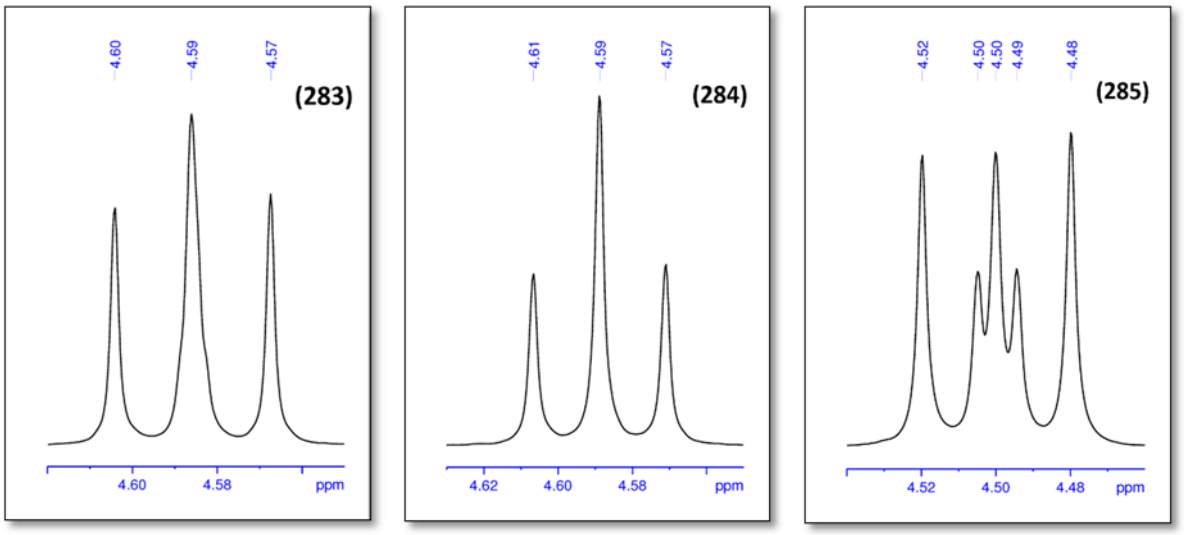


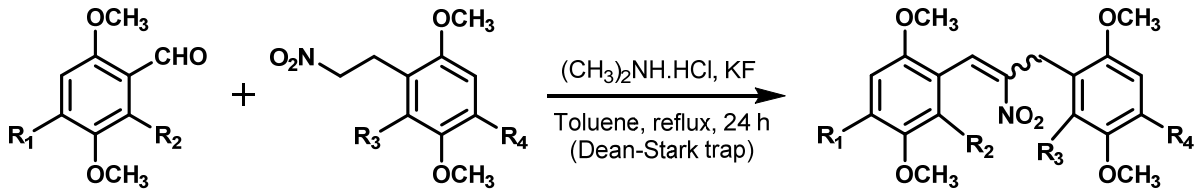
Figure 4.19: Comparison of 'triplet' signals corresponding to CH_2 protons α- to nitro group, for non-bromo (283), 4-bromo (284) and 6-bromo (285) nitroalkanes

In terms of the aromatic ring protons for the three nitroalkanes, there was slightly less resolution of the signals when compared to those of the nitrostyrenes. For non-bromo nitroalkane **(283)**, an undiscernible multiplet was observed @ δ 6.73–6.81, whereas clearly defined ABX splitting was observed for nitrostyrene **(280)**. Also, for 6-bromo nitroalkane **(285)**, the chemical shift difference ('diastereotopic shift') between the two aromatic ring protons was so small that overlap of the doublets occurred. As a result, the signals appeared as an AB quartet (ABq).

The successfully synthesised nitroalkanes were then used in the preparation of dimeric nitrostyrenes, as outlined in the next section.

4.3.1.4 Preparation of dimeric nitrostyrenes

In a second Henry-Knoevenagel condensation, a series of dimeric nitrostyrenes (of general structure **(274)**) were produced (see Figure 4.11). The synthetic methodology was different to that used for the monomeric nitrostyrenes of general structure **(272)**; the conditions used for successful monomeric nitrostyrene formation were previously found to be too mild for dimeric nitrostyrene synthesis.[248] Coupling of the three aldehydes **(72), (160)** and **(165)**, to the three nitroalkanes **(283), (284)** and **(285)** (*via* Henry-Knoevenagel condensation), would potentially produce nine novel dimeric nitrostyrenes. (Note: In theory, only six such nitrostyrenes would be required to produce the subsequent six dibenzylketones. However, all nine reactions were carried out for yield comparison purposes.)
When all nine reactions were carried out, the yields of product obtained were poor to moderate (5–48%) (Figure 4.20 and Table 4.8).



R_1=R_2=H, **(72)**
R_1=Br, R_2=H **(160)**
R_1=H, R_2=Br **(165)**

R_3=R_4=H, **(283)**
R_3=Br, R_4=H **(285)**
R_3=H, R_4=Br **(284)**

R_1=R_2=R_3=R_4=H, **(290)**
R_1=Br, R_2=R_3=R_4=H, **(291)**
R_2=Br, R_1=R_3=R_4=H, **(292)**
R_3=Br, R_1=R_2=R_4=H, **(293)**
R_4=Br, R_1=R_2=R_3=H, **(294)**
R_1=R_3=Br, R_2=R_4=H, **(295)**
R_1=R_4=Br, R_2=R_3=H, **(296)**
R_2=R_4=Br, R_1=R_3=H, **(297)**
R_2=R_3=Br, R_1=R_4=H, **(298)**

Figure 4.20: Coupling of aldehydes and nitroalkanes *via* Henry-Knoevenagel condensation

The characterisation of these compounds, together with some of their key structural features, are summarised in Table 4.8 overleaf. Included in this, is the ^{1}H-NMR δ value of the vinyl proton ('H'); the value of which may be used to tentatively assign geometric isomerism ((*E*) or (*Z*)). This will be discussed in more detail later in this Section.

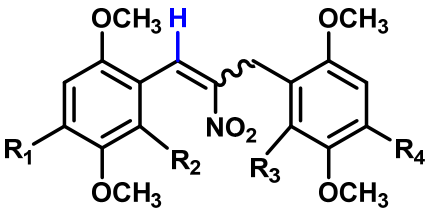


Table 4.8: Yield, R_f, m.p., IR and HRMS data, as well as some key structural features, of novel dimeric nitrostyrenes (290)–(298)

Compound No.	Yield	m.p. (°C)	R_f*	IRν_{max} (KBr) (cm^{-1})	HRMS ($M+H^+$) (*m/z*)		Ratio of *E*:*Z*▲		^{1}H-NMR δ of H (ppm)	
					Calc.	Found	Before FCC★	After FCC★	(*E*)	(*Z*)
(290)	48%	116–118 (EtOH/H_2O)	0.25	1649, 1616, 1500 (C=C), 1591, 1324 (NO_2)	360.1447	360.1443	(*E*) only	(*E*) only	8.49	–
(291)	31%	166–168 (CH_3CN)	0.48	1646, 1601, 1515 (C=C), 1571, 1323 (NO_2)	438.0552◊	438.0531	(*E*) only	9:1	8.46	6.47
(292)	35%	118–120 (MeOH)	0.14	1656, 1592, 1514 (C=C), 1573, 1330 (NO_2)	438.0552◊	438.0531	(*E*) only	(*E*) only	7.87	–
(293)	19%	127–130 (EtOH)	0.33	1644, 1510, 1490 (C=C), 1577, 1325 (NO_2)	438.0552◊	438.0544	6:1	3:1	8.13	6.28
(294)	29%	111–113 (EtOH/H_2O)	0.28	1652, 1518, 1493 (C=C), 1581, 1385 (NO_2)	438.0552◊	438.0531	15:1	3:1	8.44	6.55
(295)	23%	145–148 (EtOH)	0.32	1654, 1597, 1512 (C=C), 1578, 1335 (NO_2)	515.9657^	515.9647	4:1	3:1	8.07	6.25
(296)	40%	185–188 (EtOH)	0.39	1648, 1601, 1497 (C=C), 1568, 1328 (NO_2)	515.9657^	515.9635	(*E*) only	(*E*) only	8.41	–
(297)	43%	142–145 (EtOH)	0.25	1656, 1594, 1516 (C=C), 1570, 1332 (NO_2)	515.9657^	515.9653	(*E*) only	12:1	7.87	6.48
(298)	5%	158–161 (EtOH)	0.21	1658, 1596, 1515 (C=C), 1574, 1333 (NO_2)	515.9657^	515.9647	(*E*) only	8:1	7.70	6.02

*mobile phase = 20:80 EtOAc:hexane

★FCC = flash column chromatography

▲Based on molar ratio of alkene proton shifts in the crude reaction mixture (before FCC) and in the isolated fraction following FCC

◊molecular ion (M) calculated for ^{79}Br isotope peak

^molecular ion (M) calculated for $^{79}Br_2$ isotope peak

For the various brominated dimeric nitrostyrenes featured in Table 4.8, a number of general inferences can be made regarding which coupling methodologies are more favourable in terms of product yield:

- Coupling (to the appropriate aldehyde) of the 4-bromo **(284)** nitroalkane is much more favourable than coupling of the 6-bromo nitroalkane **(285)**.
- Coupling of two 6-bromo molecules (6-bromo aldehyde **(165)** and 6-bromo nitroalkane **(285)**) is highly unfavourable (yield of dimeric nitrostyrene **(298)** = 5%). This may not only be a consequence of unfavourable steric interaction, but also due in part to the decomposition/polymerisation of 6-bromo aldehyde **(165)**, at reflux temperature.

  (Note: This decomposition/polymerisation was evident based on the presence of a dark insoluble resinous material in the crude reaction mixture, as well as a lower than expected recovery of unreacted aldehyde (in ^{1}H-NMR spectrum of crude reaction following work-up). A similar observation was made by McNulty *et al.*,[249] whereby 2,3-dimethoxybenzaldehyde was found to be unstable under Henry reaction conditions. The phenomenon was attributed to the aldehyde undergoing phenol-formaldehyde type polymerisation.)
- In the synthesis of mono-bromo dimeric nitrostyrenes (**(291)–(294)**), incorporation of the bromine atom *via* the aldehyde (*vs.* the nitroalkane) affords higher yields.

The third point raised above may be of use to others pursuing the synthesis of halogenated dimeric nitrostyrenes. As mentioned previously, only six of the nine coupling reactions would be required to produce the six subsequent dibenzylketones. This is due to loss of asymmetry about the central nitroalkene group when it is reduced to the ketone. This means that on reduction of two different nitrostyrenes (e.g. **(291)** and **(294)**), the same dibenzylketone (**(257)**) is produced (Figure 4.21). This is also the case for dimeric nitrostyrene pairs **(292)** and **(293)**, and **(295)** and **(297)**.

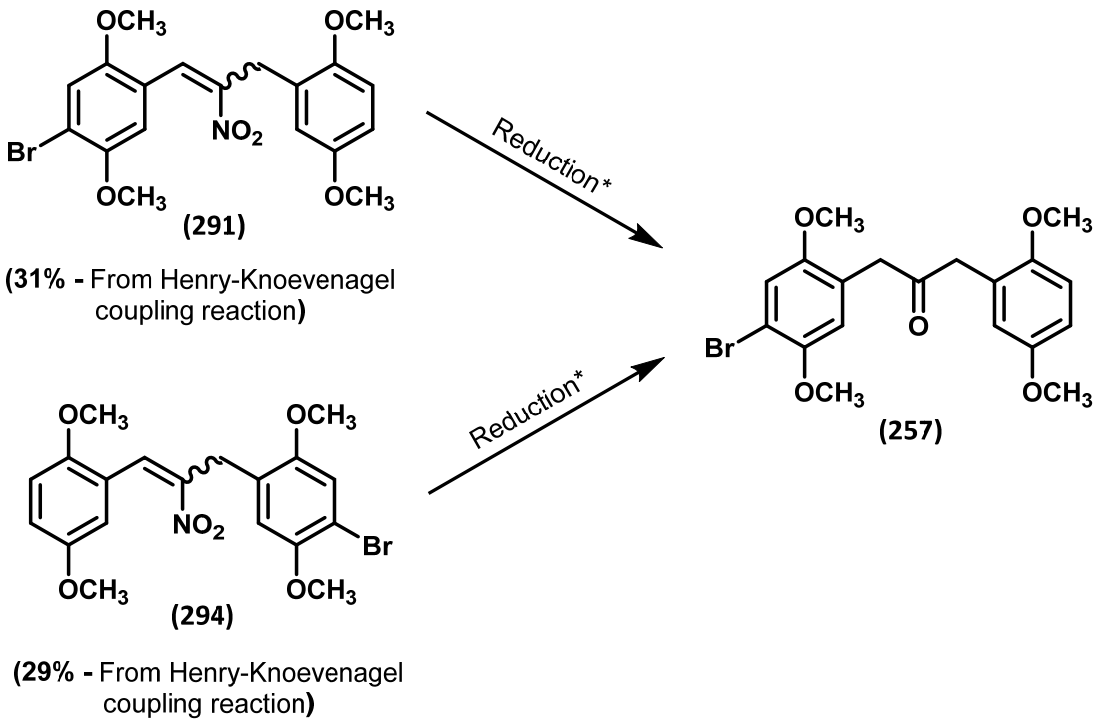


Figure 4.21: Reduction of two different dimeric nitrostyrenes, yielding dibenzylketone (257)

*(*Reaction conditions = Fe, AcOH, 90 °C, 2 h)*

For the three pairs of dimeric nitrostyrenes for which this is the case, synthesis of dibenzylketones **(257)**, **(258)** and **(259)**, may be more efficient *via* dimeric nitrostyrenes **(291)**, **(292)** and **(297)**. This is due to the fact that the yields of nitrostyrenes **(291)**, **(292)** and **(297)**, produced from their respective Henry-Knoevenagel coupling reactions are greater than the yields of nitrostyrenes **(294)**, **(293)** and **(295)**, produced from their respective Henry-Knoevenagel coupling reactions:

- Yield of **(291)** (31%) > Yield of **(294)** (29%)
- Yield of **(292)** (35%) > Yield of **(293)** (19%)
- Yield of **(297)** (43%) > Yield of **(295)** (23%)

One of the key findings from the synthesis of the dimeric nitrostyrenes (see Table 4.8), was the fact that some of the products formed as a mixture of geometric isomers. In addition to these, several others, which had initially formed exclusively in the (*E*)-conformation, were found to undergo *E*/*Z* isomerisation during flash column chromatography.

(Note: Although isomerisation on silica gel is known in the literature to occur for particular groups of compounds (e.g. branched alkenes[250]), no record of this occurring for nitrostyrenes could be found.)

These findings were initially unexpected as the literature being used at the time, pertaining to dimeric nitrostyrene synthesis, had only reported the presence of (*E*)-isomers.[240,241] On further exploration of the literature however, reports were found on the existence (to a small extent) of the (*Z*)-isomer, during

manufacture of monomeric nitrostyrenes. In a report by Guy *et al.*,[251] several nitrostyrene precursors to psychoactive phenalkylamines were prepared (Figure 4.22). During synthesis of the nitrostyrenes **(105)** and **(299)**, it was found that the conformational outcome of the product was dependant on the length of the nitroalkene side chain. In the case of the prop-1-ene compound **(105)**, the product formed exclusively as the (*E*)-isomer. However, for the chain extended but-1-ene analogue **(299)**, a small amount of the (*Z*)-isomer was also detected (ratio of *E*:*Z* = 97:3, combined yield = 19.2% following column chromatography) (Figure 4.22).

(Note: No reference was made to the *E*:*Z* ratio prior to column chromatography in this case.)

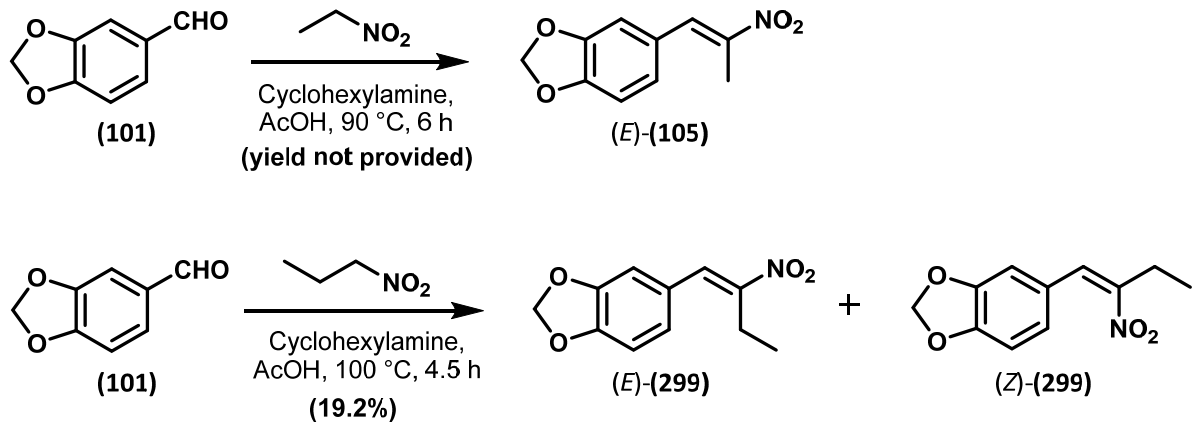
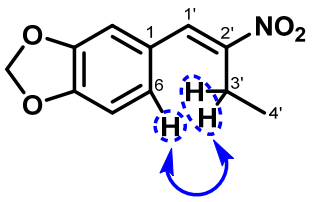


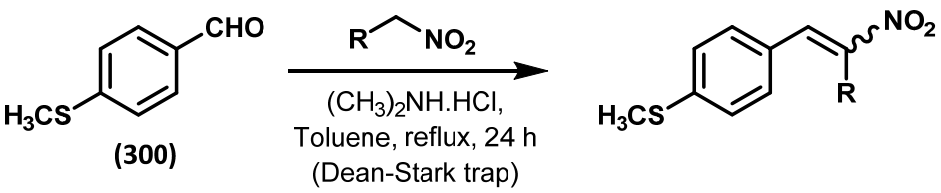
Figure 4.22: Effect of chain length on the geometric conformation of methylenedioxy-nitrostyrene product formed[251]

Although both isomers were unresolved in this particular case,[251] evidence of *E*/*Z* conformation was attained *via* NOESY NMR. The NOESY evidence used was in the form of a positive interaction between the ring proton at position six and the methylene protons (on C-3') of (*E*)-**(299)**:



(*E*)-**(299)**

A similar observation was made by Hurtado-Guzmán *et al.*[252] for a homologous series of methylthio ring-substituted nitrostyrenes, prepared from benzaldehyde **(300)**. On extension of the chain length of the nitroalkane reagent (nitromethane → nitroethane → nitropropane), the likelihood of the (*Z*)-isomer being formed increased (Figure 4.23).



R	Geometric Conformation
H	Only (*E*)
CH_3	(*E*) and trace (*Z*)*
CH_2CH_3	(*E*) + (*Z*)⋆

*Detected in crude ^{1}H-NMR spectrum, not isolated

⋆Both isomers isolated following column chromatography in a combined yield of 54% (molar ratio of *E*:*Z* in crude reaction mixture = 92:8, *E*:*Z* ratio after chromatography = 92:8)

Figure 4.23: Effect of chain length on the geometric conformation of 4-methylthio-nitrostyrene product formed[252]

Based on these results, it is not surprising that many of the dimeric nitrostyrenes outlined in Table 4.8, form as a mixture of (*E*)- and (*Z*)-isomers – these dimeric nitrostyrenes may be considered even longer chain analogues of the monomeric nitrostyrenes encountered in Figures 4.22 and 4.23. What is a little surprising is the fact that none of the literature found, pertaining to the preparation of dimeric nitrostyrenes, report formation of the (*Z*)-isomer.[240,241,253] It may be that the (*Z*)-isomer is genuinely not formed or that it is not detected, possibly for the following reasons:

1. A large difference in R_f values between the two isomers – if the difference in R_f values is sufficiently large and the reaction is purified by flash column chromatography, the two isomers may elute the column independently. The (*Z*)-isomer, which in most cases forms only to a small extent, may go unnoticed or be discarded as an unwanted by-product of the reaction.
2. Selective crystallisation of the major (*E*)-isomer – in most literature examples, the dimeric nitrostyrene, following chromatography, is purified further by recrystallisation. In the course of recrystallising the dimeric nitrostyrenes in Table 4.8, it was found in many cases that the major (*E*)-isomer selectively crystallised out of solution, over the minor (*Z*)-isomer. It may be that in the process of purifying dimeric nitrostyrenes in the literature, the (*Z*)-isomer is remaining in solution and ending up in the discarded mother liquor.

Tentative assignment of *E*/*Z* isomerism for the dimeric nitrostyrenes (in Table 4.8), was initially based on the ^{1}H-NMR δ value of the vinyl proton. The work by Hurtado-Guzmán *et al.*[252] had shown there to be a substantially large difference (Δδ = 1.69 ppm) between the δ values of this proton on (*E*)-**(301)** and (*Z*)-**(301)** (Figure 4.24).

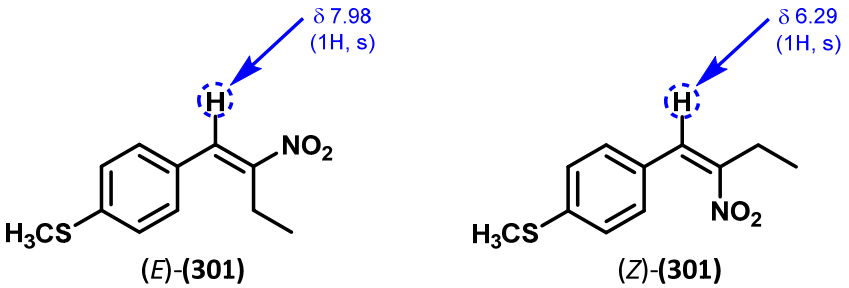


Figure 4.24: Difference in the ^{1}H-NMR δ values of the vinyl proton, between the (*E*)- and (*Z*)-isomers of methylthio-substituted nitrostyrene (301)[252]

Assignment of the conformation of each of these compounds was supported by NOESY evidence. The through-space interactions observed for (*E*)-**(301)** and (*Z*)-**(301)** are highlighted in Figure 4.25.

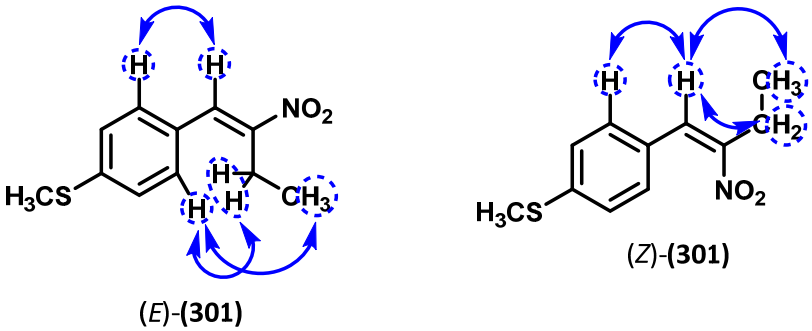
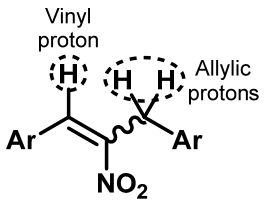


Figure 4.25: Through-space interactions observed in the NOESY spectra of (*E*)-(301) and (*Z*)-(301) nitrostyrenes[252]

Based on differences between all of the ^{1}H-NMR and ^{13}C-NMR signals for (*E*)-**(301)** and (*Z*)-**(301)**, as well as theoretical modelling experiments, an explanation for the large difference in vinyl proton δ was proposed.[252] The theoretical modelling study had shown that for (*E*)-**(301)**, the dihedral angle between the nitro group and the alkene proton was 6°. This results in the alkene double bond being highly conjugated with the electron withdrawing nitro group. For (*Z*)-**(301)**, the nitro group–alkene proton dihedral angle was 71°, the consequence of this being that conjugation, between the alkene double bond and the nitro group, is greatly diminished. This offers a logical explanation as to why the vinyl proton δ of (*E*)-**(301)** is so downfield compared to that of (*Z*)-**(301)**: the proton is deshielded by the electron-withdrawing nitro group only when it is strongly conjugated with the alkene double bond (as in (*E*)-**(301)**).

Similar to the methylthio-substituted nitrostyrene isomers (Figure 4.24), there was also found to be a substantial difference in the vinyl proton δ between the isomers of our dimeric nitrostyrenes outlined in Table 4.8. Thus, the isomers with a vinyl proton δ lying in the range of δ 7.70–8.49 were tentatively assigned (*E*)-geometry, whilst those in the range of δ 6.02–6.55 were assigned (*Z*)-.

As well as the vinyl proton δ difference between the (*E*)- and (*Z*)-isomers of the dimeric nitrostyrenes (Table 4.8), there was also found to be a subtle difference in the splitting/width of the vinyl and allylic proton signals in the ^{1}H-NMR spectra.



For all dimeric nitrostyrenes in the (*E*)-conformation, the vinyl (δ 7.70–8.49) and allylic (δ 3.83–4.36) signals showed no signs of splitting, with singlets observed for both types of signal. For many of the (*Z*)-nitrostyrenes, the vinyl proton signals (also singlets, δ 6.02–6.55) appeared to be broader than their (*E*)-counterparts and the allylic signals (δ 3.94–4.30) were observed as fine doublets (*J*=0.9–1.6 Hz).

The allylic splitting, observed only in the (*Z*)-nitrostyrenes, suggests that the vinyl proton and allylic protons probably lie closer in space for (*Z*)- (*vs*. (*E*)-) and that the vinyl C–H bond is in the same plane (θ = 0°) as one of the allylic C–H bonds (Figure 4.26). In this orientation, there is maximum overlap between the allylic C–H σ orbital and the π orbital, which enables coupling to be transmitted more efficiently.[254]

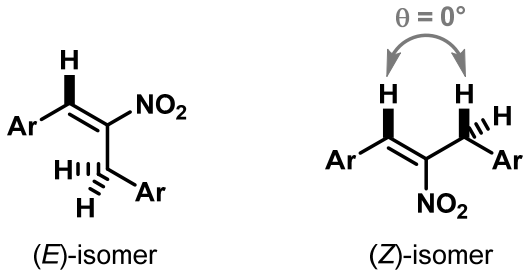


Figure 4.26: Proposed orientations of (*E*)- and (*Z*)-isomers, giving rise to the allylic splitting (only observed in (*Z*)-isomer)

The differences in vinyl proton δ and splitting of allylic protons, between (*E*)- and (*Z*)-isomers, only provides tentative or preliminary evidence of geometric conformation. For more definitive assignment of nitrostyrene conformation, it is common in the literature for NOESY experiments to be carried out.[251,252]

In this work, for dimeric nitrostyrene **(298)** in Table 4.8, a NOESY spectrum was obtained for a sample containing a mixture of (*E*)-**(298)** and (*Z*)-**(298)** isomers. For (*Z*)-**(298)**, evidence of conformation was obtained *via* the presence of an apparent interaction between the vinyl proton (@ δ 6.02) and the allylic protons (@ δ 4.30) (Figure 4.27). The interaction was corroborated by NOE difference experiments (*via* a positive irradiation↔enhancement relationship between signals). No corresponding interaction, between the vinyl proton (@ δ 7.70) and the allylic protons (@ δ 4.16) in (*E*)-**(298)**, was observed. This

NOESY/NOE difference evidence for the assignment of (*Z*)-**(298)**, corroborates the previous assignment of *E*/*Z* isomerism, based on values of vinyl proton δ.

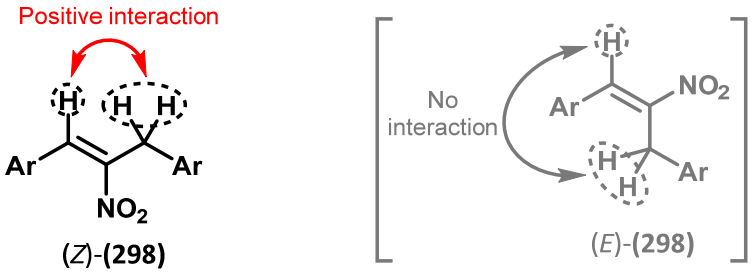
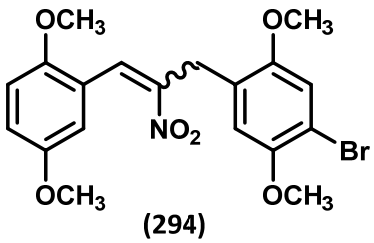


Figure 4.27: Interaction between vinyl and allylic protons on (*Z*)-nitrostyrene (298)

(Note: Ar group = 6-bromo-2,5-dimethoxyphenyl)

Definitive assignment of molecular structure can be achieved through single crystal analysis. For nitrostyrene **(294)**, pure samples of both (*E*)-**(294)** and (*Z*)-**(294)** isomers were obtained following their differential crystallisation in MeOH.



(Note: For all dimeric nitrostyrenes outlined in Table 4.8, separation of (*E*)- and (*Z*)-isomers could not be achieved by flash column chromatography. Pure samples of (*E*)- and (*Z*)-isomers were only attained for dimeric nitrostyrene **(294)**, when an isomeric mixture recovered by flash column chromatography, underwent differential crystallisation in MeOH).

Samples of both isomers of **(294)** were submitted for single crystal analysis and the resulting solved structures are outlined in Figure 4.28.

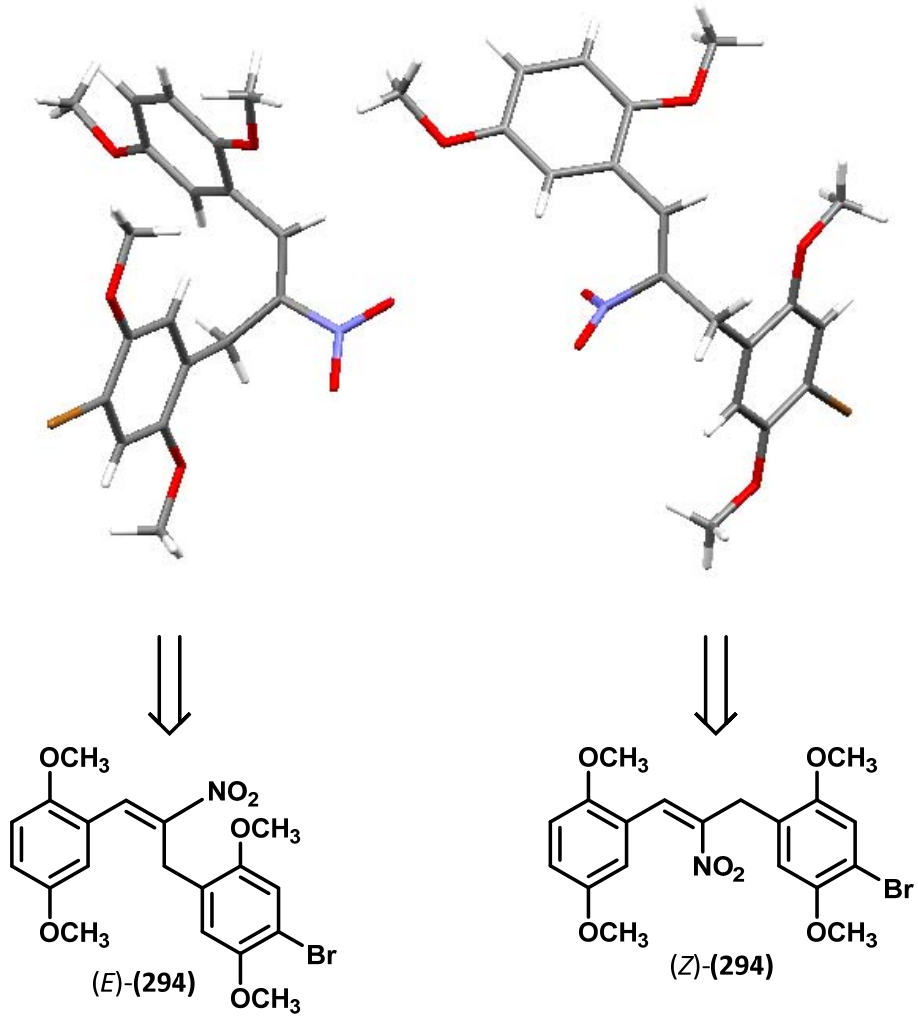


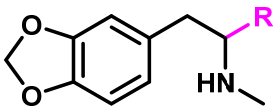
Figure 4.28: Single crystal analysis of (*E*)- and (*Z*)-isomers of dimeric nitrostyrene (294)

The confirmation of assignment of (*E*)-**(294)** and (*Z*)-**(294)**, provided by single crystal X-ray analysis, corroborated the earlier tentative assignment of geometric conformation (based on value of vinyl proton δ).

4.3.1.5 Anticancer activity of nitrostyrenes

As well as being important intermediates in chemical synthesis, nitrostyrene compounds have been shown to possess antitumor, antimicrobial and insecticidal properties.[255,256] In fact many compounds used in the synthesis of ATS, derivatives of ATS and even ATS themselves, have shown therapeutic potential. For example, MDMA **(17)** is known to be cytostatic towards Burkitt's lymphoma cell lines.[257,258] However, its low potency, psychoactivity and neurotoxicity rules-out consideration as an anticancer therapeutic drug candidate. This has led to research into "redesigning the designer drug", an attempt to create ATS analogues with increased anticancer activity and diminished psychoactivity/neurotoxicity. One such group involved in this area, successfully synthesised a range of

bulky α-aryl analogues of MDMA, that lack psychoactivity and reduce Burkitt's lymphoma cell line (L3055) viability with significantly greater potency than MDMA itself.[258] Some examples of these compounds are outlined in Figure 4.29.



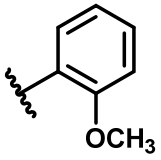
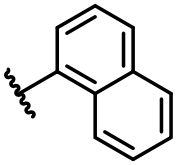
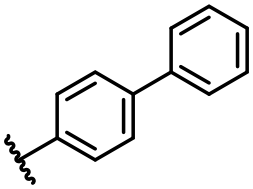
Entry	R	$IC_{50}/\mu M$
(302)		92 ± 8
(303)		12.6 ± 0.5
(304)		6 ± 1

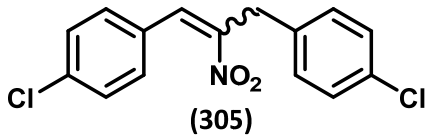
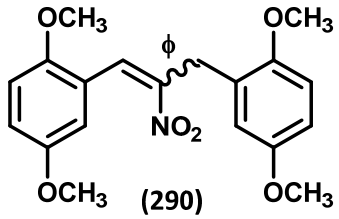
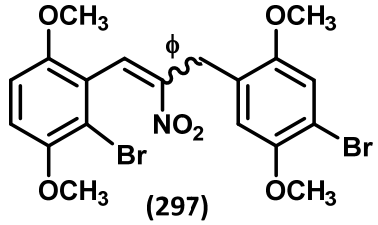
Figure 4.29: Examples of α-aryl analogues of MDMA that reduce viability of a Burkitt's lymphoma cell line (L3055)[258]

Nitrostyrene-based compounds may be used as intermediates in the synthesis of ATS (Section 1.5.1), or be used in the selective synthesis of by-products of ATS (Section 4.3.1.4). They have also, in recent years, been shown to express pro-apoptotic properties (against a rat pituitary tumour GH_3 cell line).[255] In the same study, the structure-activity relationships (SAR) of nitrostyrenes, (against related nitro compounds) as antitumor agents, was explored. This identified the nitrostyrene moiety as the essential pro-apoptotic core structure required for inhibition of serine/threonine phosphatases 1 and 2A. It also showed that substitution of the phenyl ring of nitrostyrene may enhance apoptotic potency, particularly at positions 2 and 3 by another nitro group, or at positions 3, 4 and 5 with methoxy groups.

In a more recent study by McNamara *et al.*,[241] a series of dimeric nitrostyrenes were prepared and assessed for anticancer activity. These dimeric nitrostyrenes were shown to have antiproliferative activities *in vitro* in a range of malignant cell lines, particularly against Burkitt's lymphoma. Although no specific target had been identified for the action of these compounds, they were shown to induce caspase activation, chromatin condensation and membrane blebbing in a Burkitt's lymphoma cell line, consistent with these compounds inducing apoptosis *in vitro*.

Given the structural similarity of the compounds featured in the McNamara study,[241] to those prepared in Section 4.3.1.4, it was decided to send all nine prepared nitrostyrenes (in Table 4.8) to the same group in Trinity College Dublin, for similar testing (against two Burkitt's lymphoma cell lines). To date, the activity of two of the compounds (**(290)** and **(297)**) against two cell lines (MUTU-1 and DG-75), has been established and the initial results are very promising. In comparison to the most potent (**(305)**) of the previously tested compounds, our two compounds **(290)** and **(297)**, are of 2–3 times greater potency (Table 4.9).

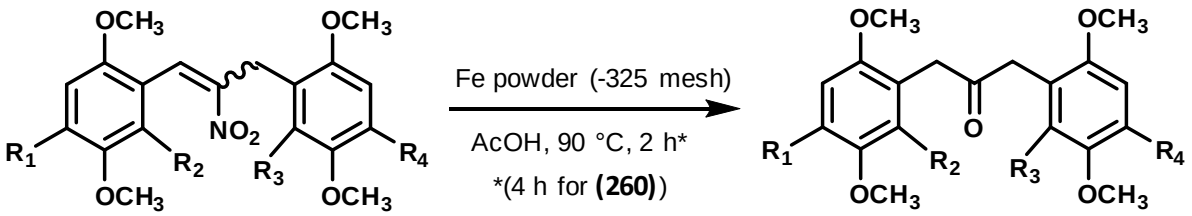
Table 4.9: *In vitro*, antiproliferative effects (EC_{50}) of previously published nitrostyrene (305) against in-house prepared nitrostyrenes (290) and (297)

	MUTU-1*	DG-75*
	EC_{50} (μM)⋆	EC_{50} (μM)
 **(305)**	0.8	3.63
 **(290)**	0.24	0.97
 **(297)**	0.37	0.31

*MUTU-1 = Malignant, chemosensitive Burkitt's lymphoma cell line.
DG-75 = Malignant, chemoresistant Burkitt's lymphoma cell line, known to be susceptible to antidepressant induced-Type-II programmed cell death.
⋆EC_{50} = 'Half maximal effective concentration' – Concentration of a drug which produces 50% of the maximum possible response, in a specified response time.
ϕSample sent for testing >95% (*E*)-isomer

4.3.1.6 Preparation of dibenzylketones

Following successful preparation of the dimeric nitrostyrenes, all six novel dibenzylketones could be prepared. This was carried out *via* iron reduction of the nitrostyrene in AcOH (Figure 4.30). This reduction procedure had been used previously in the synthesis of the monomeric ketone 2,5-P2P **(92)** (Section 3.6).



R_1=R_2=R_3=R_4=H, **(290)**
R_1=Br, R_2=R_3=R_4=H, **(291)**
R_2=Br, R_1=R_3=R_4=H, **(292)**
R_1=R_4=Br, R_2=R_3=H, **(296)**
R_2=R_4=Br, R_1=R_3=H, **(297)**
R_2=R_3=Br, R_1=R_4=H, **(298)**

R_1=R_2=R_3=R_4=H, **(221)**
R_1=Br, R_2=R_3=R_4=H, **(257)**
R_2=Br, R_1=R_3=R_4=H, **(258)**
R_1=R_4=Br, R_2=R_3=H, **(224)**
R_1=R_3=Br, R_2=R_4=H, **(259)**
R_2=R_3=Br, R_1=R_4=H, **(260)**

Figure 4.30: Preparation of dibenzylketones *via* the iron reduction of dimeric nitrostyrenes

The procedure was highly efficient and generally complete within a reaction time of 2 h. This was the case for all dibenzylketones bar one (**(260)**), where it was found that an additional 2 h of heating was required to drive reaction to completion. Reaction incompletion (after 2 h) for **(260)**, was most evident by the presence of an unknown, apparent asymmetric compound in the ^{1}H-NMR spectrum, in addition to the expected product (ratio of unknown to expected dibenzylketone **(260)** ≈ 1:1, based on crude ^{1}H-NMR evidence). HRMS data (Figure 4.31) suggests this compound to be an oxime intermediate **(306)** of the reduction reaction.

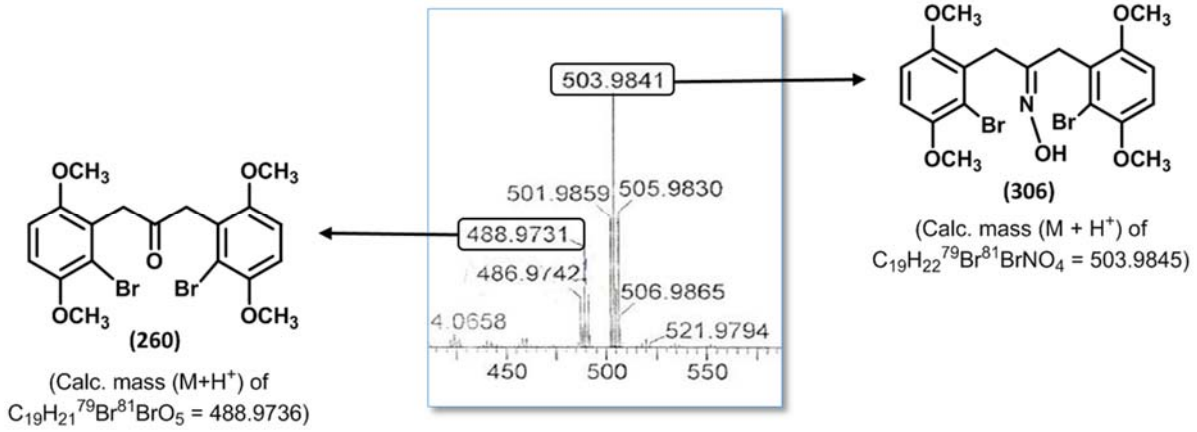


Figure 4.31: HRMS evidence for the presence of oxime intermediate (306) during the preparation of dibenzylketone (260)

A proposal for the formation of this oxime **(306)** is outlined in Figure 4.32. In this scheme, a number of successive electron transfers from iron, and proton transfers from AcOH, generate the nitroso **(307)** and *N*-hydroxyenamine **(308)** intermediates. The enamine **(308)** tautomerises to form the preferred oxime tautomer **(306)**.

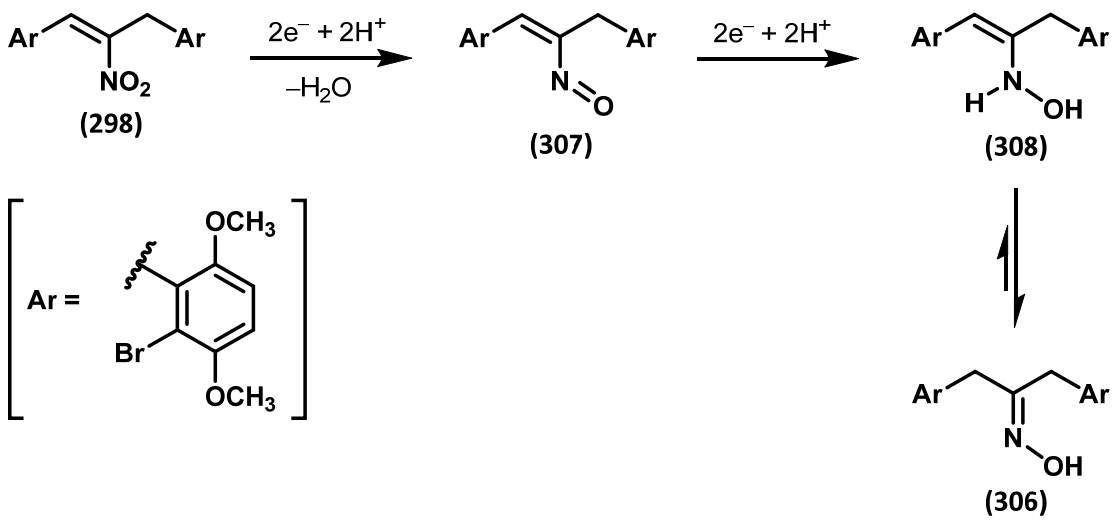
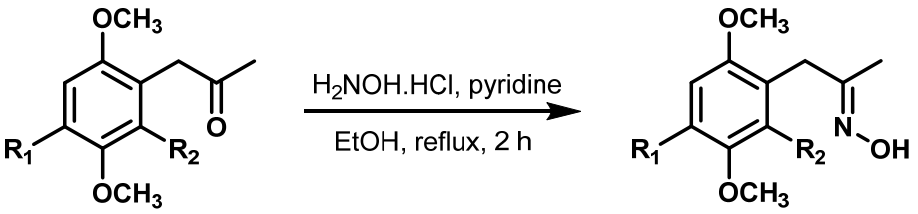


Figure 4.32: Proposed formation of oxime intermediate (306)

Although not pursued in the course of this work, definitive confirmation of the presence of this oxime intermediate **(306)** may be attained by selectively preparing a reference standard of **(306)**. This reference material may be prepared by taking the dibenzylketone product **(260)** and reacting it with hydroxylamine hydrochloride ($H_2NOH.HCl$) in pyridine and EtOH, at reflux temperature. This methodology had been used previously within the research group,[26] to prepare three monomeric oximes **(93)**, **(309)** and **(310)** (Figure 4.33).



R_1=R_2=H **(92)**
R_1=Br, R_2=H **(159)**
R_1=H, R_2=Br **(311)**

R_1=R_2=H **(93) (62%)**
R_1=Br, R_2=H **(309) (65%)**
R_1=H, R_2=Br **(310) (47%)**

Figure 4.33: Methodology used previously within the research group, to selectively prepare oxime-type impurities[26]

The issue of reaction incompletion (resulting in the presence of oxime intermediate **(306)**) was easily overcome; an additional 2 h reaction time resulted in complete consumption of this intermediate **(306)** and high yield of desired dibenzylketone **(260)**.

After sufficient reaction time, all six novel dibenzylketones were recovered in excellent yields (80–98%). The R_f, m.p., IR and MS data for dibenzylketones **(221)**, **(224)** and **(257)**–**(260)**, are outlined in Table 4.10.

Table 4.10: Yield, R_f, m.p., IR and HRMS data for novel dibenzylketones (221), (224) and (257)–(260)

Compound No.	Yield	m.p. (°C)	R_f*	IRν_{max} (KBr) (cm^{-1})	HRMS ($M+H^+$) (*m/z*)	
					Calc.	Found
(221)	98%	⋆	0.70	⋆	⋆	⋆
(257)	90%	78–80	0.74	1722 (C=O), 1593, 1501 (C=C)	409.065◊	409.0655
(258)	80%	68–70	0.63	1724 (C=O), 1578, 1502 (C=C)	409.065◊	409.0667
(224)	97%	▲	0.76	▲	▲	▲
(259)	86%	134–136	0.67	1709 (C=O), 1580, 1499 (C=C)	486.9756^	486.9764
(260)	88%	144–146 (CH_3CN)	0.55	1727 (C=O), 1578, 1480 (C=C)	486.9756^	486.9742

*mobile phase = 50:50 EtOAc:hexane
⋆compound previously characterised, see Section 3.2.1.4
▲compound previously characterised, see Section 3.3.3.4
◊molecular ion (M) calculated for ^{79}Br isotope peak
^molecular ion (M) calculated for $^{79}Br_2$ isotope peak

As these dibenzylketones were prepared as potential impurities of the bromination of non-bromo dibenzylketone **(221)**, it was decided to assess if these compounds could be efficiently resolved by HPLC. Firstly, each of the compounds were run individually in order to establish the elution order (Figure 4.34).

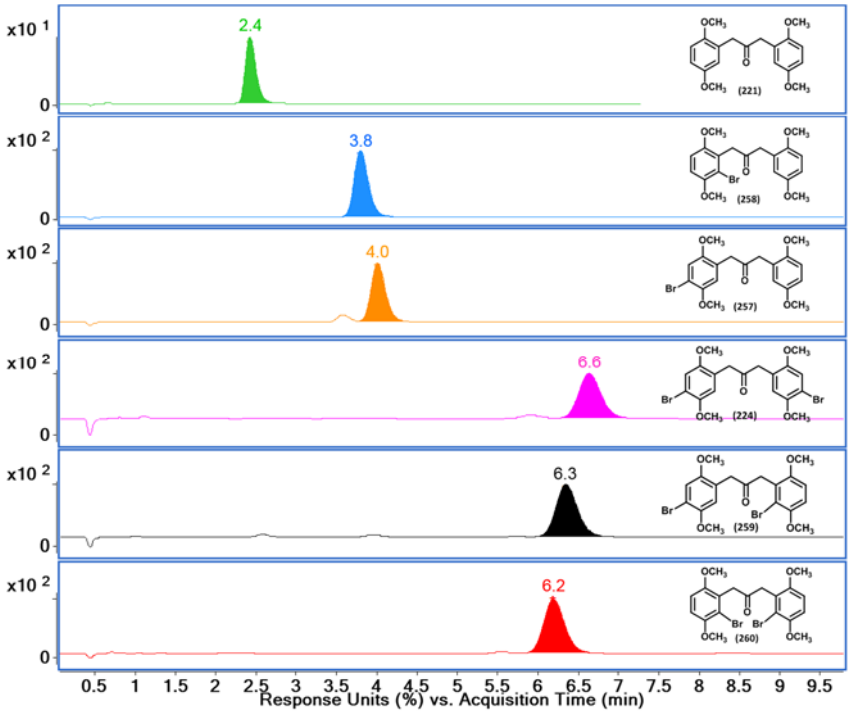


Figure 4.34: Individual HPLC runs (@ 210 nm) of all six prepared dibenzylketones

(Mobile phase = 50/50 'CH_3CN'/'H_2O' (isocratic), flow rate = 0.1 mL/min, column = Agilent Zorbax SB-C18, 3.5 µm, 2.1×30 mm @ rt)

The identity of each of the above compounds was supported by MS evidence: for regioisomeric compounds, differences in the abundance of particular daughter ions (following targeted MS/MS) may be used to distinguish between two compounds of the same mass. For example, for regioisomeric pairs **(257)** and **(258)**, and **(224)** and **(260)**, the fragmentation patterns are similar but the abundances of daughter ions are different (Figure 4.35).

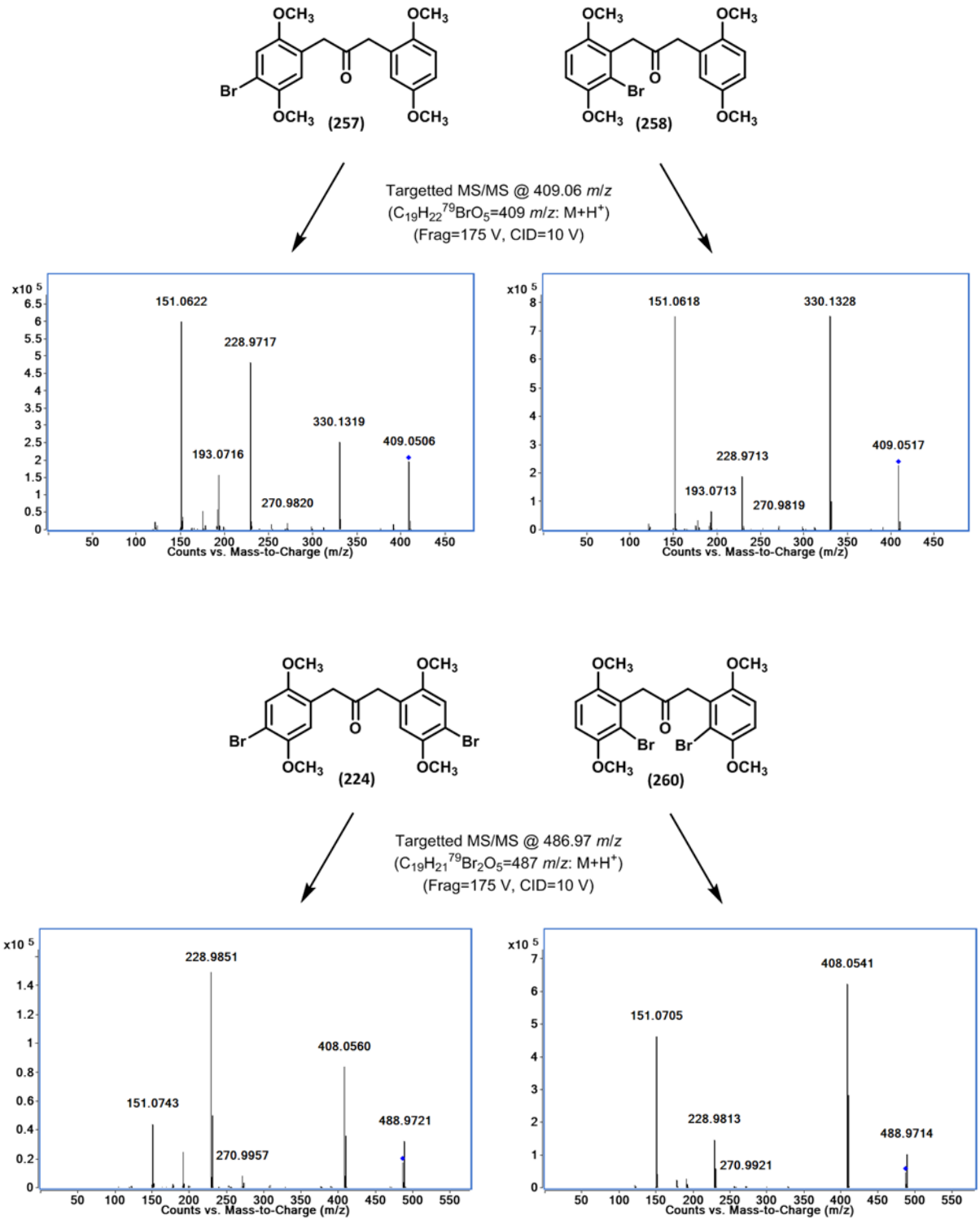


Figure 4.35: Collision-induced dissociation (CID) of regioisomeric dibenzylketone pairs, (257) and (258) (monobromo), and (224) and (260) (dibromo)

The origin of several of the most abundant daughter ions featured in Figure 4.35, is proposed in Figure 4.36.

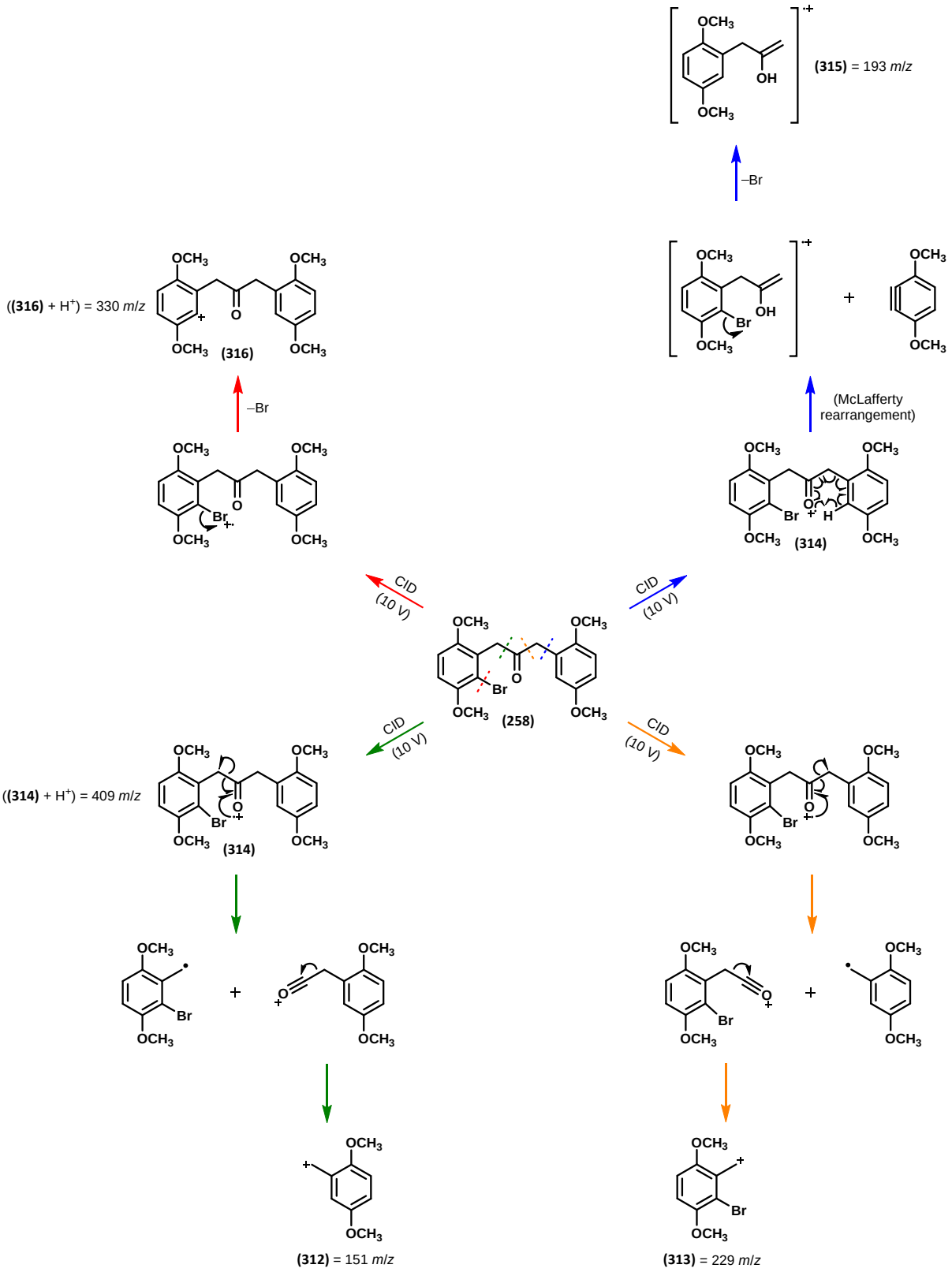


Figure 4.36: Proposed fragmentation pattern of dibenzylketone (258), giving rise to the most abundant fragment/daughter ions observed in Figure 4.35

The daughter ions are thought to arise as a result of homolytic cleavage about the central carbonyl group, followed by loss of carbon monoxide (CO), producing fragments **(312)** and **(313)**. McLafferty rearrangement of the ionised parent molecular ion **(314)** is also thought to occur, with subsequent heterolytic cleavage of bromine producing fragment **(315)**. Initial heterolytic cleavage of bromine from the parent molecular ion, may also occur resulting in cation **(316)**. Under the MS conditions used (ESI+), it is in fact the protonated *m*/*z* of **(316)** ($M+H^+$) that is observed.

The HPLC conditions used to produce the chromatograms in Figure 4.34, did not provide sufficient separation of all six dibenzylketones. Following this, optimisation of conditions was carried out using a prepared mixture of all six compounds. This optimisation included changing the type of column used, as well as modifying the organic/aqueous mobile phase ratio, flow rate and column temperature.
Separation of all six compounds was first attempted using an Agilent Zorbax SB-C18, 3.5 µm column (dimensions = 2.1×30 mm). A high organic % mobile phase ('CH_3CN'/'H_2O' = 80/20) was found to afford very poor separation (Figure 4.37, chromatogram A), with compounds of similar molecular weight remaining unresolved (monobromo compounds **(257)** and **(258)**, $t_R \approx 6.5$ min and dibromo compounds **(224)**, **(259)** and **(260)**, $t_R \approx 7.8$ min). Although marginally better separation was achieved when the % organic was lowered ('CH_3CN'/'H_2O' = 50/50) (Figure 4.37, chromatogram B), it was clear that full resolution of all peaks would not be possible using this column.

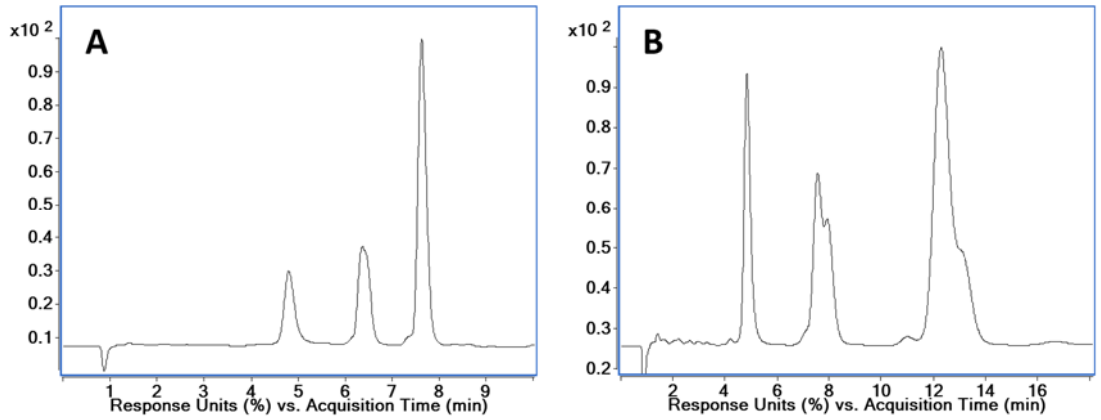


Figure 4.37: HPLC chromatograms (@ 210 nm) of attempted separation of six dibenzylketones using Agilent Zorbax SB-C18, 3.5 µm, 2.1×30 mm column

(Flow rate = 0.1 mL/min, column temperature = 22 °C, mobile phase = 80/20 'CH_3CN'/'H_2O' (chromatogram A) or 50/50 'CH_3CN'/'H_2O' (chromatogram B)

Next, separation was attempted on a slightly longer, small particle column (Agilent Zorbax Eclipse XDB-C18, 1.8 µm, 4.6×50 mm). Partial separation of the two monobromo compounds **(257)** and **(258)** ($t_R \approx$ 6.5 min) was achieved using this column (Figure 4.38, chromatogram A). Some separation of the three dibromo compounds **(224)**, **(259)** and **(260)** ($t_R \approx 9$ min, chromatogram B) was also achieved after the

column temperature was raised to 40 °C (*vs*. 22 °C for chromatogram A). Overall however, the poor peak shape (peak tailing) observed for all compounds in the mixture, suggested that full separation would be very difficult to achieve with this column also.

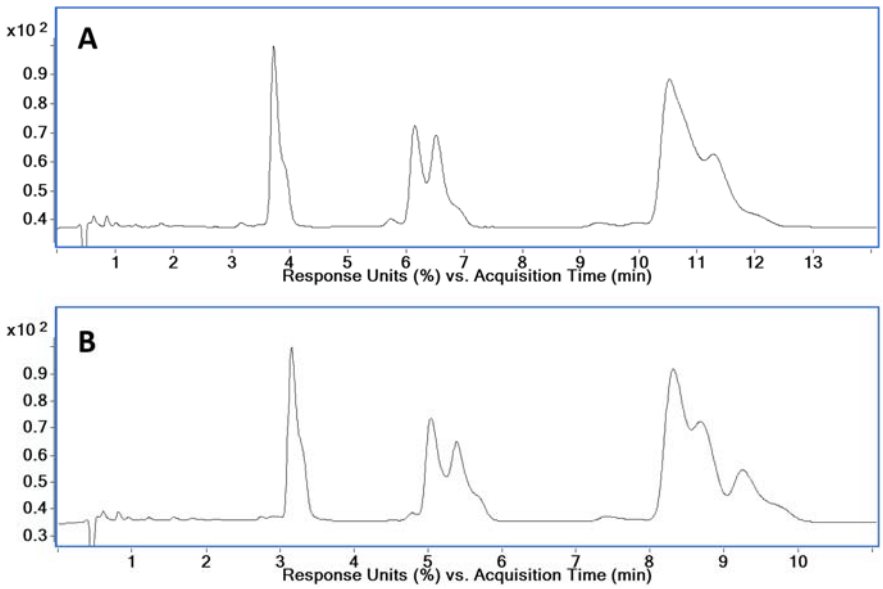


Figure 4.38: HPLC chromatograms (@ 210 nm) of attempted separation of six dibenzylketones using Agilent Zorbax Eclipse XDB-C18, 1.8 µm, 4.6×50 mm column

(Flow rate = 1 mL/min, mobile phase = 50/50 'CH₃CN'/'H₂O', column temperature = 22 °C (chromatogram A) or 40 °C (chromatogram B)

The third and final column tested (Agilent Zorbax Eclipse, XDB-C18, 3.5 µm, 4.6×75 mm), provided much improved resolution and peak shape. Using the elevated column temperature (40 °C) and even lower % organic mobile phase ('CH_3CN'/'H_2O' = 40/60), almost full baseline resolution of all six compounds was achieved. The chromatogram acquired under these conditions is shown in Figure 4.39.

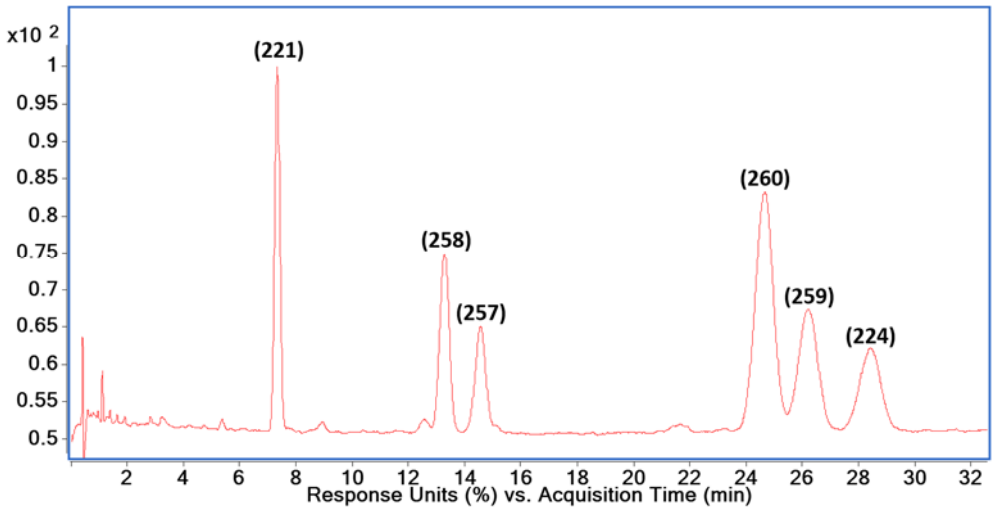


Figure 4.39: Optimised HPLC separation of six novel dibenzylketones

(Mobile phase = 40/60 'CH₃CN'/'H₂O' (isocratic), flow rate = 1.5 mL/min, column = Agilent Zorbax Eclipse XDB-C18, 3.5 µm, 4.6×75 mm @ 40 °C, signal recorded @ 210 nm)

4.3.2 Confirmation of the presence of several aromatic ring–brominated dibenzylketones, as impurities of the bromination of 1,3-bis(2,5-dimethoxyphenyl)-2-propanone (221)

As outlined in Section 4.3, numerous compounds were found to be produced from the bromination (using Br_2 in AcOH) of dibenzylketone **(221)**. With five potential brominated dibenzylketone impurities prepared, we decided to investigate if any of these compounds were present in the crude reaction mixtures of the initial bromination experiments (Section 4.3). Despite severe crowding of the methoxy/methylene proton signals (δ 3.60–3.90) and aromatic proton signals (δ 6.60–7.10) in the ^{1}H-NMR spectra of the crude bromination experiments, some of the aromatic signals corresponding to the dibenzylketone SM **(221)**, monobromo-dibenzylketone **(257)** and dibromo-dibenzylketone **(224)**, could be tentatively identified in the crude bromination experiment ^{1}H-NMR spectra. These signals in the 0.5, 1.0 and 1.5 eqv. (Br_2) experiments, as well as the protons from which they arise, are highlighted in Figure 4.40.

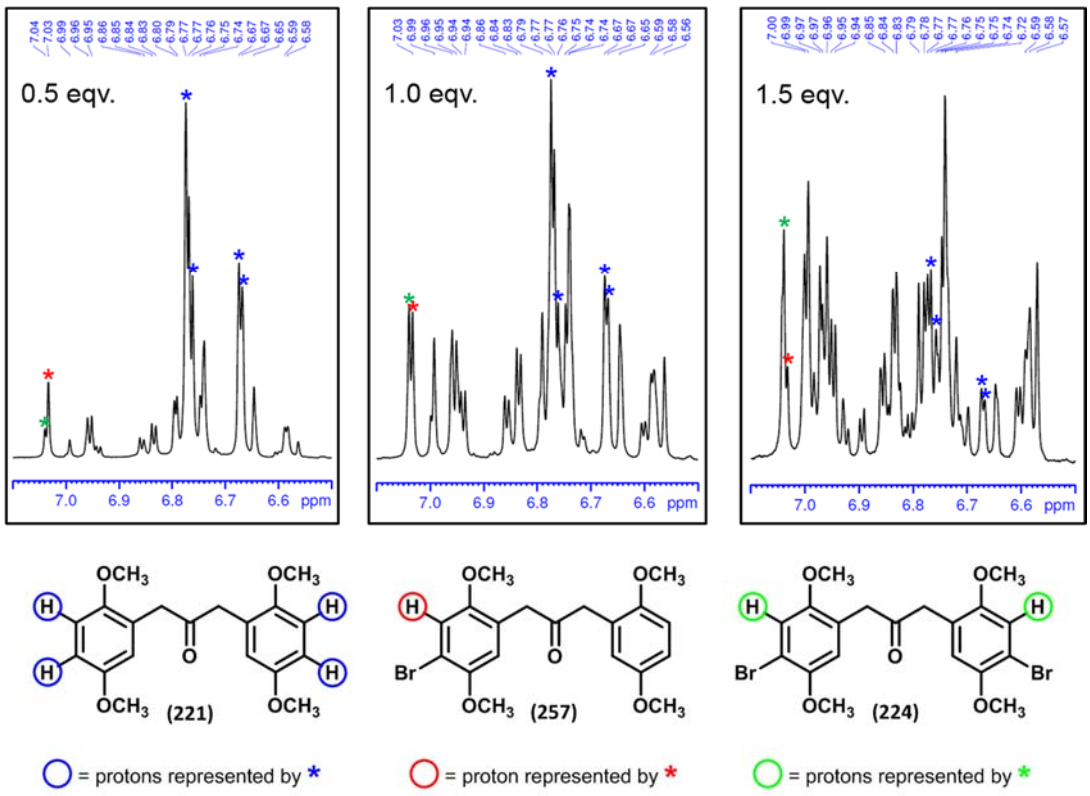


Figure 4.40: Aromatic regions of ^{1}H-NMR spectra of crude bromination experiments, showing tentative evidence for the presence of dibenzylketones (221), (257) and (224)

*(Bromination of **(221)** was carried out in Br_2/AcOH, stirring @ rt for 24 h)*

Evidence for the presence of these three compounds was corroborated by LC-MS data. When crude product samples from the bromination experiments were analysed by LC-MS, matching of the t_R, as well as the MS data, allowed for the presence of compounds **(221), (257)** and **(224)** to be confirmed. These

compounds, found as either products or unreacted SM of the bromination experiments, are highlighted in Figure 4.41.

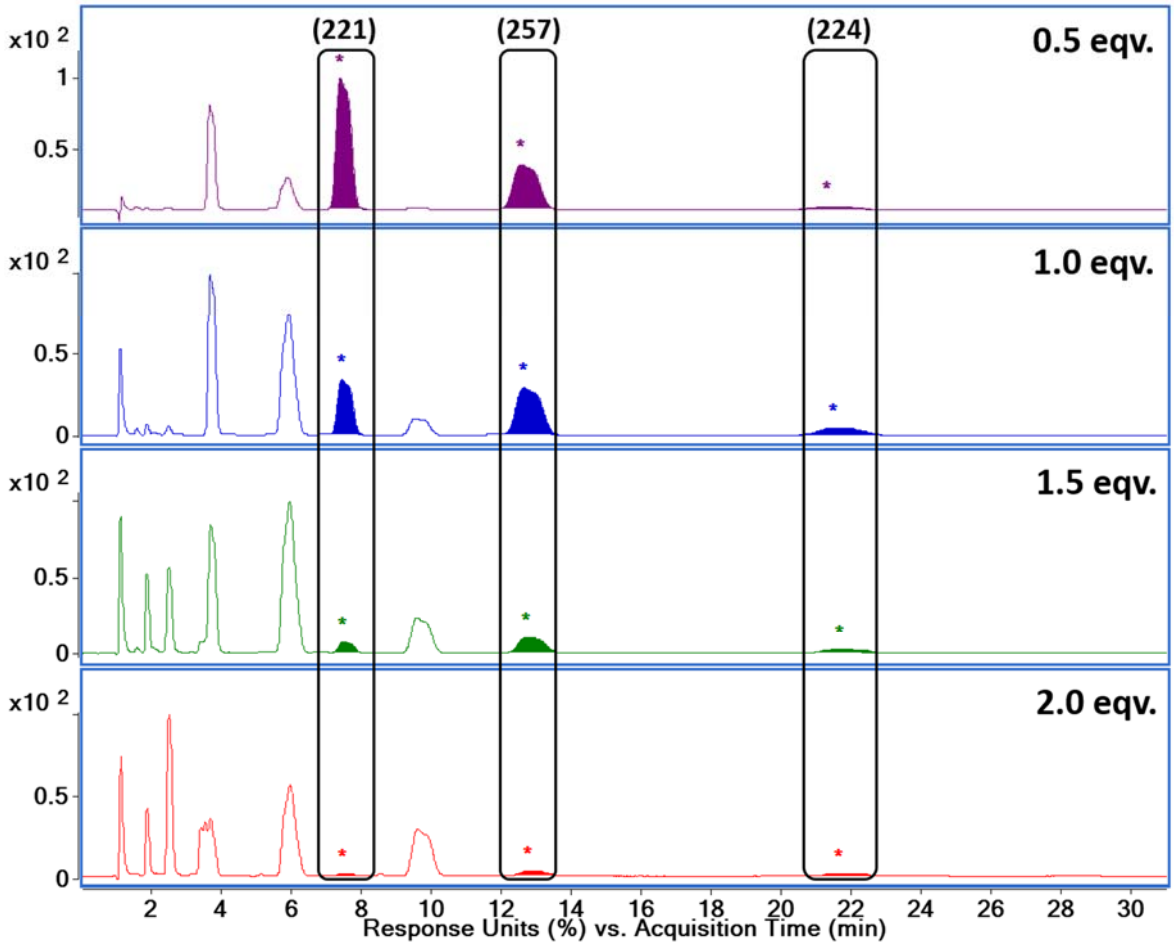


Figure 4.41: Stacked HPLC chromatograms (@ 210 nm) of crude samples from bromination experiments of (221) (in 0.5–2.0 eqv. of Br_2). Previously prepared dibenzylketones (221), (257) and (224) are outlined in boxed regions

(Mobile phase = 50/50 'CH₃CN'/'H₂O' (isocratic), flow rate = 0.4 mL/min, column = Agilent Zorbax Eclipse XDB-C18, 1.8 µm, 4.6×50 mm @ 40 °C)

Based on ^{1}H-NMR spectroscopy/LC-MS evidence from the bromination experiments, it was clear that under the conditions used (Br_2 in AcOH), bromination at any of the 6-positions (inner face of dibenzylketone), does not occur. This is evident by the absence, in the LC-MS runs (Figure 4.41), of any of the previously prepared dibenzylketones featuring a bromine atom at the 6-position (i.e. compounds **(258)**, **(259)** and **(260)**). Also, the ^{1}H-NMR and LC-MS data both suggest that increasing the number of equivalents of Br_2, greatly increases the complexity of the crude samples recovered, with several more compounds detected using 2.0 eqv. of Br_2 compared to that in which only 0.5 eqv. were used (see 1–4 min region of chromatograms in Figure 4.41). Based on ^{1}H-NMR evidence (several signals @ δ ≈6) and previous work on the bromination of 2,5-P2P **(92)** (Section 4.2), it was thought that these other

'unknown' compounds (unintegrated peaks outside boxed regions in Figure 4.41) arise when bromination of the dibenzylketone occurs at the benzylic positions.

4.3.3 Attempted synthesis and identification of suspected benzyl-bromo products

Examination of the mass spectra arising from the unknown peaks in Figure 4.41, did not shed light on the identity of the 'unknowns'; no obvious molecular ion could be identified in any of the mass spectra and no sense could be made of the several fragment/recombination product ions. This suggests that the suspected benzyl-bromo compounds ('unknowns') are labile under the MS conditions used.

In an attempt to synthesise standards of the suspected benzyl-bromo compounds, produced from the bromination (Br_2/AcOH) of dibenzylketone **(221)**, the methodology used earlier (Section 4.2.2) to selectively brominate at the benzylic site, was adopted. The radical induced, NBS bromination was carried out on the three dibenzylketones (**(221)**, **(257)** and **(224)**), previously identified as unreacted SM/products of the Br_2/AcOH bromination experiments. These reactions were carried out using different eqv. of NBS (Figure 4.42).

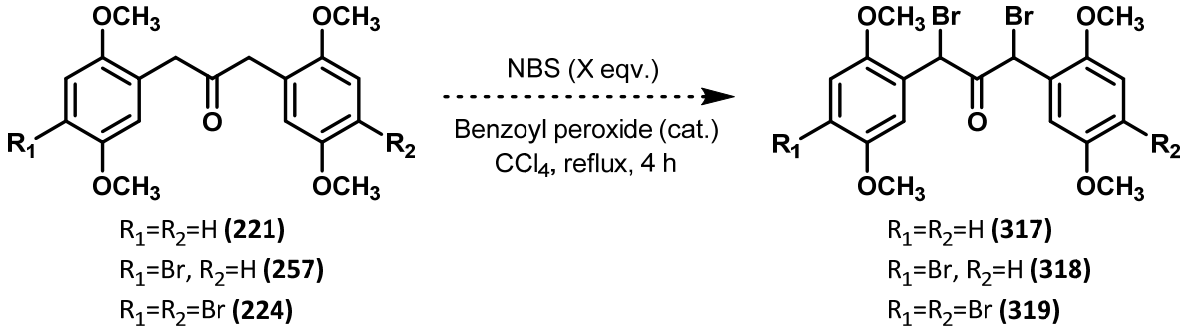


Figure 4.42: 'Selective' benzylic bromination of dibenzylketones (221), (257) and (224)

*(Benzylic bromo products **(317)**, **(318)** and **(319)** not exclusively produced, isolation of each was not pursued)*

Partial bromination (mono-bromination) of the two available benzylic sites of dibenzylketones **(221)**, **(257)** and **(224)** may be possible also, when dibenzylketone **(221)** is exposed to Br_2. With this in mind, experiments whereby a lower number of eqv. of NBS (1.1 eqv.), than is theoretically required (≈2 eqv.) for bromination at both benzylic sites, were carried out. Details of the experiments carried out are outlined in Table 4.11 (see also Experimental – Section 5.4.9).

Also included in this Table are ^{1}H-NMR δ values of shifts in the region of 6.0–6.30 ppm, observed in the spectra of the crude recovered benzyl-bromo products. These shifts are suspected to correspond to benzylic protons adjacent to a bromine atom.

Table 4.11: Attempted benzylic bromination of dibenzylketones (221), (257) and (224), using different eqv. of NBS

SM	No. of eqv. of NBS used	^{1}H-NMR δ values of prominent shifts in region of 6.0–6.3 ppm (all signals reported are singlets)
(221)	10	6.03, 6.15, 6.20
	2.2	6.03, 6.23
	1.1	6.04, 6.07, 6.23
(257)	2.2	6.01, 6.04, 6.16, 6.21
	1.1	6.02, 6.04, 6.04, 6.05, 6.16, 6.21
(224)	2.2	6.02, 6.14
	1.1	6.00, 6.03, 6.14

With regard to the initial Br_2/AcOH brominations of dibenzylketone **(221)**, benzylic bromination was suspected due to the presence of several shifts @ δ ≈6 in the ^{1}H-NMR spectra (Section 4.3). These shifts, for the 0.5–2.0 eqv. of Br_2 experiments, are summarised in Table 4.12.

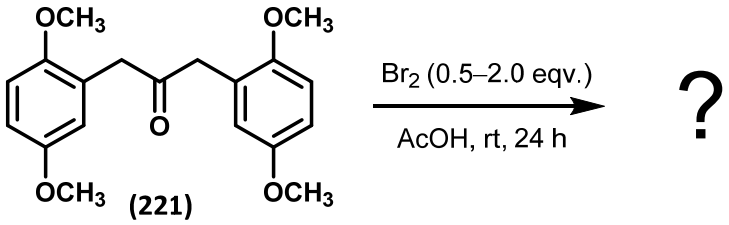


Table 4.12: ^{1}H-NMR δ values of shifts observed in the region of 6.0–6.30 ppm, following bromination of dibenzylketone (221) by Br_2

Number of eqv. of Br_2 used	^{1}H-NMR shifts observed in region of 6.0–6.30 ppm (all signals = singlets)
0.5	6.04, 6.05, 6.08
1.0	6.00, 6.04, 6.05, 6.08
1.5	6.00, 6.04, 6.04, 6.07, 6.14, 6.16, 6.21, 6.23
2.0	6.00, 6.02, 6.03, 6.04, 6.04, 6.05, 6.07, 6.14, 6.16, 6.21, 6.23

An insight into the complexity of the δ ≈6 ppm region of the ^{1}H-NMR spectrum of the 2 eqv. (of Br_2) experiment, can be gained from Figure 4.43.

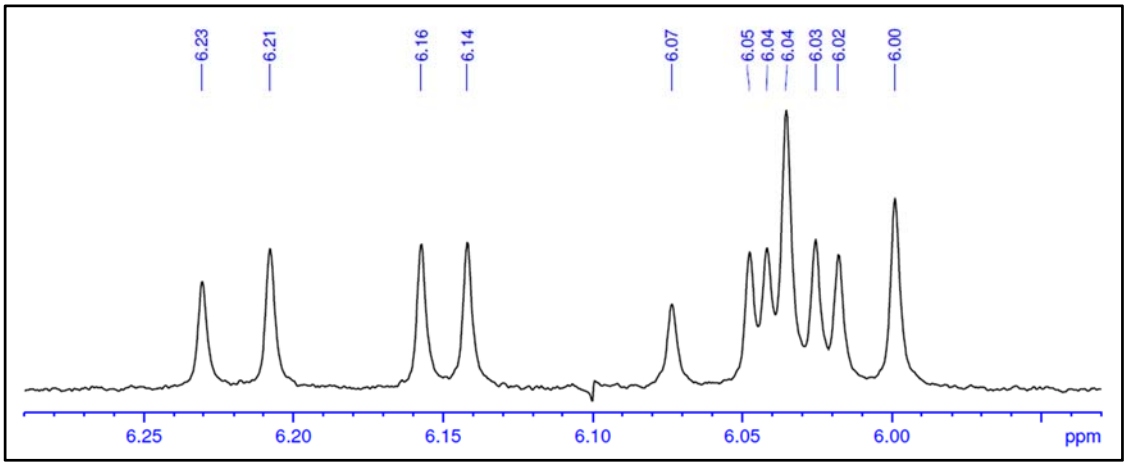


Figure 4.43: The δ 5.93–6.29 ppm region of the ^{1}H-NMR spectrum of the crude product of the bromination (2 eqv. of Br_2) of dibenzylketone (221)

The complexity of the δ ≈6 ppm region of the ^{1}H-NMR spectrum of the bromination experiments, increases with increasing number of eqv. of Br_2 (see Table 4.12 and Figure 4.43). To understand why so many signals arise, one must consider the following points:

- In addition to the dibenzylketone SM **(221)**, two other aromatic ring-brominated dibenzylketones (**(257)** and **(224)**) are known to arise, with each of these three compounds having the potential to undergo benzylic bromination to some extent.
- Bromine substitution at the benzylic positions gives rise to two stereogenic centres. The resulting benzyl-bromo isomers of each compound may give rise to multiple sets of signals (i.e. several diastereoisomers).
- The extent of bromination at the benzylic positions is difficult to control. In some cases, bromine substitution at just one of the two available benzylic sites of a given dibenzylketone ('partial bromination'), may occur. In other cases (most likely excess Br_2), dibromination at a particular benzylic site, may occur. This phenomenon was observed during the benzylic bromination of monomeric ketones in Section 4.2.3.

Although preparation of benzyl-bromo dibenzylketone standards had been attempted (Figure 4.42), no pure compounds could be isolated. This made it particularly difficult to make any correlations between the benzylic proton ^{1}H-NMR signals of the standards, and shifts present in the crude products of the bromination experiments (using Br_2) (Tables 4.11 and 4.12).

It was hoped that if correlations could be made between signals common to both Tables, evidence could be provided of the specific benzyl-bromo compounds that are formed when dibenzylketone **(221)** is subjected to Br_2. This proved to be very difficult, as a result of the high number of signals in this region and their close proximity to one another. Also, as discovered earlier, the benzyl-bromo compounds

were found to be unsuitable for analysis by MS, making their identification, in a crude reaction mixture, very difficult. In conclusion, aside from unreacted SM **(221)**, and aromatic ring-brominated products **(257)** and **(224)**, identification of other compounds produced from the bromination of dibenzylketone **(221)**, (by Br_2) proved very difficult. No further attempts to identify these compounds were pursued.

4.4 Impurity profiling of the Leuckart reaction of dibenzylketones (221) and (224) with formamide

The Leuckart route is reported to be the most common method used by clandestine chemists, for preparing amphetamine **(10)** from its ketone precursor P2P **(65)**.[115] As mentioned in Section 1.5.1.1, many impurities are known to arise during this route to P2P **(65)**, including several pyridine and pyrimidine impurities. Whilst exploring routes to the hallucinogenic amphetamine DOB **(35)**, a previous member of our research group had investigated the impurities arising during the Leuckart reaction of 2,5-P2P **(92)** with formamide (NH_2CHO).[26] The impurities isolated during this work are summarised in Figure 4.44 below.

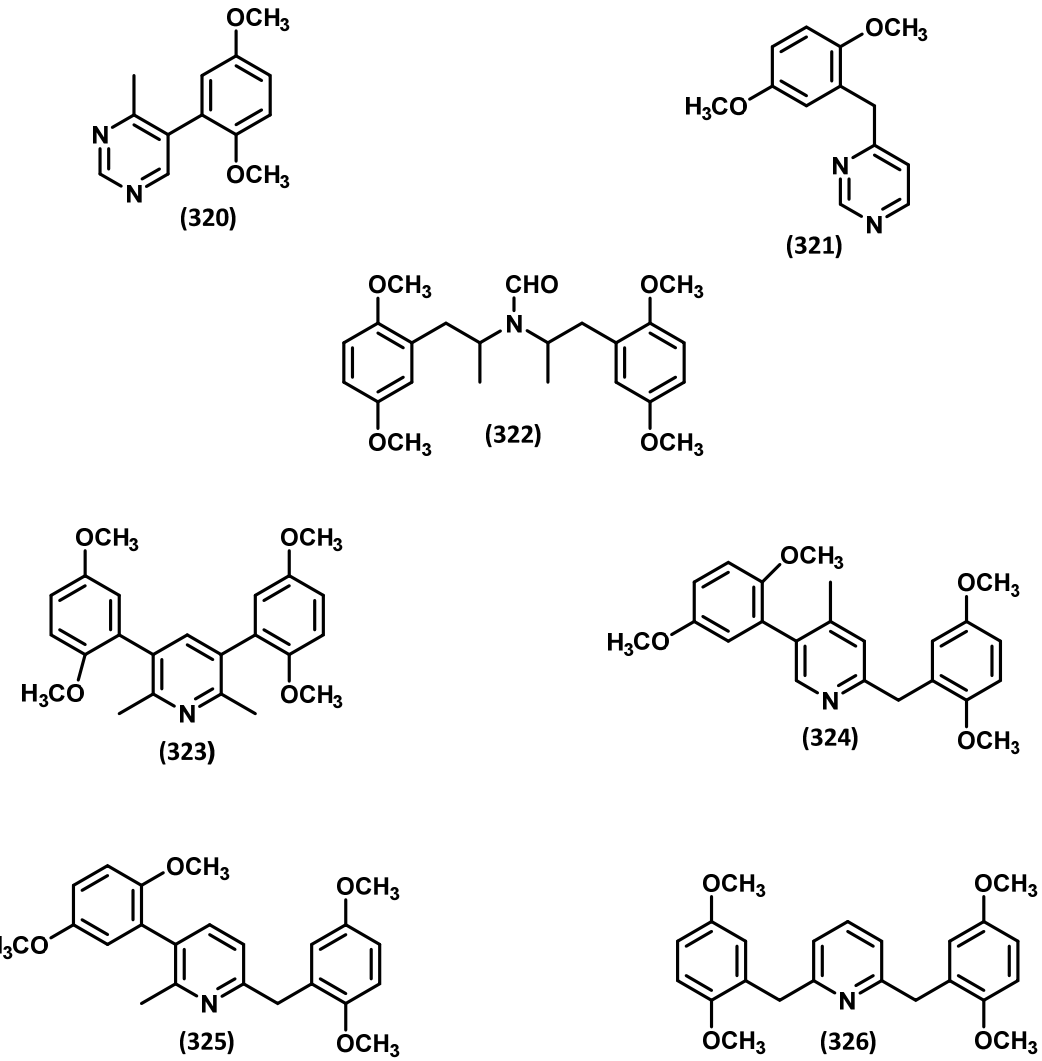


Figure 4.44: Impurities arising from the Leuckart reaction of 2,5-P2P (92) with formamide[26]

There is a substantial amount of literature pertaining to the Leuckart route to various amphetamines/methamphetamines, from their ketone precursors (see 'Impurity Profiling' – Section 1.3). These ketone precursors, if prepared in a clandestine laboratory, are likely to be impure and contain substantial amounts of impurities, such as dibenzylketones. These dibenzylketones have similar functionality to the monomeric ketone precursor and would therefore be likely to undergo similar reactions, for example, the Leuckart reaction. The impurity profile produced following exposure of these dibenzylketones to Leuckart reaction conditions, has not been well explored in the literature.[248]

Dibenzylketone **(221)**, which was shown earlier (Section 3.2.1.4) to be a likely contaminant of illicitly produced 2,5-P2P **(92)**, has similar functionality to 2,5-P2P **(92)** and would therefore be likely to possess similar reactivity. Likewise, when the aromatic 4-bromo ketone (4-Br-2,5-P2P **(159)**) is synthesised, the corresponding dibromo dibenzylketone **(224)** is formed. In this section of work, impurities produced when these dibenzylketones (**(221)** and **(224)**) are exposed to Leuckart reaction conditions, are investigated.

Using the Leuckart route to produce an amphetamine from its ketone precursor, is a two-step process. The first step involves the reaction of an appropriate alkanone with the appropriate nitrogen source e.g. formamide, to afford an intermediate *N*-formyl amphetamine. This step is a typical example of what is known as the Leuckart-Wallach reaction; the term 'Leuckart route' being derived from this. The second step involves hydrolysis of the *N*-formyl moiety to afford the desired amphetamine.
In the case whereby a dibenzylketone is used as a SM, the product (of the 2-step synthesis) would be expected to be a dimeric primary amine. The application of the Leuckart route, to the attempted synthesis of dimeric amines **(327)** and **(328)**, is outlined in Figure 4.45.

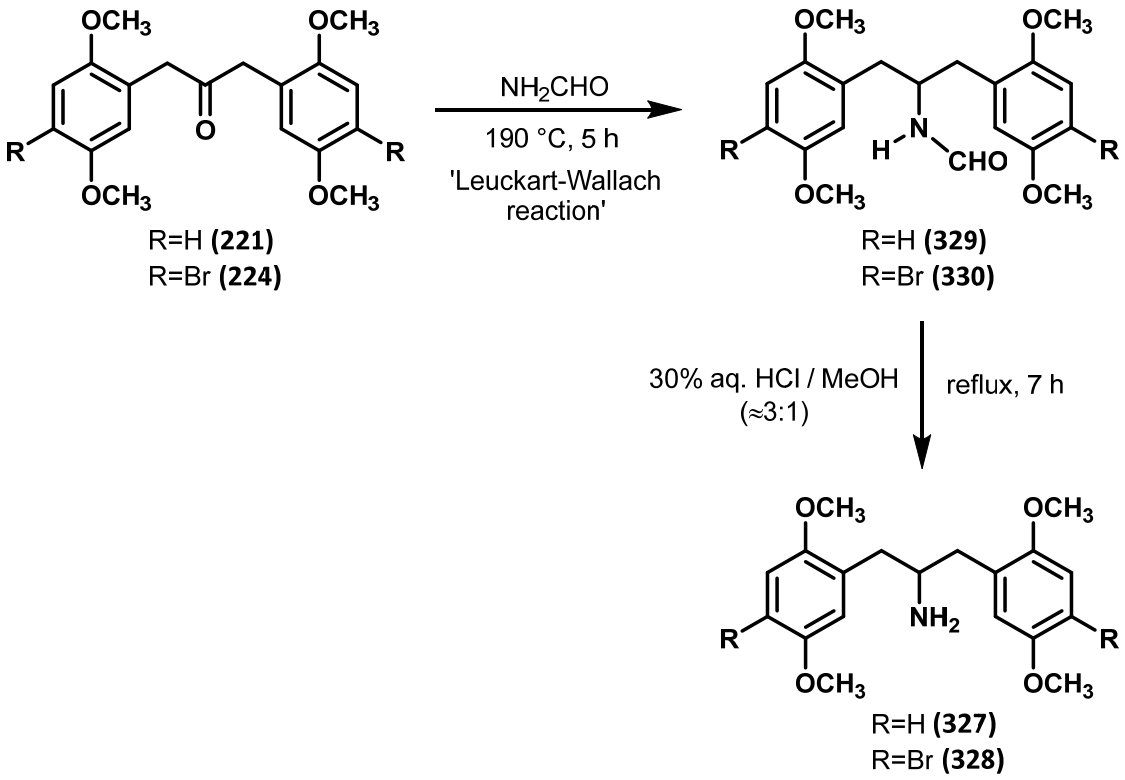


Figure 4.45: Leuckart route to dimeric amines (327) and (328) from dibenzylketones (221) and (224)

4.4.1 Step 1: The 'Leuckart-Wallach reaction'

Following the first step of the sequence (Leuckart-Wallach reaction) outlined in Figure 4.45, the crude products were subjected to flash column chromatography. Upon purification, the expected novel *N*-formyl products **(329)** and **(330)**, were isolated in yields of 47% and 61% respectively. The R_f, m.p., IR and MS data for dimeric *N*-formyl compounds **(329)** and **(330)**, are outlined in Table 4.13 below.

Table 4.13: Yield, R_f, m.p., IR and HRMS data for dimeric *N*-formyl compounds (329) and (330)

Compound No.	Yield	m.p. (°C)	R_f	IRν_{max} (KBr) (cm^{-1})	HRMS ($M+H^+$) (*m/z*)	
					Calc.	Found
(329)	47%	107–109 (Et_2O/hexane)	0.39*	3313 (N-H), 1659 (C=O), 1502 (C=C)	360.1811	360.1807
(330)	61%	148–150 (EtOH)	0.39★	3294 (N-H), 1656 (C=O), 1497 (C=C)	516.0021▲	516.0016

*mobile phase = 50:50 EtOAc:hexane

★mobile phase = 70:30 EtOAc:hexane

▲molecular ion (M) calculated for $^{79}Br_2$ isotope peak

Although there is a high degree of symmetry about the central amide bond in both *N*-formyl products **(329)** and **(330)**, hindered rotation about this bond, as well as partial double bond-like character between N and C, results in two sets of signals being observed (two 'rotamers') in the ^{1}H-NMR and ^{13}C-

NMR spectra. The double bond-like character arises due to the lone pair of electrons on the N atom being delocalised onto the O atom of the *N*-formyl carbonyl group (Figure 4.46).

The rotamer ratio observed for a particular compound may be solvent or temperature dependant. Therefore the rotamer ratio ('A':'B') may be shifted by changing either of these parameters.

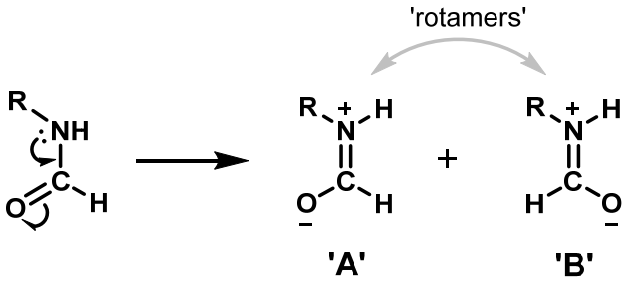
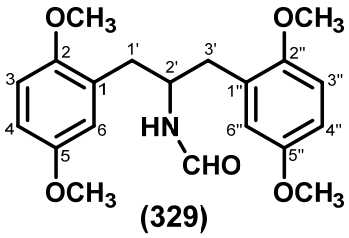


Figure 4.46: Basis for the observation of two sets on signals ('rotamers') in the ^{1}H-NMR/^{13}C-NMR spectra of some *N*-formyl compounds

Assigning ^{1}H-NMR signals to each rotamer for a particular *N*-formyl compound was difficult due to extensive signal overlap. For non-bromo *N*-formyl **(329)**, extensive rotamer signal overlap is observed for the methylene protons (on C-1'/C-3'), methoxy group protons and aromatic ring protons. In addition to the extensive rotamer signal overlap, the similarity in abundance of rotamers (rotamer ratio = 55/45 @ 20 °C in $CDCl_3$), also made it difficult to distinguish between the two.



As alluded to above, the rotamer ratio is often solvent or temperature dependant. In order to change this ratio, the ^{1}H-NMR spectrum could be acquired at a number of different temperatures. These experiments would provide spectra with varying rotamer ratios which may greatly enhance the ability to distinguish between the two sets of rotamer signals. This would be particularly useful in the case of *N*-formyl **(329)**, whereby the rotamer ratio is almost 1:1, making it extremely difficult to distinguish between the two sets of signals. Although these temperature experiments were not carried out during our work, they may be used in the future to distinguish between *N*-formyl rotamers in forensically relevant amphetamine-type drugs of abuse.

As mentioned, for *N*-formyl **(329)**, the methylene protons (on C-1'/C-3') are diastereotopic, lying α to the stereogenic centre at C-2'. Each diastereoisomer would be expected to give rise to a doublet of doublets (dd's) per diastereotopic proton. With two diastereoisomers, there is a total of eight protons

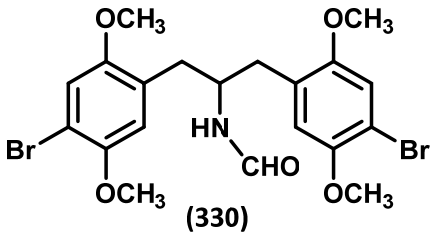
that may give rise to dd signals. However, the symmetry about C-2' makes the protons on C-1' and C-3' magnetically equivalent for a given diastereoisomer, thus simplifying the expected splitting pattern to four dd's.

For non-bromo *N*-formyl **(329)**, overlap of these dd's occurs. Only two of the dd's (@ δ 2.76 and 2.80) can be resolved in its ^{1}H-NMR spectrum and this is only achieved after the sample is run @ 600 MHz. Resolution of signals corresponding to the major and minor rotamers is only achieved for signals arising from the proton on C-2', NH proton and *N*-formyl (CHO) proton:

- Multiplets are observed for the proton on C-2', @ δ 3.87 (minor rotamer) and @ δ 4.44 (major rotamer).
- For the NH proton, coupling to the proton on C-2' is observed for the major isomer, giving rise to a doublet (@ δ 5.91, *J*=7.3 Hz). In the case of the minor rotamer, additional coupling (to the formyl proton) is evident due to the presence of a triplet (@ δ 5.70, *J*=9.6 Hz), located slightly upfield of the doublet.
- The minor and major rotamer formyl group protons are well resolved, resonating at δ 7.42 and 8.00 respectively. They also exhibit very different splitting patterns. The minor rotamer formyl proton was found earlier, to cause splitting of the NH proton. Reciprocal splitting (of the formyl proton by NH) is observed @ δ 7.42, in the form of a doublet (*J*=12.0 Hz). In contrast, there is minimal coupling of the formyl proton to NH, for the major rotamer (@ δ 8.00, *J*=0.8 Hz). The greater level of splitting experienced by the minor rotamer may indicate that its formyl and NH protons possess a more *trans* relationship (see rotamer 'B', Figure 4.46). This proposal is based on the fact that across alkenes, the splitting (*J* value) of *trans* protons is generally greater than that of *cis* protons.

As indicated in the Experimental Section (5.4.10), assignment of ^{13}C-NMR chemical shifts to each of the rotamers was not attempted. This was due to the similarity in the abundances of the two rotamers (rotamer ratio = 55/45). It is therefore not possible to assign signals to each rotamer with a high degree of certainty. There was little difference in the chemical shift values (<1 ppm) between both rotamers, for most signals in the ^{13}C-NMR spectrum. The exceptions to this were the chemical shifts corresponding to C-1'/C-3', C-2' and CHO. There was a significant difference (≈3 ppm) between the two rotamers, for each of these signals.

With regard to the novel dibromo-*N*-formyl product **(330)**, the ^{1}H-NMR and ^{13}C-NMR spectra acquired were very similar to that of non-bromo **(329)**. A rotamer ratio of ≈ 70/30 was observed (@ 20 °C in $CDCl_3$).



(330)

Similar to non-bromo-*N*-formyl **(329)**:

- Only two of the four expected dd's (@ δ 2.72 and 2.78), arising from diastereotopic protons on C-1'/C-3', are resolved in the ^{1}H-NMR spectrum.
- Some overlap of the methoxy group protons takes place, with only three singlets (@ δ 3.79, 3.83 and 3.83) observed – four '3H' singlets theoretically expected.
- For the NH proton, a doublet is observed for the major rotamer (@ δ 5.84, *J*=7.6 Hz), whilst a triplet is observed for the minor rotamer (@ δ 5.71, *J*=9.0 Hz).
- The formyl group proton splitting, arising from the major and minor rotamers, is well resolved, with that of the minor rotamer (@ δ 7.44) exhibiting a greater degree of splitting (*J*=11.9 Hz) than the major rotamer (@ δ 8.01, *J*=0.8 Hz). Again, it may be assumed that that greater level of splitting experienced by the minor rotamer, would suggest that its formyl and NH protons possess more of a *trans* relationship.

The ^{1}H-NMR spectra of both *N*-formyl compounds (non-bromo **(329)** and dibromo **(330)**) can be found in Figure 4.47.

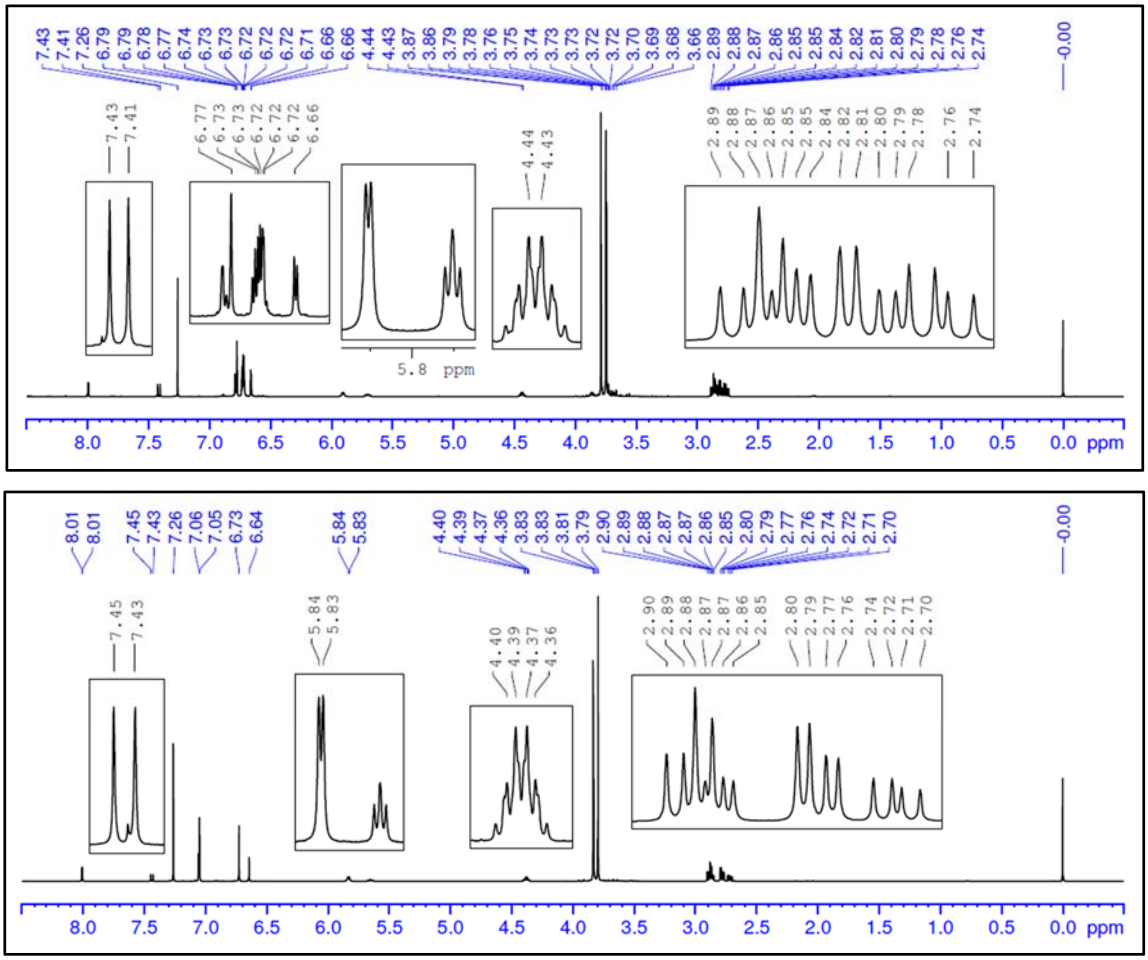


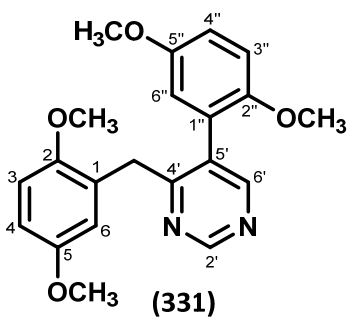
Figure 4.47: ^{1}H-NMR spectra of non-bromo (329) (top) and dibromo (330) (bottom) *N*-formyl intermediates (@ 600 MHz)

The key differences between the spectra of the non-bromo **(329)** and dibromo **(330)** *N*-formyl compounds are:

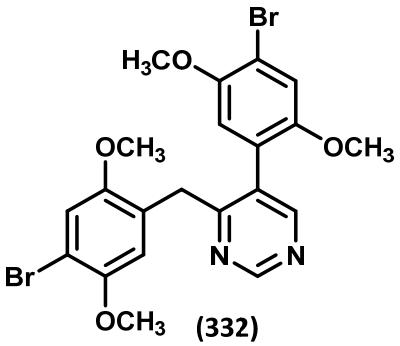
- As expected, the different ring substitution pattern of dibromo-*N*-formyl **(330)**, gives rise to a number of singlets in the aromatic region of the ^{1}H-NMR spectrum. The lack of splitting and thus inherent simplicity of the aromatic region means that, in contrast to the non-bromo compound **(329)**, the signals corresponding to each of the two rotamers can be differentiated for **(330)** (Major = δ 6.73, 7.05 [(2H, s) × 2]) and (Minor = δ 6.64, 7.06 [(0.9H, s) × 2]).
- For dibromo-*N*-formyl **(330)**, there is a greater difference in the abundance (@ 20 °C in $CDCl_3$) of the two rotamers (rotamer ratio ≈ 70/30). Thus for a given proton signal (e.g. C*H*O proton) in the ^{1}H-NMR spectrum, the major rotamer integrates for 1H, whilst the minor rotamer integrates for 0.45H. A consequence of this larger rotamer ratio is that assignment of ^{13}C-NMR signals, to one rotamer or the other (major or minor), can be performed with a greater level of certainty.

- For dibromo-*N*-formyl **(330)**, two multiplets, arising from the proton on C-2' of each rotamer, were expected in the ^{1}H-NMR spectrum (as observed for non-bromo **(329)**). In the ^{1}H-NMR spectrum acquired, only one multiplet (@ δ 4.38) was observed. Based on the integration (1H), this multiplet was assigned to the major rotamer. The other multiplet signal (which would theoretically integrate for ≈0.45H) was thought to resonate in the region of δ ≈ 3.80 – the same frequency as the methoxy group protons (17.3H, δ 3.79–3.83).

In addition to the expected dimeric *N*-formyl products (**(329)** and **(330)**) and unreacted starting materials (**(221)** ≈29% and **(224)** ≈5% recovered), one other major compound was isolated from each flash column of the two Leuckart reactions carried out. Characterisation of these compounds, as well as a knowledge of the impurities typically associated with the Leuckart route to amphetamines (Figure 4.44), allowed for plausible compound structures to be proposed. The spectroscopic data collected were consistent with compounds of the following structures:



(331)



(332)

The two novel pyrimidine impurities (**(331)** from the Leuckart reaction of dibenzylketone **(221)**, and **(332)** from the Leuckart reaction of dibromo dibenzylketone **(224)**), are thought to arise when one molecule of ketone SM condenses with two molecules of formamide, as outlined in Figure 4.48.[26] The dibenzylketone SM (**(221)** or **(224)**) undergoes nucleophilic attack (at the carbonyl carbon) by formamide, affording the carbinolamine intermediate **(333)**. Acid-catalysed dehydration, followed by nucleophilic attack by a second molecule of formamide at the acyl carbon of **(334)**, affords after protonation, carbinolimide **(335)**. A second dehydration, of species **(336)**, results in the formation of conjugated species **(337)**. Deprotonation (by ammonia*) of one of the methylene protons of **(337)** affords a carbanion, which undergoes intramolecular nucleophilic attack of the terminal formyl carbon. (*The ammonia is formed *in situ* from the partial thermal decomposition of formamide.)
Subsequent protonation of the phenoxide affords dihydropyrimidine **(338)**. An additional protonation of **(338)**, followed by dehydration, yields the observed pyrimidine (**(331)** or **(332)**).

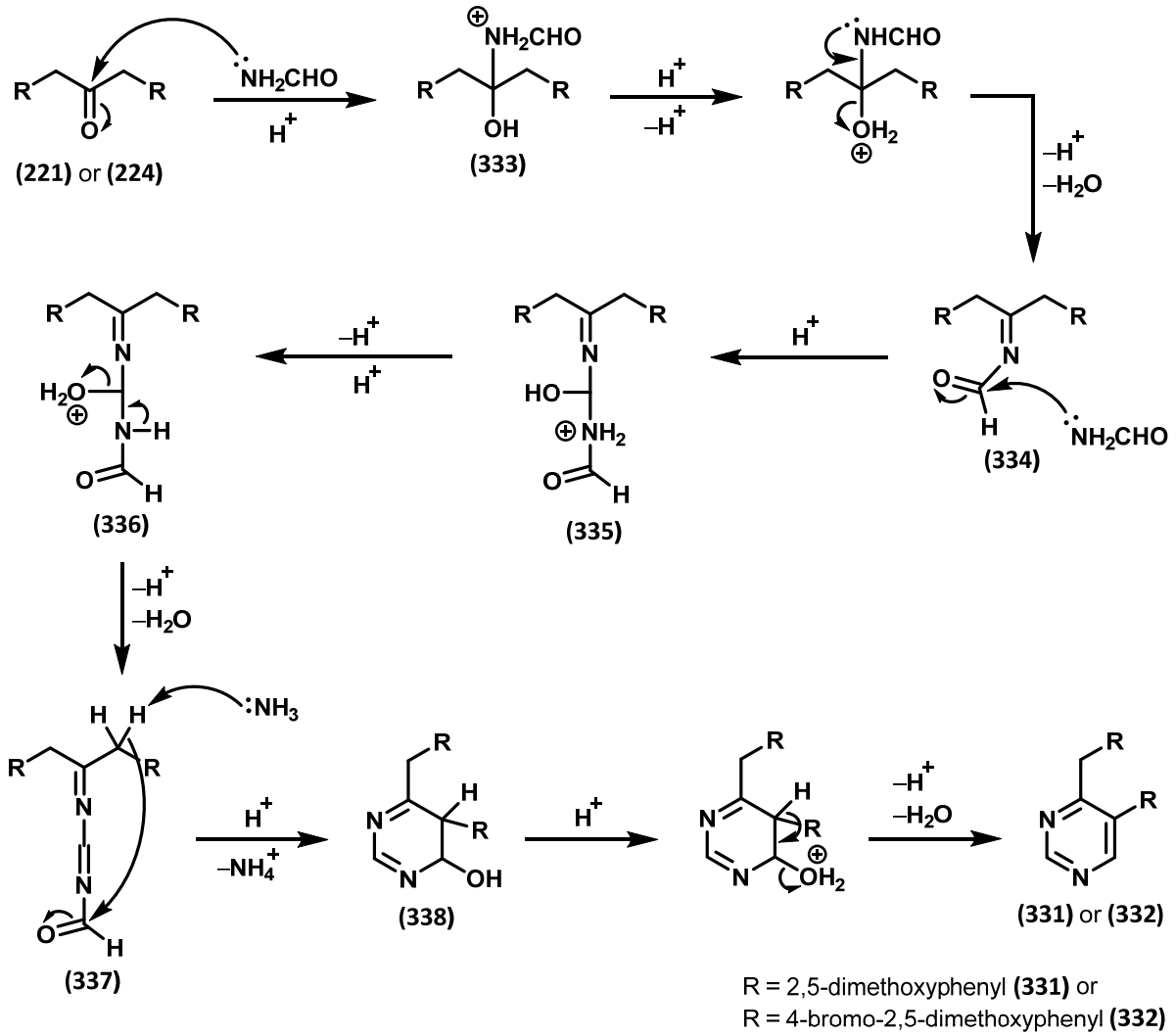


Figure 4.48: Mechanism for the formation of pyrimidines (331) and (332)

The novel pyrimidines were found to be substantial impurities of the Leuckart reaction of the dibenzylketone (either **(221)** or **(224)**) with formamide. The non-bromo pyrimidine compound **(331)** was isolated in a yield of 13%, whist the yield for the brominated analogue **(332)** was nearly twice this (25%). The R_f, m.p., IR and MS data for isolated pyrimidines **(331)** and **(332)**, are outlined in Table 4.14.

Table 4.14: Yield, R_f, m.p., IR and HRMS data for pyrimidine impurities (331) and (332)

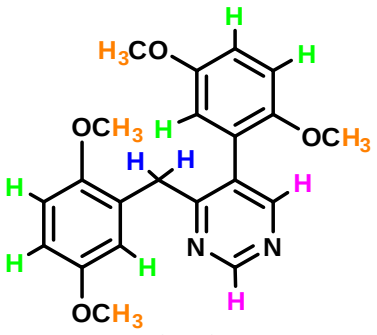
Compound No.	Yield	m.p. (°C)	R_f	IRν_{max} (KBr) (cm^{-1})	HRMS ($M+H^+$) (*m/z*)	
					Calc.	Found
(331)	13%	103–105 (Et_2O/hexane)	0.15*	1608, 1565, 1505 (C=C)	367.1658	367.1646
(332)	25%	116–118	0.45⋆	1603, 1569, 1496 (C=C)	522.9868▲	522.9871

*mobile phase = 50:50 EtOAc:hexane

⋆mobile phase = 70:30 EtOAc:hexane

▲molecular ion (M) calculated for $^{79}Br_2$ isotope peak

Assignment of signals in the ^{1}H-NMR spectra of the two pyrimidines was straightforward. The signals may be split in into four groups, according the type of proton (or group of protons) from which they arise. These include the methoxy group protons, the methylene protons, the phenyl ring protons and the pyrimidine ring protons. For the non-bromo pyrimidine compound **(331)**, these are highlighted in Figure 4.49.



(331)

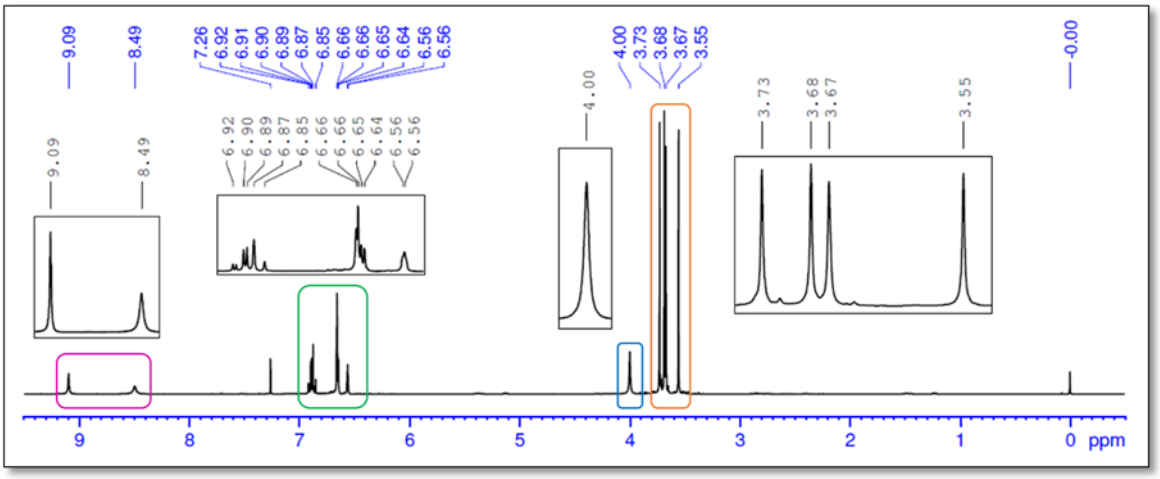


Figure 4.49: ^{1}H-NMR spectrum of pyrimidine (331) highlighting four different groups of signals

The four sets of methoxy group protons are well resolved in the ^{1}H-NMR spectrum of **(331)**, resonating at δ 3.55, 3.67, 3.68 and 3.73. The signal arising from the methylene protons is found slightly downfield of these (@ δ 4.00). The aromatic ring protons are not resolved, featuring as an undiscernible multiplet ranging from δ 6.56 to 6.92. The signals arising from the pyrimidine ring protons are the most distinguishable feature of the ^{1}H-NMR spectrum, due to their very much downfield positions (@ δ 8.49 and 9.09).

Interpretation of the ^{13}C-NMR spectrum of **(331)** was also straightforward. Crude assignment of groups of signals (e.g. aromatic ring carbons, pyrimidine ring carbons etc.) was facilitated by DEPT90 and DEPT135 spectra. In general, the ^{13}C-NMR shifts are more downfield for carbon atoms in the pyrimidine ring compared to those of the aromatic ring, presumably due to the lower π electron density associated with pyrimidine ring systems. Having said this, the general proximity of a given carbon atom to a

heteroatom has an even more substantial effect on chemical shift. This is no more so evident than for the 'quaternary'* carbons at positions 4' and 5' of the pyrimidine ring. C-4' is α to a nitrogen atom and resonates >30 ppm more downfield (@ 167.65 ppm) than its neighbouring C-5' (@ 131.80 ppm), which is β to its nearest nitrogen atom.

*(Note: In the interest of simplicity, all carbon atoms without attached protons, regardless of their hybridisation or whether heteroatoms are attached, are referred to as 'quaternary' carbons (C_q)).

An unexpected observation in the ^{13}C-NMR spectrum of **(331)**, was the exceptionally low intensity of the signal @ 131.80 ppm, corresponding to C-5' of the pyrimidine ring. The intensity of this signal was only ≈10% of the intensity of all other 'quaternary' carbons in the ^{13}C-NMR spectrum, with an approximate signal-to-noise (S/N) ratio of around 3. This meant that the signal was initially missed, and was only located after the discovery that the number of carbon atoms did not match the number of signals. In an effort to acquire additional evidence, to support the identity of this low signal as the missing 'quaternary' carbon, a DEPTq NMR experiment was conducted. The presence of this signal, in the negative phase of the DEPTq spectrum, provided sufficient evidence to support our assignment.

The low intensity of this signal is most likely due to its particularly slow relaxation, a consequence of the distance between the carbon atom and its nearest proton.[254,259] In general, 'quaternary' carbon signals tend to be of much lower intensity than those of CH_3, CH_2 and CH carbons, in a given molecule. This is due to the much slower rate of relaxation of the 'quaternary' ^{13}C nuclei and the fact that most routine ^{13}C-NMR spectra acquired, are not optimised for (i.e. do not accommodate) slowly relaxing nuclei. In order to acquire ^{13}C-NMR spectra in a reasonable time frame, pulse repetition rates (or 'relaxation delay') in instruments primed for routine analysis, are often in the range of 1–4 s. This is generally accommodating for ^{13}C nuclei directly bonded to protons, which have T_1 (Longitudinal relaxation) rates between 0.1 and 10 s. For 'quaternary' ^{13}C nuclei (no attached protons), longer values (10–300 s) are generally observed.

(Note: One of the major contributions to T_1 relaxation is the dipole-dipole interaction between the ^{13}C nucleus and its attached proton. This dipolar relaxation has also been found to be additionally affected by more distant protons.)

Therefore, a lower rate of T_1 relaxation and thus increased likelihood of observing intense signals, is largely dependent on the vicinity of protons. With regard to 'quaternary' ^{13}C nuclei in particular, it may be proposed that the more 'quaternary' carbons (C_q), attached to a given 'quaternary' carbon (C_q), the lower the likelihood of observing an intense signal (Figure 4.50).

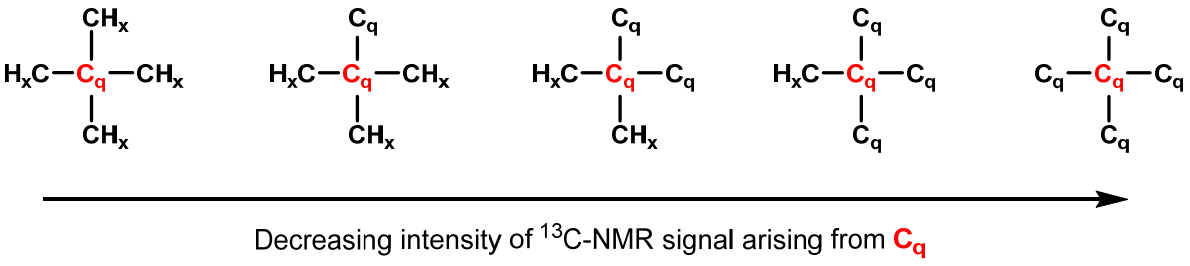


Figure 4.50: Conditions whereby the intensity of a 'quaternary' carbon signal may become diminished in a ^{13}C-NMR spectrum

Looking back at the ^{13}C-NMR spectrum of pyrimidine **(331)**, in which the 'quaternary' carbon at 131.80 ppm is of low intensity, the phenomenon may be partly explained by the reasoning described above. C-5' is bound to three other carbon atoms, two of these (C-4' and C-1'') *via* a single bond, the other (C-6') *via* a double bond. Both C-4' and C-1'' are 'quaternary' carbons which would delay relaxation of the C-5' nucleus. C-6' has one proton attached which may in theory assist the relaxation of C-5'. However, this relaxation is clearly hindered by some other factor(s) (e.g. the nature of the pyrimidine ring), as signal intensity is very low.

In an effort to increase the signal intensity of 'quaternary' carbons (or reveal the presence of hidden signals), one may extend the 'relaxation delay' parameter during acquisition of the ^{13}C-NMR spectrum. However, we did not pursue this as sufficient evidence to support signal assignment (*via* DEPTq) had already been obtained.

For the dibromo pyrimidine compound **(332)**, the ^{1}H-NMR and ^{13}C-NMR spectra are similar to those of the non-bromo compound **(331)** discussed earlier. Like the ^{1}H-NMR spectrum in Figure 4.49, the signals may be split into four groups – the methoxy group protons, the methylene protons, the aromatic ring protons and the pyrimidine ring protons. Each of the methoxy group proton signals are again resolved, resonating at δ 3.52, 3.66, 3.74 and 3.76. These are followed closely (downfield) by the methylene proton (@ δ 3.97). Signals arising from the aromatic ring protons are the next to be encountered moving downfield, and due to the *para* relationship of the two protons on each aromatic ring, four singlets are observed, resonating at δ 6.52, 6.56, 6.88 and 7.12. Lastly, the two distinctive pyrimidine ring protons can be found even further downfield, at δ 8.47 and 9.12.

In the ^{13}C-NMR spectrum, the signals can be found at similar shifts to those of the non-bromo compound **(331)**. The key difference being the disappearance of two 'C-H' signals and appearance of two new 'quaternary' carbon signals in the spectrum of the bromine-substituted pyrimidine **(332)**. As encountered previously, the signal arising from C-5' is of much lower intensity (≈60% less intense) than other 'quaternary' carbons. However, this intensity drop is not observed to the same extent as **(331)**, so the signal can be identified more easily.

A number of other potential impurities, in trace quantities, were detected (by ^{1}H-NMR spectroscopy) during the flash column chromatography of step 1 ('Leuckart-Wallach reaction'). These may include dimeric forms of the pyridine impurities outlined in Figure 4.44. These impurities however, were all recovered as mixtures and in small amounts, so characterisation was not possible. No further attempts were made (by LC-MS or otherwise) to identify these trace level impurities.

Having successfully prepared and isolated good to moderate yields of the intermediate *N*-formyl compounds (47% of **(329)**, 61% of **(330)**), hydrolysis to the dimeric amines was then attempted.

4.4.2 Step 2: Hydrolysis of *N*-formyl intermediates to produce dimeric amines

Hydrolysis of the *N*-formyl compounds **(329)** and **(330)**, was carried out under the conditions described below (procedure similar to that used by Griffin[26]). The novel dimeric amines **(327)** and **(328)**, were recovered in excellent yields without need for further purification. The R_f, m.p., IR and MS data for these are outlined in Table 4.15 below.

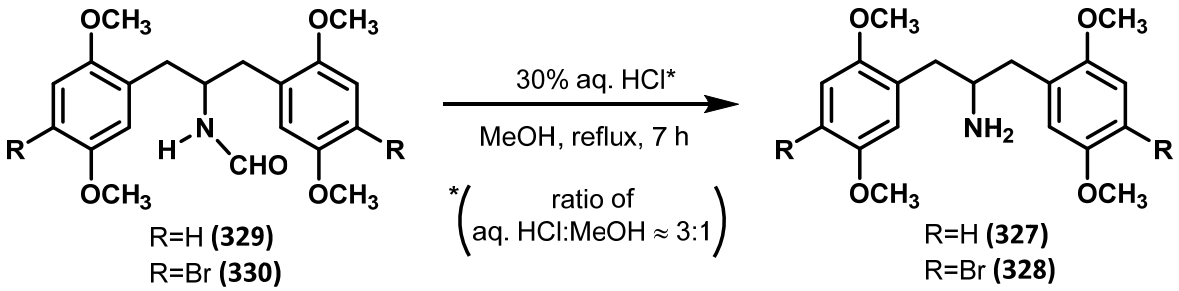


Table 4.15: Yield, R_f, m.p., IR and HRMS data for dimeric amines (327) and (328)

Compound No.	Yield	m.p. (°C)	R_f	IRν_{max} (KBr) (cm^{-1})	HRMS (M+H$^+$) (*m/z*)	
					Calc.	Found
(327)	90%	45–48	0.58*	3422 (N–H), 1593, 1503 (C=C)	332.1862	332.1852
(328)	96%	81–85	0.68★	3401 (N–H), 1605, 1497 (C=C)	488.0072▲	488.0070

*mobile phase = MeOH

★mobile phase = 80:20 DCM:MeOH

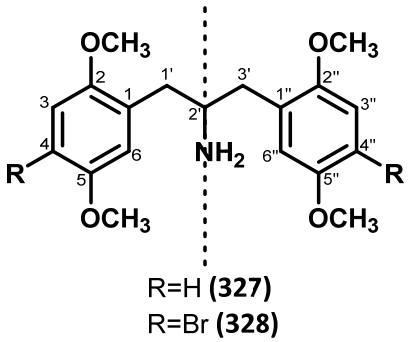
▲molecular ion (M) calculated for $^{79}Br_2$ isotope peak

The procedure used by Griffin,[26] for work-up of the monomeric amine (amphetamine **(31)**), needed to be adapted for dimeric amines **(327)** and **(328)**. During Griffin's work-up, the amine in its ionised state (due to acidic reaction conditions) remains in the aqueous phase (as the ammonium salt) until it is basified with aq. NaOH. Following this, the free base is taken up in DCM and then concentrated to yield the pure amine. Using this methodology, it was found that only a trace amount of impure dimeric amine **(327)**, was recovered. When the initial DCM portions (used in the washing of the crude aqueous

mixture) were combined, dried over $MgSO_4$ and concentrated, a ^{1}H-NMR spectrum revealed this sample to be pure amine **(327)**, in a yield of 90%. This indicates that, despite the acidic conditions of the reaction medium, the dimeric amine produced remains in a neutral state and cannot easily be taken up in an aqueous medium. This suggests that dimeric amine **(327)** is not as basic as would have been expected, possibly due to the steric hindrance imposed by the neighbouring aromatic rings.

The revised work-up procedure (whereby the crude reaction medium is washed a number of times with DCM, organic portions combined, dried and concentrated) was then used to successfully recover the dibromo-dimeric amine **(328)** in a yield of 96%.

Assignment of the ^{1}H-NMR and ^{13}C-NMR spectra of dimeric amines **(327)** and **(328)**, was straightforward; the line of symmetry about C-2' greatly simplifying the spectra.



R=H **(327)**
R=Br **(328)**

For non-bromo dimeric amine **(327)**, the geminal protons on both C-1' and C-3' are diastereotopic, so the protons in each geminal pair couple to each other, as well as to the proton on C-2'. This is manifested in the ^{1}H-NMR spectrum, as a pair of doublets of doublets (dd × 2). These resonate at δ 3.00 (dd, J_{gem}=13.9 Hz, J_{AB}=6.3 Hz) and 3.12 (dd, J_{gem}=13.9 Hz, J_{AB}=7.5 Hz). Only two methoxy signals are observed [(6H, s) × 2] due to the methoxy group protons on C-2/C-2'' and C-5/C-5'' being isochronous. The single proton on C-2' is featured as a multiplet (@ δ 3.89). The aromatic ring protons are not resolved for this structure: a multiplet ranging from δ 6.70 to 6.82 is observed. Finally, a slight kink in the baseline ('broad singlet', spanning over ≈1 ppm) is observed at δ 8.12, arising from the protons of the central amine group.

A similar pattern of signals was observed for the dibromo-dimeric amine **(328)**. The key difference being of course, the signals arising from the aromatic ring protons. For dimeric amine **(328)**, these protons, having a *para* relationship, are not sufficiently close to experience signal splitting and are observed as singlets (@ δ 6.79 and 6.97) in the ^{1}H-NMR spectrum.

General assignment of the ^{13}C-NMR spectra was also very straightforward due to the symmetric nature of the molecules. Only ten signals were observed in each of the spectra of **(327)** and **(328)**, despite the compounds having molecular formulae of $C_{19}H_{25}NO_4$ and $C_{19}H_{23}Br_2NO_4$ respectively. The assignment of these signals is outlined in Sections 5.4.10 and 5.4.11.

4.5 Summary

The key finding in this chapter was that the bromination (using Br_2/AcOH) of ketone-based intermediates or by-products, led to non-descript bromine substitution, often at multiple sites of a particular molecule. This non-descript bromination does not occur for other starting materials/intermediates. For example, in contrast to the clean and efficient bromination of 2,5-PAA **(108)** (single, aromatic-4-bromo product, 82% yield), five compounds were detected following bromination of 2,5-P2P **(92)**, with bromine substitution taking place at the 'benzylic' and 'terminal' carbons of the side-chain, as well as at the 4-position of the aromatic ring (Figure 4.51). These compounds were identified either by their isolation (and characterisation) from the bromination experiment, or by comparison with an independently synthesised standard.

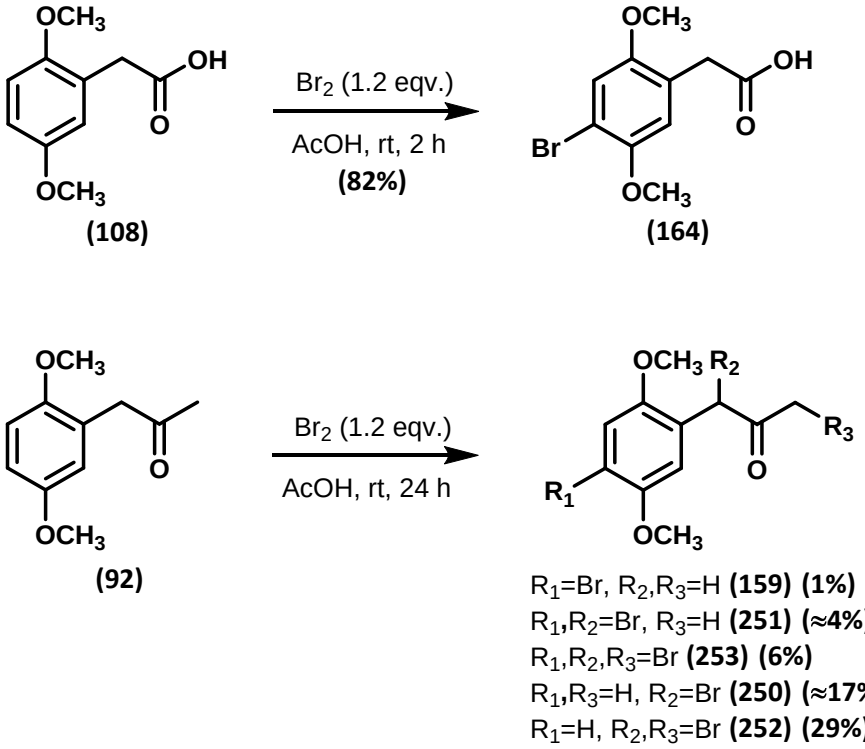


Figure 4.51: Comparison of the regioselectivity of bromine substitution, following bromination (Br_2/AcOH) of compounds (108) and (92)

The number of equivalents (eqv.) of Br_2 used in the reaction was also found to have a significant impact on the nature of the compounds produced. This may have important implications on the impurity profile of brominated amphetamines/phenethylamines. For example, in the case of bromination of 2,5-P2P **(92)** (shown in Figure 4.51), when the number of eqv. of Br_2 used is increased to 2.2 (from 1.2), further bromine substitution of the side chain appears to take place. This is evident by the low abundance of signals in the region of $\delta \approx 2$ in the ^{1}H-NMR spectrum of the crude reaction mixture. Signals found in this region are indicative of the presence of terminal methyl groups (non-brominated).

Initial attempts to establish an impurity profile of the bromination of dibenzylketone **(221)**, were unsuccessful. When analysed by ^{1}H-NMR, crude samples of the bromination were found to contain complex mixtures of compounds, the complexity increasing with increasing eqv. of Br_2. Also, attempts to isolate any of the compounds formed, by flash column chromatography, were ineffective – only mixtures of unknowns were recovered. Independent synthesis of a range of aromatic ring-substituted and benzyl-substituted bromo-dibenzylketones was then pursued.

For the independent synthesis of the aromatic ring-substituted bromo-dibenzylketones, a four step synthesis was chosen that befitted synthesis of both symmetric and asymmetric compounds. The key step in this sequence and the one most detrimental to overall product yield, was a 'Henry-Knoevenagel condensation', used to couple an aromatic aldehyde to an aromatic ring-substituted nitroalkane. Although the yields for this coupling reaction were low to moderate, improvements may possibly be brought about by modifying reaction conditions (e.g. by using ultrasound or microwave technology[249,260]), as described in recent literature.

Despite low overall yields, five novel aromatic ring-brominated dibenzylketones were successfully prepared and characterised. Together with the non-bromo dibenzylketone **(221)**, it was demonstrated that all six compounds could be efficiently separated on a standard C18 HPLC column and that MS/MS could be used to distinguish between regioisomeric compounds of equal mass.

In terms of benzyl-substituted bromo-dibenzylketones, strong evidence for their presence, following bromination (by Br_2) of dibenzylketone **(221)**, was provided by ^{1}H-NMR; several shifts in the region of δ ≈6, were indicative of benzylic bromination. However, establishing the identity of each of these compounds proved difficult. The main difficulty was the inability to acquire comprehensible mass spectra; these suspected benzylic-bromo compounds were found to undergo extensive fragmentation/recombination within the mass spectrometer, producing complex spectra with no obvious (protonated) molecular ions ($M+H^+$).

Also, it was hoped that tentative identification of benzylic-bromo dibenzylketones could be carried out by comparison of ^{1}H-NMR signals found in the crude bromination experiments, with those in the spectra of 'selectively' synthesised standards. Unfortunately, the syntheses were not very selective and as a result, no standards of benzylic-bromo dibenzylketones were isolated. Also, due to the large number of potential benzylic-bromo impurities and their diastereotopic nature, even the spectra of the selectively synthesised standards were often complex, containing multiple shifts in the region of δ ≈6. The sheer number of signals in this region, in both the products of the bromination experiments and the selectively synthesised standards, made it impossible to match common shifts, and thus draw any conclusions regarding the identity of any benzylic-bromo compounds formed during bromination (Br_2/AcOH) of dibenzylketone **(221)**.

In the final sections of this chapter, compounds arising from the Leuckart reaction of dibenzylketones **(221)** and **(224)** with formamide, were investigated. These compounds were envisaged as potential impurities of DOB **(35)** and other 'D series' amphetamines synthesised from impure* ketone intermediates.

(*Contaminated with dibenzylketone-based impurity)

Following the two-step synthesis, the novel dimeric *N*-formyl intermediates (**(329)** and **(330)**) and novel dimeric amine products (**(327)** and **(328)**) were isolated and characterised. These compounds are potential impurities of illicitly produced 'D series' amphetamines, although they may not be route specific. Of greater potential importance are the novel pyrimidine-based by-products isolated from these Leuckart reactions. The novel pyrimidines isolated (**(331)** and **(332)**) would be considered secondary impurities (or 'impurities of impurities') given that they arise as a by-product of an impurity (dibenzylketone) that undergoes a secondary reaction (Leuckart route). This phenomenon is depicted in Figure 4.52 for pyrimidine **(331)**.

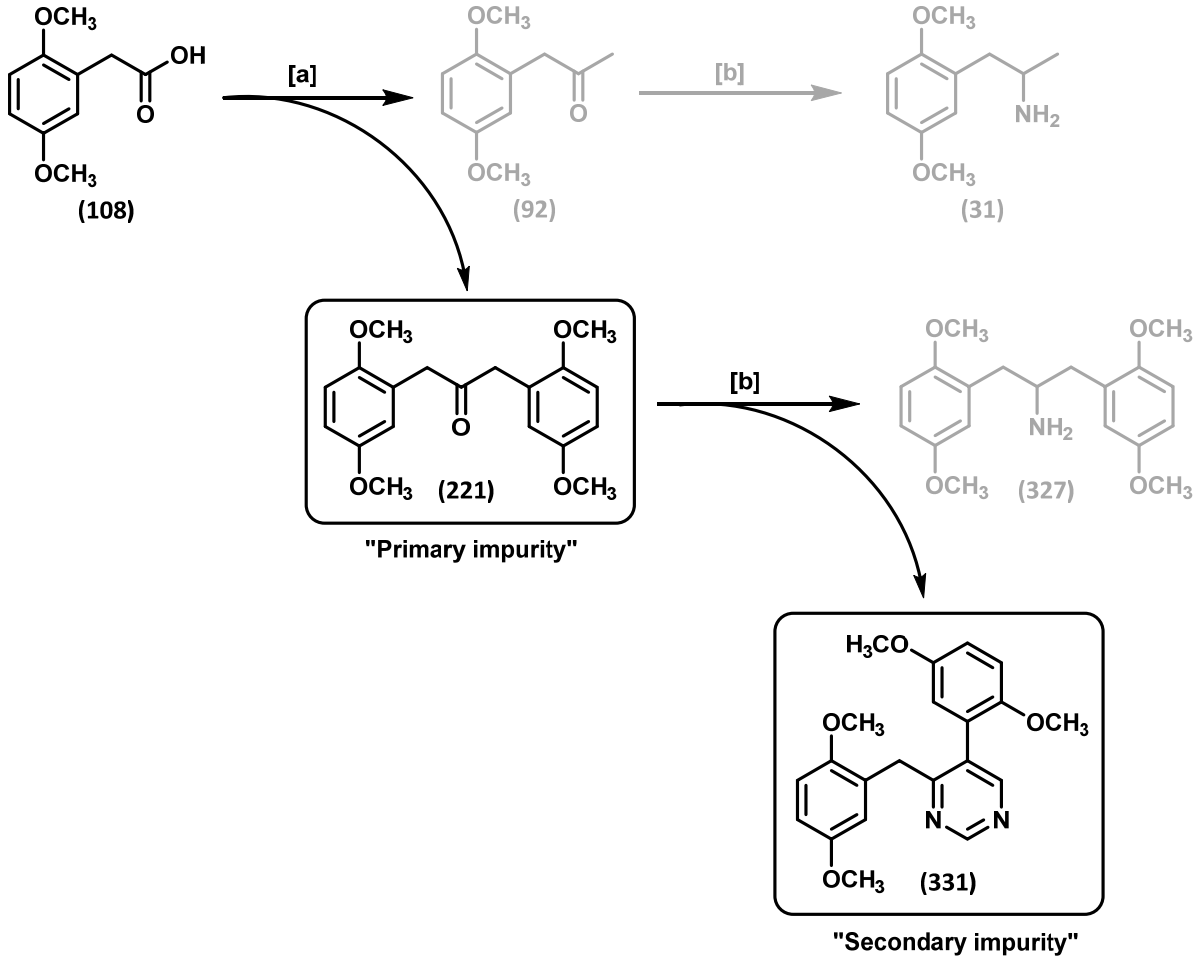


Figure 4.52: Pyrimidine (331), a secondary impurity of DMA (31), synthesised *via* the PAA and Leuckart routes

([a] = Ac_2O, pyridine, reflux, 7 h; [b] = 1. NH_2CHO, 190 °C, 5 h; 2. 30% aq. HCl, MeOH, reflux, 7 h)

What this means is that their presence may not only indicate that the illicit amphetamine was prepared *via* the Leuckart route (from a ketone intermediate **(92)**), but also that the ketone intermediate used (contaminated with dibenzylketone **(221)**) was in turn prepared form a phenylacetic acid starting material **(108)**. Impurities of this nature may be considered multi-route-specific or sequence-specific, due to the additional information they provide about the several steps involved in the synthesis of illicit amphetamines.

Chapter 5 – Experimental

5.1 General procedures

Infra-red (IR) spectra were recorded on a Perkin Paragon 1000 FT-IR spectrometer. Band positions are given in units of cm^{-1}. Solid samples were analysed as potassium bromide (KBr) discs; oils were analysed as neat films (or dissolved in a small amount of DCM) on sodium chloride (NaCl) plates.

R_f values are quoted for thin layer chromatography (TLC) on pre-coated silica gel plates (Merck Silica Gel 60, PF254) and visualisation of the plates was by ultra violet (UV) light detection (either short wave (254 nm) or long wave (365 nm)).

Flash column chromatography was carried out using Kieselgel 60 silica (particle size 0.040–0.063 mm). Unless stated otherwise, all solvents used were bulk grade and were not pre-treated in any way before use. Solvents that are preceded with "dry" were distilled as follows: DCM was distilled over phosphorous pentoxide, whilst toluene and THF were dried using a mixture of benzophenone (indicator) and sodium. All commercial reagents purchased were used without any additional purification.

^{1}H-NMR and ^{13}C-NMR spectra were recorded at 20 °C on either a Bruker Avance 300, 400 or 600 spectrometer: ^{1}H (300.13 MHz, 400.13 MHz or 600.13 MHz); ^{13}C (75.47 MHz, 100.61 MHz or 150.90 MHz) in either $CDCl_3$ (internal standard tetramethylsilane (TMS)) or DMSO. All NOESY spectra were recorded on the Bruker 600 spectrometer, whilst all DEPT, HSQC and COSY were recorded on either the 300 or 600 instruments. For $CDCl_3$, ^{1}H-NMR spectra were assigned relative to the TMS peak at 0.00 δ, ^{13}C-NMR spectra were assigned relative to the middle $CDCl_3$ triplet at 77.00 ppm. Coupling constants are reported in Hertz (Hz). For ^{1}H-NMR assignments, chemical shifts are reported as follows: shift value (δ) (number of protons, splitting pattern, coupling constant(s) where applicable, proton assignment). Splitting patterns in ^{1}H-NMR spectra are designated as follows: s (singlet), br s (broad singlet), d (doublet), t (triplet), q (quartet), ABq (AB quartet), dd (doublet of doublets), dq (doublet of quartets), qd (quartet of doublets) and m (multiplet). Splitting patterns that are exhibited between two single ditto marks signify an apparent or pseudo splitting pattern; the pattern observed has otherwise been shown to arise due to unusual signal overlap, resulting in a signal of lesser complexity than would be expected. For example, 'qd' signifies a pseudo quartet of doublets (see Section 5.3.4, compound **(239)** for an example of this). For ^{13}C-NMR, assignments are reported in parts per million (ppm).

For inseparable mixtures of isomers, rotamers or diastereoisomers, assignment of individual signals is attempted where feasible. Signals are either listed separately for each individual isomer/rotamer or listed together, with signals distinguished from one another through the use of a superscripted symbols after the assignment (e.g. ('signal')^E = denotes signal assigned to *E*-isomer). The symbol "*" is used to signify direct overlap of signals arising from two different isomers/rotamers.

Low resolution mass spectra were acquired on a Waters/Micromass LCT Premier Time-of-Flight (TOF) spectrometer (ESI). All high resolution mass spectra (HRMS) outlined in this chapter, were acquired on a Waters/Micromass Quattro Micro Triple Quadrupole (QQQ) spectrometer (ESI). All experimentally derived ("found") HRMS *m*/*z* values listed, are within 5 ppm mass accuracy of the theoretical ("calc.") values. Several other mass spectra, depicted in Figures throughout this thesis, were acquired on the 'Agilent LC-MS system' (see details below). Those mass spectra acquired using this system are clearly specified in the footnotes accompanying these Figures.

Most of the HPLC chromatograms featured in this body of work were acquired on the 'Agilent LC-MS system' (see below). The HPLC chromatograms contained in Figure 3.38 were acquired on the 'Waters Alliance system'. This system was made up of a Waters 600 Quaternary pump, a Waters 600 Controller, a Waters 717 Plus Autosampler and a 2996 Photodiode Array Detector. The samples were made up in 50/50 CH_3CN/H_2O at a concentration of ≈1 mg/mL. Other conditions pertaining to these chromatograms (column used, mobile phases etc.) can be found under Figure 3.38.

The 'Agilent LC-MS system' used was made up of the following hardware (see Figure 5.1):

HPLC (Agilent 1200 series):

1. Binary Pump ('BinPump-SL'), Model = G1312B
2. Autosampler ('ALS'), Model = G1329B
3. Thermastated Column Compartment ('Column-SL'), Model = G1316B
4. Diode Array Detector ('DAD-SL'), Model = G1315C

MS (Agilent QTOF with ESI): Model = G6510A

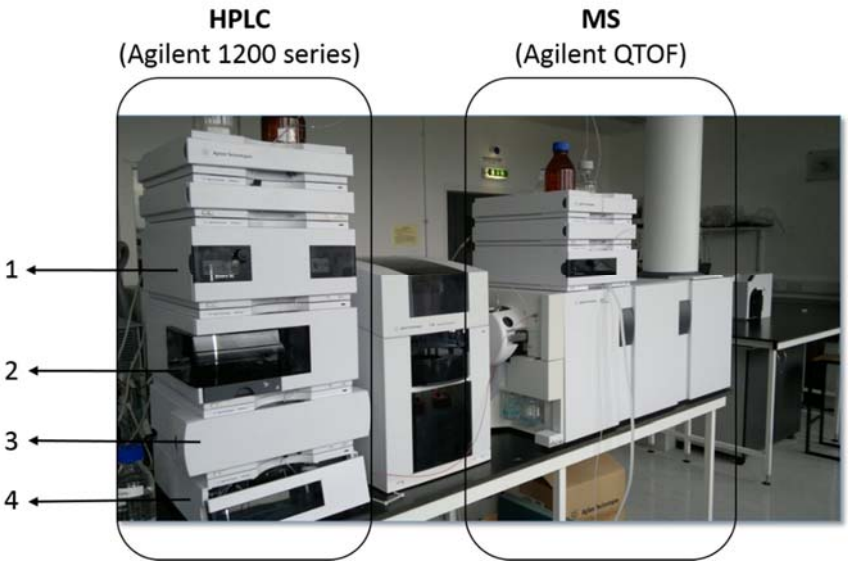


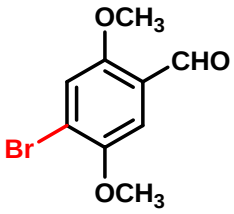
Figure 5.1: 'Agilent LC-MS system', Chemistry Department, University College Cork

Conditions specific to each run acquired using the 'Agilent LC-MS system' (e.g. flow rates, mobile phase ratio etc.) are specified under the title of each Figure. Some of the more general experimental conditions are as follows:

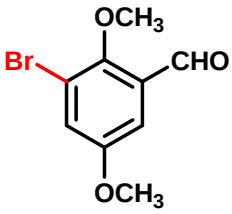
- Mobile phases: All reagents used (CH_3CN, H_2O etc.) were LC-MS grade. The 'CH_3CN' (organic based) mobile phase consisted of 95% CH_3CN, 5% H_2O and 'ionisation additive' and the 'H_2O' (aqueous based) mobile phase consisted of 95% H_2O, 5% CH_3CN and 'ionisation additive'. For ESI+, 'ionisation additive' = 0.1% HCOOH; for ESI–, 'ionisation additive' = 5 mMol ammonium formate.
- Sample preparation: All samples were made up in 50/50 CH_3CN/H_2O at a concentration of ≈1 mg/mL and were placed in an ultrasonic bath for ≈5 min. Samples not completely dissolved following this, were filtered through a 0.2 µm syringe filter.
- General MS conditions: Acquisition mode MS1 = 100–3000 *m*/*z* range, source gas temp. = 325 °C, source gas (N_2) flow = 5.0 L/min, nebuliser = 30 psi, Vcap = 3500 V, fragmentor 175 V, skimmer1 = 65 V, octoploeRFPeak = 750 V.

The microwave-assisted reactions described in Chapter 2 (General procedure 5.2.2.3), were carried out using a *CEM Discover® SP* reactor. The reagents were placed in a sealed glass microwave tube (capacity ≈10 mL) and stirred under microwave irradiation at ≈100 °C for 15 min (max. 300 W). The temperature was maintained by means of an internal temperature probe.

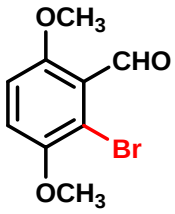
The atom numbering system used for compounds in this chapter does not always follow IUPAC rules. In order to avoid confusion, a simplified system that provides more consistent compound names is used. An example demonstrating this deviation from IUPAC, for the sake of simplicity, can be found in Figure 5.2. In this Figure can be found three of the earliest encountered compounds in this Chapter. These compounds are regioisomeric, differing only in the position of the bromine atom on the phenyl ring. However, the IUPAC system may make it more difficult for the reader to comprehend the relationship between the three compounds. It also makes the comparison of ^{1}H-NMR/^{13}C-NMR signals, of structurally similar compounds, more straightforward.



(160)



(169)



(165)

	'IUPAC system'		'customised system'
(160)	4-bromo-2,5-dimethoxybenzaldehyde	=	4-bromo-2,5-dimethoxybenzaldehyde
(169)	3-bromo-2,5-dimethoxybenzaldehyde	=	3-bromo-2,5-dimethoxybenzaldehyde
(165)	2-bromo-3,6-dimethoxybenzaldehyde	≠	6-bromo-2,5-dimethoxybenzaldehyde

Figure 5.2: Comparison of IUPAC and customised compound naming systems

Some of the general rules used in this customised system are as follows:

- For monomeric compounds (containing one phenyl ring) the carbon atoms on the ring are numbered in a counter-clockwise fashion, with the methoxy groups always in the 2- and 5-positions (i.e. carbons 1, 2, 3, 4, 5 and 6). This generally results in any formyl group/alkyl chain etc., extending from the ring, being at position 1.
- For dimeric compounds (containing two phenyl rings separated by a 2–4 carbon chain), the second ring (at the rightmost position) is numbered similarly to the first (methoxy groups at 2- and 5-positions). However, the ring position numbers are proceeded by a double prime symbol (‘’) in order to distinguish between the two rings (i.e. carbons 1’’, 2’’, 3’’, 4’’, 5’’ and 6’’) and are generally numbered in a clockwise fashion. The 2–4 carbon chain linking the two rings is generally numbered from left to right, with the number proceeded by a single prime symbol (‘).
- For the purpose of assigning ^{1}H-NMR/^{13}C-NMR signals, unique functional groups within a given compound (e.g. formyl/acetyl groups) are often not numbered specifically. Instead, they are simply referred to in terms of their atomic composition (e.g. formyl group = CHO, acetyl group = $COCH_3$), with the specific atom being assigned shown in italics (e.g. $CO\mathit{C}H_3$ for carbon or $COC\mathit{H}_3$ for protons).

For clarity, the atom numbering system is depicted on the structure of several compounds throughout this Chapter.

5.2 Experimental details pertaining to work outlined in Chapter 2

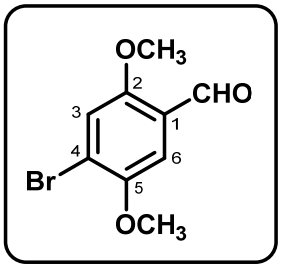
5.2.1 Impurity profiling of the bromination of 2,5-dimethoxybenzaldehyde (72)

General procedure 5.2.1.1

To a stirred solution of 2,5-dimethoxybenzaldehyde **(72)** (24.08 mmol, 4 g) in glacial acetic acid (12 mL), a solution of bromine (33.75 mmol, 1.73 mL, 4.40 g) in glacial acetic acid (4 mL), was added dropwise. The flask was covered in aluminium foil to exclude light and left stirring at room temperature for 24 h. The reaction mixture was diluted with de-ionised water (30 mL), and a 5% aq. sodium thiosulfate ($Na_2S_2O_3$) solution was added dropwise until the orange colour faded to cream. Dichloromethane (DCM) (40 mL) was added to the mixture and the phases were separated. The aqueous phase was extracted with DCM (2 × 50 mL). The combined organic phases were washed with 5% aq. $Na_2S_2O_3$ (3 × 50 mL), saturated aq. sodium bicarbonate ($NaHCO_3$) (3 × 50 mL), de-ionised water (2 × 50 mL), dried over magnesium sulfate ($MgSO_4$), filtered and concentrated *in vacuo* to give the crude product as a light brown solid. This was subjected to silica gel flash column chromatography in order to purify the products.

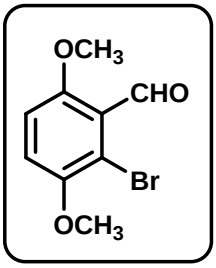
(Note: Further purification of selected impurities was carried out by acid/base extraction as follows: The selected column fraction was dissolved in Et_2O (30 mL) and added to a separating funnel. To this, 5% aq. NaOH (20 mL) was added, the flask shaken and the phases separated. The organic phase (Et_2O) was washed with de-ionised water (2 × 15 mL), dried over $MgSO_4$, filtered and concentrated *in vacuo*. The aqueous phase was acidified with 10% aq. HCl, Et_2O (20 mL) was added and the phases were separated. This new organic layer (Et_2O), was then washed with de-ionised water (2 × 15 mL), dried over $MgSO_4$, filtered and concentrated *in vacuo*.)

4-Bromo-2,5-dimethoxybenzaldehyde (160)



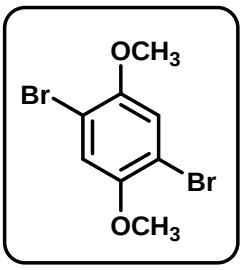
Prepared according to general procedure 5.2.1.1, the 4-bromo aldehyde **(160)** was isolated by flash column chromatography (eluent: 8/92 EtOAc/hexane) as a cream solid (17.82 mmol, 4.37 g, 74%); R_f 0.60 (30:70 EtOAc:hexane); m.p. 129–131 °C ($EtOH/H_2O$), (lit. m.p. 132–134 °C)[160]; IRν_{max} (KBr) 1678 (C=O), 1604, 1575, 1484 (C=C) cm^{-1}; ^{1}H-NMR δ (400 MHz, $CDCl_3$): 3.89, 3.90 ((3H, s) × 2, 2-OCH_3, 5-OCH_3), 7.25 (1H, s, H-6), 7.34 (1H, s, H-3), 10.40 (1H, s, CHO); ^{13}C-NMR ppm (75 MHz, $CDCl_3$): 56.33, 56.67 (2-OCH_3, 5-OCH_3), 109.52 (C-3), 117.58 (C-6), 120.24 (C-4), 124.07 (C-1), 150.35, 156.13 (C-2, C-5), 188.70 (CHO); *m/z* 245 ($M+H^+$, isotope ^{79}Br, 100%), 247 ($M+H^+$, isotope ^{81}Br, 98%); HRMS calc. for $C_9H_{10}{}^{79}BrO_3$: ($M+H^+$) 244.9813, found: 244.9821.

6-Bromo-2,5-dimethoxybenzaldehyde (165)



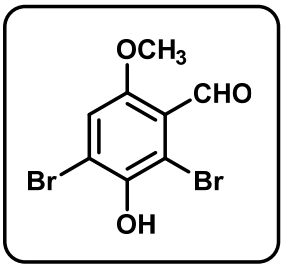
Prepared according to general procedure 5.2.1.1, the 6-bromo aldehyde **(165)** was isolated by flash column chromatography (eluent: 20/80 EtOAc/hexane) as a cream solid (3.61 mmol, 886 mg, 15%); R_f 0.26 (30:70 EtOAc:hexane); m.p. 100–101 °C (DCM/hexane), (lit m.p. 97–98 °C)[166]; IRν_{max} (KBr) 1690 (C=O), 1599, 1567, 1479 (C=C) cm^{-1}; ^{1}H-NMR δ (400 MHz, $CDCl_3$): 3.87, 3.88 ((3H, s) × 2, 2-OCH_3, 5-OCH_3), 6.93 (1H, d, $J_{3,4}$=9.1 Hz, H-3), 7.07 (1H, d, $J_{4,3}$=9.1 Hz, H-4), 10.41 (1H, s, CHO); ^{13}C-NMR ppm (75 MHz, $CDCl_3$): 56.58, 57.17 (2-OCH_3, 5-OCH_3), 111.47, 117.12 (C-3, C-4), 114.71 (C-6), 124.84 (C-1), 150.45, 155.40 (C-2, C-5), 190.83 (CHO); *m/z* 245 (M+H$^+$, isotope ^{79}Br, 100%), 247 (M+H$^+$, isotope ^{81}Br, 98%); HRMS calc. for $C_9H_{10}{}^{79}BrO_3$: (M+H$^+$) 244.9813, found: 244.9808.

3,6-Dibromo-2,5-dimethoxybenzene (168)



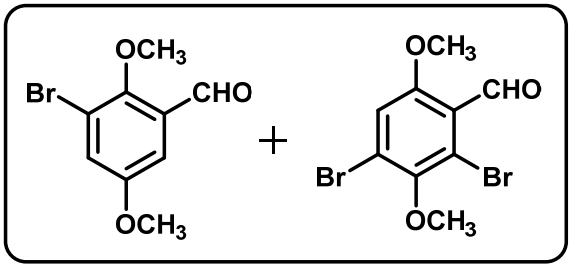
The dibromo compound **(168)** was partially purified, by flash column chromatography (eluent: 1/99 EtOAc/hexane) and then isolated by acid/base extraction (see note), as an impurity from the synthesis of 4-bromo aldehyde **(160)** by general procedure 5.2.1.1. Dibromo **(168)** was recovered as a cream solid (1.06 mmol, 314 mg, 4.4%); R_f 0.73 (30:70 EtOAc:hexane); m.p. 143–145 °C (EtOH), (lit. m.p. 142–143 °C)[174]; IRν_{max} (KBr) 1700, 1494 (C=C) cm^{-1}; ^{1}H-NMR δ (400 MHz, $CDCl_3$): 3.85 (6H, s, 2-OCH_3, 5-OCH_3), 7.11 (2H, s, H-3, H-6); ^{13}C-NMR ppm (75 MHz, $CDCl_3$): 57.00 (2-OCH_3, 5-OCH_3), 110.49 (C-2, C-5), 117.14 (C-3, C-6), 150.52 (C-1, C-4); Anal. calc. for $C_8H_8Br_2O_2$: C (32.47) H (2.72), found: C (32.43) H (2.63) %.

4,6-Dibromo-5-hydroxy-2-methoxybenzaldehyde (167)



The novel phenol **(167)** was partially purified, by flash column chromatography (eluent: 1/99 EtOAc/hexane) and then isolated by acid/base extraction (see note), as an impurity from the synthesis of 4-bromo aldehyde **(160)** by general procedure 5.2.1.1. Phenol **(167)** was recovered as a yellow solid (0.70 mmol, 216 mg, 2.9%); R_f 0.76 (30:70 EtOAc:hexane); m.p. 139–140 °C (EtOH); IRν_{max} (KBr) ≈3000 (OH), 1649 (C=O), 1593, 1577, 1561 (C=C) cm^{-1}; ^{1}H-NMR δ (400 MHz, $CDCl_3$): 3.90 (3H, s, 2-OCH_3), 7.42 (1H, s, H-3), 10.39 (1H, s, CHO), 12.14 (1H, s, OH); ^{13}C-NMR ppm (75 MHz, $CDCl_3$): 57.61 (2-OCH_3), 110.41, 115.75, 118.06 (C-1, C-4, C-6), 124.64 (C-3), 149.30, 154.25 (C-2, C-5), 197.67 (CHO); *m/z* 307 (M–H$^+$, isotope $^{79}Br_2$, 51%), 309 (M–H$^+$, isotope $^{79}Br^{81}Br$, 100%), 311 (M–H$^+$, isotope $^{81}Br_2$, 49%); HRMS calc. for $C_8H_5{}^{79}Br_2O_3$: (M–H$^+$) 306.8605, found: 306.8604.

3-Bromo-2,5-dimethoxybenzaldehyde (169) and 4,6-dibromo-2,5-dimethoxybenzaldehyde (170)



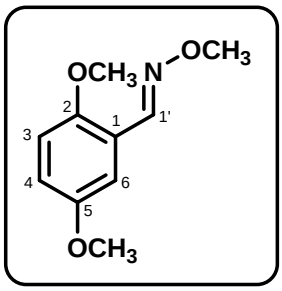
Compounds **(169)** and **(170)** were recovered, as an inseparable mixture, by flash column chromatography (eluent: 2/98 EtOAc/hexane) during the synthesis of the 4-bromo aldehyde **(160)** by general procedure 5.2.1.1, in a combined yield of <2%. R_f 0.64 and R_f 0.65 (30:70 EtOAc:hexane). Tentative identification was carried out based on the ^{1}H-NMR spectrum of the mixture. As full characterisation was not possible when pure samples were not recovered, selective syntheses of **(169)** and **(170)** (for use as standards) was carried out in Section 5.2.3 (for 3-bromo aldehyde **(169)**) and in Section 5.2.7 (for 4,6-dibromo aldehyde **(170)**). Confirmation of structure for both compounds was achieved by comparing the ^{1}H-NMR spectra of the selectively synthesised standards with that of the recovered mixture, as well as matching the chromatography and MS profile of the compounds by LC-MS.

5.2.2 Selective synthesis of 6-bromo-2,5-dimethoxybenzaldehyde (165)

General procedure 5.2.2.1

To a stirred solution of methoxyamine hydrochloride (7.22 mmol, 603 mg) and pyridine (24.08 mmol, 1.94 mL, 1.91 g) in dry DCM (20 mL), was added 2,5-dimethoxybenzaldehyde **(72)** (6.02 mmol, 1 g). The solution was left stirring for 1 h at room temperature, after which the volatiles were evaporated *in vacuo*. The remaining residue was dissolved in DCM (30 mL) and filtered through a short pad of silica gel containing a small amount of $MgSO_4$. The silica/$MgSO_4$ pad was washed through again with DCM (2 × 40 mL) and the combined DCM filtrates were concentrated *in vacuo* to give the pure product in almost quantitative yield.

(*E*)-2,5-Dimethoxybenzaldehyde *O*-methyloxime (180)

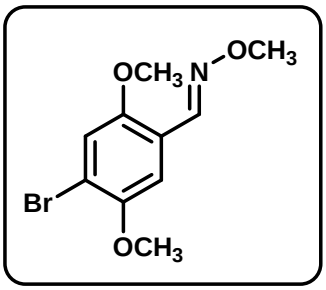


Prepared according to general procedure 5.2.2.1, the novel *O*-methyl oxime **(180)** was recovered as a yellow oil (5.72 mmol, 1.12 g, 95%), exclusively in the (*E*)-conformation; R_f 0.77 (50:50 EtOAc:hexane); IRν_{max} (NaCl) 1577, 1600 (C=N, C=C), 1495 (C=C) cm^{-1}; ^{1}H-NMR δ (400 MHz, $CDCl_3$): 3.79, 3.80 ((3H, s) × 2, 2-OCH_3, 5-OCH_3), 3.96 (3H, s, $NOCH_3$), 6.82 (1H, d, $J_{3,4}$=8.8 Hz, H-3), 6.90 (1H, dd, $J_{4,3}$=9.0 Hz, $J_{4,6}$=3.0 Hz, H-4), 7.33 (1H, d, $J_{6,4}$=3.2 Hz, H-6), 8.42 (1H, s, H-1'); ^{13}C-NMR ppm (75 MHz, $CDCl_3$): 55.77, 56.29 (2-OCH_3, 5-OCH_3), 61.88 ($NOCH_3$), 110.06, 112.73, 117.55 (C-3, C-4, C-6), 121.30 (C-1), 144.59 (C-1'), 152.12, 153.64 (C-2, C-5); *m/z* 196 ($M+H^+$, 100%); HRMS calc. for $C_{10}H_{14}NO_3$: ($M+H^+$) 196.0974, found: 196.0969.

General procedure 5.2.2.2

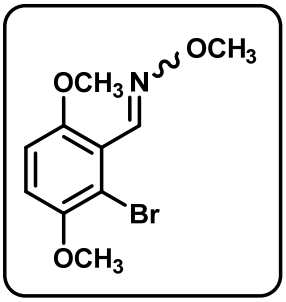
In a sealed flask, (*E*)-2,5-dimethoxybenzaldehyde *O*-methyloxime **(180)** (22.64 mmol, 4.42 g) was added to a solution of *N*-bromosuccinimide (22.64 mmol, 4.03 g), silver trifluoroacetate ($AgOCOCF_3$) (2.26 mmol, 500 mg) and palladium acetate ($Pd(OAc)_2$) (2.26 mmol, 508 mg) in 1,2-dichloroethane (76 mL). The resulting mixture was stirred and heated at 90 °C for 24 h. After cooling, DCM (200 mL) was added and the contents were transferred to a separating funnel. To this, de-ionised water (150 mL) was added and the phases separated. Both phases were then filtered individually through a pad of Celite®. The aqueous filtrate was washed with DCM (40 mL) and the resulting organic layer was separated and added to the original organic filtrate. These combined organic portions were dried over $MgSO_4$, filtered and concentrated *in vacuo* to give the crude product as a brown oil.

(*E*)-4-Bromo-2,5-dimethoxybenzaldehyde *O*-methyloxime (182)



The novel 4-bromo *O*-methyl oxime **(182)** was isolated as an impurity during the synthesis of the 6-bromo product, according to general procedure 5.2.2.2. 4-Bromo **(182)** was purified by silica gel flash column chromatography (eluent: 3/97 Et_2O/hexane) as a colourless solid (1.02 mmol, 279 mg, 4.5%), exclusively in the (*E*)-conformation; R_f 0.77 (50:50 Et_2O:hexane); m.p. 85–87 °C (MeOH); IRv_{max} (KBr) 1591, 1611 (C=N, C=C), 1499 (C=C) cm^{-1}; ^{1}H-NMR δ (400 MHz, $CDCl_3$): 3.79 (3H, s, 5-OCH_3), 3.89 (3H, s, 2-OCH_3), 3.97 (3H, s, $NOCH_3$), 7.10 (1H, s, H-6), 7.35 (1H, s, H-3), 8.36 (1H, s, H-1'); ^{13}C-NMR ppm (75 MHz, $CDCl_3$): 56.43, 56.76 (2-OCH_3, 5-OCH_3), 62.01 ($NOCH_3$), 108.81 (C-3), 113.90 (C-4), 116.96 (C-6), 120.54 (C-1), 143.95 (C-1'), 150.24, 151.94 (C-2, C-5); *m/z* 274 ($M+H^+$, isotope ^{79}Br, 100%), 276 ($M+H^+$, isotope ^{81}Br, 98%); HRMS calc. for $C_{10}H_{13}{}^{79}BrNO_3$: ($M+H^+$) 274.0079, found: 274.0082.

(*Z*)- and (*E*)-6-Bromo-2,5-dimethoxybenzaldehyde *O*-methyloxime (181)



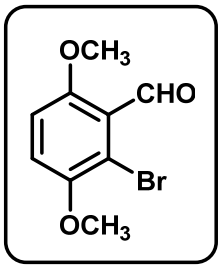
The ^{1}H-NMR spectrum of the crude product from general procedure 5.2.2.2, revealed that the intended product, 6-bromo *O*-methyloxime **(181)**, formed as a mixture of (*Z*)- and (*E*)- geometric isomers in a ratio of 1:2 (*Z*/*E*). Following silica gel flash column chromatography, the two isomers were recovered in a combined yield of 67% (15.17 mmol, 4.15 g). A small amount of pure sample of each of the two isomers was recovered by flash column chromatography, allowing for full characterisation of both isomers. The novel **(*Z*)-isomer** was isolated by flash column chromatography (4/96 Et_2O/hexane) as a white solid; R_f 0.49 (50:50 Et_2O:hexane); m.p. 100–103 °C (MeOH); IRv_{max} (KBr) 1572, 1626 (C=N, C=C), 1596, (C=C) cm^{-1}; ^{1}H-NMR δ (400 MHz, $CDCl_3$): 3.79, 3.85 ((3H, s) × 2, 2-OCH_3, 5-OCH_3), 3.91 (3H, s, $NOCH_3$), 6.84, 6.87 (2H, ABq, J_{AB}=9.0 Hz, H-3, H-4), 7.38 (1H, s, H-1'); ^{13}C-NMR ppm (75 MHz, $CDCl_3$): 56.46, 56.78 (2-OCH_3, 5-OCH_3), 62.14 ($NOCH_3$), 110.43, 112.38 (C-

3, C-4), 112.00 (C-6), 123.84 (C-1), 143.03 (C-1'), 150.28, 151.32 (C-2, C-5); *m/z* 274 ($M+H^+$, isotope ^{79}Br, 100%), 276 ($M+H^+$, isotope ^{81}Br, 98%); HRMS calc. for $C_{10}H_{13}{}^{79}BrNO_3$: ($M+H^+$) 274.0079, found: 274.0090. The novel **(*E*)-isomer** was also isolated by flash column chromatography (5/95 Et_2O/hexane) as a white solid; R_f 0.47 (50:50 Et_2O:hexane); m.p. 89–91 °C (MeOH); IRν_{max} (KBr) 1573, 1608 (C=N, C=C), 1483, (C=C) cm^{-1}; ^{1}H-NMR δ (400 MHz, $CDCl_3$): 3.81, 3.86 ((3H, s) × 2, 2-OCH_3, 5-OCH_3), 4.01 (3H, s, $NOCH_3$), 6.86, 6.89 (2H, ABq, J_{AB}=9.1 Hz, H-3, H-4), 8.26 (1H, s, H-1'); ^{13}C-NMR ppm (75 MHz, $CDCl_3$): 56.74, 56.93 (2-OCH_3, 5-OCH_3), 62.07 ($NOCH_3$), 111.02, 112.91 (C-3, C-4), 114.35 (C-6), 122.47 (C-1), 145.96 (C-1'), 150.51, 152.73 (C-2, C-5); *m/z* 274 ($M+H^+$, isotope ^{79}Br, 100%), 276 ($M+H^+$, isotope ^{81}Br, 98%); HRMS calc. for $C_{10}H_{13}{}^{79}BrNO_3$: ($M+H^+$) 274.0079, found: 274.0084.

General procedure 5.2.2.3

In a small sealed microwave vial, *p*-toluenesulfonic acid (1.6 mmol, 304 mg) and paraformaldehyde (8 mmol, 240 mg) were added to a solution of (*E*/*Z*)-6-bromo-2,5-dimethoxybenzaldehyde *O*-methyloxime **(181)** (0.8 mmol, 219 mg) in a 10/1 mixture of THF/H_2O (4 mL). The solution was stirred at 100 °C for 15 min under microwave irradiation (≤ 300 W). The solvent was then removed *in vacuo* and the crude residue dissolved in DCM (20 mL) and filtered through a short pad of silica gel. The silica pad was washed further with DCM (2 × 10 mL) and the combined filtrates were concentrated *in vacuo* to give the pure product.

6-Bromo-2,5-dimethoxybenzaldehyde (165)



Prepared according to general procedure 5.2.2.3, 6-bromo **(165)** was recovered as a cream solid (without need for further purification) in a yield of 99% (0.79 mmol, 196 mg). As this compound had been previously synthesised, isolated and characterised (*via* general procedure 5.2.1.1), structure confirmation was achieved by comparison of the spectroscopic data (^{1}H-NMR/^{13}C-NMR) with an authentic sample.

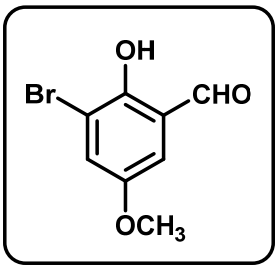
5.2.3 Preparation of 3-bromo-2,5-dimethoxybenzaldehyde (169)

General procedure 5.2.3.1

To a stirred solution of 2-hydroxy-5-methoxybenzaldehyde **(187)** (12.02 mmol, 1.5 mL, 1.83 g) in glacial acetic acid (60 mL), was added sodium acetate (19.23 mmol, 1.58 g). To this, a solution of bromine (14.42 mmol, 0.74 mL, 2.30 g) in glacial acetic acid (4 mL) was added dropwise. The flask was covered in aluminium foil to exclude light and left stirring at room temperature for 1 h. The reaction mixture was diluted with de-ionised water (100 mL), and 5% aq. $Na_2S_2O_3$ was added dropwise until the orange colour faded to cream. DCM (100 mL) was added to the mixture and the phases were separated. The

aqueous phase was extracted with DCM (2 × 40 mL). The combined organic phases were washed with 5% aq. $Na_2S_2O_3$ (3 × 50 mL), saturated aq. $NaHCO_3$ (3 × 50 mL) and de-ionised water (2 × 50 mL), dried over $MgSO_4$, filtered and concentrated *in vacuo* to give the crude product as a yellow solid. Recrystallisation from EtOH yielded pure product.

3-Bromo-2-hydroxy-5-methoxybenzaldehyde (188)

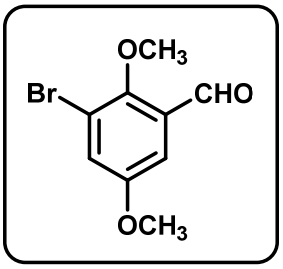


Prepared according to general procedure 5.2.3.1, the pure 3-bromo product **(188)** was recovered following recrystallisation from EtOH, as fine yellow crystals (9.74 mmol, 2.25 g, 81%); R_f 0.74 (50:50 EtOAc:hexane); m.p. 108–109 °C (EtOH), (lit. m.p. 108 °C)[169]; IRν_{max} (KBr) 1655 (C=O), 1611, 1456 (C=C) cm^{-1}; ^{1}H-NMR δ (400 MHz, $CDCl_3$): 3.83 (3H, s, 5-OCH_3), 7.04 (1H, d, $J_{6,4}$=3.0 Hz, H-6), 7.42 (1H, d, $J_{4,6}$=3.0 Hz, H-4), 9.83 (1H, s, CHO), 11.13 (1H, d, J=0.3 Hz, OH); ^{13}C-NMR ppm (75 MHz, $CDCl_3$): 56.11 (5-OCH_3), 111.45 (C-3), 115.70 (C-6), 120.35 (C-1), 127.34 (C-4), 152.37, 152.75 (C-2, C-5), 195.61 (CHO); *m/z* 229 (M–H$^+$, isotope ^{79}Br, 100%), 231 (M–H$^+$, isotope ^{81}Br, 98%); HRMS calc. for $C_8H_8{}^{79}BrO_3$: (M+H$^+$) 230.9657, found: 230.9654.

General procedure 5.2.3.2

To a stirred solution of 3-bromo-2-hydroxy-5-methoxybenzaldehyde **(188)** (4.33 mmol, 1 g) in dimethylformamide (DMF) (18 mL), was added potassium carbonate (K_2CO_3) (6.06 mmol, 837 mg) and dimethylsulfate (6.06 mmol, 0.57 mL, 764 mg). The resulting mixture was allowed to stir for 24 h at room temperature. After 24 h, de-ionised water (40 mL) and EtOAc (30 mL) were added and the phases separated. The aqueous portion was washed with EtOAc (3 × 40 mL) and these EtOAc washes were added to the original organic portion. The combined organic phases were then washed with brine (40 mL), dried over $MgSO_4$, filtered and concentrated *in vacuo* to give the crude product as a cream solid. The crude product was then purified by silica gel flash column chromatography to give the pure dimethoxy product.

3-Bromo-2,5-dimethoxybenzaldehyde (169)



Prepared according to general procedure 5.2.3.2, dimethoxy product **(169)** was isolated by flash column chromatography on silica gel (eluent: 5/95 EtOAc/hexane) as a cream solid (4.03 mmol, 987 mg, 93%); R_f 0.50 (20:80 EtOAc:hexane); m.p. 64–66 °C (EtOH), (lit. m.p. 68 °C)[169]; IRν_{max} (KBr) 1690 (C=O), 1603, 1474 (C=C) cm^{-1}; ^{1}H-NMR δ (400 MHz, $CDCl_3$): 3.82 (3H, s, 5-OCH_3), 3.94 (3H, s, 2-OCH_3), 7.28 (1H, d, $J_{6,4}$=3.2 Hz, H-6), 7.39 (1H, d, $J_{4,6}$=3.1 Hz, H-4), 10.32 (1H, s, CHO); ^{13}C-NMR ppm (75 MHz, $CDCl_3$): 55.93 (5-OCH_3), 63.76 (2-OCH_3), 110.07 (C-6), 118.50 (C-3), 126.48 (C-4), 130.43 (C-1), 154.32, 156.34 (C-2, C-5), 188.99 (CHO); *m/z* 245 (M+H$^+$,

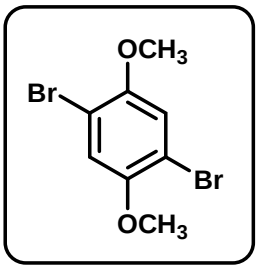
isotope ^{79}Br, 100%), 247 ($M+H^+$, isotope ^{81}Br, 98%); HRMS calc. for $C_9H_{10}{}^{79}BrO_3$: ($M+H^+$) 244.9813, found: 244.9807.

5.2.4 Preparation of 3,6-dibromo-2,5-dimethoxybenzene (168)

General procedure 5.2.4.1

To a stirred solution of 1,4-dimethoxybenzene **(190)** (14.47 mmol, 2 g) in glacial acetic acid (25 mL), a solution of bromine (34.73 mmol, 1.78 mL, 5.52 g) in glacial acetic acid (5 mL) was added dropwise. The flask was covered in aluminium foil to exclude light and left stirring at room temperature for 24 h. The reaction mixture was diluted with de-ionised water (10 mL), and 5% aq. $Na_2S_2O_3$ was added dropwise until the orange colour faded to cream. DCM (50 mL) was added to the mixture and the phases were separated. The aqueous phase was extracted with DCM (2 × 40 mL). The combined organic phases were washed with 5% aq. $Na_2S_2O_3$ (3 × 40 mL), saturated aq. $NaHCO_3$ (3 × 40 mL) and de-ionised water (2 × 40 mL), dried over $MgSO_4$, filtered and concentrated *in vacuo* to give the crude product as a white solid. Recrystallisation from EtOH yielded pure product.

3,6-Dibromo-2,5-dimethoxybenzene (168)



Prepared according to general procedure 5.2.4.1, dibromo **(168)** was recovered following recrystallisation from EtOH, as colourless crystals (12.73 mmol, 3.77 g, 88%); R_f 0.65 (20:80 EtOAc:hexane). As this compound had been previously isolated as an impurity from the bromination of 2,5-dimethoxybenzaldehyde (*via* procedure 5.2.1.1) and had been fully characterised, structure confirmation was achieved by comparison of the spectroscopic data (^{1}H-NMR) with that of the impurity, as well as matching of the chromatography and MS profile of the two compounds by LC-MS.

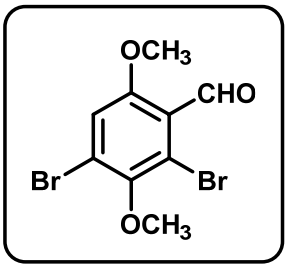
5.2.5 Attempted synthesis of 4,6-dibromo-2,5-dimethoxybenzaldehyde (170) *via* 6-bromo aldehyde (165)

General procedure 5.2.5.1

To a stirred solution of 6-bromo-2,5-dimethoxybenzaldehyde **(165)** (1.22 mmol, 300 mg) in glacial acetic acid (3 mL), a solution of bromine (1.47 mmol, 0.075 mL, 233 mg) in glacial acetic acid (1 mL) was added dropwise. The flask was covered in aluminium foil to exclude light and left stirring at room temperature for 24 h. The reaction mixture was diluted with de-ionised water (10 mL), and 5% aq. $Na_2S_2O_3$ was added dropwise until the orange colour faded to cream. DCM (20 mL) was added to the mixture and the phases were separated. The aqueous phase was extracted with DCM (2 × 15 mL). The combined organic phases

were washed with 5% aq. $Na_2S_2O_3$ (3 × 20 mL), saturated aq. $NaHCO_3$ (3 × 20 mL), de-ionised water (2 × 20 mL), dried over $MgSO_4$, filtered and concentrated *in vacuo* to give the crude product as a yellow solid.

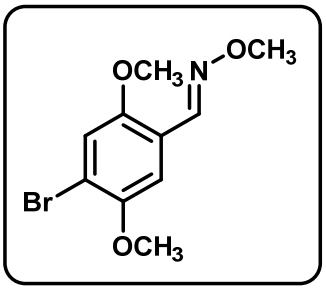
4,6-Dibromo-2,5-dimethoxybenzaldehyde (170)



The crude ^{1}H-NMR spectrum of the above reaction revealed only about 6% conversion to the desired product **(170)** was achieved. As this would result in a very low isolated yield, flash column chromatography was not pursued, as clearly this is not an efficient method of synthesising 4,6-dibromo-2,5-dimethoxybenzaldehyde **(170)**.

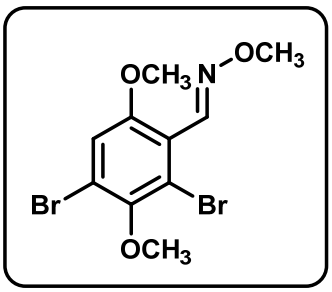
5.2.6 Attempted synthesis of 4,6-dibromo-2,5-dimethoxybenzaldehyde (170) *via* 4-bromo aldoxime (182)

(*E*)-4-Bromo-2,5-dimethoxybenzaldehyde *O*-methyloxime (182)



4-Bromo-2,5-dimethoxybenzaldehyde **(160)** (10.20 mmol, 2.5 g) was added to a stirred solution of methoxyamine hydrochloride (12.24 mmol, 1.02 g) and pyridine (40.8 mmol, 3.29 mL, 3.23 g) in dry DCM (31 mL), and the reaction was carried out according to general procedure 5.2.2.1. The pure product was recovered as a white solid in a yield of 98% (10.0 mmol, 2.74 g). As this compound has been previously isolated as an impurity during the synthesis of 6-bromo-2,5-dimethoxybenzaldehyde *O*-methyloxime **(181)** *via* procedure 5.2.2.2, and had been fully characterised, structure confirmation was achieved by comparison of the spectroscopic data (^{1}H-NMR, ^{13}C-NMR) with an authentic sample.

4,6-Dibromo-2,5-dimethoxybenzaldehyde *O*-methyloxime (191)

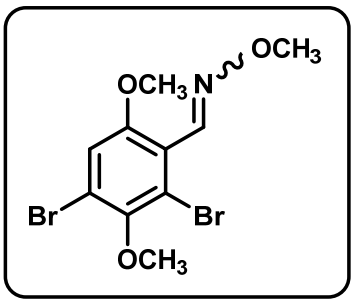


Two attempts were made to synthesise **(191)** by slightly modifying general procedure 5.2.2.2. Firstly, (*E*)-4-bromo-2,5-dimethoxybenzaldehyde *O*-methyloxime **(182)** (10.03 mmol, 2.75 g) was placed under similar conditions to those outlined in procedure 5.2.2.2, but the reaction temperature was increased to 100 °C and reaction time increased to 48 h. In a second attempt, (*E*)-4-bromo-2,5-dimethoxybenzaldehyde *O*-methyloxime **(182)** (3.65 mmol, 1 g) was reacted as in 5.2.2.2 but the reaction temperature was increased to 105 °C, and 1 eqv. (3.65 mmol, 0.21 mL) of glacial acetic acid was added with the reagents at the beginning of the experiment. The crude ^{1}H-NMR spectrum did not provide any evidence for product formation, with a substantial amount of starting material remaining. Even after attempted

purification by silica gel flash column chromatography (eluent: 1/99 to 10/90 Et_2O/hexane), the ^{1}H-NMR spectra of the subsequent fractions did not provide any further evidence for product formation.

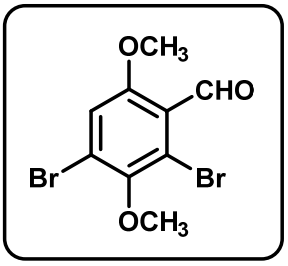
5.2.7 Selective synthesis of 4,6-dibromo-2,5-dimethoxybenzaldehyde (170) *via* 6-bromo aldoxime (181)

(*Z*)- and (*E*)-4,6-Dibromo-2,5-dimethoxybenzaldehyde *O*-methyloxime (191)



Using the bromination procedure as described in general procedure 5.2.1.1, the mixture of isomers (*Z*)- and (*E*)-6-bromo-2,5-dimethoxybenzaldehyde *O*-methyloxime **(181)** (1.82 mmol, 500 mg) were reacted with bromine (2.18 mmol, 0.11 mL, 341 mg), to produce the novel dibromo *O*-methyloxime product as a mixture of (*Z*)- and (*E*)-geometric isomers in a ratio of 1:2.5 (*Z*/*E*). After subjecting to flash column chromatography, a total combined yield of 29% (0.53 mmol, 186 mg) was recovered. A small amount of pure sample of each of the two geometric isomers was recovered, allowing for full characterisation of both isomers. The **(*E*)-isomer** was isolated by flash column chromatography (1/99 Et_2O/hexane) as a white solid; R_f 0.58 (20:80 Et_2O:hexane); m.p. 70–72 °C (MeOH); IRν_{max} (KBr) 1582 (C=N), 1545 (C=C) cm^{-1}; ^{1}H-NMR δ (400 MHz, $CDCl_3$): 3.81, 3.88 ((3H, s) × 2, 2-OCH_3, 5-OCH_3), 4.03 (3H, s, $NOCH_3$), 7.10 (1H, s, H-3), 8.26 (1H, s, H-1'); ^{13}C-NMR ppm (75 MHz, $CDCl_3$): 56.86 (2-OCH_3), 62.01, 62.29 (5-OCH_3, $NOCH_3$), 112.72, 117.23 (C-4, C-6), 116.27 (C-3), 128.39 (C-1), 145.27 (C-1'), 149.73, 152.88 (C-2, C-5); *m/z* 352 (M+H$^+$, isotopes $^{79}Br_2$, 51%), 354 (M+H$^+$, isotopes $^{79}Br^{81}Br$, 100%), 356 (M+H$^+$, isotopes $^{81}Br_2$, 49%); HRMS calc. for $C_{10}H_{12}{}^{79}Br_2NO_3$: (M+H$^+$) 351.9184, found: 351.9171. The **(*Z*)-isomer** was also isolated by flash column chromatography (3/97 Et_2O/hexane) as a white solid; R_f 0.50 (20:80 Et_2O:hexane); m.p. 70–72 °C (MeOH); IRν_{max} (KBr) 1582, 1552 (C=N, C=C), 1622 (C=C) cm^{-1}; ^{1}H-NMR δ (400 MHz, $CDCl_3$): 3.76, 3.88, 3,92 ((3H, s) × 3, 2-OCH_3, 5-OCH_3, $NOCH_3$), 7.08 (1H, s, H-3), 7.43 (1H, s, H-1'); ^{13}C-NMR ppm (75 MHz, $CDCl_3$): 56.80 (2-OCH_3), 61.65, 62.31 (5-OCH_3, $NOCH_3$), 110.14, 115.92 (C-4, C-6), 115.98 (C-3), 129.89 (C-1), 142.42 (C-1'), 148.51, 152.90 (C-2, C-5); *m/z* 352 (M+H$^+$, isotopes $^{79}Br_2$, 51%), 354 (M+H$^+$, isotopes $^{79}Br^{81}Br$, 100%), 356 (M+H$^+$, isotopes $^{81}Br_2$, 49%); HRMS calc. for $C_{10}H_{12}{}^{79}Br_2NO_3$: (M+H$^+$) 351.9184, found: 351.9175.

4,6-Dibromo-2,5-dimethoxybenzaldehyde (170)



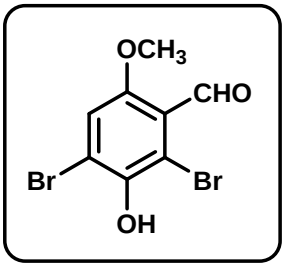
p-Toluenesulfonic acid (0.74 mmol, 141 mg) and paraformaldehyde (3.68 mmoL, 111 mg) were added to a solution of (*E*/*Z*)-4,6-dibromo-2,5-dimethoxybenzaldehyde *O*-methyloxime **(191)** (0.37 mmol, 130 mg) in a 10/1 mixture of THF/H_2O (2 mL), and the reaction was carried out according to general procedure 5.2.2.3. The novel aldehyde **(170)** was recovered pure, and as a cream solid (0.36 mmol, 116 mg, 96%); R_f 0.67 (50:50 Et_2O:hexane); m.p. 98–99.5 °C (DCM/hexane); IRν_{max} (KBr) 1693 (C=O), 1579, 1546 (C=C) cm^{-1}; ^{1}H-NMR δ (400 MHz, $CDCl_3$): 3.88, 3.92 ((3H, s) × 2, 2-OCH_3, 5-OCH_3), 7.27 (1H, s, H-3), 10.30 (1H, s, CHO); ^{13}C-NMR ppm (75 MHz, $CDCl_3$): 57.05 (2-OCH_3), 63.28 (5-OCH_3), 112.95 (C-4), 117.87 (C-6), 119.62 (C-3), 130.70 (C-1), 151.64, 153.03 (C-2, C-5), 190.16 (CHO); *m/z* 323 ($M+H^+$, isotopes $^{79}Br_2$, 51%), 325 ($M+H^+$, isotopes $^{79}Br^{81}Br$, 100%), 327 ($M+H^+$, isotopes $^{81}Br_2$, 49%); HRMS calc. for $C_9H_9{}^{79}Br_2O_3$: ($M+H^+$) 322.8918, found: 322.8906.

5.2.8 Selective synthesis of 4,6-dibromo-5-hydroxy-2-methoxybenzaldehyde (167)

General procedure 5.2.8.1

Conc. H_2SO_4 (2 mL) was slowly added (with stirring) to 4,6-dibromo-2,5-dimethoxybenzaldehyde **(170)** (prepared in Section 5.2.7) (0.30 mmol, 100 mg) at 0 °C. When addition of H_2SO_4 was complete, the mixture was heated to 55 °C for 48 h. The crude reaction mixture was then poured onto ice/water (50 mL), Et_2O (20 mL) was added, the mixture was transferred to a separating funnel and the phases were separated. The aqueous portion was washed further with Et_2O (2 × 20 mL) and these washes were added to the original organic wash. The combined organic layers were then extracted with 5% aq. NaOH (40 mL) and the aqueous portion was acidified with dilute aq. HCl. The acidified aqueous portion was then extracted with Et_2O (3 × 20 mL) and these combined Et_2O washes were dried over $MgSO_4$, filtered and concentrated *in vacuo* to give the pure product.

4,6-Dibromo-5-hydroxy-2-methoxybenzaldehyde (167)



Prepared according to general procedure 5.2.8.1, the novel phenol **(167)** was recovered as a pale yellow solid (0.057 mmol, 18 mg, 19%). As this compound had been previously isolated as an impurity from the bromination of 2,5-dimethoxybenzaldehyde (*via* procedure 5.2.1.1) and had been fully characterised, structure confirmation was achieved by comparison of the spectroscopic data (^{1}H-NMR) with that of the impurity, as well as matching the chromatography and MS profile of the two compounds by LC-MS.

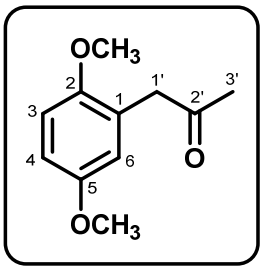
5.3 Experimental details pertaining to work outlined in Chapter 3

5.3.1 Preparation and impurity profiling of 2,5-dimethoxyphenyl-2-propanone (92) *via* the 'PAA route'

General procedure 5.3.1.1

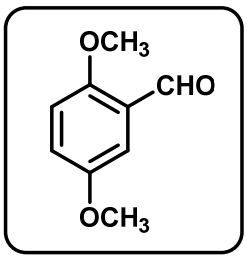
To a stirred solution of 2,5-dimethoxyphenylacetic acid **(108)** (5.1 mmol, 1 g) in Ac_2O (30.6 mmol, 2.90 mL, 3.14 g), was added pyridine (30.6 mmol, 2.47 mL, 2.43 g). This solution was refluxed under nitrogen for 7 h. Upon cooling, the reaction mixture was diluted with 10% aq. HCl (30 mL) and extracted with Et_2O (3 × 40 mL). The combined organic phases were dried over $MgSO_4$, filtered and concentrated *in vacuo* to give the crude product as a dark amber oil. This crude mixture was then subjected to flash column chromatography on silica gel to isolate the desired 2,5-dimethoxyphenyl-2-propanone **(92)**, as well as other impurities/by-products.

2,5-Dimethoxyphenyl-2-propanone (92)



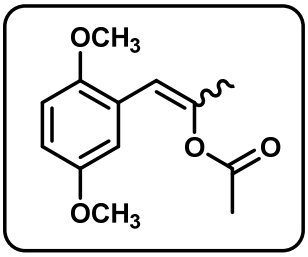
Prepared according to procedure 5.3.1.1, ketone **(92)** was isolated by flash column chromatography on silica gel (eluent: 10/90 Et_2O/hexane) as a pale amber oil[261] (1.79 mmol, 347 mg, 35%); R_f 0.66 (70:30 Et_2O:hexane); IRv_{max} (NaCl) 1715 (C=O), 1593, 1505 (C=C) cm^{-1}; ^{1}H-NMR δ (400 MHz, $CDCl_3$): 2.13 (3H, s, H-3'), 3.64 (2H, s, H-1'), 3.76, 3.77 ((3H, s) × 2, 2-OCH_3, 5-OCH_3), 6.71-6.82 (3H, m, H-3, H-4, H-6); ^{13}C-NMR ppm (75 MHz, $CDCl_3$): 29.15 (C-3'), 45.54 (C-1'), 55.62, 55.83 (2-OCH_3, 5-OCH_3), 111.38 (C-3), 112.67 (C-4), 117.20 (C-6), 124.56 (C-1), 151.57, 153.47 (C-2, C-5), 206.74 (C-2'); *m/z* 195 ($M+H^+$, 100%); HRMS calc. for $C_{11}H_{14}O_3$: ($M+H^+$) 195.1021, found: 195.1015.

2,5-Dimethoxybenzaldehyde (72)



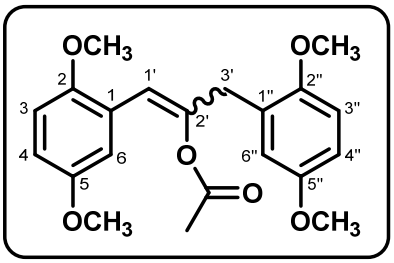
Aldehyde **(72)** was detected as an impurity from the preparation of ketone **(92)** by general procedure 5.3.1.1, and isolated by flash column chromatography on silica gel (eluent: 8/92 Et_2O/hexane) yielding a pale yellow solid (≈1%); R_f 0.71 (70:30 Et_2O:hexane); m.p. 46–48 °C (DCM/hexane), (lit. m.p. 45–48 °C)[262]; IRv_{max} (KBr) 1677 (C=O), 1618, 1499 (C=C) cm^{-1}; ^{1}H-NMR δ (400 MHz, $CDCl_3$): 3.81, 3.90 ((3H, s) × 2, 2-OCH_3, 5-OCH_3), 6.95 (1H, d, $J_{3,4}$=9.2 Hz, H-3), 7.13 (1H, dd, $J_{4,3}$=9.2 Hz, $J_{4,6}$=3.2 Hz, H-4), 7.33 (1H, d, $J_{6,4}$=3.6 Hz, H-6), 10.45 (1H, s, CHO); ^{13}C-NMR ppm (75 MHz, $CDCl_3$): 55.76, 56.12 (2-OCH_3, 5-OCH_3), 110.40 (C-3), 113.31 (C-4), 123.41 (C-6), 124.90 (C-1), 153.57, 156.67 (C-2, C-5), 189.51 (CHO); *m/z* 167 ($M+H^+$, 100%).

(*E*)/(*Z*)-1-(2,5-Dimethoxyphenyl)prop-1-en-2-yl acetate (219)



Produced as an impurity from the preparation of **(92)** by general procedure 5.3.1.1, and purified by flash column chromatography on silica gel (eluent: 8/92 Et_2O/hexane), the novel 1-(2,5-dimethoxyphenyl)prop-1-en-2-yl acetate, was recovered as a mixture of *Z*/*E* isomers (ratio of *Z*:*E* = 4:1) that were inseparable by flash column chromatography. The E/Z mixture was recovered as a pale yellow oil in a total combined yield of 5% (0.26 mmol, 60 mg); R_f 0.68 (70:30 Et_2O:hexane); IRν_{max} (NaCl) 1756 (C=O), 1678 (C=C), 1606, 1583 (aromatic C=C) cm^{-1}; **(*Z*)-(219):** ^{1}H-NMR δ (400 MHz, $CDCl_3$): 2.10 (3H, d, $J_{3',1'}$=1.2 Hz, H-3'), 2.15 (3H, s, $COCH_3$), 3.75, 3.77 ((3H, s) × 2, 2-OCH_3, 5-OCH_3), 6.21 (1H, s, H-1'), 6.72–6.85 (2H, m, H-3, H-4), 7.06 (1H, d, $J_{6,4}$=3.2 Hz, H-6); ^{13}C-NMR ppm (150 MHz, $CDCl_3$): 20.77 (C-3'), 21.11 (CO*C*H_3), 55.59, 56.12 (2-OCH_3, 5-OCH_3), 110.87, 111.60, 113.05, 114.57 (C-3, C-4, C-6, C-1'), 124.02 (C-1), 146.46, 150.90, 153.18 (C-2, C-5, C-2'), 168.64 (*C*OCH_3); **(*E*)-(219):** ^{1}H-NMR δ (400 MHz, $CDCl_3$): 2.07 (3H, d, $J_{3',1'}$=0.8 Hz, H-3'), 2.17 (3H, s, $COCH_3$), 3.77 (6H, s, 2-OCH_3, 5-OCH_3), 6.32 (1H, s, H-1'), 6.72–6.85 (3H, m, H-3, H-4, H-6); ^{13}C-NMR ppm (150 MHz, $CDCl_3$): 17.00 (C-3'), 21.09 (CO*C*H_3), 55.73, 56.05 (2-OCH_3, 5-OCH_3), 111.43, 112.82, 114.19, 115.95 (C-3, C-4, C-6, C-1'), 124.58 (C-1), 147.88, 151.44, 153.12 (C-2, C-5, C-2'), 169.51 (*C*OCH_3); *m/z* 237 ($M+H^+$, 100%); HRMS calc. for $C_{13}H_{17}O_4$: ($M+H^+$) 237.1127, found: 237.1122.

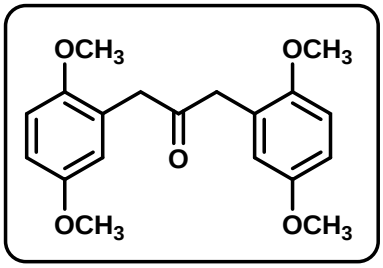
(*Z*)-1,3-Bis(2,5-dimethoxyphenyl)prop-1-en-2-yl acetate (220)



The novel dimeric acetate **(220)** was isolated by flash column chromatography on silica gel (eluent: 10/90 Et_2O/hexane) as a pale amber oil (≈1.5%); R_f 0.56 (70:30 Et_2O:hexane); IRν_{max} (NaCl) 1756 (C=O), 1672 (C=C), 1608, 1584 (aromatic C=C) cm^{-1}; ^{1}H-NMR δ (400 MHz, $CDCl_3$): 2.09 (3H, s, $COCH_3$), 3.72 (5H, s, H-3' overlapping with 2''-OCH_3 or 5''-OCH_3), 3.75, 3.76, 3.78 ((3H, s) × 3, 2-OCH_3, 5-OCH_3, 2''-OCH_3 or 5''-OCH_3), 6.31 (1H, s, H-1'), 6.70–6.86 (5H, m, H-3, H-4, H-3'', H-4'', H-6''), 7.08 (1H, d, $J_{6,4}$=2.8 Hz, H-6); ^{13}C-NMR ppm (75 MHz, $CDCl_3$): 21.08 (CO*C*H_3), 34.99 (C-3'), 55.65, 55.69, 56.12, 56.30 (2-OCH_3, 5-OCH_3, 2''-OCH_3, 5''-OCH_3), 111.60, 111.64, 111.88, 112.25, 113.32, 116.64 (C-3, C-4, C-1', C-3'', C-4'', C-6''), 114.47 (C-6), 124.12, 127.04 (C-1, C-1''), 148.15, 151.10, 151.97, 153.20, 153.45 (C-2, C-5, C-2', C-2'', C-5''), 168.68 (*C*OCH_3); *m/z* 373 ($M+H^+$, 100%); HRMS calc. for $C_{21}H_{25}O_6$: ($M+H^+$) 373.1651, found: 373.1649.

Note: A repeat ^{1}H-NMR run of the same sample about 11 months later revealed that isomerisation had taken place, with the ratio of *Z* to *E* at ≈1.6:1. The signals corresponding to the *E*-isomer (not isolated) are tentatively assigned as follows: ^{1}H-NMR δ (600 MHz, $CDCl_3$): 2.06 (3H, s, $COCH_3$), 3.65, 3.71, 3.74, 3.78 ((3H, s) × 4, 2-OCH_3, 5-OCH_3, 2''-OCH_3, 5''-OCH_3), 3.80 (2H, s, H-3'), 6.49 (1H, s, H-1'), 6.70–6.90 (6H, m, H-3, H-4, H-6, H-3'', H-4'', H-6'').

1,3-Bis(2,5-dimethoxyphenyl)-2-propanone (221)



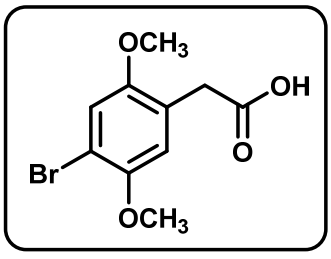
Novel dibenzylketone **(221)** was detected as an impurity from the preparation of **(92)** by general procedure 5.3.1.1, and isolated by flash column chromatography on silica gel (eluent: 10/90 Et_2O/hexane) as a pale yellow solid (0.36 mmol, 63 mg, 7%); R_f 0.54 (70:30 Et_2O:hexane); m.p. 59–60 °C; IRν_{max} (KBr) 1718 (C=O), 1616, 1592, 1506 (C=C) cm^{-1}; ^{1}H-NMR δ (300 MHz, $CDCl_3$): 3.69 (4H, s, H-1', H-3'), 3.74 (12H, s, 2-OCH_3, 5-OCH_3, 2''-OCH_3, 5''-OCH_3), 6.67–6.80 (6H, m, H-3, H-4, H-6, H-3'', H-4'', H-6''); ^{13}C-NMR ppm (75 MHz, $CDCl_3$): 43.95 (C-1', C-3'), 55.62, 55.87 (2-OCH_3, 5-OCH_3, 2''-OCH_3, 5''-OCH_3), 111.31, 112.60, 117.27 (C-3, C-4, C-6, C-3'', C-4'', C-6''), 124.62 (C-1, C-1''), 151.66, 153.37 (C-2, C-5, C-2'', C-5''), 206.09 (C=O); *m/z* 331 ($M+H^+$, 100%); HRMS calc. for $C_{19}H_{23}O_5$: ($M+H^+$) 331.1545, found: 331.1531.

5.3.2 Preparation of 4-bromo-2,5-dimethoxyphenylacetic acid (164)

General procedure 5.3.2.1

To a stirred solution of 2,5-dimethoxyphenylacetic acid **(108)** (5.1 mmol, 1 g) in glacial acetic acid (10 mL), a solution of bromine (6.12 mmol, 0.31 mL, 974 mg) in glacial acetic acid (2 mL) was added dropwise. The flask was covered in aluminium foil to exclude light and left stirring at room temperature for 2 h. The reaction mixture was then poured onto ice/water (50 mL) and filtered to give a cream solid. This cream solid was dissolved in DCM (50 mL) and transferred to a separating funnel. De-ionised water (40 mL) was added to the separating funnel and the phases separated. The aqueous phase was extracted with DCM (2 × 20 mL). The combined organic phases were washed with 5% aq. $Na_2S_2O_3$ (3 × 20 mL) and de-ionised water (2 × 20 mL), dried over $MgSO_4$, filtered and concentrated *in vacuo* to give the pure product as a cream solid.

4-Bromo-2,5-dimethoxyphenylacetic acid (164)



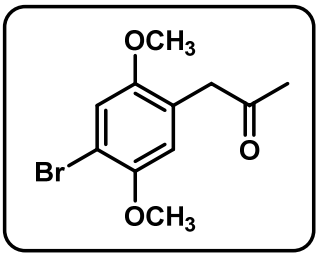
Prepared according to general procedure 5.3.2.1, the carboxylic acid **(164)** was recovered (without need for further purification) as a cream solid (4.18 mmol, 1.15 g, 82%); R_f 0.49 (50:50 THF:hexane); m.p. 125–127 °C (EtOH/H_2O), (lit. m.p. 124–126 °C)[39]; IRν_{max} (KBr) 1706 (C=O), 1501 (C=C) cm^{-1}; ^{1}H-NMR δ (400 MHz, $CDCl_3$): 3.63 (2H, s, H-1'), 3.79, 3.84 ((3H, s) × 2, 2-OCH_3, 5-OCH_3), 6.79 (1H, s, H-6), 7.08 (1H, s, H-3); ^{13}C-NMR ppm (75 MHz, $CDCl_3$): 35.53 (C-1'), 56.32, 56.93 (2-OCH_3, 5-OCH_3), 110.75 (C-4), 115.24, 116.23 (C-3, C-6), 122.21 (C-1), 149.98, 151.87 (C-2, C-5), 177.00 (COOH); *m/z* 275 ($M+H^+$, isotope ^{79}Br, 100%), 277 ($M+H^+$, isotope ^{81}Br, 98%); HRMS calc. for $C_{10}H_{12}{}^{79}BrO_4$: ($M+H^+$) 274.9919, found: 274.9908.

5.3.3 Preparation and impurity profiling of 4-bromo-2,5-dimethoxyphenyl-2-propanone (159) *via* the 'PAA route'

General procedure 5.3.3.1

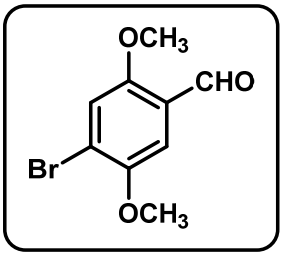
To a stirred solution of 4-bromo-2,5-dimethoxyphenylacetic acid **(164)** (3.64 mmol, 1 g) in Ac_2O (21.8 mmol, 2.06 mL, 2.23 g), was added pyridine (21.8 mmol, 1.76 mL, 1.73 g). This solution was refluxed under nitrogen for 7 h. Upon cooling, the reaction mixture was diluted with 10% aq. HCl (30 mL) and extracted with Et_2O (3 × 40 mL). The combined organic phases were dried over $MgSO_4$, filtered and concentrated *in vacuo* to give the crude product as a dark amber oil. This crude mixture was then subjected to flash column chromatography on silica gel, to isolate the desired 4-bromo-2,5-dimethoxyphenyl-2-propanone **(159)**, as well as other impurities/by-products.

4-Bromo-2,5-dimethoxyphenyl-2-propanone (159)



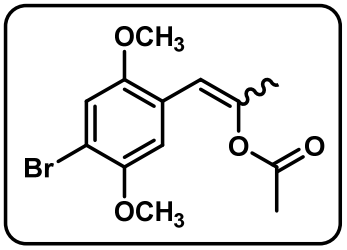
Prepared according to procedure 5.3.3.1, ketone **(159)** was recovered by flash column chromatography on silica gel (eluent: 10/90 Et_2O/hexane) as a mixture with dimeric acetate impurity **(222)**. Recrystallisation of the mixture from MeOH, resulted in the desired product **(159)** being recovered from the mother liquor (following concentration *in vacuo*) as a cream solid (1.38 mmol, 378 mg, 38%); R_f 0.48 (70:30 Et_2O:hexane); m.p. 59–60.5 °C (DCM/hexane), (lit. m.p. 55–57 °C)[26]; IRv_{max} (KBr) 1709 (C=O), 1498 (C=C) cm^{-1}; ^{1}H-NMR δ (300 MHz, $CDCl_3$): 2.16 (3H, s, H-3'), 3.64 (2H, s, H-1'), 3.77, 3.84 ((3H, s) × 2, 2-OCH_3, 5-OCH_3), 6.72 (1H, s, H-6), 7.07 (1H, s, H-3); ^{13}C-NMR ppm (75 MHz, $CDCl_3$): 29.34 (C-3'), 45.16 (C-1'), 56.12, 56.89 (2-OCH_3, 5-OCH_3), 110.27 (C-4), 115.26, 116.04 (C-3, C-6), 123.49 (C-1), 150.00, 151.68 (C-2, C-5), 206.06 (C-2'); *m/z* 273 ($M+H^+$, isotope ^{79}Br, 100%), 275 ($M+H^+$, isotope ^{81}Br, 98%); HRMS calc. for $C_{11}H_{14}{}^{79}BrO_3$: ($M+H^+$) 273.0126, found: 273.0124.

4-Bromo-2,5-dimethoxybenzaldehyde (160)



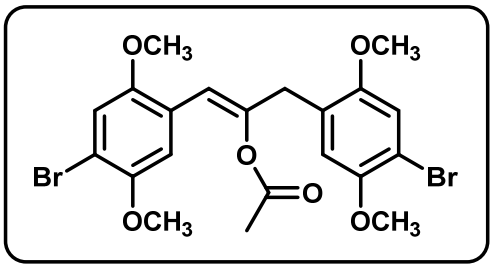
Aldehyde **(160)** was detected as an impurity from the preparation of **(159)** by general procedure 5.3.3.1, and isolated by flash column chromatography on silica gel (eluent: 7/93 Et_2O/hexane) yielding a white solid (<1%); R_f 0.85 (70:30 Et_2O:hexane). As this compound had already been synthesised (*via* general procedure 5.2.1.1) and fully characterised, structure determination was based on the matching of the spectroscopic data (^{1}H-NMR/^{13}C-NMR) of this compound, with that of an authentic sample.

(*E*)/(*Z*)-1-(4-Bromo-2,5-dimethoxyphenyl)prop-1-en-2-yl acetate (223)



Produced as an impurity from the preparation of **(159)** by general procedure 5.3.3.1, and purified by flash column chromatography on silica gel (eluent: 8/92 Et_2O/hexane), the novel acetate **(223)** was recovered as a mixture of *Z*/*E* isomers (ratio 7:1). The E/Z mixture was recovered as a cream solid, in a total combined yield of 14% (0.51 mmol, 161 mg). Following more extensive flash column chromatography, a quantity of pure **(*Z*)-(223)** was isolated and characterised. **(*Z*)-(223):** R_f 0.79 (70:30 Et_2O:hexane); m.p. 63.5–65 °C (DCM/hexane); IRν_{max} (KBr) 1748 (C=O), 1682 (C=C), 1491 (aromatic C=C) cm^{-1}; ^{1}H-NMR δ (400 MHz, $CDCl_3$): 2.10 (3H, d, $J_{3',1'}$=1.0 Hz, H-3'), 2.15 (3H, s, $COCH_3$), 3.77, 3.82 ((3H, s) × 2, 2-OCH_3, 5-OCH_3), 6.16 (1H, d, $J_{1',3'}$=0.6 Hz, H-1'), 7.03 (1H, s, H-3), 7.09 (1H, s, H-6); ^{13}C-NMR ppm (75 MHz, $CDCl_3$): 20.75 (C-3'), 21.06* (CO*C*H_3), 56.31, 56.75 (2-OCH_3, 5-OCH_3), 110.30 (C-4), 110.61, 112.96, 116.12 (C-3, C-6, C-1'), 123.20 (C-1), 146.85, 149.67, 151.10 (C-2, C-5, C-2'), 168.34 (*C*OCH_3); **(*E*)-(223)** (not isolated)**:** ^{1}H-NMR δ (400 MHz, $CDCl_3$): 2.05 (3H, d, $J_{3',1'}$=1.2 Hz, H-3'), 2.18 (3H, s, $COCH_3$), 3.78, 3.85 ((3H, s) × 2, 2-OCH_3, 5-OCH_3), 6.26 (1H, s, H-1'), 6.83 (1H, s, H-3), 7.05 (1H, s, H-6); ^{13}C-NMR ppm (75 MHz, $CDCl_3$): 17.05 (C-3'), 21.05* (CO*C*H_3 – signal overlaps with equivalent proton in (*Z*)-isomer), 56.19, 56.94 (2-OCH_3, 5-OCH_3), 110.39 (C-4), 113.82, 114.03, 115.92 (C-3, C-6, C-1'), 123.58 (C-1), 148.11, 149.61, 151.51 (C-2, C-5, C-2'), 169.46 (*C*OCH_3); *m/z* 315 ($M+H^+$, isotope ^{79}Br, 100%), 317 ($M+H^+$, isotope ^{81}Br, 98%); HRMS calc. for $C_{13}H_{16}{}^{79}BrO_4$: ($M+H^+$) 315.0232, found: 315.0225.

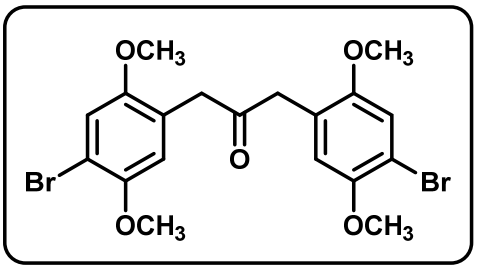
(*Z*)-1,3-Bis(4-bromo-2,5-dimethoxyphenyl)prop-1-en-2-yl acetate (222)



As described previously, a mixture of 4-bromo-2,5-dimethoxyphenyl-2-propanone **(159)** and dimeric acetate impurity **(222)** was recovered from the flash chromatography column (eluent: 10/90 Et_2O/hexane). Recrystallisation of the mixture resulted in the precipitation of the novel dimeric acetate impurity **(222)** (with ketone **(159)** remaining in solution). This precipitate was then filtered to yield the pure (*Z*)-dimeric acetate **(222)** as a white crystalline solid (0.18 mmol, 96 mg, 5%); R_f 0.53 (70:30 Et_2O:hexane); m.p. 139–141 °C (MeOH); IRν_{max} (KBr) 1764 (C=O), 1673 (C=C), 1496 (aromatic C=C) cm^{-1}; ^{1}H-NMR δ (300 MHz, $CDCl_3$): 2.09 (3H, s, $COCH_3$), 3.69 (2H, s, H-3') 3.75, 3.79, 3.80, 3.85 ((3H, s) × 4, 2-OCH_3, 5-OCH_3, 2''-OCH_3, 5''-OCH_3), 6.21 (1H, s, H-1'), 6.85 [1H, s], 7.03 [1H, s] and 7.08 [2H, s] (H-3, H-6, H-3''and H-6''); ^{13}C-NMR ppm (75 MHz, $CDCl_3$): 20.99 (CO*C*H_3), 34.84 (C-3'), 56.36, 56.40, 56.80, 56.99 (2-OCH_3, 5-OCH_3, 2''-OCH_3, 5''-OCH_3), 109.94, 110.59 (C-4, C-4''), 111.40, 112.90, 115.08, 116.28, 116.32 (C-3, C-6, C-1', C-3'', C-6''), 123.09, 125.74 (C-1, C-1''), 148.15, 149.72, 150.07, 151.26, 152.18 (C-2, C-5, C-2', C-2'', C-5''), 168.31

(*C*OCH$_3$); *m/z* 529 (M+H$^+$, isotopes $^{79}Br_2$, 51%), 531 (M+H$^+$, isotopes $^{79}Br^{81}Br$, 100%), 533 (M+H$^+$, isotopes $^{81}Br_2$, 49%); HRMS calc. for $C_{21}H_{23}{}^{79}Br_2O_6$: (M+H$^+$) 528.9861, found: 528.9861.

1,3-Bis(4-bromo-2,5-dimethoxyphenyl)-2-propanone (224)



Novel dibenzylketone **(224)** was isolated as an impurity from the preparation of **(159)** by general procedure 5.3.3.1, and purified by flash column chromatography on silica gel (eluent: 15/85 Et_2O/hexane) as a cream solid (0.33 mmol, 78 mg, 9%); R_f 0.40 (70:30 Et_2O:hexane); m.p. 147–149 °C; IRν_{max} (KBr) 1723 (C=O), 1604, 1583, 1500 (C=C) cm^{-1}; ^{1}H-NMR δ (400 MHz, $CDCl_3$): 3.67 (4H, s, H-1', H-3'), 3.73 (6H, s, 2-OCH$_3$, 2''-OCH$_3$), 3.81 (6H, s, 5-OCH$_3$, 5''-OCH$_3$), 6.64 (2H, s, H-6, H-6''), 7.04 (2H, s, H-3, H-3''); ^{13}C-NMR ppm (75 MHz, $CDCl_3$): 43.67 (C-1', C-3'), 56.08, 56.81 (2-OCH$_3$, 5-OCH$_3$, 2''-OCH$_3$, 5''-OCH$_3$), 110.12 (C-4, C-4''), 115.28, 115.86 (C-3, C-6, C-3'', C-6''), 123.24 (C-1, C-1''), 149.86, 151.66 (C-2, C-5, C-2'', C-5''), 205.19 (C=O); *m/z* 487 (M+H$^+$, isotopes $^{79}Br_2$, 51%), 489 (M+H$^+$, isotopes $^{79}Br^{81}Br$, 100%), 491 (M+H$^+$, isotopes $^{81}Br_2$, 49%); HRMS calc. for $C_{19}H_{21}{}^{79}Br_2O_5$: (M+H$^+$) 486.9756, found: 486.9753.

5.3.4 Preparation and impurity profiling of 2,5-dimethoxyphenyl-2-propanone (92) *via* the 'Darzens reaction'

General procedure 5.3.4.1 ('Procedure A')[218]

To a stirred solution of 2,5-dimethoxybenzaldehyde **(72)** (6.02 mmol, 1 g) in MeOH (8 mL), was added methyl 2-chloropropionate (8.43 mmol, 1.07 mL, 1.03 g). Whilst keeping the reaction mixture at 15 °C, sodium methoxide (NaOMe) (8.43 mmol, 573 mg) in 5 mL of MeOH, was added portionwise over 10 min. When all alkoxide had been added, the reaction mixture was allowed to come to room temperature and stirred for 1 h. The reaction mixture was then added to 5 mL of a 20% aq. NaOH solution and stirred overnight. 15% aq. HCl was then added until pH 3.5 was reached and the resulting solution was heated to 65 °C for 2 h. The MeOH was removed *in vacuo* and the resulting residue was reconstituted in Et_2O (20 mL) and transferred to a separating funnel. To this, de-ionised water (20 mL) was added and the phases separated. The aqueous extract was washed with Et_2O (2 × 15 mL) and these Et_2O washes were added to the original organic portion. These combined organic phases were dried over $MgSO_4$, filtered and concentrated *in vacuo* to give the crude product.

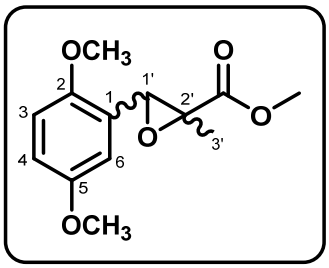
General procedure 5.3.4.2 ('Procedure B')

To a stirred solution of 2,5-dimethoxybenzaldehyde **(72)** (6.02 mmol, 1 g) in Et_2O (5 mL), was added methyl or ethyl 2-chloropropionate (8.43 mmol). Whilst keeping the reaction mixture at 15 °C, the

appropriate alkoxide (NaOMe or NaOEt) (8.43 mmol) in 5 mL of Et_2O, was added portionwise over 10 min. When all alkoxide had been added, the reaction mixture was heated to 30 °C and left stirring overnight. The following day, the cooled reaction mixture was poured onto 20 mL of ice/water and the solution was acidified to pH 4 using glacial AcOH. This solution was then transferred to a separating funnel and Et_2O (25 mL) was added. The phases were separated and the aqueous extract was washed further with Et_2O (2 × 20 mL). The combined organic extracts were washed with sat. aq. $NaHCO_3$ (2 × 25 mL) and de-ionised water (20 mL), dried over $MgSO_4$, filtered and concentrated *in vacuo* to give the pure glycidate intermediate.

To convert to the ketone, the glycidate intermediate (1 g) was dissolved in 4 mL of the appropriate alcohol (MeOH or EtOH) and added slowly to a 20% aq. NaOH solution (3 mL). This solution was stirred at reflux for 4 h and upon cooling, the alcohol was removed *in vacuo* with gentle heating. The resulting residue was diluted with de-ionised water (20 mL), transferred to a separating funnel and washed with Et_2O (15 mL). The aqueous portion was acidified with 10% aq. HCl and washed with Et_2O (2 × 20 mL). These organic portions were then washed with de-ionised water (2 × 20 mL), dried over $MgSO_4$, filtered and concentrated without heating to give the crude glycidic acid intermediate. This was dissolved in a small amount of toluene (1 mL), stirred and heated at 115 °C for 2 h and then at 120 °C for a further 1–2 h. After cooling, the toluene was removed *in vacuo* and the residue dissolved in Et_2O (20 mL). This was washed with de-ionised water (2 × 20 mL) and brine (20 mL), dried over $MgSO_4$, filtered and concentrated *in vacuo* to give the crude ketone product. This was finally purified by flash column chromatography on silica gel to give pure ketone product.

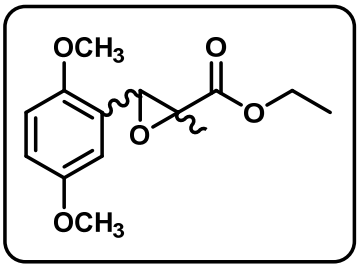
***cis*/*trans*-Methyl 2-methyl-3-(2,5-dimethoxyphenyl)glycidate (161)**



The glycidate **(161)** was recovered as an intermediate in the synthesis of ketone **(92)**. Using general procedure A (5.3.4.1), as well as additional heating (to 55 °C) and stirring for 40 h, the isomeric glycidate mixture **(161)** was recovered, following flash column chromatography (eluent: 5/95 Et_2O/hexane), as a pale yellow oil (2.77 mmol, 699 mg, 46%) consisting of a mixture of *cis* and *trans* isomers (ratio 1:1). Using general procedure B (5.3.4.2), (with methyl 2-chloropropionate as reagent and NaOMe as base), glycidate **(161)** was isolated (without need for further purification) as a pale yellow solid (5.54 mmol, 1.40 g, 92%) exclusively in the *trans* form. ***trans*-(161):** R_f 0.59 (70:30 Et_2O:hexane); m.p. 46–48 °C; IRv_{max} (KBr) 1729 (C=O), 1591, 1500 (C=C) cm^{-1}; ^{1}H-NMR δ (400 MHz, $CDCl_3$): 1.30 (3H, s, H-3'), 3.77, 3.79, 3.83 ((3H, s) × 3, 2-OCH_3, 5-OCH_3, CO_2CH_3), 4.39 (1H, s, H-1'), 6.79–6.84 (3H, m, H-3, H-4, H-6); ^{13}C-NMR ppm (75 MHz, $CDCl_3$): 12.80 (C-3'), 52.68, 55.78, 55.91 (2-OCH_3, 5-OCH_3, CO_2CH_3), 59.60 (C-2'), 59.82 (C-1'), 111.18, 113.35, 113.93 (C-3, C-4, C-6), 123.54 (C-1), 152.20, 153.44 (C-2, C-5), 171.45 (CO_2CH_3); *m/z* 253 ($M+H^+$, 100%); HRMS calc. for $C_{13}H_{17}O_5$: ($M+H^+$) 253.1076, found: 253.1072. A small sample of pure *cis*-isomer was recovered

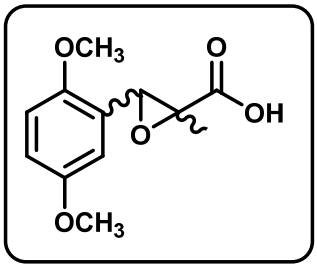
after it differentially crystallised from the *trans*-isomer in a number of fractions during flash column chromatography using general procedure A (5.3.4.1). The crystallised solid was carefully removed from these fractions, combined and characterised: ***cis*-(161):** R_f 0.58 (70:30 Et_2O:hexane); m.p. 78–79.5 °C (Et_2O/hexane); IRν_{max} (KBr) 1754 (C=O), 1612, 1499 (C=C) cm^{-1}; ^{1}H-NMR δ (400 MHz, $CDCl_3$): 1.75 (3H, s, H-3'), 3.50 (3H, s, CO_2CH_3), 3.76, 3.80 ((3H, s) × 2, 2-OCH_3, 5-OCH_3), 4.16 (1H, s, H-1'), 6.75–6.81 (2H, m, H-3, H-4), 6.91 (1H, d, *J*=3.2 Hz, H-6); ^{13}C-NMR ppm (75 MHz, $CDCl_3$): 19.41 (C-3'), 51.91, 55.80, 56.20 (2-OCH_3, 5-OCH_3, CO_2CH_3), 60.92 (C-1'), 62.65 (C-2'), 111.31, 112.41, 114.60 (C-3, C-4, C-6), 123.26 (C-1), 152.12, 153.34 (C-2, C-5), 169.18 (CO_2CH_3); *m/z* 253 ($M+H^+$, 100%); HRMS calc. for $C_{13}H_{17}O_5$: ($M+H^+$) 253.1076, found: 253.1076.

***cis*/*trans*-Ethyl 2-methyl-3-(2,5-dimethoxyphenyl)glycidate (239)**



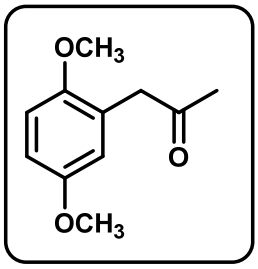
The novel glycidate **(239)** was recovered as an intermediate in the synthesis of ketone **(92)**. Using general procedure A (5.3.4.1), but using EtOH as solvent, ethyl 2-chloropropionate as reagent, NaOEt as base and stirring for 16 h at rt (*vs.* 1 h), glycidate **(239)** was recovered following flash column chromatography (eluent: 8/92 Et_2O/hexane) as a pale yellow oil (3.37 mmol, 898 mg, 56%) consisting of a mixture of *cis* and *trans* isomers (ratio 1:1). Using general procedure B (5.3.4.2), (with ethyl 2-chloropropionate as reagent and NaOEt as base), glycidate **(239)** was isolated (without need for further purification) as a pale amber solid (5.30 mmol, 1.41 g, 88%) exclusively in the *trans* form. ***trans*-(239):** R_f 0.63 (70:30 Et_2O:hexane); m.p. ≈30 °C; IRν_{max} (NaCl) 1732 (C=O), 1592, 1505 (C=C) cm^{-1}; ^{1}H-NMR δ (400 MHz, $CDCl_3$): 1.29 (3H, s, H-3'), 1.34 (3H, t, *J*=7.2 Hz, $CO_2CH_2CH_3$), 3.76, 3.78, ((3H, s) × 2, 2-OCH_3, 5-OCH_3), 4.28 (2H, 'qd', *J*=7.2, 1.6 Hz, $CO_2CH_2CH_3$), 4.38 (1H, s, H-1'), 6.80–6.81 (3H, m, H-3, H-4, H-6); ^{13}C-NMR ppm (75 MHz, $CDCl_3$): 12.76, 14.09 (C-3', $CO_2CH_2CH_3$), 55.73, 55.91 (2-OCH_3, 5-OCH_3), 59.60 (C-2'), 59.73 (C-1'), 61.64 ($CO_2CH_2CH_3$), 111.18, 113.34, 113.82 (C-3, C-4, C-6), 123.68 (C-1), 152.18, 153.42 (C-2, C-5), 170.94 ($CO_2CH_2CH_3$); *m/z* 267 ($M+H^+$, 100%); HRMS calc. for $C_{14}H_{19}O_5$: ($M+H^+$) 267.1232, found: 267.1230. ***cis*-(239):** (not isolated) ^{1}H-NMR δ (400 MHz, $CDCl_3$): 0.94 (3H, t, *J*=7.1 Hz, $CO_2CH_2CH_3$), 1.74 (3H, s, H-3'), 3.76, 3.79 ((3H, s) × 2, 2-OCH_3, 5-OCH_3), 3.95 (2H, 'qd', *J*=7.1, 2.1 Hz, $CO_2CH_2CH_3$), 4.14 (1H, s, H-1'), 6.74–6.80 (2H, m, H-3, H-4), 6.93 (1H, d, *J*=3.0 Hz, H-6); ^{13}C-NMR ppm (75 MHz, $CDCl_3$): 13.76 ($CO_2CH_2CH_3$), 19.25 (C-3'), 55.72, 56.13 (2-OCH_3, 5-OCH_3), 60.88 (direct overlap of C-1' and $CO_2CH_2CH_3$), 62.38 (C-2'), 111.16, 112.75, 114.28 (C-3, C-4, C-6), 123.38 (C-1), 152.05, 153.23 (C-2, C-5), 168.72 ($CO_2CH_2CH_3$).

2-Methyl-3-(2,5-dimethoxyphenyl)glycidic acid (241)



The glycidic acid **(241)** was isolated as an intermediate in the synthesis of ketone **(92)** from glycidates **(161)** and **(239)**. Using general procedure B (5.3.4.2), the acid **(241)** was recovered as a cream solid (87% from glycidate **(161)** and 88% from glycidate **(239)**); R_f 0.15 (50:50 EtOAc:hexane); m.p. 95–98 °C; IRν_{max} (KBr) ≈3000 (O–H), 1715 (C=O), 1498 (C=C) cm^{-1}; ^{1}H-NMR δ (300 MHz, $CDCl_3$): 1.33 (3H, s, H-3'), 3.77, 3.81 ((3H, s) × 2, 2-OCH_3, 5-OCH_3), 4.44 (1H, s, H-1'), 6.79–6.86 (3H, m, H-3, H-4, H-6), 9.89 (br s, COOH); ^{13}C-NMR ppm (75 MHz, $CDCl_3$): 12.29 (C-3'), 55.78, 55.90 (2-OCH_3, 5-OCH_3), 59.44 (C-2'), 60.19 (C-1'), 111.23, 113.29, 114.16 (C-3, C-4, C-6), 122.98 (C-1), 152.22, 153.40 (C-2, C-5), 176.15 (COOH); *m/z* 237 ($M–H^+$, 100%); HRMS calc. for $C_{12}H_{15}O_5$: ($M+H^+$) 239.0919, found: 239.0920.

2,5-Dimethoxyphenyl-2-propanone (92)



Prepared according to general procedure B (5.3.4.2), from glycidic acid **(241)**, ketone **(92)** was isolated by flash column chromatography on silica gel (eluent: 8/92 Et_2O/hexane) to yield a pale yellow oil (65%). As this compound had been previously synthesised, isolated and characterised, structure confirmation was achieved by comparison of the spectroscopic data (^{1}H-NMR/^{13}C-NMR) with those of an authentic sample.

5.3.5 Preparation and impurity profiling of 4-bromo-2,5-dimethoxyphenyl-2-propanone (159) *via* the 'Darzens reaction'

General procedure 5.3.5.1 ('Procedure A')[218]

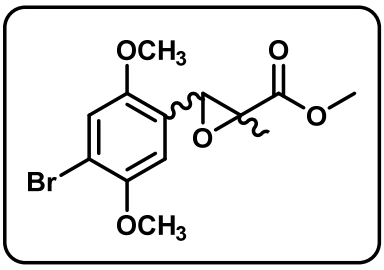
To a stirred solution of 4-bromo-2,5-dimethoxybenzaldehyde **(160)** (1.22 mmol, 300 mg) in MeOH (5 mL), was added methyl 2-chloropropionate (1.71 mmol, 0.19 mL, 210 mg). Whilst keeping the reaction mixture at 15 °C, NaOMe (1.71 mmol, 93 mg) in 3 mL of MeOH, was added portionwise over 10 min. When all alkoxide had been added the reaction mixture was allowed to come to room temperature and stirred for 1 h. The reaction mixture was then added to 3 mL of a 20% aq. NaOH solution and stirred overnight. The following day, 15% aq. HCl was added until pH 3.5 was reached and the resulting solution was heated to 65 °C for 2 h. The MeOH was removed *in vacuo* and the resulting residue was reconstituted in Et_2O (20 mL) and transferred to a separating funnel. To this, de-ionised water (20 mL) was added and the phases separated. The aqueous extract was washed with Et_2O (2 × 15 mL) and these Et_2O washes were added to the original organic portion. These combined organic phases were dried over $MgSO_4$, filtered and concentrated *in vacuo* to give the crude product.

General procedure 5.3.5.2 ('Procedure B')

To a stirred solution of 4-bromo-2,5-dimethoxybenzaldehyde **(160)** (1.22 mmol, 300 mg) in Et_2O (2 mL), was added methyl or ethyl 2-chloropropionate (1.71 mmol). Whilst keeping the reaction mixture at 15 °C, the appropriate alkoxide (NaOMe or NaOEt) (1.71 mmol) in 2 mL of Et_2O, was added portionwise over 10 min. When all alkoxide had been added, the reaction mixture was heated to 30 °C and left stirring overnight. The following day, the cooled reaction mixture was poured onto 20 mL of ice/water and the solution was acidified to pH 4 using glacial AcOH. This solution was then transferred to a separating funnel and Et_2O (25 mL) was added. The phases were separated and the aqueous extract was washed further with Et_2O (2 × 20 mL). The combined organic extracts were washed with sat. aq. $NaHCO_3$ (2 × 25 mL) and de-ionised water (20 mL), dried over $MgSO_4$, filtered and concentrated *in vacuo* to give the pure glycidate intermediate.

To convert to the ketone, the glycidate intermediate (335 mg) was dissolved in 5 mL of the appropriate alcohol (MeOH or EtOH) and added slowly to a 20% aq. NaOH solution (2 mL). This solution was stirred at reflux for 4 h and upon cooling, the alcohol was removed *in vacuo* with gentle heating. The resulting residue was diluted with de-ionised water (20 mL), transferred to a separating funnel and washed with Et_2O (15 mL). The aqueous portion was acidified with 10% aq. HCl and washed with Et_2O (2 × 20 mL). These organic portions were then washed with de-ionised water (2 × 20 mL), dried over $MgSO_4$, filtered and concentrated without heating to give the crude glycidic acid intermediate. This was then dissolved in a small amount of toluene (1 mL), stirred and heated at 115 °C for 2 h and then at 120 °C for a further 1–2 h. After cooling, the toluene was removed *in vacuo* and the residue dissolved in Et_2O (20 mL). This was washed with de-ionised water (2 × 20 mL) and brine (20 mL), dried over $MgSO_4$, filtered and concentrated *in vacuo* to give the crude ketone product. This was finally purified by flash column chromatography on silica gel to give to pure ketone product.

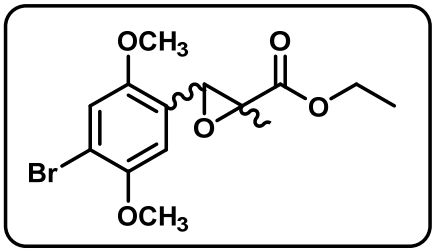
***cis*/*trans*-Methyl 2-methyl-3-(4-bromo-2,5-dimethoxyphenyl)glycidate (162)**



The novel glycidate **(162)** was recovered as an intermediate in the synthesis of ketone **(159)**. Using general procedure A (5.3.5.1) (with additional heating to 65 °C and a reaction time of two days), glycidate **(162)** was recovered, following flash column chromatography (eluent: 5/95 Et_2O/hexane) as a cream solid (0.49 mmol, 162 mg, 40%) consisting of a mixture of *cis* and *trans* isomers (ratio 1:1). Using general procedure B (5.3.5.2), (with methyl 2-chloropropionate as reagent and NaOMe as base), glycidate **(162)** was isolated (without need for further purification) as a pale yellow solid (1.01 mmol, 335 mg, 83%), exclusively in the *trans* form. ***trans*-(162):** R_f 0.65 (70:30 Et_2O:hexane); m.p. 105–106 °C (MeOH); IRν_{max} (KBr) 1738 (C=O), 1496 (C=C) cm^{-1}; ^{1}H-NMR δ (400 MHz, $CDCl_3$): 1.29 (3H, s, H-3'), 3.79,

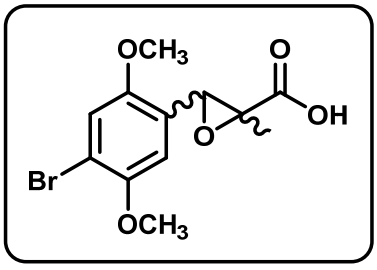
3.83, 3.85 ((3H, s) × 3, 2-OCH_3, 5-OCH_3, CO_2CH_3), 4.35 (1H, s, H-1'), 6.80 (1H, s, H-6), 7.08 (1H, s, H-3); ^{13}C-NMR ppm (75 MHz, $CDCl_3$): 12.82 (C-3'), 52.76, 56.13, 56.96 (2-OCH_3, 5-OCH_3, $CO_2\mathit{C}H_3$), 59.59 (C-1'), 59.61 (C-2'), 111.31 (C-4), 111.60, 115.78 (C-3, C-6), 122.73 (C-1), 150.02, 152.19 (C-2, C-5), 171.12 ($\mathit{C}O_2CH_3$); *m/z* 331 ($M+H^+$, isotope ^{79}Br, 100%), 333 ($M+H^+$, isotope ^{81}Br, 98%); HRMS calc. for $C_{13}H_{16}{}^{79}BrO_5$: ($M+H^+$) 331.0181, found: 331.0174. ***cis*-(162):** (Not isolated) ^{1}H-NMR δ (400 MHz, $CDCl_3$): 1.74 (3H, s, H-3'), 3.51 (3H, s, CO_2CH_3), 3.80, 3.85 ((3H, s) × 2, 2-OCH_3, 5-OCH_3), 4.11 (1H, s, H-1'), 6.95 (1H, s, H-6), 7.03 (1H, s, H-3); ^{13}C-NMR ppm (75 MHz, $CDCl_3$): 19.37 (C-3'), 52.06, 56.30, 56.81 (2-OCH_3, 5-OCH_3, $CO_2\mathit{C}H_3$), 60.53 (C-1'), 62.78 (C-2'), 111.01 (C-4), 111.34, 115.60 (C-3, C-6), 122.40 (C-1), 149.74, 152.06 (C-2, C-5), 168.83 ($\mathit{C}O_2CH_3$).

cis/_trans_-Ethyl 2-methyl-3-(4-bromo-2,5-dimethoxyphenyl)glycidate (240)



The novel glycidate **(240)** was recovered as an intermediate in the synthesis of ketone **(159)**. Using general procedure B (5.3.5.2), (with ethyl 2-chloropropionate as reagent and NaOEt as base), glycidate **(240)** was recovered (without need for further purification), as a cream solid (1.04 mmol, 358 mg, 85%) exclusively in the *trans* form. Using general procedure A (5.3.5.1), glycidate **(240)** was only detected in a trace amount in the crude ^{1}H-NMR spectrum, so purification was not pursued. ***trans*-(240):** R_f 0.68 (70:30 Et_2O:hexane); m.p. 94–96 °C (MeOH); IRν_{max} (KBr) 1736 (C=O), 1496 (C=C) cm^{-1}; ^{1}H-NMR δ (400 MHz, $CDCl_3$): 1.28 (3H, s, H-3'), 1.34 (3H, t, *J*=7.0 Hz, $CO_2CH_2C\mathit{H}_3$), 3.79, 3.84 ((3H, s) × 2, 2-OCH_3, 5-OCH_3), 4.28 (2H, 'qd', *J*=6.8, 2.0 Hz, $CO_2C\mathit{H}_2CH_3$), 4.34 (1H, s, H-1'), 6.80 (1H, s, H-6), 7.08 (1H, s, H-3); ^{13}C-NMR ppm (75 MHz, $CDCl_3$): 12.78, 14.10 (C-3', $CO_2CH_2\mathit{C}H_3$), 56.14, 56.93 (2-OCH_3, 5-OCH_3), 59.52 (C-1'), 59.63 (C-2'), 61.78 ($CO_2\mathit{C}H_2CH_3$), 111.21 (C-4), 111.60, 115.77 (C-3, C-6), 122.87 (C-1), 150.00, 152.17 (C-2, C-5), 170.63 ($\mathit{C}O_2CH_3$); *m/z* 345 ($M+H^+$, isotope ^{79}Br, 100%), 347 ($M+H^+$, isotope ^{81}Br, 98%); HRMS calc. for $C_{14}H_{18}{}^{79}BrO_5$: ($M+H^+$) 345.0338, found: 345.0323.

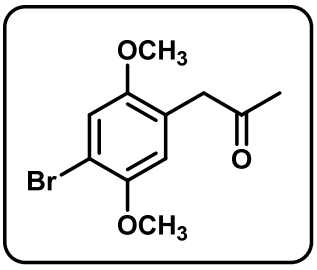
2-Methyl-3-(4-bromo-2,5-dimethoxyphenyl)glycidic acid (242)



The novel glycidic acid **(242)** was isolated as an intermediate in the synthesis of ketone **(159)** from glycidates **(162)** and **(240)**. Using general procedure B (5.3.5.2), the acid **(242)** was recovered as a cream solid (95% from glycidate **(162)** and 97% from glycidate **(240)**); R_f 0.09 (50:50 EtOAc:hexane); m.p. 121–123 °C; IRν_{max} (KBr) ≈3000 (O–H), 1705 (C=O), 1495 (C=C) cm^{-1}; ^{1}H-NMR δ (300 MHz, $CDCl_3$): 1.32 (3H, s, H-3'), 3.81, 3.86 ((3H, s) × 2, 2-OCH_3, 5-OCH_3), 4.40 (1H, s, H-1'), 6.79 (1H, s, H-6), 7.10 (1H, s, H-3), 8.87 (br s, COOH); ^{13}C-NMR ppm (75 MHz, $CDCl_3$): 12.33 (C-3'), 56.13, 56.95 (2-OCH_3, 5-OCH_3), 59.45 (C-2'), 59.98 (C-1'), 111.42, 115.79 (C-3, C-6), 111.58 (C-4), 122.05 (C-1), 149.99, 152.16 (C-2, C-5), 176.00

(COOH); *m/z* 315 ($M–H^+$, isotope ^{79}Br, 100%), 317 ($M–H^+$, isotope ^{81}Br, 98%); HRMS calc. for $C_{12}H_{14}{}^{79}BrO_5$: ($M+H^+$) 317.0025, found: 317.0023.

4-Bromo-2,5-dimethoxyphenyl-2-propanone (159)



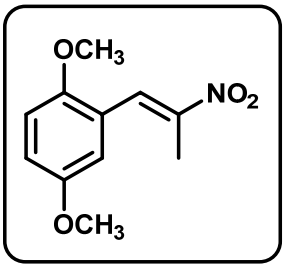
Prepared according to general procedure B (5.3.5.2), from glycidic acid **(242)**, ketone **(159)** was isolated by flash column chromatography on silica gel (eluent: 12/88 Et_2O/hexane) yielding a cream solid (71%). As this compound had been previously synthesised, isolated and characterised, structure confirmation was achieved by comparison of the spectroscopic data (^{1}H-NMR/^{13}C-NMR) with those of an authentic sample.

5.3.6 Preparation of 2,5-P2P (92) *via* the 'nitrostyrene route'

General procedure 5.3.6.1

To a stirred solution of 2,5-dimethoxybenzaldehyde **(72)** (120.4 mmol, 20 g) in glacial acetic acid (140 mL), nitroethane (240.8 mmol, 17.30 mL, 18.08 g) was added, followed by the dropwise addition of cyclohexylamine (120.4 mmol, 13.81 mL, 11.94 g). The reaction mixture was heated to 90 °C and stirred for 6 h. Upon cooling, de-ionised water (140 mL) was added and the mixture was left to stand overnight. The precipitated nitrostyrene was then isolated by filtration and recrystallised to give the pure product. If the acetic acid had not been fully removed by filtration, the precipitated crystals would have had to be dissolved in DCM and washed with 5% aq. $Na_2S_2O_3$ before recrystallisation.

(*E*)-1-(2,5-Dimethoxyphenyl)-2-nitroprop-1-ene (73)

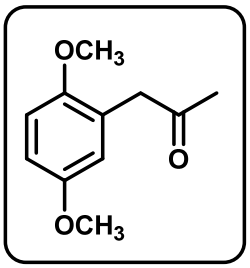


Recrystallisation of the precipitated crystals from MeOH, yielded the pure nitrostyrene **(73)** as orange crystals (98.73 mmol, 22.04 g, 82%); R_f 0.49 (50:50 Et_2O:hexane); m.p. 73–75 °C (MeOH), (lit. m.p. 72–74 °C)[261]; IRν_{max} (KBr) 1646, 1611, 1586 (C=C), 1512, 1353 (NO_2) cm^{-1}; ^{1}H-NMR δ (300 MHz, $CDCl_3$): 2.40 (3H, d, *J*=1.0 Hz, H-3'), 3.80, 3.84 ((3H, s) × 2, 2-OCH_3, 5-OCH_3), 6.85 (1H, d, $J_{6,4}$=3.0 Hz, H-6), 6.87 (1H, d, $J_{3,4}$=9.1 Hz, H-3), 6.95 (1H, dd, $J_{4,3}$=9.0 Hz, $J_{4,6}$=2.9 Hz, H-4), 8.24 (1H, s, H-1'); ^{13}C-NMR ppm (75 MHz, $CDCl_3$): 14.12 (C-3'), 55.80, 55.98 (2-OCH_3, 5-OCH_3), 111.69, 115.77, 116.02 (C-3, C-4, C-6), 122.04 (C-1), 129.61 (C-1'), 147.70 (C-2'), 152.40, 153.10 (C-2, C-5); *m/z* 224 ($M+H^+$, 100%); HRMS calc. for $C_{11}H_{14}NO_4$: ($M+H^+$) 224.0923, found: 224.0919.

General procedure 5.3.6.2

A suspension of iron powder (–325 mesh) (82.43 mmol, 4.60 g) in glacial acetic acid (20 mL), was heated to 90 °C for 20 min. Simultaneously (*E*)-1-(2,5-dimethoxyphenyl)-2-nitroprop-1-ene **(73)** (17.92 mmol, 4 g) in glacial acetic acid (20 mL), was heated in a conical flask to ≈90 °C for 20 min. The nitrostyrene solution was added portionwise to the iron suspension over a 20 min period using a glass pipette. The reaction mixture was maintained at 90 °C for 2 h. After cooling, the reaction mixture was poured onto ice/water (50 mL), filtered through Celite® in a sintered glass funnel and rinsed with DCM (60 mL). The phases were separated and the aqueous phase was extracted with DCM (3 × 40 mL). The combined organic phases were washed with 15% aq. NaOH (3 × 40 mL) and de-ionised water (3 × 40 mL), dried over $MgSO_4$, filtered and concentrated *in vacuo* to give the pure product.

2,5-Dimethoxyphenyl-2-propanone (92)



Prepared according to procedure 5.3.6.2, ketone **(92)** was recovered as a pale amber oil (15.77 mmol, 3.06 g, 88%); R_f 0.66 (70:30 Et_2O:hexane). As this compound had been previously synthesised, isolated and characterised, structure confirmation was achieved by comparison of the spectroscopic data (^{1}H-NMR/^{13}C-NMR) with those of an authentic sample.

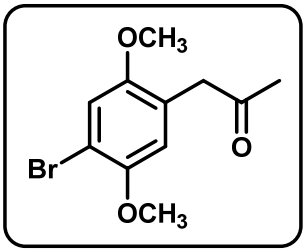
5.4 Experimental details pertaining to work outlined in Chapter 4

5.4.1 Impurity profiling of the bromination of 2,5-dimethoxyphenyl-2-propanone (92)

General procedure 5.4.1.1

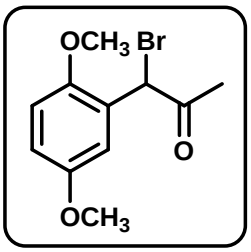
To a stirred solution of 2,5-dimethoxyphenyl-2-propanone **(92)** (2.57 mmol, 500 mg) in glacial acetic acid (3 mL), a solution of bromine (3.09 mmol, 0.16 mL, 496 mg) in glacial acetic acid (2 mL), was added dropwise. The flask was covered in aluminium foil to exclude light and left stirring at room temperature for 24 h. The reaction mixture was diluted with de-ionised water (10 mL), and 5% aq. $Na_2S_2O_3$ was added dropwise until the orange colour faded to cream. DCM (20 mL) was added to the mixture and the phases were separated. The aqueous phase was extracted with DCM (2 × 20 mL). The combined organic phases were then washed with 5% aq. $Na_2S_2O_3$ (2 × 20 mL), saturated aq. $NaHCO_3$ (3 × 20 mL) and de-ionised water (2 × 20 mL), dried over $MgSO_4$, filtered and concentrated *in vacuo* to give the crude product as a yellow oil. This crude mixture was then subjected to flash column chromatography on silica gel to isolate the products.

4-Bromo-2,5-dimethoxyphenyl-2-propanone (159)



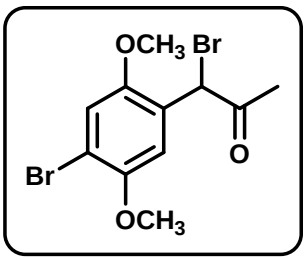
Prepared according to general procedure 5.4.1.1, ketone **(159)** was isolated by flash column chromatography on silica gel (eluent: 30/70 Et_2O/hexane) to yield a cream solid (1%). As this compound had been previously synthesised, isolated and characterised, structure confirmation was achieved by comparison of the spectroscopic data (^{1}H-NMR/^{13}C-NMR) with those of an authentic sample.

1-Bromo-1-(2,5-dimethoxyphenyl)-2-propanone (250)



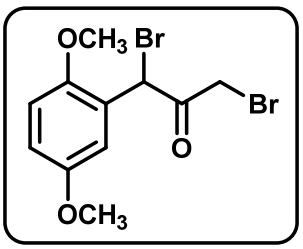
Prepared according to general procedure 5.4.1.1, ketone **(250)** was recovered by flash column chromatography on silica gel (eluent: 7/93 Et_2O/hexane), as a mixture with other structurally similar products. Although not isolated, ketone **(250)** was identified by comparison of the spectroscopic data (^{1}H-NMR/^{13}C-NMR) with those of an authentic sample that had been independently synthesised and characterised (by general procedure 5.4.2.1).

1-Bromo-1-(4-bromo-2,5-dimethoxyphenyl)-2-propanone (251)



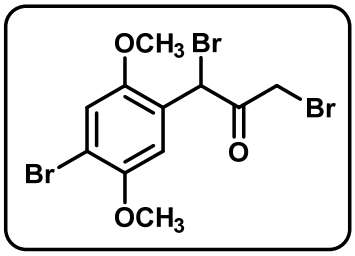
Prepared according to general procedure 5.4.1.1, ketone **(251)** was recovered by flash column chromatography on silica gel (eluent: 7/93 Et_2O/hexane), as a mixture with other structurally similar products. Although not isolated, ketone **(251)** was identified by comparison of the spectroscopic data (^{1}H-NMR/^{13}C-NMR) with those of an authentic sample that had been independently synthesised and characterised (by general procedure 5.4.3.1).

1,3-Dibromo-1-(2,5-dimethoxyphenyl)-2-propanone (252)



Prepared according to general procedure 5.4.1.1, the novel dibromo compound **(252)** was isolated by flash column chromatography on silica gel (eluent: 5/95 Et_2O/hexane), to yield a cream solid (0.75 mmol, 262 mg, 29%); R_f 0.68 (70:30 Et_2O:hexane); m.p. 80–82 °C (EtOH); IRν_{max} (KBr) 1742 (C=O), 1588, 1502 (C=C) cm^{-1}; ^{1}H-NMR δ (400 MHz, $CDCl_3$): 3.78, 3.82 ((3H, s) × 2, 2-OCH_3, 5-OCH_3), 4.12 [1H, d, J=13.2 Hz] and 4.18 [1H, d, J=13.2 Hz] (H_A-3', H_B-3'), 6.12 (1H, s, H-1'), 6.83 (1H, d, $J_{3,4}$=9.0 Hz, H-3), 6.88 (1H, dd, $J_{4,3}$=9.0 Hz, $J_{4,6}$=3.0 Hz, H-4), 7.01 (1H, d, $J_{6,4}$=2.9 Hz, H-6); ^{13}C-NMR ppm (75 MHz, $CDCl_3$): 31.43 (C-3'), 47.75 (C-1'), 55.80, 56.27 (2-OCH_3, 5-OCH_3), 112.38, 116.06, 116.23 (C-3, C-4, C-6), 124.28 (C-1), 150.47, 153.91 (C-2, C-5), 193.12 (C-2'); *m/z* 351 (M+H$^+$, isotopes $^{79}Br_2$, 51%), 353 (M+H$^+$, isotopes $^{79}Br^{81}Br$, 100%), 355 (M+H$^+$, isotopes $^{81}Br_2$, 49%); HRMS calc. for $C_{11}H_{13}{}^{79}Br_2O_3$: (M+H$^+$) 350.9231, found: 350.9225.

1,3-Dibromo-1-(4-bromo-2,5-dimethoxyphenyl)-2-propanone (253)



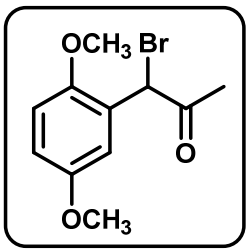
Prepared according to general procedure 5.4.1.1, the novel tribromo compound **(253)** was isolated by flash column chromatography on silica gel (eluent: 5/95 Et_2O/hexane), to yield a colourless oil (0.15 mmol, 66 mg, 6%); R_f 0.81 (70:30 Et_2O:hexane); IRν_{max} (NaCl) 1733 (C=O), 1578, 1506 (C=C) cm^{-1}; ^{1}H-NMR δ (400 MHz, $CDCl_3$): 3.84, 3.87 ((3H, s) × 2, 2-OCH_3, 5-OCH_3), 4.13 [1H, d, *J*=13.1 Hz] and 4.20 [1H, d, *J*=13.1 Hz] (H_A-3', H_B-3'), 6.14 (1H, s, H-1'), 7.05 (1H, s, H-3), 7.11 (1H, s, H-6); ^{13}C-NMR ppm (75 MHz, $CDCl_3$): 31.37 (C-3'), 46.26 (C-1'), 56.55, 56.92 (2-OCH_3, 5-OCH_3), 113.70 (C-4), 114.40, 116.79 (C-3, C-6), 123.14 (C-1), 150.46, 150.57 (C-2, C-5), 192.92 (C-2'); *m/z* 429 ($M+H^+$, isotopes $^{79}Br_3$, 34%), 431 ($M+H^+$, isotopes $^{79}Br_2{}^{81}Br$, 100%), 433 ($M+H^+$, isotopes $^{79}Br{}^{81}Br_2$, 98%), 435 ($M+H^+$, isotopes $^{81}Br_3$, 32%); HRMS calc. for $C_{11}H_{12}{}^{79}Br_3O_3$: ($M+H^+$) 428.8337, found: 428.8326.

5.4.2 Preparation of 1-bromo-1-(2,5-dimethoxyphenyl)-2-propanone (250)

General procedure 5.4.2.1

To a stirred solution of 2,5-dimethoxyphenyl-2-propanone **(92)** (1.54 mmol, 300 mg) in carbon tetrachloride (CCl_4) (4 mL), was added NBS (1.54 mmol, 275 mg) and a catalytic amount of benzoyl peroxide (4 mg). The mixture was heated at reflux temperature for 4 h. The cooled reaction mixture was then filtered to remove insoluble succinimide. The filtrate was concentrated to give an amber oil. This crude reaction mixture was subjected to flash column chromatography to isolate the desired 1-bromo-1-(2,5-dimethoxyphenyl)-2-propanone **(250)**.

1-Bromo-1-(2,5-dimethoxyphenyl)-2-propanone (250)



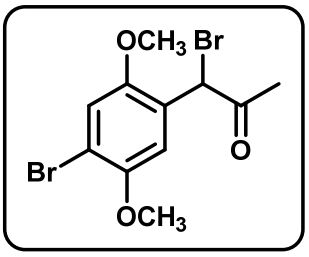
Prepared according to procedure 5.4.2.1, ketone **(250)** was isolated from the crude reaction mixture, by flash column chromatography on silica gel (eluent: 5/95 Et_2O/hexane), as a pale amber oil (1.14 mmol, 311 mg, 74%); R_f 0.58 (70:30 Et_2O:hexane); IRν_{max} (NaCl) 1734 (C=O), 1588, 1506 (C=C) cm^{-1}; ^{1}H-NMR δ (400 MHz, $CDCl_3$): 2.27 (3H, s, H-3'), 3.77, 3.82 ((3H, s) × 2, 2-OCH_3, 5-OCH_3), 5.87 (1H, s, H-1'), 6.82 (1H, d, $J_{3,4}$ =9.0 Hz, H-3), 6.86 (1H, dd, $J_{4,3}$ =9.2 Hz, $J_{4,6}$ =3.0 Hz, H-4), 7.00 (1H, d, $J_{6,4}$ =3.0 Hz, H-6); ^{13}C-NMR ppm (75 MHz, $CDCl_3$): 26.54 (C-3'), 51.45 (C-1'), 55.75, 56.18 (2-OCH_3, 5-OCH_3), 112.19, 115.54, 116.04 (C-3, C-4, C-6), 125.12 (C-1), 150.55, 153.83 (C-2, C-5), 199.18 (C-2'); *m/z* 273 ($M+H^+$, isotope ^{79}Br, 100%), 275 ($M+H^+$, isotope ^{81}Br, 98%); HRMS calc. for $C_{11}H_{14}{}^{79}BrO_3$: ($M+H^+$) 273.0126, found: 273.0120.

5.4.3 Preparation of 1-bromo-1-(4-bromo-2,5-dimethoxyphenyl)-2-propanone (251)

General procedure 5.4.3.1

To a stirred solution of 4-bromo-2,5-dimethoxyphenyl-2-propanone **(159)** (0.70 mmol, 190 mg) in CCl_4 (3 mL), was added NBS (0.70 mmol, 124 mg) and a catalytic amount of benzoyl peroxide (2 mg). The mixture was heated at reflux temperature for 4 h. The cooled reaction mixture was then filtered to remove insoluble succinimide. The filtrate was concentrated to give an amber oil. This crude reaction mixture was subjected to flash column chromatography to isolate the desired 1-bromo-1-(4-bromo-2,5-dimethoxyphenyl)-2-propanone **(251)**.

1-Bromo-1-(4-bromo-2,5-dimethoxyphenyl)-2-propanone (251)



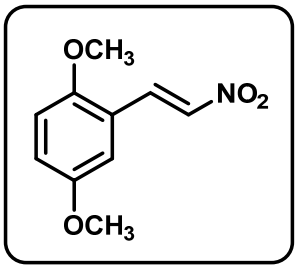
Prepared according to procedure 5.4.3.1, ketone **(251)** was isolated from the crude reaction mixture, by flash column chromatography on silica gel (eluent: 5/95 Et_2O/hexane), as a clear oil (0.37 mmol, 131 mg, 53%); R_f 0.72 (70:30 Et_2O:hexane); IRν_{max} (NaCl) 1733 (C=O), 1576, 1496 (C=C) cm^{-1}; ^{1}H-NMR δ (400 MHz, $CDCl_3$): 2.30 (3H, s, H-3'), 3.84, 3.87 ((3H, s) × 2, 2-OCH_3, 5-OCH_3), 5.86 (1H, s, H-1'), 7.01 (1H, s, H-6), 7.11 (1H, s, H-3); ^{13}C-NMR ppm (75 MHz, $CDCl_3$): 26.81 (C-3'), 50.16 (C-1'), 56.44, 56.88 (2-OCH_3, 5-OCH_3), 113.10 (C-4), 114.27, 116.61 (C-3, C-6), 124.04 (C-1), 150.48, 150.50 (C-2, C-5), 198.82 (C-2'); *m/z* 351 ($M+H^+$, isotopes $^{79}Br_2$, 51%), 353 ($M+H^+$, isotopes $^{79}Br^{81}Br$, 100%), 355 ($M+H^+$, isotopes $^{81}Br_2$, 49%); HRMS calc. for $C_{11}H_{13}{}^{79}Br_2O_3$: ($M+H^+$) 350.9231, found: 350.9240.

5.4.4 Preparation of monomeric nitrostyrenes (280), (281) and (282)

General procedure 5.4.4.1

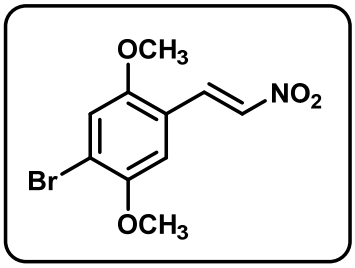
To a stirred solution of 2,5-dimethoxybenzaldehyde **(72)** (6.02 mmol, 1 g) in glacial acetic acid (8 mL) in a sealed container, was added nitromethane (CH_3NO_2) (12.04 mmol, 0.65 mL, 739 mg), followed by the dropwise addition of cyclohexylamine (6.02 mmol, 0.69 mL, 597 mg). The reaction mixture was stirred at 90 °C for 6 h. Upon cooling, de-ionised water (10 mL) was added and the mixture was left to stand overnight. The precipitated nitrostyrene was then isolated by filtration and recrystallised to yield the pure product. If the acetic acid had not been fully removed by filtration, the precipitated crystals would have had to be dissolved in DCM and washed with 5% aq. $NaHCO_3$ before recrystallisation.

(*E*)-1-(2,5-Dimethoxyphenyl)-2-nitroethene (280)



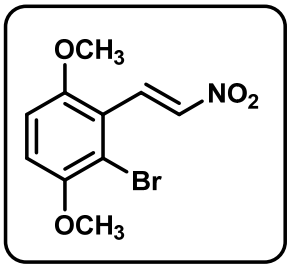
Using general procedure 5.4.4.1, an orange solid was recovered following filtration. Recrystallisation of the recovered solid from EtOH/H_2O, yielded the pure nitrostyrene **(280)** as orange crystals (5.12 mmol, 1.07 g, 85%); R_f 0.47 (50:50 Et_2O:hexane); m.p. 116–118 °C (EtOH/H_2O), (lit. m.p. 118–119 °C)[263]; IRv_{max} (KBr) 1621, 1579 (C=C), 1350 (NO_2) cm^{-1}; ^{1}H-NMR δ (300 MHz, $CDCl_3$): 3.81, 3.91 ((3H, s) × 2, 2-OCH_3, 5-OCH_3), 6.91 (1H, d, $J_{3,4}$=9.0 Hz, H-3), 6.97 (1H, d, $J_{6,4}$=3.0 Hz, H-6), 7.02 (1H, dd, $J_{4,3}$=8.7 Hz, $J_{4,6}$=3.1 Hz, H-4), 7.86 (1H, d, $J_{2',1'}$=13.6 Hz, H-2'), 8.12 (1H, d, $J_{1',2'}$=13.6 Hz, H-1'); ^{13}C-NMR ppm (75 MHz, $CDCl_3$): 55.79, 55.94 (2-OCH_3, 5-OCH_3), 112.34, 116.27, 119.10 (C-3, C-4, C-6), 119.40 (C-1), 135.25 (C-2'), 138.41 (C-1'), 153.45, 153.90 (C-2, C-5); *m/z* 210 ($M+H^+$, 100%); HRMS calc. for $C_{10}H_{12}NO_4$: ($M+H^+$) 210.0766, found: 210.0757.

(*E*)-1-(4-Bromo-2,5-dimethoxyphenyl)-2-nitroethene (281)



4-Bromo-2,5-dimethoxybenzaldehyde **(160)** (12.24 mmol, 3 g) in glacial acetic acid (90 mL), CH_3NO_2 (24.48 mmol, 1.33 mL, 1.50 g) and cyclohexylamine (12.24 mmol, 1.40 mL, 1.21 g) were used as described in general procedure 5.4.4.1, yielding the nitrostyrene **(281)** as fine, yellow, needle-like crystals (9.30 mmol, 2.68 g, 76%); R_f 0.63 (50:50 Et_2O:hexane); m.p. 156–158 °C (EtOH/H_2O), (lit. m.p. 159.5–160.5 °C (*i*PrOH))[264]; IRv_{max} (KBr) 1628, 1604, 1502 (C=C), 1563, 1346 (NO_2) cm^{-1}; ^{1}H-NMR δ (300 MHz, $CDCl_3$): 3.90, 3.92 ((3H, s) × 2, 2-OCH_3, 5-OCH_3), 6.93 (1H, s, H-6), 7.20 (1H, s, H-3), 7.87 (1H, d, $J_{2',1'}$=13.6 Hz, H-2'), 8.07 (1H, d, $J_{1',2'}$=13.6 Hz, H-1'); ^{13}C-NMR ppm (75 MHz, $CDCl_3$): 56.30, 56.85 (2-OCH_3, 5-OCH_3), 114.30, 116.97 (C-3, C-6), 117.08, 118.54 (C-1, C-4), 134.57 (C-2'), 138.61 (C-1'), 150.29, 153.78 (C-2, C-5); *m/z* 288 ($M+H^+$, isotope ^{79}Br, 100%), 290 ($M+H^+$, isotope ^{81}Br, 98%); HRMS calc. for $C_{10}H_{11}{}^{79}BrNO_4$: ($M+H^+$) 287.9871, found: 287.9882.

(*E*)-1-(6-Bromo-2,5-dimethoxyphenyl)-2-nitroethene (282)



6-Bromo-2,5-dimethoxybenzaldehyde **(165)** (9.39 mmol, 2.3 g) in glacial acetic acid (30 mL), CH_3NO_2 (18.77 mmol, 1.02 mL, 1.15 g) and cyclohexylamine (9.39 mmol, 1.07 mL, 930 mg) were used as described in general procedure 5.4.4.1, yielding the novel nitrostyrene **(282)** as yellow, needle-like crystals (8.64 mmol, 2.49 g, 92%); R_f 0.39 (50:50 Et_2O:hexane); m.p. 124–126 °C (EtOH/H_2O); IRv_{max} (KBr) 1630, 1595, 1510 (C=C), 1570, 1342 (NO_2) cm^{-1}; ^{1}H-NMR δ (300 MHz, $CDCl_3$): 3.89, 3.93 ((3H, s) × 2, 2-OCH_3, 5-OCH_3), 6.91 (1H, d, $J_{4,3}$=9.2 Hz, H-4), 7.00 (1H, d, $J_{3,4}$=9.2 Hz, H-3), 8.06 (1H, d, $J_{2',1'}$=13.5 Hz, H-2'), 8.54 (1H, d, $J_{1',2'}$=13.5 Hz, H-1'); ^{13}C-NMR ppm (300 MHz, $CDCl_3$): 56.21, 57.06 (2-OCH_3, 5-OCH_3), 110.22, 115.09 (C-3, C-4), 118.47, 120.27

(C-1, C-6), 134.32 (C-2'), 141.64 (C-1'), 150.83, 154.46 (C-2, C-5); *m/z* 288 ($M+H^+$, isotope ^{79}Br, 100%), 290 ($M+H^+$, isotope ^{81}Br, 98%); HRMS calc. for $C_{10}H_{11}{}^{79}BrNO_4$: ($M+H^+$) 287.9871, found: 287.9878.

5.4.5 Preparation of monomeric nitroalkanes (283), (284) and (285)

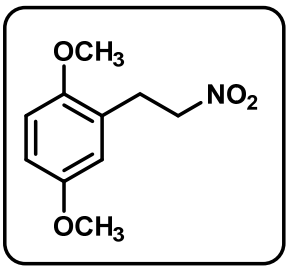
General procedure 5.4.5.1 ('Procedure A')

To a stirred solution of sodium borohydride ($NaBH_4$) (9.92 mmol, 375 mg) in *i*PrOH (6 mL) in a round bottom flask at 0 °C, was added 1-(2,5-dimethoxyphenyl)-2-nitroethene **(280)** (2.39 mmol, 500 mg) dissolved in dry THF (24 mL) (*via* a pressure equalising addition funnel) slowly over 30 min. Once all of the nitrostyrene had been added, the reaction was left to stir for 1 h. After this time, the reaction was quenched by the dropwise addition of a 32% aq. HCl solution (≈2 mL). The quenched reaction mixture was then transferred to a separating funnel and de-ionised water (20 mL) and Et_2O (20 mL) were added. The two layers were separated and the aqueous portion was washed with Et_2O (2 × 20 mL). These Et_2O washes were combined with the original organic portion and this combined portion was washed with brine (3 × 20 mL) and de-ionised water (20 mL), dried over $MgSO_4$, filtered and concentrated *in vacuo* to give the crude product.

General procedure 5.4.5.2 ('Procedure B')

To a vigorously stirred solution of 1-(2,5-dimethoxyphenyl)-2-nitroethene **(280)** (14.34 mmol, 3 g), silica gel (30 g), *i*PrOH (45 mL) and chloroform ($CHCl_3$) (220 mL) (at room temperature in a conical flask), was added $NaBH_4$ (59.51 mmol, 2.25 g) portionwise over 30 min. Once all of the $NaBH_4$ had been added, the reaction was left to stir for an additional 1 h (or until the colour faded to cream/colourless). Excess $NaBH_4$ was quenched with the slow addition of conc. aq. HCl (≈7 mL). This mixture was then filtered through a sintered glass funnel and washed through with DCM (80 mL). To the filtrate, de-ionised water (50 mL) was added. The mixture was transferred to a separating funnel and the layers separated. The organic layer was removed and washed with brine (3 × 40 mL) and de-ionised water (40 mL), dried over $MgSO_4$, filtered and concentrated *in vacuo* to give the pure product.

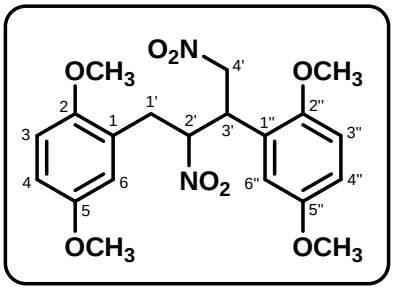
1-(2,5-Dimethoxyphenyl)-2-nitroethane (283)



Nitroethane **(283)** was recovered as a pale amber oil (general procedure A - 5.4.5.1, 73% after silica gel column chromatography (eluent: 5/95 Et_2O:hexane)) and (general procedure B – 5.4.5.2, 96%, no purification necessary); R_f 0.68 (50:50 Et_2O:hexane); IRν_{max} (NaCl) 1503 (C=C), 1552, 1379 (NO_2) cm^{-1}; ^{1}H-NMR δ (300 MHz, $CDCl_3$): 3.27 (2H, t, $J_{1'2'}$=7.3 Hz, H-1'), 3.75, 3.80 (2-OCH_3, 5-OCH_3), 4.60 (2H, t, $J_{2'1'}$=7.3 Hz, H-2') 6.73–6.81 (3H, m, H-3, H-4, H-6); ^{13}C-NMR ppm (300 MHz, $CDCl_3$): 29.21 (C-1'), 55.62, 55.64 (2-OCH_3, 5-OCH_3), 74.58 (C-2'),

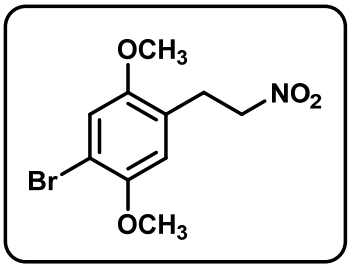
111.09, 112.78, 116.94 (C-3, C-4, C-6), 124.75 (C-1), 151.56, 153.41 (C-2, C-5); *m/z* 212 ($M+H^+$, 100%); HRMS calc. for $C_{10}H_{14}NO_4$: ($M+H^+$) 212.0923, found: 212.0918.

1,1''-(2',4'-Dinitrobutane-1',3'-diyl)-bis-(2,5-dimethoxybenzene) (286)



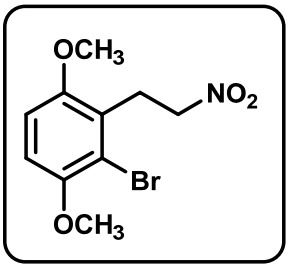
Novel dimeric nitroalkane **(286)** was isolated as an impurity during the synthesis of 1-(2,5-dimethoxyphenyl)-2-nitroethane **(283)** (*via* general procedure A – 5.4.5.1) by flash column chromatography (eluent: 5/95 Et_2O:hexane), in the form of a white solid (0.17 mmol, 70 mg, 7%); R_f 0.25 (50:50 Et_2O:hexane); m.p. 140–143 °C (EtOH); IRv_{max} (KBr) 1589, 1505 (C=C), 1554, 1375 (NO_2) cm^{-1}; ^{1}H-NMR δ (400 MHz, $CDCl_3$): 3.04 [1H, m] and 3.27 [1H, dd, J_{gem}=14.2 Hz, J_{AB}=3.2 Hz] (H-1'), 3.71, 3.73 [(3H, s) × 2] and 3.81 [6H, s] (2-OCH_3, 5-OCH_3, 2''-OCH_3, 5''-OCH_3), 4.28 (1H, m, H-3'), 4.95 (2H, m, H-4'), 5.40 (1H, m, H-2'), 6.60–6.84 (6H, m, H-3, H-4, H-6, H-3'', H-4'', H-6''); ^{13}C-NMR ppm (75 MHz, $CDCl_3$): 33.29 (C-1'), 43.98 (C-3'), 55.66, 55.68, 55.69, 55.90 (2-OCH_3, 5-OCH_3, 2''-OCH_3, 5''-OCH_3), 75.39 (C-4'), 87.67 (C-2'), 111.14, 112.25, 113.25, 114.42, 116.62, 117.10 (C-3, C-4, C-6, C-3'', C-4'', C-6''), 123.01, 124.16 (C-1, C-1''), 151.35 [two overlapping signals] and 153.48, 153.59 (C-2, C-5, C-2'', C-5''); *m/z* 421 ($M+H^+$, 100%); HRMS calc. for $C_{20}H_{25}N_2O_8$: ($M+H^+$) 421.1611, found: 421.1624.

1-(4-Bromo-2,5-dimethoxyphenyl)-2-nitroethane (284)



To a solution of 1-(4-bromo-2,5-dimethoxyphenyl)-2-nitroethene **(281)** (16.97 mmol, 4.89 g), silica gel (34 g), *i*PrOH (60 mL) and $CHCl_3$ (300 mL) was added $NaBH_4$ (70.44 mmol, 2.66 g), and the reaction was carried out according to general procedure B – 5.4.5.2. The novel product **(284)** was recovered pure, in the form of a white solid (16.80 mmol, 4.87 g, 99%); R_f 0.45 (50:50 Et_2O:hexane); m.p. 74–76 °C (EtOH); IRv_{max} (KBr) 1500 (C=C), 1545, 1379 (NO_2) cm^{-1}; ^{1}H-NMR δ (300 MHz, $CDCl_3$): 3.26 (2H, t, $J_{1'2'}$=7.0 Hz, H-1'), 3.80, 3.84 (2-OCH_3, 5-OCH_3), 4.60 (2H, t, $J_{2'1'}$=7.0 Hz, H-2'), 6.74 (1H, s, H-6), 7.06 (1H, s, H-3); ^{13}C-NMR ppm (75 MHz, $CDCl_3$): 29.10 (C-1'), 55.93, 56.90 (2-OCH_3, 5-OCH_3), 74.35 (C-2'), 110.55 (C-4), 114.96, 115.79 (C-3, C-6), 123.81 (C-1), 149.95, 151.65 (C-2, C-5); *m/z* 290 ($M+H^+$, isotope ^{79}Br, 100%), 292 ($M+H^+$, isotope ^{81}Br, 98%); HRMS calc. for $C_{10}H_{13}{}^{79}BrNO_4$: ($M+H^+$) 290.0028, found: 290.0034.

1-(6-Bromo-2,5-dimethoxyphenyl)-2-nitroethane (285)



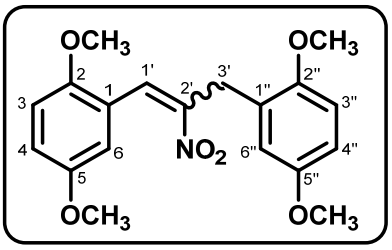
To a solution of 1-(6-bromo-2,5-dimethoxyphenyl)-2-nitroethene **(282)** (8.54 mmol, 2.46 g), silica gel (18 g), *i*PrOH (40 mL) and $CHCl_3$ (200 mL) was added $NaBH_4$ (35.44 mmol, 1.34 g), and the reaction was carried out according to general procedure B – 5.4.5.2. The novel product **(285)** was recovered pure, in the form of a cream solid (7.94 mmol, 2.30 g, 93%); R_f 0.35 (50:50 Et_2O:hexane); m.p. 61–63 °C; IRν_{max} (KBr) 1598, 1580 (C=C), 1550, 1386 (NO_2) cm^{-1}; ^{1}H-NMR δ (400 MHz, $CDCl_3$): 3.60 (2H, m, H-1'), 3.80, 3.85 (2-OCH_3, 5-OCH_3), 4.50 (2H, m, H-2'), 6.79, 6.83 (2H, ABq, J_{AB}=9.2 Hz, H-3, H-6); ^{13}C-NMR ppm (75 MHz, $CDCl_3$): 28.36 (C-1'), 56.06, 56.78 (2-OCH_3, 5-OCH_3), 72.88 (C-2'), 109.59, 111.12 (C-3, C-4), 115.66 (C-6), 125.29 (C-1), 150.42, 152.37 (C-2, C-5); *m/z* 290 ($M+H^+$, isotope ^{79}Br, 100%), 292 ($M+H^+$, isotope ^{81}Br, 98%); HRMS calc. for $C_{10}H_{13}{}^{79}BrNO_4$: ($M+H^+$) 290.0028, found: 290.0027.

5.4.6 Preparation of dimeric nitrostyrenes (290)–(298)

General procedure 5.4.6.1

A mixture of 2,5-dimethoxybenzaldehyde **(72)** (14.2 mmol, 2.36 g), 1-(2,5-dimethoxyphenyl)-2-nitroethane **(283)** (14.2 mmol, 3 g), dimethylamine hydrochloride ($(CH_3)_2$NH.HCl) (28.4 mmol, 2.32 g) and potassium fluoride (KF) (2.13 mmol, 125 mg) in toluene (20 mL) was stirred and heated at reflux (beneath a Dean-Stark trap), for 24 h. To the cooled reaction mixture, toluene (80 mL) was added and the contents transferred to a separating funnel. This solution was washed with 10% aq. HCl (3 × 30 mL). The organic portion was then dried over $MgSO_4$, filtered and concentrated *in vacuo* to give the crude product. This crude product was subjected to silica gel flash column chromatography in order to isolate the dimeric nitrostyrene.

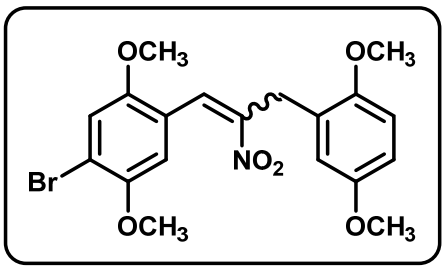
(*E*)-1,3-Bis(2,5-dimethoxyphenyl)-2-nitro-1-propene (290)



The novel dimeric nitrostyrene **(290)** was prepared according to general procedure 5.4.6.1. The crude ^{1}H-NMR spectrum suggested that the product existed exclusively in the (*E*)-conformation. The crude mixture was then purified by flash column chromatography (eluent: 5/95 Et_2O/hexane) and the isolated dimeric nitrostyrene **(290)** was recrystallised from EtOH/H_2O to yield yellow crystals (6.18 mmol, 2.45 g, 48%); R_f 0.25 (20:80 EtOAc:hexane); m.p. 116–118 °C (EtOH/H_2O); IRν_{max} (KBr) 1649, 1616, 1500 (C=C), 1591, 1324 (NO_2) cm^{-1}; ^{1}H-NMR δ (400 MHz, $CDCl_3$): 3.49 (3H, s, 5-OCH_3), 3.71, 3.76 ((3H, s) × 2, 2''-OCH_3, 5''-OCH_3), 3.83 (3H, s, 2-OCH_3), 4.16 (2H, s, H-3'), 6.65 [1H, d, *J*=2.8 Hz], 6.72 [1H, dd, *J*=9.7 and 2.9 Hz], 6.77–6.80 [2H, m], 6.85 [1H, d, *J*=9.0 Hz] and 6.91 [1H, dd, *J*=9.0 and 2.9 Hz] (H-3, H-4, H-6, H-3'', H-4'', H-6''), 8.49 (1H,

s, H-1'); ^{13}C-NMR ppm (75 MHz, $CDCl_3$): 28.26 (C-3'), 55.26, 55.64, 55.75, 56.03 (2-OCH_3, 5-OCH_3, 2''-OCH_3, 5''-OCH_3), 111.12, 111.66, 111.79, 114.09, 114.68, 117.62 (C-3, C-4, C-6, C-3'', C-4'', C-6''), 121.60, 126.18 (C-1, C-1''), 131.45 (C-1'), 149.05, 151.34, 152.65, 153.16, 153.66 (C-2', C-2, C-5, C-2'', C-5''); *m/z* 360 ($M+H^+$, 100%); HRMS calc. for $C_{19}H_{22}NO_6$: ($M+H^+$) 360.1447, found: 360.1443.

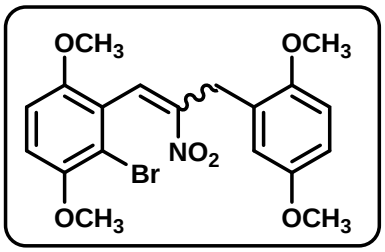
(*E*)-1-(4-Bromo-2,5-dimethoxyphenyl)-3-(2,5-dimethoxyphenyl)-2-nitro-1-propene (291)



4-Bromo-2,5-dimethoxybenzaldehyde **(160)** (2.41 mmol, 591 mg), 1-(2,5-dimethoxyphenyl)-2-nitroethane **(283)** (2.41 mmol, 509 mg), $(CH_3)_2NH.HCl$ (4.82 mmol, 393 mg) and KF (0.36 mmol, 21 mg) in toluene (20 mL) were reacted according to general procedure 5.4.6.1. The crude ^{1}H-NMR spectrum suggested that the novel product existed exclusively in the (*E*)-conformation. The crude mixture was then purified by flash column chromatography (eluent: 3/97 EtOAc/hexane) and the isolated dimeric nitrostyrene **(291)** was recrystallised from CH_3CN to yield yellow crystals (0.75 mmol, 327 mg, 31%); R_f 0.48 (20:80 EtOAc:hexane); m.p. 166–168 °C (CH_3CN); $IR\nu_{max}$ (KBr) 1646, 1601, 1515 (C=C), 1571, 1323 (NO_2) cm^{-1}; ^{1}H-NMR δ (400 MHz, $CDCl_3$): 3.39 (3H, s, 5-OCH_3), 3.71, 3.76 ((3H, s) × 2, 2''-OCH_3, 5''-OCH_3), 3.84 (3H, s, 2-OCH_3), 4.14 (2H, s, H-3'), 6.62 (1H, d, $J_{6'',4''}$=2.9 Hz, H-6''), 6.72–6.76 (2H, m, H-6, H-4''), 6.80 (1H, d, $J_{3'',4''}$=8.9 Hz, H-3''), 7.12 (1H, s, H-3), 8.46 (1H, s, H-1'); ^{13}C-NMR ppm (75 MHz, $CDCl_3$): 28.64 (C-3'), 55.69, 55.73, 55.89, 56.31 (2-OCH_3, 5-OCH_3, 2''-OCH_3, 5''-OCH_3), 111.03, 111.63, 112.59, 114.74, 116.24 (C-3, C-6, C-3'', C-4'', C-6''), 114.70 (C-4), 120.64, 126.07 (C-1, C-1''), 130.79 (C-1'), 148.87, 149.82, 151.22, 152.61, 153.76 (C-2', C-2, C-5, C-2'', C-5''); *m/z* 438 ($M+H^+$, isotope ^{79}Br, 100%), 440 ($M+H^+$, isotope ^{81}Br, 98%); HRMS calc. for $C_{19}H_{21}{}^{79}BrNO_6$: ($M+H^+$) 438.0552, found: 438.0531.

Note: ^{1}H-NMR spectra of the fractions collected during flash column chromatography, suggested that *E*/*Z* isomerisation had taken place to a small extent on the column (ratio of *E*:*Z* after flash column chromatography ≈9:1). This was most evident by the appearance, in the ^{1}H-NMR spectrum, of new signals at δ 3.95 (2H, d, $J_{3',1'}$=0.9 Hz, H-3') and δ 6.47 (1H, s, H-1'), corresponding to the (*Z*)-isomer.

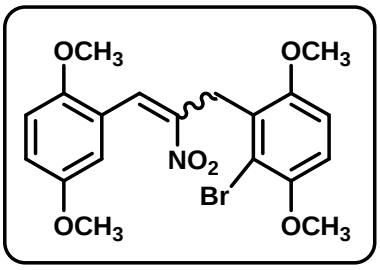
(*E*)-1-(6-Bromo-2,5-dimethoxyphenyl)-3-(2,5-dimethoxyphenyl)-2-nitro-1-propene (292)



6-Bromo-2,5-dimethoxybenzaldehyde **(165)** (2.41 mmol, 591 mg), 1-(2,5-dimethoxyphenyl)-2-nitroethane **(283)** (2.41 mmol, 509 mg), $(CH_3)_2NH.HCl$ (4.82 mmol, 393 mg) and KF (0.36 mmol, 21 mg) in toluene (20 mL) were reacted according to general procedure 5.4.6.1. The crude ^{1}H-NMR spectrum suggested that the novel product existed exclusively in the (*E*)-conformation. The crude mixture was then purified by flash column chromatography (eluent: 10/90 EtOAc/hexane) and the isolated dimeric nitrostyrene **(292)** was

recrystallised from MeOH to yield yellow crystals (0.84 mmol, 370 mg, 35%); R_f 0.14 (20:80 EtOAc:hexane); m.p. 118–120 °C (MeOH); IRν_{max} (KBr) 1656, 1592, 1514 (C=C), 1573, 1330 (NO_2) cm^{-1}; ^{1}H-NMR δ (400 MHz, $CDCl_3$): 3.66, 3.69, 3.70, 3.86 ((3H, s) × 4, 2-OCH_3, 5-OCH_3, 2''-OCH_3, 5''-OCH_3), 3.83 (2H, s, H-3'), 6.62–6.70 (3H, m, H-3'', H-4'', H-6''), 6.81 [1H, d, *J*=9.1 Hz] and 6.88 [1H, d, *J*=9.0 Hz] (H-3, H-4), 7.87 (1H, s, H-1'); ^{13}C-NMR ppm (75 MHz, $CDCl_3$): 28.42 (C-3'), 55.64, 55.80, 55.91, 56.84 (2-OCH_3, 5-OCH_3, 2''-OCH_3, 5''-OCH_3), 110.16, 111.06, 112.19, 112.54, 115.11 (C-3, C-4, C-3'', C-4'', C-6''), 114.03 (C-6), 123.88, 125.47 (C-1, C-1''), 130.54 (C-1'), 150.33, 151.07, 151.36, 152.67, 153.26 (C-2', C-2, C-5, C-2'', C-5''); *m/z* 438 ($M+H^+$, isotope ^{79}Br, 100%), 440 ($M+H^+$, isotope ^{81}Br, 98%); HRMS calc. for $C_{19}H_{21}{}^{79}BrNO_6$: ($M+H^+$) 438.0552, found: 438.0531.

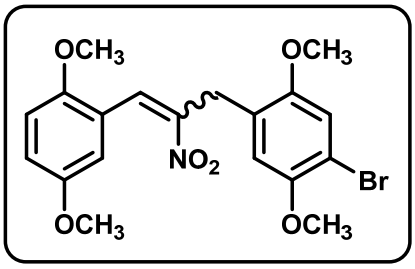
(*E*/*Z*)-1-(2,5-Dimethoxyphenyl)-3-(6-bromo-2,5-dimethoxyphenyl)-2-nitro-1-propene (293)



2,5-Dimethoxybenzaldehyde **(72)** (2.41 mmol, 400 mg), 1-(6-bromo-2,5-dimethoxyphenyl)-2-nitroethane **(285)** (2.41 mmol, 700 mg), $(CH_3)_2$NH.HCl (4.82 mmol, 393 mg) and KF (0.36 mmol, 21 mg) in toluene (20 mL) were reacted according to general procedure 5.4.6.1. The ^{1}H-NMR spectrum of the crude mixture revealed that the novel nitrostyrene product **(293)** existed as a mixture of (*E*)- and (*Z*)-isomers in a ratio of ≈6:1. (An analytically pure sample of the (*E*)-isomer was isolated after repeated recrystallisations from EtOH). The crude product was purified by flash column chromatography (eluent: 8/92 EtOAc/hexane) and the recovered dimeric nitrostyrene **(293)** was recrystallised from EtOH to yield yellow crystals (0.46 mmol, 201 mg, 19%); R_f 0.33 (20:80 EtOAc:hexane); m.p. 127–130 °C (EtOH); IRν_{max} (KBr) 1644, 1510, 1490 (C=C), 1577, 1325 (NO_2) cm^{-1}; **(*E*)-(293)**: ^{1}H-NMR δ (400 MHz, $CDCl_3$): 3.62, 3.64, 3.79*, 3.82 ((3H, s) × 4, 2-OCH_3, 5-OCH_3, 2''-OCH_3, 5''-OCH_3), 4.36 (2H, s, H-3'), 6.71, 6.74 (2H, ABq, J_{AB}=9.0 Hz, H-3'', H-4''), 6.76 (1H, d, $J_{6,4}$=3.0 Hz, H-6), 6.81 (1H, d, $J_{3,4}$=9.0 Hz, H-3), 6.87 (1H, dd, $J_{4,3}$=9.0 Hz, $J_{4,6}$=3.0 Hz, H-4), 8.13 (1H, s, H-1'); ^{13}C-NMR ppm (75 MHz, $CDCl_3$): 30.57 (C-3'), 55.52, 55.94, 56.14, 56.81 (2-OCH_3, 5-OCH_3, 2''-OCH_3, 5''-OCH_3), 110.40, 110.55, 111.52, 114.96, 116.34 (C-3, C-4, C-6, C-3'', C-4''), 115.90 (C-6''), 122.23, 126.60 (C-1, C-1''), 129.35 (C-1'), 150.30, 150.51, 152.12, 152.53, 153.08 (C-2', C-2, C-5, C-2'', C-5''); **(*Z*)-(293)**: (not isolated) ^{1}H-NMR δ (400 MHz, $CDCl_3$): 3.70 [6H, s], 3.79* [(3H, s) overlapping with OCH_3 of (*E*)-isomer] and 3.86 [3H, s] (2-OCH_3, 5-OCH_3, 2''-OCH_3, 5''-OCH_3), 4.24 (2H, d, $J_{3',1'}$=1.5 Hz, H-3'), 6.28 (1H, s, H-1'), 6.69 (1H, d, $J_{6,4}$=2.8 Hz, H-6), 6.75 (1H, d, $J_{3,4}$=8.9 Hz, H-3), 6.79 (1H, dd, $J_{4,3}$=8.0 Hz, $J_{4,6}$=2.9 Hz, H-4), 6.83, 6.86 (2H, ABq, J_{AB}=9.0 Hz, H-3'', H-4''); ^{13}C-NMR ppm (100 MHz, $CDCl_3$): 33.69 (C-3'), 55.73, 56.15, 56.29, 56.80 (2-OCH_3, 5-OCH_3, 2''-OCH_3, 5''-OCH_3), 110.06, 111.35, 112.24, 114.11, 115.53 (C-3, C-4, C-6, C-3'', C-4''), 116.19 (C-6''), 121.72 (C-1'), 122.41, 126.11 (C-1, C-1''), 148.48, 150.55, 151.19, 152.67, 153.40 (C-2', C-2, C-5, C-2'', C-5''); *m/z* 438 ($M+H^+$, isotope ^{79}Br, 100%), 440 ($M+H^+$, isotope ^{81}Br, 98%); HRMS calc. for $C_{19}H_{21}{}^{79}BrNO_6$: ($M+H^+$) 438.0552, found: 438.0544.

Note: Further *E*/*Z* isomerisation took place during flash column chromatography with the *E*/*Z* ratio changing from ≈6:1 (based on ^{1}H-NMR of crude reaction) to ≈3:1.

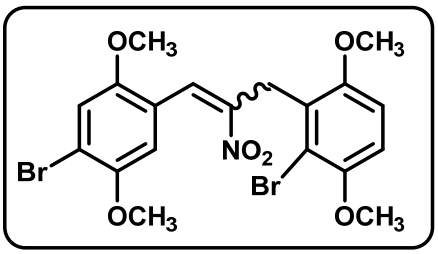
(*E*/*Z*)-1-(2,5-Dimethoxyphenyl)-3-(4-bromo-2,5-dimethoxyphenyl)-2-nitro-1-propene (294)



2,5-Dimethoxybenzaldehyde **(72)** (2.41 mmol, 400 mg), 1-(4-bromo-2,5-dimethoxyphenyl)-2-nitroethane **(284)** (2.41 mmol, 700 mg), $(CH_3)_2NH.HCl$ (4.82 mmol, 393 mg) and KF (0.36 mmol, 21 mg) in toluene (20 mL) were reacted according to general procedure 5.4.6.1. The ^{1}H-NMR spectrum of the crude mixture revealed that the novel nitrostyrene product **(294)** existed as a mixture of (*E*)- and (*Z*)-isomers in a ratio of ≈15:1. (Analytically pure samples of each of the (*E*)- and (*Z*)-isomers were recovered, after they crystallised independently from MeOH.) The crude product was purified by flash column chromatography (eluent: 6/94 Et_2O/hexane) and the recovered dimeric nitrostyrene **(294)** was recrystallised from EtOH/H_2O to yield yellow crystals (0.70 mmol, 306 mg, 29%); R_f 0.28 (20:80 EtOAc:hexane); m.p. 111–113 °C (EtOH/H_2O); IRν_{max} (KBr) 1652, 1518, 1493 (C=C), 1581, 1385 (NO_2) cm^{-1}; **(*E*)-(294)**: ^{1}H-NMR δ (400 MHz, $CDCl_3$): 3.58 (3H, s, 5-OCH_3), 3.73, 3.76 ((3H, s) × 2, 2''-OCH_3, 5''-OCH_3), 3.83 (3H, s, 2-OCH_3), 4.12 (2H, s, H-3'), 6.66 (1H, s, H-6''), 6.78 (1H, d, $J_{6,4}$=3.0 Hz, H-6), 6.86 (1H, d, $J_{3,4}$=9.0 Hz, H-3), 6.93 (1H, dd, $J_{4,3}$=9.0 Hz, $J_{4,6}$=3.0 Hz, H-4), 7.04 (1H, s, H-3''), 8.44 (1H, s, H-1'); ^{13}C-NMR ppm (75 MHz, $CDCl_3$): 28.17 (C-3'), 55.47, 55.99, 56.04, 57.00 (2-OCH_3, 5-OCH_3, 2''-OCH_3, 5''-OCH_3), 109.84 (C-4''), 111.83, 113.02, 114.57, 115.86, 117.11 (C-3, C-4, C-6, C-3'', C-6''), 121.64, 125.14 (C-1, C-1''), 131.64 (C-1'), 148.97, 150.16, 151.61, 152.55, 153.27 (C-2', C-2, C-5, C-2'', C-5''); **(*Z*)-(294)**: ^{1}H-NMR δ (400 MHz, $CDCl_3$): 3.72, 3.74, 3.81, 3.84 ((3H, s) × 4, 2-OCH_3, 5-OCH_3, 2''-OCH_3, 5''-OCH_3), 3.94 (2H, br s, H-3'), 6.55 (1H, s, H-1'), 6.72 (1H, d, $J_{6,4}$=2.9 Hz, H-6), 6.79 (1H, d, $J_{3,4}$=9.0 Hz, H-3), 6.82–6.86 (2H, m, H-4, H-6''), 7.08 (1H, s, H-3''); ^{13}C-NMR ppm (75 MHz, $CDCl_3$): 34.14 (C-3'), 55.75, 55.87, 56.25, 56.93 (2-OCH_3, 5-OCH_3, 2''-OCH_3, 5''-OCH_3), 110.60 (C-4''), 111.92, 114.34, 114.64, 115.63, 116.34 (C-3, C-4, C-6, C-3'', C-6''), 122.06, 124.08 (C-1, C-1''), 123.40 (C-1'), 149.06, 150.11, 151.17, 151.97, 153.36 (C-2', C-2, C-5, C-2'', C-5''); *m/z* 438 (M+H$^+$, isotope ^{79}Br, 100%), 440 (M+H$^+$, isotope ^{81}Br, 98%); HRMS calc. for $C_{19}H_{21}{}^{79}BrNO_6$: (M+H$^+$) 438.0552, found: 438.0531.

Note: Further *E*/*Z* isomerisation took place during flash column chromatography with the *E*/*Z* ratio changing from ≈15:1 (based on ^{1}H-NMR of crude reaction) to ≈3:1.

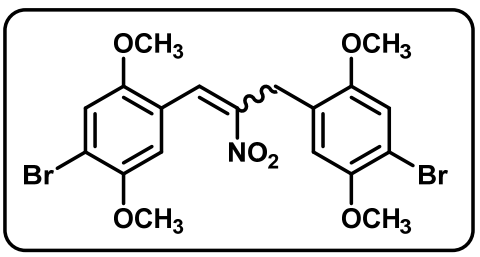
(*E*/*Z*)-1-(4-Bromo-2,5-dimethoxyphenyl)-3-(6-bromo-2,5-dimethoxyphenyl)-2-nitro-1-propene (295)



4-Bromo-2,5-dimethoxybenzaldehyde **(160)** (2.41 mmol, 591 mg), 1-(6-bromo-2,5-dimethoxyphenyl)-2-nitroethane **(285)** (2.41 mmol, 700 mg), $(CH_3)_2NH.HCl$ (4.82 mmol, 393 mg) and KF (0.36 mmol, 21 mg) in toluene (20 mL) were reacted according to general procedure 5.4.6.1. The ^{1}H-NMR spectrum of the crude mixture revealed that the novel nitrostyrene product **(295)** existed as a mixture of (*E*)- and (*Z*)-isomers in a ratio of ≈4:1. (An analytically pure sample of the (*E*)-isomer was isolated after repeated recrystallisations from EtOH.) The crude product was purified by flash column chromatography (eluent: 6/94 EtOAc/hexane) and the recovered dimeric nitrostyrene **(295)** was recrystallised from EtOH to yield yellow crystals (0.55 mmol, 287 mg, 23%); R_f 0.32 (20:80 EtOAc:hexane); m.p. 145–148 °C (EtOH); IRv_{max} (KBr) 1654, 1597, 1512 (C=C), 1578, 1335 (NO_2) cm^{-1}; **(*E*)-(295)**: ^{1}H-NMR δ (400 MHz, $CDCl_3$): 3.60, 3.64, 3.79*, 3.82 ((3H, s) × 4, 2-OCH_3, 5-OCH_3, 2''-OCH_3, 5''-OCH_3), 4.33 (2H, s, H-3'), 6.69 (1H, s, H-6), 6.72, 6.75 (2H, ABq, J_{AB}=9.0 Hz, H-3'', H-4''), 7.06 (1H, s, H-3), 8.07 (1H, s, H-1'); ^{13}C-NMR ppm (75 MHz, $CDCl_3$): 30.79 (C-3'), 55.16, 55.19, 56.38, 56.80* (2-OCH_3, 5-OCH_3, 2''-OCH_3, 5''-OCH_3), 110.55, 110.59, 113.08, 116.00 (C-3, C-6, C-3'', C-4''), 113.66, 115.75 (C-4, C-6''), 121.24, 126.39 (C-1, C-1''), 128.55 (C-1'), 149.69, 150.43, 150.57, 152.03, 152.38 (C-2', C-2, C-5, C-2'', C-5''); **(*Z*)-(295)**: (not isolated) ^{1}H-NMR δ (400 MHz, $CDCl_3$): 3.71, 3.78, 3.79* [(3H, s) overlapping with OCH_3 of (*E*)-isomer] and 3.87 ((3H, s) × 4, 2-OCH_3, 5-OCH_3, 2''-OCH_3, 5''-OCH_3), 4.23 (2H, d, $J_{3',1'}$=1.5 Hz, H-3'), 6.25 (1H, s, H-1'), 6.71 (1H, s, H-6), 6.84, 6.87 (2H, ABq, J_{AB}=9.0 Hz, H-3'', H-4''), 7.03 (1H, s, H-3); ^{13}C-NMR ppm (100 MHz, $CDCl_3$): 33.72 (C-3'), 56.27, 56.32, 56.79, 56.84* [(3H, s) overlapping with OCH_3 of (*E*)-isomer] (2-OCH_3, 5-OCH_3, 2''-OCH_3, 5''-OCH_3), 110.05, 111.39, 112.53, 116.56 (C-3, C-6, C-3'', C-4''), 112.70 (C-4), 116.15 (C-6''), 120.77 (C-1'), 121.35, 125.85 (C-1, C-1''), 148.81, 149.98, 150.55, 151.26, 152.62 (C-2', C-2, C-5, C-2'', C-5''); *m/z* 516 ($M+H^+$, isotopes $^{79}Br_2$, 51%), 518 ($M+H^+$, isotopes $^{79}Br^{81}Br$, 100%), 520 ($M+H^+$, isotopes $^{81}Br_2$, 49%); HRMS calc. for $C_{19}H_{20}{}^{79}Br_2NO_6$: ($M+H^+$) 515.9657, found: 515.9647.

Note: Further *E*/*Z* isomerisation took place during flash column chromatography with the *E*/*Z* ratio changing from ≈4:1 (based on ^{1}H-NMR of crude reaction) to ≈3:1.

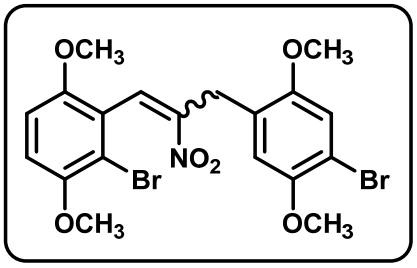
(*E*)-1,3-Bis(4-bromo-2,5-dimethoxyphenyl)-2-nitro-1-propene (296)



4-Bromo-2,5-dimethoxybenzaldehyde **(160)** (2.41 mmol, 591 mg), 1-(4-bromo-2,5-dimethoxyphenyl)-2-nitroethane **(284)** (2.41 mmol, 700 mg), $(CH_3)_2NH.HCl$ (4.82 mmol, 393 mg) and KF (0.36 mmol, 21 mg) in toluene (20 mL) were reacted according to general procedure 5.4.6.1. The crude ^{1}H-NMR spectrum suggested that the novel product **(296)** existed exclusively in the (*E*)-conformation. The crude mixture was then purified by flash column chromatography (eluent: 4/96 EtOAc/hexane) and the

isolated dimeric nitrostyrene **(296)** was recrystallised from EtOH to yield yellow crystals (0.96 mmol, 499 mg, 40%); R_f 0.39 (20:80 EtOAc:hexane); m.p. 185–188 °C (EtOH); IRν_{max} (KBr) 1648, 1601, 1497 (C=C), 1568, 1328 (NO_2) cm^{-1}; ^{1}H-NMR δ (400 MHz, $CDCl_3$): 3.50 (3H, s, 5-OCH_3), 3.74, 3.76 ((3H, s) × 2, 2''-OCH_3, 5''-OCH_3), 3.84 (3H, s, 2-OCH_3), 4.10 (2H, s, H-3'), 6.64, 6.73, 7.05, 7.14 ((1H, s) × 4, H-3, H-6, H-3'', H-6''), 8.41 (1H, s, H-1'); ^{13}C-NMR ppm (75 MHz, $CDCl_3$): 28.53 (C-3'), 55.99, 56.21, 56.31, 57.07 (2-OCH_3, 5-OCH_3, 2''-OCH_3, 5''-OCH_3), 110.03 (C-4''), 112.52, 112.83, 115.76, 116.39 (C-3, C-6, C-3'', C-6''), 114.96 (C-4), 120.51, 124.89 (C-1, C-1''), 131.02 (C-1'), 148.68, 149.91, 150.23, 151.44, 152.56 (C-2', C-2, C-5, C-2'', C-5''); *m/z* 516 ($M+H^+$, isotopes $^{79}Br_2$, 51%), 518 ($M+H^+$, isotopes $^{79}Br^{81}Br$, 100%), 520 ($M+H^+$, isotopes $^{81}Br_2$, 49%); HRMS calc. for $C_{19}H_{20}{}^{79}Br_2NO_6$: ($M+H^+$) 515.9657, found: 515.9635.

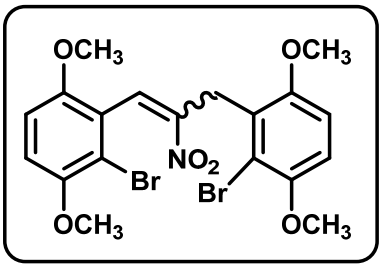
(*E*)-1-(6-Bromo-2,5-dimethoxyphenyl)-3-(4-bromo-2,5-dimethoxyphenyl)-2-nitro-1-propene (297)



6-Bromo-2,5-dimethoxybenzaldehyde **(165)** (2.41 mmol, 591 mg), 1-(4-bromo-2,5-dimethoxyphenyl)-2-nitroethane **(284)** (2.41 mmol, 700 mg), $(CH_3)_2$NH.HCl (4.82 mmol, 393 mg) and KF (0.36 mmol, 21 mg) in toluene (20 mL) were reacted according to general procedure 5.4.6.1. The crude ^{1}H-NMR spectrum suggested that the novel product **(297)** existed exclusively in the (*E*)-conformation. The crude mixture was then purified by flash column chromatography (eluent: 10/90 EtOAc/hexane) and the isolated dimeric nitrostyrene **(297)** was recrystallised from EtOH to yield yellow crystals (1.04 mmol, 536 mg, 43%); R_f 0.25 (20:80 EtOAc:hexane); m.p. 142–145 °C (EtOH); IRν_{max} (KBr) 1656, 1594, 1516 (C=C), 1570, 1332 (NO_2) cm^{-1}; ^{1}H-NMR δ (400 MHz, $CDCl_3$): 3.65, 3.71, 3.76, 3.87 ((3H, s) × 4, 2-OCH_3, 5-OCH_3, 2''-OCH_3, 5''-OCH_3), 3.81 (2H, s, H-3'), 6.64 (1H, s, H-6''), 6.82 [1H, d, J_{AB}=9.0 Hz] and 6.89 [1H, d, J_{AB}=8.0 Hz] (H-3, H-4), 6.93 (1H, s, H-3''), 7.87 (1H, s, H-1'); ^{13}C-NMR ppm (75 MHz, $CDCl_3$): 28.37 (C-3'), 55.97, 56.01 and 56.85 [direct overlap of 2 signals] (2-OCH_3, 5-OCH_3, 2''-OCH_3, 5''-OCH_3), 109.44 (C-4''), 110.23, 112.60, 113.57, 115.52 (C-3, C-4, C-3'', C-6''), 113.92 (C-6), 123.73, 124.58 (C-1, C-1''), 130.73 (C-1'), 149.64, 150.37, 150.94, 151.51, 152.22 (C-2', C-2, C-5, C-2'', C-5''); *m/z* 516 ($M+H^+$, isotopes $^{79}Br_2$, 51%), 518 ($M+H^+$, isotopes $^{79}Br^{81}Br$, 100%), 520 ($M+H^+$, isotopes $^{81}Br_2$, 49%); HRMS calc. for $C_{19}H_{20}{}^{79}Br_2NO_6$: ($M+H^+$) 515.9657, found: 515.9653.

Note: ^{1}H-NMR spectra of the fractions collected during flash column chromatography, suggested that *E*/*Z* isomerisation had taken place to a small extent (ratio of *E*:*Z* after flash column chromatography ≈12:1). This was most evident by the appearance, in the ^{1}H-NMR spectrum, of new signals at δ 4.01 (2H, br s, H-3') and δ 6.48 (1H, s, H-1') corresponding to the (*Z*)-isomer.

(*E*)-1,3-Bis(6-bromo-2,5-dimethoxyphenyl)-2-nitro-1-propene (298)

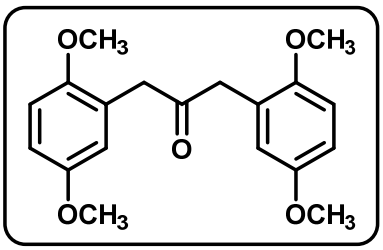


6-Bromo-2,5-dimethoxybenzaldehyde **(165)** (2.41 mmol, 591 mg), 1-(6-bromo-2,5-dimethoxyphenyl)-2-nitroethane **(285)** (2.41 mmol, 700 mg), $(CH_3)_2NH.HCl$ (4.82 mmol, 393 mg) and KF (0.36 mmol, 21 mg) in toluene (20 mL) were reacted according to general procedure 5.4.6.1. The crude ^{1}H-NMR spectrum suggested that the novel product **(298)** existed exclusively in the (*E*)-conformation. The crude mixture was then purified by flash column chromatography (eluent: 8/92 EtOAc/hexane) and the isolated dimeric nitrostyrene **(298)** was recrystallised from EtOH to yield yellow crystals (0.12 mmol, 62 mg, 5%); R_f 0.21 (20:80 EtOAc:hexane); m.p. 158–161 °C (EtOH); IRν_{max} (KBr) 1658, 1596, 1515 (C=C), 1574, 1333 (NO_2) cm^{-1}; ^{1}H-NMR δ (400 MHz, $CDCl_3$): 3.63, 3.64, 3.76, 3.82 ((3H, s) × 4, 2-OCH_3, 5-OCH_3, 2''-OCH_3, 5''-OCH_3), 4.16 (2H, s, H-3'), 6.58, 6.65, 6.68, 6.81 ((1H, d) × 4, *J*=9 Hz, H-3, H-4, H-3'', H-4''), 7.70 (1H, s, H-1'); ^{13}C-NMR ppm (75 MHz, $CDCl_3$): 29.95 (C-3'), 55.66, 55.80, 56.90, 56.92 (2-OCH_3, 5-OCH_3, 2''-OCH_3, 5''-OCH_3), 109.20, 109.72, 110.45, 112.49 (C-3, C-4, C-3'', C-4''), 113.74, 115.73 (C-6, C-6''), 123.53, 126.53 (C-1, C-1''), 128.75 (C-1'), 149.98, 150.07, 150.97, 152.35, 152.83 (C-2', C-2, C-5, C-2'', C-5''); *m/z* 516 (M+H$^+$, isotopes $^{79}Br_2$, 51%), 518 (M+H$^+$, isotopes $^{79}Br^{81}Br$, 100%), 520 (M+H$^+$, isotopes $^{81}Br_2$, 49%); HRMS calc. for $C_{19}H_{20}{}^{79}Br_2NO_6$: (M+H$^+$) 515.9657, found: 515.9647.

Note: ^{1}H-NMR spectra of the fractions collected during flash column chromatography, suggested that *E*/*Z* isomerisation had taken place to a small extent (ratio of *E*:*Z* after flash column chromatography ≈8:1). This was most evident by the appearance, in the ^{1}H-NMR spectrum, of new signals at δ 4.30 (2H, d, $J_{3',1'}$=1.6 Hz, H-3') and δ 6.02 (1H, s, H-1') corresponding to the (*Z*)-isomer.

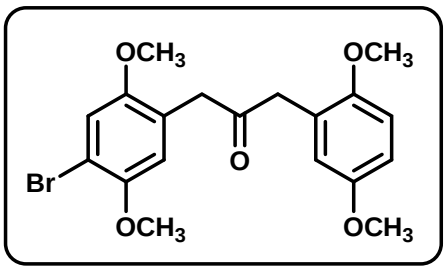
5.4.7 Preparation of dibenzylketones (221), (224) and (257)–(260) *via* dimeric nitrostyrenes (290)–(298)

1,3-Bis(2,5-dimethoxyphenyl)-2-propanone (221)



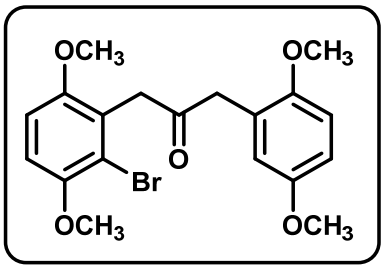
1,3-Bis(2,5-dimethoxyphenyl)-2-nitro-1-propene **(290)** (3.34 mmol, 1.2 g) in glacial acetic acid (45 mL), was added to a solution of iron powder (15.39 mmol, 860 mg) in glacial acetic acid (8 mL), and the reaction was carried out according to general procedure 5.3.6.2. Novel dibenzylketone **(221)** was recovered pure, as a pale yellow solid (3.27 mmol, 1.08 g, 98%); R_f 0.70 (50:50 EtOAc:hexane). As this compound had been previously isolated as an impurity in the synthesis of monomeric ketone **(92)** by general procedure 5.3.1.1, and had been fully characterised, structure confirmation was achieved by comparison of the spectroscopic data (^{1}H-NMR/^{13}C-NMR) with those of an authentic sample.

1-(4-Bromo-2,5-dimethoxyphenyl)-3-(2,5-dimethoxyphenyl)-2-propanone (257)



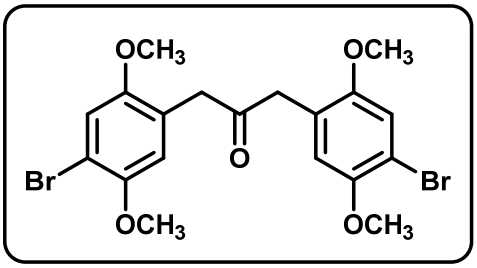
1-(4-Bromo-2,5-dimethoxyphenyl)-3-(2,5-dimethoxyphenyl)-2 -nitro-1-propene **(291)** (0.34 mmol, 150 mg) in glacial acetic acid (20 mL), was added to a solution of iron powder (1.58 mmol, 88 mg) in glacial acetic acid (3 mL), and the reaction was carried out according to general procedure 5.3.6.2. Novel dibenzylketone **(257)** was recovered pure, as a pale yellow solid (0.31 mmol, 126 mg, 90%); R_f 0.74 (50:50 EtOAc:hexane); m.p. 78–80 °C; IRν_{max} (KBr) 1722 (C=O), 1593, 1501 (C=C) cm^{-1}; ^{1}H-NMR δ (400 MHz, $CDCl_3$): 3.67, 3.69 ((2H, s) × 2, H-1', H-3'), 3.73 [6H, s], 3.74, 3.80 [(3H, s) × 2] (2-OCH_3, 5-OCH_3, 2''-OCH_3, 5''-OCH_3), 6.65 (1H, s, H-6), 6.67–6.80 (3H, m, H-3'', H-4'', H-6''), 7.03 (1H, s, H-3); ^{13}C-NMR ppm (75 MHz, $CDCl_3$): 43.48, 44.14 (C-1', C-3'), 55.64, 55.86, 56.10, 56.81 (2-OCH_3, 5-OCH_3, 2''-OCH_3, 5''-OCH_3), 109.96 (C-4), 111.30, 112.67, 117.25 (C-3'', C-4'', C-6''), 115.37, 115.86 (C-3, C-6), 123.57, 124.32 (C-1, C-1''), 149.82, 151.59, 151.75, 153.41 (C-2, C-5, C-2'', C-5''), 205.68 (C=O); *m/z* 409 ($M+H^+$, isotope ^{79}Br, 100%), 411 ($M+H^+$, isotope ^{81}Br, 98%); HRMS calc. for $C_{19}H_{22}{}^{79}BrO_5$: ($M+H^+$) 409.0651, found: 409.0655.

1-(6-Bromo-2,5-dimethoxyphenyl)-3-(2,5-dimethoxyphenyl)-2-propanone (258)



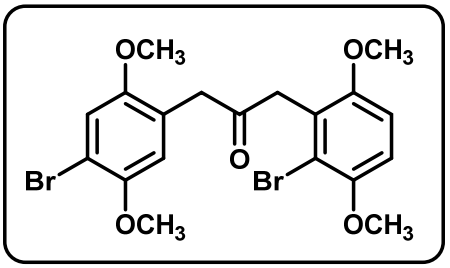
1-(6-Bromo-2,5-dimethoxyphenyl)-3-(2,5-dimethoxyphenyl)-2-nitro -1-propene **(292)** (0.37 mmol, 160 mg) in glacial acetic acid (14 mL), was added to a solution of iron powder (1.71 mmol, 95 mg) in glacial acetic acid (3 mL), and the reaction was carried out according to general procedure 5.3.6.2. Novel dibenzylketone **(258)** was recovered pure, as a pale yellow solid (0.30 mmol, 121 mg, 80%); R_f 0.63 (50:50 EtOAc:hexane); m.p. 68–70 °C; IRν_{max} (KBr) 1724 (C=O), 1578, 1502 (C=C) cm^{-1}; ^{1}H-NMR δ (400 MHz, $CDCl_3$): 3.72 (2H, s, H-3'), 3.72, 3.75, 3.78, 3.84 ((3H, s) × 4, 2-OCH_3, 5-OCH_3, 2''-OCH_3, 5''-OCH_3), 4.01 (2H, s, H-1'), 6.72–6.81 (5H, m, H-3, H-4, H-3'', H-4'', H-6''); ^{13}C-NMR ppm (75 MHz, $CDCl_3$): 43.80, 44.23 (C-1', C-3'), 55.68, 55.92, 56.21, 56.72 (2-OCH_3, 5-OCH_3, 2''-OCH_3, 5''-OCH_3), 109.60, 110.66 (C-3, C-4), 111.32, 112.74, 117.24 (C-3'', C-4'', C-6''), 116.11 (C-6), 124.47, 126.16 (C-1, C-1''), 150.30, 151.72, 152.43, 153.38 (C-2, C-5, C-2'', C-5''), 204.71 (C=O); *m/z* 409 ($M+H^+$, isotope ^{79}Br, 100%), 411 ($M+H^+$, isotope ^{81}Br, 98%); HRMS calc. for $C_{19}H_{22}{}^{79}BrO_5$: ($M+H^+$) 409.0651, found: 409.0667.

1,3-Bis(4-bromo-2,5-dimethoxyphenyl)-2-propanone (224)



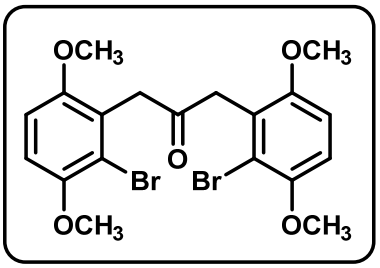
1,3-Bis(4-bromo-2,5-dimethoxyphenyl)-2-nitro-1-propene **(296)** (4.85 mmol, 2.51 g) in glacial acetic acid (125 mL), was added to a solution of iron powder (22.37 mmol, 1.25 g) in glacial acetic acid (25 mL), and the reaction was carried out according to general procedure 5.3.6.2. Novel dibenzylketone **(224)** was recovered pure, as a cream solid (4.70 mmol, 2.30 g, 97%); R_f 0.76 (50:50 EtOAc:hexane). As this compound had been previously isolated as an impurity in the synthesis of monomeric ketone **(159)** by general procedure 5.3.3.1, and had been fully characterised, structure confirmation was achieved by comparison of the spectroscopic data (^{1}H-NMR/^{13}C-NMR) with those of an authentic sample.

1-(4-Bromo-2,5-dimethoxyphenyl)-3-(6-bromo-2,5-dimethoxyphenyl)-2-propanone (259)



1-(6-Bromo-2,5-dimethoxyphenyl)-3-(4-bromo-2,5-dimethoxy phenyl)-2-nitro-1-propene **(297)** (0.38 mmol, 200 mg) in glacial acetic acid (35 mL), was added to a solution of iron powder (1.78 mmol, 100 mg) in glacial acetic acid (4 mL), and the reaction was carried out according to general procedure 5.3.6.2. Novel dibenzylketone **(259)** was recovered pure, as a cream solid (0.33 mmol, 160 mg, 86%); R_f 0.67 (50:50 EtOAc:hexane); m.p. 134–136 °C; IRν_{max} (KBr) 1709 (C=O), 1580, 1499 (C=C) cm^{-1}; ^{1}H-NMR δ (400 MHz, $CDCl_3$): 3.70 (2H, s, H-1'), 3.72, 3.77, 3.82, 3.84 ((3H, s) × 4, 2-OCH_3, 5-OCH_3, 2''-OCH_3, 5''-OCH_3), 4.02 (2H, s, H-3'), 6.72 (1H, s, H-6), 6.77 [1H, d, J_{AB}=9.2 Hz], 6.81 [1H, d, J_{AB}=8.8 Hz] (H-3'', H-4''), 7.05 (1H, s, H-3); ^{13}C-NMR ppm (75 MHz, $CDCl_3$): 43.68, 43.97 (C-1', C-3'), 56.14, 56.18, 56.71, 56.85 (2-OCH_3, 5-OCH_3, 2''-OCH_3, 5''-OCH_3), 109.57, 110.71 (C-3'', C-4''), 109.99 (C-4), 115.32, 115.87 (C-3, C-6), 116.06 (C-6''), 123.42, 125.85 (C-1, C-1''), 149.82, 150.30, 151.77, 152.36 (C-2, C-5, C-2'', C-5''), 204.22 (C=O); *m/z* 487 (M+H$^+$, isotopes $^{79}Br_2$, 51%), 489 (M+H$^+$, isotopes $^{79}Br^{81}Br$, 100%), 491 (M+H$^+$, isotopes $^{81}Br_2$, 49%); HRMS calc. for $C_{19}H_{21}{}^{79}Br_2O_5$: (M+H$^+$) 486.9756, found: 486.9764.

1,3-Bis(6-bromo-2,5-dimethoxyphenyl)-2-propanone (260)



1,3-Bis(6-bromo-2,5-dimethoxyphenyl)-2-nitro-1-propene **(298)** (0.05 mmol, 26 mg) in glacial acetic acid (7 mL), was added to a solution of iron powder (0.24 mmol, 14 mg) in glacial acetic acid (2 mL), and the reaction was carried out according to general procedure 5.3.6.2, with the exception that the reaction time was 4 h (*vs*. 2 h). Novel dibenzylketone **(260)** was recovered pure, as a pale yellow solid

(0.044 mmol, 21 mg, 88%); R_f 0.55 (50:50 EtOAc:hexane); m.p. 144–146 °C (CH_3CN); IRν_{max} (KBr) 1727 (C=O), 1578, 1480 (C=C) cm^{-1}; ^{1}H-NMR δ (400 MHz, $CDCl_3$): 3.77 (6H, s, 2-OCH_3, 2''-OCH_3), 3.84 (6H, s, 5-OCH_3, 5''-OCH_3), 4.02 (4H, s, H-1', H-3'), 6.77–6.82 (4H, m, H-3, H-4, H-3'', H-4''); ^{13}C-NMR ppm (75 MHz, $CDCl_3$): 44.06 (C-1', C-3'), 56.30, 56.76 (2-OCH_3, 5-OCH_3, 2''-OCH_3, 5''-OCH_3), 109.66, 110.75 (C-3, C-4, C-3'', C-4''), 116.18 (C-6, C-6''), 126.08 (C-1, C-1''), 150.34, 152.54 (C-2, C-5, C-2'', C-5''), 203.27 (C=O); *m/z* 487 ($M+H^+$, isotopes $^{79}Br_2$, 51%), 489 ($M+H^+$, isotopes $^{79}Br^{81}Br$, 100%), 491 ($M+H^+$, isotopes $^{81}Br_2$, 49%); HRMS calc. for $C_{19}H_{21}{}^{79}Br_2O_5$: ($M+H^+$) 486.9756, found: 486.9742.

5.4.8 Impurity profiling of the bromination of 1,3-bis-(2,5-dimethoxyphenyl)-2-propanone (221)

General procedure 5.4.8.1

To a stirred solution of 1,3-bis-(2,5-dimethoxyphenyl)-2-propanone **(221)** (3.03 mmol, 1 g) in glacial acetic acid (12 mL), a solution of bromine★ in glacial acetic acid (2 mL), was added dropwise. The flask was covered in aluminium foil to exclude light and left stirring at room temperature for 24 h. The reaction mixture was diluted with de-ionised water (20 mL), and 5% aq. $Na_2S_2O_3$ was added dropwise until the orange colour faded to cream. DCM (40 mL) was added to the mixture and the phases were separated. The aqueous phase was extracted with DCM (2 × 20 mL). The combined organic phases were washed with 5% aq. $Na_2S_2O_3$ (2 × 30 mL), saturated aq. $NaHCO_3$ (3 × 30 mL) and de-ionised water (2 × 30 mL), dried over $MgSO_4$, filtered and concentrated *in vacuo* to give the crude product as a pale yellow solid. Purification by flash column chromatography on silica gel was attempted for the reaction in which 2.0 eqv. of Br_2 were used. However, only mixtures of unknown compounds were recovered. Crude samples from all four experiments (0.5, 1.0, 1.5 and 2.0 eqv. of Br_2), were subjected to analysis by LC-MS.

★The reaction was carried out four times, with different eqv. of Br_2. The quantities of Br_2 used in each of these experiments were as follows:

0.5 eqv. = 1.52 mmol, 77 µL, 242 mg
1.0 eqv. = 3.03 mmol, 154 µL, 484 mg
1.5 eqv. = 4.55 mmol, 231 µL, 726 mg
2.0 eqv. = 6.06 mmol, 308 µL, 968 mg

5.4.9 Attempted selective synthesis of benzyl-bromo dibenzylketones

General procedure 5.4.9.1

To a stirred solution of the appropriate dibenzylketone (**(221)**, **(257)** or **(224)**)★ in CCl_4 (2 mL), was added NBS (1.1, 2.2 or 10 eqv.)★ and a catalytic amount of benzoyl peroxide (≈2 mg). The mixture was heated

at reflux temperature for 4 h. The cooled reaction mixture was then filtered to remove insoluble succinimide. The filtrate was concentrated to give an amber oil. Purification of the crude reaction mixture was not pursued.

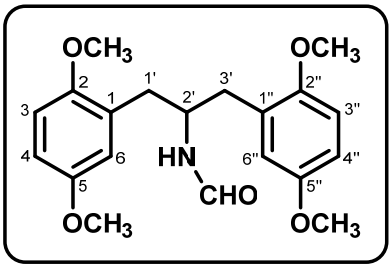
*[For dibenzylketone **(221)** (0.6 mmol, 200 mg), carried out reactions using 10 eqv. (6.0 mmol, 1.08 g), 2.2 eqv. (1.33 mmol, 237 mg) and 1.1 eqv. (0.66 mmol, 119 mg) of NBS.
For dibenzylketone **(257)** (0.49 mmol, 200 mg), carried out reactions using 2.2 eqv. (1.08 mmol, 191 mg) and 1.1 eqv. (0.54 mmol, 96 mg) of NBS.
For dibenzylketone **(224)** (0.41 mmol, 200 mg), carried out reactions using 2.2 eqv. (0.90 mmol, 160 mg) and 1.1 eqv. (0.45 mmol, 80 mg) of NBS.]

5.4.10 Impurity profiling of the Leuckart reaction of 1,3-bis(2,5-dimethoxyphenyl)-2-propanone (221) and formamide

General procedure 5.4.10.1

A mixture of 1,3-bis(2,5-dimethoxyphenyl)-2-propanone **(221)** (6.06 mmol, 2 g) and formamide (181.61 mmol, 7.2 mL, 8.165 g) was heated to reflux (190 °C) for 5 h. After cooling, de-ionised water (30 mL) and EtOAc (40 mL) were added and the mixture transferred to a separating funnel. The phases were separated and the aqueous layer was extracted with EtOAc (4 × 20 mL). These EtOAc washes were combined with the original organic layer and this was washed with de-ionised water (3 × 20 mL), dried over $MgSO_4$, filtered and concentrated *in vacuo* to give the crude product.

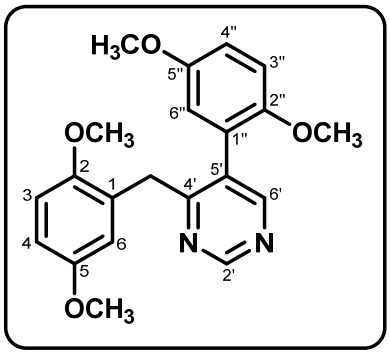
***N*-(1,3-Bis(2,5-dimethoxyphenyl)propan-2-yl)formamide (329)**



Prepared according to general procedure 5.4.10.1, the novel *N*-formyl product **(329)** was isolated by silica gel flash column chromatography (eluent: 45/55 EtOAc/hexane) as a cream solid (2.85 mmol, 1.02 g, 47%) with a rotamer ratio of 55/45 (or 1:0.8); R_f 0.39 (50:50 EtOAc:hexane); m.p. 107–109 °C (Et_2O/hexane); $IR\nu_{max}$ (KBr) 3313 (N-H), 1659 (C=O), 1502 (C=C) cm^{-1}; (Significant overlap between signals in ^{1}H-NMR and ^{13}C-NMR spectra of Major^M and minor^m rotamers): ^{1}H-NMR δ (600 MHz, $CDCl_3$): 2.76 [1.6H, dd, J_{gem}=13.6 Hz, ^3J=9.1 Hz], 2.80 [2H, dd, J_{gem}=13.7 Hz, ^3J=5.8 Hz] and 2.86 [3.6H, m], (H-1', H-3')$^{M+m}$, 3.74 [s], 3.75 [s], 3.79 [s] (19.8H, 2-OCH_3, 5-OCH_3, 2''-OCH_3, 5''-OCH_3)$^{M+m}$, 3.87 (0.8H, m, H-2')^m, 4.44 (1H, m, H-2')^M, 5.70 (0.8H, t, J=9.6 Hz, NH)^m, 5.91 (1H, d, J=7.3 Hz, NH)^M, 6.66–6.79 (11H, m, H-3, H-4, H-6, H-3'', H-4'', H-6'')$^{M+m}$, 7.42 (0.8H, d, J=12.0 Hz, CHO)^m, 8.00 (1H, d, J=0.8 Hz, CHO)^M; ^{13}C-NMR ppm (75 MHz, $CDCl_3$): 34.52, 37.26 (C-1', C-3')$^{M+m}$, 50.62, 53.99 (C-2')$^{M+m}$, 55.63, 55.64, 55.77, 55.98 (2-OCH_3, 5-OCH_3, 2''-OCH_3, 5''-OCH_3)$^{M+m}$, 111.29, 111.44, 111.95, 111.97 (C-3, C-4, C-3'', C-4'')$^{M+m}$, 117.11, 117.52 (C-6, C-6'')$^{M+m}$, 127.22, 127.96 (C-1)$^{M+m}$, 151.73, 151.88, 153.44, 153.51 (C-2, C-5, C-2'',

C-5'')$^{M+m}$, 160.69, 163.92 (CHO)$^{M+m}$; *m/z* 360 ($M+H^+$, 100%); HRMS calc. for $C_{20}H_{26}NO_5$: ($M+H^+$) 360.1811, found: 360.1807.

4,5-Di-(2,5-dimethoxyphenyl)pyrimidine (331)

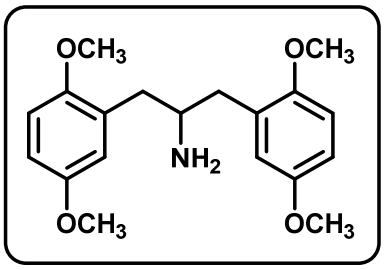


The novel pyrimidine **(331)** was detected as an impurity during the preparation of *N*-formyl **(329)** by general procedure 5.4.10.1, and isolated by silica gel flash column chromatography (eluent: 35/65 EtOAc/hexane) as an amber solid (0.79 mmol, 289 mg, 13%); R_f 0.15 (50:50 EtOAc:hexane); m.p. 103–105 °C (Et_2O/hexane); IRν_{max} (KBr) 1608, 1565, 1505 (C=C) cm^{-1}; ^{1}H-NMR δ (400 MHz, $CDCl_3$): 3.55, 3.67, 3.68, 3.73 ((3H, s) × 4, 2-OCH_3, 5-OCH_3, 2''-OCH_3, 5''-OCH_3), 4.00 (2H, s, CH_2), 6.56–6.92 (6H, m, H-3, H-4, H-6, H-3'', H-4'', H-6''), 8.49 (1H, s, H-6'), 9.09 (1H, s, H-2'); ^{13}C-NMR ppm (75 MHz, $CDCl_3$): 35.81 (CH_2), 55.55, 55.70, 55.74, 55.77 (2-OCH_3, 5-OCH_3, 2''-OCH_3, 5''-OCH_3), 111.14, 111.75, 111.83, 114.56, 116.62, 116.91 (C-3, C-4, C-6, C-3'', C-4'', C-6''), 125.41, 127.91 (C-1, C-1''), 131.79 (C-5'), 150.90, 151.42, 153.30, 153.40 (C-2, C-5, C-2'', C-5''), 157.16, 157.40 (C-2', C-6'), 167.65 (C-4'); *m/z* 367 ($M+H^+$, 100%); HRMS calc. for $C_{21}H_{23}N_2O_4$: ($M+H^+$) 367.1658, found: 367.1646.

General procedure 5.4.10.2

To a stirred solution of *N*-(1,3-bis(2,5-dimethoxyphenyl)propan-2-yl)formamide **(329)** (1.67 mmol, 600 mg) in MeOH (3 mL), was added 30% aq. HCl (10 mL) and the solution was heated to reflux for 7 h. After cooling to room temperature, de-ionised water (20 mL) was added and the mixture transferred to a separating funnel. To this, DCM (25 mL) was added and the phases separated. The aqueous portion was washed further with DCM (2 × 15 mL) and the combined DCM portions were washed with de-ionised water (20 mL), dried over $MgSO_4$, filtered and concentrated *in vacuo* to give the pure product.

1,3-Bis(2,5-dimethoxyphenyl)propan-2-amine (327)



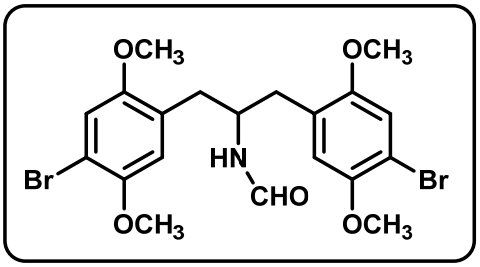
Prepared according to general procedure 5.4.10.2, the novel dimeric amine **(327)** was recovered pure, as a light purple solid (1.50 mmol, 495 mg, 90%); R_f 0.58 (MeOH); m.p. 45–48 °C; IRν_{max} (KBr) 3422 (N-H), 1593, 1503 (C=C) cm^{-1}; ^{1}H-NMR δ (400 MHz, $CDCl_3$): 3.00 [2H, dd, J_{gem}=13.9 Hz, ^3J=6.3 Hz] and 3.12 [2H, dd, J_{gem}=13.9 Hz, ^3J=7.5 Hz] (H-1', H-3'), 3.68, 3.74 ((6H, s) × 2, 2-OCH_3, 5-OCH_3, 2''-OCH_3, 5''-OCH_3), 3.89 (1H, m, H-2'), 6.70–6.82 (6H, m, H-3, H-4, H-6, H-3'', H-4'', H-6''), 8.12 (br s, NH_2); ^{13}C-NMR ppm (75 MHz, $CDCl_3$): 34.42 (C-1', C-3'), 52.47 (C-2'), 55.67, 55.69 (2-OCH_3, 5-OCH_3, 2''-OCH_3, 5''-OCH_3), 111.35, 112.90, 117.62 (C-3, C-4, C-6, C-3'', C-4'', C-6''), 125.53 (C-1, C-1''), 151.74, 153.31 (C-2, C-5, C-2'', C-5''); *m/z* 332 ($M+H^+$, 100%); HRMS calc. for $C_{19}H_{26}NO_4$: ($M+H^+$) 332.1862, found: 332.1852.

5.4.11 Impurity profiling of the Leuckart reaction of 1,3-bis(4-bromo-2,5-dimethoxyphenyl)-2-propanone (224) and formamide

General procedure 5.4.11.1

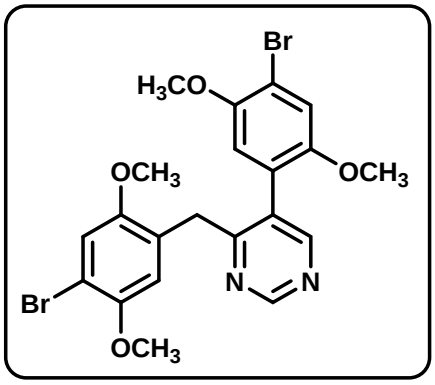
A mixture of 1,3-bis(4-bromo-2,5-dimethoxyphenyl)-2-propanone **(224)** (4.10 mmol, 2 g) and formamide (122.91 mmol, 4.88 mL, 5.53 g) was heated to reflux (190 °C) for 5 h. After cooling, de-ionised water (30 mL) and EtOAc (40 mL) were added and the mixture transferred to a separating funnel. The phases were separated and the aqueous layer was extracted with EtOAc (4 × 20 mL). These EtOAc washes were combined with the original organic layer and this was washed with de-ionised water (3 × 20 mL), dried over $MgSO_4$, filtered and concentrated *in vacuo* to give the crude product.

***N*-(1,3-Bis(4-bromo-2,5-dimethoxyphenyl)propan-2-yl)formamide (330)**



Prepared according to general procedure 5.4.11.1, the novel *N*-formyl product **(330)** was isolated by silica gel flash column chromatography (eluent: 55/45 EtOAc/hexane) as a cream solid (2.50 mmol, 1.29 g, 61%) with a rotamer ratio of 70/30 (or 1:0.45); R_f 0.39 (70:30 EtOAc:hexane); m.p. 148–150 °C (EtOH); IRν_{max} (KBr) 3294 (N-H), 1656 (C=O), 1497 (C=C) cm^{-1}; (Major^M and minor^m rotamers) ^{1}H-NMR δ (600 MHz, $CDCl_3$): 2.72 [0.9H, dd, J_{gem}=13.6 Hz, ^3J=9.1 Hz], 2.78 [2H, dd, J_{gem}=13.9 Hz, ^3J=5.9 Hz] and 2.87 [2.9H, m] (H-1', H-3')$^{M+m}$, 3.79 [s], 3.83 [s], 3.83 [s] (17.4H, 2-OCH_3, 5-OCH_3, 2''-OCH_3, 5''-OCH_3)$^{M+m}$, 4.38 (1H, m, H-2')^M, 5.71 (0.45H, t, *J*=9.0 Hz, NH)^m, 5.84 (1H, d, *J*=7.6 Hz, NH)^M, 6.64 (0.9H, s, H-6, H-6'')^m, 6.73 (2H, s, H-6, H-6'')^M, 7.05 (2H, s, H-3, H-3'')^M, 7.06 (0.9H, s, H-3, H-3'')^m, 7.44 (0.45H, d, *J*=11.9 Hz, CHO)^m, 8.01 (1H, d, *J*=0.8 Hz, CHO)^M; ^{13}C-NMR ppm (75 MHz, $CDCl_3$): 34.34 (C-1', C-3')^M, 37.24 (C-1', C-3')^m, 50.45 (C-2')^M, 53.37 (C-2')^m, 56.03, 57.02 (2-OCH_3, 5-OCH_3, 2''-OCH_3, 5''-OCH_3)^m, 56.21, 56.97 (2-OCH_3, 5-OCH_3, 2''-OCH_3, 5''-OCH_3)^M, 109.48 (C-4, C-4'')^M, 110.05 (C-4, C-4'')^m, 115.16, 116.03* (C-3, C-3'', C-6, C-6'')^M, 115.54, 116.03* (C-3, C-3'', C-6, C-6'')^m, 126.00 (C-1, C-1'')^m, 126.84 (C-1, C-1'')^M, 150.03, 151.84 (C-2, C-5, C-2'', C-5'')^m, 150.07, 151.94, (C-2, C-2'', C-5, C-5'')^M, 160.71 (CHO)^M, 163.77 (CHO)^m; *m/z* 516 (M+H$^+$, isotopes $^{79}Br_2$, 51%), 518 (M+H$^+$, isotopes $^{79}Br^{81}Br$, 100%), 520 (M+H$^+$, isotope $^{81}Br_2$, 49%); HRMS calc. for $C_{20}H_{24}{}^{79}Br_2NO_5$: (M+H$^+$) 516.0021, found: 516.0016.

4,5-Di-(4-bromo-2,5-dimethoxyphenyl)pyrimidine (332)

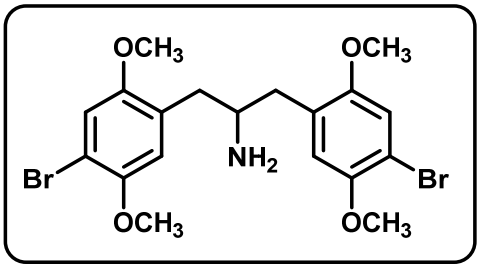


The novel pyrimidine **(332)** was detected as an impurity during the preparation of *N*-formyl **(330)** by general procedure 5.4.11.1, and isolated by silica gel flash column chromatography (eluent: 40/60 EtOAc/hexane) as an amber solid (1.03 mmol, 537 mg, 25%); R_f 0.45 (70:30 EtOAc:hexane); m.p. 116–118 °C; IRv_{max} (KBr) 1603, 1569, 1496 (C=C) cm^{-1}; ^{1}H-NMR δ (400 MHz, $CDCl_3$): 3.52, 3.66, 3.74, 3.76 ((3H, s) × 4, 2-OCH_3, 5-OCH_3, 2''-OCH_3, 5''-OCH_3), 3.97 (2H, s, CH_2), 6.52, 6.56 ((1H, s) × 2, H-6, H-6''), 6.88, 7.12 ((1H, s) × 2, H-3, H-3''), 8.47 (1H, s, H-6'), 9.12 (1H, s, H-2'); ^{13}C-NMR ppm (75 MHz, $CDCl_3$): 35.79 (CH_2), 55.84, 56.01, 56.80, 56.83 (2-OCH_3, 5-OCH_3, 2''-OCH_3, 5''-OCH_3), 109.61, 112.18 (C-4, C-4''), 114.55, 114.96, 115.44, 116.23 (C-3, C-6, C-3'', C-6''), 124.09, 126.42 (C-1, C-1''), 131.12 (C-5'), 149.75, 150.00, 150.90, 151.36 (C-2, C-5, C-2'', C-5''), 157.20, 157.56 (C-2', C-6'), 167.27 (C-4'); *m/z* 523 ($M+H^+$, isotopes $^{79}Br_2$, 51%), 525 ($M+H^+$, isotopes $^{79}Br^{81}Br$, 100%), 527 ($M+H^+$, isotopes $^{81}Br_2$, 49%); HRMS calc. for $C_{21}H_{21}{}^{79}Br_2N_2O_4$: ($M+H^+$) 522.9868, found: 522.9871.

General procedure 5.4.11.2

To a stirred solution of *N*-(1,3-bis(4-bromo-2,5-dimethoxyphenyl)propan-2-yl)formamide **(330)** (1.01 mmol, 520 mg) in MeOH (4 mL), was added 30% aq. HCl (7 mL) and the solution was heated to reflux for 7 h. After cooling to room temperature, de-ionised water (20 mL) was added and the mixture transferred to a separating funnel. To this, DCM (20 mL) was added and the phases separated. The aqueous portion was washed further with DCM (2 × 15 mL) and the combined DCM portions were washed with de-ionised water (20 mL), dried over $MgSO_4$, filtered and concentrated *in vacuo* to give the pure product.

1,3-Bis(4-bromo-2,5-dimethoxyphenyl)propan-2-amine (328)



Prepared according to general procedure 5.4.11.2, the novel dimeric amine **(328)** was recovered pure, as a pale amber solid (0.97 mmol, 473 mg, 96%); R_f 0.68 (80:20 DCM:MeOH); m.p. 81–85 °C; IRv_{max} (KBr) 3401 (N-H), 1605, 1497 (C=C) cm^{-1}; ^{1}H-NMR δ (300 MHz, $CDCl_3$): 2.91 [2H, dd, J_{gem}=13.8 Hz, ^3J=7.3 Hz] and 3.07 [2H, dd, J_{gem}=13.8 Hz, ^3J=6.6 Hz] (H-1', H-3'), 3.69, 3.80 ((6H, s) × 2, 2-OCH_3, 5-OCH_3, 2''-OCH_3, 5''-OCH_3), 3.90 (1H, m, H-2'), 6.79 ((1H, s) × 2, H-6, H-6''), 6.97 ((1H, s) × 2, H-3, H-3''), 8.27 (br s, NH_2); ^{13}C-NMR ppm (75 MHz, $CDCl_3$): 34.54 (C-1', C-3'), 51.53 (C-2'), 55.96, 57.10 (2-OCH_3, 5-OCH_3, 2''-OCH_3, 5''-OCH_3), 110.40 (C-4, C-4''), 115.85, 116.04 (C-3, C-6, C-3'', C-6''), 124.44 (C-1, C-1''), 149.89, 151.92 (C-2, C-5, C-2'', C-5''); *m/z* 488 ($M+H^+$, isotopes $^{79}Br_2$,

51%), 490 ($M+H^+$, isotopes $^{79}Br^{81}Br$, 100%), 492 ($M+H^+$, isotope $^{81}Br_2$, 49%); HRMS calc. for $C_{19}H_{24}{}^{79}Br_2NO_4$: ($M+H^+$) 488.0072, found: 488.0070.

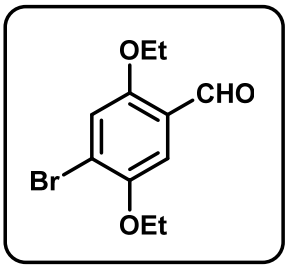
5.5 Appendix

Bromination of 2,5-diethoxybenzaldehyde (184)

General procedure 5.5.1

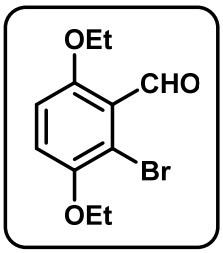
To a stirred solution of 2,5-diethoxybenzaldehyde **(184)** (2.57 mmol, 500 mg) in glacial acetic acid (4 mL), a solution of bromine (3.09 mmol, 0.16 mL, 492 mg) in glacial acetic acid (1 mL), was added dropwise. The flask was covered in aluminium foil to exclude light and left stirring at room temperature for 24 h. The reaction mixture was then diluted with de-ionised water (10 mL), and 5% aq. $Na_2S_2O_3$ was added dropwise until the orange colour faded to cream. DCM (20 mL) was added to the mixture and the phases were separated. The aqueous phase was extracted with DCM (2 × 15 mL). The combined organic phases were washed with 5% aq. $Na_2S_2O_3$ (3 × 20 mL), saturated aq. $NaHCO_3$ (3 × 20 mL) and de-ionised water (2 × 20 mL), dried over $MgSO_4$, filtered and concentrated *in vacuo* to give the crude product as a cream solid. This was subjected to silica gel flash column chromatography in order to purify the products.

4-Bromo-2,5-diethoxybenzaldehyde (339)



Prepared according to general procedure 5.5.1, 4-bromo **(339)** was isolated by flash column chromatography (eluent: 1/99 Et_2O/hexane) as a white solid (1.00 mmol, 274 mg, 39%), (An additional ≈20% co-eluted with residual starting material); R_f 0.75 (50:50 Et_2O:hexane); m.p. 130–132 °C (MeOH); IRν_{max} (KBr) 1679 (C=O), 1599, 1572 (C=C) cm^{-1}; ^{1}H-NMR δ (300 MHz, $CDCl_3$): 1.43–1.48 (6H, m, 2-OCH$_2$C*H$_3$*, 5-OCH$_2$C*H$_3$*), 4.06–4.14 (4H, m, 2-OC*H$_2$*CH$_3$, 5-OC*H$_2$*CH$_3$), 7.23 (1H, s, H-3), 7.32 (1H, s, H-6), 10.41 (1H, s, CHO); ^{13}C-NMR ppm (75 MHz, $CDCl_3$): 14.61 (overlap of 2-OCH$_2$*C*H$_3$ and 5-OCH$_2$*C*H$_3$), 65.03, 65.37 (2-O*C*H$_2$CH$_3$, 5-O*C*H$_2$CH$_3$), 110.69 (C-3), 118.45 (C-6), 120.81, 124.21 (C-1, C-4), 149.67, 155.54 (C-2, C-5), 188.92 (CHO); *m/z* 273 (M+H$^+$, isotope ^{79}Br, 100%), 275 (M+H$^+$, isotope ^{81}Br, 98%); HRMS calc. for $C_{11}H_{14}{}^{79}BrO_3$: (M+H$^+$) 273.0126, found: 273.0132.

6-Bromo-2,5-diethoxybenzaldehyde (183)

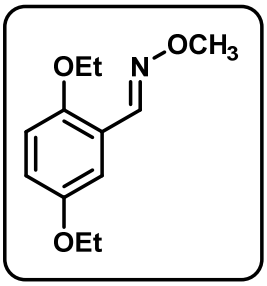


Prepared according to general procedure 5.5.1, 6-bromo **(183)** was isolated by flash column chromatography (eluent: 3/97 Et_2O/hexane) as a white solid (0.54 mmol, 147 mg, 21%); R_f 0.45 (50:50 Et_2O:hexane); m.p. 92–94 °C (MeOH); IRν_{max} (KBr) 1698 (C=O), 1596, 1567 (C=C) cm^{-1}; ^{1}H-NMR δ (300 MHz, $CDCl_3$): 1.37–1.48 (6H, m, 2-OCH$_2$C*H$_3$*, 5-OCH$_2$C*H$_3$*), 4.00–4.11 (4H, m, 2-OC*H$_2$*CH$_3$, 5-OC*H$_2$*CH$_3$), 6.90 (1H, d, *J*=9.1 Hz, H-3), 7.05 (1H, d, *J*=9.1 Hz, H-4), 10.41 (1H, s, CHO); ^{13}C-NMR ppm (75 MHz, $CDCl_3$): 14.62, 14.75 (2-OCH$_2$*C*H$_3$, 5-OCH$_2$*C*H$_3$), 65.37, 66.16 (2-O*C*H$_2$CH$_3$, 5-O*C*H$_2$CH$_3$), 112.65 (C-4), 114.56 (C-6), 119.11

(C-3), 125.06 (C-1), 149.87, 155.21 (C-2, C-5), 190.75 (CHO); *m/z* 273 ($M+H^+$, isotope ^{79}Br, 100%), 275 ($M+H^+$, isotope ^{81}Br, 98%); HRMS calc. for $C_{11}H_{14}{}^{79}BrO_3$: ($M+H^+$) 273.0126, found: 273.0125.

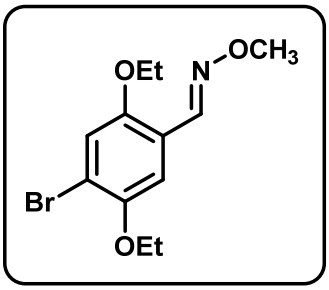
Selective synthesis of 6-bromo-2,5-diethoxybenzaldehyde (183)

(*E*)-2,5-Diethoxybenzaldehyde *O*-methyloxime (185)



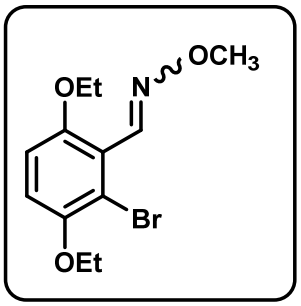
2,5-Diethoxybenzaldehyde **(184)** (5.15 mmol, 1 g) was added to a stirred solution of methoxyamine hydrochloride (6.18 mmol, 516 mg) and pyridine (20.6 mmol, 1.66 mL, 1.63 g) in dry DCM (16 mL), and the reaction was carried out according to general procedure 5.2.2.1 to yield the novel *O*-methyl oxime **(185)** as a white solid (4.53 mmol, 1.01 g, 88%), exclusively in the (*E*)-conformation; R_f 0.72 (50:50 Et_2O:hexane); m.p. 43–46 °C (MeOH); IRv_{max} (KBr) 1600, 1580 (C=C, C=N), 1500 (C=C) cm^{-1}; ^{1}H-NMR δ (300 MHz, $CDCl_3$): 1.36, 1.40 ((3H, t) × 2, *J*=2.7 Hz, 2-OCH_2CH_3, 5-OCH_2CH_3), 3.95–4.05 (7H, m, 2-OCH_2CH_3, 5-OCH_2CH_3, $NOCH_3$), 6.80 (1H, d, $J_{3,4}$=9.0 Hz, H-3), 6.88 (1H, dd, $J_{4,3}$=9.0 Hz, $J_{4,6}$=3.0 Hz, H-4), 7.33 (1H, d, $J_{6,4}$=3.0 Hz, H-6), 8.44 (1H, s, H-1'); ^{13}C-NMR ppm (75 MHz, $CDCl_3$): 14.86 (overlap of 2-OCH_2CH_3 and 5-OCH_2CH_3), 61.86 ($NOCH_3$), 64.03, 64.90 (2-OCH_2CH_3, 5-OCH_2CH_3), 110.73, 114.02, 118.23 (C-3, C-4, C-6), 121.54 (C-1), 144.76 (C-1'), 151.45, 152.96 (C-2, C-5); *m/z* 224 ($M+H^+$, 100%); HRMS calc. for $C_{12}H_{18}NO_3$: ($M+H^+$) 224.1287, found: 224.1280.

(*E*)-4-Bromo-2,5-diethoxybenzaldehyde *O*-methyloxime (340)



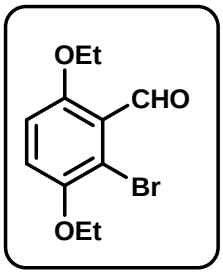
4-Bromo *O*-methyloxime **(340)** was detected as an impurity during the synthesis of 6-bromo *O*-methyloxime **(186)** using general procedure 5.2.2.2. It was isolated by silica gel flash column chromatography (eluent: 1/99 Et_2O/hexane) as a white solid (0.20 mmol, 62 mg, 5%), exclusively in the (*E*)-conformation; R_f 0.66 (20:80 Et_2O:hexane); m.p. 93–95 °C (MeOH); IRv_{max} (KBr) 1612, 1587, 1560 (C=C, C=N), 1494 (C=C) cm^{-1}; ^{1}H-NMR δ (400 MHz, $CDCl_3$): 1.39, 1.45 ((3H, t) × 2, *J*=7.0 Hz, 2-OCH_2CH_3, 5-OCH_2CH_3), 3.96–4.02 (5H, m, 2-OCH_2CH_3 or 5-OCH_2CH_3, $NOCH_3$), 4.10 (2H, q, *J*=6.8 Hz, 2-OCH_2CH_3 or 5-OCH_2CH_3), 7.09 (1H, s, H-6), 7.35 (1H, s, H-3), 8.38 (1H, s, H-1'); ^{13}C-NMR ppm (75 MHz, $CDCl_3$): 14.75, 14.78 (2-OCH_2CH_3, 5-OCH_2CH_3), 61.99 ($NOCH_3$), 65.09, 65.63 (2-OCH_2CH_3, 5-OCH_2CH_3), 110.41 (C-3), 114.72 (C-4), 117.99 (C-6), 120.73 (C-1), 144.18 (C-1'), 149.67, 151.41 (C-2, C-5); *m/z* 302 ($M+H^+$, isotope ^{79}Br, 100%), 304 ($M+H^+$, isotope ^{81}Br, 98%); HRMS calc. for $C_{12}H_{17}{}^{79}BrNO_3$: ($M+H^+$) 302.0392, found: 302.0380.

(*Z*)- and (*E*)-6-Bromo-2,5-diethoxybenzaldehyde *O*-methyloxime (186)



(*E*)-2,5-Diethoxybenzaldehyde *O*-methyloxime **(185)** (4.08 mmol, 910 mg) was added to a solution of NBS (4.08 mmol, 726 mg), $AgOCOCF_3$ (0.408 mmol, 90 mg) and $Pd(OAc)_2$ (0.408 mmol, 92 mg) in 1,2-dichloroethane (15 mL), and the reaction was carried out according to general procedure 5.2.2.2. The crude ^{1}H-NMR spectrum revealed that the novel 6-bromo *O*-methyloxime product **(186)** formed as a mixture of (*Z*)- and (*E*)-isomers in a ratio of 1:2.3 (*Z*/*E*), in a total combined yield of 68% (2.77 mmol, 838 mg). Following silica gel flash column chromatography (eluent: 2/98 Et_2O:hexane), the 6-bromo product was isolated but the two isomers were not resolved. The (*Z*/*E*) mixture was recovered as a cream solid; R_f 0.35 (20:80 Et_2O:hexane); m.p. 76–79 °C (MeOH); IRν_{max} (NaCl) 1595, 1570 (C=C, C=N), 1484 (C=C) cm^{-1}; ^{1}H-NMR δ (400 MHz, $CDCl_3$): 1.34–1.46 (m, (2-OCH$_2$C*H*$_3$)^E, (5-OCH$_2$C*H*$_3$)^E, (2-OCH$_2$C*H*$_3$)^Z, (5-OCH$_2$C*H*$_3$)^Z), 3.91–4.07 (m, (2-OC*H*$_2$CH$_3$)^E, (5-OC*H*$_2$CH$_3$)^E, (NOCH$_3$)^E, (2-OC*H*$_2$CH$_3$)^Z, (5-OC*H*$_2$CH$_3$)^Z, (NOCH$_3$)^Z), 6.79–6.88 (m, (H-3)^E, (H-4)^E, (H-3)^Z, (H-4)^Z), 7.38 (s, H-1')^Z, 8.26 (s, H-1')^E; ^{13}C-NMR ppm (150 MHz, $CDCl_3$): **(*E*)-(186)**: 14.79 (overlap of 2-OCH$_2$*C*H$_3$ and 5-OCH$_2$*C*H$_3$), 62.02 (NOCH$_3$), 65.70, 65.89 (2-O*C*H$_2$CH$_3$, 5-O*C*H$_2$CH$_3$), 112.89, 114.93 (C-3, C-4), 114.94 (C-6), 122.91 (C-1), 145.92 (C-1'), 150.02, 150.20 (C-2, C-5); **(*Z*)-(186)**: 14.73 (overlap of 2-OCH$_2$*C*H$_3$ and 5-OCH$_2$*C*H$_3$), 61.98 (NOCH$_3$), 64.96, 65.67 (2-O*C*H$_2$CH$_3$, 5-O*C*H$_2$CH$_3$), 111.73, 114.24 (C-3, C-4), 112.69 (C-6), 124.03 (C-1), 143.20 (C-1'), 149.65, 150.70 (C-2, C-5); *m/z* 302 (M+H$^+$, isotope ^{79}Br, 100%), 304 (M+H$^+$, isotope ^{81}Br, 98%); HRMS calc. for $C_{12}H_{17}{}^{79}BrNO_3$: (M+H$^+$) 302.0392, found: 302.0381.

6-Bromo-2,5-diethoxybenzaldehyde (183)



p-Toluenesulfonic acid (2 mmol, 378 mg) and paraformaldehyde (10 mmol, 298 mg), were added to a solution of (*E*/*Z*)-6-bromo-2,5-diethoxybenzaldehyde *O*-methyloxime **(186)** (1 mmol, 300 mg) in a 10/1 mixture of THF/H_2O (5 mL), and the reaction was carried out according to general procedure 5.2.2.3. The aldehyde **(183)** was recovered as a cream solid (0.98 mmol, 268 mg, 98%). As this compound had been previously synthesised, isolated and characterised (*via* general procedure 5.5.1), structure confirmation was achieved by comparison of the spectroscopic data (^{1}H-NMR/^{13}C-NMR) of the isolated impurity with those of an authentic sample.

Overall summary and future work

In chapter 2, impurities arising from the bromination of 2,5-dimethoxybenzaldehyde **(72)** were investigated. This simple bromination reaction (using Br_2/AcOH) may be carried out in clandestine laboratories, as the first step in the multistage synthesis of ring-brominated ATS, such as the phenethylamine 2C-B **(18)** and the amphetamine DOB **(35)**. Although the reaction may provide a satisfactory yield (45–74%) of the desired 4-bromo regioisomer **(160)**, we found that several other compounds were detected in the crude reaction mixture. Only one of these compounds (the 6-bromo regioisomer **(165)**) had been previously reported in the literature, as a product of this reaction. In addition to this, we identified four other compounds (**(167)**, **(168)**, **(169)** and **(170)**) in the mixture. These were identified based on their spectroscopic (^{1}H-NMR/^{13}C-NMR) and MS data, in addition to their comparison against reference standards that were independently prepared in-house.

Potentially, any of these compounds could be carried forward through subsequent reaction steps (with 4-bromo **(160)**) and be detected in street samples of the illicit ATS (e.g. compounds **(18)** or **(35)**). It is possibly more likely however, that these compounds will not make it to the final target ATS, without being modified in some way, i.e. they may undergo transformations similar to 4-bromo **(160)**, in subsequent reaction steps. This would lead to the formation of secondary/tertiary by-products, the origins of which may be difficult to establish without prior knowledge of the impurity profile of each reaction step. Bearing this in mind, future work in this area may explore the exposure of these impurities (formed in the initial bromination step) to reaction conditions that would be experienced by the intended intermediates, during the multistep synthesis to the target ATS (e.g. nitrostyrene route and Leuckart route). In addition to this potential future work, other impurities of the bromination of **(72)** may be investigated; it was recently postulated that the work-up procedure employed during this step (see general procedure 5.2.1.1), which involves a basic wash, may result in removal of potential acidic components present in the crude reaction mixture. A re-work of the aqueous phase removed following this basic wash, or elimination of the basic wash altogether during work-up, may reveal the presence of acidic components, such as benzoic acid-type by-products. It may also enhance the yield of the acidic component (phenol **(167)**) isolated previously. These potentially overlooked acidic components were not considered at the time that this work was being carried out.

Chapter 3 focussed on routes that may be employed in the synthesis of ketone precursors to ‘D series’ amphetamines. This included the direct precursor to DOB – ketone 4-Br-2,5-P2P **(159)** and the more versatile, unsubstituted analogue 2,5-P2P **(92)**. The well-known ‘phenylacetic acid route’, which is commonly used in the synthesis of ATS precursors, was attempted using the 2,5-dimethoxy substituted starting material **(108)** and the 4-bromo-2,5-dimethoxy substituted starting material **(164)**. Low yields (35–38%) of the expected ketone products were isolated. In addition to these expected products, four

other impurities were isolated from each reaction. Among these was an impurity possessing a dibenzylketone core, the yield of which is said to be greatly influenced by the number of eqv. of acetic anhydride (Ac_2O) reagent used in the reaction. Having carried out several experiments, whereby the number of eqv. of Ac_2O was varied, it was found that the yield of 'dibenzylketone' remained low (7–9%) when a large amount (≥6 eqv.) of Ac_2O was used, whereas at lower levels (≈1 eqv.) of Ac_2O, the yield of 'dibenzylketone' was substantially higher (20–26%). It was particularly noteworthy that even when a significant excess of Ac_2O was used (12 eqv.), the formation of the 'dibenzylketone' could not be eliminated. Therefore, the 'dibenzylketone' is likely to always be a contaminant of the ketone precursor to 'D series' amphetamines.

Although having only ever been reported for use in amphetamine and MDMA precursor synthesis, the 'Darzens route' was assessed for its viability in 2,5-P2P **(92)** and 4-Br-2,5-P2P **(159)** manufacture. Following optimisation of a procedure published on 'erowid.com' (site dedicated to clandestine drug manufacture), it was found that the ketones **(92)** and **(159)** could be produced in yields of 50–60%. This confirms the viability of this method for use in the synthesis of 'D series' amphetamine precursors.
In addition to the 'Darzens route', another route which has only emerged in recent years for the synthesis of ketone precursors to ATS, is one involving an α-phenylacetoacetonitrile ('APAAN') intermediate **(81)**. This route has not been reported for use in the synthesis of 'D-series' amphetamines. An assessment of the viability of this route, for the manufacture of precursors to these 'D-series' amphetamines, could be explored in the future. The impurity profiling of this reaction may provide very interesting data also; recent reports indicate that very distinctive naphthalene-based impurities can be recovered from this reaction. These impurities may be used as marker compounds, possibly aiding the assignment of synthetic route used, in the manufacture of illicit ATS.

The degradation of 2,5-P2P **(92)** was also examined in Chapter 3. It was found that over time, the ketone **(92)** degraded into several components, a significant one of these being benzaldehyde **(72)**. Based on the presence of **(72)** in the mixture, it was postulated that this degradation may be occurring as a result of light-induced α-cleavage of the ketone **(92)**, with the resultant benzyl radicals reacting with atmospheric oxygen to form benzaldehyde **(72)**. It is important to highlight this phenomenon, as a search of the literature found the presence of such benzaldehyde-type compounds to be attributed to their use as pre-precursor chemicals (and not as a degradation product of the ketone), in some cases. This assumption may possibly lead to the incorrect assignment of the route of manufacture, during the impurity profiling of an illicit ATS.

In Chapter 4, impurity profiling of the bromination of both the monomeric ketone **(92)** and 'dibenzylketone' **(221)**, was carried out. In the case of 2,5-P2P **(92)**, standard bromination (using Br_2/AcOH) was found to produce several compounds, as a result of bromine substitution taking place at

several different sites on the molecule. The key finding from this work was that bromine substitution of a compound of this structure, was non-regiospecific and the extent of bromine substitution was very difficult to control. When similar bromination experiments were carried out using the larger 'dibenzylketone' molecule **(221)**, the complexity of the resultant crude product mixtures was even greater than that observed for 2,5-P2P **(92)**. When subjected the flash column chromatography, not a single product of the bromination reaction (of **(221)**), could be isolated and identified. Despite carrying out the independent synthesis of several reference compounds (as potential products of the bromination), only two ring-brominated dibenzylketones could be confirmed as products of the bromination reaction, in addition to unreacted starting material **(221)**. The remaining unidentified products (suspected to be benzyl-substituted dibenzylketones), could not be confirmed due to the inability to synthesise pure reference standards. Possible future work in this area may involve the exploration of more selective preparation methods for the synthesis of benzyl-substituted dibenzylketone reference standards. Optimisation of MS parameters may also be investigated, in an attempt to provide more meaningful data for use in structure elucidation.

The library of impurity compounds identified throughout this thesis (and their spectroscopic/analytical data), may play a valuable role in the future impurity profiling of 'D-series' amphetamines. The data may it be used in an attempt to assign route of manufacture, as well as helping to establish the origins of potential secondary/tertiary by-products. The data may also be useful from a pharmacological/toxicological prospective. Little is known about the potential toxicity of these impurity compounds and some of these may pose a greater threat to human health than the active ATS compound itself, in street samples of the drug. A prior knowledge of theses impurities, their analytical data, and in many cases methods for their selective preparation, would help those working in toxicological assessment, to identify potentially harmful compounds much quicker. Availability of reference standards of these compounds, many of which are novel, would also allow for specific toxicity assessments to be carried out.

Dissemination of research findings

Communication of my research to date, has been carried out *via* poster and oral presentations. The details of these have been provided below:

Oral presentations:

- Mar 2011 – Presentation to staff and postgraduate students of the UCC Chemistry Department as part of Postgraduate Organic and Pharmaceutical Chemistry module CM 7002.
- Apr 2012 – Presentation to staff and postgraduate students of the UCC Chemistry Department as part of Postgraduate Organic and Pharmaceutical Chemistry module CM 7003.
- Aug 2012 – Presentation to staff and postgraduate students of the UCC Chemistry Department as part of 3rd year PhD assessment.
- Sep 2012 – Presentation to staff and postgraduate students of the UCC Chemistry Department, and representatives from Eli Lilly, as part of "10th Eli Lilly Symposium in Organic and Pharmaceutical Chemistry" held in University College Cork, Cork, Ireland.

Poster presentations:

- Jun 2011 – Poster entitled *Forensic Impurity Profiling and Synthesis of the Hallucinogenic Amphetamine DOB* presented at "63rd Irish Universities Chemistry Research Colloquium 2011" held in University College Dublin, Dublin, Ireland.
- Aug 2011 – Poster entitled *Forensic Impurity Profiling and Synthesis of the Hallucinogenic Amphetamine DOB* presented to staff and postgraduate students of the UCC Chemistry Department as part of 2nd year PhD assessment.
- Mar 2012 – Poster entitled *Forensic Impurity Profiling and Synthesis of Precursors to the Hallucinogenic Amphetamine DOB* presented at "First International Conference on Novel Psychoactive Substances" held in Budapest, Hungary.
- Jun 2013 – Poster entitled *Forensic Impurity Profiling and Synthesis of Precursors to the Hallucinogenic Amphetamine DOB* presented at "7th Conference on Analytical Sciences, Ireland (CASi)" held in University College Cork, Cork, Ireland (Awarded 1st prize in poster competition).

Preparation of manuscripts for submission to peer reviewed journals, will take place in the coming months. Provisional titles for submissions are as follows:

- *Trace impurities of the bromination of 2,5-dimethoxybenzaldehyde*
- *Impurity profiling of 2,5-dimethoxyphenyl-2-propanone ('2,5-P2P') – A key precursor to the hallucinogenic class of 'D series' amphetamines*

- *Bromination of 2,5-dimethoxyphenyl-2-propanone ('2,5-P2P') and its dimeric 'dibenzylketone' analogue*

These will be aimed for submission to the peer reviewed journals '*Forensic Science International*' (Elsevier) and '*Drug Testing and Analysis'* (Wiley online).

References

1. Bell, S., *Forensic Chemistry*, Pearson Prentice Hall, West Viginia University, 1st ed, **2006**, ISBN: 0-13-147835-4.
2. Hill, S.L. and Thomas, S.H.L., Clinical toxicology of newer recreational drugs, *Clin. Toxicol.*, **2011**, 49(*8*), 705-719.
3. Boos, T., *Designer Drugs*, D.E. Agency, **2011**.
4. *Global Synthetic Drugs Assessment 2014 - Amphetamine Type Substances and NPS*, United Nations Office on Drugs and Crime, Vienna, **2014**.
5. http://www.a1b2c3.com/drugs/amp01.htm, History of Amphetamines, (accessed: 12/10/2010).
6. Rasmussan, N., *On Speed: The Many Lives of Amphetamine*, NYU Press, **2008**, ISBN: 0814776272.
7. http://www.eclectible.com/3d/benzedrine.jpg, Benzedrine Inhaler, (accessed: 13/10/2010).
8. Hanson, G.R., Venturelli, P.J., and Fleckenstein, A.E., *Drugs and Society*, Jones & Bartlett Learning, 9th ed, **2004**, ISBN: B003TDTEA2.
9. Sulzer, D., Sonders, M.S., Poulsen, N.W., and Galli, A., Mechanisms of neurotransmitter release by amphetamines: A review, *Prog. Neurobiol.*, **2005**, 75(*6*), 406-433.
10. Iverson, L., *Drugs: A Very Short Introduction*, Oxford University Press, **2001**, ISBN: 978-0-19-285431-5.
11. King, L.A., New phenethylamines in Europe, *Drug Test. Anal.*, **2013**, 6(*7-8*), 808-818.
12. Shulgin, A. and Shulgin, A., *Pihkal - A Chemical Love Story*, Transform Press, San Francisco, 1st ed, **1991**, ISBN: 0-9630096-0-5.
13. *Recommended Methods for the Identification and Analysis of Amphetamine, Methamphetamine and their Ring-substituted Analogues in Seized Materials*, United Nations Office on Drugs and Crime, Vienna, **2006**.
14. Maurer, H.H., Chemistry, pharmacology, and metabolism of emerging drugs of abuse, *Ther. Drug Monit.*, **2010**, 32(*5*), 544-549.
15. Freeman, S. and Alder, J.F., Arylethylamine psychotropic recreational drugs: a chemical perspective, *Eur. J. Med. Chem.*, **2002**, 37(*7*), 527-539.
16. Ewald, A.H., *The 2,5-Dimethoxyamphetamines – A new Class of Designer Drugs*, (Unpublished doctoral thesis), Natural Sciences and Technical Sciences III - Chemistry, Pharmacy and Materials Science, Saarland University, Saarbrücken, **2008**.
17. Jacob III, P. and Shulgin, A.T., Structure-activity relationships of the classic hallucinogens and their analogs, *NIDA Research monograph*, **1994**, 146, 74-91.
18. Snyder, S.H., *Drugs and the Brain*, Scientific American Library: Distributed by W.H. Freeman, **1996**, ISBN: 9780716760177.
19. Nichols, D.E., Structure-activity relationships of phenethylamine hallucinogens, *J. Pharm. Sci.*, **1981**, 70(*8*), 839-849.
20. Shulgin, A.T., Sargent, T., and Naranjo, C., 4-Bromo-2,5-dimethoxyphenylisopropylamine, a new centrally active amphetamine analog, *Pharmacology*, **1971**, 5(*2*), 103-107.
21. Glennon, R.A., Titeler, M., Seggel, M., and Lyon, R.A., *N*-Methyl derivatives of the 5-HT_2 agonist 1-(4-bromo-2,5-dimethoxyphenyl)-2-aminopropane, *J. Med. Chem.*, **1987**, 30(*5*), 930-932.
22. Oberlender, R., Ramachandran, P.V., Johnson, M.P., Huang, X., and Nichols, D.E., Effect of a chiral 4-alkyl substituent in hallucinogenic amphetamines, *J. Med. Chem.*, **1995**, 38(*18*), 3593-3601.
23. Glennon, R.A., Bondarev, M.L., Khorana, N., Young, R., May, J.A., Hellberg, M.R., McLaughlin, M.A., and Sharif, N.A., β-Oxygenated analogues of the 5-HT_{2A} serotonin receptor agonist 1-(4-bromo-2,5-dimethoxyphenyl)-2-aminopropane, *J. Med. Chem.*, **2004**, 47(*24*), 6034-6041.
24. Monte, A.P., Marona-Lewicka, D., Parker, M.A., Wainscott, D.B., Nelson, D.L., and Nichols, D.E., Dihydrobenzofuran analogues of hallucinogens. 3. Models of 4-substituted (2,5-

dimethoxyphenyl)alkylamine derivatives with rigidified methoxy groups, *J. Med. Chem.*, **1996**, 39(*15*), 2953-2961.
25. Nichols, D.E., The medicinal chemistry of phenethylamine psychedelics, *The Heffter Review of Psychedelic Research*, **1998**, 1, 40-45.
26. Griffin, D., *Studies in the Synthesis and Impurity Profiling of 2,5-Dimethoxy Amphetamines* (Unpublished doctoral thesis), University College Cork, Cork, Ireland, **2009**.
27. Ries, R.K., Fiellin, D.A., Miller, S.C., and Saitz, R., *Principles of Addiction Medicine*, Lippincott Williams & Wilkins, 4th ed, **2009**, ISBN: 0781774772.
28. Arunotayanun, W. and Gibbons, S., Natural product 'legal highs', *Nat. Prod. Rep.*, **2012**, 29(*11*), 1304-1316.
29. Gouzoulis-Mayfrank, E. and Hermle, L., *Are the "entactogens" a distinct psychoactive substance class?*, in *The Heffter Review of Psychedelic Research*, Heffter Research Institute, D.E. Nichols, **1998**, Vol. 1.
30. *Precursors and Chemicals Frequently Used in the Illicit Manufacture of Narcotic Drugs and Psychotropic Substances, 2013*, INCB and United Nations Office on Drugs and Crime, New York, **2014**.
31. Collins, M., Some new psychoactive substances: Precursor chemicals and synthesis-driven end-products, *Drug Test. Anal.*, **2011**, 3(*7-8*), 404-416.
32. http://basic-clinical-pharmacology.net/chapter%2032_%20drugs%20of%20abuse.htm, Pharmacology of amphetamine, (accessed: 08/01/2010).
33. http://mongboards.com/Pharmacology/Amphetamines.htm, Mechanism of action of amphetamine-like drugs, (accessed: 07/07/2014).
34. Chambers, J.J., Kurrasch-Orbaugh, D.M., Parker, M.A., and Nichols, D.E., Enantiospecific synthesis and pharmacological evaluation of a series of super-potent, conformationally restricted 5-$HT_{2A/2C}$ receptor agonists, *J. Med. Chem.*, **2001**, 44(*6*), 1003-1010.
35. Nelson, D.L., Lucaites, V.L., Wainscott, D.B., and Glennon, R.A., Comparisons of hallucinogenic phenylisopropylamine binding affinities at cloned human 5-HT_{2A}, 5-HT_{2B} and 5-HT_{2C} receptors, *Naunyn-Schmiedeberg's Arch. Pharmacol.*, **1999**, 359(*1*), 1-6.
36. Fiorella, D., Rabin, R.A., and Winter, J.C., The role of the 5-HT_{2A} and 5-HT_{2C} receptors in the stimulus effects of hallucinogenic drugs I: Antagonist correlation analysis, *Psychopharmacology*, **1995**, 121(*3*), 347-356.
37. Vernier, P., Cardinaud, B., Valdenaire, O., Philippe, H., and Vincent, J.-D., An evolutionary view of drug-receptor interaction: the bioamine receptor family, *Trends Pharmacol. Sci.*, **1995**, 16(*11*), 375-381.
38. Ettrup, A., Hansen, M., Santini, M.A., Paine, J., Gillings, N., Palner, M., Lehel, S., Herth, M.M., Madsen, J., Kristensen, J., Begtrup, M., and Knudsen, G.M., Radiosynthesis and *in vivo* evaluation of a series of substituted ^{11}C-phenethylamines as 5-HT_{2A} agonist PET tracers, *Eur. J. Nucl. Med. Mol. Imaging*, **2011**, 38(*4*), 681-693.
39. Juncosa, J.I., Hansen, M., Bonner, L.A., Cueva, J.P., Maglathlin, R., McCorvy, J.D., Marona-Lewicka, D., Lill, M.A., and Nichols, D.E., Extensive rigid analogue design maps the binding conformation of potent *N*-benzylphenethylamine 5-HT_{2A} serotonin receptor agonist ligands, *ACS Chem, Neurosci.*, **2012**, 4(*1*), 96-109.
40. http://www.cnsforum.com/content/pictures/imagebank/hirespng/5HT_struc_level2.png, 5-HT receptor, (accessed: 10/01/2011).
41. Nichols, D.E., Differences between the mechanism of action of MDMA, MBDB, and the classic hallucinogens. Identification of a new therapeutic class: entactogens, *J. Psychoactive Drugs*, **1986**, 18(*4*), 305-313.
42. *Illicit Drug Data Report 2008-09 - Amphetamine-Type Stimulants*, Australian Crime Commission, Canberra, **2009**.
43. *World Drug Report 2013*, United Nations Office on Drugs and Crime, Vienna, **2014**.
44. *European Drug Report 2014: Trends and Developments*, European Monitoring Centre for Drugs and Drug Addiction, Lisbon, **2014**.
45. *Annual Report of An Garda Siochana*, An Garda Siochana, Garda Headquarters, Phoenix Park, Dublin, **2003**.

46. *Annual Report of An Garda Siochana*, An Garda Siochana, Garda Headquarters, Phoenix Park, Dublin, **2004**.
47. *Annual Report of An Garda Siochana*, An Garda Siochana, Garda Headquarters, Phoenix park, Dublin, **2005**.
48. *Annual Report of An Garda Siochana*, An Garda Siochana, Garda Headquarters, Phoenix Park, Dublin, **2006**.
49. *Annual Report of An Garda Siochana*, An Garda Siochana, Garda Headquarters, Phoenix Park, Dublin, **2007**.
50. *Annual Report of An Garda Siochana*, An Garda Siochana, Garda Headquarters, Phoenix Park, Dublin, **2008**.
51. *Annual Report of An Garda Siochana*, An Garda Siochana, Garda Headquarters, Phoenix park, Dublin, **2009**.
52. *Annual Report of An Garda Siochana*, An Garda Siochana, Garda Headquarters, Phoenix Park, Dublin, **2010**.
53. *Annual Report of An Garda Siochana*, An Garda Siochana, Garda Headquarters, Phoenix Park, Dublin, **2011**.
54. *Annual Report of An Garda Siochana*, An Garda Siochana, Garda Headquarters, Phoenix Park, Dublin, **2012**.
55. *Drug Use in Ireland and Northern Ireland*, National Advisory Committee on Drugs (NACD) and Drug and Alcohol Information and Research Unit (DAIRU), **2008**.
56. *2010 Annual Report on the State of the Drugs Problem in Europe*, European Monitoring Centre for Drugs and Drug Addiction, Lisbon, **2010**.
57. *Amphetamine: a European Union Perspective in the Global Context*, Europol and European Monitoring Centre for Drugs and Drug Addiction, Lisbon, **2011**.
58. *Amphetamine-Type Stimulants in the European Union 1998-2007*, Europol, The Hague, **2007**.
59. *European Drug Report 2013: Trends and Developments*, European Monitoring Centre for Drugs and Drug Addiction, Lisbon, **2013**.
60. Dujourdy, L., Dufey, V., Besacier, F., Miano, N., Marquis, R., Lock, E., Aalberg, L., Dieckmann, S., Zrcek, F., and Bozenko Jr, J.S., Drug intelligence based on organic impurities in illicit MA samples, *Forensic Sci. Int.*, **2008**, 177(*2-3*), 153-161.
61. *EU Drug Markets Report: A Strategic Analysis*, Europol and the European Monitoring Centre for Drugs and Drug Addiction, Luxemburg, **2013**.
62. http://treaties.un.org/Pages/Treaties.aspx?id=6&subid=A&lang=en, United Nations Treaty Collection, (accessed: 15/04/2011).
63. http://isomerdesign.com/Cdsa/legislationUS.php?structure=C, Controlled Substances Act, 1970, (accessed: 15/04/2011).
64. http://www.legislation.gov.uk/ukpga/1971/38/schedule/2, Misuse of Drugs Act, 1971, (accessed: 15/04/2011).
65. http://www.irishstatutebook.ie/1977/en/act/pub/0012/index.html, Misuse of Drugs Act, 1977 (accessed: 15/04/2011).
66. O'Mahony Carey, S., *Psychoactive substances - A guide to ethnobotanical plants and herbs, synthetic chemicals, compounds and products*, Substance Misuse Service South Tipperary, **2007**.
67. *Drug Policy Profiles - Ireland*, European Monitoring Centre for Drugs and Drug Addiction, Lisbon, **2013**.
68. *Dáil passes emergency legislation after Court of Appeal rules possession of ecstasy and other psychoactive drugs legal*, rte.ie, **11/03/2015**.
69. http://www.oireachtas.ie/viewdoc.asp?fn=/documents/bills28/bills/2015/2115/b2115d.pdf, Misuse of Drugs (Ammendment) Bill 2015, (accessed: 07/04/2015).
70. da Costa, J.L., Wang, A.Y., Micke, G.A., Maldaner, A.O., Romano, R.L., Martins-Júnior, H.A., Neto, O.N., and Tavares, M.F.M., Chemical identification of 2,5-dimethoxy-4-bromoamphetamine (DOB), *Forensic Sci. Int.*, **2007**, 173(*2-3*), 130-136.
71. Ewald, A.H., Fritschi, G., Bork, W.-R., and Maurer, H.H., Designer drugs 2,5-dimethoxy-4-bromo-amphetamine (DOB) and 2,5-dimethoxy-4-bromo-methamphetamine (MDOB): studies

on their metabolism and toxicological detection in rat urine using gas chromatographic/mass spectrometric techniques, *J. Mass Spectrom.*, **2006**, 41(*4*), 487-498.
72. Bell, S.E.J., Fido, L.A., Sirimuthu, N.M.S., Speers, S.J., Peters, K.L., and Cosbey, S.H., Screening tablets for DOB using surface-enhanced raman spectroscopy, *J. Forensic Sci.*, **2007**, 52, 5.
73. Winek, C.L., Collom, W.D., and Bricker, J.D., A death due to 4-bromo-2,5-dimethoxyamphetamine, *Clin. Toxicol.*, **1981**, 18(*3*), 267-271.
74. Balíková, M., Nonfatal and fatal DOB (2,5-dimethoxy-4-bromamphetamine) overdose, *Forensic Sci. Int.*, **2005**, 153(*1*), 85-91.
75. Buhrich, N., Morris, G., and Cook, G., Bromo-DMA - The Australasian hallucinogen, *Australasian and N.Z. J. of Psychiatry*, **1983**, 17(*3*), 275-279.
76. Sargent, T., Kalbhen, D.A., Shulgin, A.T., Braun, G., Stauffer, H., and Kusubov, N., *In vivo* human pharmacodynamics of the psychodysleptic 4-Br-2,5-dimethoxyphenylisopropylamine labelled with ^{82}Br or ^{77}Br, *Neuropharmacology*, **1975**, 14(*3*), 165-174.
77. Beránková, K., Szkutová, M., and Balíková, M., Distribution profile of 2,5-dimethoxy-4-bromoamphetamine (DOB) in rats after oral and subcutaneous doses, *Forensic Sci. Int.*, **2007**, 170(*2-3*), 94-99.
78. Shulgin, A.T., Manning, T., and Daley, P.F., *The Shulgin Index: Vol 1: Psychedelic Phenethylamines and Related Compounds*, Transform Press, **2011**, ISBN: 9780963009630.
79. http://www.justice.gov/dea/pr/micrograms.shtml, DEA micrograms, (accessed: 10/04/2014).
80. http://www.erowid.org/chemicals/showimage.php?i=dob/dobpowderi2005e1617disp.jpg, Powdered DOB, (accessed: 19/04/2011).
81. http://www.justice.gov/dea/programs/forensicsci/microgram/mg1106/mg1106.pdf, DOB empregnated onto blotting paper, (accessed: 19/04/2011).
82. *Dangerous new drug seized in Mayo*, *Hot Press*, **25/11/2003**.
83. *Fresh warnings over "snowballs"*, *Irish Daily Star*, **29/11/2003**.
84. *New Cork drug danger*, Cooke, N., *The Evening Echo*, Cork, **2003**.
85. *Drugs snowballing out of control*, Clark, S., *thepost.ie*, **16/11/2003**.
86. http://www.emcdda.europa.eu/stats13#display:/stats13/szrtab21, Drug seizures not included in other SZR tables, 2004-2011, (accessed: 03/04/2015).
87. Delliou, D., 4-Bromo-2,5-dimethoxyamphetamine: Psychoactivity, toxic effects and analytical methods, *Forensic Sci. Int.*, **1983**, 21(*3*), 259-267.
88. Cole, M.D., Lea, C., and Oxley, N., 4-Bromo-2,5-dimethoxyphenethylamine (2C-B): a review of the public domain literature, *Sci. Justice*, **2002**, 42(*4*), 223-224.
89. Kanai, K., Takekawa, K., Kumamoto, T., Ishikawa, T., and Ohmori, T., Simultaneous analysis of six phenethylamine-type designer drugs by TLC, LC-MS, and GC-MS, *Forensic Toxicol.*, **2008**, 26(*1*), 6-12.
90. *Drug Characterization/Impurity Profiling*, United Nations Office on Drugs and Crime, Vienna, **2004**.
91. Milliet, Q., Weyermann, C., and Esseiva, P., The profiling of MDMA tablets: A study of the combination of physical characteristics and organic impurities as sources of information, *Forensic Sci. Int.*, **2009**, 187(*1-3*), 58-65.
92. Qi, Y., Evans, I., and McCluskey, A., New impurity profiles of recent Australian imported 'ice': Methamphetamine impurity profiling and the identification of (pseudo)ephedrine and Leuckart specific marker compounds, *Forensic Sci. Int.*, **2007**, 169(*2-3*), 173-180.
93. Kunalan, V., Nic Daéid, N., Kerr, W.J., Buchanan, H.A.S., and McPherson, A.R., Characterization of route specific impurities found in methamphetamine synthesized by the Leuckart and Reductive Amination methods, *Anal. Chem.*, **2009**, 81(*17*), 7342-7348.
94. Singh, S., Handa, T., Narayanam, M., Sahu, A., Junwal, M., and Shah, R.P., A critical review on the use of modern sophisticated hyphenated tools in the characterization of impurities and degradation products, *J. Pharm. Biomed. Anal.*, **2012**, 69, 148-173.
95. http://chemweb.ucc.ie/courses/CM4106/GCpart2.pdf, Hyphenated analytical technologies, (accessed: 22/04/2011).
96. Nic Daéid, N. and Waddell, R.J.H., The analytical and chemometric procedures used to profile illicit drug seizures, *Talanta*, **2005**, 67(*2*), 280-285.

97. Dujourdy, L. and Besacier, F., Headspace profiling of cocaine samples for intelligence purposes, *Forensic Sci. Int.*, **2008**, 179(*2-3*), 111-122.
98. Krawczyk, W. and Parczewski, A., Application of chemometric methods in searching for illicit Leuckart amphetamine sources, *Anal. Chim. Acta*, **2001**, 446(*1-2*), 107-114.
99. Stojanovska, N., Fu, S., Tahtouh, M., Kelly, T., Beavis, A., and Kirkbride, K.P., A review of impurity profiling and synthetic route of manufacture of methylamphetamine, 3,4-methylenedioxymethylamphetamine, amphetamine, dimethylamphetamine and *p*-methoxyamphetamine, *Forensic Sci. Int.*, **2013**, 224(*1*), 8-26.
100. Ballany, J., Caddy, B., Cole, M., Finnon, Y., Aalberg, L., Janhunen, K., Sippola, E., Andersson, K., Bertler, C., Dahlén, J., Kopp, I., Dujourdy, L., Lock, E., Margot, P., Huizer, H., Poortman, A., Kaa, E., and Lopes, A., Development of a harmonised pan-European method for the profiling of amphetamines, *Sci. Justice*, **2001**, 41(*3*), 193-196.
101. Aalberg, L., Andersson, K., Bertler, C., Borén, H., Cole, M.D., Dahlén, J., Finnon, Y., Huizer, H., Jalava, K., Kaa, E., Lock, E., Lopes, A., Poortman-van der Meer, A., and Sippola, E., Development of a harmonised method for the profiling of amphetamines: I. Synthesis of standards and compilation of analytical data, *Forensic Sci. Int.*, **2005**, 149(*2-3*), 219-229.
102. Camilleri, A., Johnston, M.R., Brennan, M., Davis, S., and Caldicott, D.G.E., Chemical analysis of four capsules containing the controlled substance analogues 4-methylmethcathinone, 2-fluoromethamphetamine, α-phthalimidopropiophenone and *N*-ethylcathinone, *Forensic Sci. Int.*, **2010**, 197(*1-3*), 59-66.
103. Finnon, Y.S., Waddell, R.J.H., Nic Daéid, N., and Carter, K.C., Preliminary investigation of the toxicity levels of amphetamine impurities, *Sci. Justice*, **2001**, 41(*3*), 229-230.
104. Cheng, J.Y.K., Chan, M.F., Chan, T.W., and Hung, M.Y., Impurity profiling of ecstasy tablets seized in Hong Kong by gas chromatography-mass spectrometry, *Forensic Sci. Int.*, **2006**, 162(*1-3*), 87-94.
105. Koper, C., van den Boom, C., Wiarda, W., Schrader, M., de Joode, P., van der Peijl, G., and Bolck, A., Elemental analysis of 3,4-methylenedioxymethamphetamine (MDMA): A tool to determine the synthesis method and trace links, *Forensic Sci. Int.*, **2007**, 171(*2-3*), 171-179.
106. Baer, I. and Margot, P., Analysis of fatty acids in ecstasy tablets, *Forensic Sci. Int.*, **2009**, 188(*1-3*), 68-74.
107. Weyermann, C., Marquis, R., Delaporte, C., Esseiva, P., Lock, E., Aalberg, L., Bozenko Jr, J.S., Dieckmann, S., Dujourdy, L., and Zrcek, F., Drug intelligence based on MDMA tablets data: I. Organic impurities profiling, *Forensic Sci. Int.*, **2008**, 177(*1*), 11-16.
108. Swist, M., Wilamowski, J., and Parczewski, A., Determination of synthesis method of ecstasy based on the basic impurities, *Forensic Sci. Int.*, **2005**, 152(*2-3*), 175-184.
109. Świst, M., Wilamowski, J., Zuba, D., Kochana, J., and Parczewski, A., Determination of synthesis route of 1-(3,4-methylenedioxyphenyl)-2-propanone (MDP-2-P) based on impurity profiles of MDMA, *Forensic Sci. Int.*, **2005**, 149(*2–3*), 181-192.
110. Dufey, V., Dujourdy, L., Besacier, F., and Chaudron, H., A quick and automated method for profiling heroin samples for tactical intelligence purposes, *Forensic Sci. Int.*, **2007**, 169(*2-3*), 108-117.
111. Verweij, A.M.A., Impurities in illicit drug preparations: Amphetamine and methamphetamine, *Forensic Sci. Rev.*, **1989**, 1(*1*), 1-11.
112. Zhang, J.X., Zhang, D.M., and Han, X.G., Identification of impurities and statistical classification of methamphetamine hydrochloride drugs seized in China, *Forensic Sci. Int.*, **2008**, 182(*1-3*), 13-19.
113. Dayrit, F.M. and Dumlao, M.C., Impurity profiling of methamphetamine hydrochloride drugs seized in the Philippines, *Forensic Sci. Int.*, **2004**, 144(*1*), 29-36.
114. Błachut, D., Wojtasiewicz, K., Krawczyk, K., Maurin, J., Szawkało, J., and Czarnocki, Z., Identification and synthesis of by-products found in 4-methylthioamphetamine (4-MTA) produced by the Leuckart method, *Forensic Sci. Int.*, **2012**, 216(*1–3*), 108-120.
115. Soine, W.H., Clandestine drug synthesis, *Med. Res. Rev.*, **1986**, 6(*1*), 41-74.
116. http://aisforatlanta.com/2010/12/when-bad-homes-happen-to-good-people/, Small scale methamphetamine laboratory, (accessed: 04/08/2010).

117. *Amphetamines and Ecstasy, 2011 Global ATS Assessment*, United Nations Office on Drugs and Crime, Vienna, **2011**.
118. *Police discover largest synthetic drugs production site ever found in the EU*, Europol, The Hague, the Netherlands, **23/10/2013**.
119. *World Drug Report 2010*, United Nations Office on Drugs and Crime, Vienna, **2010**.
120. *Perspectives on drugs: Synthetic drug production in Europe*, European Monitoring Centre for Drugs and Drug Addiction, Lisbon, **2013**.
121. http://www.rte.ie/news/2008/0722/drugs1.html, Methamphetamine seized in Offaly raid, (accessed: 03/03/2011).
122. *Cold medicines being used to manufacture crystal meth*, rte.ie, **17/09/2012**.
123. krawczyk, W., Kunda, T., and Perowska, I., *Impurity profiling/comparitive analyses of samples of 1-phenyl-2-propanone*, Central forensic laboratory of the police, Warsaw, **2005**.
124. Di Giovanni, S., Varriale, A., Marzullo, V.M., Ruggiero, G., Staiano, M., Secchi, A., Pierno, L., Fiorello, A.M., and D'Auria, S., Determination of benzyl methyl ketone - a commonly used precursor in amphetamine manufacture, *Anal. Methods*, **2012**, 4(*11*), 3558-3564.
125. Frank, R.S., The clandestine drug laboratory situation in the United States, *J. Forensic Sci.*, **1983**, 28(*1*), 18-31.
126. Schneiders, S., Holdermann, T., and Dahlenburg, R., Comparative analysis of 1-phenyl-2-propanone (P2P), an amphetamine-type stimulant precursor, using stable isotope ratio mass spectrometry: Presented in part as a poster at the 2nd meeting of the Joint European Stable Isotope User Meeting (JESIUM), Giens, France, September 2008, *Sci. Justice*, **2009**, 49(*2*), 94-101.
127. Snow, O., *Amphetamine Syntheses: Industrial*, Thoth Press, **2002**, ISBN: 9780966312836.
128. 'Uncle-Fester', *Secrets of Methamphetamine Manufacture: Including Recipes for MDA, Ecstasy, and Other Psychedelic Amphetamines*, Loompanics Unlimited, **1996**, ISBN: 9781559501446.
129. http://designer-drugs.com/pte/12.162.180.114/dcd/chemistry/phenylacetone.html, Synthesis of phenyl-2-propanone (P2P), (accessed: 03/12/10).
130. Herbst, R.M. and Manske, R.H., Methyl benzyl ketone, *Org. Synth.*, **1938**, 18, 54.
131. Błachut, D., Wojtasiewicz, K., and Czarnocki, Z., Identification and synthesis of some contaminants present in 4-methoxyamphetamine (PMA) prepared by the Leuckart method, *Forensic Sci. Int.*, **2002**, 127(*1–2*), 45-62.
132. Power, J.D., Clarke, K., McDermott, S.D., McGlynn, P., Barry, M., White, C., O'Brien, J., and Kavanagh, P., The identification of 4-methylamphetamine and its synthesis by-products in forensic samples, *Forensic Sci. Int.*, **2013**, 228(*1–3*), 115-131.
133. Müller, L., Martin, N., Rößler, T., and Pütz, M. *APAAN – a new precursor substance for the illicit production of amphetamine* at *XVIIIth GTFCh-Symposium Including Satellite Symposium on "New Techniques and New Drugs – Impact on Forensic Chemistry and Toxicology"*, **2013**, Vol. 80, 280.
134. Inoue, H., Iwata, Y.T., and Kumamoto, T., Characaterization and profiling of methamphetamine seizures, *J. Health Sci.*, **2008**, 54(*6*), 615-622.
135. *World Drug Report 2012*, United Nations Office on Drugs and Crime, Vienna, **2012**.
136. Newman, M.S. and Magerlein, B.J., *The Darzens Glycidic Ester Condensation*, in *Organic Reactions*, John Wiley & Sons, Inc., **1949**, ISBN: 9780471264187.
137. Elks, J. and Hey, D.H., β-3 : 4-Methylenedioxyphenylisopropylamine, *J. Chem. Soc.*, **1943**, 15-16.
138. Dal cason, T.A., An evaluation of the potential for clandestine manufacture of 3,4-methylenedioxyamphetamine (MDA) analogs and homologs, *J. Forensic Sci.*, **1990**, 35(*3*), 675-697.
139. Collins, M., Heagney, A., Cordaro, F., Odgers, D., Tarrant, G., and Stewart, S., Methyl 3-[3',4'-(methylenedioxy)phenyl]-2-methyl glycidate: An ecstasy precursor seized in Sydney, Australia, *J. Forensic Sci.*, **2007**, 52(*4*), 898-903.
140. *Global SMART Update 2012*, United Nations Office on Drugs and Crime, **2012**, Vol. 7.
141. *'Determined' gang jailed over £5m drugs plot*, Tubb, G., *skynews.com*, **14/03/2013**.

142. *Synthetic drug precursor traficking network broken up*, Europol, The Hague, Netherlands, **03/04/2014**.
143. *The illicit drug trade through south-eastern Europe*, United Nations Office on Drugs and Crime, Vienna, **2014**.
144. Tsujikawa, K., Kuwayama, K., Miyaguchi, H., Kanamori, T., Iwata, Y.T., and Inoue, H., Chemical profiling of seized methamphetamine putatively synthesized from phenylacetic acid derivatives, *Forensic Sci. Int.*, **2013**, 227(*1*), 42-44.
145. http://www.erowid.org/archive/rhodium/chemistry/eleusis/bisulfite.html, Purification of ketones by sodium bisulfite, (accessed: 21/04/2014).
146. Forbes, I.J. and Kirkbride, K.P., Origin of alkenes in illicit amphetamine: An examination of the illicit synthesis of phenyl-2-propanone *J. Forensic Sci.*, **1992**, 37(*5*), 8.
147. *The Challenge of New Psychoactive Substances*, United Nations Office on Drugs and Crime, Global SMART Programme, **2013**.
148. Mechoulam, R., Lander, N., University, A., and Zahalka, J., Synthesis of the individual, pharmacologically distinct, enantiomers of a tetrahydrocannabinol derivative, *Tetrahedron: Asymmetry*, **1990**, 1(*5*), 315-318.
149. Lugassy, D.M., *Clinical Toxicology, An Issue of Emergency Medicine Clinics of North America*, Elsevier Health Sciences, **2014**, ISBN: 9780323266550.
150. Jankovics, P., Váradi, A., Tölgyesi, L., Lohner, S., Németh-Palotás, J., and Kőszegi-Szalai, H., Identification and characterization of the new designer drug 4′-methylethcathinone (4-MEC) and elaboration of a novel liquid chromatography–tandem mass spectrometry (LC–MS/MS) screening method for seven different methcathinone analogs, *Forensic Sci. Int.*, **2011**, 210(*1–3*), 213-220.
151. Zuba, D., Sekuła, K., and Buczek, A., Identification and characterization of 2,5-dimethoxy-4-nitro-β-phenethylamine (2C-N) – A new member of 2C-series of designer drug, *Forensic Sci. Int.*, **2012**, 222(*1–3*), 298-305.
152. Sainsbury, P.D., Kicman, A.T., Archer, R.P., King, L.A., and Braithwaite, R.A., Aminoindanes—the next wave of 'legal highs'?, *Drug Test. Anal.*, **2011**, 3(*7-8*), 479-482.
153. Shulgin, A. and Shulgin, A., *Tihkal: The Continuation*, Transform Press (CA), **1997**, ISBN: 9780963009692.
154. *New psychoactive substances: European Commission proposal gets green light from the European Parliament (IP/14/461)*, European Commission, Strasbourg, **2014**.
155. *Global SMART Update 2013 v10*, United Nations Office on Drugs and Crime, **2013**, Vol. 10.
156. Simmons, R.L., Yu, R.T., and Myers, A.G., Storable arylpalladium(II) reagents for alkene labeling in aqueous media, *J. Am. Chem. Soc.*, **2011**, 133(*40*), 15870-15873.
157. Koo, J.Y., Oh, S., Cho, S.-R., Koh, M., Oh, W.-K., Choi, H.-S., and Park, S.B., Total synthesis of eryvarin H and its derivatives and their biological activity as ERR[γ] inverse agonist, *Org. Biomol. Chem.*, **2013**, 11(*35*), 5782-5786.
158. Radomkit, S., Sarnpitak, P., Tummatorn, J., Batsomboon, P., Ruchirawat, S., and Ploypradith, P., Pt(IV)-catalyzed generation and [4+2]-cycloaddition reactions of *o*-quinone methides, *Tetrahedron*, **2011**, 67(*21*), 3904-3914.
159. Tisdale, E.J., Kochman, D.A., and Theodorakis, E.A., Total synthesis of atroviridin, *Tetrahedron Lett.*, **2003**, 44(*16*), 3281-3284.
160. Bedford, R.B., Bowen, J.G., and Weeks, A.L., Synthesis of murrayaquinone A and analogues *via* ring-closing C–H arylation, *Tetrahedron*, **2013**, 69(*22*), 4389-4394.
161. Barfknecht, C.F. and Nichols, D.E., Potential psychotomimetics: Bromomethoxyamphetamines and structural congeners of lysergic acid, *J. Med. Chem.*, **1971**, 14(*4*), 370-372.
162. Sardessai, M.S. and Abramson, H.N., The bromination of 2,5-dimethoxybenzaldehyde - Structural proof of the 6-isomer *via* 3,6-dimethoxybenzocyclobutene, *Org. Prep. Proced. Int.*, **1991**, 23(*4*), 419-424.
163. Craig, B.D. and Anderson, D.S., *Handbook of Corrosion Data*, ASM International, **1994**, ISBN: 9780871705181.

164. Takao, K.-i., Nanamiya, R., Fukushima, Y., Namba, A., Yoshida, K., and Tadano, K.-i., Total synthesis of (+)-clavilactone A and (−)-clavilactone B by ring-opening/ring-closing metathesis, *Org. Lett.*, **2013**, 15(*21*), 5582-5585.
165. Sato, K., Asao, N., and Yamamoto, Y., Efficient method for synthesis of angucyclinone antibiotics *via* gold-catalyzed intramolecular [4+2] benzannulation: Enantioselective total synthesis of (+)-ochromycinone and (+)-rubiginone B2, *J. Org. Chem.*, **2005**, 70(*22*), 8977-8981.
166. Li, C., Johnson, R.P., and Porco, J.A., Total synthesis of the quinone epoxide dimer (+)-torreyanic acid: Application of a biomimetic oxidation/electrocyclization/Diels−Alder dimerization cascade, *J. Am. Chem. Soc.*, **2003**, 125(*17*), 5095-5106.
167. Dubost, E., Fossey, C., Cailly, T., Rault, S., and Fabis, F., Selective *ortho*-bromination of substituted benzaldoximes using Pd-Catalyzed C–H activation: Application to the synthesis of substituted 2-bromobenzaldehydes, *J. Org. Chem.*, **2011**, 76(*15*), 6414-6420.
168. Gordon, M.S., Sojka, S.A., and Krause, J.G., Carbon-13 NMR of *para*-substituted hydrazones, phenylhydrazones, oximes, and oxime methyl ethers: substituent effects on the iminyl carbon, *J. Org. Chem.*, **1984**, 49(*1*), 97-100.
169. Evano, G., Schaus, J.V., and Panek, J.S., A convergent synthesis of the macrocyclic core of cytotrienins: Application of RCM for macrocyclization, *Org. Lett.*, **2004**, 6(*4*), 525-528.
170. Swenton, J.S. and Raynolds, P.W., A regiospecific synthesis of the anthracycline aglycons, daunomycinone and adriamycinone, *J. Am. Chem. Soc.*, **1978**, 100(*19*), 6188-6195.
171. Glennon, R.A., Liebowitz, S.M., and Anderson, G.M., Serotonin receptor affinities of psychoactive phenalkylamine analogs, *J. Med. Chem.*, **1980**, 23(*3*), 294-299.
172. Rubenstein, L., CCLXX.-Substitution in derivatives of quinol ethers, *J. Chem. Soc. Perkin-Trans 1*, **1925**, 127, 1998-2004.
173. Tsutsui, S., Tanaka, H., and Sakamoto, K., Preparation, structures, and theoretical calculations of novel silacalixarene derivatives: Silacalix[4]quinone and silacalix[4]hydroquinone octamethyl ether, *Organometallics*, **2004**, 23(*15*), 3719-3726.
174. Ungnade, H.E. and Zilch, K.T., Phenoxyquinones. II. The diphenoxyquinones, *J. Org. Chem.*, **1951**, 16(*1*), 64-69.
175. Moy, C.L., Kaliappan, R., and McNeil, A.J., Aryl trihydroxyborate salts: Thermally unstable species with unusual gelation abilities, *J. Org. Chem.*, **2011**, 76(*20*), 8501-8507.
176. Adimurthy, S., Ramachandraiah, G., Bedekar, A.V., Ghosh, S., Ranu, B.C., and Ghosh, P.K., Eco-friendly and versatile brominating reagent prepared from a liquid bromine precursor, *Green Chem.*, **2006**, 8(*10*), 916-922.
177. Kadokawa, J.-i., Tanaka, Y., Yamashita, Y., and Yamamoto, K., Synthesis of poly(spiropyran)s by polycondensation and their photoisomerization behaviors, *Eur. Polym. J.*, **2012**, 48(*3*), 549-559.
178. Lee, K.-S. and Lee, J.-S., Synthesis of highly fluorinated poly(arylene ether sulfide) for polymeric optical waveguides, *Chem. Mater.*, **2006**, 18(*18*), 4519-4525.
179. Yadav, R.R., Battini, N., Mudududdla, R., Bharate, J.B., Muparappu, N., Bharate, S.B., and Vishwakarma, R.A., Deformylation of indole and azaindole-3-carboxaldehydes using anthranilamide and solid acid heterogeneous catalyst *via* quinazolinone intermediate, *Tetrahedron Lett.*, **2012**, 53(*17*), 2222-2225.
180. Rangisetty, J.B., Dukat, M., Dowd, C.S., Herrick-Davis, K., DuPre, A., Gadepalli, S., Teitler, M., Kelley, C.R., Sharif, N.A., and Glennon, R.A., 1-[2-Methoxy-5-(3-phenylpropyl)]-2-aminopropane unexpectedly shows 5-HT_{2A} serotonin receptor affinity and antagonist character, *J. Med. Chem.*, **2001**, 44(*20*), 3283-3291.
181. Ulrich, H., Rao, D.V., Tucker, B., and Sayigh, A.A.R., Selective demethylation of 2,5-dimethoxybenzaldehyde to 5-hydroxy-2-methoxybenzaldehyde, *J. Org. Chem.*, **1974**, 39(*16*), 2437-2438.
182. Du, Z.-T., Lu, J., Yu, H.-R., Xu, Y., and Li, A.-P., A facile demethylation of *ortho* substituted aryl methyl ethers promoted by $AlCl_3$, *J. Chem. Res.*, **2010**, 34(*4*), 222-227.
183. Maruyama, S., Kikuchi, K., Hirano, T., Urano, Y., and Nagano, T., A novel, cell-permeable, fluorescent probe for ratiometric imaging of zinc ion, *J. Am. Chem. Soc.*, **2002**, 124(*36*), 10650-10651.

184. Lanfranchi, D.A. and Hanquet, G., Asymmetric Diels−Alder reactions of a new enantiomerically pure sulfinylquinone: A straightforward access to functionalized Wieland−Miescher ketone analogues with (*R*) absolute configuration, *J. Org. Chem.*, **2006**, 71(*13*), 4854-4861.
185. Zou, C.-L., Ji, H., Xie, G.-B., Chen, D.-L., and Wang, F.-P., An effective *O*-demethylation of some C19-diterpenoid alkaloids with HBr–glacial acetic acid, *J. Asian Nat. Prod. Res.*, **2008**, 10(*11*), 1063-1067.
186. Przybyl, A.K., Flippen-Anderson, J.L., Jacobson, A.E., and Rice, K.C., Practical and high-yield syntheses of dihydromorphine from tetrahydrothebaine and efficient syntheses of (8S)-8-bromomorphide, *J. Org. Chem.*, **2003**, 68(*5*), 2010-2013.
187. Nicholson, J.W. and Wilson, A.D., The conversion of carboxylic acids to ketones: A repeated discovery, *J. Chem. Educ.*, **2004**, 81(*9*), 1362.
188. Dakin, H.D. and West, R., A general reaction of amino acids, *J. Biol. Chem.*, **1928**, 78(*1*), 91-104.
189. Allinger, N.L., Wang, G.L., and Dewhurst, B.B., Kinetic and mechanistic studies of the Dakin-West reaction, *J. Org. Chem.*, **1974**, 39(*12*), 1730-1735.
190. Buchanan, G.L., The Dakin-West reaction, *Chem. Soc. Rev.*, **1988**, 17, 91-109.
191. Tran, K.-V. and Bickar, D., Dakin−West synthesis of β-aryl ketones, *J. Org. Chem.*, **2006**, 71(*17*), 6640-6643.
192. King, J.A. and McMillan, F.H., The decarboxylative acylation of α-substituted acids, *J. Am. Chem. Soc.*, **1955**, 77(*10*), 2814-2816.
193. Allen, A.C., Stevenson, M.L., Nakamura, S.M., and Ely, R.A., Differentiation of illicit phenyl-2-propanone synthesized from phenylacetic acid with acetic anhydride versus lead (II) acetate, *J. Forensic Sci.*, **1992**, 37(*1*), 301-322.
194. Ammermann, S., Hrib, C., Jones, P.G., du Mont, W.-W., Kowalsky, W., and Johannes, H.-H., Pyrrolo[1,2-*a*]quinoxalines: Novel synthesis *via* annulation of 2-alkylquinoxalines, *Org. Lett.*, **2012**, 14(*19*), 5090-5093.
195. Jozwiak, K., Khalid, C., Tanga, M.J., Berzetei-Gurske, I., Jimenez, L., Kozocas, J.A., Woo, A., Zhu, W., Xiao, R.-P., Abernethy, D.R., and Wainer, I.W., Comparative molecular field analysis of the binding of the stereoisomers of fenoterol and fenoterol derivatives to the β2 adrenergic receptor, *J. Med. Chem.*, **2007**, 50(*12*), 2903-2915.
196. Hurd, C.D., Christ, R., and Thomas, C.L., Preparation and pyrolysis of dibenzyl ketone, phenylacetic anhydride and diphenylacetic anhydride, *J. Am. Chem. Soc.*, **1933**, 55(*6*), 2589-2592.
197. Smith, G.G., Preparation of ketones and their enol esters by the base-catalyzed condensation of acids and acid derivatives with anhydrides, *J. Am. Chem. Soc.*, **1953**, 75(*5*), 1134-1137.
198. House, H.O., Czuba, L.J., Gall, M., and Olmstead, H.D., Chemistry of carbanions. XVIII. Preparation of trimethylsilyl enol ethers, *J. Org. Chem.*, **1969**, 34(*8*), 2324-2336.
199. Nishiguchi, I., Oki, T., Hirashima, T., and Shiokawa, J., Electroreductive acylation of benzyl chlorides with acid anhydrides. Stereoselective formation of (*E*)-enol esters from benzyl alkyl ketones, *Chem. Lett.*, **1991**, 20(*11*), 2005-2008.
200. Hurd, C.D. and Thomas, C.L., Preparation of dibenzyl ketone and phenylacetone, *J. Am. Chem. Soc.*, **1936**, 58(*7*), 1240-1240.
201. Magidson, O.Y. and Garkusha, G.A., The synthesis of β-phenylisopropylamine (phenamine), *Chemical abstracts*, **1941**, 35, 7.
202. King, J.A. and McMillan, F.H., The decarboxylative acylation of arylacetic acids, *J. Am. Chem. Soc.*, **1951**, 73(*10*), 4911-4915.
203. Waldman, S.R., Monte, A.P., Bracey, A., and Nichols, D.E., One-pot Claisen rearrangement/*O*-methylation/alkene isomerization in the synthesis of *ortho*-methoxylated phenylisopropylamines, *Tetrahedron Lett.*, **1996**, 37(*44*), 7889-7892.
204. Rowe, D., *Chemistry and Technology of Flavours and Fragrances*, Wiley, **2009**, ISBN: 9781405148078.
205. Crouch, R.D., Holden, M.S., and Romany, C.A., The Darzens condensation: Structure determination through spectral analysis and understanding substrate reactivity, *J. Chem. Educ.*, **2004**, 81(*5*), 711.

206. Mhamdi, L., Bohli, H., Moussaoui, Y., and Salem, R.b., Phase transfer catalysis of Henry and Darzens reactions, *International Journal of Organic Chemistry*, **2011**, 1, 119-124.
207. Billman, J.H. and Tonnis, J.A., Substituted aralkyl aldehydes: Preparation and antitumor evaluation, *J. Pharm. Sci.*, **1971**, 60(*8*), 1188-1192.
208. Ban, Y. and Oishi, T., The preparation of 2-(Substituted phenyl) ethanols, *Chem. Pharm. Bull.*, **1958**, 6(*5*), 574-576.
209. Skaddan, M.B. and Katzenellenbogen, J.A., Integrated "3+1" oxorhenium(V) complexes as estrogen mimics, *Bioconjugate Chem.*, **1998**, 10(*1*), 119-129.
210. Roux-Schmitt, M.C., Seyden-Penne, J., and Wolfe, S., Stereochemistry of the aldol condensation of benzaldehydes with alpha-chloro esters : An example of the gauche effect of adjacent polar bonds, *Tetrahedron*, **1972**, 28(*19*), 4965-4979.
211. Dullaghan, M.E. and Nord, F.F., Studies on the chemistry of heterocyclics. XXI. The Darzens reaction, *J. Org. Chem.*, **1952**, 17(*9*), 1183-1186.
212. Nelson, N.K. and Morris, H.H., Decarboxylation of α-substituted glycidic acids, *J. Am. Chem. Soc.*, **1953**, 75(*14*), 3337-3339.
213. Clegg, N.J., Paruthiyil, S., Leitman, D.C., and Scanlan, T.S., Differential response of estrogen receptor subtypes to 1,3-diarylindene and 2,3-diarylindene ligands, *J. Med. Chem.*, **2005**, 48(*19*), 5989-6003.
214. Johnson, C.R. and Bade, T.R., Dianions derived from α-halo acids. The Darzens condensation revisited, *J. Org. Chem.*, **1982**, 47(*7*), 1205-1212.
215. Valente, V.R. and Wolfhagen, J.L., The stereospecific synthesis of *cis* and *trans* isomers of glycidic esters and products of the Darzens synthesis, *J. Org. Chem.*, **1966**, 31(*8*), 2509-2512.
216. Josa, D., Peña-Gallego, A., Rodríguez-Otero, J., and Cabaleiro-Lago, E., Theoretical study of the decomposition of ethyl and ethyl 3-phenyl glycidate, *J. Mol. Model.*, **2013**, 19(*1*), 315-320.
217. Blanchard, E.P. and Buchi, G., A new method for the conversion of glycidic esters to aldehydes and ketones, *J. Am. Chem. Soc.*, **1963**, 85(*7*), 955-958.
218. http://www.erowid.org/archive/rhodium/chemistry/25dmp2p.html, 2,5-dimethoxyphenylacetone *via* Darzen Condensation, (accessed: 05/12/2013).
219. Tung, C.C., Speziale, A.J., and Frazier, H.W., The Darzens condensation. II. Reaction of chloroacetamides with aromatic aldehydes, *J. Org. Chem.*, **1963**, 28(*6*), 1514-1521.
220. Günther, H., *NMR Spectroscopy: Basic Principles, Concepts and Applications in Chemistry*, Wiley, **2013**, ISBN: 9783527674756.
221. http://www.chem.wisc.edu/areas/reich/nmr/notes-5-hmr-13-ABX3.pdf, ABX_3 Spectra, (accessed: 07/10/2014).
222. Kagan, J., *Organic Photochemistry - Principles and Applications*, Academic Press Limited, San Diego, **1993**, ISBN: 0-12-394320-5.
223. Turro, N.J. and Weed, G.C., Micellar systems as supercages for reactions of geminate radical pairs. Magnetic effects, *J. Am. Chem. Soc.*, **1983**, 105(*7*), 1861-1868.
224. Aspee, A., Maretti, L., and Scaiano, J.C., Monitoring photodecomposition of dibenzyl ketone within NaY zeolite with a pre-fluorescent nitroxide compound, *Photochem Photobiol Sci*, **2003**, 2(*11*), 1125-9.
225. Ruzicka, R., Baráková, L., and Klán, P., Photodecarbonylation of dibenzyl ketones and trapping of radical intermediates by copper(II) chloride in frozen aqueous solutions, *J. Phys. Chem. B*, **2005**, 109(*19*), 9346-9353.
226. Houk, K.N., The photochemistry and spectroscopy of β,γ-unsaturated carbonyl compounds, *Chem. Rev.*, **1976**, 76(*1*), 1-74.
227. Wan, P. and Yates, K., Photochemistry of α-aryl carbonyl compounds in aqueous solution, *J. Chem. Soc., Chem. Commun.*, **1982**, (*5*), 275-276.
228. Xu, Y., Hixon, M.S., Yamamoto, N., McAllister, L.A., Wentworth, A.D., Wentworth, P., Jr., and Janda, K.D., Antibody-catalyzed anaerobic destruction of methamphetamine, *Proc. Natl. Acad. Sci. USA*, **2007**, 104(*10*), 3681-6.
229. Tada, N., Hattori, K., Nobuta, T., Miura, T., and Itoh, A., Facile aerobic photooxidation of methyl group in the aromatic nucleus in the presence of an organocatalyst under VIS irradiation, *Green Chem.*, **2011**, 13(*7*), 1669-1671.

230. Step, E.N. and Turro, N.J., Photolysis of ketones in oxygen-saturated micellar solution: oxygen scavenging of C-centered radicals in microheterogeneous media, *J. Photochem. Photobiol., A*, **1994**, 84(*3*), 249-256.
231. Choi, H.Y. and Chi, D.Y., Nonselective bromination−selective debromination strategy: Selective bromination of unsymmetrical ketones on singly activated carbon against doubly activated carbon, *Org. Lett.*, **2003**, 5(*4*), 411-414.
232. Lagoja, I.M., Pannecouque, C., Van Aerschot, A., Witvrouw, M., Debyser, Z., Balzarini, J., Herdewijn, P., and De Clercq, E., *N*-Aminoimidazole derivatives inhibiting retroviral replication *via* a yet unidentified mode of action, *J. Med. Chem.*, **2003**, 46(*8*), 1546-1553.
233. Megiel, E., Kaim, A., and Cyrański, M.K., Theoretical and experimental studies on stability of the C-ON bond in new ketone functionalized *N*-alkoxyamines, *J. Phys. Org. Chem.*, **2010**, 23(*12*), 1146-1154.
234. Takahashi, N., Ito, T., Matsuda, Y., Kogure, N., Kitajima, M., and Takayama, H., Determination of absolute configuration of trimeric indole alkaloid, psychotrimine, by first asymmetric total synthesis, *Chem. Commun.*, **2010**, 46(*14*), 2501-2503.
235. Podgoršek, A., Stavber, S., Zupan, M., and Iskra, J., Visible light induced 'on water' benzylic bromination with *N*-bromosuccinimide, *Tetrahedron Lett.*, **2006**, 47(*7*), 1097-1099.
236. Mann, J., Wilde, P.D., and Finch, M.W., Synthesis and reactions of 2-aryl-8-oxabicycloc[3.2.1]oct-6-en-3-ones, *Tetrahedron*, **1987**, 43(*22*), 5431-5441.
237. McMurry, J., *Organic Chemistry, Enhanced Edition*, Cengage Learning, **2009**, ISBN: 9780538733953.
238. Lange, J.H.M., Attali, A., van der Neut, M.A.W., Wals, H.C., Mulder, A., Zilaout, H., Duursma, A., van Aken, H.H.M., and van Vliet, B.J., Two distinct classes of novel pyrazolinecarboxamides as potent cannabinoid CB1 receptor agonists, *Bioorg. Med. Chem. Lett.*, **2010**, 20(*17*), 4992-4998.
239. Matsumoto, K., Okada, A., Girek, T., Ikemi, Y., Kim, J.C., Hayashi, N., Yoshida, H., and Kakehi, A., Synthesis of 2-methyl-4,6-diaryl-1,2,3-triazinones *via* diarylcyclopropenones, *Heterocycl. Commun.*, **2002**, 8(*4*), 325-328.
240. Kodukulla, R.P.K., Trivedi, G.K., Vora, J.D., and Mathur, H.H., Synthesis, chemical transformation and antimicrobial activity of a novel class of nitroolefins: 1,3-diaryl-2-nitroprop-1-enes, *Synth. Commun.*, **1994**, 24(*6*), 819-832.
241. McNamara, Y.M., Cloonan, S.M., Knox, A.J.S., Keating, J.J., Butler, S.G., Peters, G.H., Meegan, M.J., and Williams, D.C., Synthesis and serotonin transporter activity of 1,3-bis(aryl)-2-nitro-1-propenes as a new class of anticancer agents, *Biorg. Med. Chem.*, **2011**, 19(*3*), 1328-1348.
242. North, M., *Principles and Applications of Stereochemistry*, Taylor & Francis, **1998**, ISBN: 9780748739943.
243. http://designer-drugs.com/pte/12.162.180.114/dcd/chemistry/2cb.beaker.html, 2C-B synthesis without LAH, (accessed: 03/12/10).
244. Shechter, H., Ley, D.E., and Roberson, E.B., Nitroalkanes from conjugated nitroalkenes by reduction with complex hydrides, *J. Am. Chem. Soc.*, **1956**, 78(*19*), 4984-4991.
245. Coutts, R.T. and Malicky, J.L., The synthesis of some analogs of the hallucinogen 1-(2,5-dithethoxy-4-methylphenyl)-2-aminopropane (DOM), *Can. J. Chem.*, **1972**, 51, 1402-1409.
246. Meyers, A.I. and Sircar, J.C., Reduction of nitroalkenes to nitroalkanes with aqueous sodium borohydride, *J. Org. Chem.*, **1967**, 32(*12*), 4134-4136.
247. Sinhababu, A.K. and Borchardt, R.T., Silica gel-assisted reduction of nitrostyrenes to 2-aryl-1-nitroalkanes with sodium borohydride, *Tetrahedron Lett.*, **1983**, 24(*3*), 227-230.
248. Keating, J.J., *Studies in the Synthesis and Impurity Profiling of Methylenedioxy and Alkylthioamphetamines*, (Unpublished doctoral thesis), Trinity College Dublin, Dublin, Ireland, **2001**.
249. McNulty, J., Steere, J.A., and Wolf, S., The ultrasound promoted Knoevenagel condensation of aromatic aldehydes, *Tetrahedron Lett.*, **1998**, 39(*44*), 8013-8016.
250. Gallaway, W.S. and Murray, M.J., Isomerization of certain olefins by silica gel at room temperature, *J. Am. Chem. Soc.*, **1948**, 70(*7*), 2584-2586.

251. Guy, M., Freeman, S., Alder, J.F., and Brandt, S.D., The Henry reaction: Spectroscopic studies of nitrile and hydroxylamine by-products formed during synthesis of psychoactive phenylalkylamines, *Cent. Eur. J. Chem*, **2008**, 6(*4*), 526-534.
252. Hurtado-Guzman, C., Iturriaga-Vasquez, P., Zapata-Torres, G., and Cassels, B.K., Geometrical isomerism in β-nitrostyrenes: Preferred conformations of (*E*)- and (*Z*)-1-(4-methylthiophenyl)-2-nitrobutenes, *J. Chil. Chem. Soc.*, **2004**, 49, 257-260.
253. Yamamura, K. and Watarai, S., Phenylations of β-nitrostyrene derivatives with benzene by the use of palladium(II) acetate, *Bull. Chem. Soc. Jpn.*, **1975**, 48(*12*), 3757-3758.
254. Pavia, D., Lampman, G., Kriz, G., and Vyvyan, J., *Introduction to Spectroscopy*, Cengage Learning, **2014**, ISBN: 9781305177826.
255. Kaap, S., Quentin, I., Tamiru, D., Shaheen, M., Eger, K., and Steinfelder, H.J., Structure activity analysis of the pro-apoptotic, antitumor effect of nitrostyrene adducts and related compounds, *Biochem. Pharmacol.*, **2003**, 65(*4*), 603-610.
256. Milhazes, N., Calheiros, R., Marques, M.P.M., Garrido, J., Cordeiro, M.N.D.S., Rodrigues, C., Quinteira, S., Novais, C., Peixe, L., and Borges, F., β-Nitrostyrene derivatives as potential antibacterial agents: A structure–property–activity relationship study, *Biorg. Med. Chem.*, **2006**, 14(*12*), 4078-4088.
257. Wasik, A., Gandy, M., McIldowie, M., Holder, M., Chamba, A., Challa, A., Lewis, K., Young, S., Scheel-Toellner, D., Dyer, M., Barnes, N., Piggott, M., and Gordon, J., Enhancing the anti-lymphoma potential of 3,4-methylenedioxymethamphetamine ('ecstasy') through iterative chemical redesign: mechanisms and pathways to cell death, *Invest. New Drugs*, **2011**, 1-13.
258. Gandy, M.N., McIldowie, M., Lewis, K., Wasik, A.M., Salomonczyk, D., Wagg, K., Millar, Z.A., Tindiglia, D., Huot, P., Johnston, T., Thiele, S., Nguyen, B., Barnes, N.M., Brotchie, J.M., Martin-Iverson, M.T., Nash, J., Gordon, J., and Piggott, M.J., Redesigning the designer drug ecstasy: non-psychoactive MDMA analogues exhibiting Burkitt's lymphoma cytotoxicity, *MedChemComm*, **2010**, 1(*4*), 287-293.
259. Richards, S.A. and Hollerton, J.C., *Essential Practical NMR for Organic Chemistry*, Wiley, **2010**, ISBN: 9780470977224.
260. Rodríguez, J.M. and Dolors Pujol, M., Straightforward synthesis of nitroolefins by microwave- or ultrasound-assisted Henry reaction, *Tetrahedron Lett.*, **2011**, 52(*21*), 2629-2632.
261. Rosowsky, A., Mota, C.E., Wright, J.E., Freisheim, J.H., Heusner, J.J., McCormack, J.J., and Queener, S.F., 2,4-Diaminothieno[2,3-d]pyrimidine analogs of trimetrexate and piritrexim as potential inhibitors of Pneumocystis carinii and Toxoplasma gondii dihydrofolate reductase, *J. Med. Chem.*, **1993**, 36(*21*), 3103-3112.
262. Kantam, M.L., Arundhathi, R., Likhar, P.R., and Damodara, D., Reusable copper-aluminum hydrotalcite/rac-BINOL system for room temperature selective aerobic oxidation of alcohols, *Adv. Synth. Catal.*, **2009**, 351(*16*), 2633-2637.
263. Cheng, A.C. and Castagnoli, N., Synthesis and physicochemical and neurotoxicity studies of 1-(4-substituted-2,5-dihydroxyphenyl)-2-aminoethane analogs of 6-hydroxydopamine, *J. Med. Chem.*, **1984**, 27(*4*), 513-520.
264. Cassels, B.K., Herreros, S., Ibanez, C., Rezende, M.C., and Sebastian, C., Synthesis of antitumoral 1-aryl-2-nitroalkenes, *An. Asoc. Quim. Argent.*, **1982**, 70, 283-288.